

UNCLASSIFIED

AD NUMBER

ADB017286

LIMITATION CHANGES

TO:

Approved for public release; distribution is unlimited.

FROM:

Distribution authorized to U.S. Gov't. agencies only; Test and Evaluation; JAN 1977. Other requests shall be referred to Air Force Rocket Propulsion Lab., Edwards AFB, CA 93523.

AUTHORITY

AFRPL ltr 10 Mar 1986

THIS PAGE IS UNCLASSIFIED

AD BO 17 286

AUTHORITY:

AFRPL

145 10 MAR 86





✓  
AFRPL-TR-77-7 ✓

(2)



LOW COST MOTOR DEMONSTRATION PROGRAM  
PHASE 1 REPORT, VOLUME I

THIOKOL/HUNTSVILLE DIVISION ✓  
HUNTSVILLE, ALABAMA 35807

AUTHORS: W. R. SUMMERS  
G. P. ROYS, ET AL.

F E B R U A R Y 1 9 7 7

Interim Report for Period June 1975 to November 1976.

Distribution limited to U.S. Government agencies only;  
Test and Evaluation, January 1977. Other requests for  
this document must be referred to AFRPL/STINFO/DOZ,  
Edwards AFB, California 93523.

**COPY AVAILABLE TO DDC DOES NOT  
PERMIT FULLY LEGIBLE PRODUCTION**

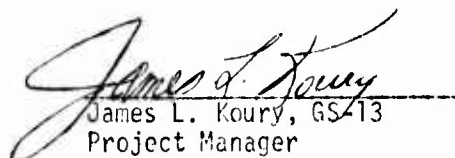
Prepared for:  
AIR FORCE ROCKET PROPULSION LABORATORY  
DIRECTOR OF SCIENCE AND TECHNOLOGY  
AIR FORCE SYSTEMS COMMAND  
EDWARDS AFB, CALIFORNIA 93523

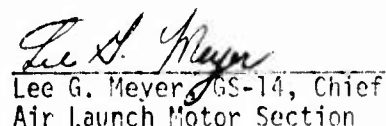
ADBO17286

## FOREWORD

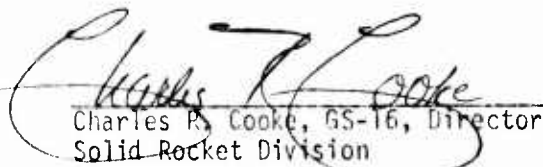
This report was submitted by Thiokol Corporation/Huntsville Division at Huntsville, Alabama 35807 under Contract Number F04611-75-C-0059, Job Order 314810GV with the Air Force Rocket Propulsion Laboratory, Edwards AFB, California 93523.

This technical report has been reviewed and is approved for publication and distribution in accordance with the distribution statement on the cover and on the DD Form 1473.

  
James L. Koury, GS-13  
Project Manager

  
Lee G. Meyer, GS-14, Chief  
Air Launch Motor Section

FOR THE COMMANDER

  
Charles R. Cooke, GS-16, Director  
Solid Rocket Division

## NOTICES

When U.S. Government drawings, specifications, or other data are used for any purpose other than a definitely related government procurement operation, the Government thereby incurs no responsibility nor any obligation whatsoever, and the fact that the Government may have formulated, furnished, or in any way supplied the said drawings, specifications or other data, is not to be regarded by implication or otherwise, or in any manner licensing the holder or any other person or corporation, or conveying any rights or permission to manufacture, use, or sell any patented invention that may in any way be related thereto.

ACCESSION No.	White Section	<input type="checkbox"/>
RTS	Red Section	<input type="checkbox"/>
SEC		
UNANNOUNCED		
JUSTIFICATION		
BY	DISTRIBUTION/AVAILABILITY CODES	
Dist.	Avail. and of SPECIAL	
		

UNCLASSIFIED

SECURITY CLASSIFICATION OF THIS PAGE (When Data Entered)

REPORT DOCUMENTATION PAGE		READ INSTRUCTIONS BEFORE COMPLETING FORM	
1. REPORT NUMBER AFRPL-TR-77-7	2. GOVT ACCESSION NO.	3. RECIPIENT'S CATALOG NUMBER	
4. TITLE (and Subtitle) LOW COST MOTOR DEMONSTRATION PROGRAM, <del>PILOT REPORT</del> VOLUME 1		5. TYPE OF REPORT & PERIOD COVERED Interim Report. Jun 1975 thru Nov 1976 on Phase I	
6. AUTHOR(s) George P. Roys, et. al.		7. CONTRACT OR GRANT NUMBER(s) F04611-75-C-0059	
8. PERFORMING ORGANIZATION NAME AND ADDRESS Thiokol/Huntsville Division A Division of Thiokol Corporation Huntsville, Alabama 35807		9. PROGRAM ELEMENT, PROJECT, TASK AREA & WORK UNIT NUMBERS Project 3148 JON3148106V	
10. CONTROLLING OFFICE NAME AND ADDRESS Air Force Rocket Propulsion Laboratory/MKMB Edwards AFB, CA 93523		11. REPORT DATE February 1977	
12. MONITORING AGENCY NAME & ADDRESS (if different from Controlling Office)		13. NUMBER OF PAGES 588	
		14. SECURITY CLASS. (of this report) UNCLASSIFIED	
		15a. DECLASSIFICATION/DOWNGRADING SCHEDULE	
16. DISTRIBUTION STATEMENT (of this Report) Distribution limited to U.S. Gov't agencies only. Test and Evaluation January 1977. Other requests for this document must be referred to AFRPL (STINFO)/DOZ, Edwards AFB, California 93523			
17. DISTRIBUTION STATEMENT (of the abstract entered in Block 20, if different from Report) Approved for Public Release, Distribution Unlimited			
18. SUPPLEMENTARY NOTES N/A			
19. KEY WORDS (Continue on reverse side if necessary and identify by block number) solid propellant rocket motors, low cost techniques and components, high volume production rate, injection molded nozzle, consumable mandrel, igniter initiators and pyrotechnics, stock tubing motor cases, impact extruded motor cases, laminated motor cases, cost/performance trade-off,			
20. ABSTRACT (Continue on reverse side if necessary and identify by block number) The program objective is to identify materials, designs, and manufacturing techniques that will significantly reduce the cost of tactical rocket motors in production and to demonstrate in pilot production quantities the validity of such identities. Phase I evaluated design options for each motor component through tests and analyses. Eleven full-scale four-inch diameter motors and ten sub-scale nozzle material evaluation motors were static tested. A low cost grain manufacturing technique of pour casting deaerated			

DD FORM 1 JAN 73 1473

EDITION OF 1 NOV 65 IS OBSOLETE

UNCLASSIFIED

SECURITY CLASSIFICATION OF THIS PAGE (When Data Entered)

next page

bpg

UNCLASSIFIED

SECURITY CLASSIFICATION OF THIS PAGE(When Data Entered)

19. Key Words (Continued)

ambient temperature cured adhesive, thermoplastic and mastic insulation, grain forming experiments, joining techniques for closures and nozzles, adhesives, minimum cost/minimum weight combinations.

cont

20. Abstract (Continued)

propellant without benefit of vacuum was evaluated by manufacturing two motors. Technology in ambient-temperature (80°F) propellants developed under AFRPL contract was satisfactorily transferred and combined with in-house technology to produce improved propellant.

Components and other manufacturing techniques evaluated were consumable grain-forming mandrels, igniter initiators and pyrotechnics, nozzle ablative materials, nozzle configuration, steel and aluminum stock tubing cases, aluminum impact extruded cases, metal and plastic laminated cases, techniques for joining nozzles and forward closures to cases, thermoplastic and mastic case insulations and adhesives.

Performance analyses were made to determine effects of nozzle throat erosion rate, case strength level, thrust profile, and propellant formulation on missile performance. Cost and weight data were combined to determine the best combinations of forward closure with its joining technique, case, and nozzle with its joining technique.



UNCLASSIFIED

SECURITY CLASSIFICATION OF THIS PAGE(When Data Entered)

## TABLE OF CONTENTS

	<u>Page</u>
<u>Section I.</u> <u>INTRODUCTION</u>	1
<u>Section II.</u> <u>SUMMARY AND CONCLUSIONS</u>	5
BASELINE MOTOR	7
PROPELLANT	7
POUR CASTING	8
FULL-SCALE MOTORS TESTS	8
CONSUMABLE MANDREL	8
IGNITER	9
NOZZLE	9
CASE	10
CLOSURE/JOINING TECHNIQUE	10
INSULATION/LINER	11
PERFORMANCE AND COST TRADE-OFFS	11
NEEDED ADDITIONAL INVESTIGATIONS	12
REFERENCES	12
<u>Section III.</u> <u>BASELINE MOTOR PRELIMINARY DESIGN</u>	15
<u>Section IV.</u> <u>PROPELLANT TAILORING AND CHARACTERIZATION</u>	31
PROPELLANT REQUIREMENTS	34
PROPELLANT FORMULATIONS AND	
CHARACTERISTICS	34
MOTOR LOADINGS AND PROPELLANT	35
Mix T-600 (TP-H8245)	37
Mix T-607 (TP-H8245)	47
Aerojet Formulation	60
Mix T-630 (DTS-7984)	64
Mix T-656 (DTS-7984)	78
Mix T-684 (DTS-7984)	78
Reproducibility and Control of Ambient Temperature	
Cure Propellants	81
Processing Aids	86
Process Hot/Ambient Cure	86
CONCLUSIONS	91
REFERENCES	91
<u>Section V.</u> <u>POUR-CASTING TECHNIQUE FOR MOTOR</u>	
<u>MANUFACTURING</u>	93
PROPELLANT SELECTION	95
PROPELLANT CASTING	96
DTS-7984, Mix T-630	96
TP-H8208, Mix T-640	102

TABLE OF CONTENTS (Continued)

	<u>Page</u>
COMPARISON OF MOTOR QUALITY AND PROPELLANTS	107
CONCLUSIONS	107
REFERENCE	109
<u>Section VI.</u>	
<u>SUMMARY OF TX-631 STATIC TESTS</u>	111
PREDICTED PERFORMANCE	113
STATIC TEST RESULTS	117
Group No. 1	117
Group No. 2	126
Group No. 3	126
Group No. 4	136
Group No. 5	140
Post-Test Investigation of T684-2	147
REFERENCES	172
<u>Section VII.</u>	
<u>CONSUMABLE MANDREL</u>	173
MANDREL MANUFACTURE	176
Mandrel Material	176
"Low Density" Mandrels	179
"High Density" Mandrels	193
MOLD RELEASE AGENT	193
MOTOR TEST RESULTS	194
CONCLUSIONS	194
REFERENCES	196
<u>Section VIII.</u>	
<u>IGNITER/CONSUMABLE MANDREL STUDY</u>	197
LABORATORY TEST EVALUATION	199
Series I Tests	203
Series II Tests	208
Series III Tests	208
Alternate Approach	212
CONCEPTS EVALUATION	212
Pyrotechnics	212
Initiators	214
Atlas Electric Match	216
Electric Match and Welding	225
CONCEPT SELECTION	225
FULL-SCALE MOTOR TESTS	228
First Test Group	228
Second Test Group	233
Third Test Group	237
Fourth Test Group	247

## TABLE OF CONTENTS (Continued)

	<u>Page</u>
Fifth Test Group	250
CONCLUSIONS	256
REFERENCES	258
 <u>Section IX.</u>	
<u>NOZZLE STUDY</u>	259
APPROACH	261
MATERIAL SELECTION	263
STRUCTURAL ANALYSIS	265
Nozzle Geometries	265
Method of Analysis	273
Results	273
THROAT EROSION	282
AVAILABILITY	306
COSTS	306
SUMMARY AND CONCLUSIONS	315
VENDORS	320
 <u>Section X.</u>	
<u>CASE STUDIES</u>	321
<u>STOCK TUBING STUDY</u>	323
Initial Investigation	323
Expanded Investigation	324
Summary of Tubing Characteristics	325
IMPACT EXTRUDED CASE STUDY	325
Summary and Conclusions	334
Integral Forward Closure (R53148)	337
Integral Nozzle Shell (R53152)	339
WOUND METAL/PLASTIC LAMINATE CASE	342
Wound Metal Cases	342
Plastic Laminate Case	343
VENDOR CONTACTS	349
Stock Tubing	349
Case Impact Extrusions	349
Strip Laminate Case	349
REFERENCE	349
 <u>Section XI.</u>	
<u>CLOSURE/JOINING STUDY</u>	351
STRESS ANALYSIS	357
LABORATORY TESTS	357
Friction Welding	357
Weldbonding	364
Rivethbonding	369
Tapered Bondline	369
Electromagnetic Forming (EMF)	369



## TABLE OF CONTENTS (Continued)

	<u>Page</u>
COMPARISON OF JOINING METHODS	371
Welding Methods	371
Adhesive Bonding	374
Mechanical Retainers	377
Closure Cost Studies	377
SUMMARY	379
REFERENCES	381
VENDOR CONTACTS	381
Closure Manufacture	381
Welding Equipment and Services	382
Machining and Welding Vendors	383
Adhesives	383
Electromagnetic Forming	383
Tube Forming	384
Plastic Closures	384
 <u>Section XII.</u>	
<u>INSULATION/LINER STUDY</u>	385
INITIAL SCREENING	388
Liner	388
Mastic Insulation	388
Insulation Sleeve	390
Adhesives	390
Summary	390
LINER	390
MASTIC INSULATION	398
INSULATION SLEEVE	414
Cartridge Sleeve Fabrication	420
FULL-SCALE MOTOR TESTS	420
MATERIAL SELECTION	424
SUMMARY AND RECOMMENDATIONS	430
 <u>Section XIII.</u>	
<u>GRAIN DESIGN AND PERFORMANCE STUDY</u>	433
GENERALIZED PERFORMANCE STUDY	435
RELATIONSHIP BETWEEN COST AND PERFORMANCE	455
BURN RATE STUDY	458
GRAIN DESIGN STUDY	460
Assumption for Cost Comparisons	464
Comparison of Cartridge and Case-Bonded Grains	464
GAP BETWEEN INSULATION SLEEVE AND CASE	478
EFFECT OF INSULATION THICKNESS ON PERFORMANCE	483
EFFECT OF CASE STRENGTH ON PERFORMANCE	487



# TABLE OF CONTENTS (Continued)

	<u>Page</u>
VENDOR CONTACTS	487
REFERENCES	487
<u>Section XIV. COST COMPARISONS</u>	489
<u>Section XV. PHASE II MOTOR CONFIGURATIONS</u>	499
<u>Appendix A. BALLISTIC ANALYSIS OF TP-H8245 PROPELLANT</u>	
(MIX T-600)	507
BURNING RATE	509
TX-395 Motors	509
Cured Strands	510
TEMPERATURE EFFECTS	510
$\pi_k$	510
$\sigma_k$	511
<u>Appendix B. STOCK TUBING STUDY</u>	525
STEEL TUBULAR PRODUCTS	527
Background	527
Preliminary Screening	530
Seamless Versus Welded Steel Tubing	532
Welded Tubing Considerations	536
Summary of Preliminary Screening of Steel	
Tubular Products	538
ALUMINUM TUBULAR PRODUCTS	539
Background	539
Materials	539
Preliminary Screening	539
MATERIAL COMPARISONS	542
Mechanical Properties	543
Processing Properties	543
Physical Properties	543
Economic Properties	543
Corrosion Resistance (General)	543
Stress Corrosion	544
Tensile Properties	545
Temperature Effects on Mechanical Properties	545
Fracture Toughness Properties	547
Weldability	548
Formability	550
Machinability	551
Heat Treating Characteristics	552
Wall Thicknesses and Weights	554
Mill Tolerances	555

# TABLE OF CONTENTS (Continued)

	<u>Page</u>
Cost	555
Summary of Material Considerations	555
Cost Versus Performance	559
EXPANDED INVESTIGATIONS	564
Tubing Wall Thicknesses	564
Tubing Weights	570
Loaded Tubing Mass Fraction	570
Properties of 6061-T6 Aluminum	575
VENDOR CONTACTS	578
REFERENCES	579
Military Handbooks	580
Federal Specifications	581
Military Specifications	581
 <u>Appendix C.</u>	
<u>DRAG COEFFICIENT FOR 4-INCH DIAMETER</u>	
<u>LOW-COST MOTOR</u>	583
 <u>Appendix D.</u>	
<u>PROPELLANT FORMULATIONS</u>	Volume 2 -1

## LIST OF TABLES

<u>No.</u>	<u>TITLE</u>	<u>Page</u>
II-1	Lowest Cost/Lowest Weight Combinations	13
II-2	Phase II Motor Configuration	14
III-1	Baseline Motor Design	22
III-2	Properties and Ballistics of HTPB Type Propellant	25
IV-1	Summary of Phase I Five-Gallon Mixes	36
IV-2	Characteristics of TP-H8245 Propellant	39
IV-3	Determination of Cure Time	41
IV-4	TP-H8245 Broad Spectrum Mechanical Properties	43
IV-5	Aging of TP-H8245 Propellant	45
IV-6	Summary of Thiokol End-Of-Mix Viscosity Experience	50
IV-7	Characteristics of Mix T-607	
IV-8	Mix T-607 Broad Spectrum Mechanical Properties	54
IV-9	Response of Physical Properties to NCO/OH	55
IV-10	Physical Properties in One-Gallon Mixes	57
IV-11	Comparison of Thiokol and Aerojet Physical Properties	58
IV-12	Summary of Aerojet Aging Data	59
IV-13	Strand Burn Rate Measurements	62
IV-14	Aerojet Formulation Manufactured at Thiokol	65
IV-15	TP-H8245 Rheology Improvements	67
IV-16	Characteristics of Mix T-630	73
IV-17	Effect of Cure Temperature on Mix T-630 Properties	74
IV-18	Post-Cure Reduced by Obtaining Complete Cures	76
IV-19	Further Comparison of Aerojet and Thiokol Propellants	77
IV-20	Properties of Propellant for Bond Evaluation	79
IV-21	DTS-7984 Propellant Physical Properties	83
IV-22	Summary of DTS-7984 Propellant Results	84
IV-23	Processing Aids to Improve TP-H8245 Propellant Rheology	88
IV-24	Alternate Cure System Processed Hot, Cured Ambient	89
V-1	Comparison of Propellant Rheology	108
VI-1	Test Summary TX-631 Motors for Component Evaluation	114
VI-2	Summary of TX-631 Ballistic Parameters	120
VI-3	Possible Failure Mechanisms for T684-2	165
VI-4	Bond of Propellant to Liner and Insulation	167
VI-5	Physical Properties of Mix T-684	169
VII-1	Foam Density Versus Tube Length - Pour No. 1	177
VII-2	Foam Density Versus Tube Length - Pour No. 2	178
VII-3	Foam Density Versus Tube Length - Pour No. 3	180
VII-4	Foamed Mandrel (Core) Casting Procedure	183
VII-5	TX-631 Motors with Consumable Mandrels	192
VII-6	Results of Tests on TX-631 Motors with Consumable Mandrels	195

# LIST OF TABLES (Continued)

<u>No.</u>	<u>TITLE</u>	<u>Page</u>
VIII-1	Igniter Design Requirements and Guidelines	200
VIII-2	Igniter Concepts for Initial Screening	201
VIII-3	Characteristics of Magnesium/Teflon Ignition Materials	204
VIII-4	Characteristics of SP-168 Type 1, Class 1, Boron-Potassium Nitrate	205
VIII-5	Series I Test Data	207
VIII-6	Series II Test Data	209
VIII-7	Series III Test Data	210
VIII-8	Characteristics of Pyrofuze Wire	211
VIII-9	Initiator Concept Ratings	215
VIII-10	Electric Match Composition	218
VIII-11	Characteristics of M-100 Electric Match	219
VIII-12	Electrical Characteristics: M-100 Series Electric Matches	220
VIII-13	Static Sensitivity of Initiators	223
VIII-14	Initiator Comparison	224
VIII-15	Weld-Bond Initiator Sensitivity Tests	227
VIII-16	Igniter/Consumable Mandrel Tests	231
VIII-17	TX-631 Ballistic Data Ignition Phase	234
VIII-18	TX-631 Motor Ballistic Data: First and Second Test Groups and Reference Firing	238
VIII-19	Igniter/Consumable Mandrel Temperature Effects	241
VIII-20	TX-631 Motor Ballistic Data-Third, Fourth, and Fifth Test Groups	242
IX-1	Low Cost Motor-Nozzle Candidate Materials	264
IX-2	Material Property Table	274
IX-3	Induced Stresses and Margins of Safety for Designs Baseline Through Five	281
IX-4	Results of Analysis of Shell	283
IX-5	Maximum Stress and Margin of Safety for Nozzle with Steel Support Shell	285
IX-6	Nozzle Material Erosion Tests	286
IX-7	Nozzle Material Erosion Tests	287
IX-8	Summary of Erosion Data	308
IX-9	Estimated Probability of Ten-Year Continued Economical Availability	309
IX-10	Nozzle Total Costs	316
IX-11	Index of Technical Merit Matrix	317
IX-12	Ranking of Best Candidates	319
X-1	Tensile Properties for Steel Tubing	326
X-2	Tensile Properties (Room Temperature)	327
X-3	Tolerance Comparison for 4-Inch Outside Diameter Tubing	328

LIST OF TABLES (Continued)

<u>No.</u>	<u>TITLE</u>	<u>Page</u>
X-4	Tolerance for Drawn Aluminum Tubing	329
X-5	Summary of Advantages and Disadvantages Selected Tubings	330
X-6	Alloys for Impact Extruded Cases	332
X-7	Design Mechanical Properties of Several Case Mandrels	345
XI-1	Potential Arrangements	354
XI-2	Joining Method Summary	355
XI-3	Results of Stress Analysis of Weld Bonded Head End Closure	360
XI-4	Results of Stress Analysis of Friction Welded Head End Closure	361
XI-5	Material Property Table	362
XI-6	Comparison of Joining Methods	372
XI-7	Joining Cost Evaluation	373
XI-8	Closure Cost Evaluation	378
XI-9	Total Costs for Combinations of Closures and Joining Techniques	380
XII-1	Rationale for Material Selection Liner and Mastic Insulation	389
XII-2	Rationale for Material Selection Insulation Sleeve Material	391
XII-3	Rationale for Material Selection Insulation Sleeve/Case Adhesive	392
XII-4	Rationale for Material Selection	393
XII-5	Materials Selected for Evaluation	394
XII-6	Materials for Liner and Insulation Studies	395
XII-7	Cost of Materials	396
XII-8	Liner Formulation	397
XII-9	Propellant Bond to TA-H732A Liner	400
XII-10	Mastic Insulation Curing Aging and Catalyst Study	401
XII-11	Formulation for Mastic Insulations	404
XII-12	Properties of TI-H706A Insulation	405
XII-13	Properties of TI-H707A Insulation	406
XII-14	Properties of TI-H708A Insulation	407
XII-15	Mastic Insulation-Processing Characteristics	409
XII-16	Mastic Insulation Bond, Physical, and Erosion Properties	410
XII-17	Effect of Bond Promoter HX-868 on Mastic Insulation Bond to Propellant	411
XII-18	Oxygen/Acetylene Torch Erosion Test	413
XII-19	Adhesives for Insulation Sleeves	416
XII-20	Bond of Selected Sleeve Systems	417
XII-21	Propellant Bond to Insulation Sleeve	418
XII-22	Physical Properties for Insulation Sleeve Materials	419
XII-23	Summary of Liner/Insulation Materials Selected for Phase II Evaluation	426

LIST OF TABLES (Continued)

<u>No.</u>	<u>TITLE</u>	<u>Page</u>
XII-24	Costs for Case-To-Insulation Sleeve Bond System	429
XII-25	Costs for Propellant-To-Insulation Sleeve Bond System	431
XIII-1	Propellant Characteristics	436
XIII-2	Effects of Thrust History	445
XIII-3	Processing Steps for Type I Insulation System	468
XIII-4	Processing Steps for Type II Insulation System	469
XIII-5	Processing Steps for Type III Insulation System	470
XIII-6	Comparison of Processing Steps	471
XIII-7	Type I Grain Cost Penalties	473
XIII-8	Type II Grain Cost Penalties	474
XIII-9	Type III Grain Cost Penalties	477
XIII-10	Comparison of Cost and Performance Case Insulation	486
XIV-1	Component Weights and Costs	492
XIV-2	Case Comparisons	494
XIV-3	Lowest Cost/Lowest Weight Combinations	497
XV-1	Phase II Motor Configurations	504
A-1	TX-395 Motor Data for TP-H8245 Propellant	513
A-2	Cured Strand Data for TP-H8245 Propellant	514
B-1	Tolerance Comparison for 4-Inch Outside Diameter Tubing	534
B-2	Tensile Properties for Steel Tubing	537
B-3	Tensile Properties of Tubing (Ambient Temperature)	546
B-4	Critical Plane Strain Fracture Toughness	549
B-5	Cost of 4-Inch I. D. Tubing Materials	558
B-6	Factors of Comparison for Select Tubing (2024 T8=Base)	561
B-7	Summary of Advantages and Disadvantages of Selected Stock Tubing	562
B-8	Tolerance Comparison Steel Tubing (DOM) Versus Aluminum Tubing	556
B-9	Price and Availabilities of "Basic" Quantities	566
<u>VOLUME 2</u>		
D-1	Phase I Propellant Formulations	2
D-2	Characteristics of Mix T-600	3
D-3	Aerojet Formulation Manufactured at Thiokol	4
D-4	Comparison of Thiokol and Aerojet Propellant	5
D-5	Alternate Cure System Processed Hot, Cured Ambient	6

# LIST OF FIGURES

<u>No.</u>	<u>Title</u>	<u>Page</u>
III-1	Bore Strain in Case Bonded Grain	19
III-2	Bore Strain in Free-Standing Grain with slip-fit Aluminum Case	20
III-3	Baseline Design For 4-Inch Low Cost Motor	21
III-4	Pressure and Thrust versus time, Baseline Design, Vacuum and 70 F	26
III-5	Velocity Versus Time, Baseline Design	27
III-6	Variation of Burn Rate with Chamber Pressure, Showing Three Basic Rates of Typical Ambient Temperature Cure Propellants	28
III-7	Effect of Burn Rate on Baseline Motor Performance	30
IV-1	Pot Life of TP-H8245 Propellant (Mix T-600)	38
IV-2	Shear Stress and Viscosity Versus Shear Rate of TP-H8245	40
IV-3	Effect of Temperature on Physical Properties of TP-H8245 Propellant	44
IV-4	Strand Burning Rate, TP-H8245, Mix T-600	46
IV-5	Pot Life of TP-H8245 Propellant (Mix T-607)	51
IV-6	Pot Life Comparison of Five-Gallon Mixes	52
IV-7	Failure Boundary of TP-H8245 Propellant, Mix T-607	61
IV-8	Strand Burn Rate, Mix T-607	63
IV-9	Shear Stress Versus Shear Rate of DTS-7980 (15Q-403)	66
IV-10	Shear Stress and Viscosity Versus Shear Rate of DTS-7984 (15Q-422) Without Curing Agent	68
IV-11	Shear Stress Versus Shear Rate of DTS-7984 (T-630) Without Curing Agent	69
IV-12	Shear Stress Versus Shear Rate of DTS-7984 (T-630) with Curing Agent	70
IV-13	Effective Casting Life, Mix T-630, DTS-7984 Propellant.	71
IV-14	Shear Stress and Viscosity Versus Shear Rate of DTS-7984 (T-656)	80
IV-15	Effective Casting Life, Mix T-684, DTS-7984 Propellant.	82
IV-16	Stress and Strain of DTS-7984 as a function of Modulus at 77 F	85
IV-17	Effect of NCO/OH on Modulus of DTS-7984 Propellant	87
IV-18	Effect of Temperature on Pot Life, Mix BP-1428	90
V-1	Pour-Casting Set-Up for TX-631 Motor	97
V-2	Pour-Cast Sample from Mix T-630, Showing Good Quality of Propellant	98
V-3	Radiograph of Forward Portion of TX-631 Motor, Mix T-631, Charge 1	99



# LIST OF FIGURES (Continued)

<u>No.</u>	<u>Title</u>	<u>Page</u>
V-4	Radiograph of Center Portion of TX-631 Motor, Mix T-630, Charge 1	100
V-5	Radiograph of Aft Portion of TX-631 Motor, Mix T-630, Charge 1	101
V-6	Shear Stress and HAAKE Viscosity Versus Shear Rate for TP-H8208 (Mix T-640) with Cure Agent	103
V-7	Radiograph of Forward Portion of TX-631 Motor, Mix T-640, Charge 1	104
V-8	Radiograph of Center Portion of TX-631 Motor, Mix T-640, Charge 1	105
V-9	Radiograph of Aft Portion of TX-631 Motor, Mix T-640, Charge 1	106
VI-1	TX631-1 Test Motor	115
VI-2	Ballistic Prediction of TX-631 Motor with TP-H8208 Propellant, Fired at 70°F	116
VI-3	TX-631, Mix T-634, Charge 1, In Test Cell Before Test	118
VI-4	TX-631, Mix T-634, Charge 1, In Test Cell After Test	119
VI-5	Ballistic History, TX-631 Motor, Mix T-622, Charge 1, Fired at 70°F	121
VI-6	Ballistic History, TX-631 Motor, Mix T-622, Charge 2, Fired at 70°F	122
VI-7	Comparison of Measured and Simulated Ballistics, TX631, Mix T622-1	125
VI-8	Ballistic History, TX-631 Motor, Mix T-634, Charge 1, Fired at 70°F	127
VI-9	Ballistic History, TX-631 Motor, Mix T-640, Charge 1, Fired at 70°F	129
VI-10	Ballistic History, TX-631 Motor, Mix T-640, Charge 2, Fired at 70°F	130
VI-11	Ballistic History, TX-631 Motor, Mix T-630, Charge 1, Fired at 70°F	132
VI-12	Ignition Phase of TX631, Mix T630-1	133
VI-13	Comparison of Ignition Phases of T622-2	134
VI-14	Ballistic Prediction of TX-631 Motor with DTS-7883/ DTS-7984 Propellant, Fired at 70°F	135
VI-15	Ballistic Prediction of TX-631 Motor with DTS-7984 Propellant and T622-1 Erosive Burning, Fired at 70°F	137
VI-16	Thrust and Pressure Histories for TX-631, Mix T-643-1, -65°F	138
VI-17	Ballistic History, TX-631 Motor, Mix T-643, Charge 2, Fired at 165°F	139



# LIST OF FIGURES (Continued)

<u>No.</u>	<u>Title</u>	<u>Page</u>
VIII-1	Igniter Laboratory Test Fixture	202
VIII-2	Function Time of Pyrofuze Wire	206
VIII-3	Polyurethane Foam Test Igniter	213
VIII-4	Atlas M-100 Electric Match	217
VIII-5	Function Time versus Current for M-100 Electric Match	221
VIII-6	Weld-Bond Initiator Sensitivity Test Set-Up	226
VIII-7	Concept A, Leave-In-Place Igniter/Mandrel for TX-631 Motor	229
VIII-8	Concept B, Leave-In-Place Igniter/Mandrel for TX-631 Motor	230
VIII-9	Leave-In-Place Igniter/Mandrel for TX-631 Motor, Mix T-634, Charge 1	232
VIII-10	TX-631 Motor Ignition Transients, First Test Group and References	235
VIII-11	Igniter/Mandrel for TX-631 Motors, Mix T-640, Charges 1 and 2	236
VIII-12	TX-631 Motor Ignition Transients, First and Second Test Groups	239
VIII-13	Ballistic History, TX-631 Motor, Mix T-643, Charge 1, Fired at $-65^{\circ}\text{F}$	244
VIII-14	Igniter Operation, TX-631 Motor, Mix T-643, Charge 2, Fired at $165^{\circ}\text{F}$	245
VIII-15	Ballistic History, TX-631 Motor, Mix T-643, Charge 2, Fired at $165^{\circ}\text{F}$	246
VIII-16	Pressurization Test at $70^{\circ}\text{F}$ on TX-631 Motor, Mix T-634, Charge 2	248
VIII-17	Pressurization Test at $165^{\circ}\text{F}$ on TX-631 Motor, Mix T-634, Charge 2	249
VIII-18	Ignition Phase, TX-631 Motor, Mix T-634, Charge 2, Fired at $165^{\circ}\text{F}$	251
VIII-19	Ballistic History, TX-631 Motor, Mix T-634, Charge 2, Fired at $165^{\circ}\text{F}$	252
VIII-20	Igniter/Mandrel for TX-631 Motors, Mix T-684, Charges 1 and 2	253
VIII-21	Ignition Phase, TX-631 Motor, Mix T-684, Charge 1, Fired at $70^{\circ}\text{F}$	254
VIII-22	Ballistic History, TX-631 Motor, Mix T-684, Charge 1, Fired at $70^{\circ}\text{F}$	255
VIII-23	Ballistic History, Igniter and TX-631 Motor, Mix T684, Charge 2, Fired at $70^{\circ}\text{F}$	257
IX-1	Baseline Design	266

LIST OF FIGURES (Continued)

<u>No.</u>	<u>Title</u>	<u>Page</u>
VI-18	Ballistic History, TX-631 Motor, Mix T-634, Charge 2, Fired at 165° F	141
VI-19	Ignition Phase, TX-631 Motor, Mix T-634, Charge 2, Fired at 165° F	142
VI-20	Igniter Operation, TX-631 Motor, Mix T-634, Charge 2, Fired at 165° F	143
VI-21	Ballistic History, TX-631 Motor, Mix T-684, Charge 1, Fired at 70° F	145
VI-22	Ignition Phase, TX-631 Motor, Mix T-684, Charge 1, Fired at 70° F	146
VI-23	Igniter Operation, TX-631 Motor, Mix T-684, Charge 1, Fired at 70° F	148
VI-24	Ballistic History, TX-631 Motor, Mix T-684, Charge 2, Fired at 70° F	149
VI-25	Igniter Operation, TX-631 Motor, Mix T-684, Charge 2, Fired at 70° F	150
VI-26	Parts Recovered in Test Cell After Test of TX-631 Motor, Mix T-684, Charge 2	152
VI-27	Inner Surface of Propellant Recovered from TX-631 Motor, Mix T-684, Charge 2	154
VI-28	Insulation/Propellant Interface Surface on Propellant Recovered From TX-631 Motor, Mix T-684, Charge 2	155
VI-29	Aft End of Propellant Recovered From TX-631 Motor, Mix T-684, Charge 2	156
VI-30	Diametric Crack and Adhering Foam Mandrel on Propellant Recovered from TX-631 Motor, Mix T-684, Charge 2	157
VI-31	TX-631 Motor, Mix T-684, Charge 2, Post-Test Position	158
VI-32	Comparison of Measured Pressure From TX631 Motors, Mix T643-2 and T684-2	160
VI-33	Post Test Calculation of Burning Surface For T643-2 and T684-2	162
VI-34	Comparison of Calculated and Measured Pressure Response of T-631, Mix T-684-2	164
VII-1	Consumable Mandrel Mold, Disassembled	185
VII-2	Consumable Mandrel Mold, Assembled, Standing Vertical	186
VII-3	Foam Mixture Being Poured into Mold	187
VII-4	Early Foamed Mandrel with Wires Imbedded in Foam	188
VII-5	Foamed Mandrel with Wires Inserted in Spaghetti Tubing	189
VII-6	Forward End of Foamed Mandrel Showing Molded Cavity	190
VII-7	Close-Up of Forward End and Cavity of Foamed Mandrel	191

# LIST OF FIGURES (Continued)

<u>No.</u>	<u>Title</u>	<u>Page</u>
IX-2	Nozzle Baseline Design (Grid and Material Outline)	267
IX-3	Design 1 (Grid and Material Outline)	268
IX-4	Design 2 (Grid and Material Outline)	269
IX-5	Design 3 (Grid and Material Outline)	270
IX-6	Design 4 (Grid and Material Outline)	271
IX-7	Design (Grid and Material Outline)	272
IX-8	Effect of Varying Modulus on the Maximum Hoop Stress in Baseline Design	275
IX-9	Effect of Varying Modulus on Maximum Hoop Stress in Design 1	276
IX-10	Effect of Varying Modulus on the Maximum Hoop Stress in Design 2	277
IX-11	Effect of Varying Modulus on the Maximum Hoop Stress in Design 3	278
IX-12	Effect of Varying Modulus on the Maximum Hoop Stress in Design 4	279
IX-13	Effect of Varying Modulus on the Maximum Hoop Stress in Design 5	280
IX-14	Effect of Structural Support Stiffness on Stress	284
IX-15	Post Test Condition of FM16771 in TX-3 Motor, Charge 1	288
IX-16	Post Test Condition of 110 RPD in TX-3 Motor, Charge 3	289
IX-17	Post Test Condition of 153 RPD in TX-3 Motor, Charge 4	290
IX-18	Post Test Condition of D16090 in TX-3 Motor, Charge 5	291
IX-19	Post Test Condition of D22532 in TX-3 Motor, Charge 6	292
IX-20	Post Test Condition of D791 in TX-3 Motor, Charge 7	293
IX-21	Post Test Condition of FM3510 in TX-3 Motor, Charge 8	294
IX-22	Post Test Condition of D23639 in TX-3 Motor, Charge 9	295
IX-23	Post Test Condition of R25406 in TX-3 Motor, Charge 10	296
IX-24	Post Test Condition of D23570 in TX-3 Motor, Charge 11	297
IX-25	Unit Cost Versus TX-3 Throat Erosion	298
IX-26	Post Test Condition of FM16771 in TX-631 Motor, Mix T-622, Charge 1	299
IX-27	Post Test Condition of RYTON R4 in TX-631 Motor, Mix T-622, Charge 2	300
IX-28	Post Test Condition of FM16771 in TX-631 Motor, Mix T-634, Charge 1	301
IX-29	Post Test Condition of 100RPD in TX-631 Motor, Mix T-643, Charge 1	302
IX-30	Post Test Condition of 153RPD in TX-631 Motor, Mix T-643, Charge 2	303
IX-31	Post Test Condition of D22532 in TX-631 Motor, Mix T-634, Charge 2	304

# LIST OF FIGURES (Continued)

<u>No.</u>	<u>Title</u>	<u>Page</u>
IX-32	Post Test Condition of D23570 in TX-631 Motor, Mix T-684, Charge 1	305
IX-33	Correlation of Erosion In TX-3 and TX-631 Motors	307
IX-34	Costing Design 1	310
IX-35	Costing Design 2	311
IX-36	Costing Design 3	312
IX-37	Costing Design 4	313
IX-38	Low Cost Motor Nozzle Materials	314
IX-39	Cost Versus Index of Merit	318
X-1	Integral Forward Closure Impact Extruded Case	335
X-2	Integral Nozzle Support For Impact Extruded Case	336
X-3	Modified Design of Integral Forward Closure	338
X-4	Modified Design of Integral Nozzle Shell Case	341
X-5	Strip Laminate Case Assembly	344
X-6	Comparison of Filament Wound Case Materials	347
X-7	Filament Wound Composite Cases	348
XI-1	Weld Bonded Head End Closure	358
XI-2	Friction Welded Head End Closure	359
XI-3	Friction Weld Test Chamber	363
XI-4	Weldbond Test Specimens	365
XI-5	Weldbond Test Chamber	367
XI-6	Electromagnetic Formed Test Chamber	370
XII-1	Effect of DBTL Concentration on Cure Rate of Liner	399
XII-2	Mastic Insulation Cure Time with Various Curing Agents and Catalysts	402
XII-3	Cure Rate of Mastic Insulation	408
XII-4	Double Plate Test Device for Insulation Sleeve Materials	415
XII-5	Molded Integral Case Insulation Concept	421
XII-6	Extruded Insulation Sleeve Concept	422
XII-7	Molded Forward Closure Insulation Concept	423
XII-8	Erosion Patterns on ABS and Polycarbonate Insulation Samples in TX-631, Mix T684-1	425
XII-9	Selected Insulation Systems	428
XIII-1	Variation of Maximum Pressure With Slot Length	438
XIII-2	Variation of Burnout Velocity with Slot Length	439
XIII-3	Variation of Thrust Profile with Slot Length	440
XIII-4	Typical Pressure and Thrust Histories	441
XIII-5	Effect of Initial Launch Angle on Slant Range	442
XIII-6	Relationship Between Burnout Velocity and Impact Velocity for Selected Conditions	443

# LIST OF FIGURES (Continued)

<u>No.</u>	<u>Title</u>	<u>Page</u>
XIII-7	Performance Map of Possible Motor Designs, $\sigma_u = 78,000$ psi	446
XIII-8	Performance Map of Possible Motor Designs, $\sigma_u = 60,000$ psi	447
XIII-9	Performance Map of Possible Motor Designs, 88% Total Solids	448
XIII-10	Performance Map of Possible Motor Designs, 86% Total Solids	449
XIII-11	Performance Map of Possible Motor Designs, 86% Total Solids	450
XIII-12	Effect of Maximum Pressure on Burnout Velocity	452
XIII-13	Effect of Burn Rate on Missile Performance	453
XIII-14	Relationship Between Burnout Velocity and Velocity Out of Launch Tube at Constant Burn Rate	454
XIII-15	Cost of Stock Tubing Cases	456
XIII-16	Cost to Obtain Specified Burnout Velocity	457
XIII-17	Effect of Thrust History on Stock Tubing Case Costs	459
XIII-18	Typical Pressure and Thrust Histories of Flight Motor, Fired at 70° F	461
XIII-19	Variation of Missile Performance With Propellant Burn Rate	462
XIII-20	Insulation/Grain Systems to be Studied	466
XIII-21	Cost Effects of Mastic Insulation Compared to Case Bonded Thermoplastic Insulation	479
XIII-22	Capabilities of Insulation Sleeve Materials	481
XIII-23	Effect of Insulation Thickness on Missile Velocity	485
XIII-24	Effect of Case Material and Insulation Thickness on Burnout Velocity	488
XIV-1	Cost Comparisons	496
XV-1	Motor Configuration Selected For Phase II Evaluation	505
A-1	Ballistic History, TX-395 Motors, Mix T-600, Charges 1 and 2, Fired at -65° F	515
A-2	Ballistic History, TX-395 Motors, Mix T-600, Charges 3 and 4, Fired at -65° F	516
A-3	Ballistic History, TX-395 Motors, Mix T-600, Charges 5 and 6, Fired at 70° F	517
A-4	Ballistic History, TX-395 Motors, Mix T-600, Charges 7 and 8, Fired at 70° F	518
A-5	Ballistic History, TX-395 Motors, Mix T-600, Charges 9 and 10, Fired at 160° F	519

# LIST OF FIGURES (Continued)

<u>No.</u>	<u>Title</u>	<u>Page</u>
A-6	Ballistic History, TX-395 Motors, Mix T-600, Charges 11 and 12, Fired at 160° F	520
A-7	Burning Rate versus Pressure for TP-H8245 Propellant (Mix T-600)	521
A-8	Temperature Effect on Burning Rate Exponent, TP-H8245 Propellant (Mix T-600)	522
A-9	Temperature Effect on Pressure, TP-H8245 Propellant (Mix T-600)	523
A-10	Temperature Effect on Burning Rate, TP-H8245 Propellant (Mix T-600)	524
B-1	Steel Tubular Products	528
B-2	Aluminum Tubular Products	540
B-3	Aluminum Tubular Products Applicable Standard Tolerances	556
B-4	Relative Performance Versus Cost of Selected Stock Tubing	560
B-5	Allowable Maximum Pressure at 70° F Versus Wall Thickness for Selected Stock Tubing	568
B-6	Cost of Selected Stock Tubing Versus Wall Thickness	569
B-7	Allowable Maximum Pressure at 70° F Versus Cost of Selected Stock Tubing	571
B-8	Weight of Selected Stock Tubing Versus Wall Thickness	572
B-9	Weight of Selected Stock Tubing Versus Allowable Maximum Pressure at 70° F	573
B-10	Effects of Wall Thickness on Loaded Case Mass Fraction for Selected Stock Tubing	574
B-11	Loaded Case Mass Fraction as Function of Allowable Maximum Pressure at 70° F	576
B-12	Loaded Case Min. Friction Versus Cost of Selected Stock Tubing	577
C-1	Ratio of Power on $C_D$ to Power Off $C_D$ for Sparrow Missile	586
C-2	Drag Coefficients for Low Cost Motor Trajectory Studies	587

## CONTRIBUTORS

The following individuals made significant contributions to the accomplishments of the program:

R. D. Atchley	-	Preliminary Motor Design
D. W. Booth	-	Propellant
W. T. Boyd	-	Nozzle
J. A. Burka	-	Closure/Joining
J. D. Byrd	-	Liner/Insulation
J. P. Caldwell, Jr.	-	Ballistic Analysis
K. E. Junior	-	Liner/Insulation
J. H. Kelly	-	Grain Design
J. E. Lloyd	-	Process Engineer
H. E. Manning	-	Adhesives and Plastics
J. W. McCain	-	Igniter
P. B. Renfroe	-	Engineering Technician
C. G. Stokes	-	Nozzle
F. A. Urban	-	Stock Tubing
S. L. Vance	-	Consumable Mandrel
R. P. Ware	-	Report Editor
T. F. Wilson	-	Nozzle

SECTION I

INTRODUCTION



## SECTION I INTRODUCTION

The objective of this program is to identify materials, designs and manufacturing techniques that will significantly reduce the cost of tactical rocket motors (4-inch to 8-inch diameter) in production, and to demonstrate in pilot production quantities the validity of the identities made by study and analysis.

Design simplicity is perhaps the greatest single contributor to the development of high production rate, low cost solid rocket motors. Design simplicity implies fewer components, fewer suppliers, less inspection, and fewer manufacturing steps, all of which contribute to lowering motor cost. Inasmuch as possible, commercially available materials with relaxed manufacturing tolerances and surface finishes will be used. The use of O-rings and their specially prepared seal surfaces will be minimized. Design concepts will emphasize high volume manufacturing processes and minimum inspection requirements, without compromising safety, reliability, and long service life. Component functions will be combined wherever possible. Selected designs will be made available to potential subcontractors so that competitive bids for motor production can be obtained. Also, designs will include provisions for automated quality control functions where feasible. Data generated by Booz, Allen under Contract F04611-72-C-0074 will be used during the design phase. Design analyses will include detailed cost estimates in order to establish the cost effectiveness of each of the candidate concepts and methods. Tests will be designed and conducted to demonstrate the capability of selected designs to meet the temperature/vibration environmental requirements for air-launched tactical motors. Reliability and safety are paramount in the manufacture of rocket motors for manned weapon systems. To this end, development of highly repeatable, reliable techniques incorporating safe designs and processes, a minimum of hand assembly operations, and minimum manufacturing costs was stressed.

The program has three phases, of which the first, Phase I, is complete. The first phase involved the evaluation of design options for each motor component. Motor component designs and specific fabrication techniques were screened both by analysis and by component tests in order to distinguish those concepts and methods that meet performance requirements at acceptable cost levels. The second phase will consist of selecting optimum combinations of those concepts/methods determined to be successful under Phase I. These optimum combinations will be fabricated and tested in twelve motors of 4-inch diameter. Results from Phases I and II will be compiled and used to devise a manufacturing plan for Phase III. The third and final phase will be a pilot production run of 120 motors at a rate of 30 motors/day in each of four different runs, with time for analysis and modification between runs.

Analyses and tests conducted under Phase I were designed to determine the most effective way to implement recommended manufacturing methods, design techniques, and new materials for reducing the costs of air launched tactical motors. Particular attention was paid throughout Phase I to the requirements of the air launch environment and its effect on proposed designs, methods, and materials. Candidate component designs, new materials, and specific manufacturing techniques were screened during Phase I in two ways — analyses and tests. Concepts were analyzed for performance (stress, ballistics, reliability, etc.). Engineering judgement was used to screen concepts on the basis of their actual or potential merit. Concepts (materials, designs, and manufacturing techniques) were selected for detailed cost analysis. Analytical screening of concepts by cost and performance produced a set of component design and manufacturing process options. The most promising concepts in this set were selected (with AFRPL concurrence) for component tests. Results of these tests were then used to select candidate component concepts for inclusion in Phase II tests of complete motors.

Activities of Phase I are described in this Phase Report, which is divided into fifteen sections with four appendices.

<u>Section Number</u>	<u>Subject</u>
I	Introduction
II	Summary and Conclusions
III	Baseline Motor Preliminary Design
IV	Propellant Tailoring and Characterization
V	Pour Casting Technique for Manufacturing Motors
VI	Full-Scale Motor Tests
VII	Consumable Mandrel
VIII	Igniter/Consumable Mandrel Study
IX	Nozzle Study
X	Case Study
XI	Closure/Joining Technique Study
XII	Insulation/Liner Study
XIII	Grain Design and Performance Analysis
XIV	Cost Comparisons
XV	Phase II Motor Configurations

#### Appendix

A	Ballistic Analysis of Mix T600
B	Stock Tubing Study
C	Drag Coefficient
D	Propellant Formulation

Information in Appendix D is classified "Confidential" and is contained in a separate volume (Volume 2) of this report.

**SECTION II**

**SUMMARY AND CONCLUSIONS**

## SECTION II SUMMARY AND CONCLUSIONS

The following paragraphs summarize the investigations performed during Phase I and their findings. Details of the work are found in subsequent sections.

### BASELINE MOTOR

At the beginning of the program, a 4-inch diameter motor was designed that incorporated typical low cost components. Preliminary design calculations showed that the required missile performance of burnout velocity, impact velocity and range could be provided.

The margin between delivered and required performance was not great, which portended difficulties when incorporating even lower cost concepts, such as lower strength case material and nozzles with less erosion resistance.

### PROPELLANT

Technology in ambient-temperature cured propellants (i. e., 80°F) developed under AFRPL contract (Reference II-1)<sup>1</sup> was satisfactorily transferred to Thiokol and combined with in-house technology to produce improved propellant. The result is that ambient-temperature cured propellants are available for further use and evaluation and that future system evaluations can be made with a firm data base.

Improved propellant cure reproducibility and cure completeness were obtained with the identification that moisture effects were significant. It was found that detrimental moisture effects can be alleviated with mixing under a vacuum at elevated temperature prior to adding curing agent. The mix is then cooled with the cure catalyst addition delayed until late in the mix cycle to increase pot life.

The ambient-temperature cured propellant used in this program met the goals set for it:

	<u>Goals</u>	<u>Demonstrated</u>
Cure Temperature	"Ambient"	80°F
Cure Time	< 9 days	8 - 10 days
Strain at Max. Stress, -65°F	> 25%	36%
Max. Stress, 77°F	> 100 psi	140 psi
Modulus, 77°F	> 400 psi	618 psi
Temperature Capability	-65 to 165°F	

1. References are given at the end of this section.

## POUR CASTING

An attractive low cost grain manufacturing technique is "pour casting", wherein propellant is metered into the motor without benefit of the motor chamber being at vacuum conditions. The propellant is simply poured into the case. Success of this technique depends on a propellant with very low viscosity (2 to 3 kilopoise) and low yield values. Available ambient-temperature cured propellants have end-of-mix viscosities of 12 to 20 kilopoise.

Two full-scale motors were pour cast, one with an ambient-temperature cured propellant with a viscosity of about 15 kilopoise, and the other with an elevated-temperature cure (145°F) propellant with about 3 kilopoise viscosity. There was not a great difference in the final grain quality between the two motors; both were considerably worse than usually considered acceptable in the solid propellant industry. One motor was successfully static fired. The other experienced an over-pressurization which cannot be attributed to a single cause. Thus, at the present time, there are mixed results about the necessary grain quality for this class of motors.

There is a need to study the effects of mechanical energy input to the motor during casting to achieve satisfactory grain quality. The ultimate casting technique may combine elements of pure pour-casting and vacuum casting.

## FULL-SCALE MOTORS TESTS

Eleven full-scale (25 lb.) four-inch diameter motors were static fired to evaluate grain manufacturing techniques, nozzle ablative material, consumable mandrel with integral igniter, igniter configuration, and ambient-temperature cured propellant.

One of the motors successfully tested incorporated:

- o Nozzle ablative material that can be transfer molded
- o Grain manufactured with leave-in-place foam mandrel
- o Integral igniter with magnesium-teflon pyrotechnics
- o Thermoplastic insulation samples
- o Ambient-temperature cured propellant

## CONSUMABLE MANDREL

Polyurethane foam was suitably fashioned into mandrels for evaluation in full-scale motor firings. These tests demonstrated satisfactory motor operation with a single pyrotechnic charge (integral with the mandrel) to consume the mandrel and ignite the propellant. Presence of the mandrel modulated the initial high pressure. Two motors were successfully cast with ambient-temperature cured propellant and foam mandrels, which were left in the motors.

Hangfires resulted when the gap between propellant and mandrel was closed through differential thermal expansion or because cure shrinkage was not sufficient to separate the two. It was demonstrated in a full-scale motor test that increased energy output from the igniter can alleviate the hangfire without causing high pressure.

There is a need for additional experimental investigation to achieve satisfactory ignition when the consumable mandrel is used to form the grain.

### IGNITER

Analysis confirmed Reference II-2 that bi-metallic wire could not serve as a direct ignition source for the propellant because of large power requirements. Laboratory tests revealed that bi-metallic wire was impractical as an initiator for other pyrotechnics because of fragility. The lowest cost initiator found was an Atlas electric match which demonstrated satisfactory characteristics in laboratory evaluation and full-scale motor firings.

Atlas matches can be obtained with one amp no-fire characteristics, but not with one amp-one watt no fire. Thus safety considerations can influence selection of an initiator - Atlas match for about \$0.50 or one amp-one watt initiators for about \$7.00 (the latter being identified as part of the investigation).

Magnesium-teflon pellets were selected as the primary pyrotechnic charge because of cost (lower than the common  $\text{BKNO}_3$  pellets), low gas-solids ratio (which is beneficial when incorporating a consumable mandrel to reduce maximum pressure), low sensitivity to moisture when compared with  $\text{BKNO}_3$ , and acceptable delay times. Magnesium-teflon pellets with Atlas match initiators provided satisfactory ignition in full-scale motor tests.

### NOZZLE

Six nozzle ablative materials were identified through analysis and experiments to offer up to 50% reduction in cost from the glass-phenolic molding compound used as a baseline material. All six had satisfactory erosion resistance and structural capabilities.

An extensive analytical evaluation was performed which culminated in the rational selection of the best materials. Glass, cellulose, and wood flour as fillers in phenolic resin were selected for Phase II testing on the basis of this study. Factors in the study were erosion resistance (sub-scale motor screening and full-scale motor testing), structural capabilities (stress analysis), availability (resin, reinforcement, compounding and fabrication), and basic configuration. Other features of the selected nozzles were contoured exit sections and aluminum support structure.



## CASE

Steel and aluminum stock tubing were analytically evaluated as case material. Both are practical if performance losses (particularly with steel) can be tolerated. Some performance loss (using 7075-T6 as baseline) can be expected with aluminum tubing because the high strength 7075-T6 alloy was available with only one wall thickness and unless pressure capability exactly matches this wall thickness, then the higher strength is of no benefit.

On the other hand, 7075-T6 (as well as other alloys) can be furnished as impact extruded cases with integral forward closure or aft closure, with the wall thickness dictated by the specific motor design. For this improved performance capability there is an added cost.

A detailed evaluation of impact extruded aluminum cases was made; cost and design details were a result. Alloy 2014-T6 was found to be the most attractive from a cost standpoint.

Metal strip laminate cases (with appropriate closures) provide the lowest weight and greatest internal volume, but at the highest cost for the systems studied. Filament wound composite cases probably have the highest performance/lowest cost potential of all cases examined; however, there are technical misgivings about their current environmental and proof-testing aspects. Additional experimental evaluation should be performed on the filament wound case for air launch application.

## CLOSURE/JOINING TECHNIQUE

Steel, plastic and aluminum closures are all practical at reasonable cost, but some are more promising than others. The closures and joining techniques must be compatible with the case approach. Plastic closures are generally the least expensive.

Five joining techniques (friction welding, electromagnetic forming with bond, weldbonding, taper bondline, and rivet bonding) were experimentally evaluated. These five and six others (laser weld, electron beam welding in and out of vacuum, straight bondline, snap ring retainer, and threaded joint) were evaluated for costs and usability. Five techniques cost less than \$1.00 per joint (adhesive bonding with tapered and straight bondline, electromagnetic forming with bond, friction welding, electron beam welding out-of-vacuum) when applied to a high volume production run. Friction welding for empty motors and electromagnetic forming and adhesive bonding for either loaded or empty motors are the lowest cost joining techniques.

Costs of eleven closure arrangements and nine of the above joining techniques were combined to determine the lowest cost combination. Friction welding aluminum is the best for empty motors. Adhesive bonding with a straight (i.e., constant diameter) bondline and plastic closure is best for a loaded motor.

Stress analyses were performed on two test chambers (friction welded and weldbonded) to assist in evaluating test results.

Difficulty was encountered in the bond of plastic to metal with room-temperature cured adhesive where the motor was to be fired at 170°F.

#### INSULATION/LINER

Three basic areas were investigated: thermoplastics for injection or transfer molding integral case and dome insulations; mastic insulations for application directly into case; liner for use as back-up bonding agent.

It was experimentally determined that glass-filled thermoplastics can be used as case insulation. Polycarbonate, nylon and ABS were investigated. Polycarbonate had the best erosion resistance; ABS had the lowest cost. Polycarbonate has the potential for lowest cost because less is required for equal thermal protection. All demonstrated satisfactory bonding characteristics when using appropriate bonding agents. Low cost adhesives were identified to bond propellant to the thermoplastic and thus, liner, as commonly used in solid propellant rocket motors, is not needed. However, an ambient-temperature cured liner was found to be the most cost effective adhesive to bond the thermoplastic to the case.

An ambient-temperature cured mastic insulation was formulated and experimentally verified. Three filler materials- silica, carbon, glass - were evaluated. Carbon was selected for Phase II testing because it results in the lowest cost. Liner is not needed between the insulation and propellant. Laboratory tests included cure catalyst and cure agent studies, bond to propellant and to case, effects of bond promoter, physical and thermal properties, processing characteristics (pot life, cure time, viscosity), and qualitative erosion resistance.

An ambient-temperature cured liner was formulated and experimentally verified for use as a bond promoter, if needed. Laboratory evaluation consisted of cure agent and cure catalyst studies, propellant-to-liner bond and effects of bond promoter.

A cost and performance analysis determined that case-bonded propellant grains with thermoplastic insulation is the lowest cost system.

#### PERFORMANCE AND COST TRADE-OFFS

Performance analyses were made to determine effects of nozzle throat erosion rate, case strength level, thrust profile and propellant formulation on missile performance. Case strength and propellant formulation are strong drivers on missile performance. Nozzle throat erosion rate is less influential. High burnout velocity and high velocity out of a launch tube are incompatible characteristics. Steel cases cause significant performance penalties.



Cost and weight data were combined to determine the best combinations of forward closure with its joining technique, case, and nozzle with its joining technique (Table II-1).

Three motor configurations were formulated (Table II-2) that combined the best weight/cost considerations for manufacture and evaluation in Phase II (consistent with program funding limitations).

#### NEEDED ADDITIONAL INVESTIGATIONS

Several areas for additional investigations were identified during the Phase I studies:

- a. Experimentally determine igniter/mandrel interactions in a systematic manner to devise a combination that completely eliminates the hangfire tendencies.
- b. Experimentally and analytically determine the mechanical energy input spectrum optimum for reducing number of voids in propellant that is pour cast out-of-vacuum.
- c. Experimentally and analytically determine the grain quality requirements.
- d. Perform a cost comparison of propellants that cure for 8 to 10 days at ambient temperature (80°F) with those that cure one to three days at elevated temperature (145°F). Include the total manufacturing process and facilities costs in the analysis.
- e. Conduct an evaluation of room-temperature cure adhesives for bonding plastics to metals that provide high strength at elevated temperatures (170°F).

#### REFERENCES

1. "Demonstration of Ambient-Temperature Cure Propellant", Aerojet Solid Propulsion Co., Report No. AFRPL-TR-73-68, Contract No. FO-4611-72-C-0072, August 1973.
2. "Improved Low Cost Rocket Motor Processing and Component Development Study", AFRPL-TR-75-34, Fred Marks and Edward Gonzales, Booz, Allen Applied Research, July 1975.

**TABLE II-1**  
**LOWEST COST/LOWEST WEIGHT COMBINATIONS**

<u>Forward Closure</u>	<u>Forward Closure</u>	<u>Case</u>	<u>Aft Joining</u>	<u>Nozzle (b)</u>	<u>Wt. (lb)</u>	<u>Cost (\$)(d)</u>
Plastic Dome (a)	Adhesive	Steel Strip Laminate	Adhesive	D791 (c)	10.1	38.15
N/A	N/A	Integral HE (7075-T6 Alum)	EMF-Bond	D791	11.8	36.76
Taper-Plastic	Taper Bond	Alum Tubing 2014-T6	EMF-Bond	D791	12.7	35.88
Aluminum Flat Plate	Friction Weld	Alum Tubing 2014-T6	EMF-Bond	D791	13.3	35.47
N/A	N/A	Integral HE (2014-T6 Alum)	EMF-Bond	D791	13.5	35.22
Plastic Dome (a)	Snap Ring	Steel Tubing (4130N)	Snap Ring	D791	19.7	31.39
Plastic Dome (a)	Snap Ring	Steel Tubing (1026)	Snap Ring	D791	25.1	24.02

a. Conventional configuration

b. All with contoured exit section and aluminum shell

c. Wood-flour phenolic molding

d. Costs to Propulsion Contractor

TABLE II-2

PHASE II MOTOR CONFIGURATIONS

Feature	Configuration		
	No. 1	No. 2	No. 3
Propellant	Ambient-Temp. cured	Ambient-Temp. cured	Ambient-Temp. cured
Grain Configuration	Case Bonded	Case Bonded	Case Bonded
Grain Manufacturing	Pour casting with vibration	Pour casting with vibration	Pour casting with vibration
Mandrel	Foam, leave-in-place	Foam, leave-in-place	Foam, leave-in-place
Igniter Pyrotechnics	Magnesium-teflon pellets	Magnesium-teflon pellets	Magnesium-teflon pellets
Forward Closure	Plastic/taper	Alum (FW)	Alum (FW)
Forward Joining Technique	Taper-bond	Friction Weld	Friction Weld
Case	Aluminum stock tubing	Aluminum stock tubing	Aluminum stock tubing
Aft Joining Technique	EMF-Bond	EMF-Bond	Snap Ring
Nozzle Ablative	Wood-flour	Cellulose	Glass
Nozzle Support Shell	Aluminum	Aluminum	Aluminum
Case Insulation	Polycarbonate	ABS	Carbon Mastic

**SECTION III**

**BASELINE MOTOR PRELIMINARY DESIGN**

### SECTION III

#### BASELINE MOTOR PRELIMINARY DESIGN

One of the first activities in Phase I was to formulate a preliminary design of a rocket motor which would provide the specified missile performance and would incorporate typical low-cost components. This design then served as a reasonable starting point from which to evaluate changes in propellant burn rate, case strength level, nozzle throat erosion rate, insulation/liner thickness, and nozzle exit diameter.

Performance requirements for the 4-inch motor were updated:

Burnout Velocity (ft/sec)	3290
Impact Velocity (ft/sec)	2820
Slant Range (ft)	12,000
Launch Conditions	
Altitude (ft)	6000
Velocity (ft/sec)	760
Angle (deg)	-30
Missile Inert Weight (lb)	
Warhead	45
Fins	1.29
Motor External Configuration	
Outside Diameter (in)	4.0
Overall Length (in)	53
Aft End Reduced Cross- Section	
Diameter (in)	2.6 and 3.29
Length (in)	8.0

Design pressure factors were calculated:

MEOP/Max Pressure at 70°F	1.225
Burst Pressure/Max Pressure at 70°F	1.714

which were based on:

Temperature Range (MIL-R-25532)	-65 to 160°F
Temperature Coefficient of Pressure, $\pi_k$	0.001 per °F
Burst Pressure/MEOP (MIL-R-25532)	1.4
Variability of Maximum Pressure (3-sigma)	12%

1. Burnout velocity is final velocity of missile and includes the initial launch velocity (burnout velocity equals launch velocity plus  $\Delta V$  imparted by rocket motor).

## UNCLASSIFIED

As a precursor to the baseline motor design, estimates of propellant bore strain were made. Calculations were made for a case-bonded grain and for a free-standing grain where the case was slipped onto the grain. Results are shown on Figures III-1 and III-2, where pressurization and thermal strains are a function of web fraction. It was decided to limit total strains to 20%, which limits the web fraction to 0.70 for a case-bonded grain. Strains are less than 20% for a free-standing grain at 0.70 web fraction.

Drag characteristics of a 4-inch-diameter missile were determined as shown in Appendix C. The missile was launched with an initial flight angle of minus 28 degrees as a result of preliminary studies (N. B., slant range of 12,000 ft., launch altitude of 6,000 ft. corresponds to a line-of-sight launch angle of minus 30 deg. without consideration of gravity effects during flight.)

A motor design (Thiokol designation TX-649), described in subsequent figures and tables, was formulated to meet the aforementioned missile performance requirements. Preliminary calculations revealed that an aft-diameter of 2.6 inches made it unlikely that performance would be met. Thus, further calculations were made with 3.29 inch aft missile diameter.

The baseline motor utilizes an aluminum case, an all-plastic nozzle, polyisoprene insulation, and a 12% aluminum HTPB propellant formulation. The grain design (see Figure III-3) is a cylindrical perforate in the forward end transitioning to two longitudinal slots in the aft end of the motor. The longitudinal slots have a 7.5° taper on the sides. This taper is to provide the increasing radii needed to decrease the induced strains as the configuration transitions from the 14% web fraction beneath the slots to the 70% web fraction of the cylindrical perforate.

The case design is based on the strength level (78,000 psi ultimate) of 7075-T6 aluminum. The nozzle erosion characteristics are based on demonstrated performance of molded glass phenolic. The motor case insulation is TI-R300, an asbestos filled polyisoprene rubber. The liner is a HTPB system compatible with both the propellant formulation and the insulation. A complete summary of performance and general motor specifications are presented in Table III-1. A summary of propellant characteristics used in the design are shown in Table III-2. A predicted pressure-time, thrust-time history is shown on Figure III-4. A plot of missile velocity versus time is shown on Figure III-5.

Design of the baseline motor was based on a burning rate range availability of 0.39 in/sec at 1000 psia to 0.44 in/sec at 1000 psia. Plots of the variation of burning rate with pressure are shown on Figure III-6 for three rates. As may be seen from Figure III-6, as the basic rate increased, so did rate exponent. The change in exponent as the base rate increased had

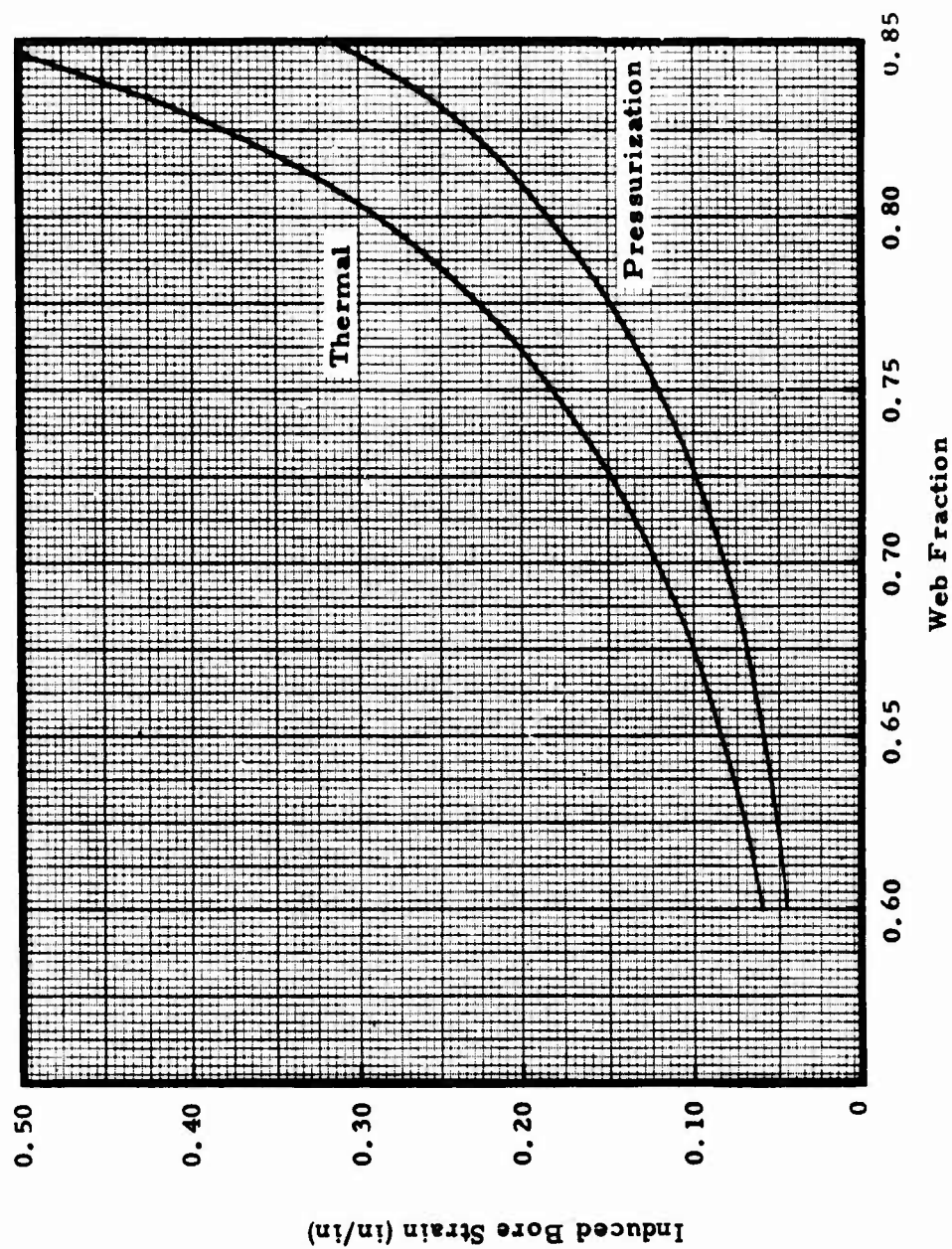


Figure III-1. Bore Strain in Case Bonded Grain



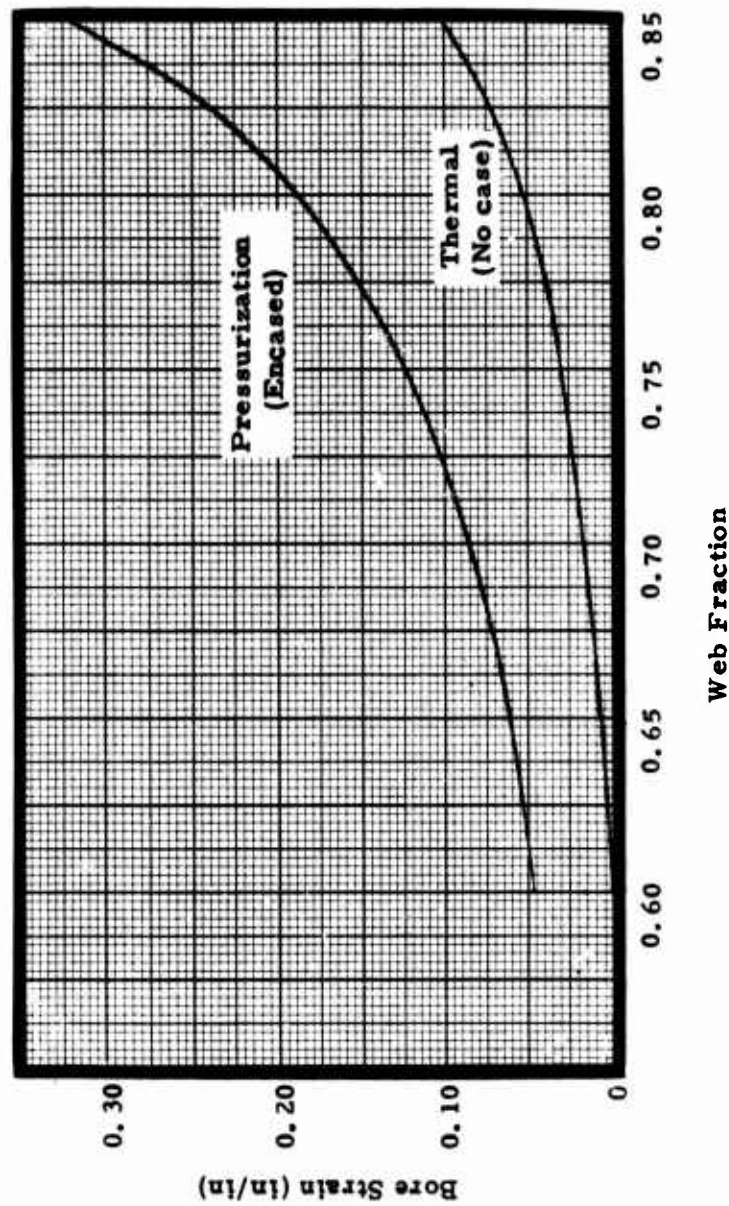
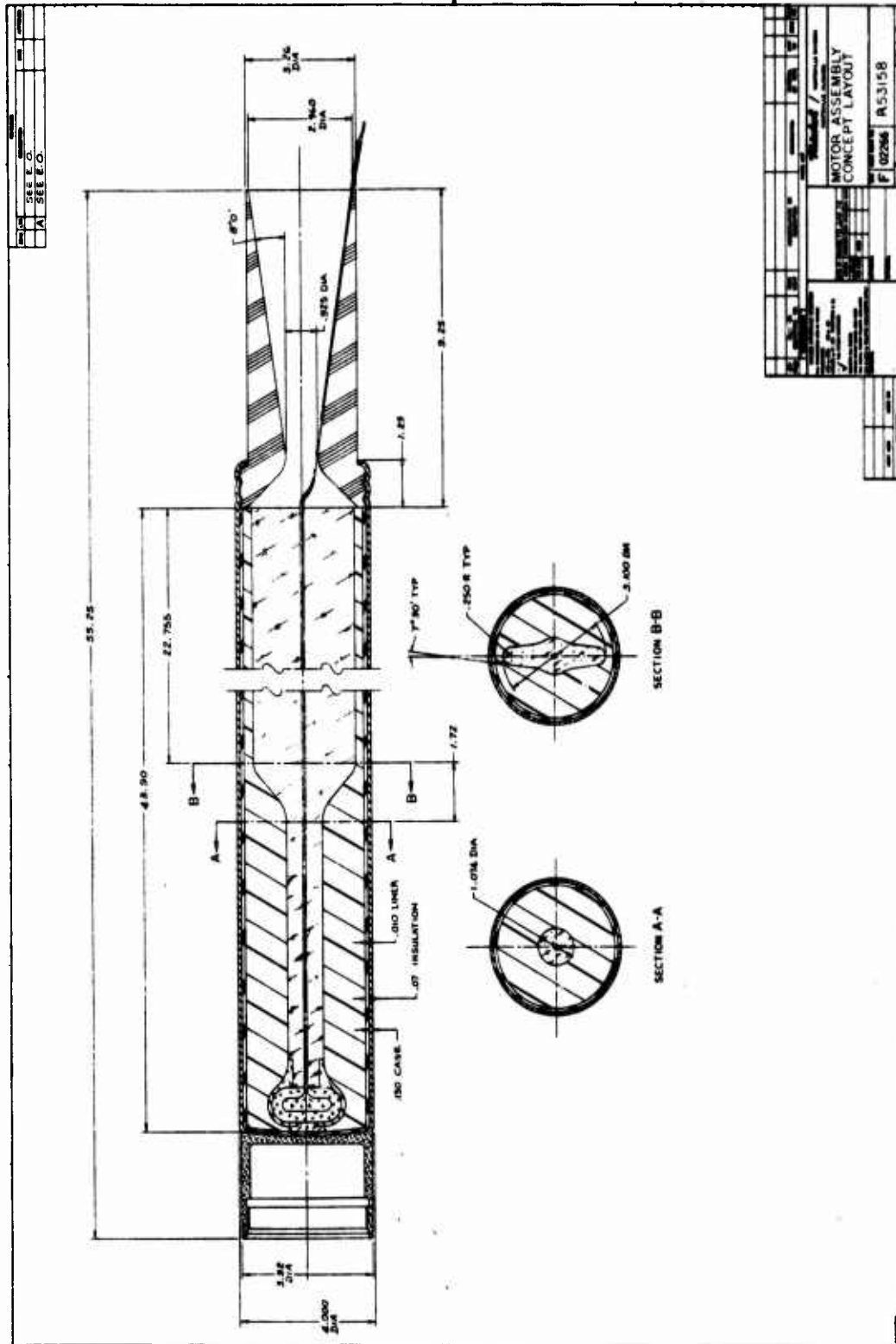


Figure III-2. Bore Strain in Free-Standing Grain with Slip-fit Aluminum Case



**Figure III-3. Baseline Design For 4-inch Low Cost Motor**

**TABLE III-1**  
**BASELINE MOTOR DESIGN**

**Motor Performance Parameters**  
**(70°F)**

	<u>Sea Level</u>	<u>Vacuum</u>
Web Burning Time, sec	1.8	1.8
Average Thrust, lb	3076	3178
Average Pressure, psia	2263	2263
Maximum Pressure, psia	2975	2975
Total Impulse, lb-sec	6013	6225
Total Impulse/Total Weight, lb-sec/lb (Flight)	167.5	173.5
Propellant Weight/Total Weight (Flight)	0.642	0.642

**General Specifications**

**Dimensions, in**

Overall Length	55.25
Outside Diameter	4.0

**Weights, lb**

Propellant	23.05
Chamber	7.01
Nozzle	3.55
Liner and Insulation	2.02
Igniter	<u>0.25</u>
TOTAL WEIGHT (Flight)	35.88
Blow-Out Mandrel	<u>0.66</u>
TOTAL WEIGHT	36.54
VEHICLE FLIGHT WEIGHT (LAUNCH)	82.25

(Continued on next page)

Table III-1. (Continued).

Trajectory

Slant Range (ft)	12,000
Burnout Velocity (ft/sec)	3,336
Impact Velocity (ft/sec)	2,978
Initial Flight Angle (deg)	-28

Propellant Geometrical Parameters

Configuration---Case Bonded, Internal Burning, CP with two longitudinal slots	
Propellant Outside Diameter, in	3.58
Volumetric Loading Density, %	0.85
Web Fraction	0.70
Geometrical Web Thickness, in	1.253
Nominal Liner Thickness, in	0.010
Initial Burning Surface/Throat Area	342
Length-Average Port Area/Throat Area	2.04

Chamber

Type	Cylindrical
Material	7075/T6 Aluminum
Ultimate Uniaxial Strength, psi	78,000
Specific Weight, lb/in <sup>3</sup>	0.10
Nominal Thickness, in	0.13
Minimum Thickness, in	0.13
Maximum Expected Operating Pressure (MEOP)	3642
Burst Pressure, psia	5100
Burst Pressure/MEOP	1.4

(Continued on next page)

Table III-1. (Continued).

Nozzle

Geometry

Type	Fixed
Expansion Section Configuration	Conical
Number of Nozzles	One
Throat Diameter, in (initial)	0.925
Exit Diameter, in (initial)	2.96
Throat Area, in <sup>2</sup> (average)	0.869
Expansion Ratio (average)	7.92

Entrance and Throat Section

Material	Molded glass phenolic <sup>(a)</sup>
Specific Weight, lb/in <sup>3</sup>	0.068

Expansion Section

Material	Molded glass phenolic <sup>(a)</sup>
Specific Weight, lb/in <sup>3</sup>	0.068

Insert

Material	Molded glass phenolic <sup>(a)</sup>
Specific Weight, lb/in <sup>3</sup>	0.068

<u>Throat Erosion Rate (in/sec)<sup>(b)</sup></u>	$r_e = 0.000111P^{0.824}$
---	---------------------------

a. FM16771 Typical Material

b. RER 915, "Nozzle Throat Erosion Rates on Mark 17 Motors",  
G. P. Roys, Thiokol/Huntsville, 6 June 1975.

TABLE III-2

PROPERTIES AND BALLISTICS  
OF HTPB-TYPE PROPELLANT

Characteristic Velocity, $c^*$ , (ft/sec)	5220 <sup>(a)</sup>
Specific Weight, $\delta_f$ , (lb/in <sup>3</sup> )	0.063 <sup>(b)</sup>
Ratio of Specific Heats, $\gamma$	1.145 <sup>(a)</sup>
Burning Rate Equation, $r = a_t P_c^n$	0.01328 $P_c^{.50}$
Temperature Coefficient of Pressure, $\pi_K$ , (%/°F)	0.10 <sup>(c)</sup>
Temperature Coefficient of Burning Rate, $\sigma_K$ , (%/°F)	0.098 <sup>(c)</sup>
Generalized Formulation (pbw)	
Aluminum	12
AP	76
HTPB Binder System	12

a. Computer Sequence T51645, 7/22/75, at 2000 psia

b. Computer Sequence T51645, corrected for cure shrinkage

c. Assumed

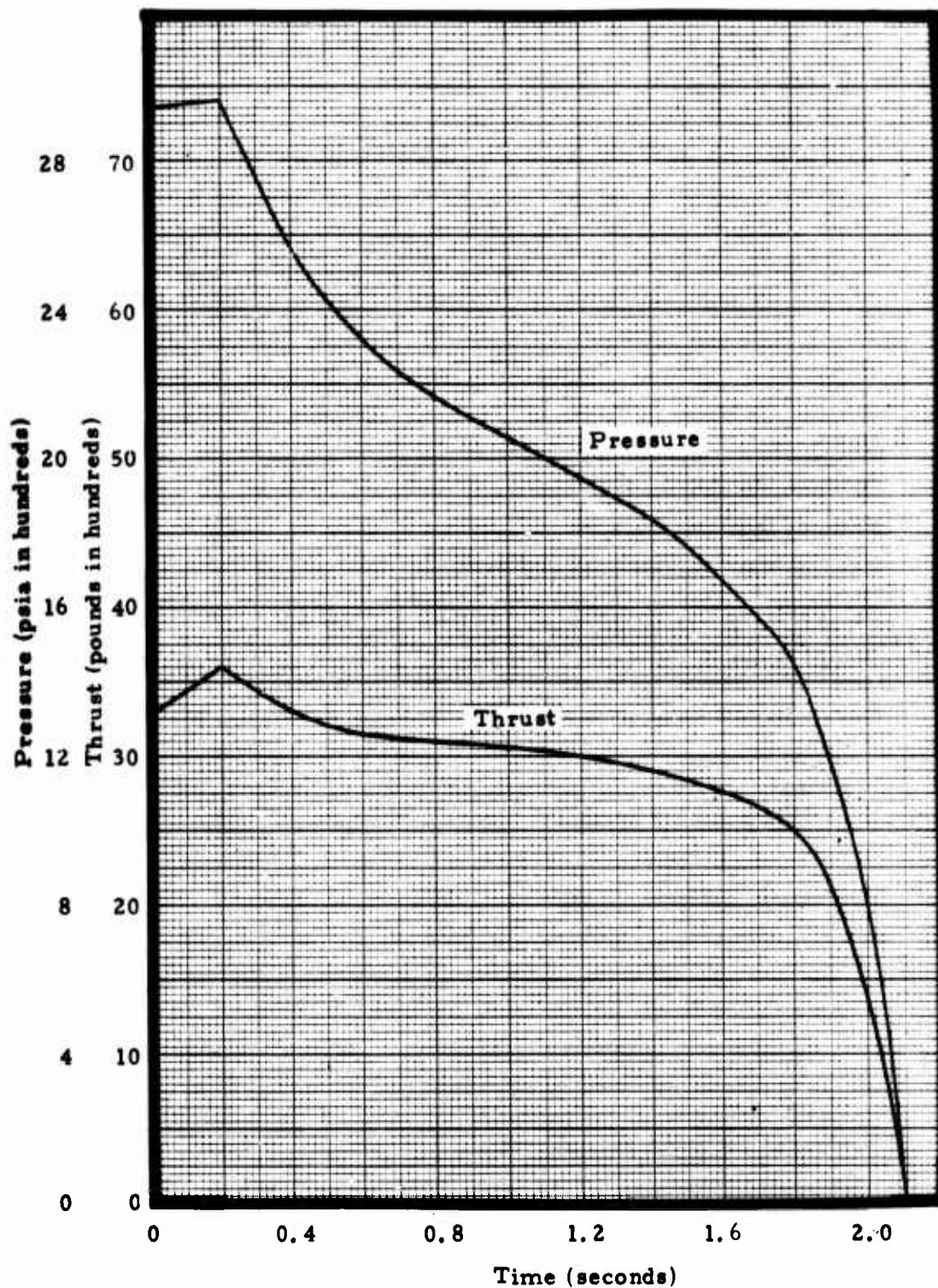


Figure III-4. Pressure and Thrust versus time, Baseline Design, Vacuum and 70°F



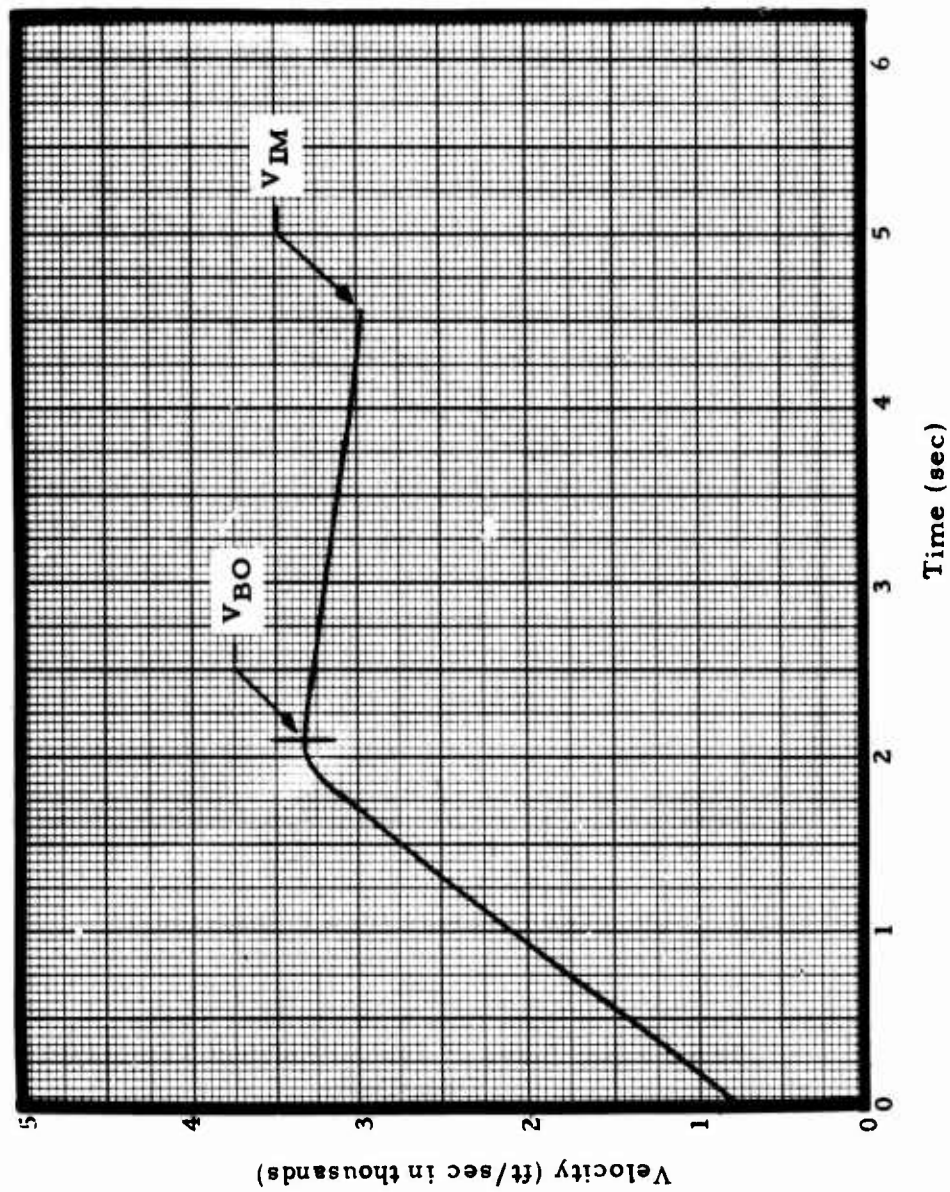


Figure III-5. Velocity Versus Time, Baseline Design

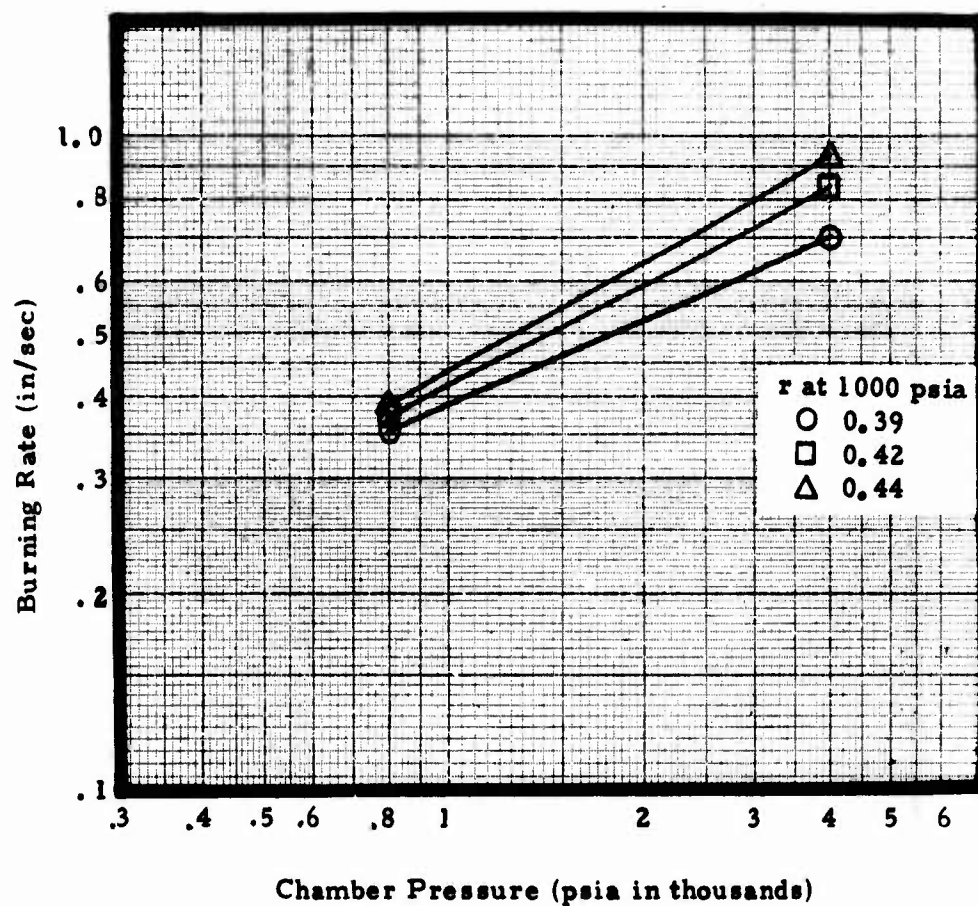


Figure III-6. Variation of Burn Rate with Chamber Pressure, Showing Three Basic Rates of Typical Ambient Temperature Cure Propellants

a significant effect on the ability of the configuration to meet the required slant range and velocity. A matrix of throat areas and burning rates was used to establish the throat and burning rate combination that would meet the requirements (Figure III-7). In using the lower burning rate range, it was found that the pressure did not change rapidly enough to produce the regressivity needed to meet the requirements. It was found that the higher burning rate range would produce the necessary regressivity; however, throat size would have to be so large that other problems would exist. The burning rate used to establish the baseline design was 0.42 inch per second at 1000 psia. In this rate range, the burning rate exponent is 0.5, high enough to provide the necessary regressivity, but not so high that pressurization problems are insurmountable.

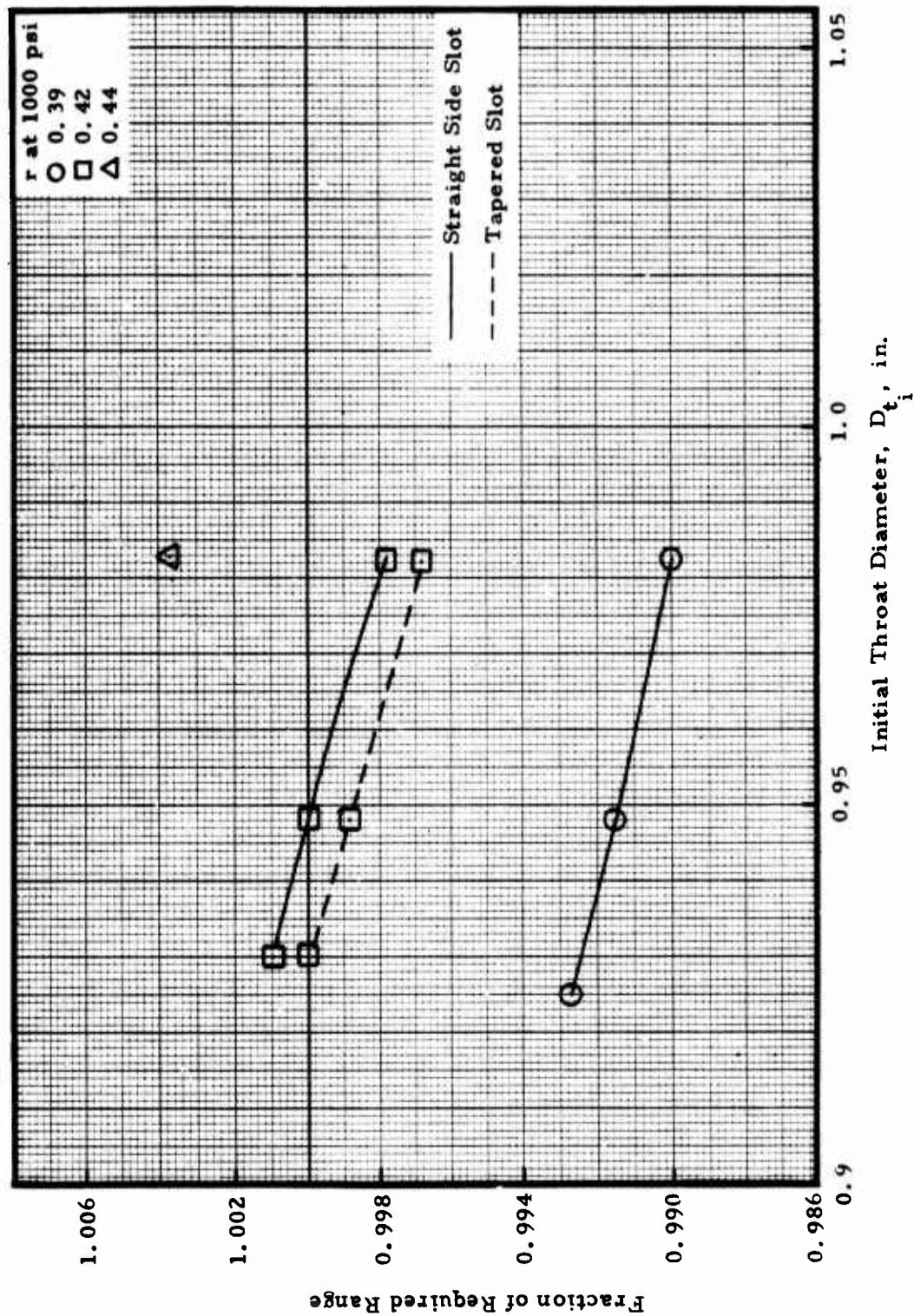


Figure III-7. Effect of Burn Rate on Baseline Motor Performance

**SECTION IV**  
**PROPELLANT TAILORING AND CHARACTERIZATION**

#### SECTION IV

#### PROPELLANT TAILORING AND CHARACTERIZATION

Ambient-temperature cured HTPB propellant used in conjunction with consumable grain-forming mandrels was identified by the Booz-Allen study (Reference IV-1)<sup>1</sup> as having high cost reduction potential. It was stated that "the payback ratio is surprisingly high because of the mix of cost-reducing elements: cheaper propellant, elimination of ovens, reduced tooling for mandrels, no mandrel withdrawal, use of the mandrel as the weather seal, and so on. It does not appear too difficult to develop ambient temperature cured HTPB, since it is lower in viscosity and pot life is less of a problem." Because these advantages for achieving lower cost were identified, the AFRPL contracted with Aerojet Solid Propulsion Company to develop an ambient-temperature cured HTPB propellant (Reference IV-2). That program demonstrated the feasibility of such a propellant system and thus ambient temperature cure propellant was dictated for use in the subject contract.

Of the advantages listed in the Booz-Allen study for this propellant/mandrel system, only the "elimination of ovens" can be attributed to use of ambient temperature cured propellant. Further details of this concept are implied in Appendix D of Reference IV-1 where propellant cure is described as occurring while the motors are "waiting for normal shipment or being shipped to a user destination." Thus, the propellant would be expected to cure at some unknown, uncontrolled, inconsistent temperature. Geographic location of the manufacturing facilities, season of the year, storage facilities at the plant and mode of shipping finished motors would all affect the temperature-time history the propellant would experience while it is curing. Experience throughout the solid propellant industry has shown that consistent propellant physical properties are obtained in large measure by consistent temperature-time history during cure. The inappropriateness of inconsistent storage conditions was implicitly recognized during the Reference III-2 program wherein those propellants were cured at 80°F for whatever time was required for the given formulation.

Even so, it is accepted that curing propellant at a controlled 80°F may be more economical than curing at the conventional 140-150°F, assuming equal cure times. However, controlling temperature to 80°F will, in most parts of the country, require both heating and cooling equipment for the curing area. The opinion is that the initial cost of an 80°F cure facility would be about the same as a 140-150°F facility, since the latter requires only heating equipment. Of course, the former would operate at considerably less energy cost. Perhaps the minimum cost cure condition (including both initial investment and operating costs) would be 100-110°F, since only heating equipment would be needed for most sections of the country and energy costs

---

1. References are given at the end of this section



would be less than for 140-150°F cure. As a result of the above considerations, Phase II scope of work was expanded to include a detailed cost analysis of various cure time/cure temperature combinations.

Initial attempts during the subject contract to load heavy-weight full scale motors with ambient temperature cure propellant were frustrated because of unacceptable grain quality and inability to complete casting operations. The initial evaluation indicated the problem was propellant rheological properties but subsequent experiences revealed that casting tooling was the culprit. In the meantime another available conventionally cured propellant was loaded in the full scale motors so that component testing could proceed. After rectifying the casting tooling deficiencies, ambient temperature cure propellant was cast in full scale motors and was used to provide bond samples for insulation systems.

#### PROPELLANT REQUIREMENTS

The propellant formulation for the Phase I motor tests was to be an ambient temperature cure HTPB system using R-45 polymer and to have solids loading of 88%. The goals for ballistic, physical and other characteristics were:

	<u>Goals</u>	<u>Demonstrated</u>
Cure Temperature	"Ambient"	80°F
Cure Time	<9 days	8 - 10 days
Strain @ Max. Stress, -65°F	>25%	36%
Max. Stress, 77°F	>100 psi	140 psi
Modulus, 77°F	>400 psi	618 psi
Temperature Capability	-65 to 165°F	

These goals were met, as listed above, with DTS-7984<sup>1</sup> propellant as manufactured in Mix T-684.

#### PROPELLANT FORMULATIONS AND CHARACTERISTICS

Three basic formulations were used in 5-gallon mixes:

1. Designated as TP-H8256 at the end of Phase I. Identified as DTS-7984 throughout this report.



<u>Designation</u>	<u>Cure Temp. (°F)</u>	<u>Comments</u>
TP-H8245	"Ambient-temperature"	Baseline formulation
DTS-7984	"Ambient-temperature"	Same as TP-H8245 except 3% plasticizer instead of 2%
TP-H8208	145	Developed for SAM-D

All three contained the same amounts of total solids and aluminum. Complete formulations of the ambient temperature cure propellants are given in Appendix D.

Theoretical thermochemical properties of TP-H8245 are:

	<u>TP-H8245</u>
Characteristic Velocity, $C^*$ (ft/sec) <sup>1</sup>	5186
Density, $\rho_f$ (lb/cu in)	0.0639
Flame Temperature <sup>1</sup>	
$T_c$ (°F)	5838
$I_{sp}$ (lb-sec/lb) <sup>2</sup>	263

Burn rate of TP-H8245 is defined in later sections. It was assumed that DTS-7984 had the same burn rate.

#### MOTOR LOADINGS AND PROPELLANT PROCESSING

Ten 5-gallon mixes were manufactured during the program (Table IV-1). Six used TP-H8208 propellant, one used TP-H8245 and three used DTS-7984. Pertinent information about the mixes is listed in Table IV-2. A 5-gallon mix (T-600) was manufactured under a corporate-sponsored (IR&D) propellant evaluation program prior to the mixes manufactured to load the

1. 1000 psia.

2. Optimum expansion from 100 psia to 14.7 psia; no divergence or nozzle losses.

**TABLE IV-1**  
**SUMMARY OF PHASE I FIVE-GALLON MIXES**

Mix Number	Date Mfg.	Propellant Type	Items Loaded	Disposition
T600 <sup>a</sup>	8/20/75	TP-H8245	12 ea. TX-395; Physical property samples	All items tested
T607	9/18/75	TP-H8245	1 ea. TX-631; Bond, physical property and hazard samples	TX-631 reject because of inadequate casting tooling; all other items tested
T616	10/16/75	TP-H8208	2 ea. TX-631 Motors	Aborted loading because of inadequate casting tooling
T622	11/12/75	TP-H8208	2 ea. TX-631 Motors	Motors static tested, 11/25/75
T630	11/21/75	DTS-7984	1 ea. TX-631 (pour cast); bond and physical property samples	TX-631 tested 1/30/76; other samples tested
T634	12/5/75	TP-H8208	2 ea. TX-631 Motors	Charge 1 static tested 12/24/75. Chg 2 pressure tested 3/8 & 3/9; static tested 3/10/76
T640	12/16/75	TP-H8208	2 ea. TX-631 Motors (Chg 1 pour cast)	Motors static tested 1/29/76
T643	12/23/75	TP-H8208	2 ea. TX-631 Motors	Static tested 2/27/76
T649	1/14/76	TP-H8208	14 ea. TX3 Motors (Nozzle Material testing)	10 Motors static tested 1/28/76
T656	1/21/76	DTS-7984	Bond Samples	Laboratory tests completed
T684	3/5/76	DTS-7984	2 ea. TX-631 Motors (foam mandrels); bond samples	Motors static tested 2/19/76; Laboratory tests completed

a. Mix T600 was manufactured as part of a corporate-sponsored propellant evaluation program. Data therefrom is presented herein for completeness and comparison with subsequent results.

component test motors. Data from Mix T-600 are presented in this report for continuity and completeness of information and for comparison with subsequent mixes.

#### Mix T-600 (TP-H8245)

Mix T-600 of TP-H8245<sup>1</sup> was made without using heat during the propellant processing. However, cooling water was not circulated and, consequently, heat buildup due to work input resulted in a propellant temperature increase. This mix processed well, and end-of-mix viscosity was 11 Kp. The temperature at end-of-mix was 105°F which is 15-20°F higher than that observed for gallon mixes. It is believed that this higher mix temperature resulted in significant reduction in propellant pot life. As seen in Table IV-2 and Figure IV-1, time to 40 Kp was only 1.5 hours. Previous mixes had pot lives of greater than four hours and the actual casting life was considered to be about eight hours as the rate of viscosity increase was still low. For future mixes, it was decided that the processing temperature be controlled to a lower temperature.

Mix T-600 was deaerated and cast at 145°F as previous experience has demonstrated that this propellant tends to stack during casting below about 80°F. Because of the short pot life, the deaeration and casting time was longer than normal and consequently the propellant was exposed to 145°F temperature longer. This extended exposure also contributed to a shorter pot life. In future mixes, it was decided that the deaeration and casting temperature be maintained at a lower level (approximately 120°F). Although this mix had a short pot life, the propellant was successfully cast and exhibited good processing characteristics two hours after curing agent addition (Figure IV-2).

Sensitivity was measured on this scale-up mix and, as expected, the propellant was relatively insensitive to impact, friction, and spark (Table IV-2). In addition, the propellant had good thermal stability based on limited exposure to 250°F.

Mechanical properties, including tensile properties versus cure time, broad spectrum, strain endurance, and short term aging, were measured. Tensile properties after seven days at 145°F and eight days at ambient indicated the propellant was softer than that from one-gallon mixes. After seven days at 145°F, the stress was 111 psi and the strain was 64.6% (Table IV-3). The 65% strain was high even for soft propellant, but might be very attractive. After eight days at ambient temperature (80°F), the stress was 76 psi and strain was 50.4%. For the next five-gallon mix, since higher stress was desired, the NCO/OH ratio was increased to 0.93.

---

1. Earlier designation was DTS-7883.

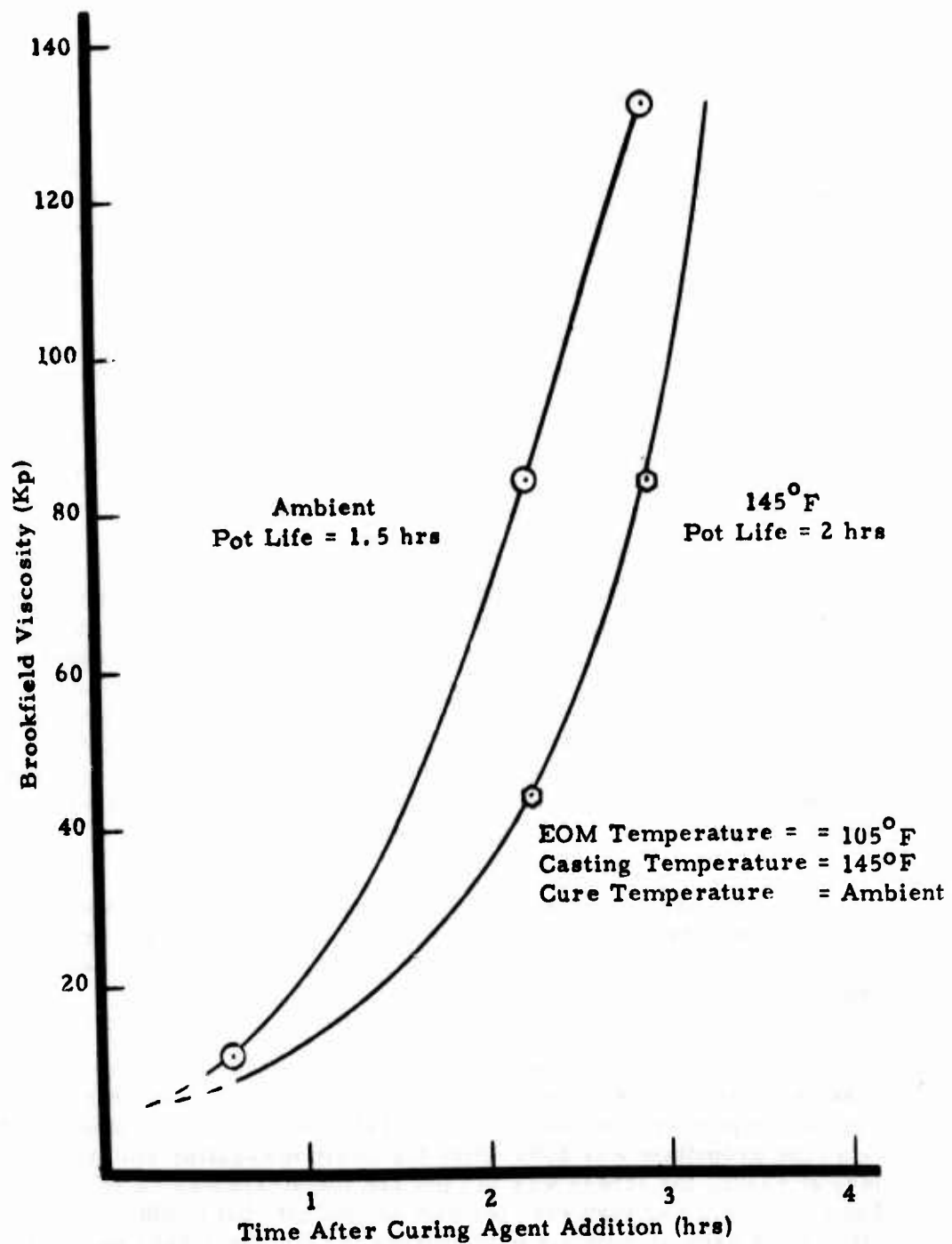


Figure IV-1. Pot Life of TP-H8245 Propellant (Mix T-600)

TABLE IV-2  
CHARACTERISTICS OF TP-H8245 PROPELLANT  
(Mix T-600)

EOM Viscosity, Kp	11
Pot Life, Hrs. to 40 Kp	1.5
Actual Cure Time, days	13
NCO/OH	0.90
<u>Sensitivity (0% fire level)</u>	
Impact, Kg-cm	110/125
Friction, lb.	>100
Spark, joules	>25
<u>Thermal Stability (No Fire) at 250°F, hrs.</u>	18
<u>Strand Burn Rate</u>	
at 1000 psi, in/sec.	0.398
at 2225 psi, in/sec.	0.580
n	0.46
<u>Physical Properties</u>	
at 77°F	Modulus, psi 342
	Maximum Stress, psi 80
	Strain at Max. Stress, % 46.8
at -65°F	Modulus, psi 10,068
	Maximum Stress, psi 530
	Strain at Max. Stress, % 35.3

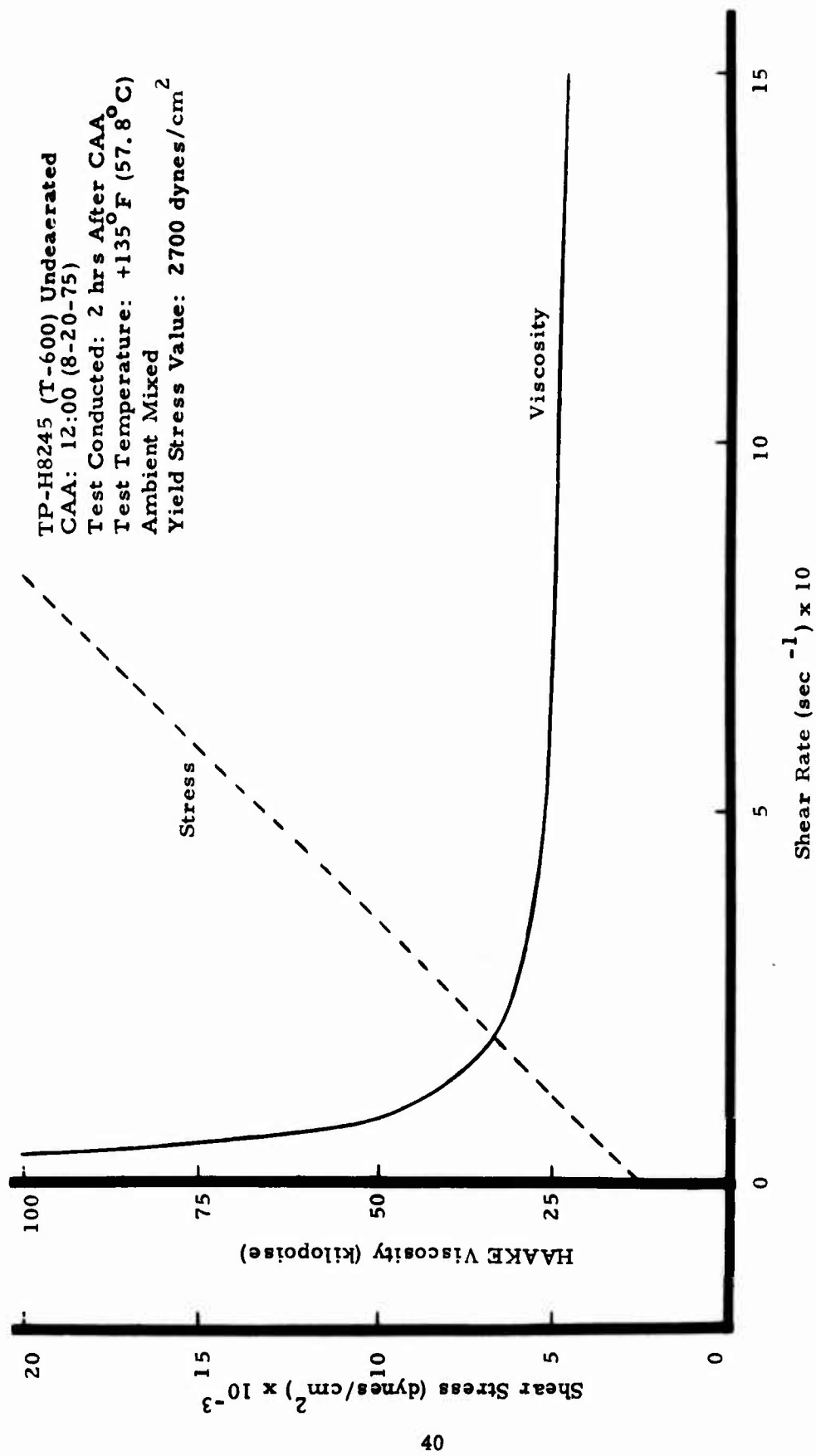


Figure IV-2. Shear Stress and Viscosity Versus Shear Rate of TP-H8245 (T-600)

**TABLE IV-3**  
**DETERMINATION OF CURE TIME**  
**(Mix T-600, NCO/OH = 0.90, TP-H8245)**

Cure Temperature	<u>Ambient</u>	<u>145°F</u>
Cure Time, days	7	5
77°F Modulus, psi	301	336
Stress, psi	78	109
Strain, %	51.9	65.3
Cure time, days	8	7
77°F Modulus, psi	296	354
Stress, psi	76	111
Strain, %	50.4	64.6
Cure Time, days	9	9
77°F Modulus, psi	232	352
Stress, psi	75	123
Strain, %	51.5	57.3
Cure time, days	13	
77°F Modulus, psi	296	
Stress, psi	71	
Strain, %	48.9	



Broad spectrum physical properties are shown in Table IV-4 and Figure IV-3 for Mix T-600. Short term aging results are listed in Table IV-5.

Twelve TX-395 (0.5 lb.) motors were static fired with DTS-7883 (TP-H8245) propellant loaded from Mix T-600. A complete ballistic analysis was performed to determine pressure and temperature characteristics and the results are reported in Appendix A. Following is a summary of the findings.

TX-395 burn rate is described:

$$r_b = a_T P^n$$

Temp. (°F)	$\frac{r_b}{a_T P^n}$	
	$a_T$	$n$
-65	0.02001	0.421
70	0.01487	0.475
160	0.01219	0.511

Burn rate at 1000 psia and 70°F is 0.395 in/sec.

Temperature coefficients of pressure and rate are functions of pressure because the pressure exponent,  $n$ , varies with temperature. Some typical values, which cover the pressure range of interest to this program, are:

Pressure (psia)	Temperature Coefficients (per °F)	
	Pressure ( $\pi_k$ )	Rate ( $\sigma_k$ )
~ 1000	0.00065	0.00086
~ 1800	0.00110	0.00114
~ 2500	0.00159	0.00162

The coefficient  $\sigma_k$  is theoretically smaller than  $\pi_k$  for propellants with constant pressure exponent,  $n$ . The subject data show  $\sigma_k$  higher than  $\pi_k$ , which is probably caused by a bias in the data.

Strands were tested at 70°F in a nitrogen-pressurized bomb with samples from Mix T-600 Figure IV-4). The rate is described by

$$r = 0.01679 P^{0.458} \quad (\text{T-600 Strands at } 70^\circ\text{F})$$

which shows a rate of 1000 psia of 0.398 in/sec. There is no statistical difference between the levels or slopes of the strand and motor 70°F regression lines.

TABLE IV - 4

## TP-H8245 BROAD SPECTRUM MECHANICAL PROPERTIES

(Mix T-600 Cured at Ambient Temperature)

Temperature (°F)	Modulus (psi)	Maximum Stress (psi)	Strain at Max. Stress (%)	Ultimate Strain (%)
160	86	53	68.9	76.2
110	194	69	50.6	59.6
77	342	80	46.8	55.2
40	554	103	46.6	53.8
0	1420	176	59.6	64.3
-25	3246	255	56.3	67.0
-45	5682	349	40.1	51.9
-65	10068	530	35.3	46.9
-75	13640	671	20.6	31.9

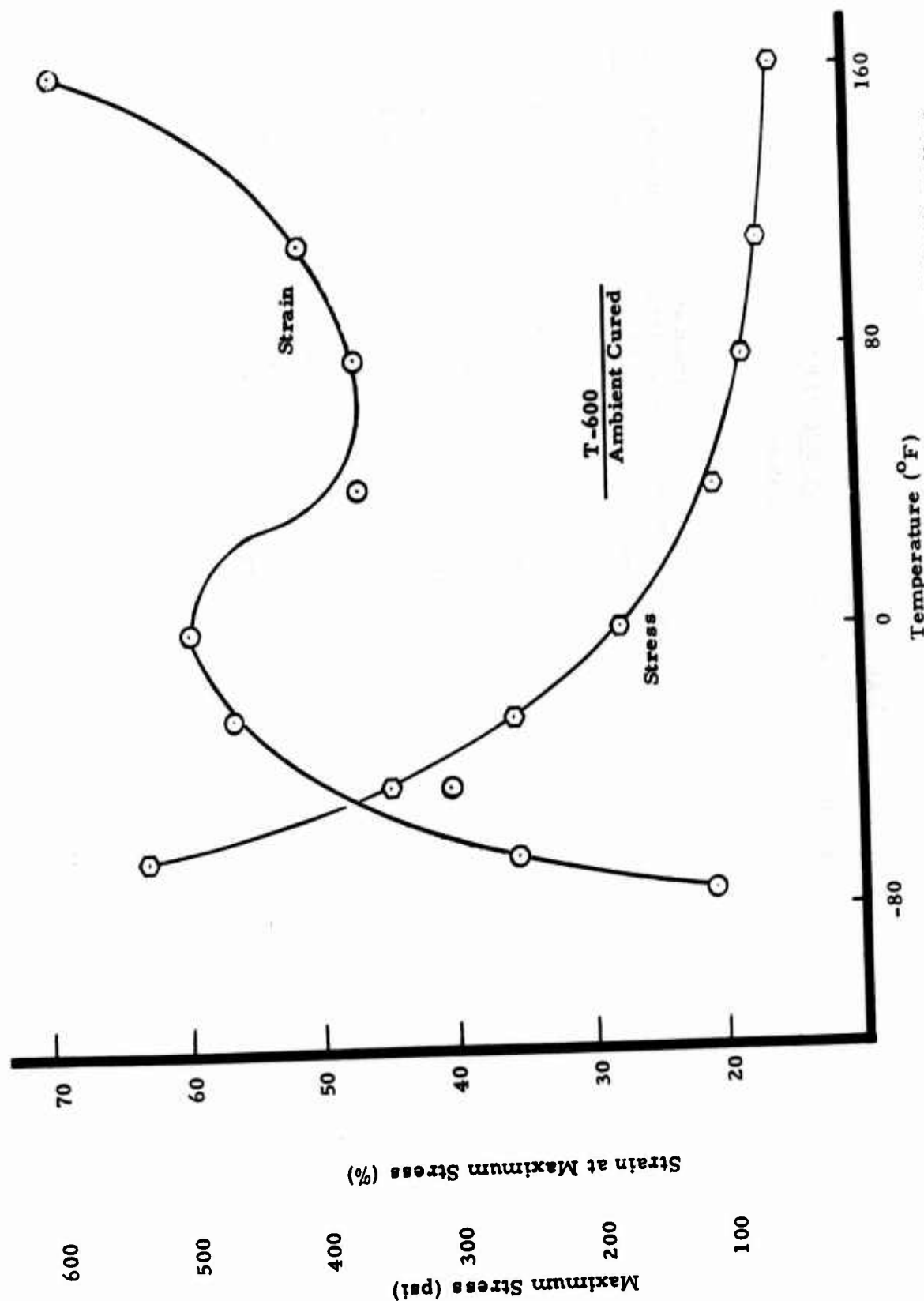


Figure IV-3. Effect of Temperature on Physical Properties of TP-H8245 Propellant

TABLE IV-5

AGING OF TP-H8245 PROPELLANT  
(Mix T-600 Cured at Ambient Temperature, Tested at 77°F)

<u>Storage Time</u> <u>(weeks)</u>	<u>Modulus</u> <u>(psi)</u>	<u>Maximum Stress</u> <u>(psi)</u>	<u>Strain @ Max.</u> <u>Stress (%)</u>
<u>Stored at 145°F</u>			
0	342	80	47
1	469	129	48
2	425	156	46
4	666	176	43
6	761	207	41
<u>Stored at ambient temperature (77°F)</u>			
0	342	80	47
1	261	83	50
2	261	92	50
4	324	106	48
6	370	119	52

N<sub>2</sub> Strands  
70°F  
2" Gage Length

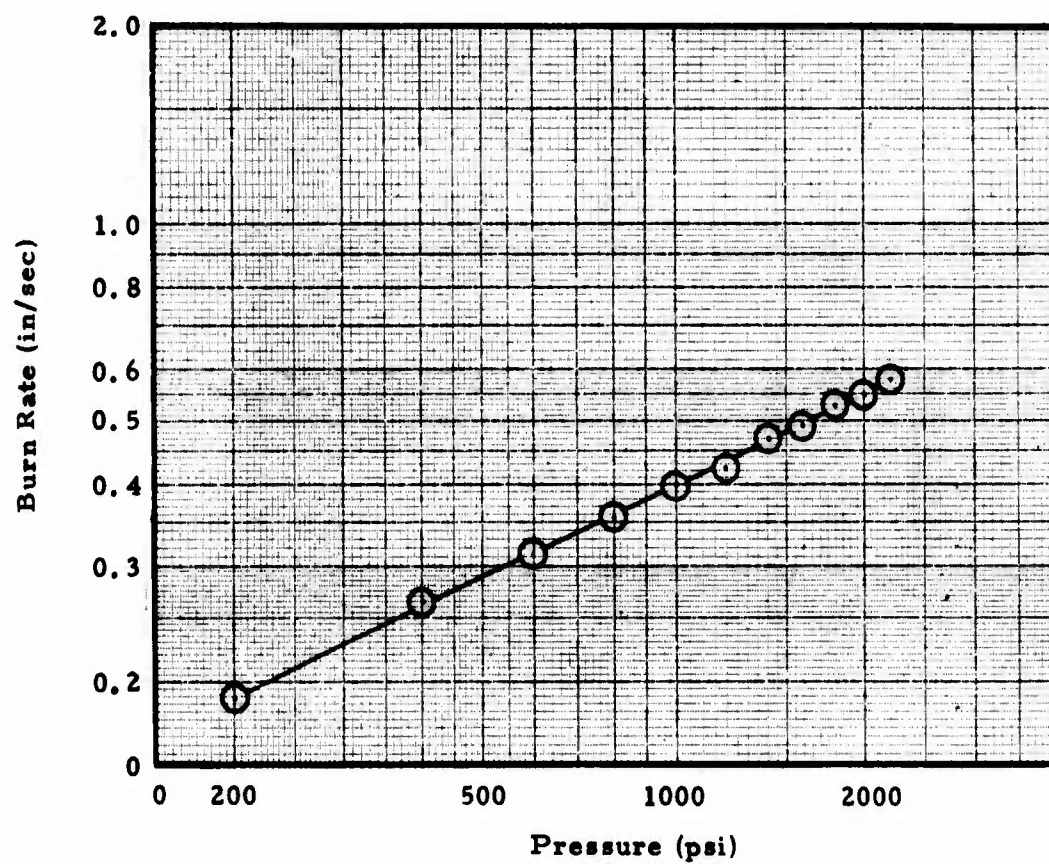


Figure IV-4. Strand Burning Rate, TP-H8245, Mix T-600

As a result of the experiences with Mix T-600, the following procedures were adopted for subsequent mixes:

1. Reduce and control maximum mix temperature
2. Reduce and control deaeration and casting temperature.
3. Minimize deaeration time.
4. Delay ZnO addition until late in mix cycle.
5. Increase NCO/OH.

#### Mix T-607 (TP-H8245)

##### Processing

The second scale-up mix of TP-H8245 propellant (Mix T-607) was manufactured but it was not possible to cast acceptable motors. Processing was hampered by mis-sized casting tooling, although at the time it was thought the major blame was propellant rheological characteristics. A subsequent mix (T-616) of TP-H8208 propellant (which has excellent rheology) using the same casting tooling also experienced severe processing difficulties, which identified the culprit as the tooling, at least in large measure. Details of the casting experience are given in the paragraphs below.

Mix T-607 was an ambient cure HTPB formulation, TP-H8245. Based on the results of Mix T-600, the following mix cycle was used:

1. Add and blend R45M polymer, DOA plasticizer, HX-752 bonding agent, and linoleic acid.
2. Add and blend oxidizer fractions.
3. Mix for 60 minutes at ambient pressure using no added heat.
4. Add and blend HMDI cure agent and ZnO catalyst.
5. Mix for 20 minutes, using cold water to hold the end-of-mix temperature to 91°F.

The propellant was used to cast ballistic, tensile, and bond samples and one TX-631 motor (4" OD x 42" long). The propellant for the samples was deaerated and pressure cast without difficulty. Midway through the vacuum casting of the TX-631 the propellant began to bridge and fill the annulus formed by the casting sleeve and the aft end of the core. The casting was interrupted to clean the sleeve/core annulus, but the plugging recurred shortly after resumption of casting. The motor was eventually filled by repeatedly interrupting the casting to clear the sleeve/core annulus. No precise data exist, but the propellant viscosity during casting is estimated to have been 20-30 kilopoise.

Radiographic inspection of the cured loaded case revealed many voids, large and small, throughout the propellant. The most probable cause of the unsuccessful casting was felt at the time to be the high viscosity of the propellant. In order to supply TX-631 motors for component evaluation, Phase I effort was redirected to use TP-H8208 (SAM-D) propellant.

Mix T-616 of TP-H8208 propellant was manufactured with standardized raw materials per current TP-H8208 manufacturing procedures. End-of-mix viscosity was 3.2 kilopoise. Two TX-631's were scheduled to be vacuum cast from this mix. With approximately two-thirds of the first motor filled, bridging in the sleeve/core annulus again occurred, necessitating several interruptions in the casting to clear the casting sleeve. Eighty minutes were required to cast the motor. Immediately after the start of casting of the second motor the casting sleeve plugging began to occur and the loading was aborted.

Visual inspection of the first loaded case after finishing showed propellant/liner separation at the aft end. Radiographic inspection revealed numerous 0.1" to 0.4" voids throughout the motor and confirmed that the propellant/liner separation was extensive. The separation was caused by over-cured liner. The loaded case was unacceptable for test.

A more critical review of the casting problems was conducted. This review concluded that, though propellant viscosity was a contributing factor, the primary cause of the bridging in the casting was casting tooling configuration. The core/sleeve annulus was 0.67-inch wide and a 0.375-inch diameter hole plate was being used to deaerate the propellant as the propellant fell into the sleeve. As a result of the small clearance, the propellant would occasionally contact and stick to either the core or sleeve, gradually filling the annulus until bridging occurred.

Corrective action for this condition was to redesign the casting tooling to increase the core/sleeve annulus and to utilize an available 3/16-inch diameter hole plate for propellant deaeration. This design provided a 1.02-inch clearance for a 0.187-inch stream of propellant. Use of this tooling was initiated with Mix T-622, which also contained TP-H8208 propellant.

As a result of these experiences, another project modified TX-631 casting tooling in a manner similar to that described here. A defect-free motor was produced with a propellant having comparable rheological characteristics as TP-H8208, thus proving that tooling configuration was the primary contributor to the TX-631 casting difficulties with both TP-H8245 and TP-H8208 propellants.



### Rheology

The end-of-mix viscosity of Mix T-607 was 20 Kp. This is a rather high viscosity to vacuum cast, but as seen in Table IV-6, this end-of-mix viscosity is exactly as predicted for this solids loading and ambient processing. Thiokol has made 10 pint, 30 one-gallon and two five-gallon mixes of this ambient cured propellant. A summary of these mixes indicates an average viscosity for this formulation is 21 Kp. As the Mix T-607 viscosity was 20 Kp, it is obvious that this viscosity is well within experimental error. As can also be seen in this table, an average end-of-mix viscosity of approximately 13.9 Kp was obtained in Reference IV-2; however, that program used a 70/30 blend of coarse-to-fine AP. With this same blend, Thiokol measured an end-of-mix viscosity of 15.5 Kp. Although the attempt to load two full scale TX-631 motors from this mix was unsuccessful, the cause, as demonstrated in other experiments, was casting equipment design as opposed to abnormally high viscosity.

Time to 40 Kp for this second five-gallon mix was 9.5 hours (Figure IV-5). Two changes were made to increase the pot life from the 1.5 hours of the first mix (T-600) to the 9.5 hours of this mix. The processing temperature was controlled to a lower value and end-of-mix temperature was 92°F. The ZnO cure catalyst addition was delayed until immediately prior to curing agent addition. Obviously, these two changes were successful as pot life was increased significantly and demonstrated that the cure chemistry is sufficiently understood to make desired formulation changes. As seen in Figure IV-6, the HMDI selection as curing agent was justified as the pot life measured by Thiokol in their second five-gallon mix exceeded that measured in the five-gallon mix in Reference IV-2. The difference in rate of viscosity rise for these two mixes is attributed to the reaction rate differences of HMDI and TDI curing agents.

### Sensitivity

Samples for extensive sensitivity tests were cast from Mix T-607. The results are summarized in Table IV-7 and indicate the propellant will be classified as a military Class II or a DOT Class B. Thiokol, however, does not have the authority to make these classifications.

### Mechanical Properties

For Mix T-607, the NCO/OH ratio was increased from 0.90 to 0.93 as the physical properties of the first five-gallon mix were considered soft. Mechanical properties were measured at temperatures from -75°F to 160°F (Table IV-8). As seen in Table IV-9, the ambient modulus was increased

TABLE IV-6

SUMMARY OF THIOKOL END-OF-MIX VISCOSITY EXPERIENCE

		AP Blend (Coarse/Fine)	
	<u>70/30</u>	<u>60/40 - 55/45</u>	<u>50/50</u>
	20	20	47
	14	22	
	18	22	
	15	16	
	12	23	
	14	18	
		20	
		32	
		28	
		32	
		11 (5 gal)	
		<u>20 (5 gal)</u>	
$\bar{X}$	<u>15.5</u>	21	<u>47</u>
$\sigma$	2.9	3.4	--
Ref. IV-2	13.9		

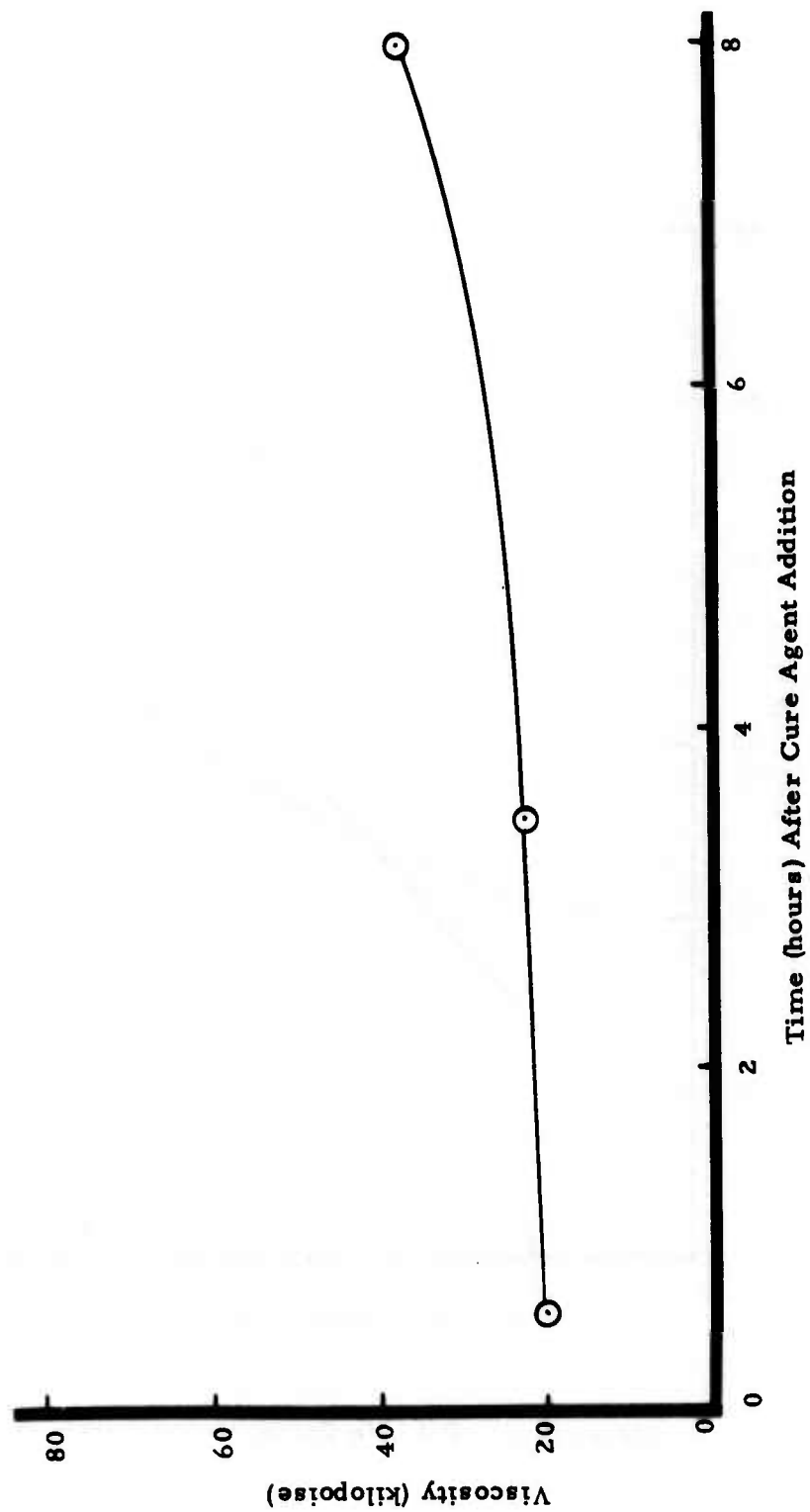


Figure IV -5. Pot Life of TP-H8245 Propellant (Mix T-607)

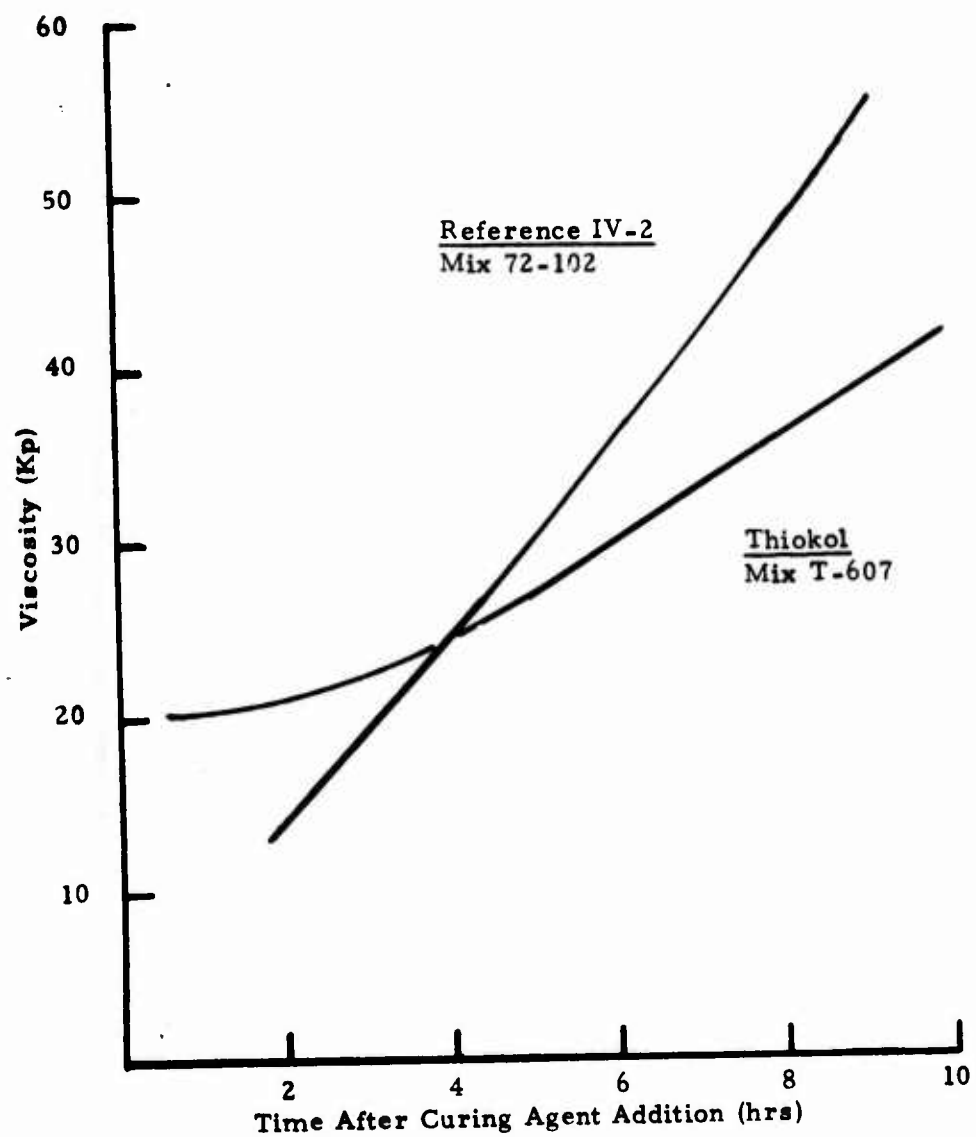


Figure IV-6. Pot Life Comparison of Five-Gallon Mixes

TABLE IV-7

CHARACTERISTICS OF MIX T-607

Propellant Type:	TP-H8245	
Mix Number	T-607	
Date Made	9/18/75	
EOM Viscosity, kp	20	
Pot Life, hours to 40 kp	9.5	
Actual Cure Time, days	11	
<u>Sensitivity</u>		
Uncured:		
Impact, kg-cm	115/125	
Friction, lbs	> 100	
Spark, joules	> 25	
Cured:		
Impact kg-cm	45/50	
Card Gap	0	
Lead Column, 5 tests	negative	
Unconfined burning	negative	
Thermal Stability - 48 hrs. at 75°C	No change	
Probable Classification:	Military Class 2 DOT Class B	
<u>Strand Burn Rate, in/sec</u>		
@ 1000 psi	0.42	
@ 2225 psi	0.61	
n	0.46	
<u>Physical Properties</u>		
NCO/OH	0.93	
Storage Time at Ambient Temp. (days)	11	54
<u>77°F</u>		
Modulus, psi	550	827
Max. Stress, psi	129	147
Strain at Max. Stress, %	50	40
<u>160°F Max. Stress, psi</u>	79	
<u>-65°F Strain at Max. Stress, %</u>	47	
Strain Endurance, %	38	
Bond to TL-H755 Liner:	Peel, pli	2.2
	Tensile, psi	80

**TABLE IV-8**  
**MIX T-607 BROAD SPECTRUM MECHANICAL PROPERTIES**  
**(TP-H8245)**

<u>Temperature (°F)</u>	<u>Modulus (psi)</u>	<u>Max. Stress (psi)</u>	<u>Strain at Max. Stress (%)</u>	<u>Ultimate Strain (%)</u>
	<b>Strain Endurance = 38%</b>			
160	225	79	53	56
110	408	109	51	53
77	550	129	50	53
40	862	160	53	57
0	1860	229	59	62
-25	3099	350	67	72
-45	5628	477	63	69
-65	9017	663	47	54
-75	13492	803	38	41
<b>Stored 54 Days at Ambient</b>				
77	827	147	40	42

TABLE IV-9

RESPONSE OF PHYSICAL PROPERTIES TO NCO/OH

	<u>T-600</u>	<u>T-607</u>
NCO/OH	0.90	0.93
Modulus (psi) at 77°F	342	550
Maximum Stress (psi) at 77°F	80	129
Strain at Maximum Stress (%) at 77°F	47	50
Maximum Stress (psi) at 165°F	53	79
Strain at Maximum Stress (%) at -65°F	35	47



from 342 to 550 psi. Stress was increased from 80 to 129 psi while strain was also increased from 47 to 50%. Normally, when modulus and stress are increased, strain is decreased. However, when the propellant cure is not complete or not optimum, it is fairly common to see an increase in both stress and strain as the cure more nearly approaches the optimum point. This type of effect was also observed at the other temperature extremes as the 165°F stress was increased from 53 to 79 psi and the strain at -65°F was increased from 35% to 47%. Mechanical properties of both five-gallon scale-up mixes were considered soft, however, because higher values were obtained reproducibly in one-gallon mixes.

As seen in Table IV-10, seven one-gallon mixes were made with the same binder cure system. The average stress for these mixes was 218 psi and strain was 29.9%. Obviously these mixes are significantly harder than the five-gallon mixes. Aging data also indicates harder propellant should be obtained at complete cure.

Historically, Thiokol has observed softer propellants when scaling from the one-gallon to the five-gallon mixer. Generally, this difference in mechanical properties has been attributed to a higher moisture content from the five-gallon mixer. The differences observed before have not been this severe. However, because these propellants are ambient cured, a small difference in moisture content, or any other slight changes in binder chemistry conceivably could cause a significant difference in mechanical properties. Complete cures and reproducible mechanical properties are one area that needs additional evaluation and development.

Although the first five-gallon scale-up mix was considered soft by Thiokol, a review of the Reference IV-2 propellant data indicated very comparable properties. Aerojet measured an ambient stress of 86 psi (uncorrected) on their five-gallon mix (Table IV-11). Comparable value from Thiokol was 80 psi. The other physical properties were of similar nature. It should be reiterated, however, that Thiokol does not consider this propellant completely cured. Furthermore, these two propellants should be different as Thiokol only uses 2% plasticizer whereas 3% was used in Reference IV-2 (Appendix D). However, review of "cured" and aging data indicates to Thiokol that the Aerojet propellant was not completely cured either (Table IV-12). The maximum stress as measured at 80°F increases from 98 psi to 147 psi after four months storage at 165°F. Under the same conditions, the modulus also increased from 490 to 783 psi. However, Thiokol does not consider this a true aging phenomenon but rather a post cure phenomenon. Results of the initial aging of Mix T-600 by Thiokol indicate similar trends demonstrated by Aerojet. A summary of the Thiokol aging data is presented in Table IV-5.

TABLE IV-10

PHYSICAL PROPERTIES IN ONE-GALLON MIXES

NCO/OH = 0.90

	<u>Modulus</u> <u>(psi)</u>	<u>Stress</u> <u>(psi)</u>	<u>Strain</u> <u>(%)</u>
	1356	225	36.8
	1644	221	23.5
	1764	226	24.6
	994	222	36.8
	1027	212	29.4
	1058	200	34.3
	<u>463</u>	<u>78</u>	<u>29.9</u>
$\bar{X}$	1108	218	29.9
$\sigma$	167	10	4.8

TABLE IV -11

COMPARISON OF THIOKOL AND AEROJET PHYSICAL PROPERTIES

<u>Thiokol</u>		<u>Aerojet</u> <sup>(a)</sup>
T-600	Mix Number	72-162
342	Modulus (psi) at 77°F	440
80	Max. Stress (psi) at 77°F	86
47	Strain at Max. Stress (%) at 77°F	35.0
53	Max. Stress (psi) at 165°F	52 <sup>(b)</sup>
35	Strain at Max. Stress (%) at -65°F	37 <sup>(b)</sup>

a. Reference IV-2

b. From 100-gallon mix

TABLE IV - 12  
SUMMARY OF AEROJET AGING DATA<sup>(a)</sup>  
(Mix 72-215 Cured at 80°F)

<u>Storage Time</u> <u>(months)</u>	<u>Modulus</u> <u>(psi)</u>	<u>Stress</u> <u>(psi)</u>	<u>Strain</u> <u>(%)</u>
<u>Stored at 165°F</u>			
0	490	98	35
0.5	578	115	36
1.0	671	127	42
2.0	677	128	35
3.0	794	144	35
4.0	783	147	35
<u>Stored at 80°F</u>			
0	490	98	35
2.0	532	103	30
4.0	521	108	32
6.0	541	112	31

a. Appendix G, page 243, Reference IV-2

One propellant slab was tested after 54 days storage at ambient conditions. At 77°F, modulus was 827 psi, stress was 147 psi and strain was 40% (Table IV-7). By comparison with zero time data, it is seen that the modulus and stress increased, and strain decreased slightly, which indicates that post cure was still occurring. However, it is believed that if these mechanical property values were obtained initially then post cure phenomena would be eliminated. As observed previously, high modulus and stress were obtained in one-gallon mixes and it was believed that they could be obtained in the five-gallon mixer by implementing alternate processing and curing conditions.

Tensile tests were performed with specimens from Mix T-607 at several temperature and strain rates to establish a failure boundary (Reference IV-3) for TP-H8245 propellant (Figure IV-7). These data represent "zero time" characteristics because they were obtained shortly after completion of cure.

#### Ballistic Properties

Only strand samples were loaded from Mix T-607 to measure the burn rate. It was intended to use the remainder of the propellant for two TX-631 motors and a limited amount of physical property measurements. The data measurements are shown in Table IV-13 and Figure IV-8. The strand rate is defined by

$$r = 0.01521 P^{0.480} \quad (\text{T-607 Strands at } 70^{\circ}\text{F})$$

which shows a rate of 1000 psia of 0.418 in/sec. Standard deviation of ln rate at a given pressure is 0.0111 (coefficient of variation of approximately 1.1%).

#### Summary

In summary, the properties of the second five gallon mix (T-607) of the ambient cured propellant (TP-H8245) were in line with the average properties calculated from the fairly large propellant data base. Although the TX-631 motor castings were unsuccessful, the propellant rheology was exactly as predicted. The casting difficulties were caused by inadequate casting tooling.

#### Aerojet Formulation

A one-gallon mix (15Q-403) was made to provide propellant for rheology testing of the Aerojet-developed ambient cure propellant.<sup>1</sup> This rheology data was desired as Aerojet had successfully scaled-up their formulation to a 300-gallon mixer and vacuum cast large-scale Sparrow motors,

---

1. Given the Thiokol designation DTS-7980 for internal records

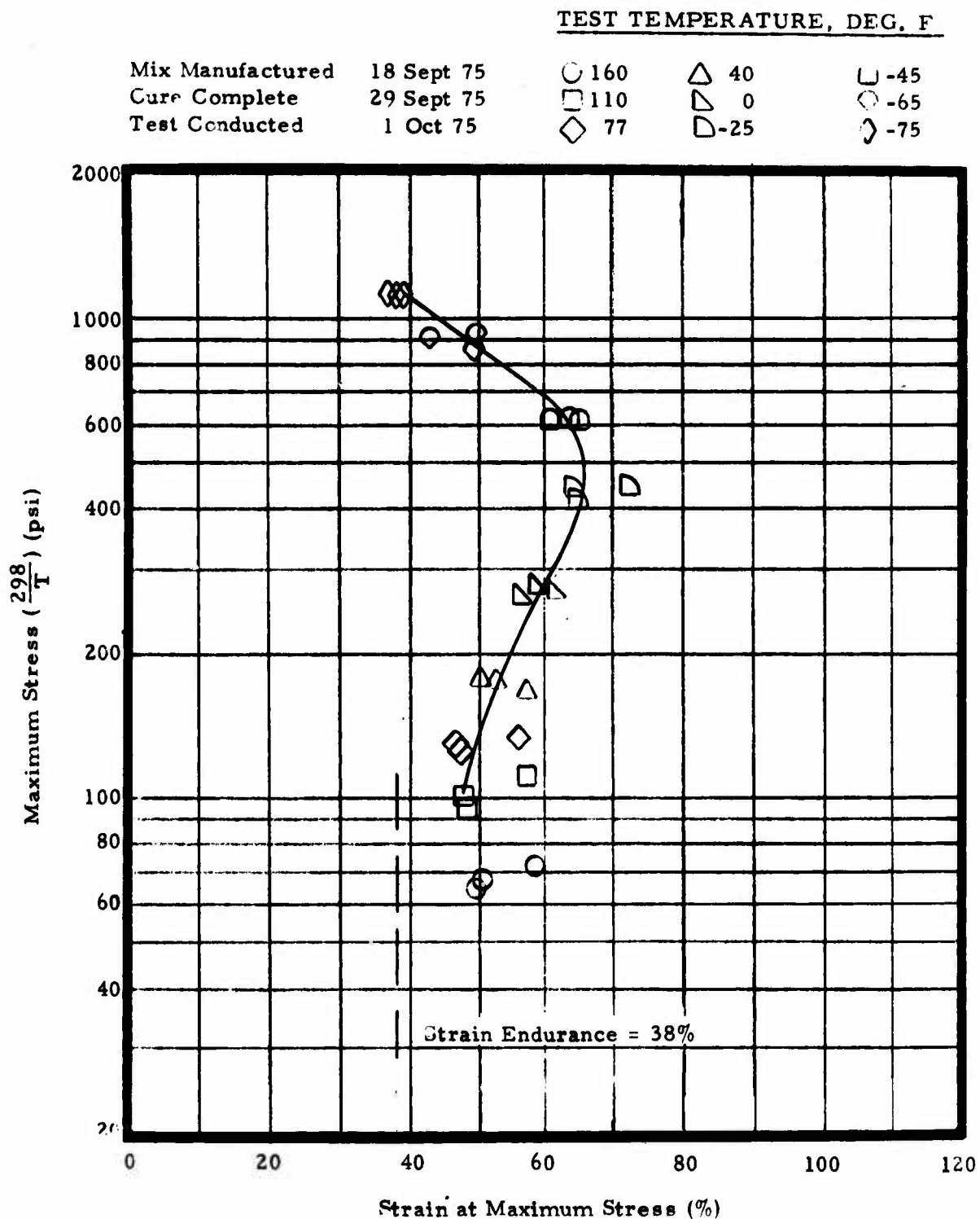


Figure IV-7. Failure Boundary of TP-H8245 Propellant, Mix T-607

TABLE IV-13

STRAND BURN RATE MEASUREMENTS

(Mix T-607, 70°F)

Nitrogen Pressurization, 2-inch Length

<u>Average Pressure (psia)</u>	<u>Rate (in./sec.)</u>
200	0.192
400	0.275
600	0.325
800	0.372
1000	0.410
1200	0.459
1400	0.493
1600	0.525
1800	0.557
2000	0.585
2200	0.606



MIX T-607  
Nitrogen Strand  
70°F, 2-inch Length

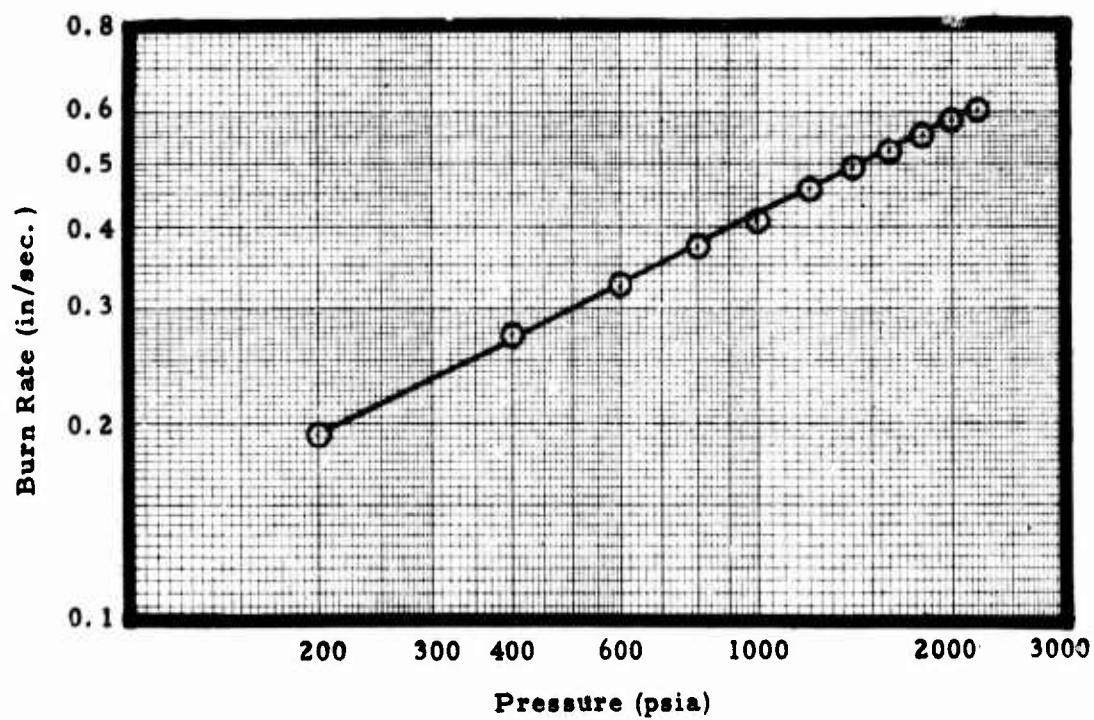


Figure IV-8. Strand Burn Rate, Mix T-607

but did not report sufficient rheology data to determine the propellant yield value. Although the propellant had the same polymer and total solids content, it included 3% plasticizer and 0.1% bonding agent (Table IV-4). End-of-mix viscosity was 14 kilopoise and yield was 300 dynes/cm<sup>2</sup> (Figure IV-9). TP-H8245 has end-of-mix viscosity of 21 kilopoise and yield of 100 dynes/cm<sup>2</sup>. Plasticizer level was considered the major formulation difference and the improved rheology was attributed to this parameter. Plasticizer content of the Thiokol formulation was increased from 2 to 3%, and this evaluation will be discussed in the next section.

High modulus and stress of Mix 15Q-403 was obtained at a 0.9 NCO/OH ratio. Modulus at 77°F was 1250 psi, stress was 158 psi and strain was 42% after eight days cure at 80°F. Stress at 165°F was 113 psi and -65°F strain was 53%. Better mechanical properties were obtained at all temperatures because more complete cure was obtained. Reference IV-2 reported routine measurements of 400 psi modulus and 90 psi stress. However, the aging data demonstrated that this propellant post cured during storage, at either 165°F or ambient, to about 800 psi modulus and 150 psi stress. Aerojet stated their propellant was completely cured because the same mechanical properties were obtained after curing at either ambient or 135°F. However, their aging data demonstrate that complete cure was not obtained and tensile properties appear to be approaching limiting values.

#### Mix T-630 (DTS-7984)

Based on the evaluation of the Reference IV-2 propellant, it appeared that the rheology properties of TP-H8245 could be improved by increasing the plasticizer content. Consequently, a one-gallon mix (15Q-422) was made with 3% IDP, which replaced the 2% DOA and 1% binder.<sup>1</sup> The end-of-mix viscosity was 12 kilopoise at 83°F (Table IV-15) and the yield was 300 dynes/cm<sup>2</sup> (Figure IV-10). The increase in plasticizer content also increased the pot life to 21 hours. Subsequently, a five-gallon mix of DTS-7984 (T-630) was manufactured to evaluate the pour-cast technique (Table IV-15). End-of-mix viscosity was 12 Kp and the yield value without cure agent was approximately 200 dynes per cm<sup>2</sup> at 80°F (Figure IV-11). One hour after cure agent addition the yield value at 80°F was 600 dynes/cm<sup>2</sup> (Figure IV-12). Time to 40 Kp was 17.5 hours and the required cure time was less than 10 days. Effective casting life at 77°F is shown in Figure IV-13.

#### Processing

Mix T-630 was processed differently in an effort to reduce the apparent moisture effect on mechanical properties. Previous five-gallon mixes were significantly softer than comparable one-gallon mixes. A review of both mixers and procedures revealed that propellant in one-gallon mixers was

---

1. The new formulation was designated DTS-7984.

TABLE IV-14

AEROJET FORMULATION MANUFACTURED AT THIOKOL  
(DTS-7980)

Mix Numbers	<u>72-215<sup>(a)</sup></u>	<u>15Q-403</u>
EOM Viscosity, kp/°F	13/?	14/84
Pot Life, hrs. to 40 kp	7	5
Yield, dynes/cm <sup>2</sup>	Not Reported	300
NCO/OH	0.91	0.90
<u>Physical Properties</u>		
Required Cure Time, Days at 80°F	8	(Aged 4 mo. @ 165°F) 8
<u>77°F</u> Modulus, psi	490	783
Stress, psi	98	147
Strain, %	35.0	35
<u>165°F</u> Stress, psi	66	---
Strain, psi	33.0	---
<u>-65°F</u> Strain, %	17	---

a. Mix reported in Reference IV-2

DTS-7980 (15Q403) W/O C.A. L.C.M.D.  
 No C.A. in Test Sample  
 Sample held at R. T. 16 hrs. before testing

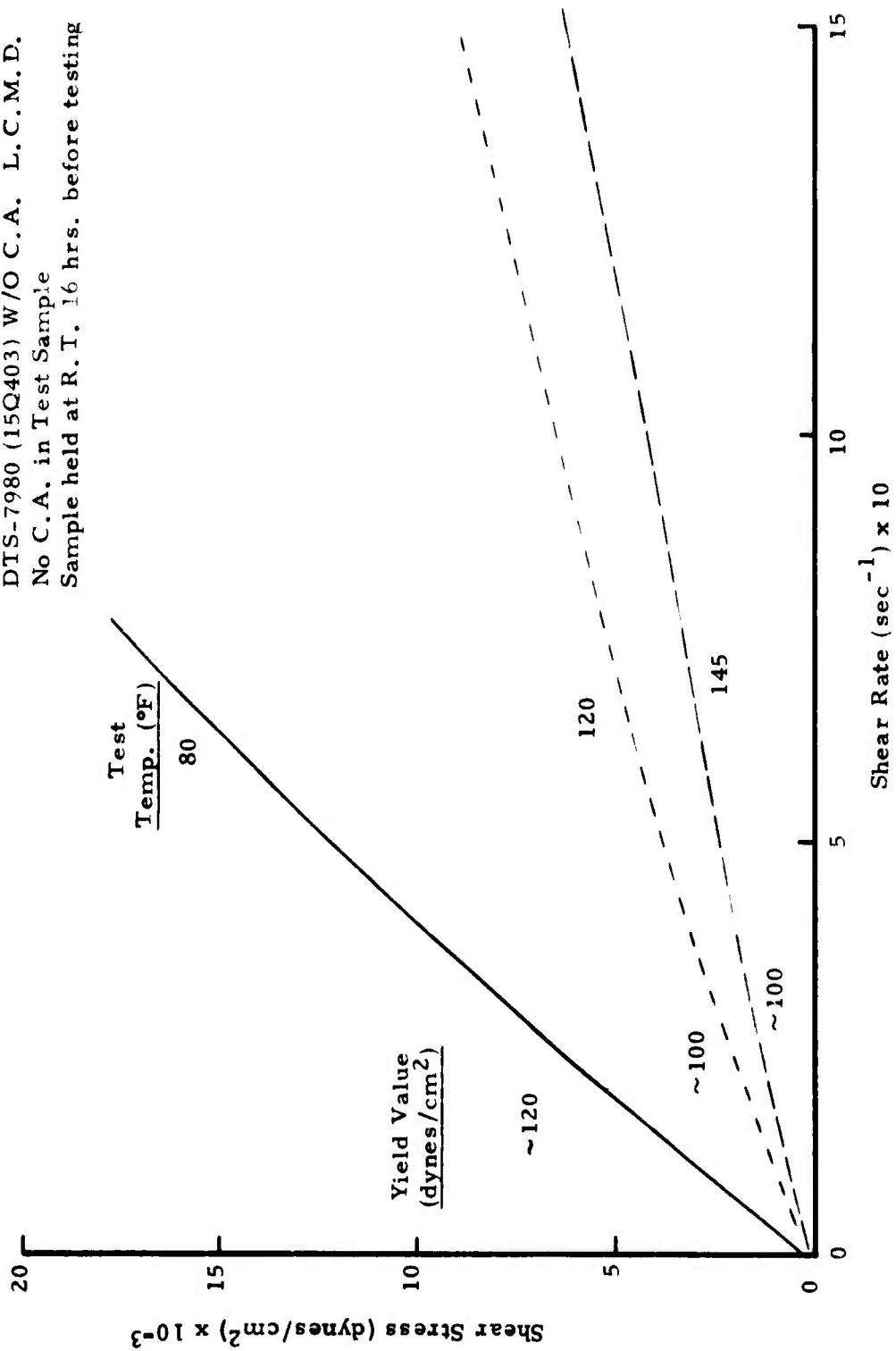


Figure IV-9. Shear Stress Versus Shear Rate of DTS-7980 (15Q-403)

TABLE IV-15  
TP-H8245 RHEOLOGY IMPROVEMENTS

Mix Numbers	<u>DTS-7984</u>		<u>TP-H8245</u>
	<u>15Q-422</u>	<u>T-630</u>	<u>T-607</u>
EOM Viscosity, kp/°F	12/83	12/90	20/91
Time to 40 kp, hrs.	21	18	9.5
Yield, dynes/cm <sup>2</sup>	300	100	---
NCO/OH	0.90	0.975	0.93

DTS-7984 (15Q422 w/o C.A.) L. C.M. D.  
 Tested Before C.A. addition  
 Test Temperature: 80°F (27°C)  
 Sample held at R.T. ~ 16 hrs. before testing  
 Yield Value: ~ 300 dynes . cm

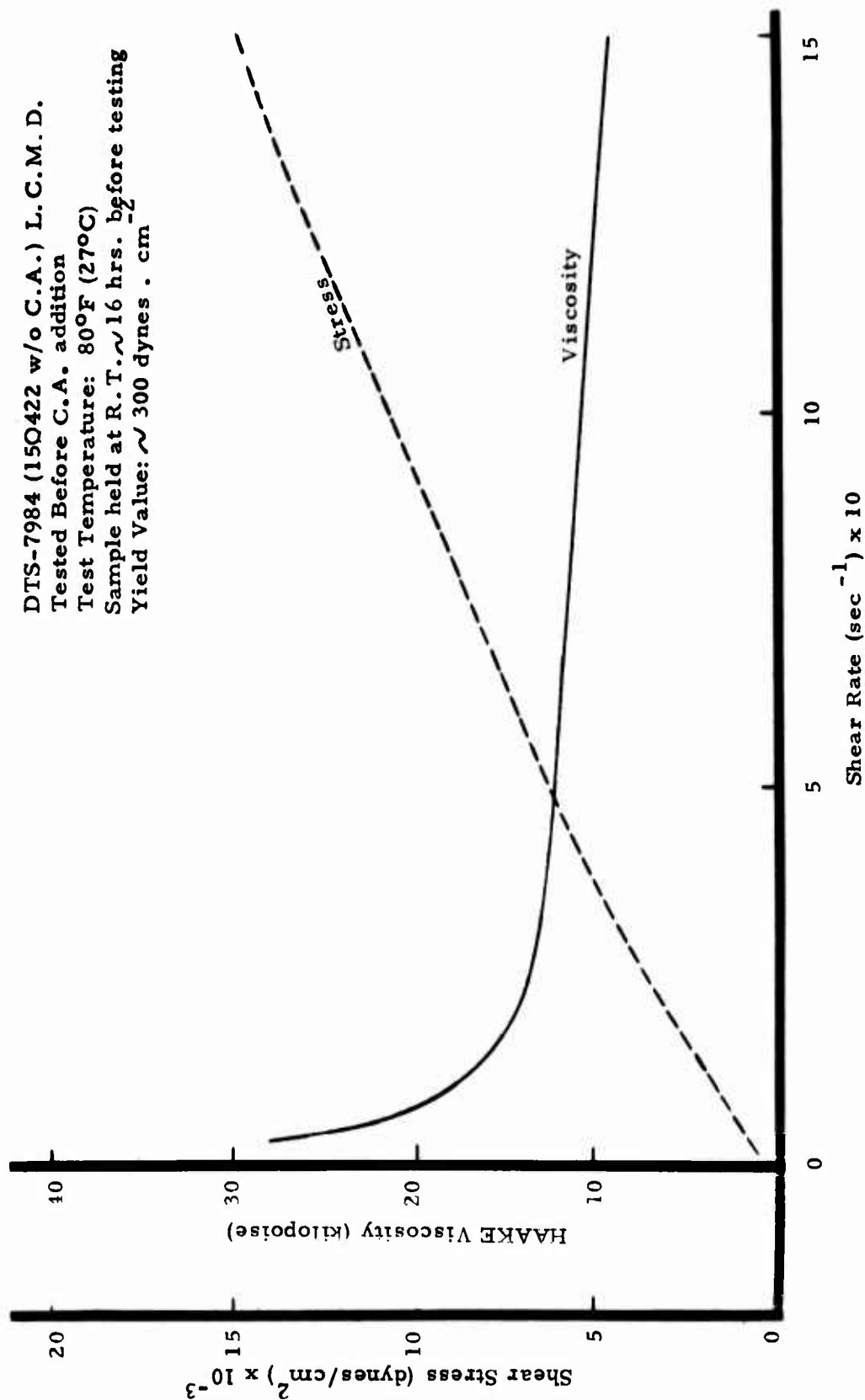


Figure IV-10. Shear Stress and Viscosity Versus Shear Rate of DTS-7984 (15Q-422) Without Curing Agent

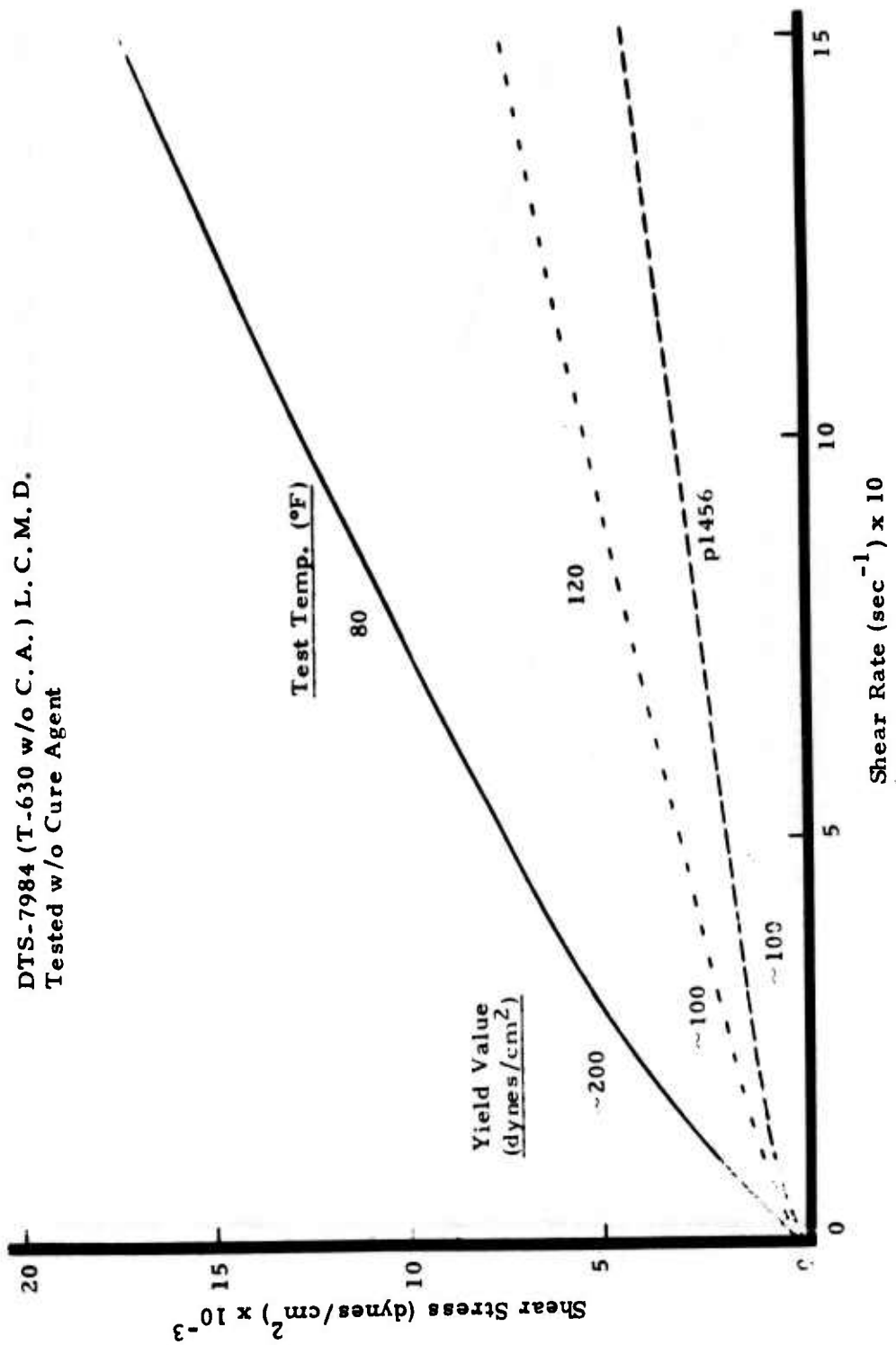


Figure IV-11. Shear Stress Versus Shear Rate of DTS-7984 (T-630) Without Curing Agent



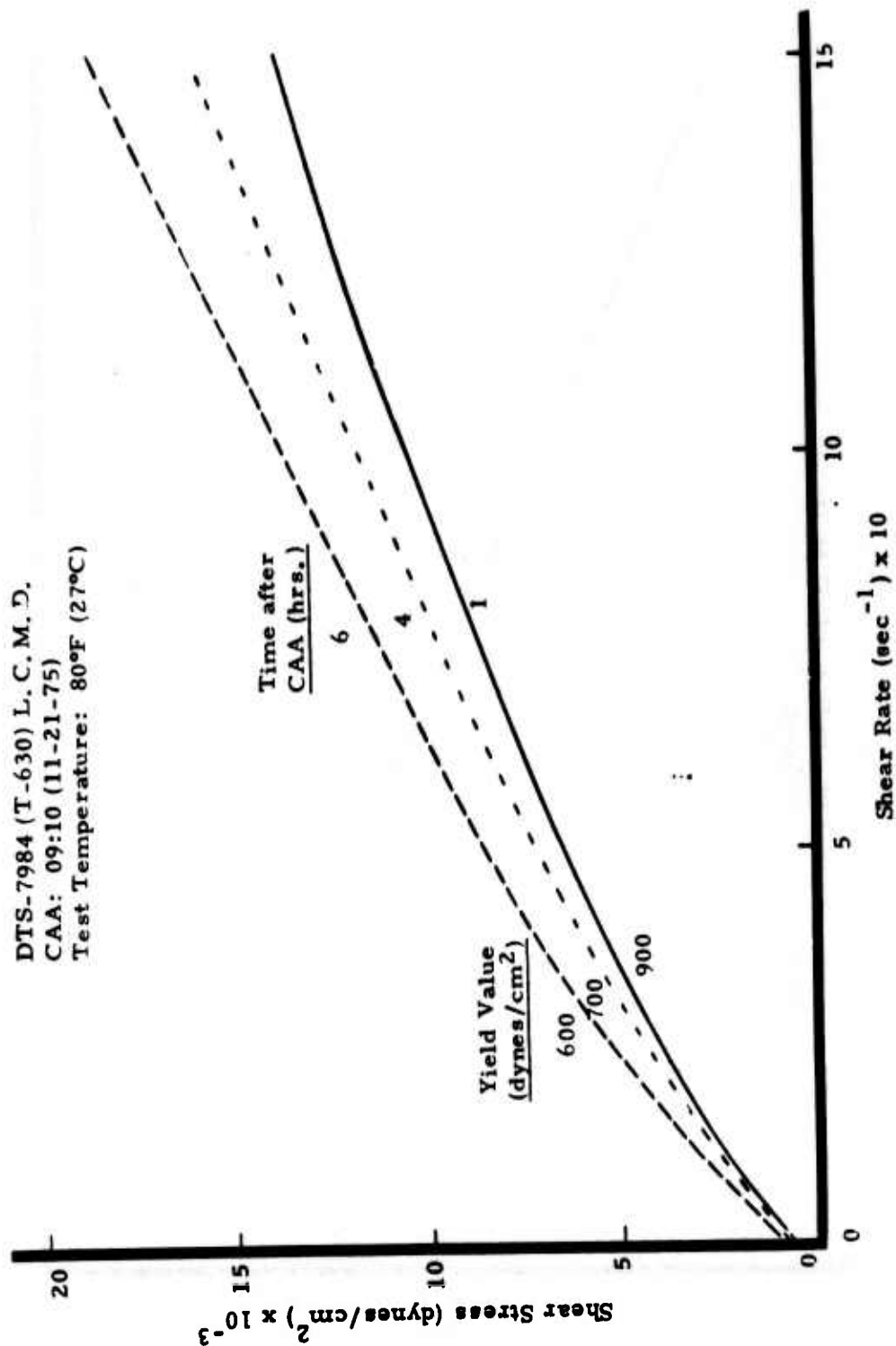


Figure IV-12. Shear Stress Versus Shear Rate of DTS-7984 (T-630) with Curing Agent

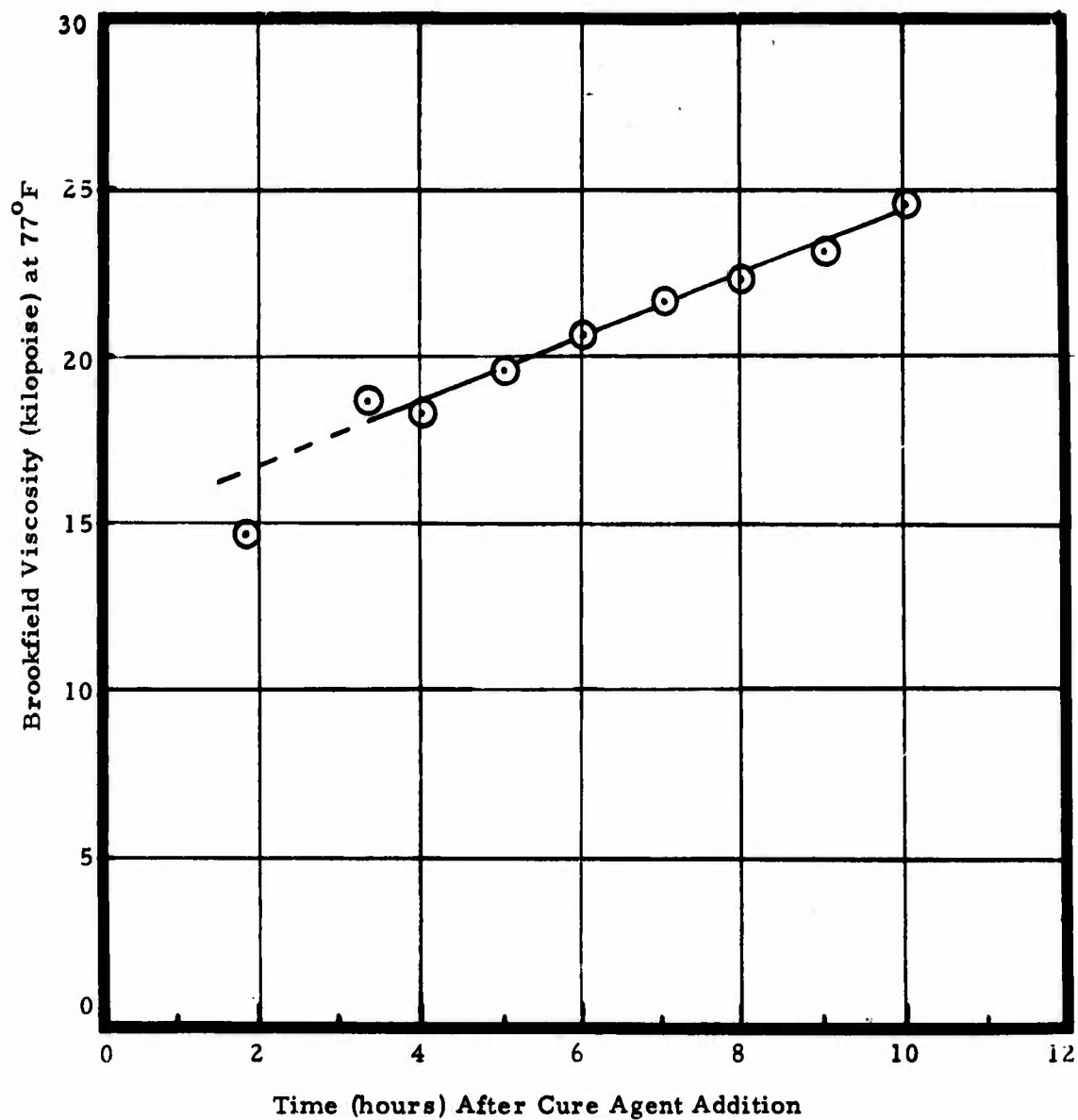


Figure IV-13. Effective Casting Life, Mix T-630, DTS-7984 Propellant.

deaerated at full vacuum and 145° F. It is believed that this small exposure to high temperature vacuum removed sufficient water to make the difference; therefore Mix T-630 was vacuum mixed at 145° F during solids addition. Prior to curing agent addition, the temperature was reduced to approximately 80° F.

1. Add and blend R45M polymer, IDP plasticizer, and HX-752 bonding agent.
2. Add and blend oxidizer fractions, using hot water to raise temperature to 133° F.
3. Mix for 60 minutes at 10-12 mm of Hg. absolute pressure, maintaining mix temperature at 135° F.
4. For scheduling convenience, the mix was stored overnight (16.9 hours). During this hold period, the mix cooled to 69° F.
5. After 5 minutes of reblending, the linoleic acid and ZnO catalysts were added and blended for 20 minutes under full line vacuum (10-12 mm of Hg. absolute pressure).
6. Add HMDI curing agent and blend for 5 minutes at ambient pressure.
7. Mix for 25 minutes under full line vacuum, using cold water to hold propellant temperature down.

NCO/OH ratio for this initial scale-up was set at 0.975 as the one-gallon checkout mix (15Q422) was soft (Table IV-15) with an NCO/OH ratio of .90. End-of-cure modulus for Mix T-630 was 1564 psi, which indicated this ratio was slightly high. Maximum stress was 264 psi and strain at maximum stress was 25.1% (Table IV-16). Samples of this mix were also cured at 145° F for eleven days (Table IV-17). This cure time was excessive but was utilized to insure complete cure. Modulus was 1661 psi, stress was 287 psi and strain was 25.9%. These properties duplicated the best ambient cure mechanical properties and further confirmed that complete cure was achieved. As these were the best properties obtained from an ambient cure, there is justification for concluding that the 145° F vacuum mixing was instrumental to obtaining good cures. Tensile properties of a pour case sample were also measured and maximum stress was 234 psi. Mechanical properties of the pour cast sample were not quite as good as the pressure cast samples. The stress and strain were lower.

TABLE IV-16  
CHARACTERISTICS OF MIX T-630  
(DTS-7984)

EOM Viscosity, kp/90°F	12
Pot Life, hours at 80°F	17.5
Yield, dynes/cm <sup>2</sup> at 80°F (w/o C.A)	200
Required cure time, days	<10
Cure Temperature, °F	80
NCO/OH	975

Physical Properties

<u>165°F</u>	Modulus, psi	1174
	Stress, psi	175
	Strain, %	21.3
	Strain, Ult., %	22.1
<u>77°F</u>	Modulus, psi	1564
	Stress, psi	264
	Strain, %	25.1
	Strain, Ult., %	26.0
<u>-65°F</u>	Modulus, psi	10,413
	Stress, psi	680
	Strain, %	19.6
	Strain, Ult., %	26.2

TABLE IV -17

EFFECT OF CURE TEMPERATURE ON MIX T-630 PROPERTIES

Cast Method	<u>Pressure</u>		<u>Pour</u>
Cure Temperature, °F	<u>80</u>	<u>145</u>	<u>80</u>
Physical Properties at 77°F:			
Modulus, psi	1564	1661	1709
Stress, psi	264	287	234
Strain, %	25.1	25.0	18.7

### Post Cure Investigation

An ambient cured propellant has been developed which has acceptable processing, pot life and complete cure. The one remaining technical problem is post cure. Both Aerojet and Thiokol/Huntsville experienced extensive post cure during short term aging at ambient and elevated temperatures. This post cure was attributed to incomplete cure. A five-gallon mix (T-630) was made which appeared to be completely cured. Samples of this mix were stored at 80°F and 145°F and the results indicated improved storage capabilities (Table IV-18).

After storage of Mix T-630 for five weeks at 145°F, modulus was 2357 psi and stress was 304 psi. Strain at maximum stress was 20.3%. Based on these limited results that indicate identical hardening at 80°F and 145°F storage, it is concluded that the post cure problem has been eliminated. Both RPL and Thiokol predicted post cure would be significantly reduced if complete cures were obtained. During storage, stress increased 10% at ambient, and 15% at 145°F. For the first time, strain decreased after storage (19% at 145°F; 23% at ambient).

Because the T-630 samples stored at 80°F and 145°F hardened to the same degree, the phenomenon is no longer considered as further polymer-isocyanate reaction. It is believed that the probable cause of the current hardening is oxidation of the double-bond in the polymer back bone. This oxidation is believed to be promoted by the zinc, which is added as a cure catalyst and is essential to obtaining ambient cures. If the cause of post cure is metallic catalyzed oxidation, a possible solution is incorporation of a metal scavenger. The mixed antioxidant system, developed during the TALM program, has some scavenger characteristics. However, previous evaluations have indicated the mixed antioxidants slow propellant cure at ambient conditions. RPL indicated sulfur may serve as scavenger, but technical details are not available. For the current program, this level of hardening is acceptable and no additional effort is planned at this time.

### Comparison of Propellants

Results of a one-gallon mix of Aerojet-developed propellant were reported previously. Two basic Thiokol formulations have been processed: TP-H8245 with 2% plasticizer and DTS-7984 with 3% plasticizer. Table IV-19 compares the processing characteristics and physical properties of these four propellants. Note that there has been no tailoring of the physical properties of DTS-7984. A high NCO/OH ratio was selected for Mix T-630 (DTS-7984) to assure complete cure so that the pour casting evaluation could be performed.

TABLE IV-18

POST-CURE REDUCED BY OBTAINING COMPLETE CURES

(DTS-7984, Mix T630)

Storage (wks)	Physical Properties (77°F)		
	Modulus (psi)	Maximum Stress (psi)	Strain at Max Stress (%)
0 <sup>(a)</sup>	1564	264	25.1
5 at 145°F	2367	304	20.3
5 at 80°F	2522	291	19.2
			26.0
			20.8
			19.6

COMPARISON OF CURE CYCLE

Physical Properties (77°F)	Cure Temperature for 11 Days	
	80°F	145°F
Modulus (psi)	1564	1661
Maximum Stress (psi)	264	287
Strain at Max. Stress (%)	25.1	25.0

a. Cured at ambient; stored at 145°F and 80°F



TABLE IV-19

FURTHER COMPARISON OF AEROJET AND THIOKOL PROPELLANTS

	<u>Aerojet Propellant</u>		<u>Thiokol Propellant</u>	
	<u>72-215<sup>(a)</sup></u>	<u>15Q-403<sup>(b)</sup></u>	<u>TP-H8245<sup>(c)</sup></u>	<u>DTS-7984<sup>(d)</sup></u>
EOM Viscosity (kp/°F)	13/80	14/84	22/80	12/90
Pot Life (hrs. to 40 kp)	7	5	10	18
Yield (dynes/cm <sup>2</sup> ) at 80°F	(e)	200(f)	800(f)	200(f)
NCO/OH	0.91	0.90	0.90	0.975(g)
Required Cure Time (Days at 80°F)	8	8	9	11
<u>Physical Properties</u>				
165°F Stress (psi)	66	113	101	175
Strain (%)	33	31	27	21
77°F Stress (psi)	98	158	218	264
Strain (%)	35	42	31	25
Modulus (psi)	490	1250	1307	1564
-65°F Strain (%)	35(c)	53	25	20

a. Mix reported in Reference IV-2

b. Thiokol mix of same formulation as in Mix 72-215

c. Typical values

d. TP-H8245 modified to have 3% IDP instead of 2% DOA as plasticizer,  
Mix T-630

e. Not reported

f. Before cure agent addition

g. Not optimized for physical properties

THIS REPORT HAS BEEN DELIMITED  
AND CLEARED FOR PUBLIC RELEASE  
UNDER DOD DIRECTIVE 5200.20 AND  
NO RESTRICTIONS ARE IMPOSED UPON  
ITS USE AND DISCLOSURE.

DISTRIBUTION STATEMENT A

APPROVED FOR PUBLIC RELEASE;  
DISTRIBUTION UNLIMITED.

### Conclusions

1. Good mechanical properties (complete ambient cure) were obtained by vacuum mixing the propellant at 145° F.
2. Post cure was eliminated--apparently by achieving complete cures.
3. Ambient cured propellants may be subject to hardening via metallic catalyzed oxidation. Incorporation of metal scavenger may eliminate this oxidation but an evaluation is not planned at this time.

### Mix T-656 (DTS-7984)

A five-gallon propellant mix, T-656, was made (1/21/76) to provide propellant (DTS-7984) for liner/propellant bond tests. This mix was processed and cured at ambient (80° F) and the propellant results are summarized in Table IV-20. The mix processed easily and EOM viscosity was a reasonable 13.2 Kp at 82° F. (First scale-up mix, T-630, had an EOM viscosity of 12 Kp at 90° F.) One hour after cure agent addition the yield was 800 degrees/cm<sup>2</sup> (Figure IV-14). Cure was complete after eight days at 80° F as indicated by the high stress propellant. At 77° F, stress was 260 psi and strain was 22.6%. Stress at 165° F was 173 psi and strain at -65° F was 18.7%. Considering that the NCO/OH ratio was reduced from 0.975 to 0.95, stress was slightly high and strain was slightly low.

This mix was processed using the 145° F vacuum mix cycle implemented for Mix T-630 to minimize the effect of water on propellant. However, the vacuum mix time was reduced from 50 to 30 minutes and mix temperature was adjusted from 145 to 80° F in the same day. Previously, temperature was reduced during overnight shutdown. The slightly lower strains may indicate 30 minutes vacuum mixing was not quite as efficient. For future mixes, a longer vacuum mix cycle (60 minutes) is recommended. Also, NCO/OH ratio should be further reduced to approximately 0.90.

### Mix T-684 (DTS-7984)

A 65-pound mix of DTS-7984 propellant was manufactured to load the two final TX-631 motors for component evaluation and cast tensile property and bond samples. An NCO/OH ratio of 0.925/1.0 and a 59.2/40.8 ratio of unground/high speed ground oxidizer fractions were selected to achieve the desired properties. The following mix cycle (patterned after Mixes T-630 and T-656) was used:

1. Add and blend R45M polymer, IDP plasticizer, and HX-752 bonding agent.

TABLE IV-20

PROPERTIES OF PROPELLANT FOR BOND EVALUATION

Mix Number	T-656
Propellant Type	DTS-7984
EOM Viscosity, Kp/°F	13.2/82
Yield, dynes/cm <sup>2</sup>	800
Pot Life, hrs. to 40 Kp	18
Required Cure Time, days	8
NCO/OH	0.95

Physical Properties(a):

<u>165°F</u>	Modulus, psi	1231
	Stress, psi	173
	Strain, %	22.0
<u>77°F</u>	Modulus, psi	1885
	Stress, psi	260
	Strain, %	22.6
<u>-65°F</u>	Modulus, psi	9,721
	Stress, psi	667
	Strain, %	18.7

---

a. Tests conducted 20 days after cure agent addition.

DTS-7984 (T-656) L. C. M. D.  
 CAA: 10:15 (1-21-76)  
 Test Conducted: 1 hour after CAA  
 Test Temperature: 80°F (27°C)  
 Yield Value: 800 dynes . cm

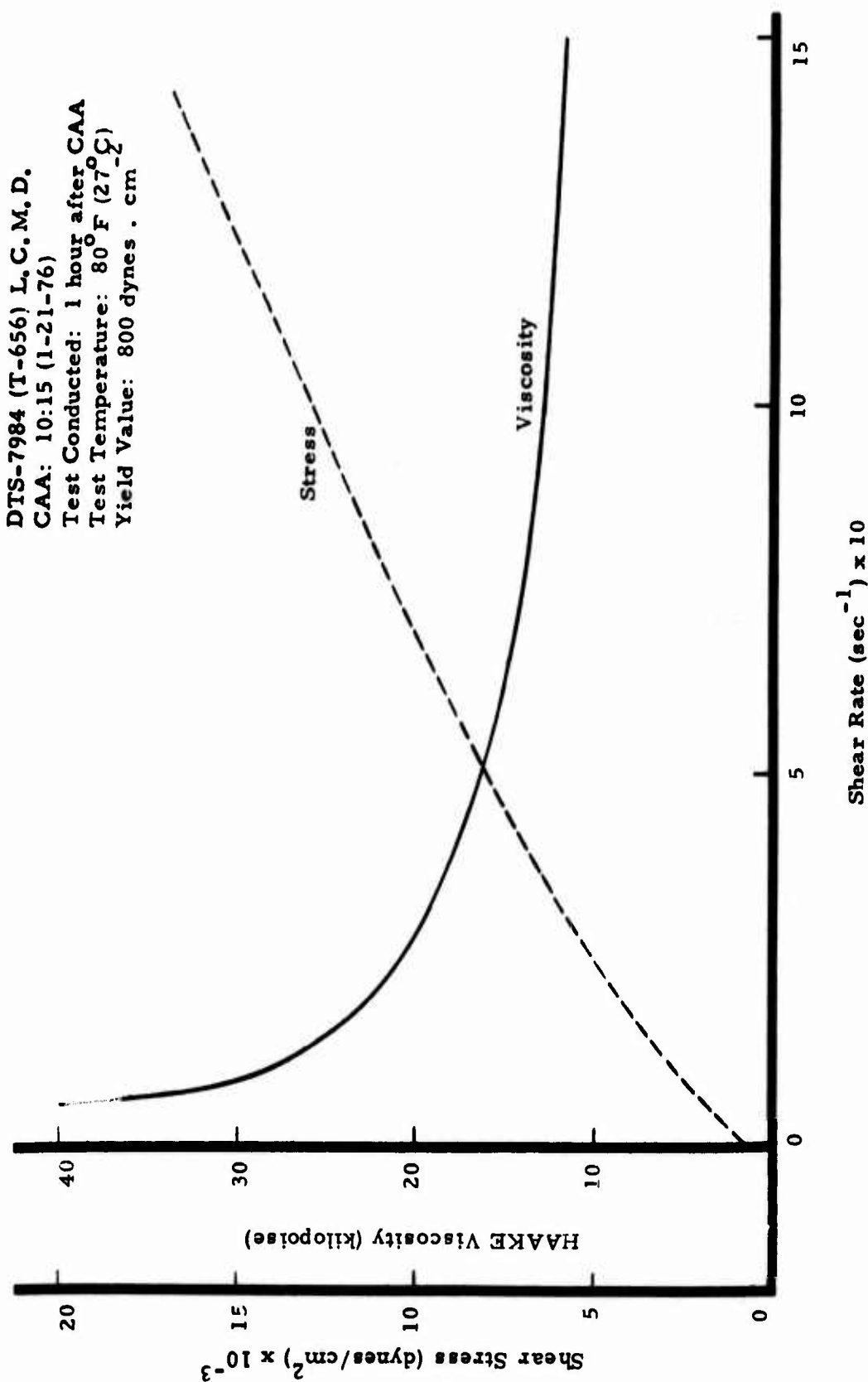


Figure IV-14. Shear Stress and Viscosity Versus Shear Rate of DTS-7984 (T-656)

2. Add and blend oxidizer fractions, using hot water to raise temperature to 145° F.
3. Mix for 30 minutes at 10-12 mm of Hg absolute pressure, maintaining mix temperature @145° F.
4. Mix for 40 minutes at ambient pressure using cold water to cool mix to 100° F.
5. The mix was stored overnight (16.5 hours) and, during this hold period, cooled further to 85° F.
6. Mix for 45 minutes, using cold water, to a temperature of 80° F.
7. Add and blend the linoleic acid and ZnO catalyst into the mix.
8. Add HMDI curing agent and blend.
9. Mix for 25 minutes at 10-12 mm of Hg. absolute pressure, using cold water to hold propellant temperature down.

The mixed propellant had an end-of-mix viscosity of 10.8 kilopoise @85° F. The effective casting life curve @77° F is shown on Figure IV-15. Physical properties are in Table IV-21.

The mixed propellant was vacuum cast into the TX-631 motors. Motor T-684-1 was cast first with no problems. Motor T-684-2 cast smoothly until the aft end of the motor was reached. Then the streams of propellant began to catch on the protruding ledge of mastic insulation and bridge to the core. This condition in Motor T-684-2 required that the casting chamber be repressurized and evacuated to complete the casting.

#### Reproducibility and Control of Ambient Temperature Cure Propellants

Four mixes (three five-gallon and one one-gallon) of DTS-7984 propellant have been ambient temperature processed and cured. NCO/OH ratio of 0.9, 0.925, 0.95 and 0.975 were used for these four mixes to further define response of mechanical properties to cure stoichiometry (Table IV-22). Although the mechanical properties varied as expected with cure levels, a plot of stress and strain versus modulus indicated both properties responded much as would be predicted (Figure IV-16). These predictable properties further indicate that propellant cure is reasonably reproducible. Furthermore, it finally appears that ambient curing of propellant is understood and controllable.

The key to ambient cure now appears to be the water content of the propellant slurry. (Reacting at lower temperatures, ambient, apparently



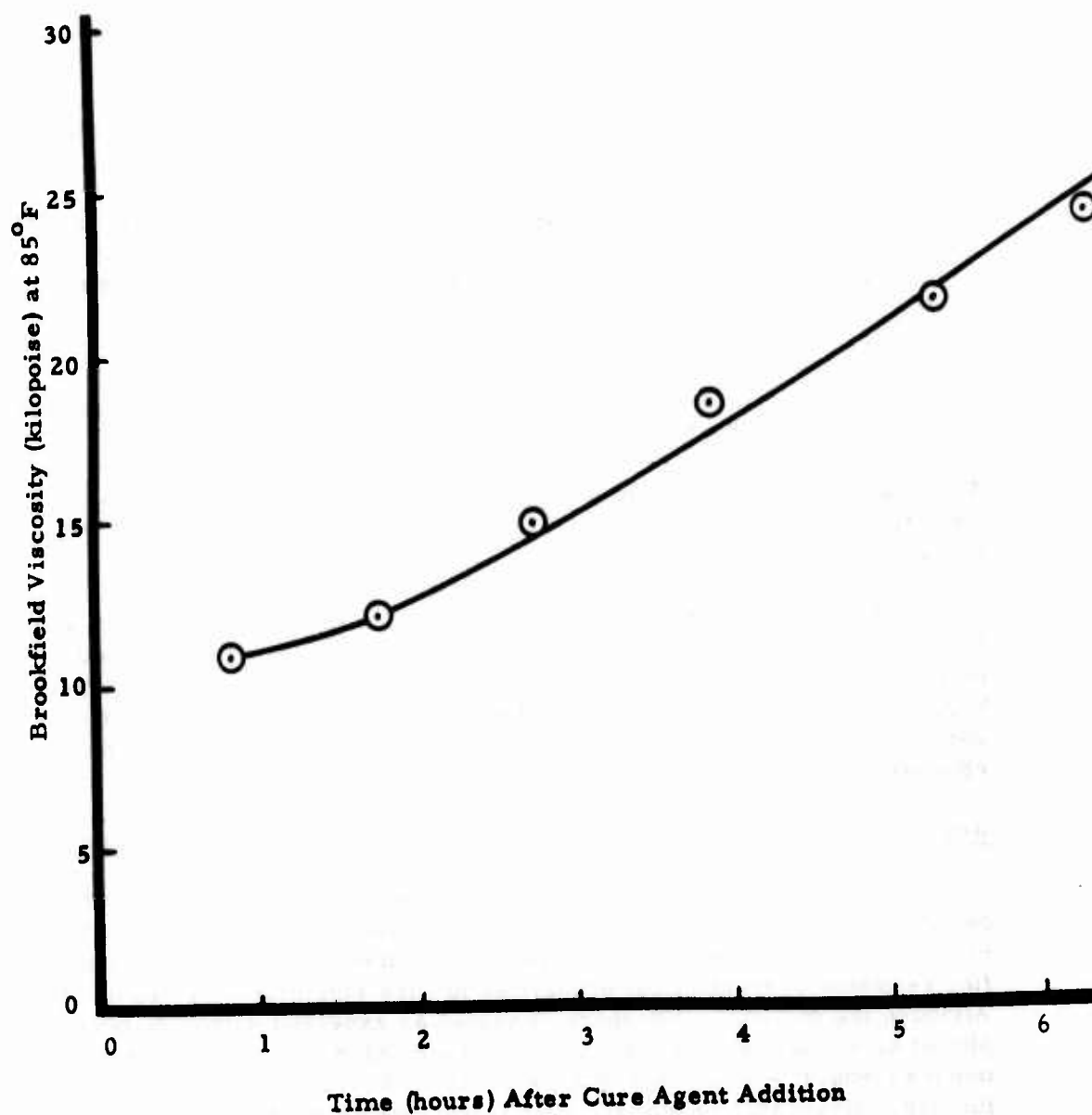


Figure IV-15. Effective Casting Life , Mix T-684, DTS-7984 Propellant.

TABLE IV-21  
DTS-7984 PROPELLANT PHYSICAL PROPERTIES<sup>(a)</sup>  
(Mix T-684)

Modulus (psi) at	
165°F	299
77°F	618
-65°F	9819
Maximum Stress (psi) at	
165°F	89
77°F	140
-65°F	577
Strain at Max. Stress (%) at	
165°F	40.7
77°F	36.6
-65°F	36.1
Strain at Cracking (%) at	
165°F	42.3
77°F	38.0
-65°F	40.9

a. "Cure" time of 19 days at 80°F



**TABLE IV-22**  
**SUMMARY OF DTS-7984 PROPELLANT RESULTS**  
**(Cured at 80°F)**

	Mix Number		
	T-630	T-656	T-684
Mix Size, lb	60	40	65
Vacuum Mix Time <sup>(a)</sup>			
@ Amb, min	45	25	25
@ 145, min	60	50	50
Overnight Soak	Yes	No.	Yes
EOM Viscosity, k <sub>p</sub>	12.0	13.2	10.8
NCO/OH	0.975	0.950	0.925
165°F Stress, psi	175	173	89
Strain, %	21.3	22.0	40.7
77°F Modulus, psi	1564	1885	618
Stress, psi	264	260	140
Strain, %	25.1	22.6	36.6
-65°F Strain, %	19.6	18.7	36.1
			15Q-422
			10
			150
			---
			No
			12
			0.900
			46
			56.2
			354
			101
			48.9
			26.0

a. Total elapsed time that binder was exposed to vacuum conditions

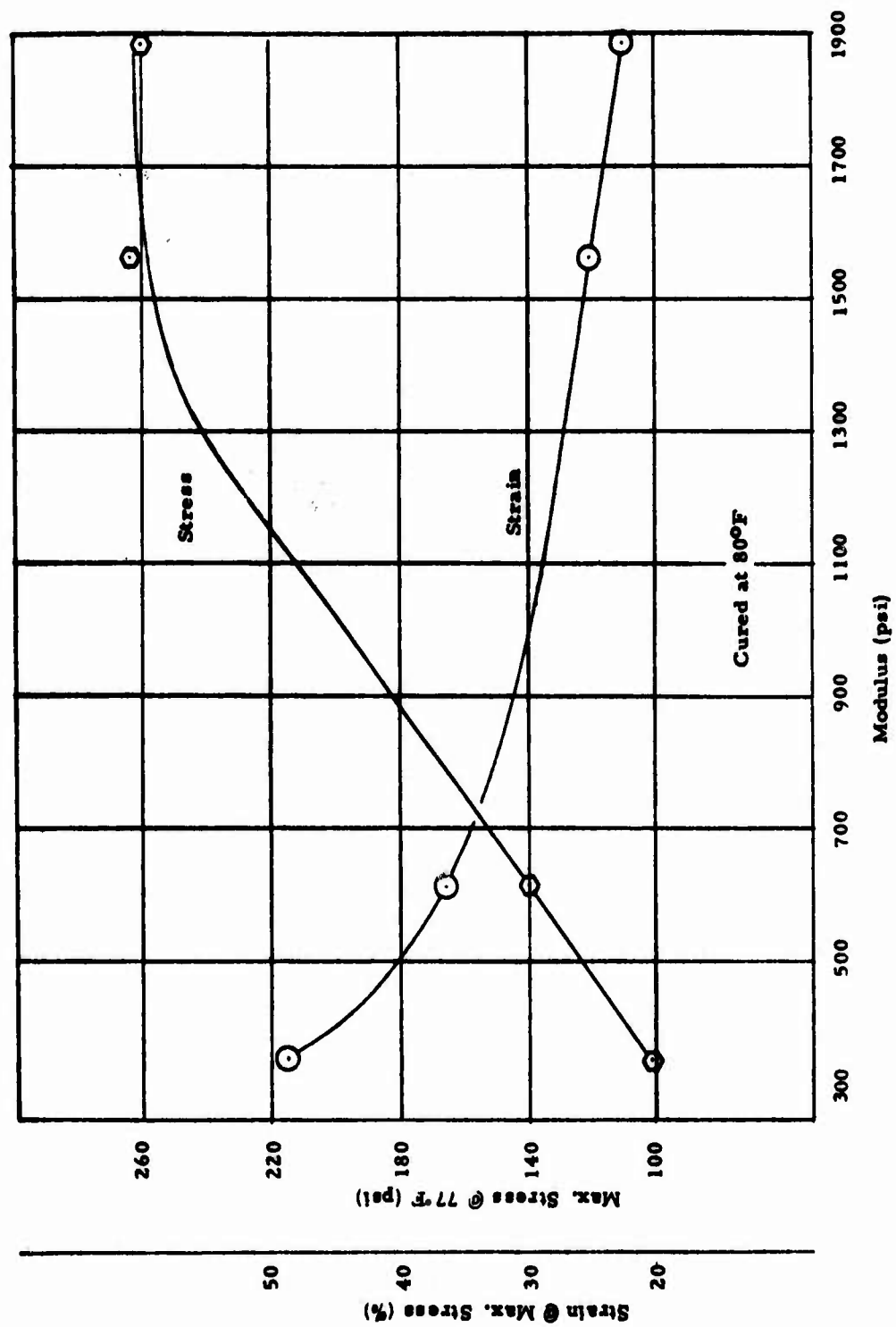


Figure IV-16. Stress and Strain of DTS-7984 as a Function of Modulus at 77°F

significantly increase the adverse effect of water contamination.) The water content can be effectively and practically controlled by efficient vacuum mixing. There appears to be a correlation between vacuum mixing efficiency and mixer load (Figure IV-17). The smaller the mix size within a mixer, the better vacuum mixing, and the higher the mechanical properties. Inherent in mix size are mixing parameters like vacuum level and mixing time. Mixing temperature is also important but the one-gallon mix indicated 145° F mixing is not necessary if mix time is sufficiently long. For practical purposes, 145° F mixing is still recommended.

#### Processing Aids

During this report period, a pint mix was made to evaluate polydimethyl siloxane. The objective of this mix was to improve the rheology characteristics of TP-H8245 propellant via a known processing additive. As seen in Table IV-23, 0.05% polydimethyl siloxane reduced the propellant yield from 1000 to 300 dynes/cm<sup>2</sup>. However, the end-of-mix viscosity was not reduced. The siloxane appeared to reduce the mechanical properties. Maximum stress was unchanged, but the strain was approximately half. This approach does not appear as attractive as increased plasticizer because high strain will be required for the tactical application.

#### Process Hot/Ambient Cure

Another means to utilize the beneficial effect of processing at 145°F is the "trigger cure". "Trigger cure" is distinguished from "quick cure" in that the binder ingredients are changed to achieve cure at ambient conditions after processing at 145°F. An antioxidant and higher concentrations of catalysts were used. (See Appendix D for the complete formulation.)

A one-pint mix (BP-1428) was processed at 145° F and EOM viscosity of 4 Kp was obtained (Table IV-24). Samples of this mix were then placed at 80°, 125° and 145° F and time to 40 Kp was measured. At 145° F, pot life of five hours was measured. When the temperature was reduced to 125° F, pot life increased to 8.5 hours. When the temperature was further reduced to 80° F, pot life was reduced to 5.5 hours. As the temperature is decreased, the viscosity of the R45M polymer and, consequently, viscosity of propellant with this polymer increases significantly as the temperature is reduced beyond about 90° F. The polymer/curing agent reaction rate is also reduced by the reduction in temperature, so there is an optimum where minimum viscosity and maximum pot life are obtained. For these combinations of ingredients, the optimum appears to be about 113° F (Figure IV-18).

As measured by penetrometer, complete cure was obtained between eight and nine days at 80° F. Modulus at 77° F was 1521 psi, stress was 208 psi and strain was 27.6%. As discussed elsewhere (Table IV-23), complete cure for TP-H8245 propellant was at a stress of 218 psi and strain of 29.9%.

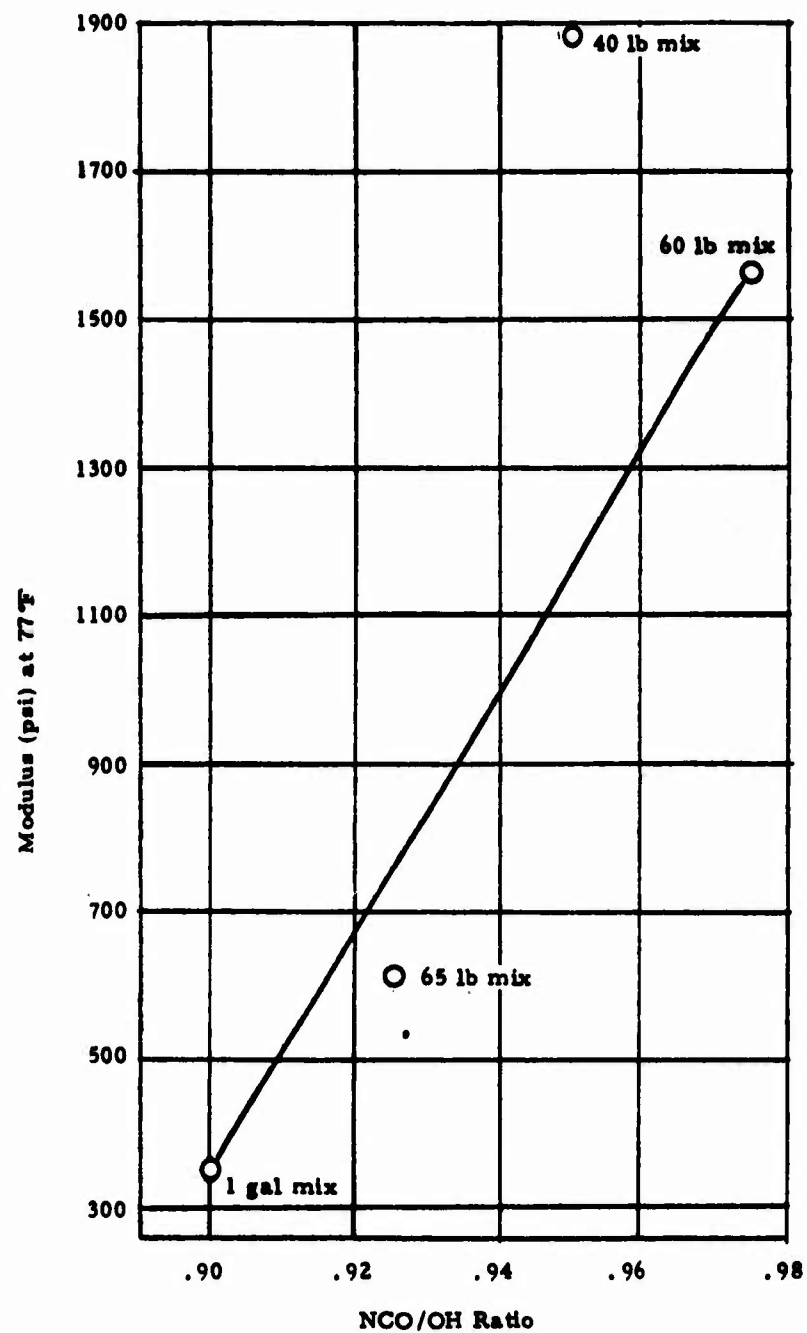


Figure IV-17. Effect of NCO/OH on Modulus of DTS-7984 Propellant

TABLE IV-23

PROCESSING AIDS TO IMPROVE TP-H8245 PROPELLANT RHEOLOGY

	<u>Control</u>	<u>0.05% PDMS<sup>(a)</sup></u>
Mix Number	Average	BP-1429
EOM Viscosity, kp	21	28
Yield, Dynes/cm <sup>2</sup>	1000	300
Cure Time, Days at ambient temperature	9	9
77°F Physical Properties		
NCO/OH	0.9	0.9
Modulus, psi	1108	2344
Stress, psi	218	226
Strain, %	29.9	18.4

---

a. Polydimethyl Siloxane

TABLE IV-24  
ALTERNATE CURE SYSTEM  
PROCESSED HOT, CURED AMBIENT

Mix No.	BP-1428
Process Temperature, °F	145
EOM Viscosity, kp	4
Pot Life, at 80°F, hrs.	5.5
at 125°F, hrs.	8.5
at 145°F, hrs.	5.0
NCO/OH	0.9
Cure Temperature, °F	80
Penetrometer, mm (10 <sup>1</sup> )	
at 8 days	42
at 9 days	25
at 10 days	30
77°F Physical Properties at 14 days	
Modulus, psi	1521
Stress, psi	208
Strain, %	27.6

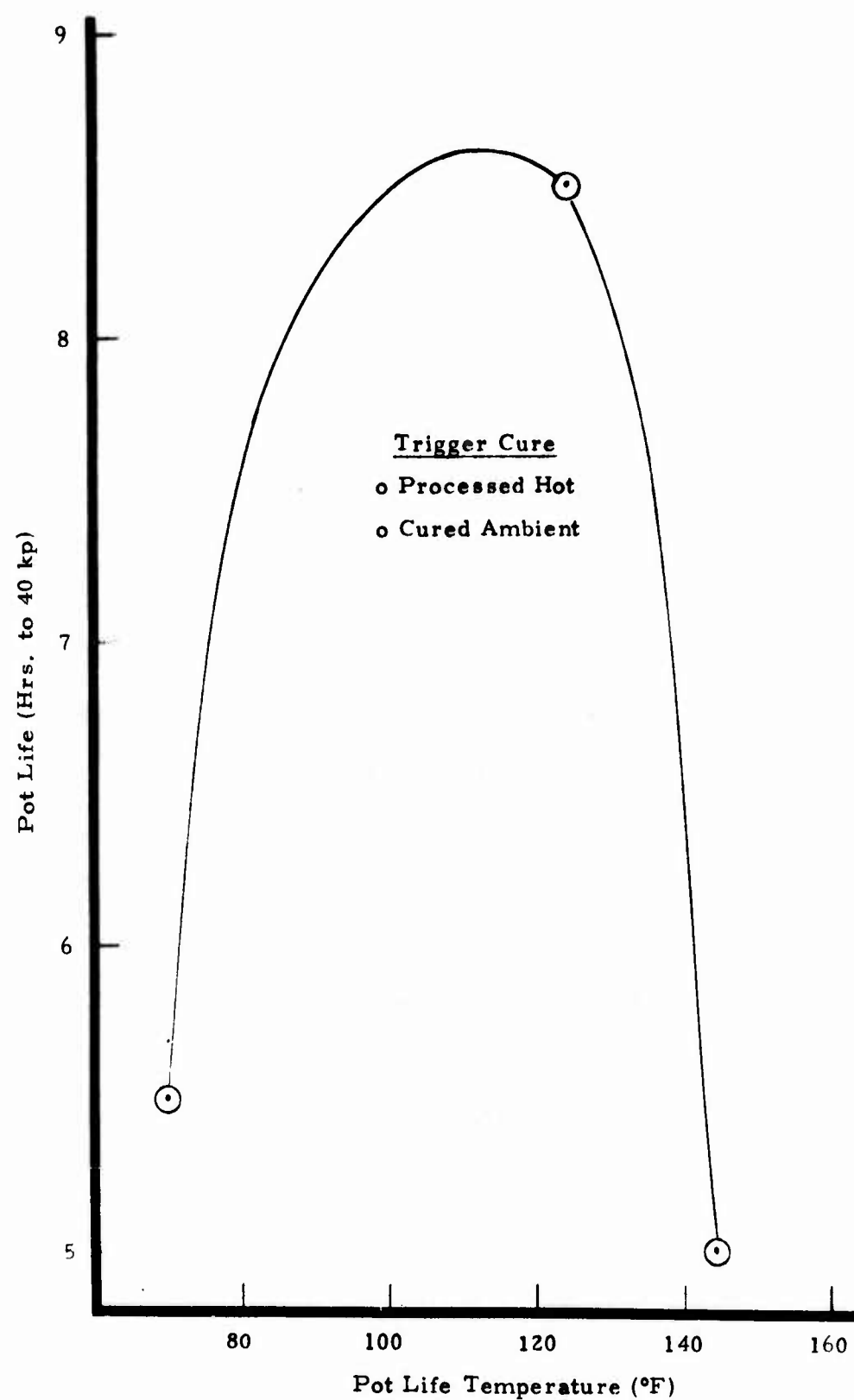


Figure IV-18. Effect of Temperature on Pot Life, Mix BP-1428

## CONCLUSIONS

Propellant studies produced the following accomplishments:

1. An ambient temperature cured propellant was successfully scaled to five-gallon mixer size and was partially characterized (rheological, hazards, ballistics and physical properties).
2. Improved rheology (viscosity and yield) was obtained even at the high fine AP content required to achieve the burn rate by increasing the plasticizer content of the baseline propellant.
3. Lower yield, which signifies better flow properties, was also achieved by incorporating polydimethyl siloxane.
4. The Aerojet developed propellant was duplicated which successfully demonstrated that ambient cure technology was transferable.
5. One of the most significant technical advances was accomplished with mechanical properties. Both Aerojet and Thiokol experienced softer than predicted propellant at end of ambient curing. Extensive post-cure further confirmed that cure was incomplete. Analysis by Thiokol indicated that excess moisture was the probable cause. The mixing procedure was altered (vacuum mixing at high temperature) and experimental results indicate the hypothesis and solution were correct. Complete cure was apparently demonstrated in a five-gallon scale-up mix. Reproducible, harder mechanical properties are now expected without post cure.
6. An alternate ambient cure system (processed hot — cured ambient) was identified which had excellent processability because of the high process temperature, good potlife, and excellent ambient cured mechanical properties.
7. Ambient-temperature cured propellants may be subject to hardening (aging) via metallic catalyzed oxidation. Additional investigations are required in this area.

## REFERENCES

1. "Improved Low-Cost Rocket Motor Processing and Component Development Study", Final Report, June 1972 - May 1975, Booz, Allen Applied Research, Report No. AFRPL-TR-75-34, Contract No. F0-4611-72-C-0074, July 1975.
2. Demonstration of Ambient-Temperature Cure Propellant", Aerojet Solid Propulsion Co., Report No. AFRPL-TR-73-68, Contract No. FO-4611-72-C-0072, August 1973.



3. Smith, T.L., "Ultimate Tensile Properties of Elastomers: I. Characterization by a Time and Temperature Independent Failure Envelope", J. Polymerific, Part A, 1, 3597-3615 (1963).

SECTION V

POUR-CASTING TECHNIQUE FOR  
MOTOR MANUFACTURING

## SECTION V

### POUR-CASTING TECHNIQUE FOR MOTOR MANUFACTURING

The low-cost propellant casting technique proposed for demonstration in Phases II and III is pour-casting. This technique consists of "pouring" the deaerated propellant into the open end of the casting assembly and allowing the propellant to fall to the bottom of the case. The pour-casting technique requires no casting tooling (e.g., bayonets, casting sleeves, or vacuum seals) such as is needed for bayonet or vacuum casting; however, it will result in a greater number of voids than the conventional higher cost casting methods. The quality of the propellant grain will be primarily dependent on propellant rheological properties and the loading rate.

The selection of pour-casting as the proposed production loading technique was predicated on the availability of a low viscosity propellant (i.e., 1 to 3 kilopoise). The limited propellant tailoring conducted to date (discussed in Section IV) and data available from the Aerojet program (reported in Reference V-1)<sup>1</sup> indicate that the final propellant formulation will have a viscosity in the 12 to 20 kilopoise range. The ability to "pour-cast" propellant at this viscosity level was questionable, and, consequently, an evaluation of pour-casting was conducted as described herein.

#### PROPELLANT SELECTION

DTS-7984 was selected for the initial evaluation because this formulation represented the best available ambient-cure propellant. The DTS-7984 formulation differs from the ambient-cure propellant (TP-H8245) used in Mix T-607 in the type and quantity of plasticizer (i.e., 3% IDP in DTS-7984 versus 2% DOA in TP-H8245). This change resulted in a propellant having a lower viscosity and a lower yield value. Both parameters are important to the success of pour-casting. The only pressure available to cause propellant flow in the motor is the head of the propellant itself. A lower yield point should result in less propellant stacking and folding. The lower viscosity should permit the propellant to fill the cavity more easily and permit large entrapped air bubbles to rise and burst.

The lower viscosity TP-H8208 propellant, which is processed at 145°F, was considered as an alternate to the ambient-cure propellants. Its low viscosity (3 to 5 kilopoise) is considered to be much lower than can be obtained with an ambient processed propellant. For this reason, the higher viscosity DTS-7984 formulation was selected to approximate the most likely final propellant formulation. The TP-H8208 was used in a later pour-casting evaluation to determine whether an acceptable pour-cast motor could be obtained even with a low viscosity propellant.

1. References are given at the end of this section.

## PROPELLANT CASTING

### DTS-7984, Mix T-630

The mixed DTS-7984 propellant was deaerated into a casting can equipped with a two-outlet spout. As shown on Figure V-1, the casting can was positioned over the lined TX-631 case so that the ends of the 3/4-inch ID spouts were 4 to 5 inches below the top of the casting sleeve and just above the aft end of the case. Initial casting pressure was 15 psig to simulate a barometric leg of propellant, but this pressure was reduced to 10 psig, and then 5 psig during the casting. Total casting time for the TX-631 motor was 45 minutes.

Propellant streamed from the spouts for 18 to 24 inches before breaking off. After breaking, the propellant then fell to the bottom of the motor without striking either core or case. Propellant would stack up 1 1/2 to 2 inches in the center of each motor half-section and fold to one side or the other. The propellant flowed well into the web behind the core points. The propellant surface was glossy and tended to level. No entrapment of large voids was observed although there were numerous small voids from the folding propellant and the roping of the propellant streams back and forth over themselves. After completion of casting, the propellant in the casting sleeve leveled almost immediately. No vibration or rocking was used to attempt to raise bubbles to the surface during casting since the small size of the entrapped bubbles would have required that the casting be stopped completely to permit surfacing of the bubbles. The motor and the samples were cured for 9 days at a room temperature of 95 - 100°F.

As indicated in Section IV, good rheology properties were obtained and the propellant appeared to have good flow properties. An experimental sample was also pour-cast for visual evaluation of voids. As shown on Figure V-2, the quality of a one-inch standard mold was excellent, with only a few surface voids. The sample was cut into half-inch dogbone specimens and each specimen was examined for voids. There were no detectable voids or flow patterns. Since the actual motor did have numerous voids, the one-inch mold was not considered a good facsimile. Because both the motor and samples were cast with the same casting equipment, the difference in quality appeared to be a function of the sample configuration. The TX-631 motor is over 4 feet long, whereas the one-inch mold is only about a half-foot long, which did not provide for the same fold-over experienced in the motor.

The loaded case was finished and radiographically inspected. The propellant contained a multitude (too numerous to count) of voids (see Figures V-3, V-4, and V-5). Void size appeared to increase, the number to decrease, and void shape to become more spherical in the aft end of the loaded case (compare Figures V-3 and V-5). This grain quality was a significant deterioration from normal standards, but it cannot yet be labeled "unacceptable".

The loaded case was conditioned at 65°F for 12 hours and then radiographically reinspected. No changes (i.e., crack formation or defect propagation) were found by the reinspection.

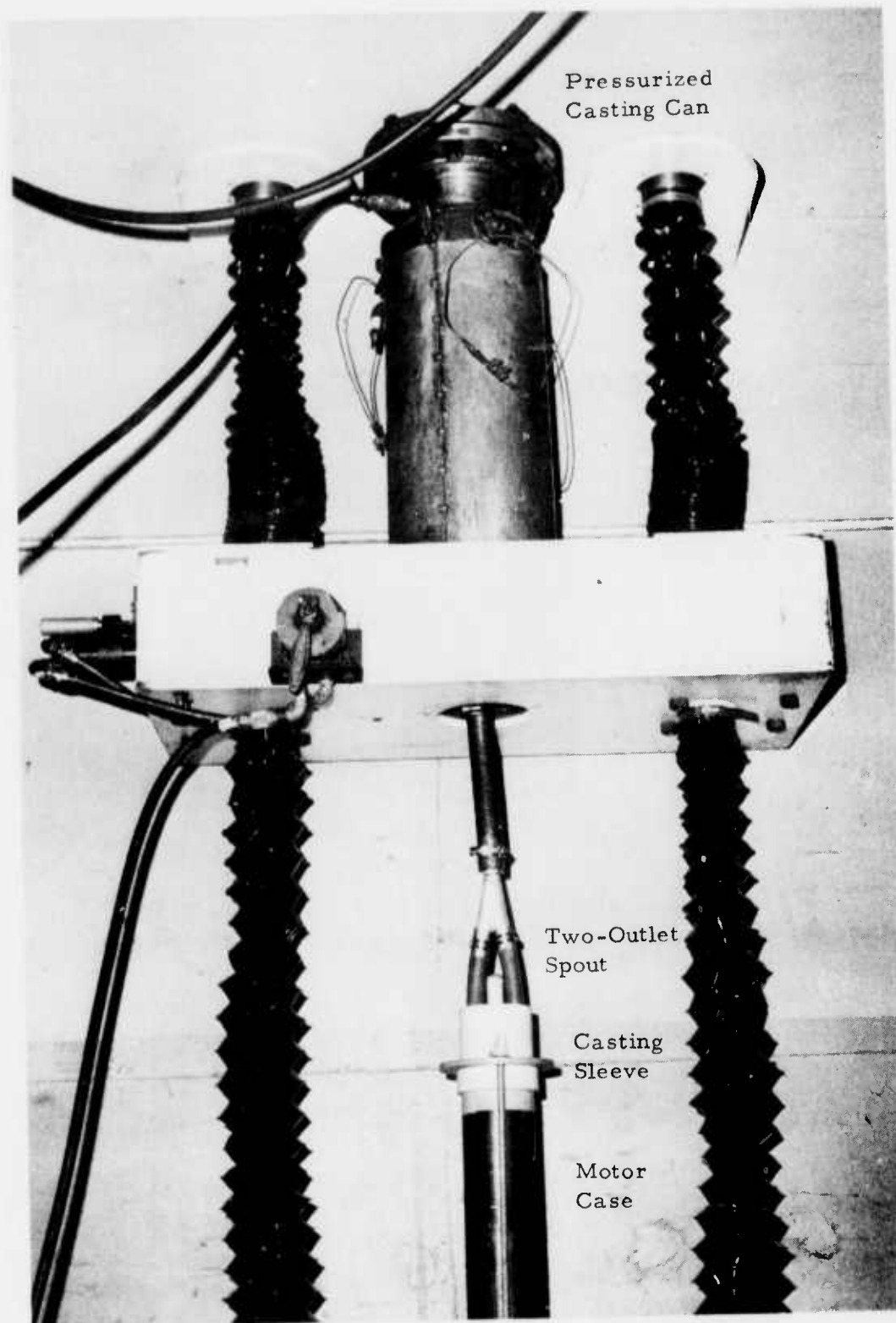


Figure V-1. Pour-Casting Set-Up for TX-631 Motor



Figure V-2. Pour-Cast Sample from Mix T-630,  
Showing Good Quality of Propellant

Photograph retouched; outlined areas show approximate shape and size of voids.

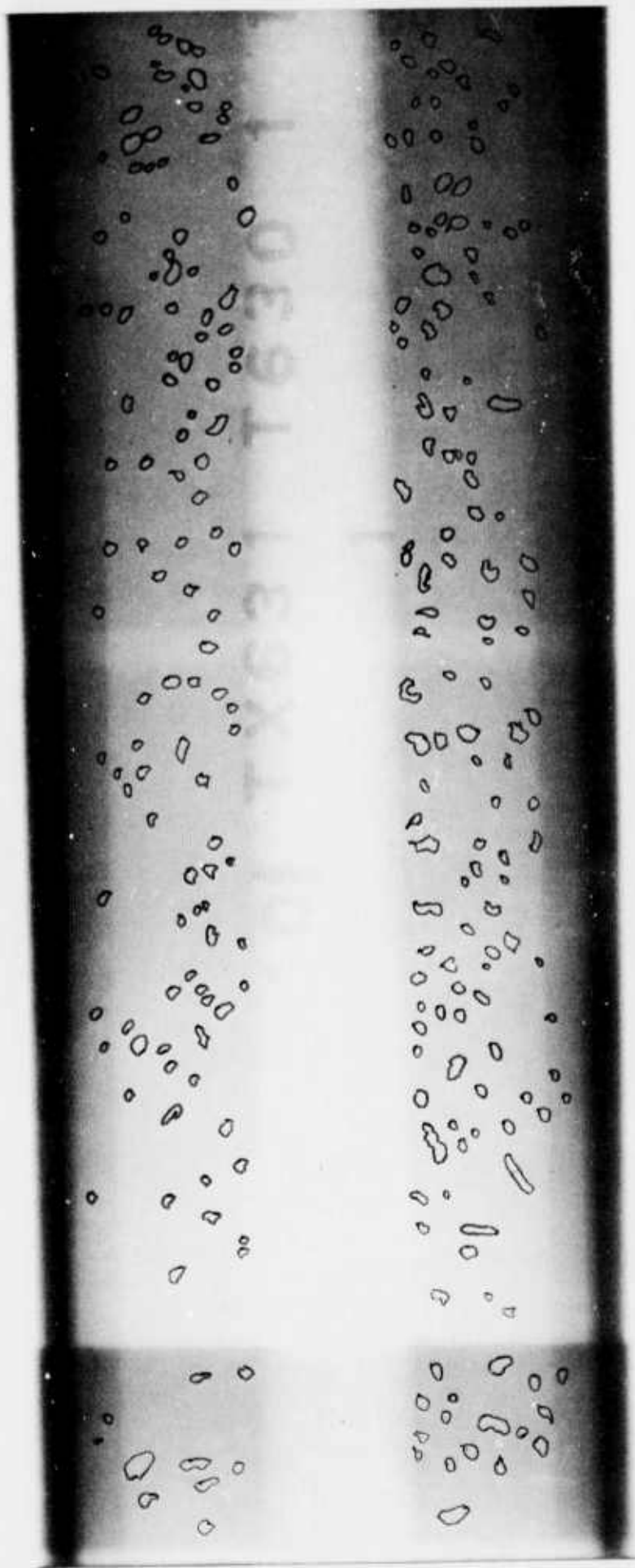


Figure V-3. Radiograph of Forward Portion of TX-631 Motor, Mix T-630, Charge 1



Photograph retouched; outlined areas show approximate shape and size of voids.

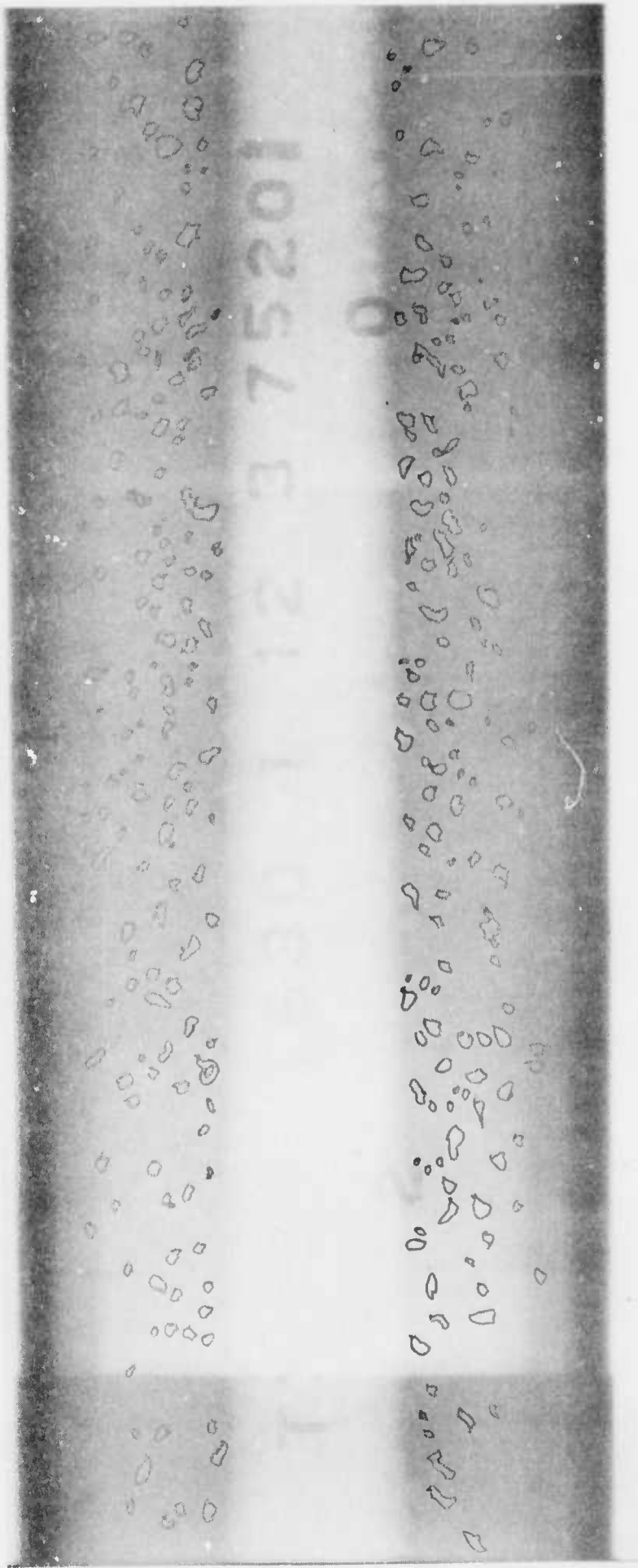


Figure V-4. Radiograph of Center Portion of TX-631 Motor, Mix T-630, Charge 1



Photograph retouched; outlined areas show approximate shape and size of voids.

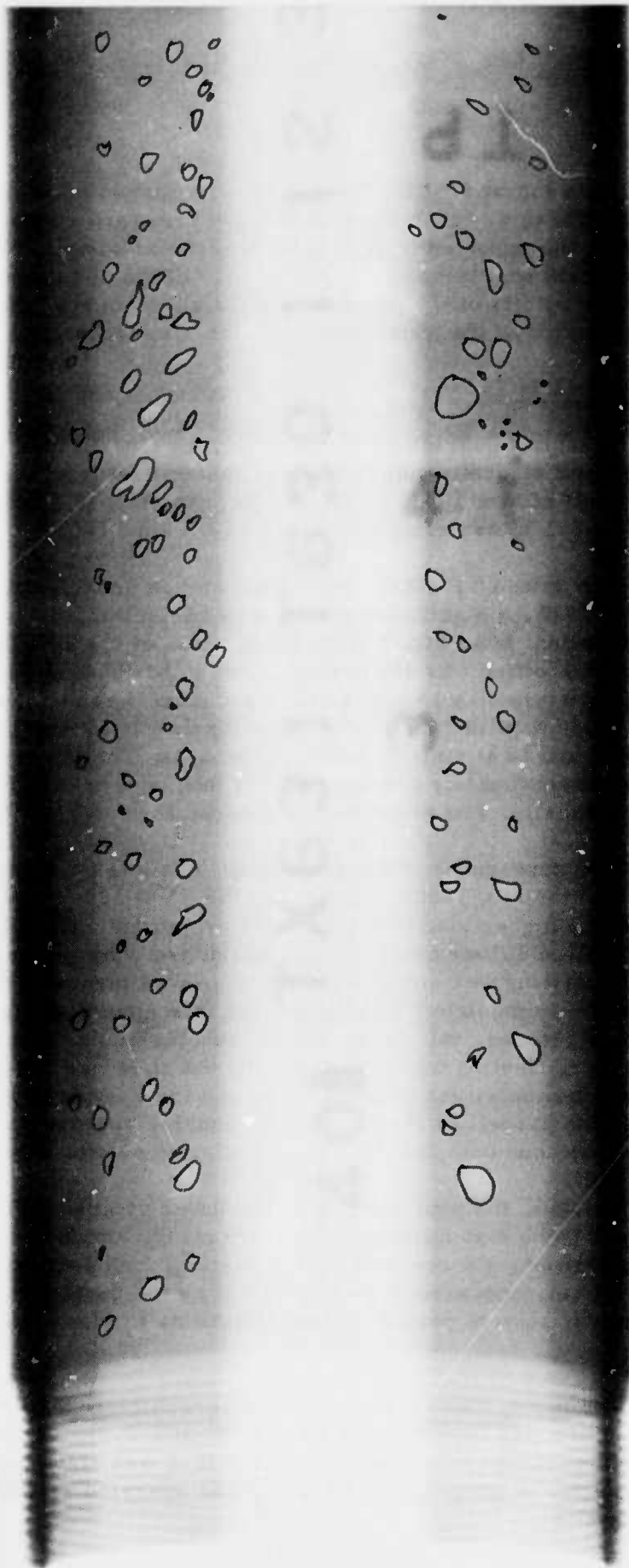


Figure V-5. Radiograph of Aft Portion of TX-631 Motor, Mix T-630, Charge 1

This motor (T-630, Charge 1) experienced an overpressurization at ignition. There was an indication that the pressure started to come to equilibrium at the expected level, but then resumed rising. There was no evidence that the grain quality was the direct cause of the abnormal pressure (see Section VI for details of the post-test analysis). However, the failure does complicate evaluation of the pour-cast manufacturing technique.

#### TP-H8208, Mix T-640

A second pour-casting experiment was performed to evaluate the effect of propellant viscosity and yield value on the quality of the loaded case. Approximately half of Mix T-640 of TP-H8208 propellant was deaerated and pour-cast into a TX-631 motor using the set-up as for Mix T-630.

The mixed TP-H8208 propellant had an end-of-mix viscosity of 2.8 kilopoise at 148°F, a significant contrast to the 12 kilopoise viscosity of the DTS-7984 propellant from Mix T-630. Yield value of the TP-H8208 two hours after cure agent addition was 400 dynes/sq cm at 145°F (see Figure V-6). The initial casting pressure was 15 psig and the pressure was maintained at this level until just prior to filling the motor. Casting was interrupted twice to level the propellant and to attempt to raise air bubbles. The interruptions occurred with the case approximately 1/2 full and 3/4 full, and in each instance, the case was rocked manually. The propellant was cured for 6 days at 145°F.

The appearance of the propellant as it was cast into the motor was similar to that for Mix T-603, except that the TP-H8208 propellant did not stack as much as the higher viscosity DTS-7984 propellant. The TP-H8208 propellant leveled well and flowed into the web behind the core points. When the case was half-full, casting was stopped and the case was manually rocked. The propellant surface immediately leveled and became smooth and glossy. After five minutes of rocking, only three or four bubbles could be observed on the propellant surface. Casting was resumed until the case was 3/4-full, at which time, it was again stopped for three minutes and the casting assembly was manually rocked. The propellant leveled, but no bubbles appeared on the surface. Casting was resumed and completed with a cumulative casting time of 34 minutes.

Overall, the pour-casting of the lower viscosity TP-H8208 propellant did not appear to be significantly different from the ambient-cure DTS-7984 propellant. In addition, air removal during casting, by imparting mechanical work to the propellant, appeared to be impractical as the casting rate would have to be prohibitively slow to permit the small bubbles to rise faster than the propellant level.

The motor was finished and radiographically inspected. It contained a multitude of voids (see Figures V-7, V-8, and V-9), as did T-630-1 in the first pour-casting evaluation. Motor T-640-1 was static tested at 70°F, with a foam mandrel in the propellant cavity, and operated satisfactorily (see Section VI for details).

TP-H8208 (T-640) L.C.M.D.  
 C.A.A.: 11:05 (12-16-75)  
 Test Conducted: 2 hrs. after C.A.A.  
 Test Temperature: +145°F (63°C)  
 Yield Value: 400 dynes · cm<sup>-2</sup>

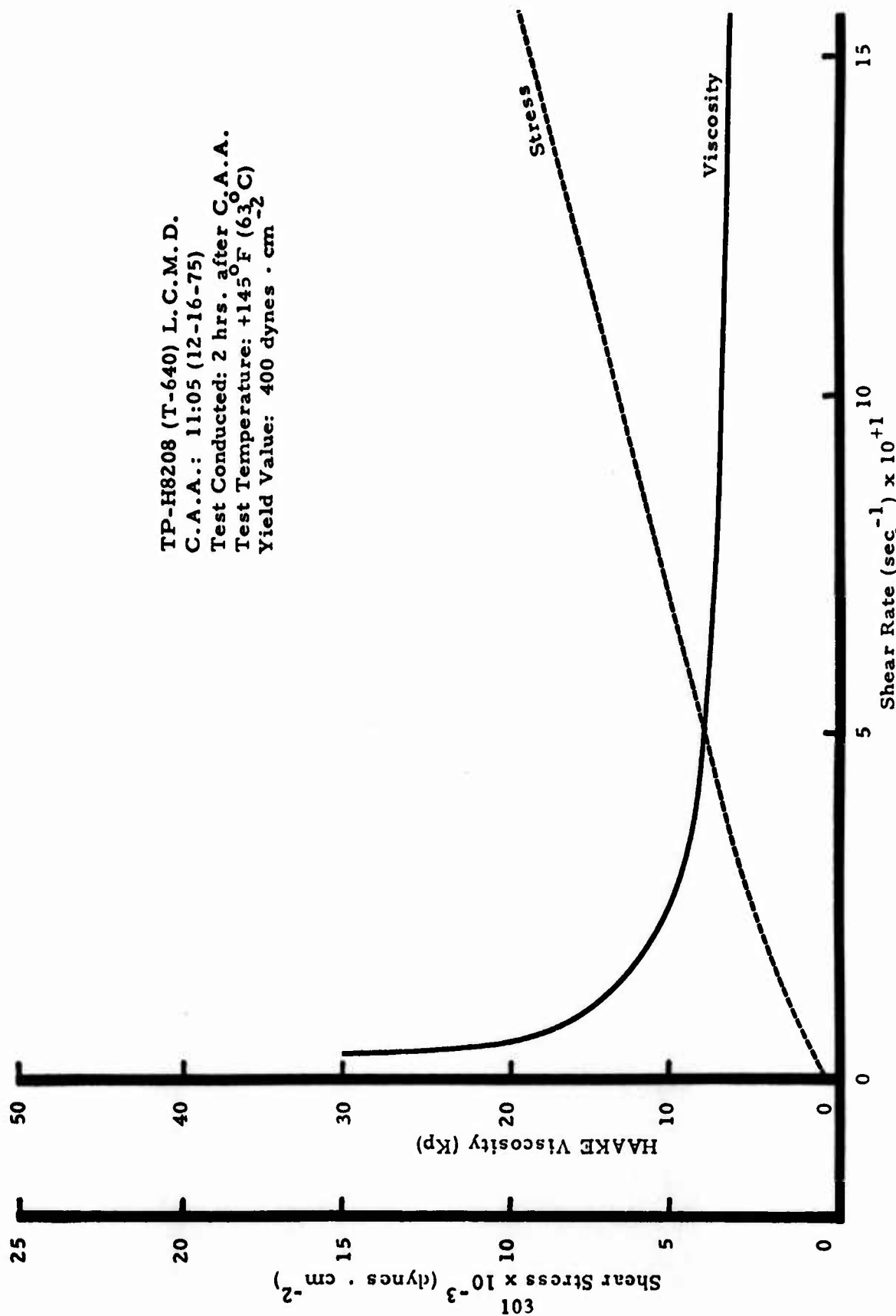


Figure V-6. Shear Stress and HAAKE Viscosity Versus Shear Rate for TP-H8208 (Mix T-640) with Cure Agent.

Photograph retouched; outlined areas show approximate shape and size of voids.



Figure V-7. Radiograph of Forward Portion of 1A-001 Motor, Mix 1-640, Charge 1

Photograph retouched; outlined areas show approximate shape and size of voids.

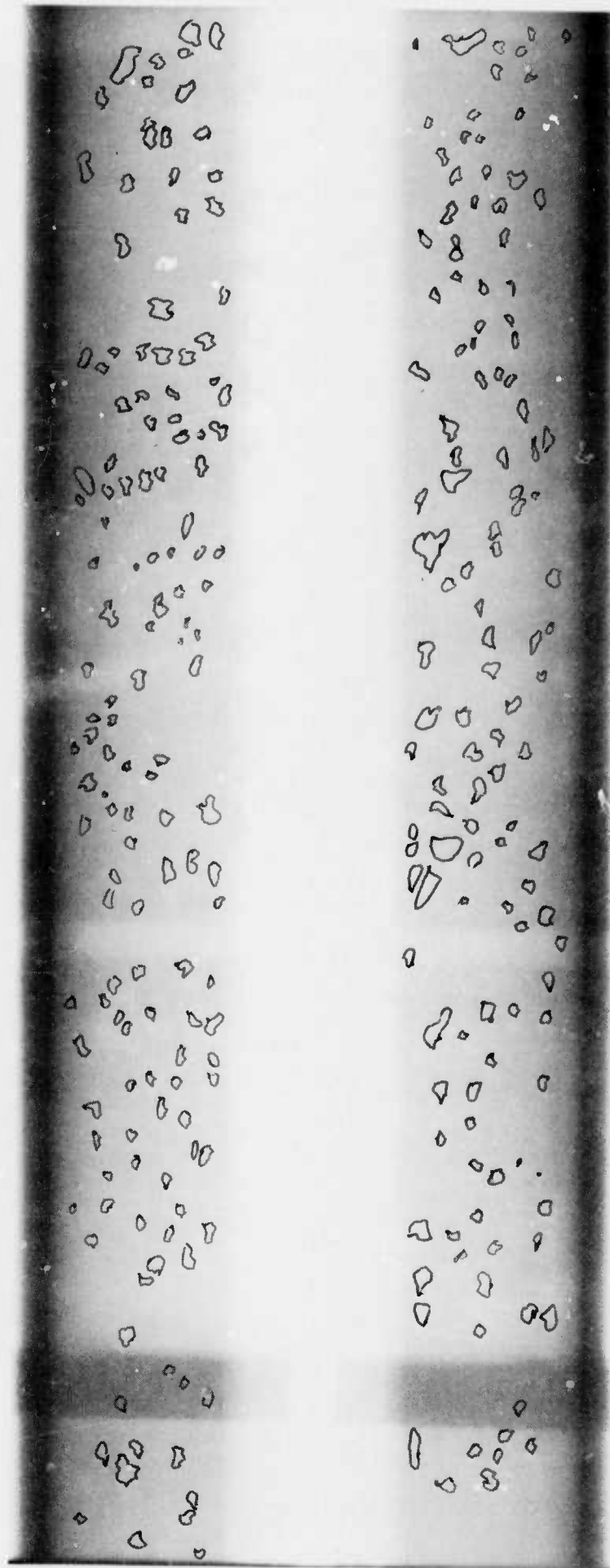


Figure V-8. Radiograph of Center Portion of TX-631 Motor, Mix T-640, Charge 1

Photograph retouched; outlined areas show approximate shape and size of voids.

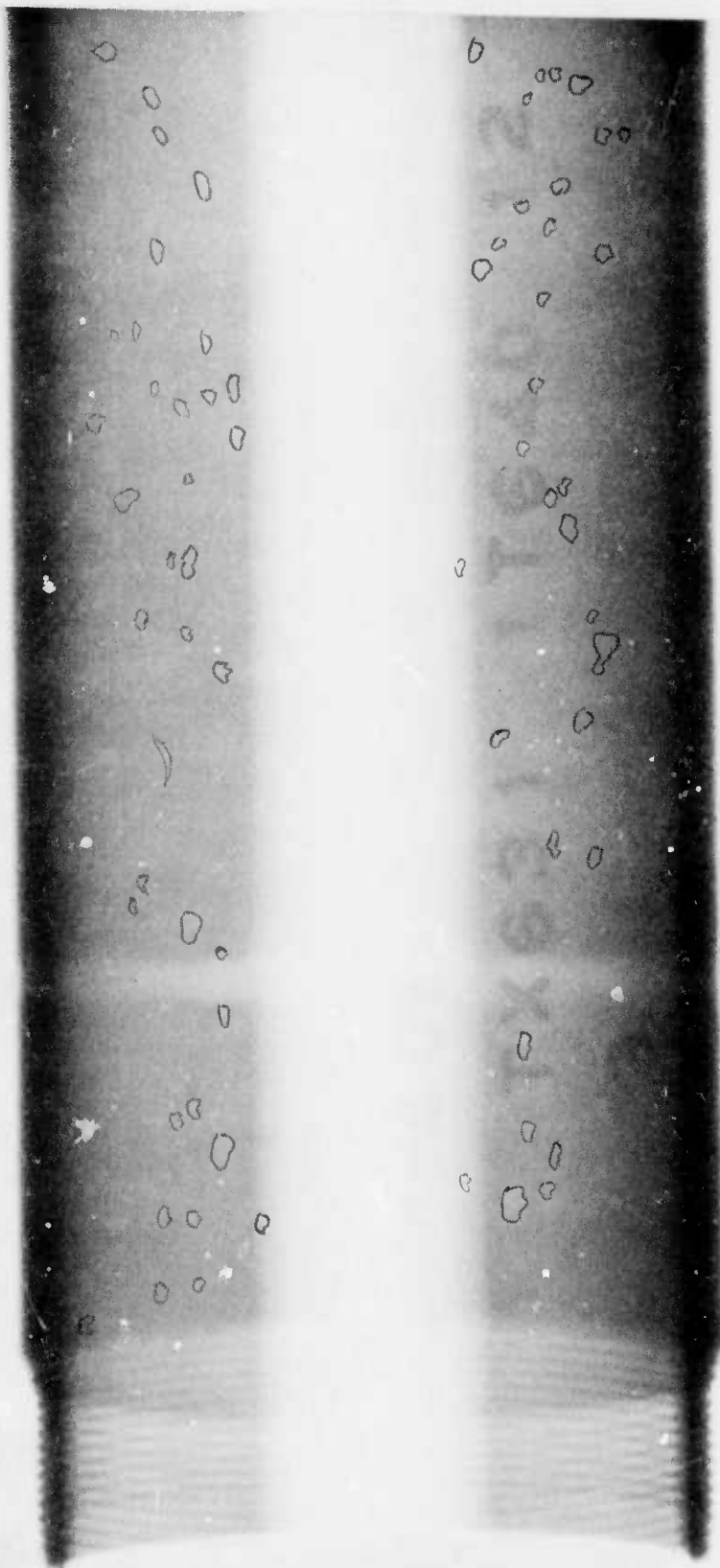


Figure V-9. Radiograph of Aft Portion of TX-631 Motor, Mix T-640, Charge 1



## COMPARISON OF MOTOR QUALITY AND PROPELLANTS

Motor T-640-1, with TP-H8208 propellant, had about the same number of voids in the forward end of the case (the "down" end during pour-casting) as Motor T-603-1, with DTS-7984 propellant, but they appeared to be smaller (Figure V-7 versus Figure V-3). In the aft end (the "up" end during pour-casting), the voids in Motor T-640-1 were fewer in number, and perhaps a little smaller (Figure V-9 versus Figure V-5).

The TP-H8208 propellant processed at 145°F offered many advantages over DTS-7984 processed at 80°F. Rheological properties are compared in Table V-1, and two sets of typical values are given below:

	<u>End-of-Mix Viscosity</u>	<u>Yield Value 2 hours after CAA</u>
TP-H8208 (Mix T-640)	3 kilopoise	400 dynes/sq cm
DTS-7984 (Mix T-630)	12 kilopoise	600 dynes/sq cm

These values show both lower viscosity and yield values for TP-H8208 and these two features resulted in some improvement in the pour-cast grain quality. However, there is a vast difference between the grain quality of even Mix T-640 and what is usually expected from conventional casting techniques (i. e., bayonet, vacuum, pressure). A formulation such as DTS-7980 (Table V-1) would offer some even further improvement in yield values, but the increased viscosity over TP-H8208 would probably counter any tendency toward fewer voids gained by the yield improvement.

## CONCLUSIONS

In summary, the pour-casting manufacturing technique for loading propellant into a TX-631-type motor introduces a significant number of voids. Even with lower viscosity and low-yield-value propellant, the entrapped air cannot be effectively removed during casting. Further investigation is needed to determine the propellant rheological properties and/or mechanical energy input spectrum that will result in a motor whose grain quality is equal to that now expected from conventional casting techniques.

The optimum casting technique for a production program probably is a combination of the vacuum casting as routinely used and pour-casting as evaluated. The two techniques are similar in that both introduce the propellant at the top of the case and allow the propellant to fall into the motor case. The inlet tooling differs and vacuum casting may utilize undeaerated propellant, whereas pour-casting requires vacuum-mixed or deaerated propellant. Vacuum casting utilizes the low pressure atmosphere to prevent void formation; pour-casting at ambient pressure relies on the propellant's rheological properties

TABLE V-1  
COMPARISON OF PROPELLANT RHEOLOGY

Propellant	Mix No.	End-of-Mix		Yield Value (dynes/sq cm)			
		Viscosity (kp)	Temp. (°F)	With Cure Agent		Without Cure Agent	
				Time (hours) After CAA	Yield	Yield	Temp. (°F)
TP-H8208 <sup>(a)</sup>	T-640	2.8	148	2	400	---	---
DTS-7984 <sup>(b)</sup>	T-630	12	90	1	600	200	80
				4	700	100	120
				6	900	100	145
DTS-7984	15Q-422	12	83	-	---	300	80
DTS-7980 <sup>(c)</sup>	15Q-403	14	84	1	200	200	80
				3	300	100	120
						100	145

- a. Developed for SAM-D motor.  
b. TP-H8245 with 3% plasticizer instead of 2%.  
c. Aerojet-developed formulation manufactured at Thiokol.



to minimize air inclusion. This latter difference is a significant quality influence. A high volume production technique may be to apply a relatively "soft" vacuum to the case interior (which reduces chances for air being pulled into the propellant through case/tooling interfaces) and then pour deaerated propellant into the case through quick connect/disconnect tooling.

Optimization of the casting technique for cost and quality will require definition of propellant rheological properties under vibrational influence and effect of casting chamber pressure on propellant quality and control of final level.

Static test results show that the grain quality did not inherently compromise the acceptability of ballistic performance. Results point out opposing inferences about the grain quality requirements with regards to manufacturing technique.

#### REFERENCE

1. "Demonstration of Ambient-Temperature Cure Propellant", Aerojet Solid Propulsion Co., Report No. AFRPL-TR-73-68, Contract No. FO-4611-72-C-0072, August 1973.

SECTION VI

SUMMARY OF TX-631 STATIC TESTS

## SECTION VI

### SUMMARY OF TX-631 STATIC TESTS

Eleven TX631 heavy-weight motors were static fired for Phase I component evaluation. The TX631 (Figure VI-1) was an available set of 4-inch diameter motor hardware which contained about 25 lbs propellant, had a regressive pressure-time history, was capable of operating at pressures of at least 4000 psia, and had a reduced-diameter aft section. All of these features were very similar to those anticipated for the 4-inch diameter application of the low cost concepts being evaluated.

A summary of the components tested on each motor is in Table VI-1. Almost every motor firing had more than one test objective, so the detailed results are discussed in the other sections of this report allocated to the individual components. The purpose of this section is to provide a summary of the test conditions and to report certain information which may not be appropriate for listing as component test results.

#### PREDICTED PERFORMANCE

As discussed in Section IV, TP-H8208 propellant was loaded in the first TX 631 motors. Performance predictions were then made with TP-H8208 ballistic properties.

A throat size was selected to produce a maximum pressure (which occurs at ignition) of 3000 psia. Nozzle material is FM16771, which has an erosion rate modeled by

$$r_e = 0.000111 P^{0.824} \text{ (on radius)}$$

based on previous firings with the same propellant and material.

Pertinent predicted parameters of the TX-631 with TP-H8208 propellant are:

Initial throat diameter (in.)	1.050
Burn Time (sec.)	2.1
Pressure (psia)	
Maximum	2970
Average	1720
Thrust (lb.)	
Maximum	3820
Average	2680

A predicted pressure and thrust history are shown in Figure VI-2.

**TABLE VI-1**  
**TEST SUMMARY TX-631 MOTORS FOR COMPONENT EVALUATION**

Mix & Chg. No	T622-1	T622-2	T634-1	T630-1	T640-1	T640-2	T643-1	T643-2	T634-2	T684-1	T684-2
Test Objectives	(1) Baseline nozzle mat'l performance with TP-H8208 prop.	(1) Nozzle material	(1) Motor operation with foam mandrel in place (2) Second baseline nozzle mat'l test with (3) Candidate igniter	(1) Pour casting technique (2) Grain quality requirements	(1) Pour casting technique (2) Grain quality requirements (3) Change in igniter charge	(1) High density foam	(1) "Low" density foam at low temperature (2) Nozzle material	(1) "Low" density foam at high temperature (2) Nozzle material	(1) "Low" density foam at extreme temperature (2) Nozzle material	(1) Motor cast with "high" density foam mandrel (2) Nozzle material (3) Mastic insulation (4) Ambient cure propellant (5) Ignition aid	(1) Motor cast with "low" density foam mandrel (2) Nozzle material (3) Mastic insulation (4) Ambient cure propellant (5) Ignition aid
Grain Processing	(a)	(a)	(a)	Pour cast	Pour cast	(a)	(a)	(a)	(a)	(b)	(b)
Propellant	TP-H8208	TP-H8208	TP-H8208	DTS-7984	TP-H8208	TP-H8208	TP-H8208	TP-H8208	TP-H8208	DTS-7984	DTS-7984
In-place Mandrel	None	None	Foam @ (c) 12 PCF	None	Foam @ (c) 12 PCF	Foam @ (c) 17 PCF	Foam @ (c) 12 PCF	Foam @ (c) 12 PCF	Foam @ (c) 12 PCF	Foam @ 14 PCF	Foam @ 12 PCF
Igniter	(d)	(d)	(e)	(d)	(f)	(f)	(f)	(f)	(g)	(f)	(h)
Nozzle	FM16771	RVTOR R4	FM16771	ATI Graphite	ATI Graphite	ATI Graphite	RM1108PD	RM153RPD	D22532	D23570	R25406
Insulation	(i)	(i)	(i)	(i)	(i)	(i)	(i)	(i)	(i)	Polycarbonate & ABS spec.	Mastic (TI-H706A)
Conditioning Temperature	70° F	70° F	70° F	70° F	70° F	70° F	-65° F	165° F	165° F	70° F	70° F
Results	Satisfactory Operation	Satisfactory Operation	Satisfactory Operation	Over-pressurization	Satisfactory Operation	Satisfactory Operation	Satisfactory Operation	2.675 sec Hangfire Nozzle data of	0.339 sec Hangfire Nozzle data of	0.155 sec Hangfire Nozzle data of	Over-pressurization preceded by 2.620 sec hangfire

- Vacuum cast through aft end with aluminum mandrel.
- Foam mandrel used to form grain (vacuum cast through aft end).
- Mandrel inserted during motor assembly.
- Pyrotechnic pellets (BKNO<sub>3</sub>) in head-end mounted metal tube (routine TX-631).
- Magnesium-terfion pellets (20 gms) with Atlas match initiator.
- Modification of (e) by replacing 10 gm pellets with 10 gm powder.
- Doubled charge weight (20 gms pellets and 20 gms powder), magnesium-terfion.
- 10 gms pellets, 10 gms powder (magnesium-terfion). Foam mandrel cut back to propellant surface in cylindrical bore for 1.5 inches at head-end.
- Polyisoprene (routine TX-631).



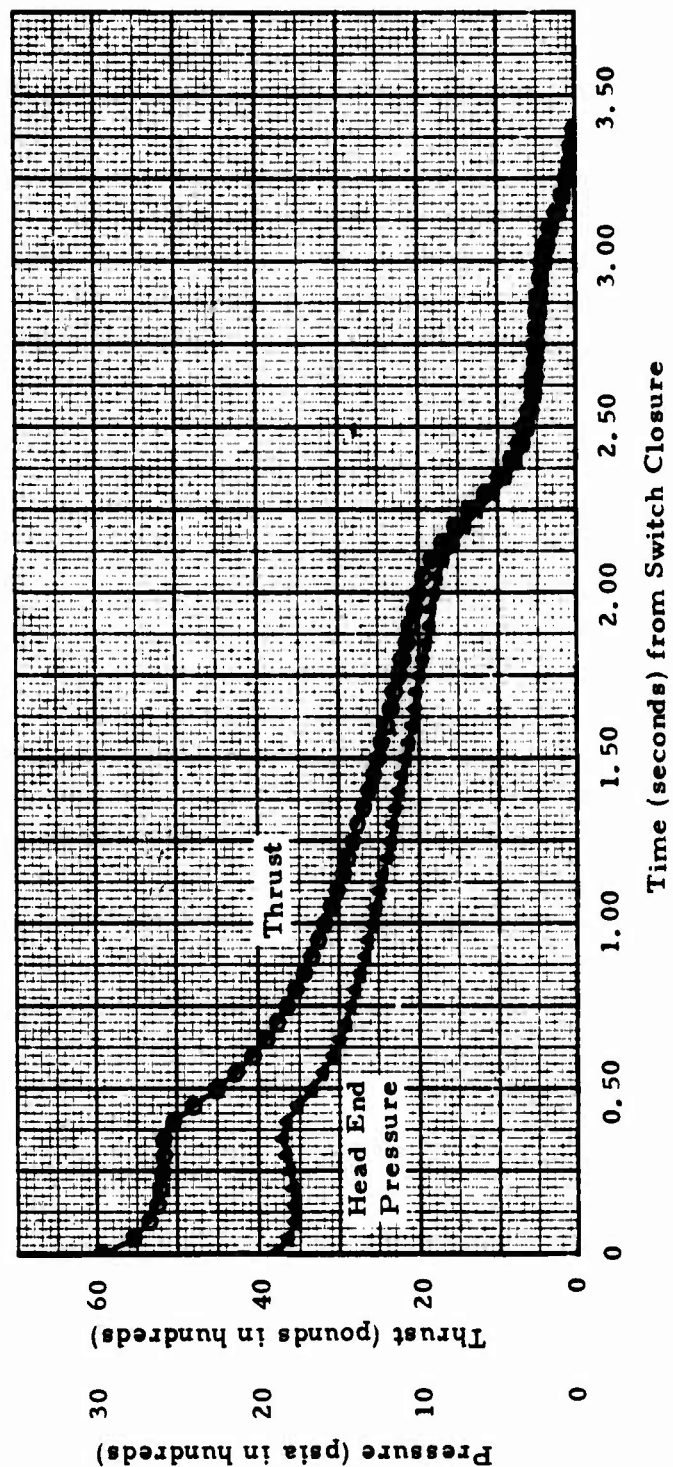


Figure VI-2. Ballistic Prediction of TX-631 Motor with TP-H8208 Propellant, Fired at 70°F

## STATIC TEST RESULTS

The TX631 test series was established to evaluate nozzle ablative materials, insulations, igniters, leave-in-place foam mandrels and grain manufacturing techniques. Even though basic motor configurations were formulated prior to the start of the series, the tests were conducted as an adaptive investigation; final selection of exact details of several components was made on the basis of tests just completed. As such, the eleven tests fell into five groups, and the results are presented in subsequent paragraphs according to that grouping.

<u>Group Number</u>	<u>Motors</u>	<u>Basic Objectives<sup>1</sup></u>
1	T622-1 T622-2	Baseline and one candidate nozzle material
2	T634-1	First test with foam mandrel and candidate integral igniter
3	T640-1 T640-2 T630-1	Pour-casting grain manufacturing technique. "High" and "low" density foam mandrels
4	T643-1 T643-2 T634-2	Igniter/mandrel interaction at temperature extremes. Change in igniter charge to alleviate hangfire
5	T684-1 T684-2	Grains manufactured with "high" and "low" density foam mandrels. Igniter configuration to alleviate hangfire.

The TX631 motor is shown in the test cell before and after one of the firings (Figures VI-3 and VI-4). Ballistic parameters measured and calculated for each of the 11 tests are summarized in Table VI-2.

### Group No. 1

Motors T622-1 and T622-2 were loaded with TP-H8208 and manufactured with conventional tooling. They had routine TX631 igniters, which were BKNO<sub>3</sub> pellets in a metal perforated head-end mounted tube. The cases were insulated with two strips of polyisoprene under each of the propellant valleys. Test objectives were to evaluate the baseline (FM16771) and a candidate thermoset (Ryton R4) nozzle materials. Thrust and pressure measurements at 70°F are shown in Figures VI-5 and VI-6.

---

1. See Table VI-1 for complete list of objectives.



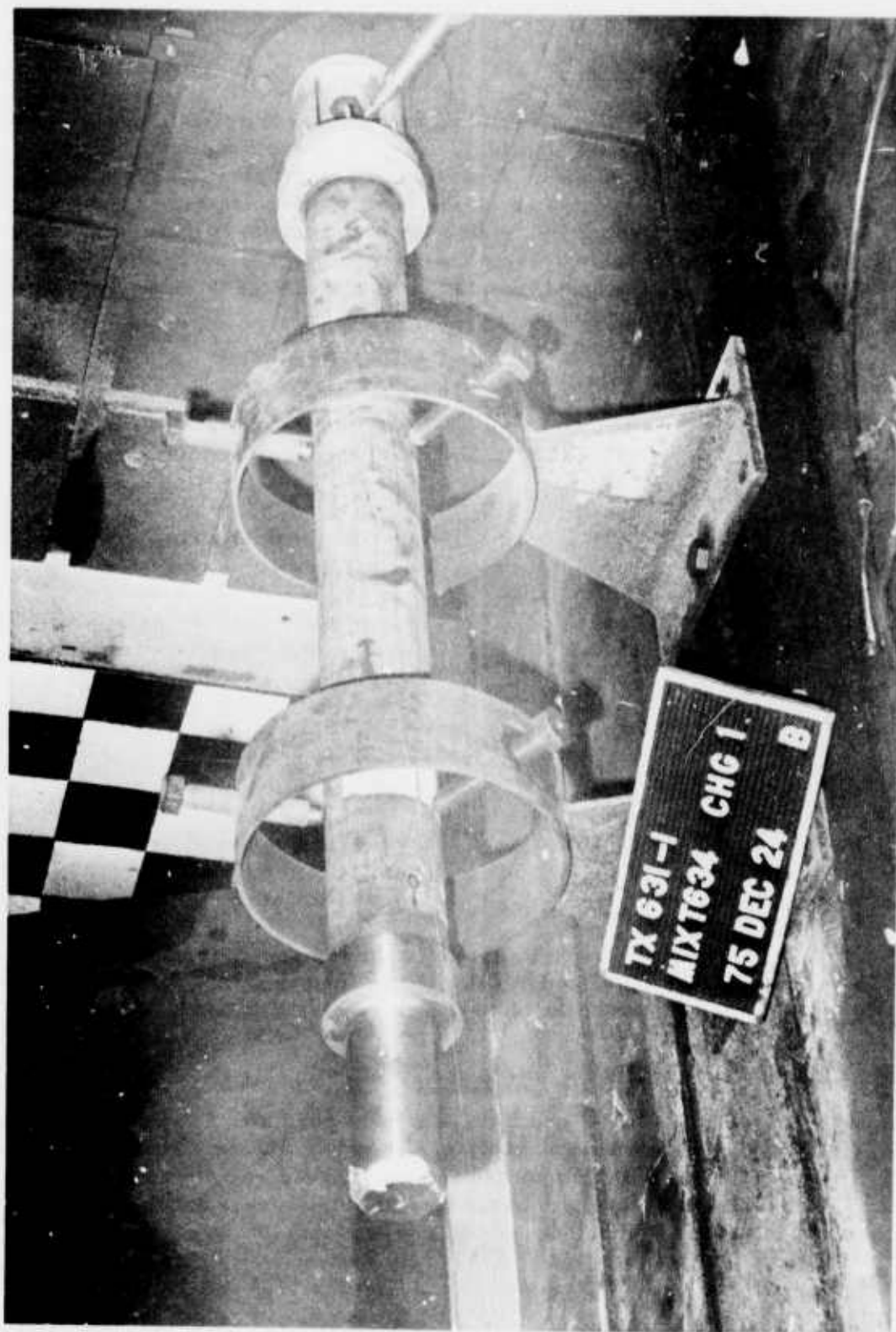


Figure VI-3. TX-631, Mix T-634, Charge 1, In Test Cell Before Test



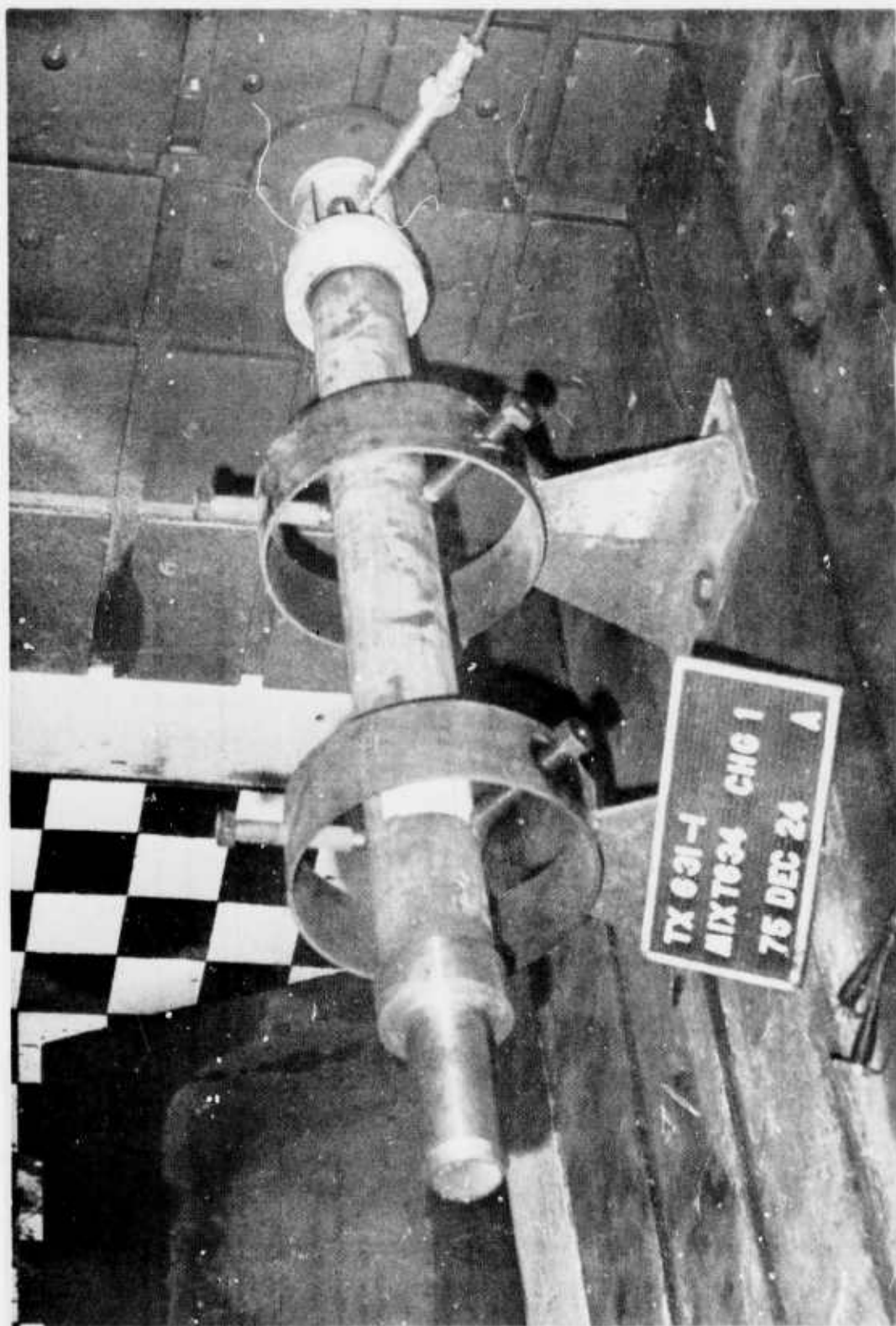


Figure VI-4. TX-631, Mix T-634, Charge 1, In Test Cell After Test

**TABLE VI-2**  
**SUMMARY OF TX-631 BALLISTIC PARAMETERS**

Mix and Charge No.	T 622-1	T 622-2	T 634-1	T 630-1 (a)	T 640-1	T 640-2	T 643-1	T 643-2 (b)	T 634-2 (b)	T 604-1 (b)	T 604-2 (a)
Conditioning Temperature (°F)	70	70	70	70	70	70	-65	165	165	70	70
Loaded Propellant Weight (lb)	25.35	25.27	25.34	25.46	25.13	25.22	25.30	25.46	25.23	24.61	19.52
Burned Weight (lb)	25.69	25.73	25.70	N/A	25.70	25.30	25.70	25.80	25.70	25.90	N/A
Throat Diameter (in)											
Before (c)	1.047	1.057 (d)	1.045	1.048	1.048	1.048	1.048	1.048	1.049	1.050	1.048
After (c)	1.310 (d)	1.709 (d)	1.235 (d)	N/A	1.096	1.096	1.336	1.332	1.256	1.248	N/A
Operating Time (sec)											
Web	2.392	3.240	2.280	N/A	2.034	2.064	2.797	1.192	2.298	1.835	N/A
Total	3.777	4.686	3.790	N/A	3.413	3.340	4.274	3.381	3.525	3.602	N/A
Pressure, Head-end (psia)											
Maximum	3853 (e)	4268	3951	N/A	3750	4963	3705	2231	2649	2758	N/A
Average, Web	1439	659	1525	N/A	1996	1974	1168	1917	1444	1766	N/A
Thrust (lb)											
Maximum	5706 (e)	5872	(f)	N/A	(f)	(f)	4840	3532	3579	(f)	N/A
Average, Web	2315	1572	(f)	N/A	(f)	(f)	1958	3005	2414	(f)	N/A
Characteristic Velocity (ft/sec) (g)	5294	4635	5101	N/A	5282	5293	5141	5133	4854	5148	N/A
Total Impulse (lb-sec)	6122	5440	(f)	N/A	(f)	(f)	6050	6119	6065	(f)	N/A

- a. Overpressurized.  
b. Hangfire.  
c. Average of four measurements taken 45° apart, except as noted.  
d. Equivalent diameter based on planimeter area measurement of tracing of throat obtained from profilometer image.  
e. Not true maxima because data system was calibrated at too low pressure and thrust.  
f. Not measured.  
g. Based on loaded propellant weight, average throat area (calculated from listed initial and final throat diameters) and head-end pressure.

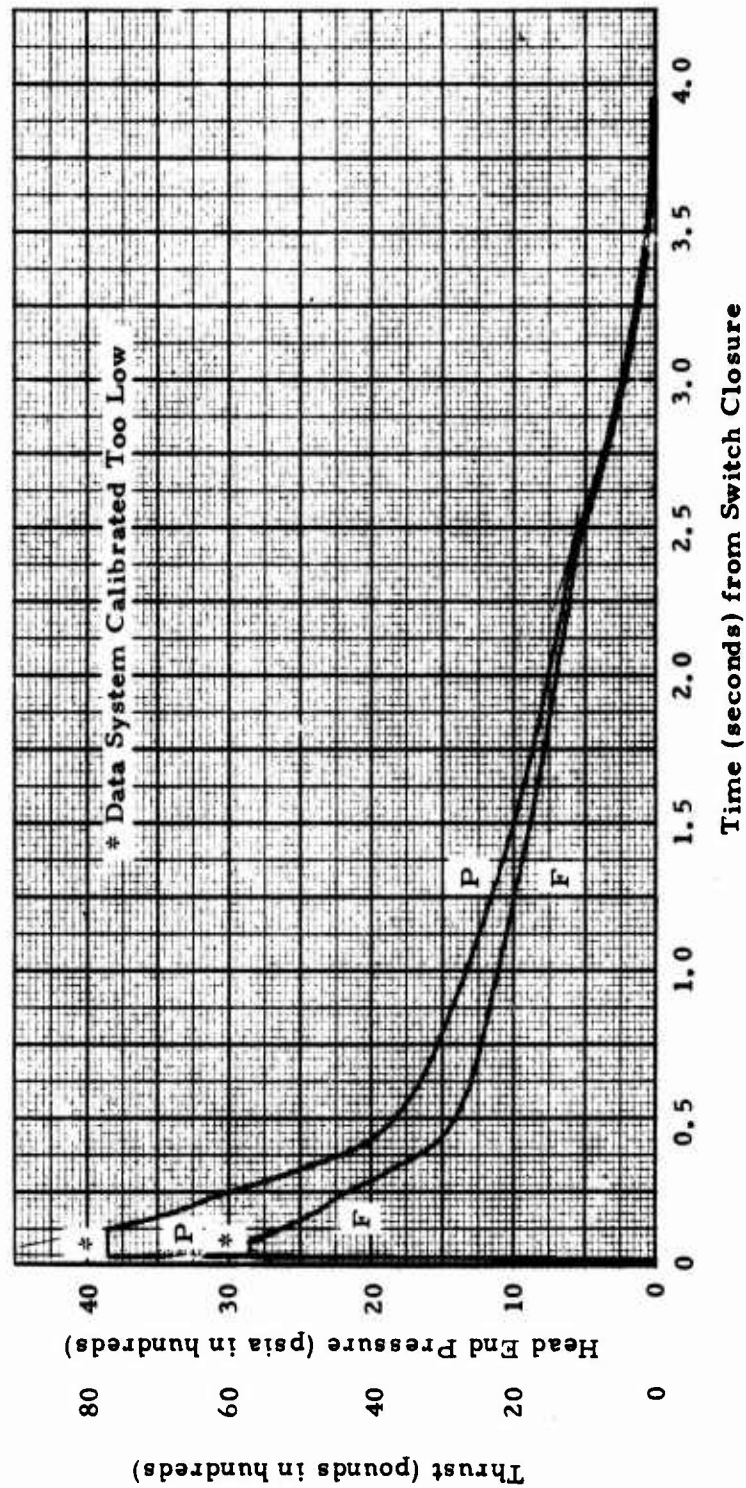


Figure VI-5. Ballistic History, TX-631 Motor, Mix T-622, Charge 1, Fired at 70°F

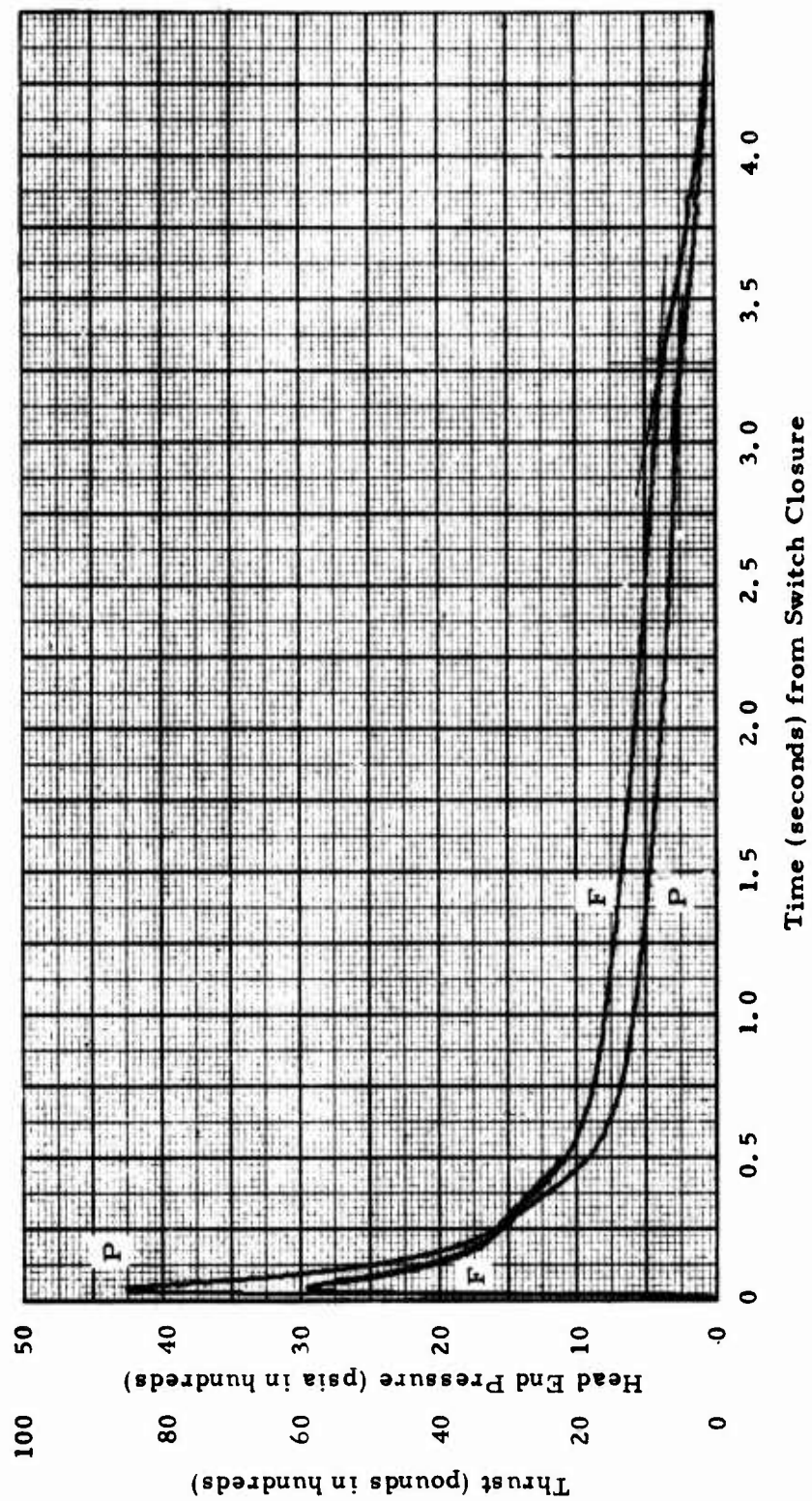


Figure VI-6. Ballistic History, TX-631 Motor, Mix T-622, Charge 2, Fired at 70°F

All components performed satisfactorily. Ignition was as expected. Maximum pressure was significantly higher than expected, >4200 psia rather than 3000 psia. The difference is attributed to an erosive burning contribution larger than anticipated. Concurrent performance analyses were indicating that pressure in a final design could be higher than 3000 psia, so it was decided to continue to operate in this regime. In addition, by keeping the throat size constant for all TX631 tests, there could be a direct comparison of nozzle throat erosion experience.

Characteristic velocity for T622-2 was significantly lower than for the other motors. The  $C^*$  parameter was calculated from

$$C^* = \frac{g A_t \int P dt}{W_f}$$

where  $A_t$  is the average of initial and final throat areas. Calculating  $A_t$  in this manner requires an assumption that throat area varies uniformly with time. If throat area varies non-uniformly, the calculated parameter  $C^*$  can be high or low from its expected value. Because  $C^*$  for T622-2 was much lower than expected, it would indicate that there was a very high erosion rate during the initial part of motor operation which very quickly caused the motor to experience a large throat area. Then the erosion rate could have drastically decreased and the motor could have operated for a majority of its duration at a large throat area. Thus, calculating average area as the average of initial and final throat areas would indicate a smaller average throat than was actually experienced. The result would be a low  $C^*$ . Post-test examination showed severe erosion of the Ryton R4 material.

Post-test ballistic simulations were performed to explain the high pressure at ignition. Igniter contributions were ruled out as a major influence primarily because previous tests with the TX631 motor had not shown similar tendencies. Results of T622-1 were compared with calculated parameters because the severe nozzle erosion of T622-2 would make meaningful comparisons difficult. Because pressure measurements were truncated, an estimate was made of the pressure and thrust above the cut-off levels. Propellant density was adjusted so that computer-calculated propellant weight agreed with loaded weight. The head-end characteristic velocity,  $C^*_{HE}$ , was adjusted to a nozzle-end value according to

$$C^*_{NE} = \left[ C^*_{HE} \right] \left[ \frac{\int P dt (\text{nozzle end})}{\int P dt (\text{head end})} \right]$$

where the ratio of pressure integrals was determined from a computerized ballistic calculation for the TX631. Actual motor thrust efficiency calculated from thrust and head-end pressure was corrected to nozzle-end conditions and used in thrust simulations.



Burning rate was modeled by three equations, with the highest rate of the three being used at any given longitudinal position at any given time during the simulated motor operation.

$$r = a P^n \quad (1)$$

$$r = \left[ a P^n \right] \left[ \frac{M}{M_{crit}} \right]^x \quad (2)$$

$$r = 0.0093 (MP)^{0.71} \quad (3)$$

where  $r$  = burn rate

$a$  = coefficient determined for particular propellant

$n$  = exponent determined for particular propellant

$P$  = local chamber pressure

$M$  = local Mach number

$M_{crit}$  = experimentally determined Mach number above which erosive burning has effect on rate

$x$  = experimentally determined exponent

Equation (1) is the familiar Vieille rate relationship. Equations (2) and (3) were developed in Reference VI-1 and VI-2<sup>1</sup>, respectively. A recent study (Reference VI-3) verified the validity of these models, particularly for "first-time" estimates. Sequential simulations with adjustments in  $M_{crit}$  and  $x$  were made to match measured and calculated motor behavior.

The final post-test simulation gave the following results, where initial pressure was treated as the primary parameter to be matched. Pressure-time histories are compared in Figure VI-7.

	<u>Measured</u>	<u>Post-Test Simulation</u> <sup>(2)</sup>
Maximum Pressure (psia)	4600 <sup>(3)</sup>	4600
Total $\int P dt$ (psia-sec)	3814 <sup>(3)</sup>	3878
Final Throat Diameter (in)	1.327	1.305
Web Burn Time (sec)	2.39	2.2
Maximum Thrust (lb)	6000 <sup>(3)</sup>	5929
Total Impulse (lb-sec)	6138 <sup>(3)</sup>	6095

Agreement between measurements and simulations is satisfactory, but abnormally high values of  $M_{crit}$  (0.08) and  $x$  (1.2) were required to achieve such a match. The critical Mach number,  $M_{crit}$ , is usually 0.03 - 0.05, while the exponent,  $x$ , is usually 0.10 - 0.15. There are several possibilities that could cause the high values of  $M_{crit}$  and  $x$  to be deduced:

1. References are listed at the end of this Section.
2. Computer Sequence T53557
3. Estimated because data records were truncated

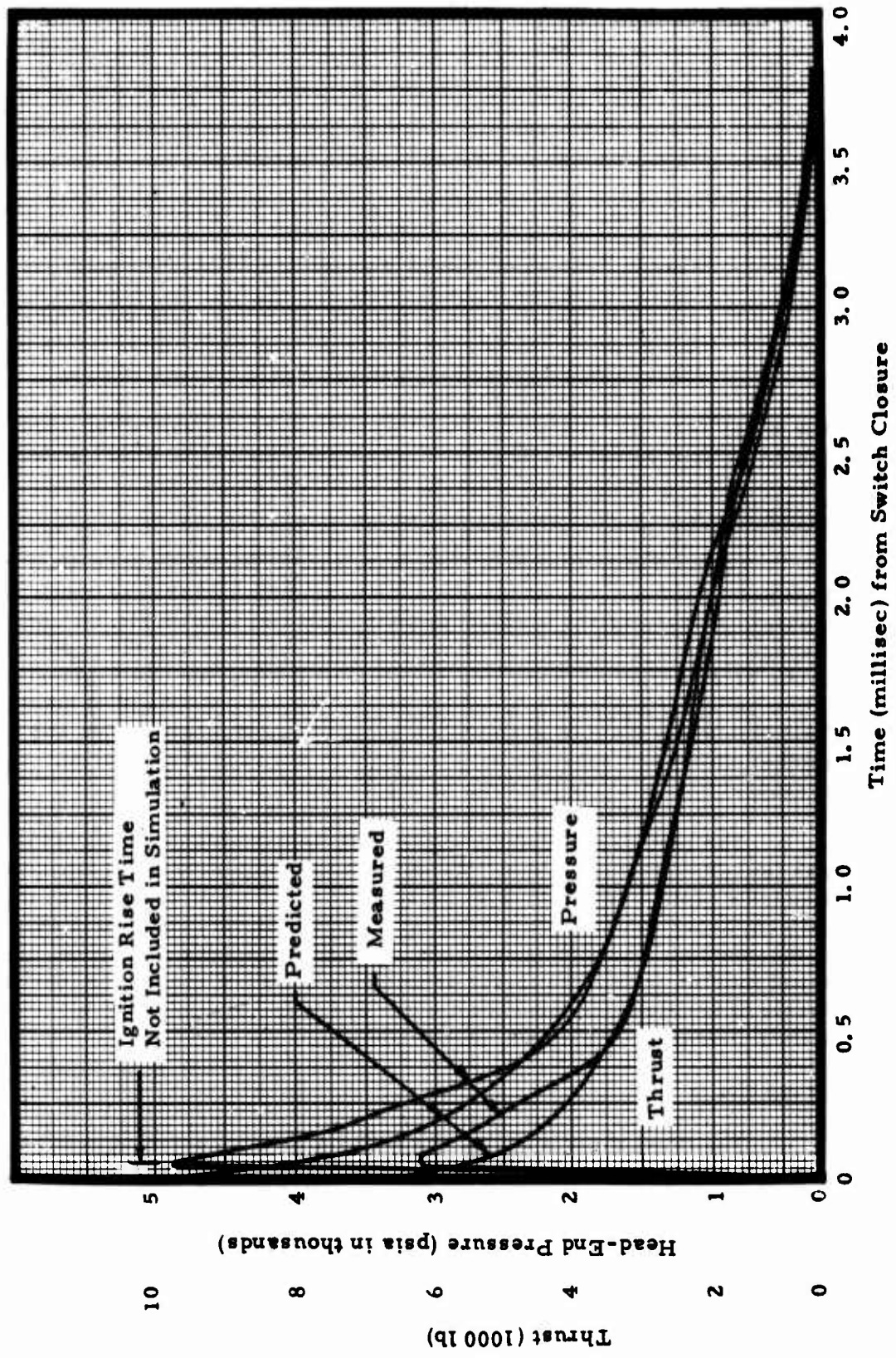


Figure VI-7. Comparison of Measured and Simulated Ballistics, TX631, Mix T622-1

- a. Burning rate of TP-H8208 propellant has been measured only up to pressures of about 2500 psia (Reference VI-4). Extrapolation to pressures of 3000 psia is not too inexact, but using the same relationship to 4500 psia leads to some uncertainties as to basic rate. In the subject analysis, these uncertainties were accommodated through adjustments in  $M_{crit}$  and  $x$ .
- b. Burning rate over a large part of the propellant surface was described by Equation (3) whenever the values of  $M_{crit}$  and  $x$  were nearer their usual values because the Mach number/pressure combination was such to cause Equation (3) to calculate a higher rate than Equation (2). The values of the coefficient and exponent for Equation (3) are not nearly so well defined for HTPB propellants in this particular Mach number/pressure regime.

For these reasons, the erosive burning parameters deduced for T622-1 should be applied only to TP-H8208 propellant burned in TX631 motors.

#### Group No. 2

Motor T634, Charge 1, was loaded with TP-H8208 propellant manufactured with conventional tooling. It had routine TX631 case insulation and a nozzle containing the baseline ablative material (FM16771). A consumable mandrel with foam density of 12 lb/cu ft was inserted into the propellant cavity after propellant cure was complete. The igniter was magnesium-teflon pellets contained in a molded cavity at the forward end of the mandrel. Test objectives were to evaluate the igniter/mandrel interaction and to have another measurement of throat erosion with the baseline material. A pressure-time history is shown in Figure IV-8.

The test was singularly successful. Maximum pressure (3951 psia) was less than experienced by the two previous motors without consumable mandrels (estimated 4600 psia and 4268 psia). Throat erosion was more uniform around the nozzle periphery, which is attributed to the slower filling of the chamber and thus less distortion of the flow field at ignition. High speed movies (4000 frames per second) did not show any debris leaving the nozzle at ignition. It appeared the mandrel was completely or almost completely consumed during the ignition phase.

#### Group No. 3

The three motors of this group had a diverse set of objectives which were all related in some way. Motor T630-1 was loaded with ambient-temperature cured propellant (DTS-7984) manufactured by the pour-cast technique using conventional tooling (see Section V). It was fired with the routine TX631 igniter and thus did not incorporate a consumable mandrel. Motor T640-1 was also pour-cast (conventional tooling), but with TP-H8208



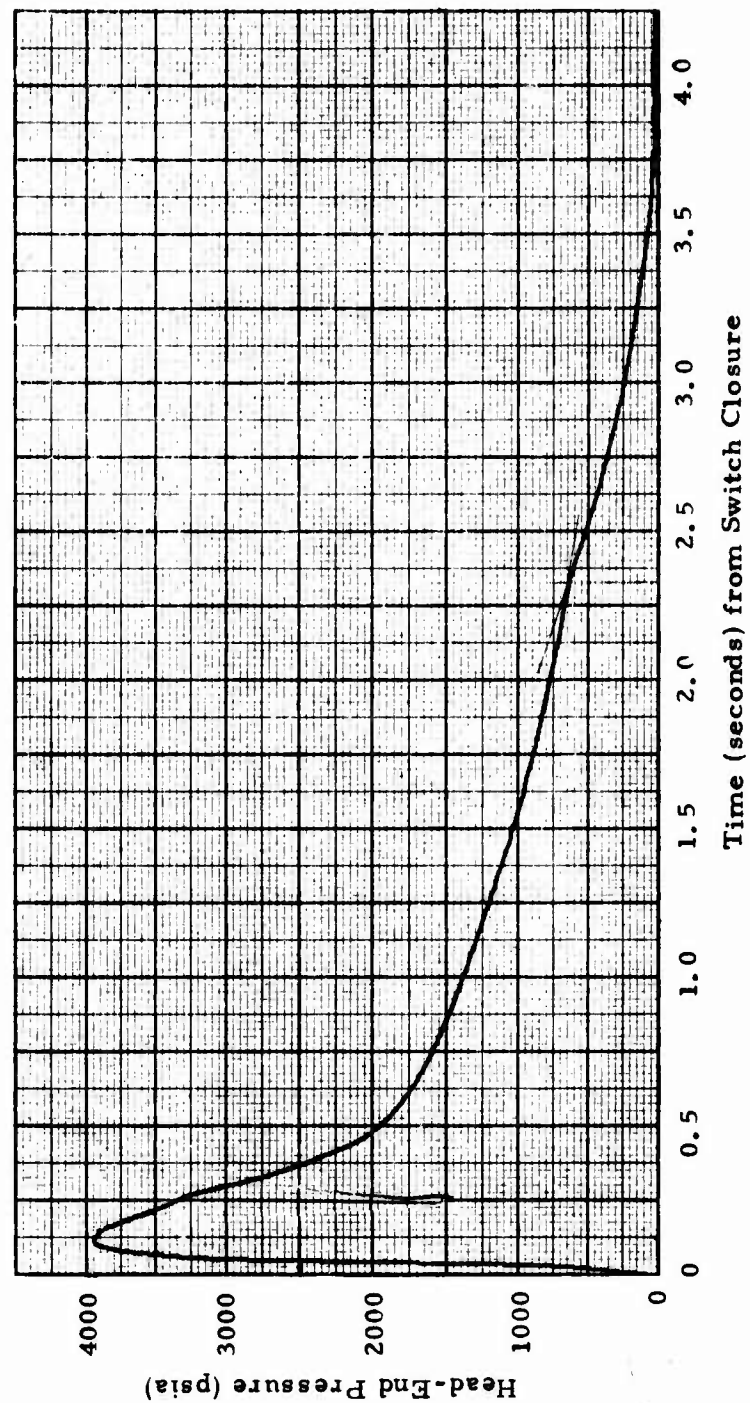


Figure VI-8. Ballistic History, TX-631 Motor, Mix T-634, Charge 1 Fired at 70°F

propellant to determine effects of propellant rheology on grain quality. A mandrel (12 lb/cu ft) was inserted into the propellant cavity. An additional objective was to determine if a modified igniter charge (50% pellets, 50% powder, instead of all pellets) would decrease pressure rise time from that of T634-1. The second motor from Mix T640, Charge 2, was vacuum cast with conventional tooling. It had a "high" density consumable mandrel (17 lb/cu ft) inserted into the propellant cavity after propellant cure was complete and an igniter with the modified charge. All three motors were equipped with routine TX631 polyisoprene insulation and ATJ graphite throat inserts.

The two motors loaded with TP-H8208 propellant from Mix T640 were successfully static tested after being conditioned to 70° F.

	Mix T640	
	Charge 1	Charge 2
Propellant Manufacturing Technique	Pour-cast	Vacuum-cast
Number of Voids	Hundreds	20
Mandrel Density (lb/cu ft)	12	17.5
Mandrel S/N	24	28
Maximum Ignition Pressure (psi)	3476	4963
Maximum Pressure (psia)	3750	4963
TD50 (sec) <sup>1</sup>	0.046	0.046

Pressure-time histories are shown in Figures VI-9 and VI-10. Pertinent performance parameters and other information are listed in Table VI-2.

Graphite nozzle throat inserts were used because the tests were considered as high risks and there was a desire to use candidate ablative materials only on tests where there was reasonable chance of obtaining useful erosion information. The graphite eroded uniformly with only slight distortion due to gas flow from the grain longitudinal slots.

Based on comparison of these two motors, the presence of the higher density foam mandrel in T640-2 caused a large increase in the ignition pressure. Because the grain of T640-2 was of higher quality than the pour-cast grain of T640-1, it is reasonably certain that the higher ignition pressure of T640-2 was caused by the foam mandrel.

---

1. Time interval from switch closure to when pressure is 50% of maximum pressure on the first sustained pressure rise.

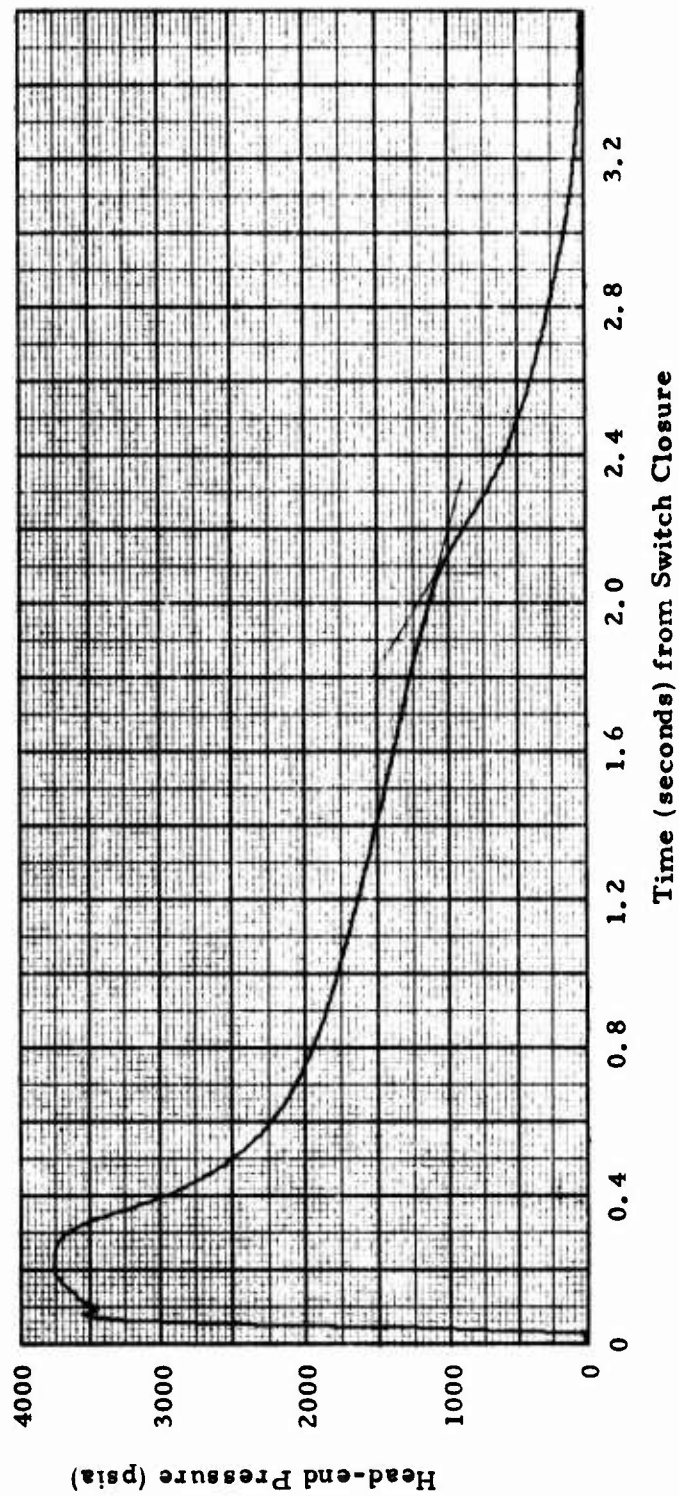


Figure VI-9. Ballistic History, TX-631 Motor, Mix T-640, Charge 1, Fired at 70°F

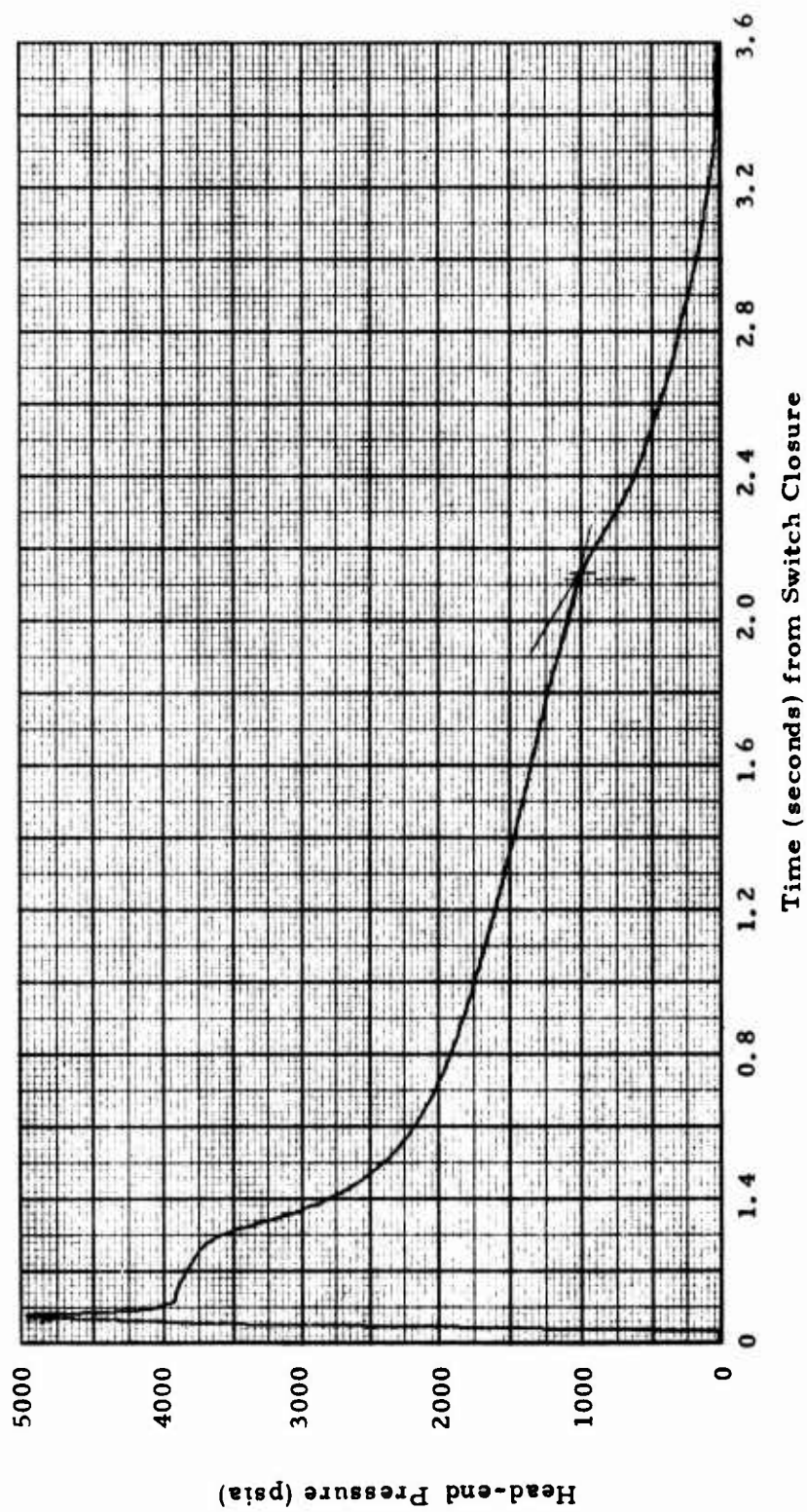


Figure VI-10. Ballistic History, TX-631 Motor. Mix T-640, Charge 2, Fired at 70°F

Motor T640-1 should be compared to T634-1 for evaluation of grain quality characteristics:

	<u>T634-1</u>	<u>T640-1</u>
Mandrel density (lb/cu ft)	12	12
Propellant	TP-H8208	TP-H8208
Grain Manufacturing Technique	Vacuum-cast	Pour-cast
Number of voids	35 (0.2" max)	Hundreds
Igniter	All pellets	Pellets/powder
Maximum Pressure (psia)	3951	3750
Ignition Pressure (psia)	3951	3476

Exact comparisons of ignition characteristics cannot be made because a change was made in igniter pellet/powder ratio at the same time the pour-cast grain was introduced. However, the successful operation of T640-1 does illustrate that the poor quality grain resulting from pour casting did not inherently compromise satisfactory motor operation.

The motor loaded with DTS-7984 propellant (ambient temperature cure) from Mix T630 failed at ignition as a result of a pressure fitting blowing out of the forward closure at a pressure between 10,000 and 12,000 psia (Figure VI-11). Gas escaping through the resultant opening burned a large hole in the forward closure; the closure retaining ring, case and nozzle were unharmed. The instrumentation system was calibrated to 6500 psia so the final failure pressure is an estimate.

The grain for Motor T630-1 was manufactured by pour-casting technique. It was of poorer quality than the T640-1 grain because the rheology of DTS-7984 is less suitable than that of TP-H8208 for pour-casting (Section V). Ignition was by BKNO<sub>3</sub> pellets in a head-end mounted tube. There was no foam mandrel in the propellant cavity. The loaded case had been cycled to -65°F conditioning temperature. Radiographic re-inspection did not show any change from the first post-cure inspection. Visual inspection of the grain ends did not reveal any separations.

Figure VI-11 pressure history and the expanded presentation of Figure VI-12 show an inflection point at about  $t = 0.04$  sec, which could be a result of the motor starting to reach an equilibrium pressure (of about the expected 4000 psia). Then pressure resumed rising at an increasing rate (until the last observation was made at  $t = 0.046$  second). Figure VI-13 shows the similarity of initial pressurization of T630-1 and T622-2, which also had the tube igniter, no consumable mandrel, and TP-H8208 propellant. A pre-test calculation with the burn rate of DTS-7883 propellant (rate of DTS-7984 was assumed to be the same, see Section IV) predicted a maximum pressure of 3500 psia (Figure VI-14). Conventional erosive burning characteristics were used in this calculation. If erosive burning parameters deduced



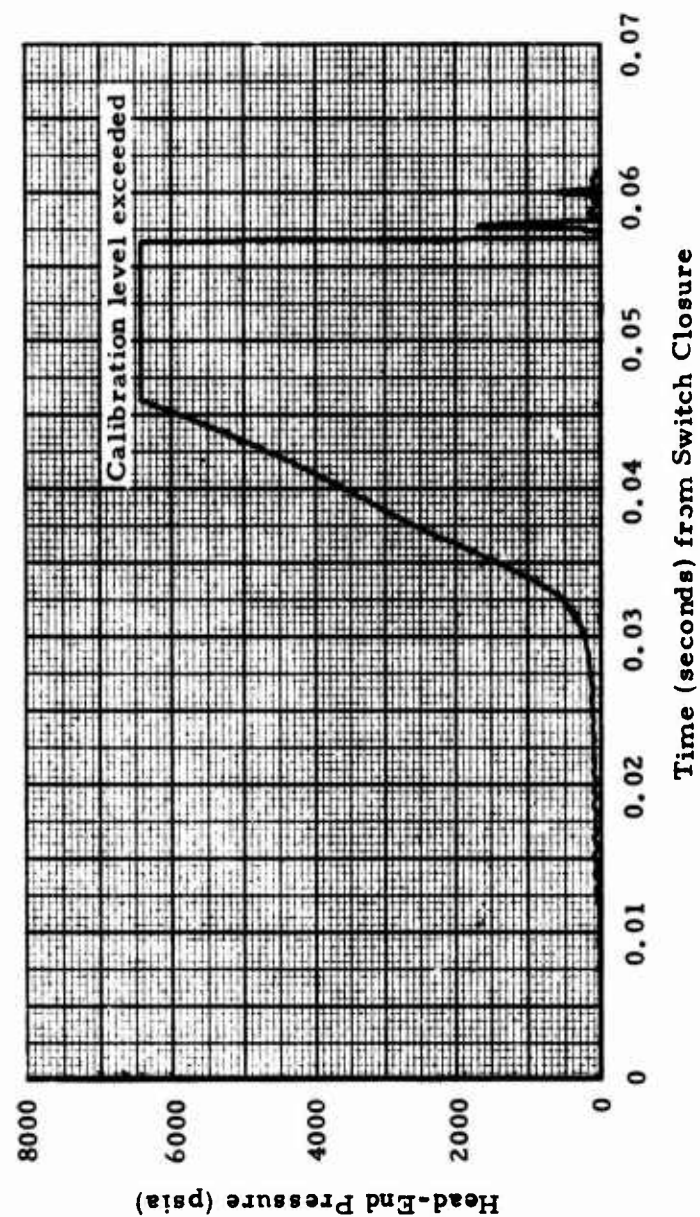


Figure VI-11. Ballistic History, TX-631 Motor, Mix T-630, Charge 1, Fired at 70°F

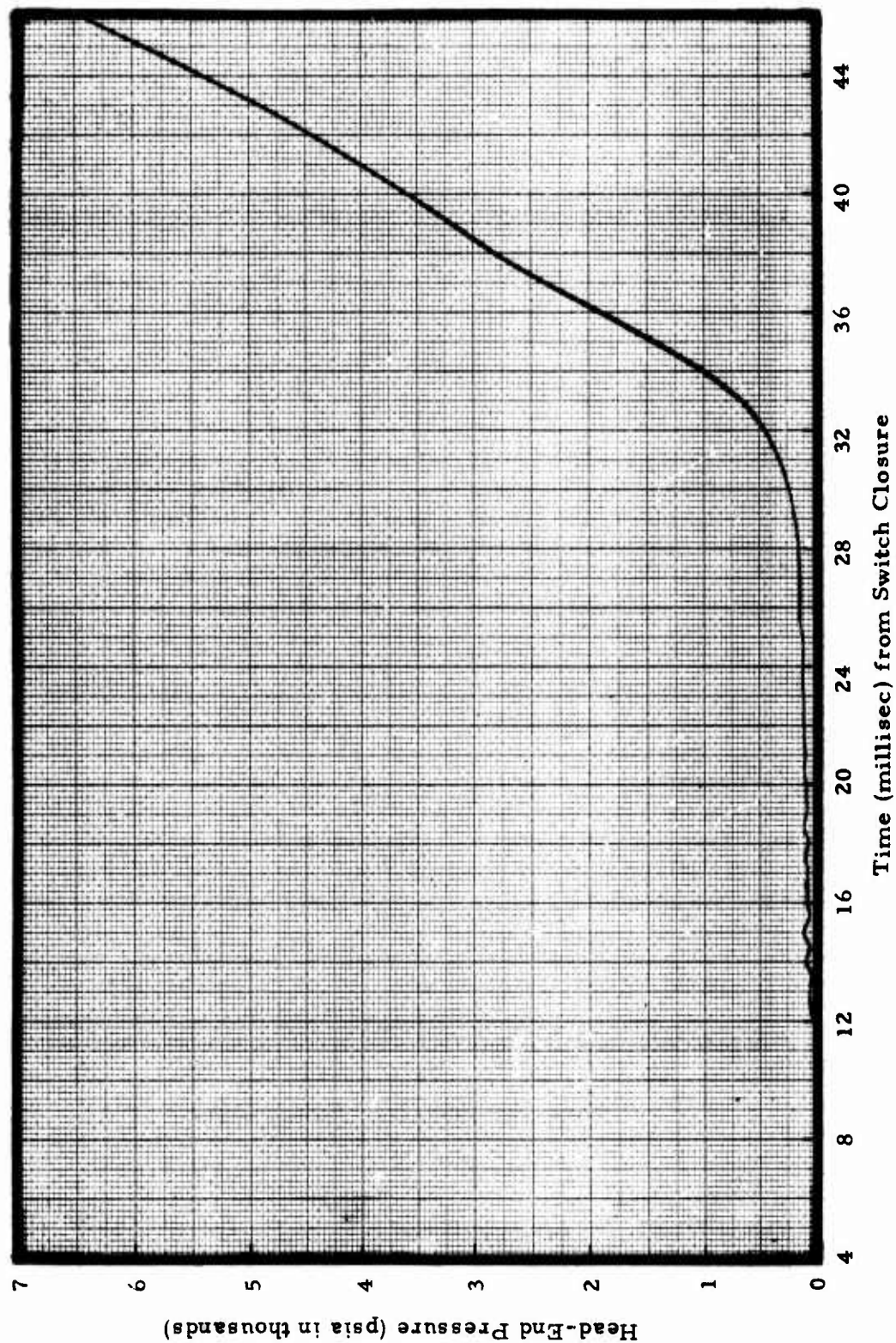


Figure VI-12. Ignition Phase of TX631, Mix T630-1



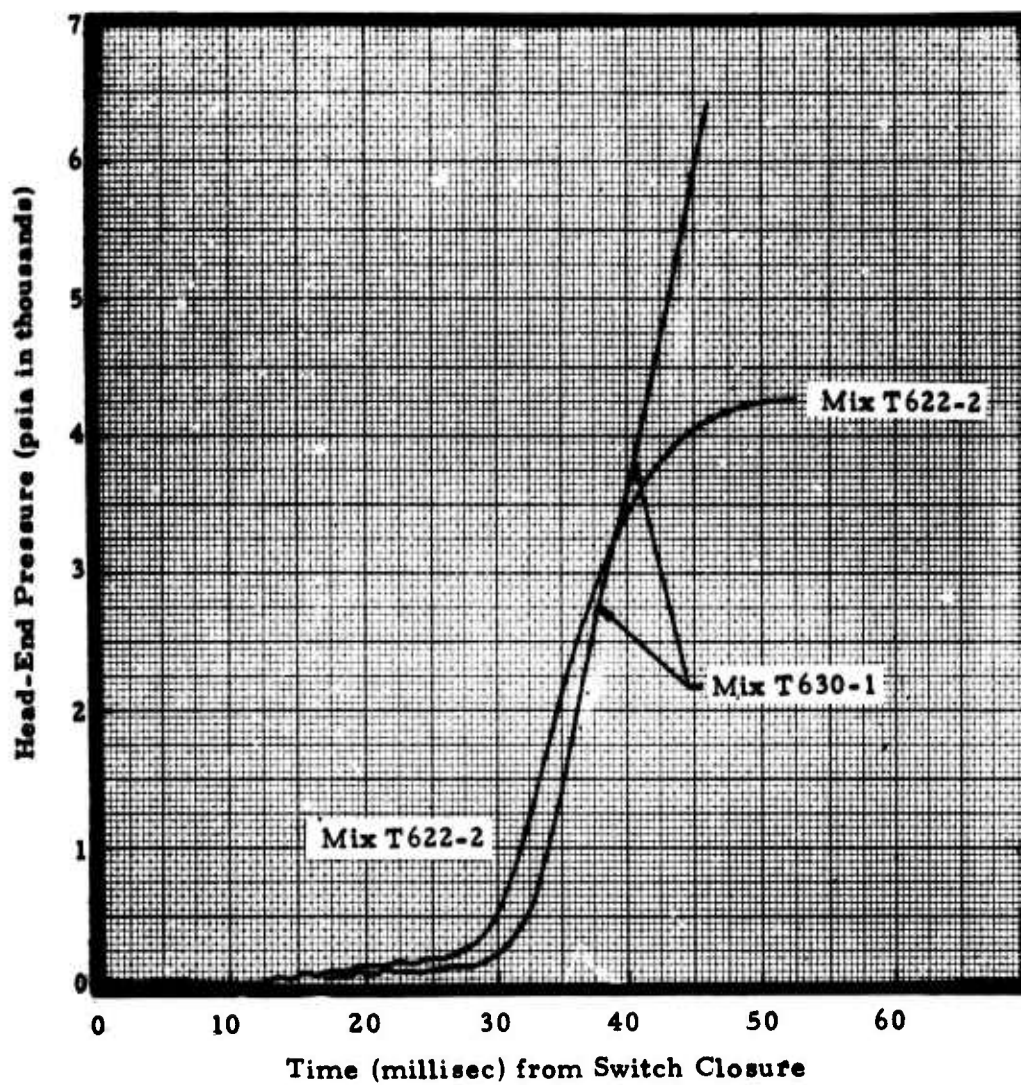


Figure VI-13. Comparison of Ignition Phases of T 622-2 and T 630-1

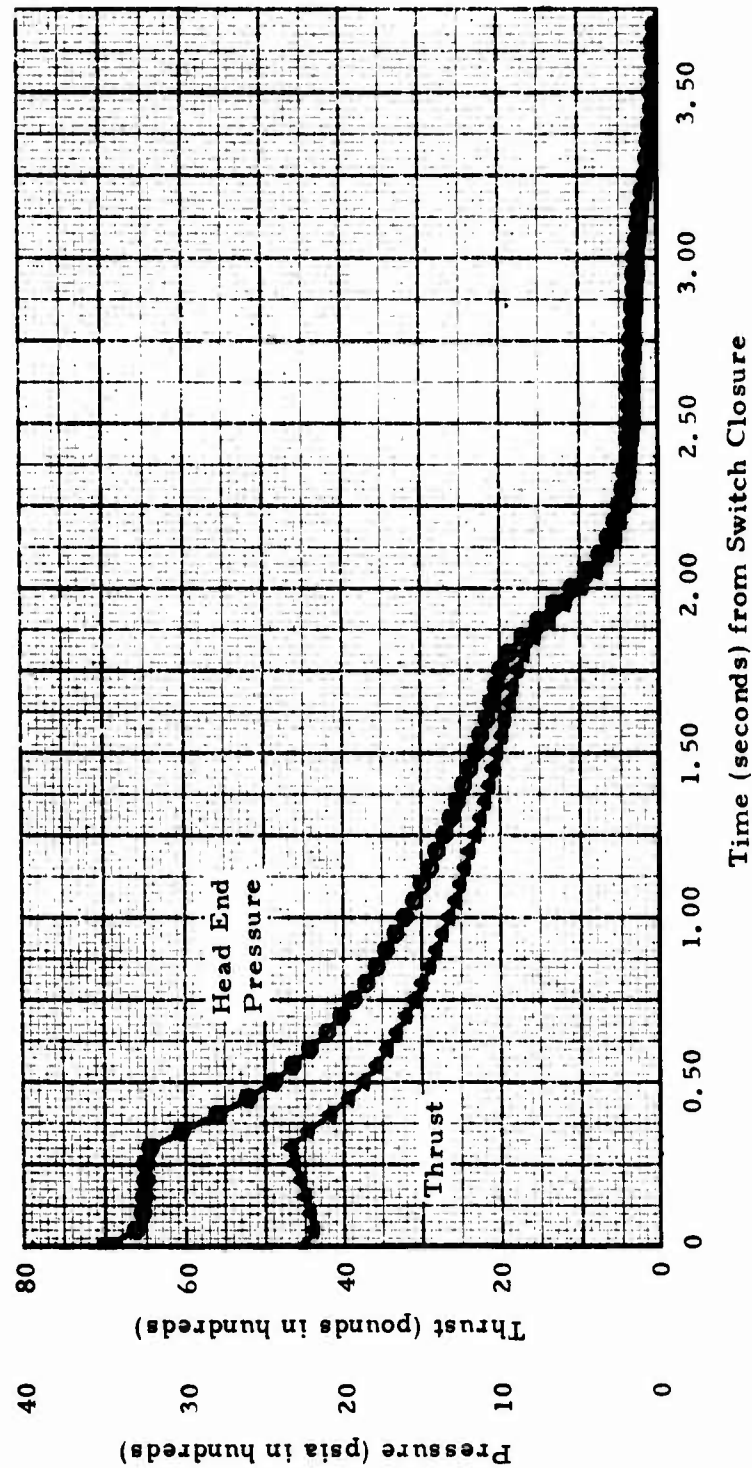


Figure VI-14. Ballistic Prediction of TX-631 Motor with DTS-7883/DTS-7984 Propellant, Fired at 70°F

from the test of T622-1 are used to establish an upper bound, the predicted maximum pressure becomes 6400 psia (Figure VI-15), keeping in mind the reservations about the validity of  $M_{crit}$  and  $x$  expressed in the preceding discussion. Because of the limited data available on propellant basic burn rate and its erosive burning characteristics, cause of T630-1 over-pressurization cannot be determined exactly. Once the motor went to pressures so much greater than 3000 psia, burn rate extrapolation becomes inexact and erosive burning characteristics are not well defined. Although it is possible the over-pressurization was caused simply by the nozzle being unable to pass the flow resulting from "normal" propellant burning, at this point there are opposing inferences about the grain quality requirements with regards to grain manufacturing techniques.

#### Group No. 4

Motors vacuum cast with TP-H8208 propellant from Mix T643 (Charges 1 and 2) were tested to determine igniter/mandrel interaction at the temperature extremes (-65°F and 165°F, respectively). Consumable mandrels (12 lb/cu ft) were coated with a mold release agent (MR-22) and inserted into the propellant cavity formed by conventional tooling. Both motors had the pellet/powder igniter charge in the mandrels. The second motor from Mix T634 (Charge 2), also with TP-H8208 propellant, was added to the test group to determine if a doubled igniter charge weight (still 50% powder, 50% pellets) would, with an identical consumable mandrel, alleviate the hangfire experienced by T643-2 at 165°F. All three motors had candidate nozzle ablative materials and routine TX631 polyisoprene case insulation.

Motor T-643-1, after being conditioned to -65°F for 12 hours, operated satisfactorily and as expected (Figure VI-16). Ignition time was comparable to that experienced in previous tests which had identical igniters, e. g., T640-1.

Mix and Charge No.	T-643-1	T-640-1
Conditioning Temperature, °F	-65	+70
Mandrel Density	12.1	12.0
TD50 (sec) <sup>1</sup>	0.0545	0.0463
Maximum Pressure (psia)	3705	3750

Motor T643-2 experienced a 2.675-second hangfire (Figure VI-17). The igniter appeared to operate properly, but full ignition did not occur. At about 2.6 seconds after switch closure chamber pressure started to rise and rose to an eventual maximum of about 2200 psia. The hangfire was attributed to differential thermal expansion between mandrel and propellant causing the gap (inherent because of slip fit at 70°F) between the two to disappear (see Section VIII for details). Throat erosion measurements still were valid.

Motor T634-2 was established as a duplicate of T643-2 (except for a

- 
1. TD50 = time interval from switch closure to when pressure is 50% of maximum pressure on the first sustained pressure rise.

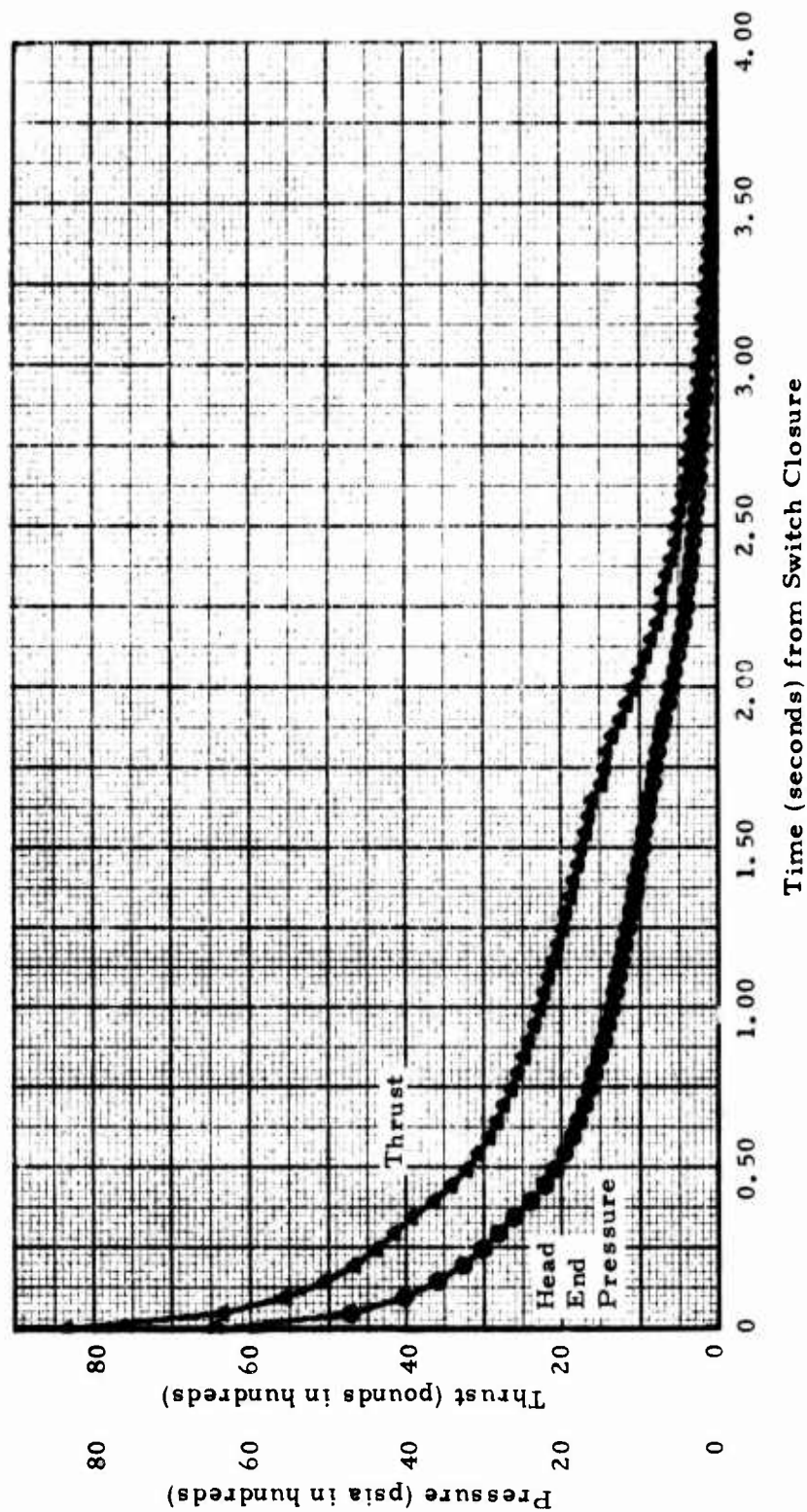


Figure VI-15. Ballistic Prediction of TX-631 Motor with DTS-7984 Propellant and T622-1 Erosive Burning, Fired at 70°F

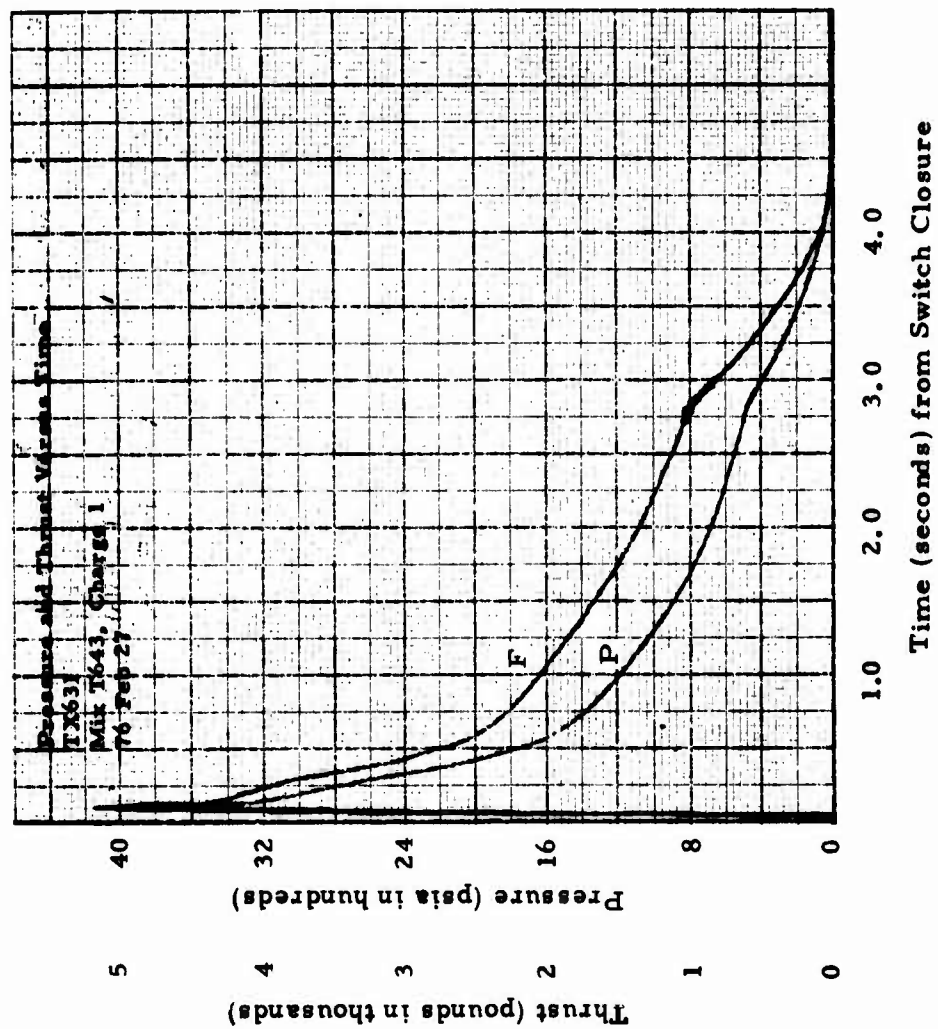


Figure VI-16. Ballistic History, TX-631 Motor, Mix T-643, Charge 1, Fired at -65°F



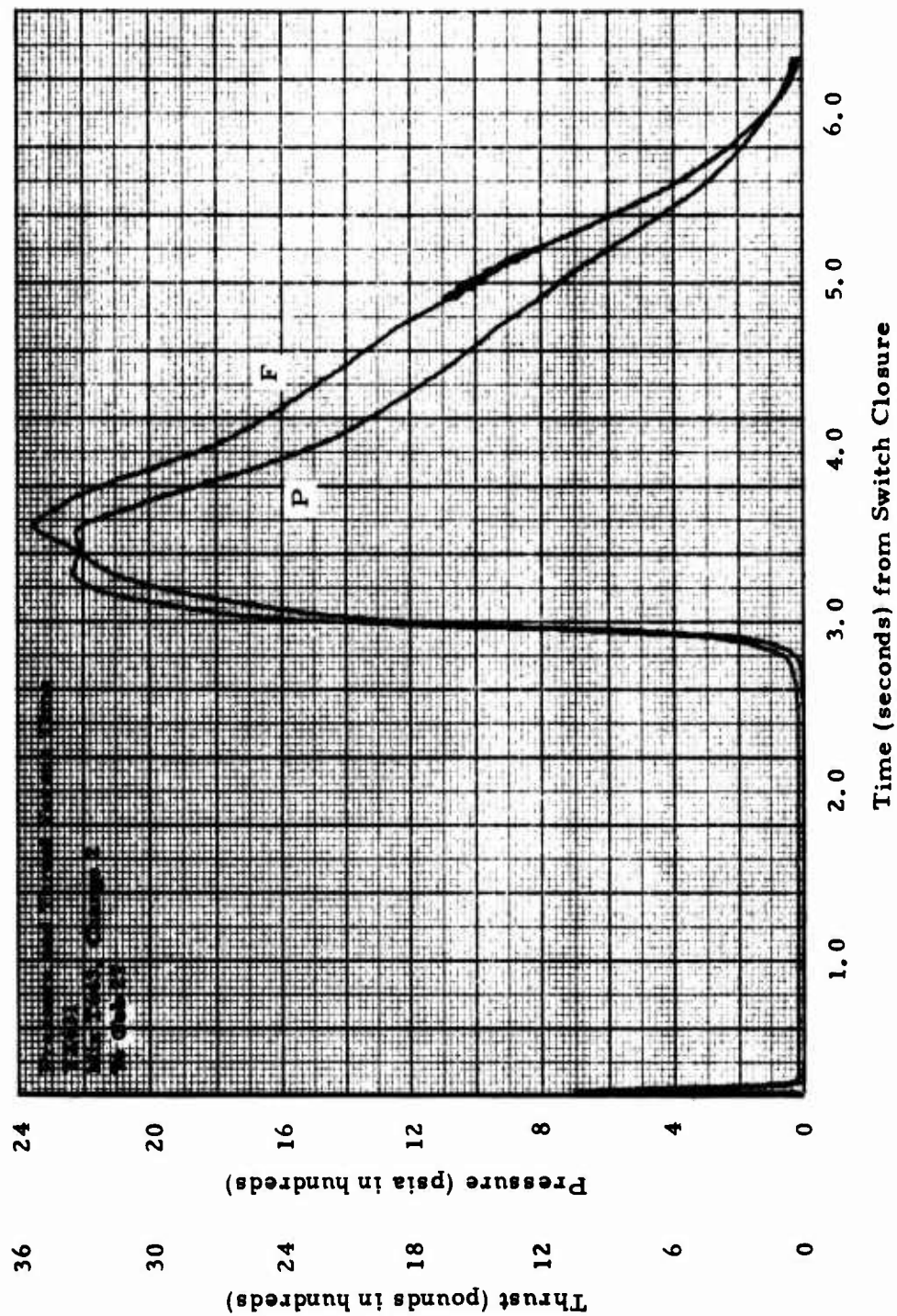


Figure VI-17. Ballistic History, TX-631 Motor, Mix T-643, Charge 2, Fired at 165°F

different candidate nozzle material). The igniter charge was doubled to 20 gm pellets and 20 gm powder to more rapidly burn away the mandrel. It was hypothesized the foam was acting as an inhibitor to the propellant surface and the increased energy output would consume the foam more rapidly. Prior to static firing T634-2, the case (with foam mandrel in place) was assembled to two forward closures. Nitrogen was introduced at the forward end and the time for a transducer at the nozzle end to respond was measured, first with the motor at 70 °F and then again with it conditioned to 165 °F. It took much longer at 165 °F, indicating that flow passages from forward end to nozzle end had been closed because of the higher temperature. (See Section VIII for more details).

Results of the static test verified the hypothesis (Figure VI-18 and VI-19), although there was still a hangfire (0.155 second). The usual point of measuring ignition response (pressure equal to 50% of maximum pressure) was not reached until about 0.40 second after switch closure, which is still an unacceptable delay. Figure VI-20 shows the igniter functioned as expected and caused a pressure not too much higher than the previous test with a 20 gm igniter (1075 psia versus 700 psia).

Characteristic velocity,  $C^*$ , calculated for T634-2 was significantly lower than the average of all other motors (5200 ft/sec, excluding T622-2). Throat erosion was moderate. As discussed in connection with T622-2, the most likely explanation is the throat diameter enlarging very rapidly at the start of motor operation, but then ablating at a much lower rate for the remainder of the test, with the result that actual average throat diameter is much greater than the post-test calculated value. "Gouging" of the D22532 material in T634-2 was among the worst experienced on the tests (Section IX).

#### Group No. 5

The two motors (Charges 1 and 2) from the last mix (T684) to be manufactured in Phase II were already loaded when results of the T634-2 test became available; so, the test objectives adapted for these two motors were tempered by the configurations available to work with. Propellant grains in both motors were formed by consumable mandrels, one with 12 lb/cu ft density, the other with 14 lb/cu ft. The mandrels were left in place following completion of propellant cure.

Since increased energy release in T634-2 had reduced the duration of hangfire, a means was sought to further increase the magnitude and duration of energy release during the "ignition phase". A section (1.5 inches long) of the cylindrical portion of the mandrel in the forward end of T684-2 was removed prior to motor assembly so that propellant surface was directly exposed to the igniter combustion products. Motor T684-2 was selected for this modification because it had a 12 lb/cu ft mandrel. The igniter charge weight was set at the original 20 gm (50% powder, 50% pellets) because the



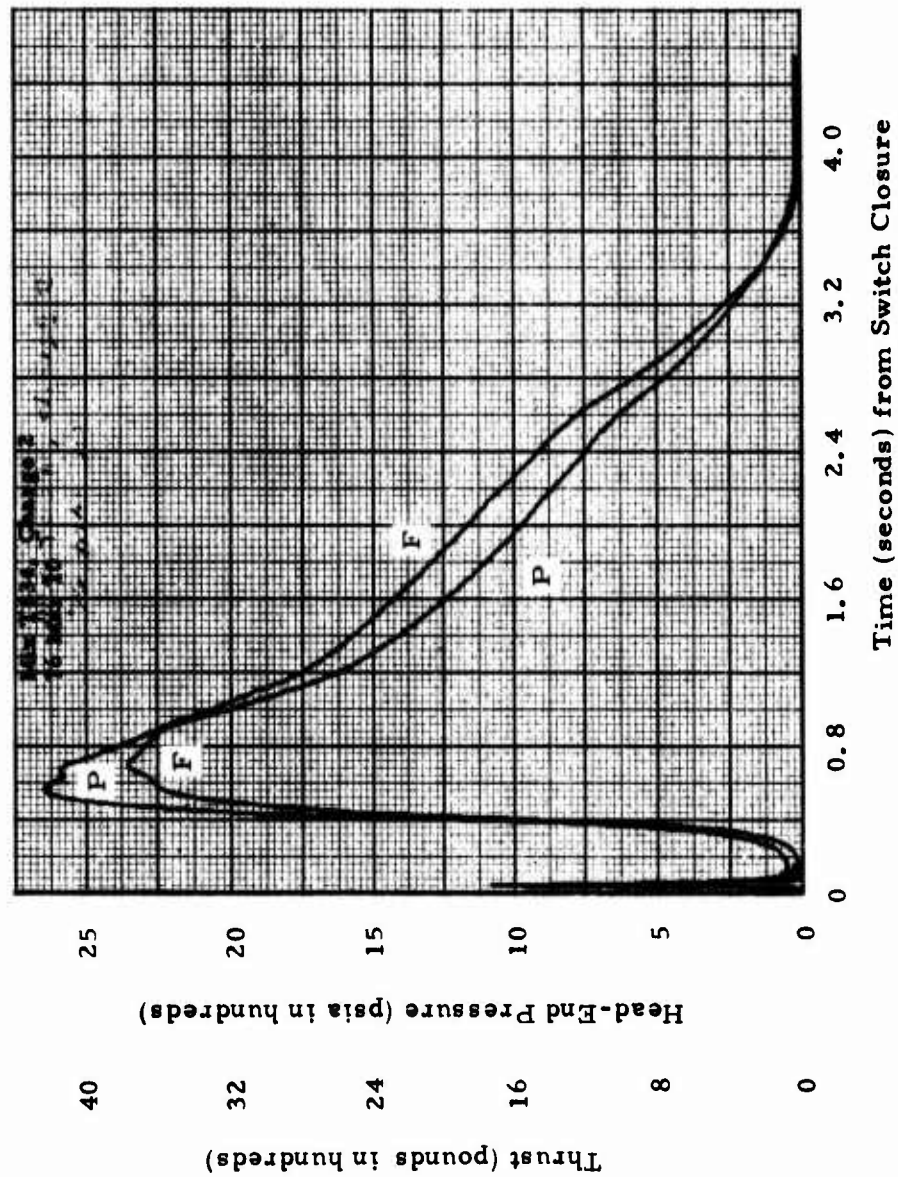


Figure VI-18. Ballistic History, TX-631 Motor, Mix T-634, Charge 2, Fired at 165°F

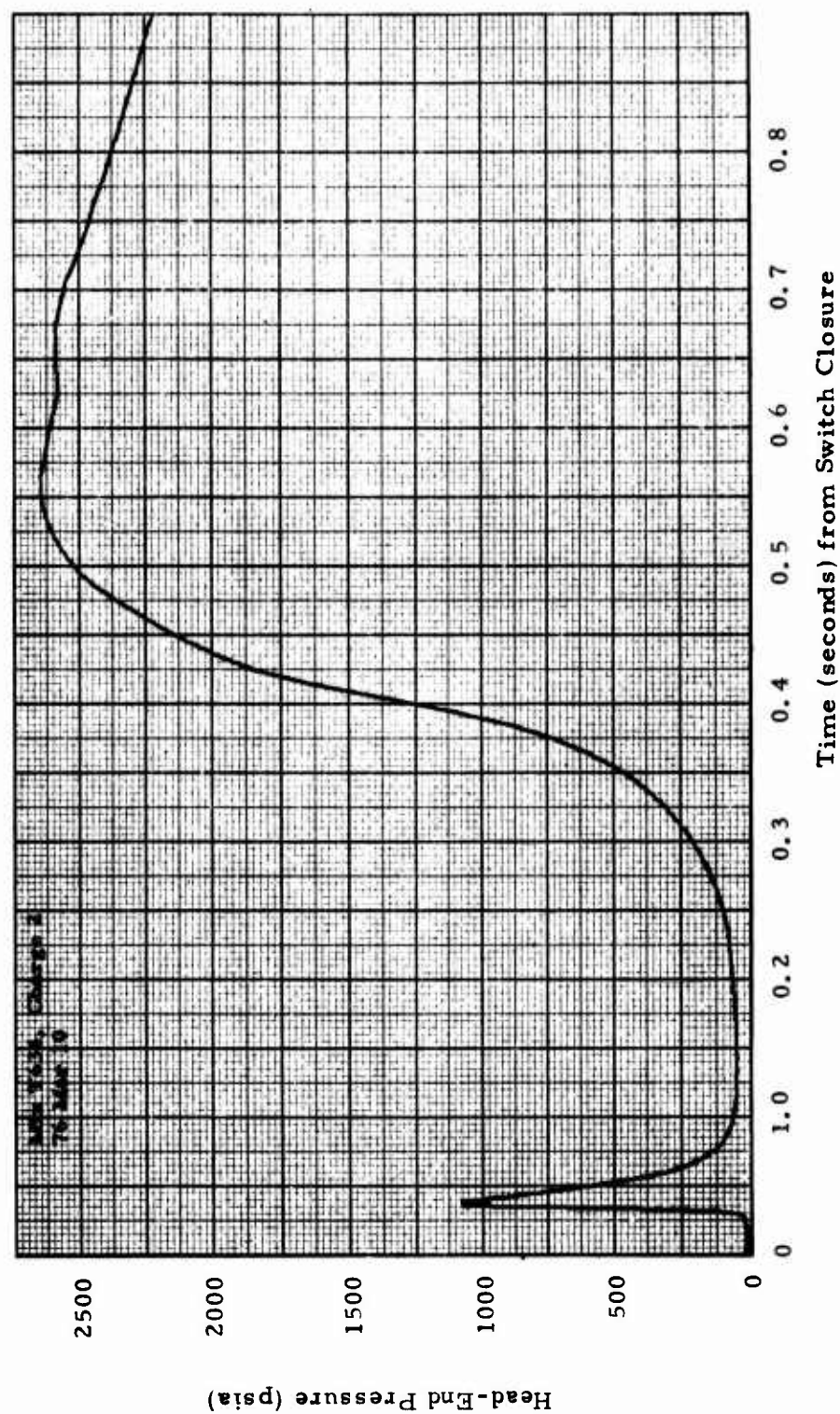


Figure VI-19. Ignition Phase, TX-631 Motor, Mix T-634, Charge 2, Fired at 165°F

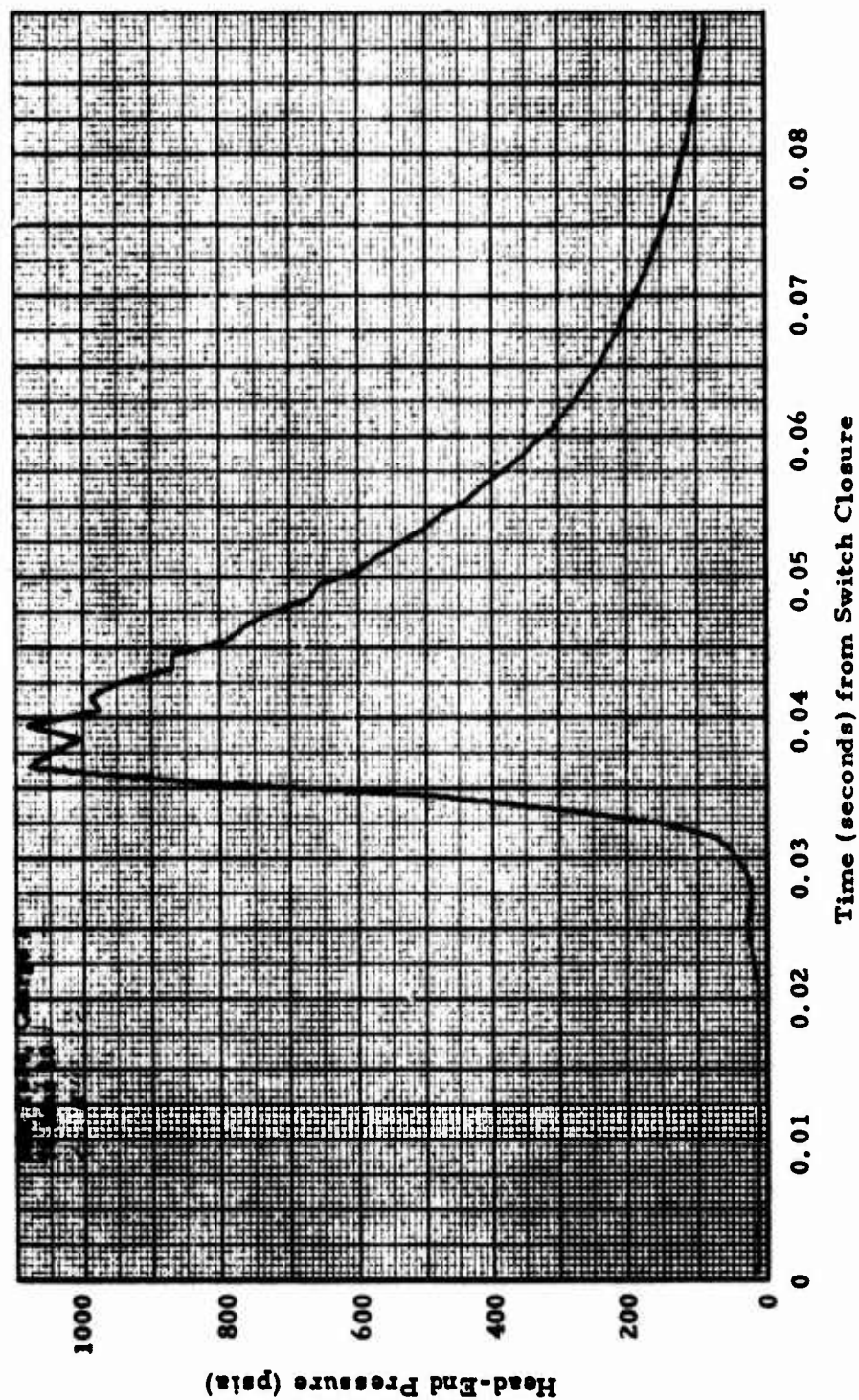


Figure VI-20. Igniter Operation, TX-631 Motor, Mix T-634, Charge 2, Fired at 165°F

motor propellant was to produce the increased heat release. The igniter charge for T684-1 was also 20 gm because it was manufactured with a "high" density mandrel (14 lb/cu ft) and there was concern for the effects this might have on maximum pressure (per T640-2).

Motor T684-1 contained the standard configuration of polyisoprene case insulation but was modified to bond samples of two candidate cartridge materials in the aft end. The insulated case was lined with TA-H732A. Motor T684-2 was insulated with 0.25 inch of TI-H706A mastic insulation over the entire interior. The mastic insulation required no liner and after insulation cure the insulated case was assembled for casting with a "low" density (12 lb/cu ft) foam mandrel.

Both mandrels were coated with MR-22 silicone mold release. The mold release was applied by spraying a solvent-diluted solution onto the mandrels and allowing the mold release to air dry to a non-tacky surface. The mandrels were centered in the casting assembly and held in place by engaging a head end stud (with O-ring) in the igniter cavity in the forward end of the mandrel. The fins on the mandrel used in T684-1 had to be trimmed to fit over the thermoplastic samples bonded in the insulated case.

The loaded motors were held at room temperature for 10 days prior to "finishing" the motors. With the foam mandrel, there is no core removal operation, but the casting fixtures must be removed and the excess propellant and mandrel trimmed from the aft end. Casting sleeve removal was difficult and in neither motor did the foam mandrel release from the propellant. When the casting sleeve propellant was peeled from the foam mandrel, the separation generally left a thin coat of propellant on the mandrel with less than 10% of the propellant releasing cleanly from the MR-22 coated mandrel.

Radiographic inspection of the loaded cases with foam mandrels in place presented a particular problem. Without extensive use of triangulation techniques, an accurate distinction could not be drawn between voids in the foam material of the mandrel and voids in the propellant. The inspection of loaded cases T684-1 and T684-2 detected 4 voids and 68 voids respectively, but no separations, unbonded areas, or cracks.

Because of the uncertainties in calculating maximum pressure with DTS-7984 propellant (discussed as part of Group No. 4 results), the initial burning surface was reduced by inhibiting both ends of the propellant grains with TA-H731A liner. Both motors were tested at 70°F because it was anticipated that there would not be much (if any) gap between mandrel and propellant; the propellant was cured at this temperature and there was visual evidence of incomplete propellant release from the mandrel.

Motor T684-1 had a short hangfire almost identical to that T634-2 (Figure VI-21 and VI-22). After the igniter operated, the motor did not experience a sustained pressure rise for about 0.15 second and 50% of



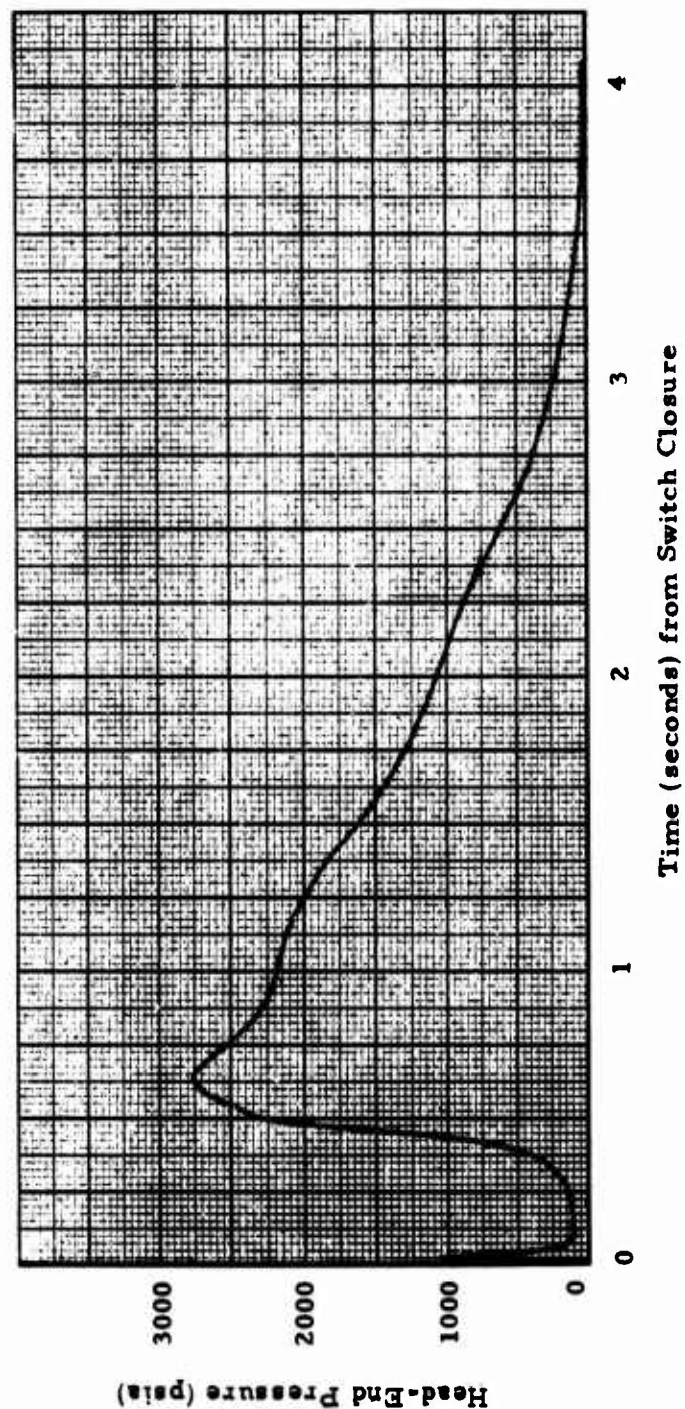


Figure VI-21. Ballistic History, TX-631 Motor, Mix T-684, Charge 1, Fired at 70°F

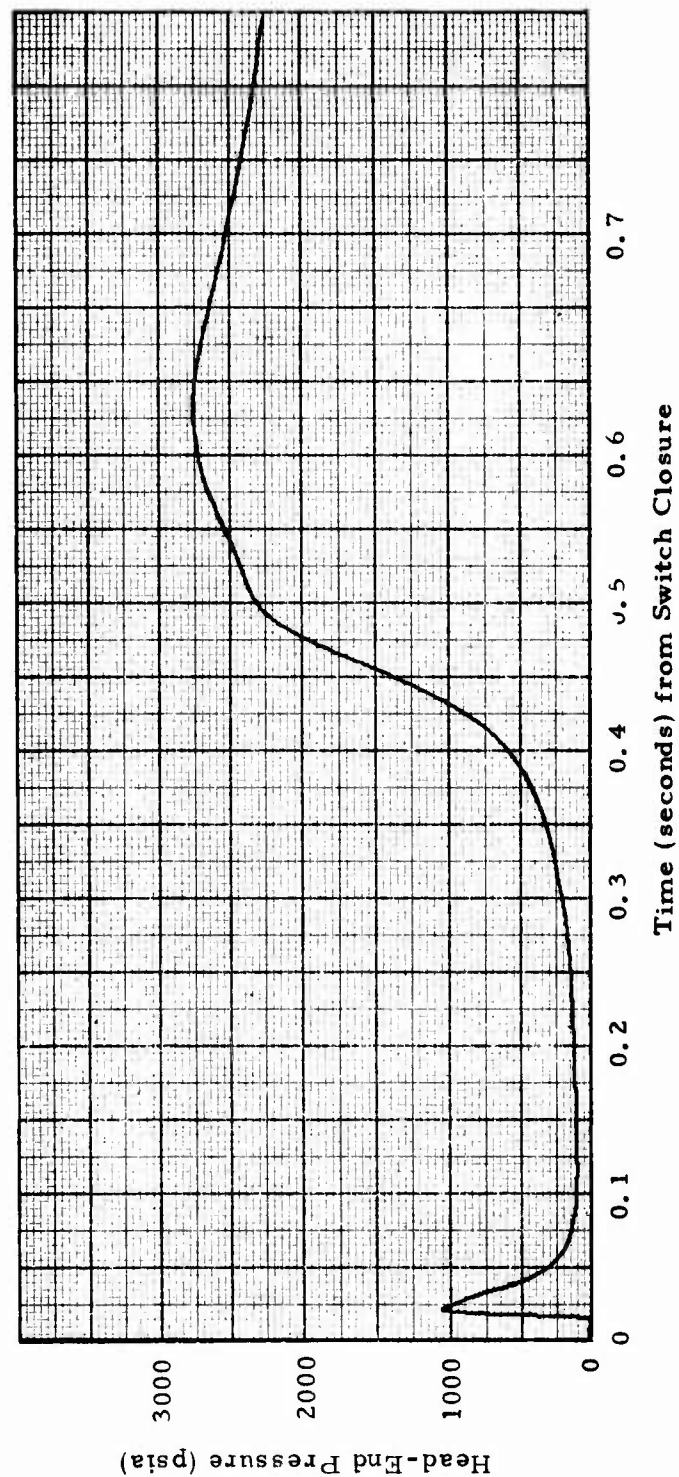


Figure VI-22. Ignition Phase, TX-631 Motor, Mix T-684, Charge 1, Fired at 70°F

maximum pressure was not achieved until about 0.44 second after switch closure. Output of the 20 gm igniter (Figure VI-23) caused about the same pressure (1060 psia) as did the 40 gm charge in T634-2, attributed to the influence of the higher density mandrel in the former. Otherwise, motor operation was satisfactory; nozzle erosion measurements are valid; an initial evaluation was obtained of erosion resistance of two candidate thermoplastic case insulations (polycarbonate and ABS, both glass filled).

Motor T684-2 had a long hangfire almost identical to that of T643-2, followed by an overpressurization that started about 2.6 seconds after switch closure (Figure VI-24). The igniter produced about the same pressure rise as previous firings (Figure VI-25). It is obvious the specially exposed propellant surface immediately adjacent to the igniter was not ignited. An extensive post-test investigation was conducted and is reported in subsequent paragraphs.

#### Post-Test Investigation of T684-2

##### Test Events

The following paragraphs describe the test using information obtained from movies, pressure records, and post test examination of the fired parts. The source of information is not always referenced but should be self-evident from the context.

Motor T684-2 was mounted in the test cell the same as all other TX631 motors (Figure VI-3). Chamber pressure was measured with a single 10,000 psi Baldwin transducer attached to the forward closure with an oil-filled 1/4-inch diameter tube approximately four inches long. Care was taken during motor assembly to insure the pressure port was open because the inhibitor applied to the grain ends somewhat restricted access from the chamber to port opening. Thrust was not measured. One high speed color movie camera operated at approximately 4000 frames per second (design speed at full line voltage); another color movie camera operated at 64 frames per second. Both cameras recorded all events.

Igniter operation was normal in all respects. Pressure in the motor chamber started to rise about 0.014 second after power was applied to the initiator and reached a maximum of 900 psia at 0.023 second<sup>1</sup>. These parameters are very similar to those recorded for other motors that experienced hangfires.

---

1. All times given in subsequent discussion are measured from when power was applied to the igniter ("Switch Closure")



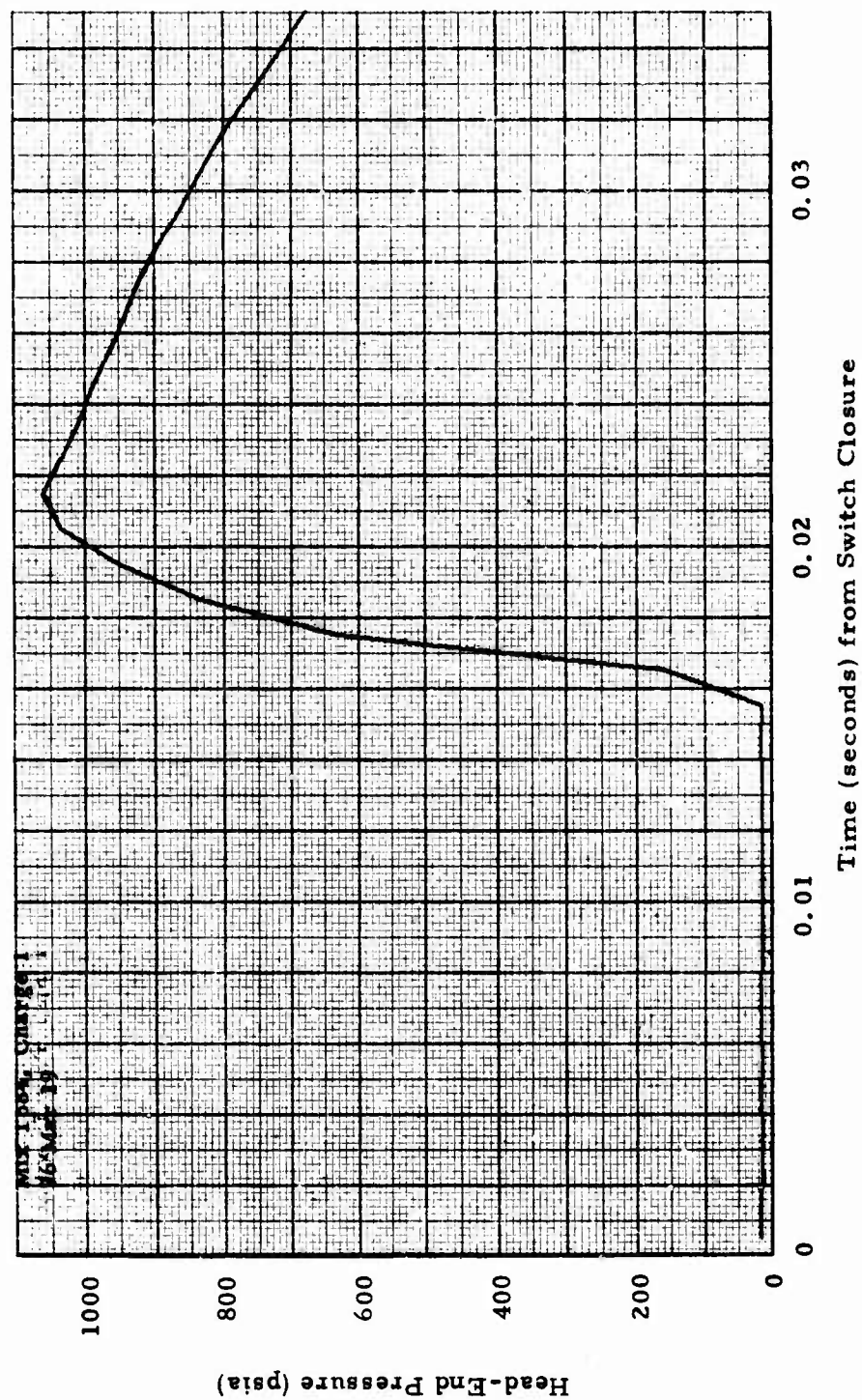


Figure VI-23. Igniter Operation, TX-631 Motor, Mix T-684, Charge 1, Fired at 70°F

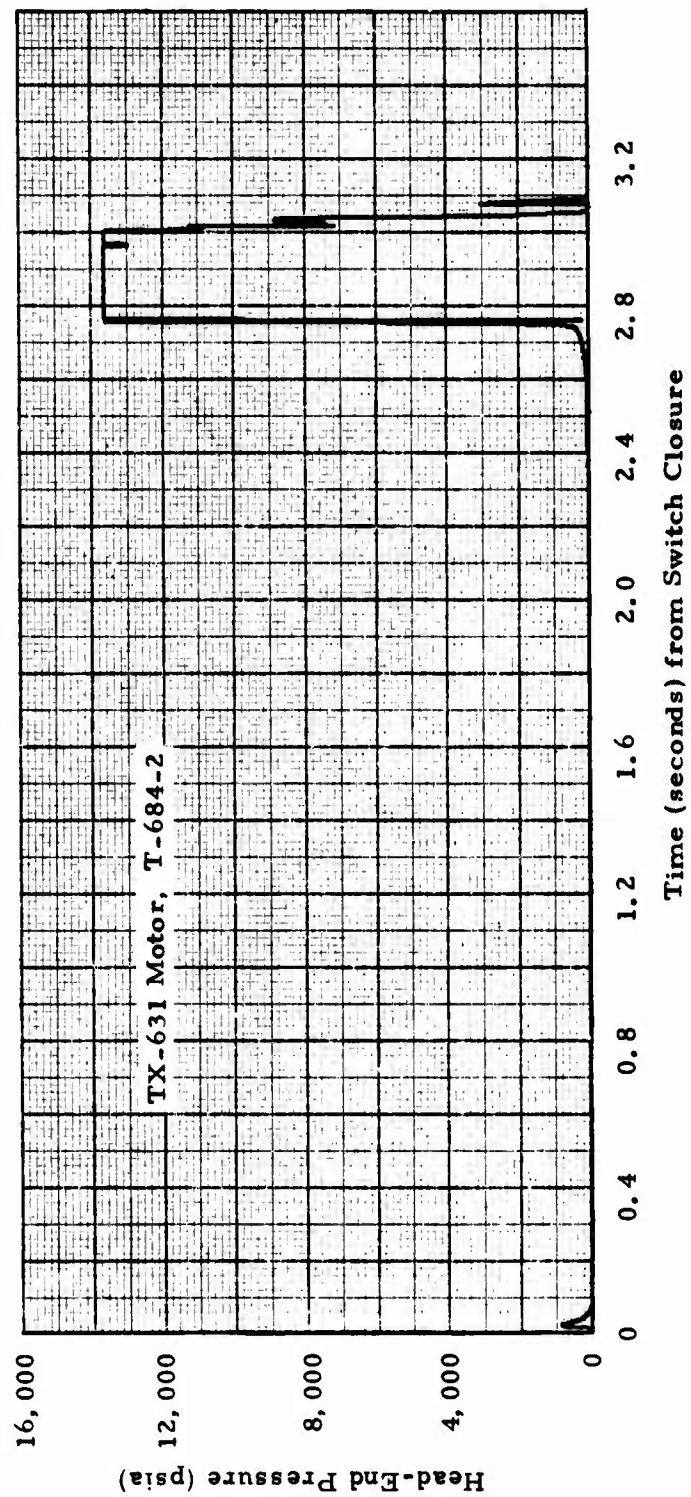


Figure VI-24, Ballistic History, TX-631 Motor, Mix T-684, Charge 2, Fired at 70°F

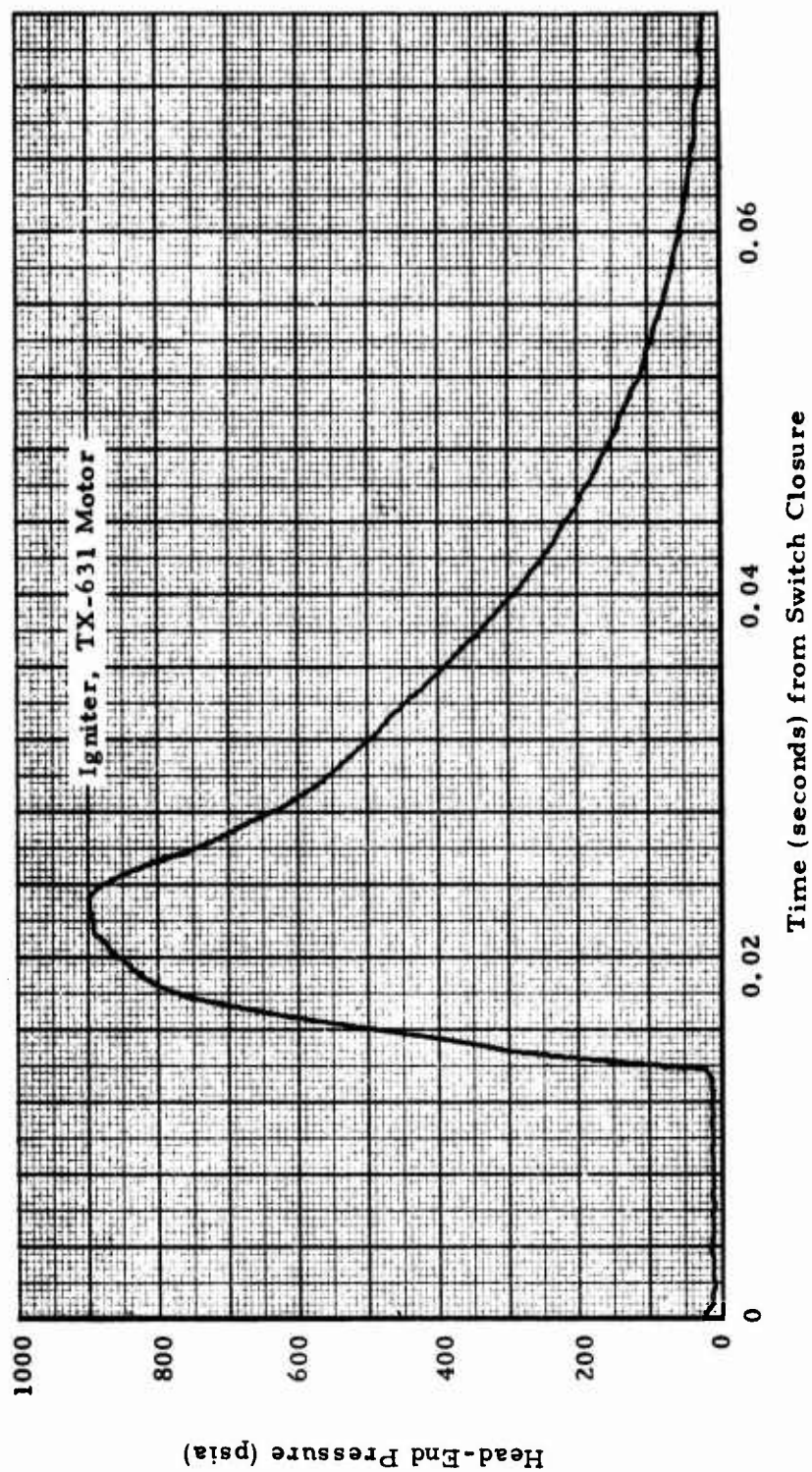


Figure VI-25. Igniter Operation, TX-631 Motor, Mix T-684, Charge 2, Fired at 70°F

	<u>Time Pressure Starts to Increase (sec)</u>	<u>Maximum Igniter Pressure (psia)</u>	<u>Time of Max. Igniter Pressure (sec)</u>
T684-2	0.014	900	0.023
T684-1	0.016	1060	0.022
T634-2	0.020	1075	0.038
T643-2	0.013	700	0.027

Smoke first appeared out of the nozzle at 0.018 second and the first flame was observed at 0.028 second. A single fireball was discharged from the motor and continued to burn as it moved away from the motor and out of the field of view. Pressure decayed to atmospheric at about 0.08 second.

Because the camera aperture was adjusted for normal operation with intense flame illumination, the onset of smoke from the motor cannot be established exactly. However, smoke did come out at least by 0.36 second and was emitted continuously until end of motor operation. Luminosity was seen at 0.73 second. Pressure in the motor was still atmospheric at this time. It was not until about 1.9 seconds that pressure started to increase (albeit very slowly) and by this time the smoke was flowing out with some velocity rather than just "drifting" out. Pressure did not reach 20 psia until about 2.4 seconds at which time still stronger flow was observed.

At 2.429 seconds all luminosity in the plume disappeared (pressure of 20 psia). Then at 2.726 seconds (when the pressure was 300 psia), the plume burst into flame. It had the appearance of normal motor operation, and showed high velocity flow.

Pressure continued to increase until 2.735 seconds in a manner almost exactly the same as experienced by motor T643-2. Indeed, up until this point the two motors had behaved almost identically. However, after 2.735 seconds, the pressure in T684-2 started a more rapid increase.

At 2.742 seconds (660 psia) the visible (luminous) portion of the plume moved away (downstream) from the nozzle exit. At 2.745 seconds (1350 psia) the region between the previously visible portion and the nozzle burst into flame over its entire length. At 2.750 seconds (6000 psia) the plume started to expand in size as would be expected from a motor operating at very high pressure with an under-expanded nozzle.

Flame from the forward end of the motor was first observed at 2.753 seconds. The opening through which the motor was exhausting was either the igniter port (which had been closed by an igniter adapter) or the pressure port (Figure VI-26). A plug in an unused pressure port remained intact. Based only on the relative damage of the two openings, it seems the igniter adapter

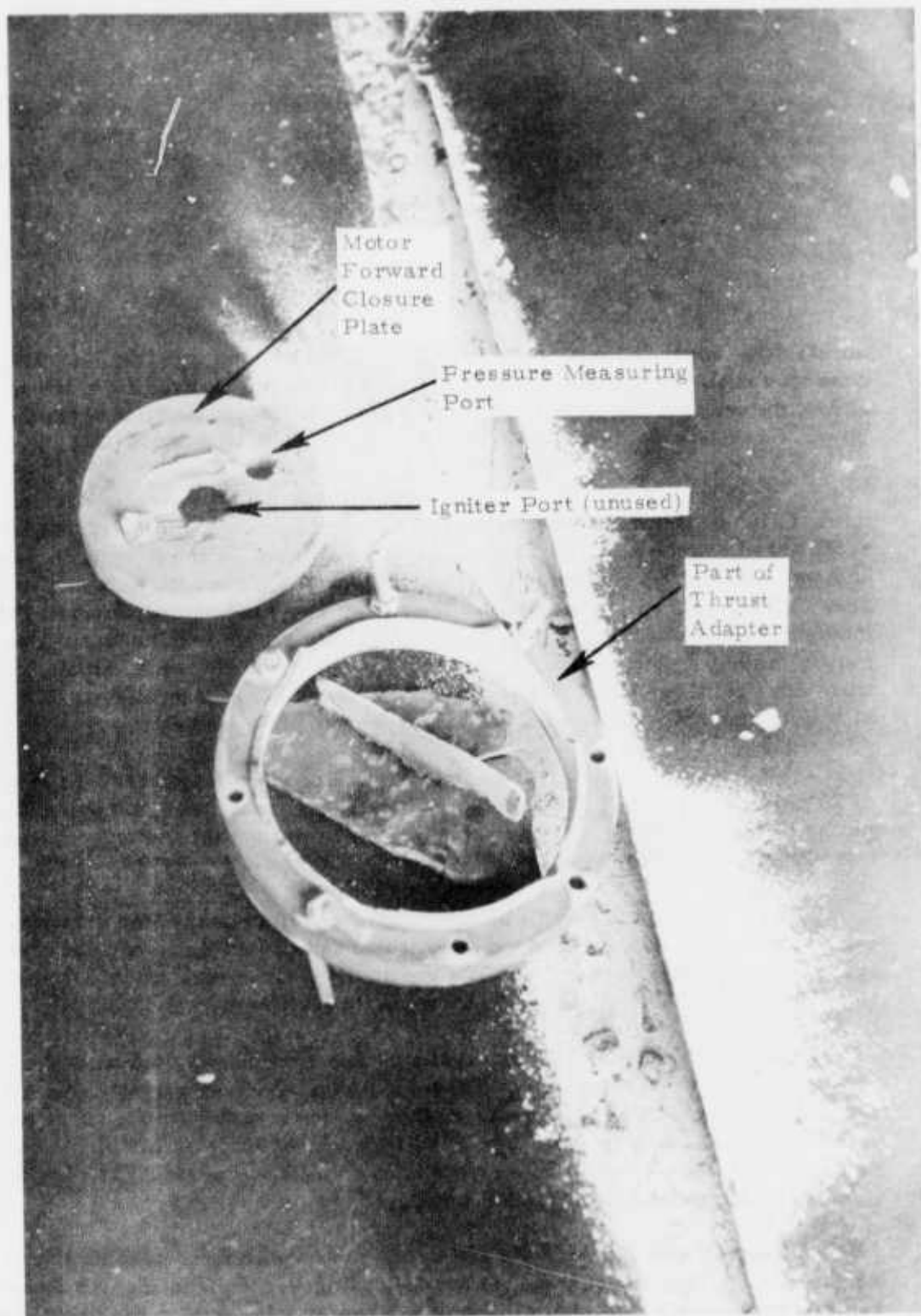


Figure VI-26. Parts Recovered in Test Cell After Test of TX-631 Motor, Mix T-684, Charge 2



was the first to be ejected. Regardless, it is reasonable to assume that pressure measurements stopped when the first flame issued from the forward closure. Pressure at this time was 13,630 psia.

Apparently pressure continued to increase because a lip on the ring holding the forward closure plate in place sheared off, allowing combustion products to flow from a full-diameter opening. The plate shown in Figure VI-26 was found in the test cell. Smoke completely filled the cell and prevented visual observations.

A few milliseconds after the first flame came out of the forward closure, the motor flew out of the thrust stand and the test cell, emerging out of the smoke and flame looking like a horizontal version of a Minuteman missile launch out of a silo. Right behind the motor came a large piece of propellant (Figure VI-27) which was already separated from the motor by about one foot before the motor was completely out of the test cell. The distance between the motor and piece of propellant was increasing as the two disappeared from the field of view. The propellant was about 9 inches long and weighed 1.7 lb.

The large piece of propellant (hereinafter referred to as the "chunk") was not burning even when it first appeared. Other small pieces of propellant were burning as they scattered about, as deduced from their bright luminosity. The chunk showed on the film as a dark object. Even if the chunk had been burning when it first appeared, it was extinguished by the time it hit the concrete and asphalt pavement just outside the test cell. Impact marks on the chunk were not smoothed by subsequent burning and pieces of loose asphalt were embedded in the chunk (Figures VI-27 and VI-28).

The propellant chunk was one-half the grain from the aft end of the motor. It separated along the slots; propellant under the slots was very thin to start with because of extra-thick insulation and some propellant was consumed before the chunk was ejected. Inhibitor was still in place, which identified it as from either the aft or forward ends. The port diameter of 1.5 inches identified it as the aft end (Figure VI-29).

The diametric cracks in the chunk (Figure VI-27 and VI-30) may or may not have occurred before the propellant was ejected. Pushing the cracks closed seemed to indicate there was some small thickness of material missing from the crack surfaces. There is not too much difference in appearance of unburned and burned-but-newly-extinguished propellant surfaces, so visual examination did not reveal anything.

The motor flew across the test area and impacted nozzle-end first on the protective dirt embankment (Figure VI-31). It landed directly downstream of the test cell after first ricocheting off the pavement directly in front of the embankment.

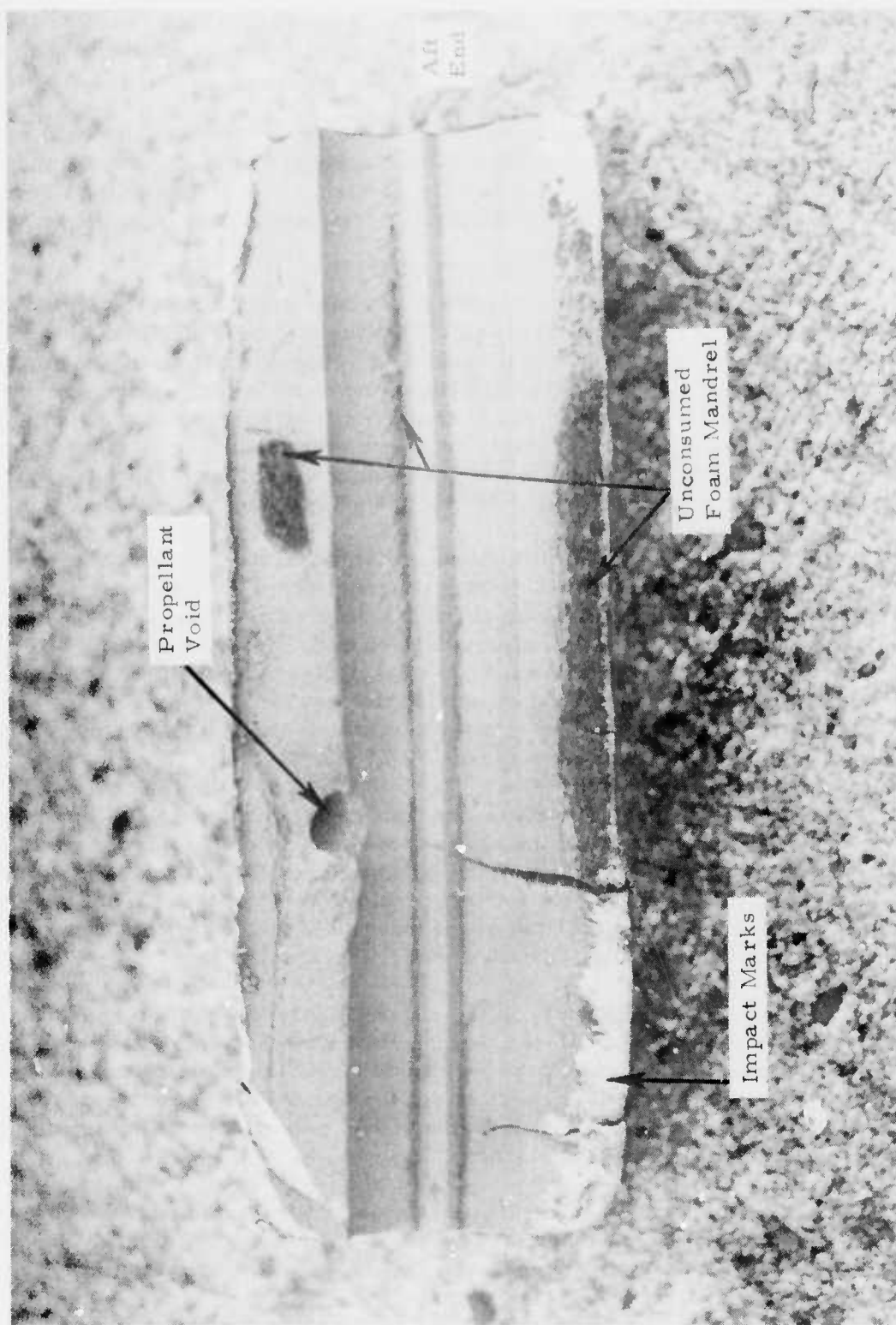


Figure VI-27. Inner Surface of Propellant Recovered from TX-631 Motor, Mix T-684, Charge 2



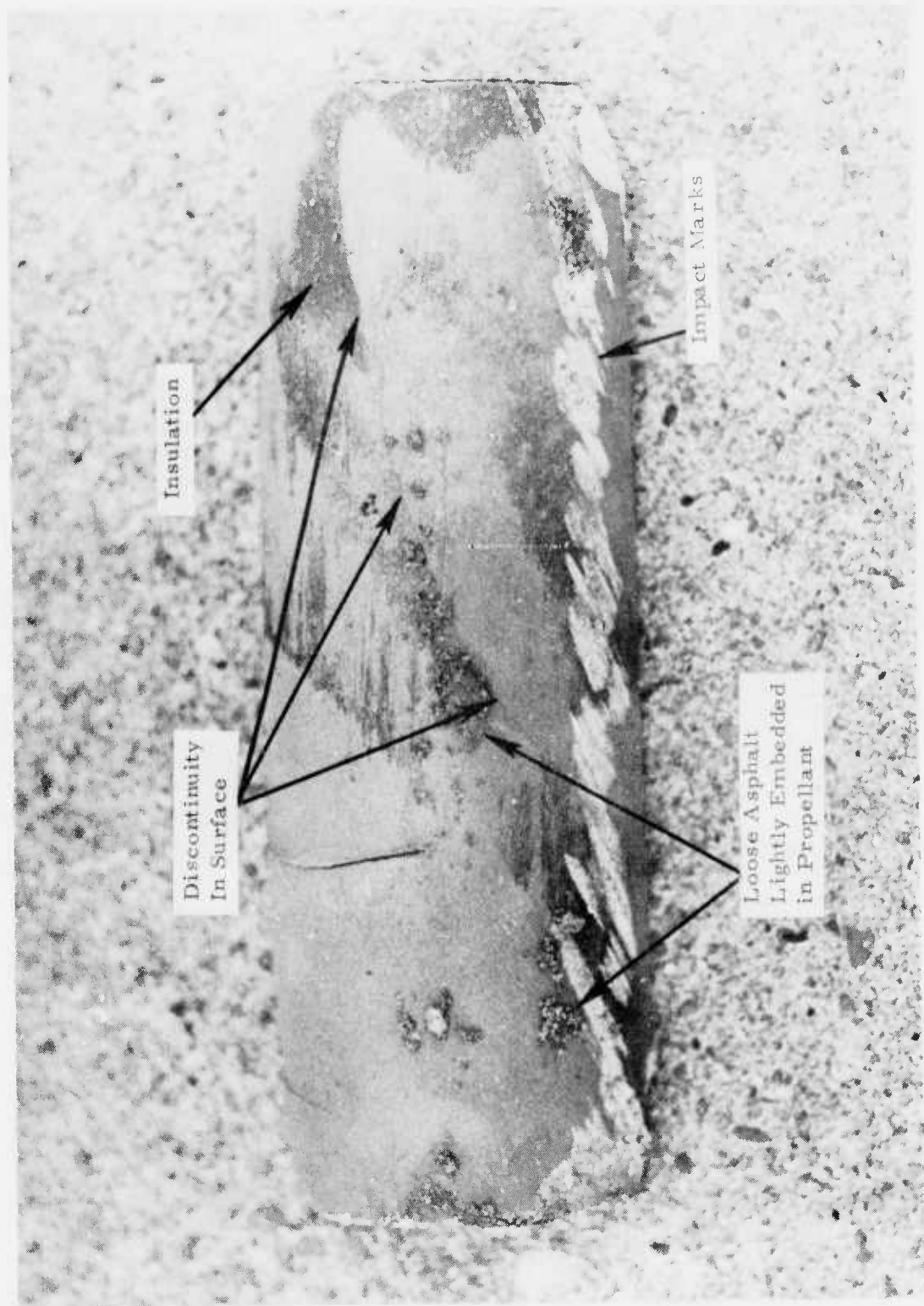


Figure VI-28. Insulation/Propellant Interface Surface on Propellant Recovered  
From TX-631 Motor, Mix T-684, Charge 2

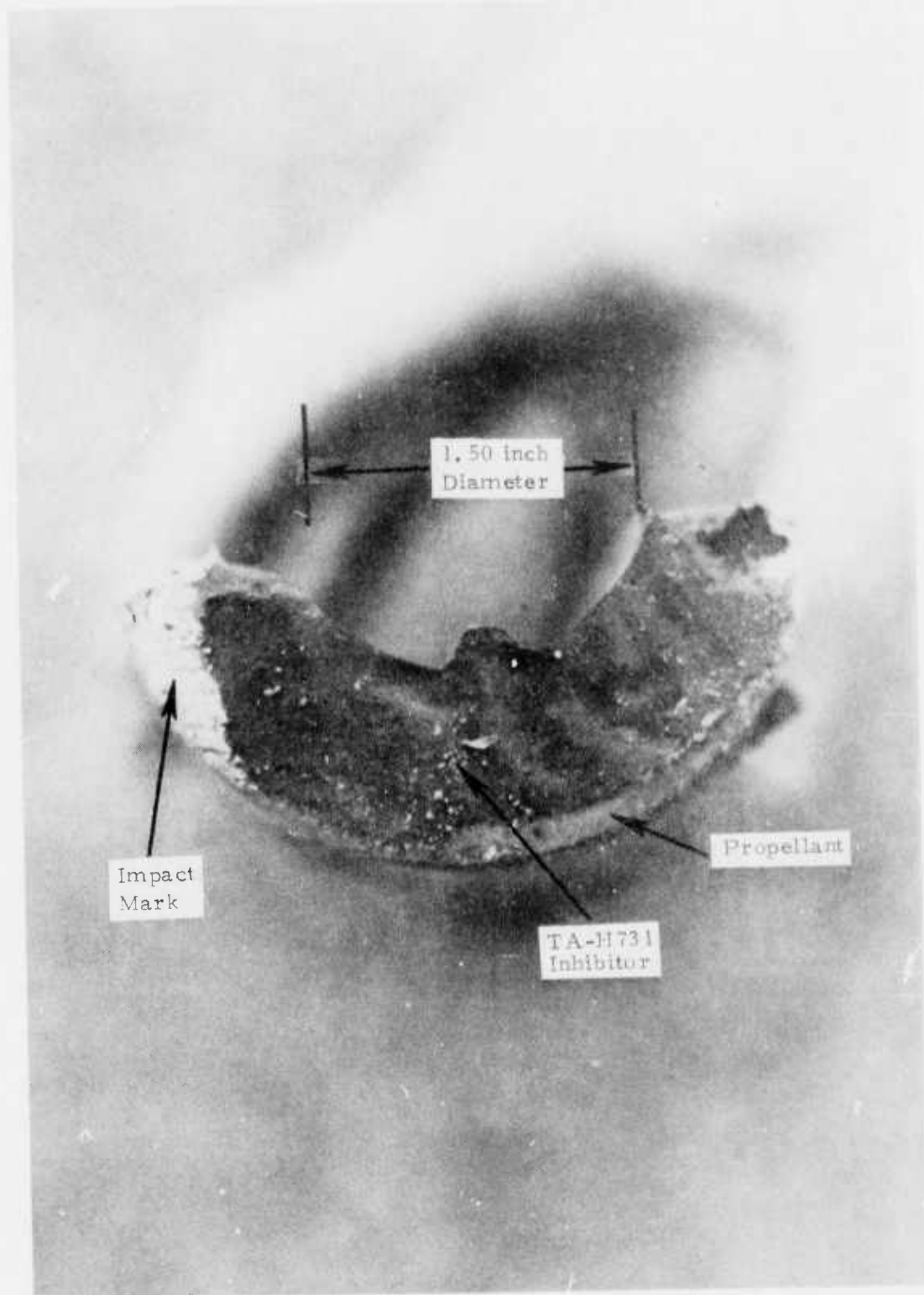


Figure VI-29. Aft End of Propellant Recovered  
From TX-631 Motor, Mix T-684, Charge 2

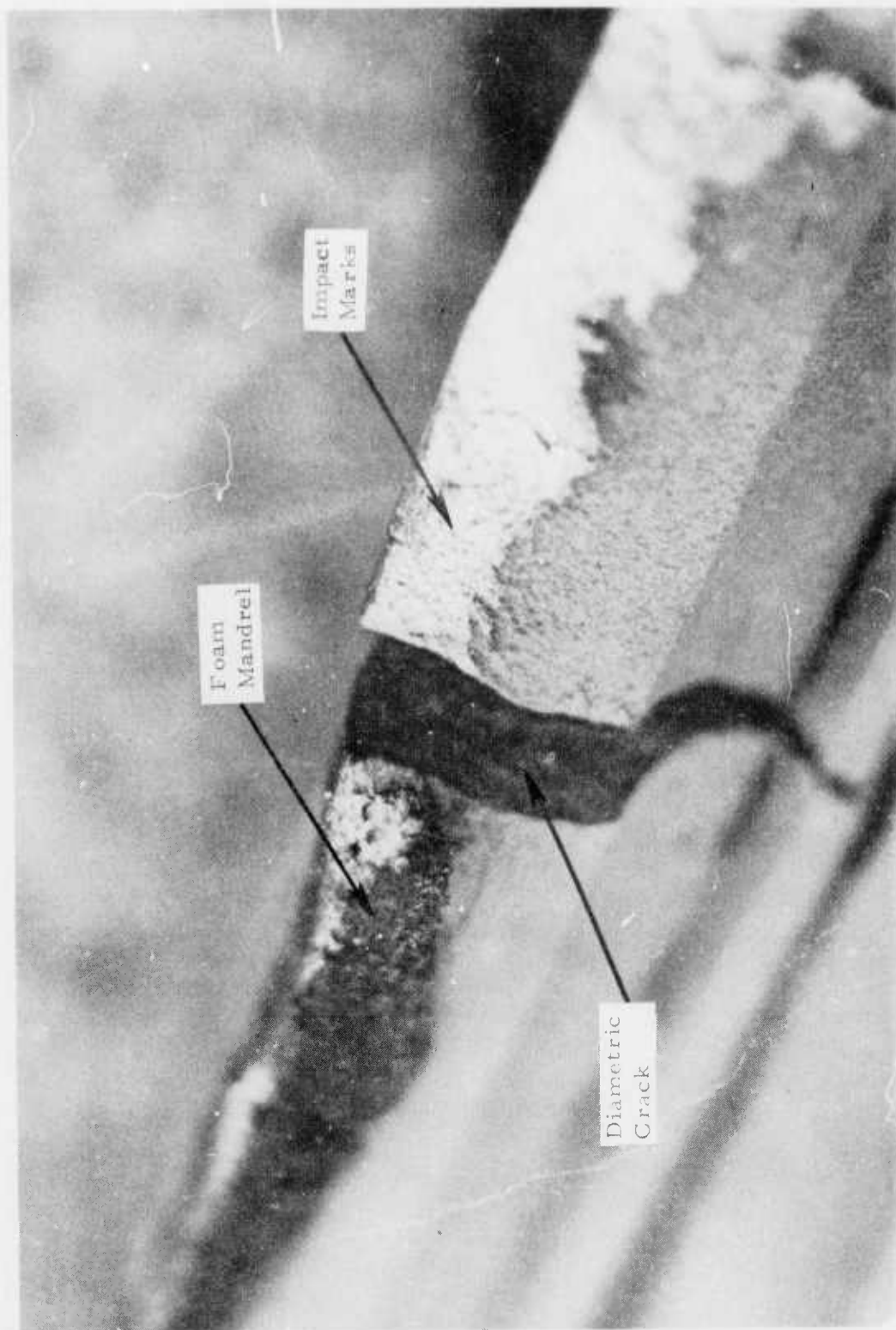


Figure VI-30. Diametric Crack and Adhering Foam Mandrel on Propellant  
Recovered from TX-631 Motor, Mix T-684, Charge 2



Figure VI-31. TX-631 Motor, Mix T-684, Charge 2, Post-Test Position

### Ballistic Analysis

From the beginning of the investigation the similarities between the behavior of T684-2 and T643-2 were recognized. Figure VI-32 is a direct comparison of pressure measured in the two motors. If the trace for T643-2 is shifted to the right only 0.020 second (out of a total operating time of 2.4 seconds) it exactly overlaps the trace of T684-2 until a pressure of about 350 psia is reached. At that point T684-2 started to rise at a very rapid rate while T643-2 made a more gradual increase.

Other comparisons were made with the movie records.

	Time From First Indication On Flash Bulb	
	T643-2	T684-2
First ignition flame	0.025	0.028
First indication of burning after igniter flame disappears	1.120	0.732
Flame disappears	2.350	2.434
Plume ignites vigorously	2.707	2.726

A flashbulb was connected in parallel to the igniter electrical circuit. When electrical power was applied to the igniter, it also fired the flashbulb. First indication of light from the flashbulb shows when power was applied to the igniter. Elapsed times shown above were calculated with frame counts and an assumed average camera speed of 4000 frames per second.

Because of these similarities, there could be some direct comparison of calculated ballistic behavior. The first calculation was that of burning surface required to produce the observed pressure. Non-equilibrium conditions were considered, in that

$$\text{Rate of mass generation} = \text{Rate of mass stored} + \text{Rate of mass discharged}$$

which leads to the following (assuming  $V$ ,  $R$ ,  $T$  and  $A_t$  to be constant over the short duration that calculations were made).

$$r A_s \left[ \delta_f - \frac{P}{12 RT} \right] = \frac{V \dot{P}}{12 RT} + \frac{g A_t P}{C^*} \quad (4)$$

Since  $\frac{P}{12 RT} \ll \delta_f$ , Equation (4) can be simplified and then rearranged to

$$A_s = \frac{\frac{V \dot{P}}{12 RT} + \frac{g A_t P}{C^*}}{r \delta_f} \quad (5)$$



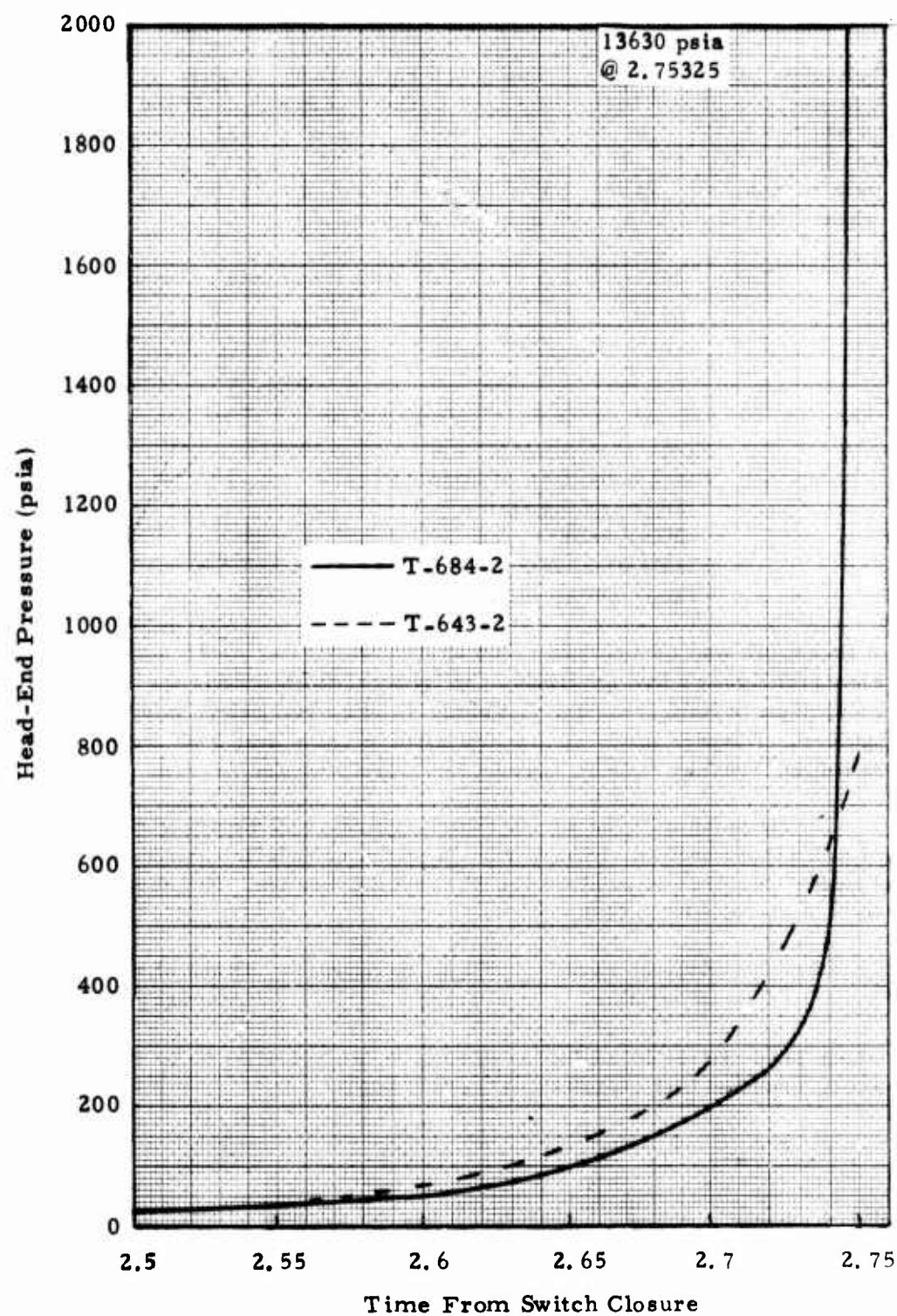


Figure VI-32. Comparison of Measured Pressure From TX631 Motors, Mix T643-2 and T684-2

where:

$A_s$	=	burning surface (sq in)
$V$	=	chamber volume = 82 cu in (initial for TX-631)
$R$	=	gas constant = 54.7 ft-lb <sub>f</sub> /lb <sub>m</sub> - °R (theoretical for DTS-7984 propellant at 1000 psia)
$T$	=	chamber temperature = 6190°R (theoretical for DTS-7984 propellant at 1000 psia)
$\dot{P}$	=	time rate of change of pressure (psia per sec)
$g$	=	gravitational constant = 32,174 lb <sub>m</sub> -ft/lb <sub>f</sub> -sec <sup>2</sup>
$A_t$	=	throat area = 0.8626 sq in (initial area for diameter = 1.049 in)
$C^*$	=	characteristic velocity = 5215 ft/sec (theoretical for DTS-7984 at 1000 psia)
$\delta_f$	=	cured propellant density = 0.063 lb/cu in
$r$	=	burning rate = $a P^n$ where $a = 0.01487$ and $n = 0.475$ for DTS-7883

Equation (5) was solved at individual time points in a rather simple manner. At time  $t_i$ ,  $\dot{P}_i$  was calculated by

$$\dot{P}_i = \frac{P_i - P_{i-1}}{t_i - t_{i-1}} \quad (6)$$

Results of calculations for motors T-643-2 and T-684-2 are shown in Figure VI-33. There is a very gradual increase in burning surface up to a time of about 2.734 seconds. Then T-684-2 shows a very sudden, very large increase in surface. Initial geometric burning surfaces for the two motors are

	Burning Surface (sq in)	
	<u>T-643-2</u>	<u>T-684-2</u>
Forward face	9.0	Inhibited
Aft face	8.1	Inhibited
Cylindrical bore	153.3	153.3
Slots	<u>183.7</u>	<u>183.7</u>
Total	354.1	337.0

Thus at the time being considered (2.735 seconds) only about half the surface was ignited (within the bounds of the assumptions and inputs used to solve Equation (5)).



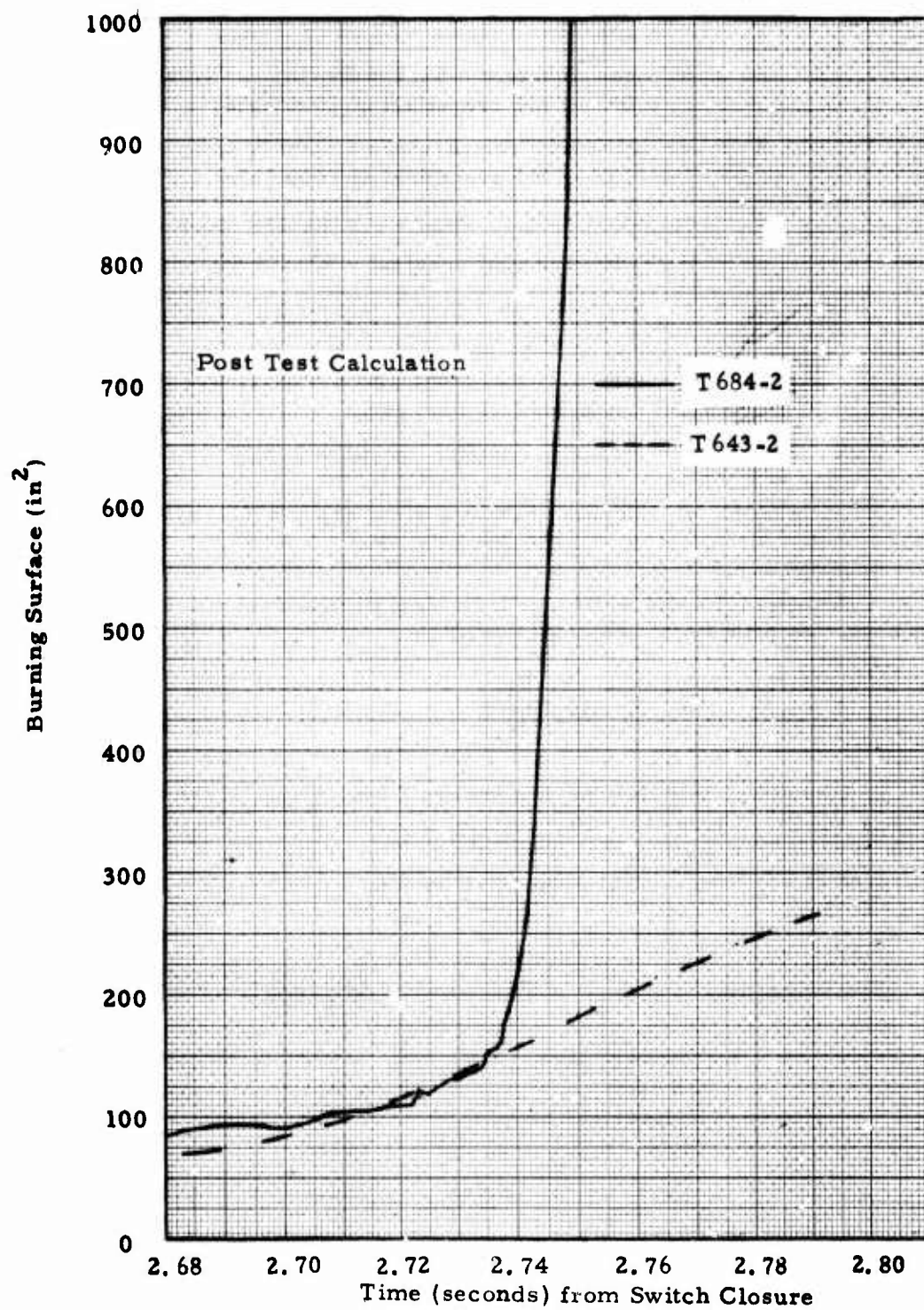


Figure VI-33. Post Test Calculation of Burning Surface For T643-2 and T684-2

Pressure deviating from the expected behavior can be caused also by unexpected changes in throat area. Equation (4) was rearranged to solve for  $\dot{P}$  and to include the effects of volume changes due to propellant consumption

$$\dot{P} = \frac{12 RT}{V} \left[ r A_s \dot{\delta}_f - \frac{g A_t P}{C^*} \right] - P r A_s \quad (6)$$

Equation (6) was integrated to obtain a pressure-time history. The integration was accomplished with an IBM Continuous System Modeling Program coded for an IBM 370 Computer.

Simulations were started at a pressure of 350 psia, surface area of 150 sq. in. and zero throat area. Two runs were made, one with the initial geometric chamber volume of 82 cu in and the other with 41 cu in to account for the presence of the foam mandrel (Figure VI-34). The calculated pressure history shows a much faster response than that measured.

#### Analysis of Possible Failure Mechanisms

There are three basic mechanisms by which a motor will over-pressurize: (1) throat area was too small; (2) burning rate was increased; (3) burning surface was increased. A fourth category can be listed to include such factors as premature failure of the pressure vessel. In the investigation of T684-2, ways by which these basic mechanisms could be implemented were examined. They are listed in Table VI-3, along with the final decision as to their contribution. Arguments by which the final decisions were reached are discussed in subsequent paragraphs.

Mandrel Blocked Nozzle: Igniter products made a hole through at least the center of the mandrel, as evidenced by flame exhausting at ignition and smoke and flame during hangfire. Once propellant started to burn, any mandrel material could have been consumed even more easily than during igniter operation. The nozzle was exhausting prior to and during time when pressure deviated from expected behavior, and, in fact, the plume was visible throughout the entire motor operation. Once propellant started to burn, there was no mechanism to force the mandrel from the slots into the throat, which would more likely happen with motors which had a gap between propellant and mandrel (gases "behind" mandrel to force it out). Conclusion: Not a contributor.

Grain Distorted to Block Nozzle: There was not enough differential load on grain to distort it all the way into the nozzle. Abnormal pressure increase started at low chamber pressure when motor was in fairly good equilibrium and loads would have been low. Conclusion: Not a contributor.

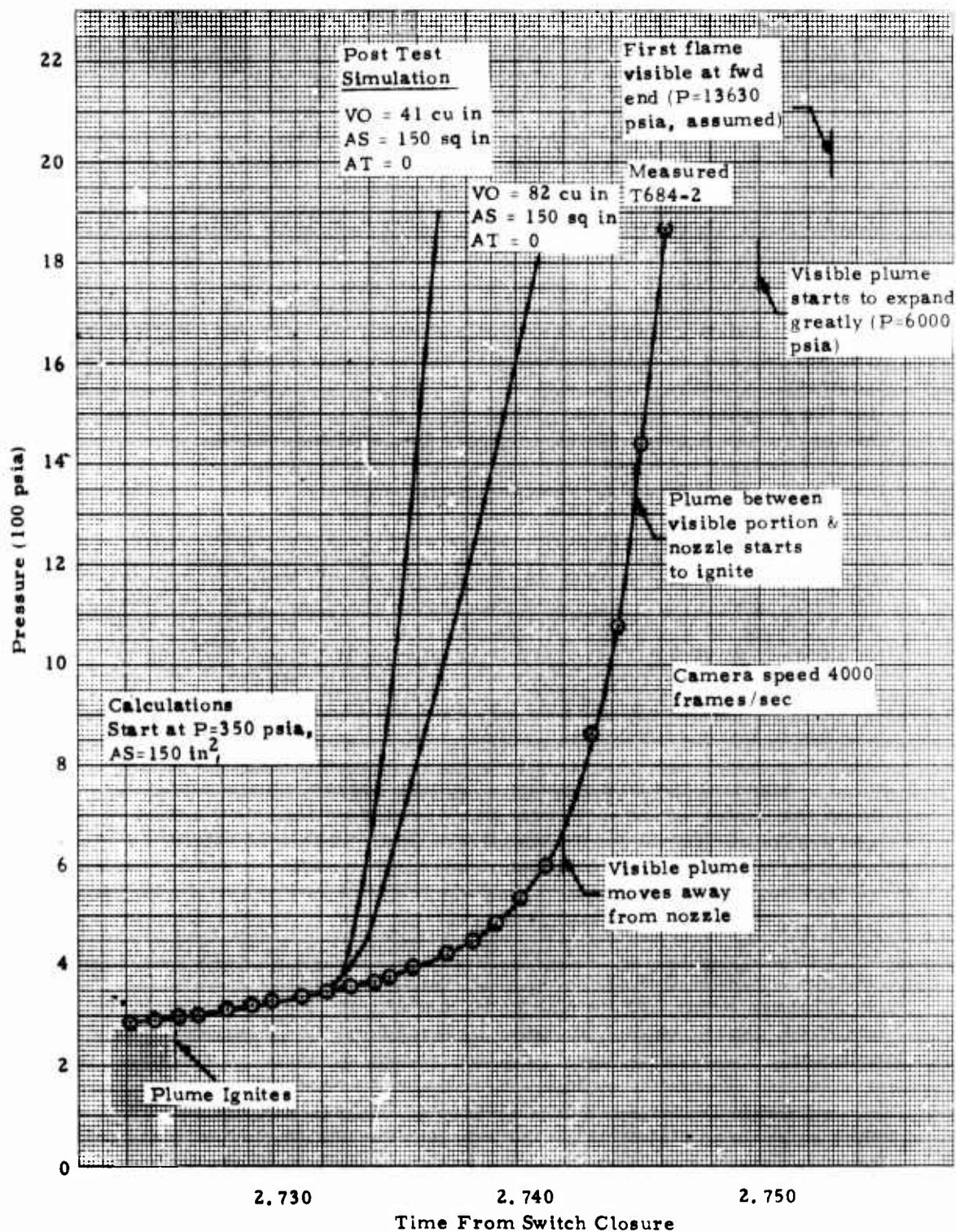


Figure VI-34. Comparison of Calculated and Measured Pressure Response of T-631, Mix T-684-2

TABLE VI-3  
POSSIBLE FAILURE MECHANISMS  
FOR T684-2

<u>Failure Mechanism</u>	<u>Effect on Final Motor Behavior</u>
<u>Throat Area Too Small</u>	
Mandrel blocked nozzle	None
Grain distorted to block nozzle	None
Throat too small for normal operation	None
<u>Increased Burning Rate</u>	
"Crack burning" in separation or crack	Contributor
Heating of surface layer of propellant during hangfire	Insignificant
<u>Increased Burning Surface</u>	
Voids crushed under pressurization	Not Likely
Differential pressure during ignition sheared grain from insulation	Not Likely
Differential pressure during ignition caused grain failure or bond failure at forward end	Possibly
Voids exposed as burning surface regresses	Not Likely
Adiabatic heating (during pressurization) of gas in voids	None
Propellant failure during cure because of partial (weak) bond of propellant to mandrel	Not Likely
Deterioration of propellant surface due to environmental storage or incompatibility with mandrel	None
Propellant not bonded to insulation	Unknown
<u>Miscellaneous</u>	
Premature failure of pressure vessel	None
Igniter contribution to total mass flow	None



Throat Too Small for Normal Operation: Companion Motor, T684-1, with same throat diameter operated satisfactorily. Conclusion: Not a contributor.

"Crack Burning" in Separation or Crack: By itself this phenomenon could not cause the over-pressurization. There must be some mechanism by which burning in a restricted volume is initiated. Conclusion: A contributor when crack or separation is ignited.

Heating of Surface Layer During Hangfire: Burning of the surface layer was already started when pressure deviated from that experienced on T643-2. Not all the surface was burning, but about half was (assuming "normal" burning rate). If rate was higher than "normal", then even less surface was burning. Initial rise to about 2.734 seconds does not indicate increased rate because there is no mechanism for suddenly increasing the heat soak effects. Furthermore, T643-2 had the same soak period and operated at a pressure lower than expected. Conclusion: Not a contributor; insignificant, if at all.

Voids Crushed Under Pressurization: There were not an extremely large number of voids on the surface, where they would have to be to be crushed by the relatively low (350 psia) pressure at which abnormal operation started. Not all voids were exposed to gases directly so that even if they were crushed they would not be ignited. The few voids that might have failed and might have ignited would not cause such a high pressure. Conclusion: Not likely a contributor.

Differential Pressure During Ignition Sheared Grain: Assuming that a differential pressure equal to the igniter-caused pressure (900 psia) acted across the grain length and that the pressure was imposed on both the propellant forward face and the mandrel, there was imposed a shear stress of 17 psi between the propellant and the insulation. There is no way to relate this directly to bond line capabilities, which were measured for Mix T684 (Table VI-4). However, the companion motor, T684-1, had a higher shear stress of 25 psi because of slightly higher ignition pressure (1060 psia) and thinner insulation at the forward end resulting in more axial load. There is not a significant difference in the bond test results with the systems shown in Table II-4. Conclusion: Not likely a candidate.

Differential Pressure During Ignition Caused Grain Failure or Bond Failure at Forward End: Weak propellant or weak bond by themselves will not cause extra burning surface to be exposed. There must also be a load on the propellant; the only load that can be conceived is the initial differential pressure caused by the igniter, assuming that for an instant all that pressure is contained at the head end of the grain. Then there might have been propellant cracking or bond failure. Why then didn't it also

TABLE VI-4

BOND OF PROPELLANT TO LINER AND INSULATION  
(DTS-7984)

	<u>Peel (pli)<sup>a</sup></u>	<u>Adhesion (psi)<sup>a</sup></u>	
	<u>Mix T-684</u>	<u>T-684</u>	<u>T-656</u>
TA-H732A	1.9 (5TCP)	75 (5P)	141
TA-H731A	3.1 (5P)	51 (5P)	---
TI-H706A	---	68 (5P)	106

a. Number and letter in parenthesis indicates number of tests and mode of failure: TCP = thin coat of propellant, P = propellant. Test temperature 77°F.

happen on T-684-1? Failure could have occurred on Charge 1, but since the chamber pressure started back up so quickly (0.2 to 0.3 second), the crack or unbond might not have had enough time to open. Propellant requires a certain "relaxation time" to respond. The long delay in Charge 2 gave enough time for the crack to open and it could have been reached eventually by combustion gas. The propellant was not particularly low strength. Physical properties measured five days after the motor was tested were not-too-unusual (Table VI-5). Maximum stress and strain at maximum stress (77°F) are somewhat lower than obtained with Mix T-656, but are still acceptable.

	<u>T-656</u>	<u>T-684</u>
Maximum Stress, 77°F (psi)	259	140
Strain at Maximum Stress, 77°F (in/in)	0.23	0.37

Note that Mix T-684 would satisfy the program propellant requirements (Section IV). There are conflicting impressions about the physical properties of Mix T-684, with the opposite position expressed earlier in this Section as a result of observations made during motor finishing operations. The short period of time (5 days) between motor finishing and physical property measurements should not have affected relative propellant conditions. The most likely explanation for the apparent difference in propellant properties is that the motor and laboratory samples cured differently, even though they were together at all times. Conclusion: Possibly a contributor.

Voids Exposed As Burning Surface Regresses: There probably was a thin layer of propellant consumed, and so, voids very near the surface could be exposed (See Figure VI-27). Voids were scattered throughout the motor and exposure at or shortly after ignition should not have caused a drastic change in pressure, but merely just operation at a somewhat higher-than-usual pressure. Conclusion: Not likely to be a significant contributor.

Adiabatic Heating of Gas in Voids: Initial pressurization could have compressed voids, heating the entrapped air to a temperature sufficiently high to initiate combustion. Assuming isentropic compression and no heat losses, the final temperature is

$$T_2 = T_1 \left[ \frac{P_2}{P_1} \right]^{\frac{\gamma-1}{\gamma}}, \text{ where } \gamma = 1.4 \text{ for air}$$

At  $P_1 = 15$  psia,  $T_1 = 530^\circ\text{R}$  and  $P_2 = 1000$  psia,  $T_2$  would be  $840^\circ\text{F}$ . This may be high enough to ignite the propellant but the pressure rise at ignition was relatively slow (0.010 second) and there would be significant heat loss before the temperature becomes high enough. Tests with more sensitive propellant and faster pressure rise failed to experience sub-surface ignition (Reference VI-5). If the



TABLE VI-5  
PHYSICAL PROPERTIES OF MIX T-684

	<u>Test Temperature (°F)</u>		
	<u>-65</u>	<u>77</u>	<u>165</u>
Modulus (psi)	9819	618	299
Maximum Stress (psi)	577	140	89
Strain at Maximum Stress (%)	36	37	41
Ultimate Strain (%)	41	38	42

voids had been ignited there should have been more effect, even to the extent of no hangfire. Instead the pressure trace is almost exactly like T643-2. Conclusion: Not a contributor.

Propellant Fails During Cure Because of Bond to Mandrel: If the bond between propellant and mandrel is sufficiently strong, cure shrinkage might cause the propellant to fail. Cure at ambient temperature alleviates this tendency somewhat since thermal strains imposed during cooldown from an elevated cure temperature are not encountered. There was no evidence of cracks on X-rays. The same effect should have been seen by Charge 1, but wasn't. Qualitative assessment of the "bond" between mandrel and propellant did not indicate a particularly strong joining. Furthermore, as given in the earlier Group No. 5 discussion, the propellant could be peeled away from the mandrel (albeit leaving a thin coating of propellant on the mandrel). If this happened in the motor, the thin layer would have been consumed quickly and the motor would have operated normally. Conclusion: Not likely a candidate.

Deterioration of Propellant Surface Due to Environmental Effects or Incompatibility with Mandrel: Motors were cast on March 5, finishing was started on March 15 and tests were conducted on March 19; there was not much time for deterioration. Motors were stored at 70°F, outdoor transportation was in mild weather, and they were sealed against moisture at all times except when being worked on. Compatibility of propellant and mandrel had already been determined. Again the most convincing argument is that Motor T-684-1 operated satisfactorily. Conclusion: Not a contributor.

Propellant Not Bonded to Insulation: Test data shown in Table VI-4 shows bond strengths lower than previously experienced with this system, but all failures were in the propellant and so the true bond strength is not known. It cannot be known for certain how bond sample strength compares with strength in the motor. The samples were cast after the motors and this sequence sometimes leads to problems. Even though the peel strengths for T-684 were low (usually like to have 10 pli), the tensile adhesion was not too far different from the "usually acceptable" value of 100 psi.

Even if there were unbond at the propellant/insulation interface, the flame must reach that point before it has any influence. Both ends of the propellant grain were inhibited, which adds protection at the exposed propellant/insulation interface. Radiographic inspection did not reveal any unbond. Inspection of the interface during motor finishing likewise did not uncover any abnormalities.

The strongest evidence for unbond is in the recovered piece of propellant. The exterior surface shows no sign of being torn from the insulation. It was not burning immediately after leaving the motor and so there was no opportunity for defects to burn away. Scratch marks on the outer surface

were caused by impact with concrete and asphalt pavement after it was extinguished.

There is a discontinuity in the outer surface of the recovered propellant (Figure VI-28) which may be caused by burning in one area. There is a mechanism by which combustion products could reach the outer surface. The clearance between mandrel star tips and the mastic insulation was very thin because of the extra insulation applied to this motor, which would have left no room for propellant to flow between the mandrel and insulation. At pressurization the case could have moved away from the propellant, opening a gap, which could have allowed combustion gases to reach an unbonded area. Charge 1 of T-684 did not have this situation because the insulation under the slots was much thinner (0.10 inch, except at the thermoplastic samples, compared with 0.250 inch in T-684-2). Conclusion: Cannot determine contribution.

Premature Failure of Pressure Vessel: The forward closure did not vent until pressure was greater than 13,000 psia. Conclusion: Not a contributor.

Igniter Contribution to Total Mass Flow: The igniter was already consumed 2.7 seconds earlier. Conclusion: Not a contributor.

### Conclusions

The following conclusions were reached as a result of the various analyses described above:

- (1) Over-pressurization was not connected with the igniter or foam mandrel.
- (2) The throat was not blocked at any time.
- (3) Inert components behaved as expected.
- (4) Over-pressurization was caused by abnormal exposure of burning surface.
- (5) Most likely mechanisms for increased burning surface were:
  - (a) Propellant or bond failure at forward face caused by differential pressure during ignition.
  - (b) Weakness at propellant/insulation interface in bottom of propellant valleys caused by close proximity of mandrel to insulation, coupled with (possibly) an unbonded condition between insulation and propellant.

The exact mechanism cannot be determined with any degree of certainty.

#### REFERENCES

1. "A Characterization of Erosive Burning for Composite H-Series Propellants", AIAA Solid Propellant Rocket Conference, C. A. Saderholm, Thiokol/Huntsville, 1964.
2. "Erosive Burning Study of TP-H8041 Propellant", Report No. C-A-61-176, C. A. Saderholm, Thiokol/Huntsville, 1961
3. "Erosive Burning", Report No. 2313-72-110, J. Baker, Thiokol/Wasatch, 1973
4. "TP-H8208 Ballistic Characteristics for TX546 Application", Report No. C-73-4516, G. P. Roys, Thiokol/Huntsville, 1973.
5. "Analysis of Data for Sprint Propellant Void Autoignition Experiments", Memorandum to F. A. Clark from B. B. Stokes, Thiokol/Huntsville, January 1968; and "Critical Void Size for Autoignition of Sprint Propellant", Unpublished Study, B. B. Stokes, Thiokol/Huntsville, 1967.

SECTION VII  
CONSUMABLE MANDREL

## SECTION VII

### CONSUMABLE MANDREL

A consumable grain-forming mandrel was identified by the Booz-Allen study (Reference VII-1)<sup>1</sup> as having high cost-reduction potential. As a result of this finding, one objective of the current program was to evaluate the technical feasibility of the consumable mandrel technique. Previous programs at Thiokol/Huntsville (Reference VII-2) used Pyrocore<sup>®</sup> to fragment the mandrel just before the igniter was initiated (using the same fire pulse). The current program emphasized low cost approaches, so a two-element ignition train is less attractive than one where the ignition and fragmentation functions are performed by one device. However, the experience gained during the Reference VII-2 work was directly related regarding mandrel materials and grain forming techniques.

Reference VII-2 results showed: First, 5-inch diameter by 12-inch long TX-11 motors were successfully cast by the "core-insertion" method using foam mandrels having densities of 3.8 to 5.0 lb/cu ft, and second, 9-inch diameter by 90-inch long TX-19 motors were successfully cast by the "bottom pressure cast" technique using foam mandrels of 4.7 to 6.2 lb/cu ft density. A much larger motor, the TX-33 with a 31-inch diameter and 202-inch length, was bayonet cast with a mandrel having a density of 3.2 lb/cu ft. In all tests, the mandrel was successfully fragmented and ejected.

It was decided that firing a motor was the surest way to determine the feasibility of using the igniter charge to break up the mandrel along with igniting the propellant. Full-scale test-weight motors (TX-631) were scheduled for Phase I component testing and, so, evaluation of the consumable mandrel was included in the test objectives. A further choice was to follow the approach of Reference VII-2: (1) Form some of the grains with conventional metal tooling and insert consumable mandrels into the grain cavity during final motor assembly and (2) Form the remaining grains with the consumable mandrels themselves. The igniter charge was contained in the consumable mandrel.

As the Phase I program progressed, the original plan was expanded to cast two motors using the foam mandrels to form the grain. An additional investigation was added to determine the effect of mandrel density on motor operation as well as on grain forming.

---

1. References are given at the end of this section.

## MANDREL MANUFACTURE

Based on Reference VII-2 results, it was decided that the initial TX-631 static tests would be conducted with a mandrel having a density of 3 to 5 lb/cu ft. It appeared that this density range would provide sufficient strength to withstand loads imposed during propellant pouring and still be low enough to have a reasonable chance of being ejected without the use of a separate fragmenting charge.

### Mandrel Material

As the Rigitane polyurethane foam system used in the Reference VII-2 program was no longer available, a substitute was sought that would have similar characteristics. Two materials<sup>1</sup> - Stepanfoam BX-249 and BX-289 from Stepan Chemical Company - were on-hand for such applications. The BX-289 was selected because it is more readily available. The BX-289 is a two-part system with the Freon 11 blowing agent already incorporated in the resin. The recommended mixing ratio of 50/50 of the two ingredients yields a nominal 2.2 lb/cu ft density when allowed to "free rise". While the mandrel (core) mold was being prepared, a number of foam batches were made to gain experience in handling and using the material. Three such batches were made to obtain density gradient data, as detailed below.

Simulated core molds, a 2-inch-ID cardboard tube 47 inches in length, were used to assess the ability of the Stepanfoam BX-289 to foam vertically in a small cross section cavity. Based on a nominal 2.2 lb/cu ft density, a 68.5 gram casting would result. A 74-gram mix was made and immediately poured into the first tube. The mix drained to the bottom, then started reacting and expanding. The foam stopped, however, when only about 22 inches had been filled. The foamed portion was cut into nominal 3-inch lengths, and density values were calculated, using the gross weight and length of each piece, and the nominal weight-per-unit-length of the cardboard tube. Although the calculated foam density is given to two decimal places, the method of calculation probably warrants rounding to only one place. As can be seen, (Table VII-1), the foam density varied only slightly over all but the upper most portion of the casting.

Based on the results from the first pour, a second mix was weighed up and poured into a second tube. This mix was 130 grams and the foamed length was 39.75 inches. When sectioned and weighed for density calculation, the results reported in Table VII-2 were obtained. As can be seen, the results were generally similar to the first pour; however, a higher density region occurred about six inches below the top and extending for about twelve inches. The top-most section, again, was low in density.

1. Both of these materials were classed as "self-extinguishing" per ASTM D-1692-67T, which means they will burn as long as there is a source of heat, but if that source is removed, the materials will not continue to burn.



TABLE VII-1

FOAM DENSITY VERSUS TUBE LENGTH - POUR NO. 1

Mold - 2 inch ID cardboard tube 47 inches long, vertical  
Nominal Weight of Tube - 8.83 grams per lineal inch  
Weight of Mix - 74 grams total of Stepan foam BX-289  
Final Foamed Length - 22 inches

<u>Section</u>	<u>Length</u>	<u>Weight, Gross</u>	<u>Foam Weight, Corrected</u>	<u>Foam Density</u>
A (bottom)	3 inches	34.3 gms.	7.8 gms.	3.15 lb. /cf.
B	3	33.9	7.4	2.99
C	3	34.3	7.8	3.15
D	2 15/16	33.9	8.0	3.30
E	3	34.3	7.8	3.15
F	3	34.7	8.2	3.31
G (top)	3	33.3	6.8	<u>2.75</u>
Avg.				3.11

TABLE VII-2

FOAM DENSITY VERSUS TUBE LENGTH - POUR NO. 2

Mold - 2 inch ID cardboard tube 47 inches long, vertical  
Nominal Weight of Tube - 5.21 grams per lineal inch  
Weight of Mix - 130 grams total of Stepan foam BX-289  
Final Foamed Length - 39 3/4 inches

<u>Section</u>	<u>Length</u>	<u>Weight, Gross</u>	<u>Foam Weight, Corrected</u>	<u>Foam Density</u>
A (bottom)	3 inches	24.3 gms.	8.7 gms.	3.52 lb. /cf.
B	3	23.6	8.0	3.23
C	3	23.2	7.6	3.07
D	3 1/16	24.0	8.1	3.20
E	2 15/16	23.3	8.0	3.30
F	3 1/16	24.6	8.7	3.44
G	3	24.0	8.4	3.39
H	2 15/16	24.6	9.3	3.84
I	3	25.4	9.8	3.96
J	3	25.9	10.3	4.16
K	3	25.8	10.2	4.12
L	3	24.2	8.6	3.47
M (top)	2 15/16	21.8	6.5	<u>2.68</u>
Avg.				3.49

A third pour, using 150 grams of material, filled the tube to within 1-1/8 inch of the top. The results (Table VII-3) are very similar to those for the second pour except that the higher density region (i. e., nominally 3.9 lb/cu ft and above) extends for a longer length. The overall variation in density was considered to be acceptable.

#### "Low Density" Mandrels

A split mold was fabricated, using an epoxy-based tooling plastic, for foaming the core for the TX-631 motors. The mold was prepared in two halves, using 2 x 4 inch lumber for framing. A TX-631 Teflon-coated steel core, DR-51963-A, was used to form the cavity. After each half of the mold had been poured, using Ren RP-3209-1 Mass Casting-Black tooling plastic, the parting surface was located and smoothed on a milling machine. Some minor surface defects remained in the mold cavity, produced by voids in the plastic, but it was decided that these could be more readily corrected by sanding the foamed part than by attempting to rework the mold. Some slight bowing of each mold half was noted, causing each to be concave at the parting plane; however, the effect was minimized when the halves are bolted together. The bow apparently was caused by a slight shrinkage of the tooling plastic during cure.

A total of twenty-one foamed mandrels was poured, using the hand-fabricated split mold, with varying degrees of success, before an acceptable unit was obtained. Problems encountered included high density (resin-rich) areas, voids, and insufficient "blowing" of the foam materials resulting in both an incomplete mold fill and in overall high density items. Pours were made with the mold at room temperature and 110°F, with the resin/halocarbon constituent at room temperature or cooled to about 40°F, and with the cure agent at either room temperature or heated to 110° - 120°F (when the resin was cold). In addition, the mixture was stirred for an extended period of time, causing the material to "blow" before it was completely poured, and the mold was tilted at various angles during pouring and during "blowing" and cure.

Finally, three mandrels (S/N 22, 23, and 24) were deemed both satisfactory for use and identical in appearance and properties. The preparation procedures to produce these three mandrels were identical, indicating a reasonably reproducible process and product. As discussed below, two particular changes in the process appeared to cause the improvement.

A series of mixes of the foam material, Stepanfoam BX-289, was made to better define the working life of the mixture and the time to completion of blowing. Fifty-gram mixes, prepared by stirring with a spatula, indicated the onset of "blowing" in a well-mixed batch occurred at 30 to 35 seconds, with completion of "blowing" after about 3 minutes in the unrestrained state. Subsequent batches, using a 250-gram batch resulted in the same times, but

TABLE VII-3

FOAM DENSITY VERSUS TUBE LENGTH - POUR NO. 3

Mold - 2 inch ID cardboard tube 47 inches long, vertical  
 Nominal Weight of Tube - 4.99 grams per lineal inch  
 Weight of Mix - 150 grams total of Stepan foam BX-289  
 Final Foamed Length - 45 7/8 inches

<u>Section</u>	<u>Length</u>	<u>Weight, Gross</u>	<u>Foam Weight, Corrected</u>	<u>Foam Density</u>
A (bottom)	2 15/16 in.	23.8 gms.	9.1 gms	3.76 lb. /cf
B	3	23.2	8.2	3.31
C	3	23.2	8.2	3.31
D	2 15/16	23.4	8.7	3.59
E	3	23.1	8.1	3.27
F	2 15/16	23.3	8.6	3.55
G	3	23.9	8.9	3.60
H	2 15/16	24.0	9.3	3.84
I	2 15/16	24.2	9.5	3.92
J	3	24.8	9.8	3.96
K	3	25.0	10.0	4.04
L	3	25.2	10.2	4.12
M	3	25.0	10.0	4.04
N	3	24.1	9.1	3.68
O (top)	2 15/16	21.4	6.7	2.76
			Avg.	3.65

indicated that mixing with a spatula by hand was unsatisfactory for batches of this size. It took 25 to 30 seconds of mixing to obtain a reasonably homogeneous blend of the two ingredients, leaving from zero to 5 seconds to get the mixture poured into the mold cavity. Batches mixed for a shorter time tended to have streaks of uncured or semicured material in them.

A Lightnin' mixer was set up and tried as a means of achieving homogeneity of the blend in a shorter period of time. A 250-gram batch mixed only 15 seconds on the Lightnin' mixer achieved good homogeneity, but started "blowing" in 20 to 25 seconds. This still allowed sufficient time to pour the liquid into the mold cavity prior to the onset of "blowing".

Efforts at casting a core continued to be unsatisfactory when the mold was either left at an angle or raised to the vertical immediately after pouring, so a different approach was tried. The mold was poured at a 60° angle, then immediately layed flat. The material completely filled the mold, and the resultant mandrel looked good, although there were several resin-rich areas on the upper surface (as poured) near the aft end. Since this pour was made with the "wings" of the cavity horizontal, the next pour was accomplished with the core "wings" vertical.

For Pour No. 22, made with the mold rotated such that the core wings remained in the vertical plane at all times, one additional change was also made. The core was at a 60° angle for pouring, but was laid horizontal immediately after the pouring was completed. The forward end was then immediately raised to drain some of the liquid back towards the aft end. The mold was then returned to the horizontal and left there until the foam had hardened. The resultant core was of excellent appearance. The next two pours, No. 23 and 24, were made as nearly identical to No. 22 as possible, with essentially identical results.

Modifications were made to the mold prior to the eighth pour to incorporate a cavity at the forward end for an ignition/core-blow-out charge. Three pours were made using a wooden dowel that had been turned on a lathe to the desired shape. The first was made with the dowel only, and was successful to the extent that a satisfactory cavity was formed; density problems at the aft end were still evident. For the second pour, lead wires for a squib were strung in the mold and imbedded in the foam during the casting. Subsequent attempts to pull the wires one way or the other through the cured mandrel caused the wires to break. The third attempt utilized a PVC spaghetti tube strung full length through the mold on a copper wire support. This concept worked quite well, although other problems caused the molded core to be rejected.

A cavity former was then machined from aluminum, both to withstand the forces required to remove the unit from the molded core, and to provide

more accurate dimensions and taper than the wooden unit gave. The last two cores were successfully cast using this cavity former and a steel support rod for the PVC tubing. After cure, the steel rod was removed and lead wires for the ignition squib were drawn through the PVC tube. The technique worked quite well.

The procedure used to produce the acceptable cores is summarized in Table VII-4. Photographs taken during previous castings are given in Figure VII-1 through VII-7, and illustrate portions of the operation. Figure VII-1 shows the disassembled mold and components. Figure VII-2 shows the fully assembled mold standing on end prior to casting. Figure VII-3 shows the mold assembly leaning at an angle, with the polyurethane mixture being poured into it through a funnel. When all the mix has been poured, the funnel is removed, and the rubber stopper is jammed into the opening as both a seal and as a support for the tube-supporting rod. Figure VII-4 shows a foamed core in which the lead wires were imbedded directly during casting. This technique was abandoned because the wires could not be pulled in either direction. Figure VII-5 shows one of the three acceptable cores, in which the vinyl spaghetti tubing was imbedded. The lead wires were inserted later. Figure VII-6 shows the lead wires protruding from the cavity molded in the forward end of the core. The cavity will contain the pyrotechnic charge and initiators used to blow the core out and to ignite the motor. Figure VII-7 gives a close-up view of the same area.

Table VII-5 lists the TX-631 motors tested during Phase I and indicates the consumable mandrels which were used.

Average density of the individual mandrels were calculated by dividing the total weight by the calculated volume. The latter was determined by making planimeter measurements of cross-sectional areas at regular intervals along the length of the grain (using enlarged drawings from Core Drawing R51963A). Numerical integration gave 70.1 cu. in. for the mandrel finished to 43.8 inches length which accounts for the cavity molded in the mandrel to contain the igniter and which agrees with a cavity volume calculated by the ballistic analysis computer program (71.3 cu. in.).

The density values shown on Table VII-5 were considerably higher than expected (i. e., 4 to 6 lb / cu ft ) so a reject core (No. 10) was sectioned to determine just what the actual density distribution is. A small block cut from the central, conical portion of the core body had a density of 4.26 lb / cu ft (in the expected range). Two specimens cut from the "wings", however, were considerably denser: 16.05 lb / cu ft and 19.72 lb / cu ft. The apparent explanation is that movement of the flowing material into the relatively narrow confines of the "wing" areas causes densification by inhibition of the blowing process. The same condition causes the foam in the central, conical region to be well above the nominal 2.2 lb / cu ft that results from free, unrestricted foam blowing.

TABLE VII-4

FOAMED MANDREL (CORE) CASTING PROCEDURE

1. Inspect interior surfaces of mold cavity and remove any foreign material and cured residues from previous castings.
2. Apply a light coat of Johnsons Paste Wax to the interior surfaces and to the surfaces of the parting joint. Buff the waxed surfaces to a shine using a soft, lint free rag.
3. Install a length of 10 gage vinyl tubing on the steel support rod, then insert the tubing/rod through the cavity former. Apply a light coat of Johnsons Paste Wax to the exterior of the cavity former, but do not buff.
4. Place the cavity former assembly in the bottom half of the mold, aligning the groove with the ridge of the mold.
5. Place the upper half of the mold on top, aligning all the bolt holes as well as the groove and ridge at the cavity former.
6. Install the clamping bolts and tighten, while ensuring the index marks on the mold halves maintain proper alignment. The aft end of the mold may require mechanical restraint to effect proper alignment.
7. Apply a light coat of Johnsons Paste Wax to the drilled rubber stopper, then insert the end of the tubing/rod through the hole.
8. Incline the mold at a  $60^{\circ}$  angle from the floor, and place the plastic casting funnel in the aft end opening, with the tubing/rod end to one side. The mold should be oriented such that the parting joint plane is normal to the floor.
9. Weigh up 250 grams of Stepanfoam BX-289.
10. Mix the polyurethane constituents with a Lightnin' mixer for exactly 15 seconds, moving the container around to ensure complete incorporation and blending of all portions of the ingredients.
11. Immediately pour the ingredients into the mold cavity through the funnel. Without delay, remove the funnel and cram the stopper into the opening, applying tension to the support rod while doing so.
12. Immediately lay the mold horizontal (while maintaining the parting joint plane normal to the floor) and elevate the forward end about  $30^{\circ}$  for about five seconds.

(Continued on next page)



TABLE VII-4 (Continued)

13. Lay the mold back horizontal, then leave as is for at least three hours.
14. Remove the rubber stopper from the aft end, then twist the cavity former with a wrench to break it free. Withdraw the support rod by pulling it straight out (the spaghetti tubing may come with it).
15. Remove the clamping bolts and carefully lift off the top half of the mold.
16. Lift the rigid core from the bottom mold half and remove the cavity former.
17. Examine the core for acceptability, then cut off the aft end, as needed, to leave a final length of 43.80 inches (or as requested by Engineering Department).
18. Insert a 16 gage copper wire (solid conductor, straightened by stretching) through the length of the core inside the spaghetti tubing (or the hole left by it).
19. Strip the insulation from the ends of the two lead wires for about 1/2 inch, then solder the wires to the copper wire at the forward end of the core.
20. Trim off any burrs at the solder joint, then pull the copper wire out the aft end, pulling the lead wires on through the core.
21. Clip the lead wires free from the copper wire and bend the lead wires back at each end of the core to minimize the possibility of slippage.
22. Deliver the core to the Igniter Lab.

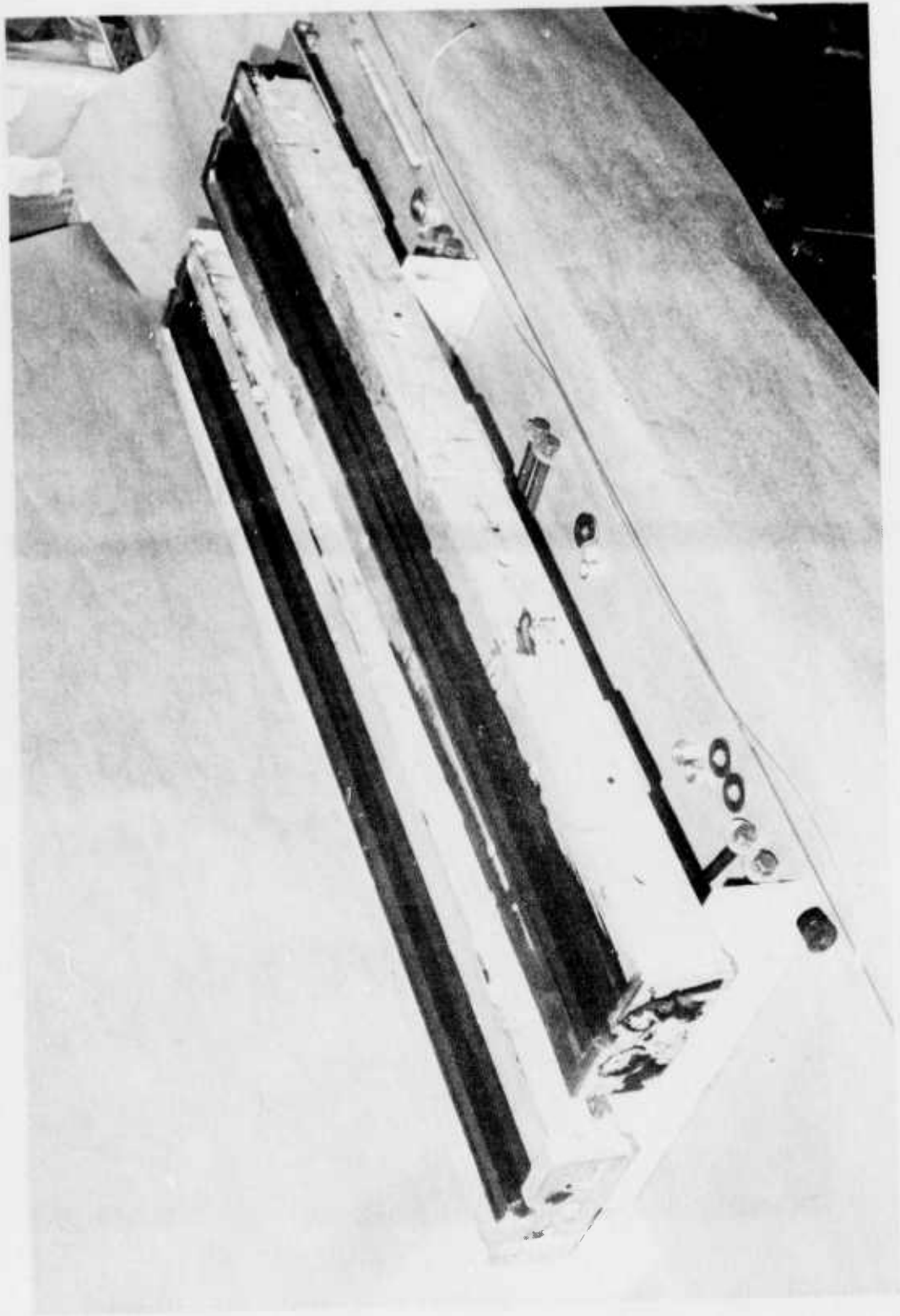


Figure VII-1. Consumable Mandrel Mold, Disassembled



Figure VII-2. Consumable Mandrel Mold, Assembled, Standing Vertical



Figure VII-3. Foam Mixture Being Poured into Mold

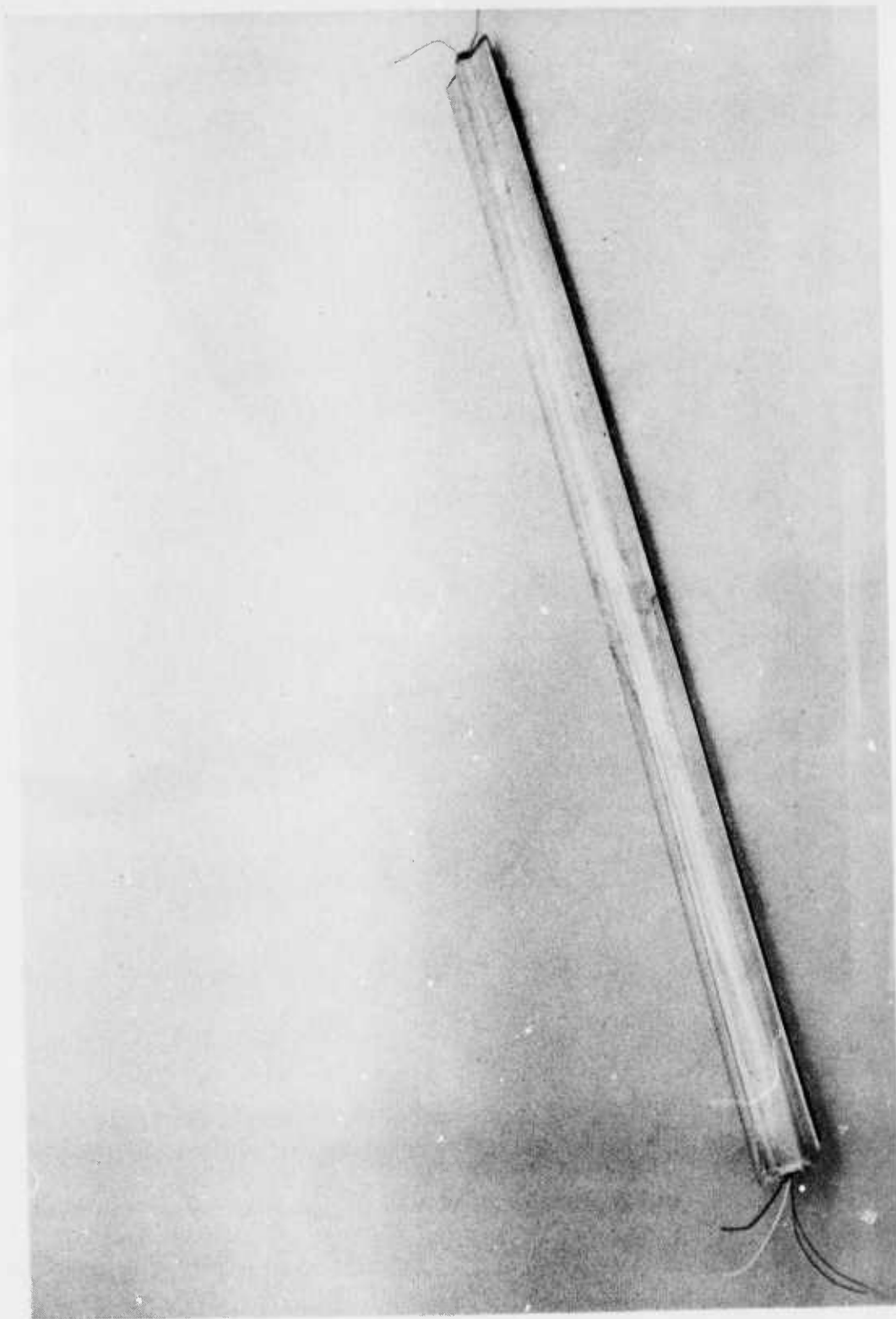


Figure VII-4. Early Foamed Mandrel with Wires Imbedded in Foam



Figure VII-5. Foamed Mandrel with Wires Inserted in Spaghetti Tubing



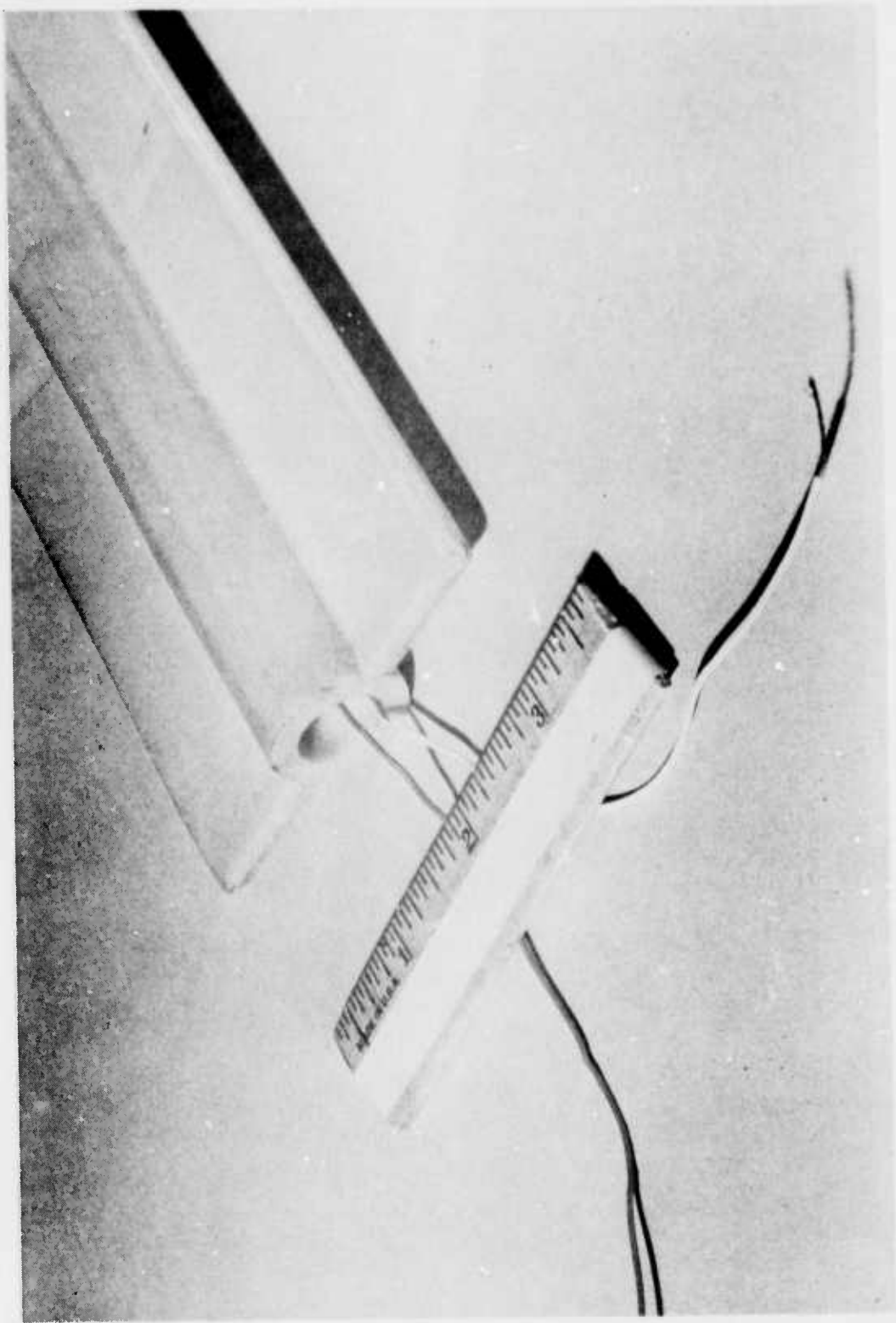


Figure VII-6. Forward End of Foamed Mandrel Showing Molded Cavity



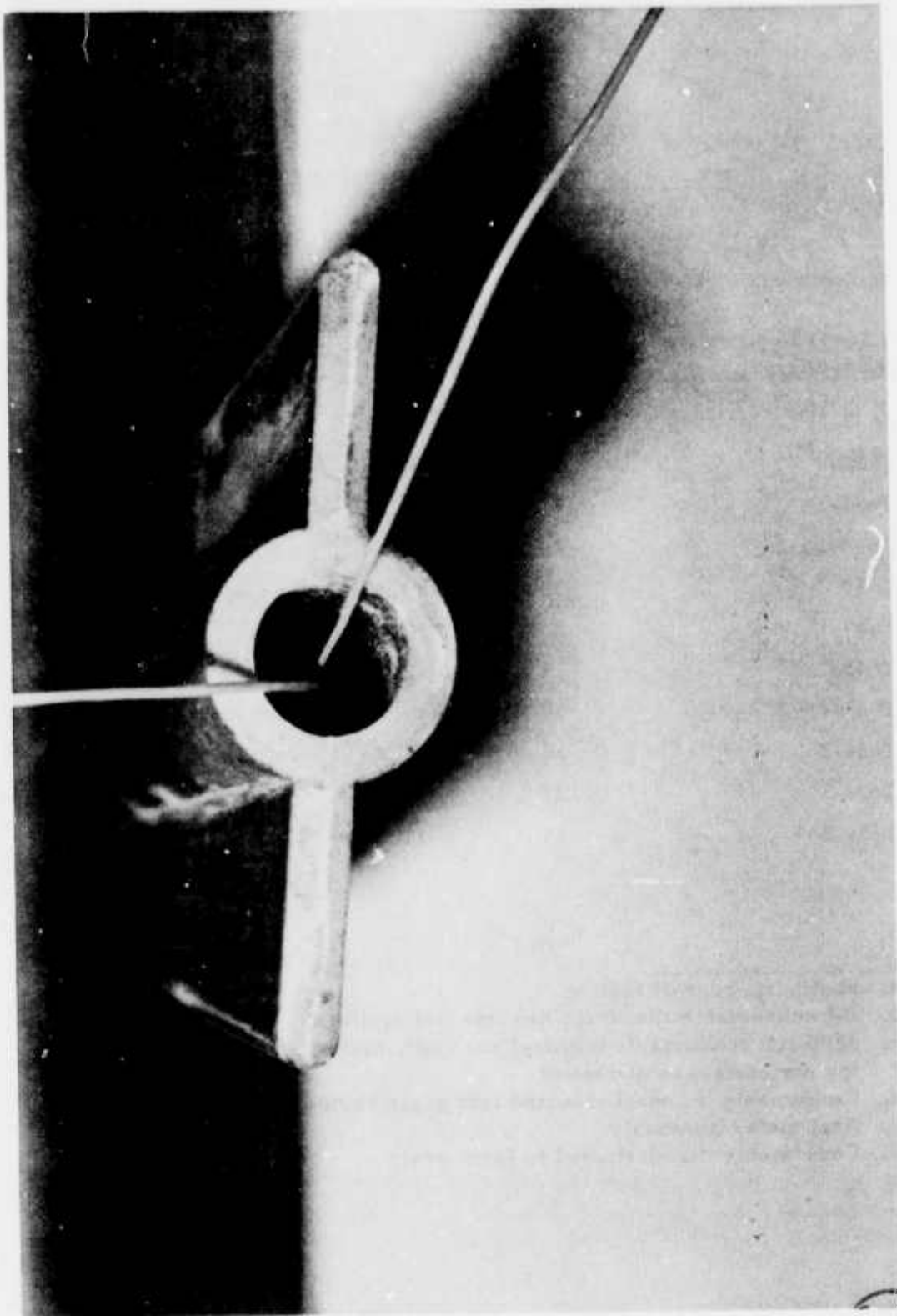


Figure VII-7. Close-Up of Forward End and Cavity of Foamed Mandrel

TABLE VII - 5

TX-631 MOTORS WITH CONSUMABLE MANDRELS

<u>TX-631 Designation<sup>(a)</sup></u> <u>(Mix-Charge)</u>	<u>Mandrel</u> <u>S/N</u>	<u>Mandrel</u> <u>Average</u> <u>Density</u> <u>(lb/cu ft)</u>	<u>Mold</u> <u>Release</u> <u>Agent</u>	<u>How</u> <u>Mandrel</u> <u>Used<sup>(b)</sup></u>
T622-1 <sup>(c)</sup>	N/A	N/A	N/A	N/A
T622-2 <sup>(c)</sup>	N/A	N/A	N/A	N/A
T634-1	22	12.5	None	d
T640-1	24	11.9	None	d
T640-2	28	17.5	None	d
T630-1 <sup>(c)</sup>	N/A	N/A	N/A	N/A
T643-1	23	12.1	MR22	d
T643-2	30	11.9	MR22	d
T634-2	36	11.7	MR22	d
T684-1	27	14.3	MR22	e
T684-2	35	11.9	MR22	e

a. Shown in order of testing

b. All consumable mandrels had integral igniters

c. Although consumable mandrel not used, motor is listed for completeness of record

d. Consumable mandrel inserted into grain cavity during final motor assembly

e. Consumable mandrel used to form grain

### "High Density" Mandrels

The initial tests with consumable mandrels of nominal 12 lb/cu ft density were very successful, presenting the opportunity to expand the goals of the Phase I investigations. Although the mandrels were much denser than those used in Reference VII-2 motor manufacturing, it appeared advantageous to use an even greater density to provide more stiffness in the high L/D mandrel.

A means was sought for obtaining a nominal 16 lb/cu ft density as the overall average for a cast core. An attempt was made to force the extra material of a standard foam mix into the mold to give the required 320-gram gross core weight. The internal pressure from the flowing process caused the mold to bow apart between clamp bolts, letting excess foam spew out. The resultant core had a density of only 14.3 lb/cu ft, and varying dimensions from the bowing.

A quantity of the R component of BX-289, which contains Freon 11, was heated in an oven to drive out all the halocarbon blowing agent. This material was used, in varying proportions with regular BX-289R, in a series of mixing and free-foaming experiments to determine whether higher core densities could be obtained by removing portions of the blowing agent. The primary criteria was mixing time required for a homogeneous blend versus working life (before blowing prevented pouring). A formulation was ultimately selected using 27.2% BX-289 without blowing agent and 72.8% regular BX-289R (with blowing agent).

Two cores were subsequently cast with the selected formulation, using a starting (mix) weight of about 395 grams. Core No. 28 weighed 342.7 grams as-cast (17.1 lb/cu ft), and 322.6 grams (17.5 lb/cu ft) after finishing. Core No. 29 was processed exactly the same way, except that the mixing cup was partially scraped-down during pouring. Its as-cast weight was 361 grams, or 18.0 lb/cu ft density. A series of cores were then cast to obtain several that were dimensionally acceptable, void free, and "high" density. As it turned out, the core used to form the grain of a motor from the final propellant mix had a density of 14 lb/cu ft.

### MOLD RELEASE AGENT

A mold release agent must be applied to the surfaces of the mandrel in contact with propellant so there will not be a bond between them. It was found during Reference VII-2 investigations that failure to use a mold release agent can cause grain fracture during cooldown from cure temperature

MR-22 is a silicone type, air-drying mold release agent that can be solvent diluted for spray-on application. It was used successfully on previous foam core studies (Reference VII-2), so was deemed a prime candidate as the mold release for the current program. A small quantity was diluted with methylene chloride and sprayed on a number of reject foam core bodies. A

shiny, smooth surface was produced, that became dry to the touch after about a half hour. The coating was almost colorless, so the only means of determining complete coverage was by surface sheen. Dyes were available at one time for coloring the spray, but these were no longer obtainable.

One core sprayed with the MR-22 mold release was heated in an oven at 150°F for several hours to speed up the air drying. No particular benefits were noted, but no problems were encountered either. To insure the methylene chloride diluent would not cause degradation of the polyurethane foam, a core was immersed in methylene chloride for about one hour. Examination of the part afterward revealed no softening, distortion, or other degradation. Although not tested for release properties with the current propellant systems, MR-22 was deemed ready for further testing usage because of similarity of propellants and release characteristics.

The mold release agent was applied to some mandrels which were later inserted in the grain cavity after propellant cure was complete (Table VII-5). There was no noticeable difference between these firings and the ones where the mandrel had no release agent.

#### MOTOR TEST RESULTS

Details of the tests on TX-631 motors are given in Section VIII, Igniter/Consumable Mandrel Studies, where igniter/mandrel interactions are discussed. To summarize here (Table VII-6), motor behavior was satisfactory with both "high" and "low" density mandrels which were inserted into the pre-formed propellant cavity and which were tested at 70°F and -65°F. At 165°F, the absence of a gap between propellant and mandrel caused a 2.675-sec. hangfire. Increasing the igniter charge weight for the next test at 165°F resulted in a 0.339-sec. hangfire. The final two motors had grains formed by the consumable mandrel and the original igniter charge weight. One of these with a "high" density mandrel experienced a 0.115-sec. hangfire. The other overpressurized due to grain failure after a 2.620-sec. hangfire. Neither the grain failure nor overpressurization were associated with either the igniter or foam mandrel.

#### CONCLUSIONS

The following conclusions were a result of the consumable mandrel effort:

- (1) A polyurethane foam material was suitable for making mandrels having densities up to a nominal of 17.1 lb/cu ft.
- (2) Propellant was successfully vacuum cast through the motor aft end with mandrels of 12 and 14 lb/cu ft density forming the grain.
- (3) The mandrel was consumed in the motor, with no evidence of material being ejected.

TABLE VII-6  
RESULTS OF TESTS ON TX-631 MOTORS WITH CONSUMABLE MANDRELS

TX631 Designation (Mix-Charge No.)	Mandrel Average Density (lb/cu ft)	How Mandrel Used	Test Temp. (°F)	Results
T634-1	12.5	(a)	70	Satisfactory operation
T640-1	11.9	(a)	70	Satisfactory operation
T640-2	17.5	(a)	70	Satisfactory operation
T643-1	12.1	(a)	-65	Satisfactory operation
T643-2	11.9	(a)	165	2.675 sec. hangfire
T634-2	11.7	(a)	165	0.339 sec. hangfire (increased igniter charge from T634-2)
T684-1	14.3	(b)	70	0.155 sec. hangfire
T684-2	11.9	(b)	70	Over-pressurization not associated with igniter/mandrel preceded by 2.620 sec. hangfire

a. Consumable mandrel inserted into grain cavity during final motor assembly

b. Consumable mandrel used to form grain

## REFERENCES

1. "Improved Low Cost Rocket Motor Processing and Component Development Study", Final Report, June 1972 - May 1975, Report No. AFRPL-TR-75-34, Contract No. F04611-72-C-0074, July 1975.
2. "Final Report, Feasibility and Test Program for Demonstration of Integral Mandrels for Large Solid Propellant Motors", R. C. Comer, Sam Zeman and M. H. Latimer, Report No. U-65-2613, Thiokol/Huntsville, June 1965.

SECTION VIII

IGNITER/CONSUMABLE MANDREL STUDY



## SECTION VIII

### IGNITER/CONSUMABLE MANDREL STUDY

The use of a consumable mandrel in combination with an igniter integral with the mandrel was determined to have exceptional cost-saving potential by the Booz-Allen study (Reference VIII-1)<sup>1</sup>. Additional results reported in Reference 1 showed it was not feasible to initiate directly the bimetallic elements in the igniter. The recommended concept consisted of a molded magnesium/Teflon (Mg/TFE) charge with a low-cost squib initiator.

Ignition system design requirements (Table VIII-1) were established at the beginning of this program for use in evaluating component performance. On the basis of these requirements, concepts were identified for initial screening (Table VIII-2). Although bimetallic wire was not feasible as the sole ignition device, it did appear attractive as the initiator for a subsequent pyrotechnic. A short length of the wire would function within an acceptable time and within the power limitations of the aircraft. The most promising pyrotechnic materials were Mg/TFE (for the reasons listed in Reference 1) and B/KNO<sub>3</sub> (because of past experience, higher heat release, and higher gas-to-solids ratio). Following this initial screening, laboratory tests were conducted as discussed below.

#### LABORATORY TEST EVALUATION

A total of 45 tests was conducted to support the initial concept screening. Tests were performed on the following concepts:

- (1) Bimetallic wire initiator with B/KNO<sub>3</sub> pellet charge.
- (2) Bimetallic wire initiator with Mg/TFE pellet charge.
- (3) Nichrome wire initiator with B/KNO<sub>3</sub> pellet charge.
- (4) Nichrome wire initiator with Mg/TFE pellet charge.
- (5) Electric Match initiator with B/KNO<sub>3</sub> pellet charge.
- (6) Electric Match initiator with Mg/TFE pellet charge.
- (7) Inert mandrel/bimetallic wire/TP-H8047 propellant charge.

The test vehicle used for Concepts 1 - 6 tests is shown on Figure VIII-1 and consists of a mild steel, vented tube fixture threaded to accept a screw-

---

1. References are listed at the end of this section.

TABLE VIII-1

IGNITER DESIGN REQUIREMENTS AND GUIDELINES

1. Delay time:

mandatory	< 0.2 sec
goal	< 0.1 sec
2. Air-launch environment:
  - (a) Firing temperature limit: -65 to 160°F
  - (b) Temperature cycling per paragraph 4.4.2.2.1 of MIL-R-25535A
  - (c) Vibration per MIL-STD-810B, Figure 514.1-2, Curve J, Two axis only
3. Low or minimum smoke is not a requirement.
4. Propellant parameters:
$$r_b = 0.019927 P^{0.428}$$
$$\delta_f = .0630 \text{ lb/cu in}$$
$$C^* = 5185 \text{ ft/sec (nozzle end)}$$
5. Motor parameters:

Initial throat diameter	~ 1.0 in
Initial free volume	~ 60 cu in
Initial burning surface	~ 250 sq in
6. Available ignition current: 3.5 amps (later revised to 9 amps)

TABLE VIII-2

IGNITER CONCEPTS FOR INITIAL SCREENING

<u>Concept No.</u>	<u>Initiation Device</u>	<u>Ignition Device</u>	<u>Mandrel</u>
1	Bi-metallic <sup>(a),(b)</sup> bridgewire	Mg/TFE	Inert <sup>(c)</sup>
2	Bi-metallic <sup>(b)</sup> bridgewire	B/KNO <sub>3</sub>	Inert
3	Bi-metallic <sup>(b)</sup> bridgewire	Mg/TFE	None
4	Bi-metallic <sup>(b)</sup> bridgewire	B/KNO <sub>3</sub>	None
5-8	Nichrome wire <sup>(b)</sup>	Repeat concepts No. 1 through No. 4	
9	Squib	Mg/TFE	Inert
10	Squib	B/KNO <sub>3</sub>	Inert
11	Squib	Bi-metallic wire	Inert
12	Detonator <sup>(d)</sup>	Pyrocore	Inert
13	Selected initiation technique		Combustible <sup>(b)</sup>

a. Pyrofuze<sup>®</sup>.

b. Initiated by current applied directly to noted device.

c. Cannot sustain combustion.

d. One amp-one watt.

e. Contains some amount of oxidizer so that combustion is sustained, once initiated.

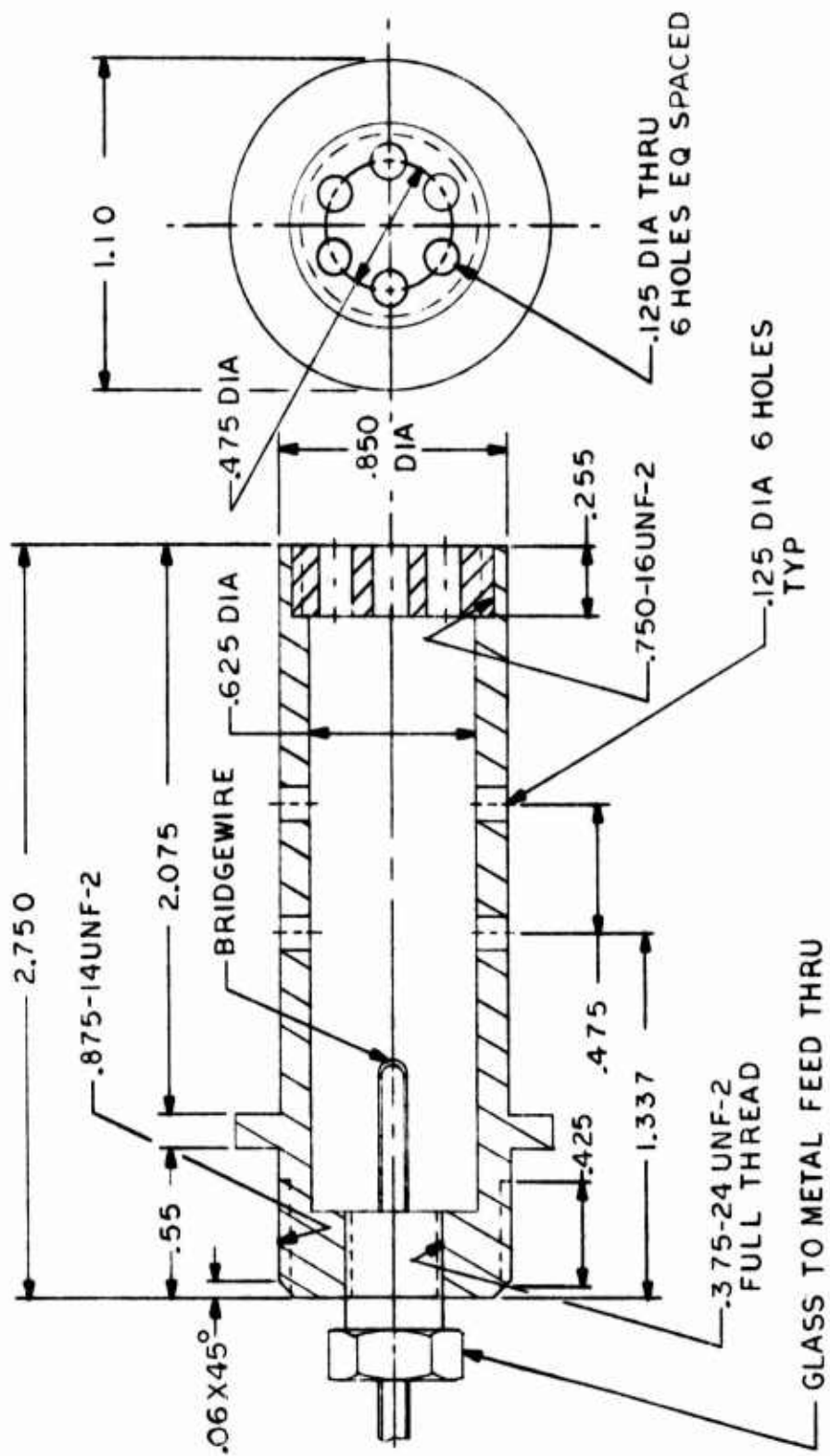


Figure VIII-1. Igniter Laboratory Test Fixture

in glass-to-metal feed-through at the head end and a vented closure on the other. The fixture was cleaned for reuse following each test. A 7-gram charge weight was selected for testing and was held constant throughout. Characteristics of the two pyrotechnics are listed in Tables VIII-3 and VIII-4. Various bridge-wire materials were either soldered or spot-welded to terminals of the glass-to-metal feed through. Photocell sensing was employed to detect igniter function and data was recorded photographically from a Tektronix<sup>®</sup> Model 7844, dual beam oscilloscope. Firing current was calculated from total circuit resistance in tests 1-12 and measured in subsequent tests. Power was provided by two 12-volt wet cell batteries.

#### Series I Tests

The first group of tests was conducted using two sizes of Pyrofuze<sup>®</sup> bimetallic wire in two bridgewire lengths. Tests were performed using B/KNO<sub>3</sub> and Mg/TFE pellets. Firing current was set for approximately 3.5 amps and calculated for each test based on total circuit resistance.

The primary objectives of this first test series were to demonstrate the bimetallic initiator/pellet charge concept and to measure the delay times for .004-inch and .005-inch diameter wires. A mandatory delay time of <0.2 second was desired with a goal of <0.1 second. The function time of the bridgewire material was firmly established which focused concern on the delay to ignite the charge. Function time of Pyrofuze<sup>®</sup> versus applied current is shown on Figure VIII-2 and has been shown to be a reproducible parameter.

At a 3.5 amp firing current level, .004-inch Pyrofuze<sup>®</sup> requires 60 msec to function; .005 requires 170 msec. Since igniter function time is dependant on bridgewire function plus pellet ignition delay, meeting the 100 msec goal at 3.5 amps would require .004 wire and very short pellet ignition delay.

Results from Series I tests are presented in Table VIII-5. For the .004-inch Pyrofuze<sup>®</sup>, 1.5-inch length/Mg/TFE combination, delays ranged from 135 to 215 msec. The .005 Pyrofuze<sup>®</sup>, with the longer bridgewire function time, exhibited delays of 260 to 340 msec. B/KNO<sub>3</sub> charges also exhibited long delays (210-280 msec) in tests 7 - 12.

Results of these tests indicated that although the Pyrofuze<sup>®</sup> initiator did ignite the pellet charge, the delay times were long and inconsistent at this current level. Variance in contact between the bridgewire and pellet charge emerged as a major factor in explaining this phenomenon. A review of igniter objectives was held with the AFRPL Project Officer. Based on these results, the decision was made to increase the firing current from 3.5 to 9.0 amps and to measure actual current on all subsequent tests.

The method of attaching the bridgewire to the feed through terminals by soldering, combined with the relatively long bridgewire lengths proved to present a situation very vulnerable to breakage both in handling of the bridgewire

TABLE VIII-3

CHARACTERISTICS OF MAGNESIUM/TEFLON  
IGNITION MATERIALS

Composition	
<u>Ingredients</u>	<u>Parts by Weight</u>
Magnesium	58.5
Teflon (TFE)	38.5
Binder (laminac)	<u>3.0</u>
	100.0
Burning Rate (in/sec)	$r = 0.060 p^{0.67}$ (from 2-88 psia)
	$r = 1.04 p^{0.033}$ (above 88 psia)
Temperature Sensitivity (%/°F), $\pi_k$	less than 0.0008
Adiabatic Flame Temperature (°F)	3000
Heat of Reaction (cal/gm)	1310 min
Auto-Ignition Temperature (°F)	920
Maximum Storage Temperature (°F)	unlimited at 500
Gas/Solid Ratio	1/99

Physical Properties, 3A Size Pellets

Size, average, inches	0.125 Dia. 0.188 Long
Shape	Cylindrical
Grain Density, min, gm/cc	1.70
Grain Weight, min, gm	0.07
Grain Crush Strength (min longitudinally), gm	8500

TABLE VIII-4  
CHARACTERISTICS OF SP-168  
TYPE I, CLASS 1 BORON-POTASSIUM NITRATE

<u>Ingredients</u>	<u>Composition</u>
	<u>Parts by Weight</u>
Boron	23.7
Potassium Nitrate	70.7
Binder (Laminac)	5.6

Combustion Properties

Heat of Explosion, cal./gm.	1600
Flame Temperature, °F	4080
Burning Rate at 1000 psi, in./sec.	1.25
Gas Volume, ml./gm.	120

Sensitivity

Autoignition Temperature, °F	700
Detonation Rate, m./sec.	Will not detonate
Electric Spark Sensitivity Classification	Not Sensitive
ICC Shipping Classification <sup>(a)</sup>	B
Military Explosive Classification	Class 2

Alkali Metal (By Weight)

Potassium in Potassium Nitrate, %	33.61
Potassium Nitrate in Pellet Composition, %	70.70

Size, Average

Diameter, in.	0.125
Length, in.	0.188

- a. Shipping classification by authority of Bureau of Explosives, Association of American Railroads, South Amboy, N. J., in a letter to Thiokol Corporation dated 2 November 1959.



Values given are for 0.001 to 0.006 -inch diameter wires

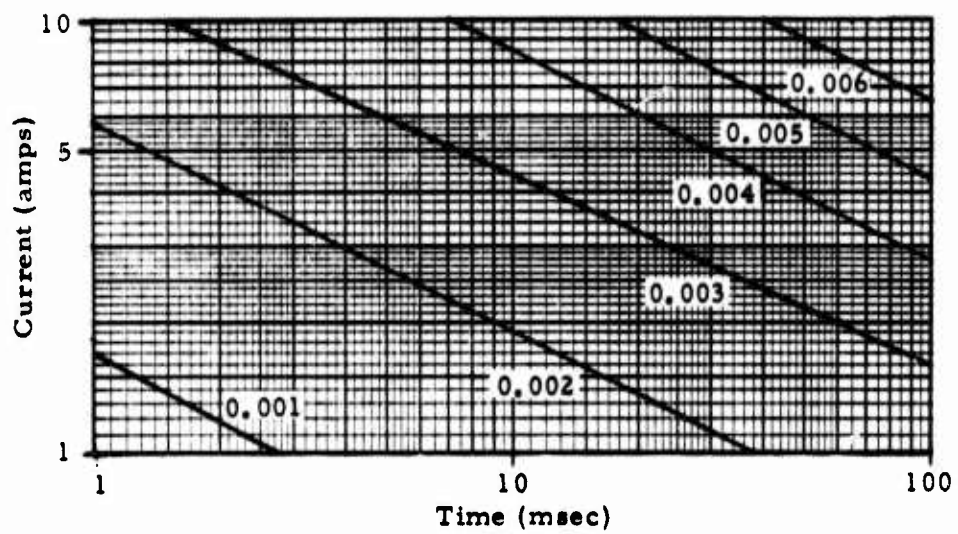


Figure VIII-2. Function Time of Pyrofuze® Wire

TABLE VIII-5  
SERIES I TEST DATA<sup>(a)</sup>

S/N	Pellet Type	Bridge Material	Length (in)	Res. ( $\Omega$ )	Current <sup>(b)</sup> (amps)	Delay <sup>(c)</sup> (msec)
1	Mg/TFE (3A)	0.004 Pyrofuze	1.5	0.60	3.12	215
2	Mg/TFE (3A)	0.004 Pyrofuze	1.5	0.51	3.15	215
3	Mg/TFE (3A)	0.004 Pyrofuze	1.5	0.47	3.86	135
4	Mg/TFE (3A)	0.004 Pyrofuze	1.5	0.54	3.82	180
5	Mg/TFE (3A)	0.005 Pyrofuze	1.5	0.35	3.94	260
6	Mg/TFE (3A)	0.005 Pyrofuze	1.5	0.31	3.67	340
7	B/KNO <sub>3</sub> (2A)	0.004 Pyrofuze	1.5	0.51	3.57	210
8	B/KNO <sub>3</sub> (2A)	0.004 Pyrofuze	1.5	0.54	3.55	---
9	B/KNO <sub>3</sub> (2A)	0.005 Pyrofuze	1.5	0.36	3.64	---
10	B/KNO <sub>3</sub> (2A)	0.005 Pyrofuze	1.5	0.32	3.66	230
11	B/KNO <sub>3</sub> (2A)	0.005 Pyrofuze	3.0	0.67	3.48	255
12	B/KNO <sub>3</sub> (2A)	0.005 Pyrofuze	3.0	0.68	3.48	280

a. Tested at 25 VDC, Ambient Temp., 7 grams pellets

b. Calculated maximum current

c. Photocell sensing

itself and from pellet contact. This is one discrete disadvantage of the bimetallic bridgewire concept.

### Series II Tests

The second series of tests involved the use of the .004-inch Pyrofuze<sup>®</sup> and .0025-inch Nichrome, exclusively. Again a 7-gram charge was employed, with photocell sensing to record delay time. In this series and all subsequent testing, firing current was recorded (voltage across a 0.66-ohm series resistance). The Pyrofuze<sup>®</sup> was attached by the solder method, whereas the Nichrome was spot-welded to the feed-through terminals.

Data are shown in Table VIII-6. The delay times were decreased significantly by the increase in firing current; however, random scatter was still apparent. It was determined in discussions with Pyrofuze Corporation that even a minute bend could fracture the wire resulting in a noticeable increase in the function time. Since braided Pyrofuze<sup>®</sup> was unbraided to obtain the single-strand material, the probabilities of fracturing the wire during the process was high. Future tests were, therefore, conducted using factory-supplied, single-strand material in an effort to reduce data scatter.

Delays using the B/KNO<sub>3</sub> pellets were below the goal of 100 msec max. along with several Mg/TFE tests. From an ignitibility standpoint, the B/KNO<sub>3</sub> has the lower autoignition temperature and generally should ignite faster.

Due to the high resistance of the Nichrome (.0025-inch diameter) bridgewire, firing current at 24 VDC was limited to 1.5 amps. Even so, delays were comparable to those exhibited by the Pyrofuze<sup>®</sup>. It was decided to include more resistance wire tests, at a higher current, in the later tests. No decided advantage was distinguishable, on the basis of these results, in using the Pyrofuze<sup>®</sup> instead of the Nichrome, although the .0025 Nichrome used was more easily broken than the .004 Pyrofuze<sup>®</sup>.

### Series III Tests

The third series of tests employed .006-inch Pyrofuze<sup>®</sup>, .005-inch Karma<sup>1</sup> Alloy #431 and the Atlas M-100 Electric Match<sup>2</sup>. Charges of B/KNO<sub>3</sub> and Mg/TFE pellets were again held constant at 7 grams weight.

Test data are shown in Table VIII-7. The larger .006-inch Pyrofuze<sup>®</sup> having twice the output of the .004-inch size (see Table VIII-8) offered much more reproducible results than previously tested sizes and gave acceptable delay times ( $\leq 100$  msec). The lower resistance Nichrome tested (32  $\Omega$ /ft, Karma #431) allowed an increase in firing current to 4.5 amps. Bridgewire burnout time (T1) was somewhat varied but was close to that observed earlier. However, shorter delays were noted with the Nichrome than with the .006-inch Pyrofuze<sup>®</sup> with B/KNO<sub>3</sub>. Longer delays were noted with the Mg/TFE with two misfires resulting.

---

1. Driver Harris Company, Harristown, N. J.

2. ICI United States, Inc., Atlas Aerospace Division, Valley Forge, Penn.

TABLE VIII-6

## SERIES II TEST DATA (a)

S/N	Pellet Type	Bridge Material	Length (in)	Res. ( $\Omega$ )	Current (b) (amps)	Delay (msec)	T <sub>1</sub> (c) (msec)
13	Mg/TFE (3A)	0.004 Pyrofuze	3.0	1.01	9.0	135	4
17	Mg/TFE (3A)	0.004 Pyrofuze	3.0	0.98	9.0	32	8
16	Mg/TFE (3A)	0.004 Pyrofuze	1.5	0.58	9.0	40	8
25	Mg/TFE (3A)	0.004 Pyrofuze	1.5	0.57	9.0	130	--
26	Mg/TFE (3A)	0.004 Pyrofuze	1.5	0.58	9.0	44	17
14	B/KNO <sub>3</sub> (2A)	0.004 Pyrofuze	3.0	1.01	9.0	24	12
15	B/KNO <sub>3</sub> (2A)	0.004 Pyrofuze	1.5	0.55	9.0	50	8
18	B/KNO <sub>3</sub> (2A)	0.004 Pyrofuze	1.5	0.54	9.0	20	8
23	B/KNO <sub>3</sub> (2A)	0.004 Pyrofuze	1.5	0.53	9.0	50	18
24	B/KNO <sub>3</sub> (2A)	0.004 Pyrofuze	1.5	0.57	9.0	52	19
19	B/KNO <sub>3</sub> (2A)	0.0025 Nichrome	1.5	13.58	1.5	68	36
20	B/KNO <sub>3</sub> (2A)	0.0025 Nichrome	1.5	14.41	1.5	68	37
21	B/KNO <sub>3</sub> (2A)	0.0025 Nichrome	1.5	13.87	1.5	64	35
22	Mg/TFE (3A)	0.0025 Nichrome	1.5	14.21	1.5	120	30

a. Tested at 25 VDC, Ambient Temp., 7 grams pellets

b. Measured maximum current

c. Bridgewire burnout

TABLE VIII-7  
SERIES III TEST DATA<sup>(a)</sup>

S/N	Pellet Type	Bridge Material	Length (in)	Res. ( $\Omega$ )	Current <sup>(b)</sup> (amps)	T <sub>1</sub> <sup>(c)</sup> (msec)	Delay (msec)
27	B/KNO <sub>3</sub> (2A)	0.006 Pyrofuze	1.5	0.26	9.0	58	90
28	B/KNO <sub>3</sub> (2A)	0.006 Pyrofuze	1.5	0.26	9.0	60	89
29	B/KNO <sub>3</sub> (2A)	0.006 Pyrofuze	1.5	0.26	9.0	57	90
35	B/KNO <sub>3</sub> (2A)	0.005 Karma #431	1.5	4.19	4.5	56	48
36	B/KNO <sub>3</sub> (2A)	0.005 Karma #431	1.5	4.01	4.5	46	62
37	B/KNO <sub>3</sub> (2A)	0.005 Karma #431	1.5	3.92	4.5	50	59
43	B/KNO <sub>3</sub> (2a)	M-100 Match	---	1.36	3.5	1.5	10
44	B/KNO <sub>3</sub> (2A)	M-100 Match	---	1.37	9.0	0.5	13
30	Mg/TFE (3A)	0.006 Pyrofuze	1.5	0.26	9.0	58	60
31	Mg/TFE (3A)	0.006 Pyrofuze	1.5	0.26	9.0	59	62
32	Mg/TFE (3A)	0.006 Pyrofuze	1.5	0.26	9.0	60	66
38	Mg/TFE (3A)	0.005 Karma #431	1.5	3.96	4.5	52	38
39	Mg/TFE (3A)	0.005 Karma #431	1.5	3.89	4.5	62	Misfire
40	Mg/TFE (3A)	0.005 Karma #431	1.5	3.87	4.5	64	Misfire
41	Mg/TFE (3A)	M-100 Match	---	1.36	9.0	0.5	44
42	Mg/TFE (3A)	M-100 Match	---	1.36	3.5	1.5	25

a. Tested at 25 VDC, Ambient Temp., 7 grams pellets

b. Measured Maximum Current

c. Bridgewire Burnout

TABLE VIII-8

CHARACTERISTICS OF PYROFUZE WIRE<sup>(a)</sup>

<u>Diameter (inches)</u>	<u>Calculated Resistance (<math>\Omega</math>/ft @ 25°C)</u>	<u>Minimum Ignition Current (amps, in air)</u>	<u>Output (cal/ft)</u>
0.001	62.00	0.30	0.4
0.002	15.50	0.60	1.4
0.003	6.90	0.95	3.1
0.004	3.86	1.30	5.8
0.005	2.50	1.70	8.9
0.006	1.72	2.10	13.2

---

a. Pyrofuze Corp., Mount Vernon, New York 10553

Four tests were conducted with the M-100 Electric Match, which was a prime candidate, low-cost initiator. The test data (Table VIII-7) showed that the function time of this device was short ( $< 5$  msec) even at a low current of 1.0 amp. As the current increased, a point was reached, however, where a slight increase in function time was noticed (Reference VIII-2). The test results indicated very short delay times ( $< 50$  msec) with reproducible results.

#### Alternate Approach

A prototype "polyurethane foam" igniter was successfully tested as a prelude to employing the concept in a TX-631 motor. The test unit (Figure VIII-3) was machined from 16 lb/cu ft polyurethane foam to the approximate bore configuration of the TX-631. A dual, parallel bridgewire of .006-inch Pyrofuze<sup>®</sup> was selected along with a TP-H8047 propellant booster charge. The test objective was to verify that ignition of the propellant charge would take place and to measure, by photocell sensing, the delay time. Bridgewire resistance was measured at .92 ohms. At 9.0 amps, 24 VDC required 80 msec to bridgewire burnout. The propellant ignited within 10 msec following bridgewire function. This test verified that sufficient energy was available from the Pyrofuze<sup>®</sup> to ignite a typical propellant within reasonable time limits.

#### CONCEPTS EVALUATION

##### Pyrotechnics

Mg/TFE, in raw material form, is about 55% of the cost of B/ $\text{KNO}_3$ , or \$5.00 per pound difference in 1,000 pound lots. Pellet manufacturing costs are about the same for the two materials. Thus, since the same cost differential (\$5.00 per pound) should be available for Mg/TFE purchased in larger quantities, about 10% savings should result in total cost.

Although Mg/TFE exhibited a higher autoignition temperature than B/ $\text{KNO}_3$  (Tables VIII-3 and VIII-4), tests showed ready ignition of the material. Thiokol tests under another demonstration program had indicated that the motor ignition characteristics with an aft-end-inserted igniter at low temperature ( $-65^\circ\text{F}$ ) were superior (shorter delay) using the Mg/TFE than B/ $\text{KNO}_3$  tests. The low (1:99) gas/solids ratio permits achievement of 'soft' motor ignition and permits use of a plastic tube, 'shotgun' igniter where B/ $\text{KNO}_3$  will not perform satisfactorily (higher  $dp/dt$  ruptures tubes at locations other than the end). Therefore, Mg/TFE is considered superior over B/ $\text{KNO}_3$  as a low cost pyrotechnic candidate for aft end ignition systems.

For an aft-end igniter or a leave-in-place mandrel-type igniter, a pellet or combination pellet/powder charge would be employed. Since a soft ignition is usually desired for both cases, the relatively slow-burning pellet approach is a likely choice. However, to assure good ignition of the entire igniter charge and to improve motor ignition reproducibility at low temperatures it is often necessary to supplement the pellets with powder (i. e., 20/80 mesh). Use of an all-powder charge would normally result in



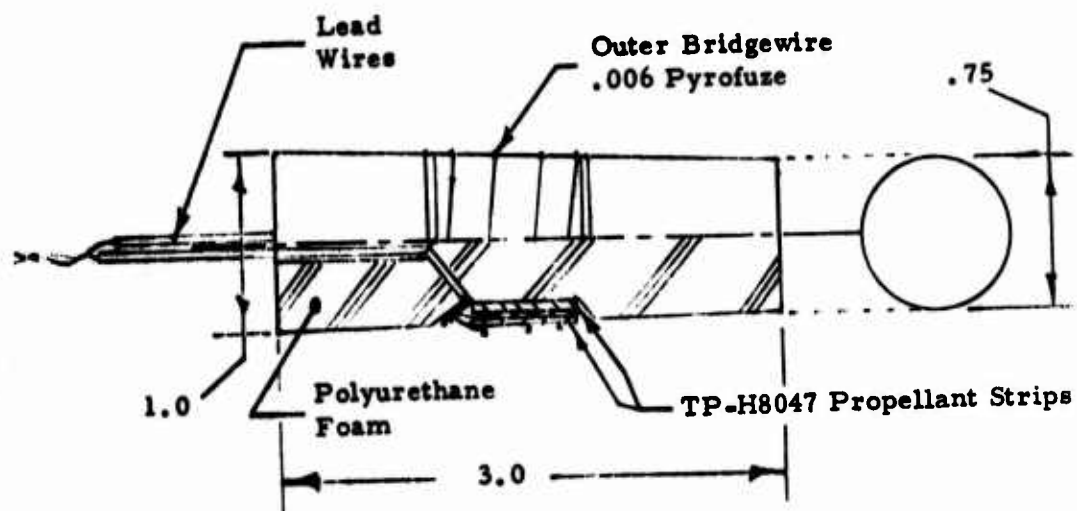


Figure VIII-3. Polyurethane Foam Test Igniter

a higher-than-desirable  $dp/dt$ . The lower gas-to-solids ratio of Mg/TFE makes it particularly attractive for "soft" igniters.

In summary, the Mg/TFE pyrotechnic, with its low gas/solids ratio, good ignition capabilities, and lower cost over standard materials is the most appropriate candidate.

### Initiators

All three types of initiators tested —bimetallic wire, Nichrome, and Atlas Match —represent significant cost savings over most conventional squib initiators. The first two types, although they did meet ignition delay goals, have disadvantages over the latter, those being their potential sensitivity to handling and to shock and vibration. The relatively long bridgewire lengths make them fragile. The bridgewire length could be a disadvantage from a manufacturing standpoint, also, since most automated squib producing machines are designed for short bridgewires. This might be overcome in production, however.

Table VIII-9 lists the initiators tested, ranked according to their overall acceptability based on the low-cost technology philosophy.

The Atlas Match is rated first due to its lower cost and good performance (short delays at low current). The simplicity of the design makes reliability inherent. The match has demonstrated good performance at low temperature and low firing current. The fact that it is automatically produced gives it an edge in cost over other concepts. More detailed discussion is under the following sub-section.

Pyrofuze<sup>®</sup> is rated second and Nichrome third with the Pyrofuze<sup>®</sup> bridgewire (.004-.006 dia.) showing superiority in resistance to breakage over the Nichrome (.0025-.005 dia.). Both the Nichrome and the Pyrofuze<sup>®</sup> exhibit good electrostatic and radio frequency (RF) sensitivity characteristics. Both concepts would require further development to adapt their assembly to fully automated techniques due to the long (1.0-3.0 inch) bridgewire lengths.

The fragile characteristics of primarily the Nichrome, and to some extent the Pyrofuze<sup>®</sup>, bridgewires would present problems when applying the concept to conventional 'loose-load' type igniters. A pellet or powder type pyrotechnic could actually vibrate enough in use to break the bridgewire unless special precautions were taken to pack the pellets. Damage could also occur during loading of the pellets into the container. Casting or dipping the assembled bridgewire in a pyrotechnic could improve this situation.

In summary, the Atlas Match has emerged as the leading contender of the group of initiators tested for the Low Cost Motor Demonstration Program. Short delays, even at low current and low temperature, were demonstrated. The initiator design permits its adaptation for use in practically any conventional type igniter, including the leave-in-place mandrel type.

TABLE VII-9  
INITIATOR CONCEPT RATINGS

<u>Rating</u>	<u>Initiator Concept</u>	<u>Status</u>	<u>Relative Cost</u>	<u>Performance</u>	<u>Advantages</u>	<u>Disadvantages</u>
1	Atlas Match	Demonstrated approach used in Test Motor Igniters and thermal batteries	Lowest Cost	Good	Short function time, low firing current, simple design with good reliability, rigid mass produced	May have poor high temp. storage at high humidity
2	Pyrofuse® Bridgewire (single-strand)	Demonstrated approach used for EED bridge-wires, destruct systems, fusing, etc.	Low Cost	Satisfactory	High alloying temperature (2800°C) Lowest Electrostatic and RF Sensitivity	Somewhat fragile. Long function time. Requires high current. Hand labor required. Minimum initiation temperature 650°C means high temperature available to ignite pyrotechnic
3	Nichrome	Demonstrated approach used in hot-wire and bag igniters	Low Cost	Satisfactory	High melting temperature (1400°C). Low Electrostatic & RF Sensitivity	Very fragile. Requires spot welding. Long function times. high current required. Hand labor required.

### Atlas Electric Match

The Atlas M-100 Electric Match is a standard, off-the-shelf item in high rate production by ICI United States, Inc., Atlas Aerospace Division. The match is fired by supplying sufficient electrical energy to the bridgewire to cause it to become hot enough to ignite the adjacent pyrotechnic mix.

The M-100 series, shown in Figure VIII-4, is characterized by high reliability and low cost based on simplicity of design and exacting control over automated production techniques. The electrode body of the match incorporates resin-impregnated paper, laminated on both sides with 0.0028 inch copper. The laminate is tin plated 0.0005 - 0.0008 inch on each side. The pyrotechnic bead is dip deposited and consists of several discrete coats. Bead composition and dip sequence are listed in Table VIII-10.

Atlas matches have soldered, Nichrome bridgewires. Soldering is done in accordance with MIL-S-6872A, using solder per QQ-S-571B, SN-60. The wire is soldered to each electrode using 60-40 tin-lead solder. Matches are available with or without soldered wire leads.

Characteristics of the M-100 match are listed in Table VIII-11 and Table VIII-12 list data for other 100-series matches. Function time versus firing current for the M-100 match are shown in Figure VIII-5. Tests conducted by Thiokol/Huntsville have verified the operation of the match when used to ignite the Mg/TFE charge and ignition delays (switch closure to  $P_{max}$ ) of < 20 msec have been demonstrated at -75 °F and 1.0 amp firing current, using a single M-100 match.

Atlas matches have been used extensively as thermal battery initiators and in test motor igniters (bag and 'torpedo' types). Early uses of 'match' initiators in sounding rockets and other experimental rockets were common.

There is some indication that the Atlas Match may be susceptible to a high temperature, high humidity environment. Tests run by the Army (Reference VIII-2) showed that the match failed to function when conditioned at 100% relative humidity at 160°F for 24 hours. The firing current was 5 amperes. Tests indicated, however, that the match did function properly after submersion for 24 hours under 1 foot of water (ambient temperature).

Tests conducted by Thiokol/Huntsville have indicated proper match function after storage at 150°F for 15 days at a low (<10%) relative humidity. Firing current was 3.5 amps with no apparent degradation in performance (function time  $\leq 2$  msec).

Since most ignition systems are sealed from high humidity and high temperatures are experienced only for short periods of time, this characteristic of the match may not be a point of major concern. If it should prove to be a problem, steps could be taken to further seal the match and improve its storage capabilities.

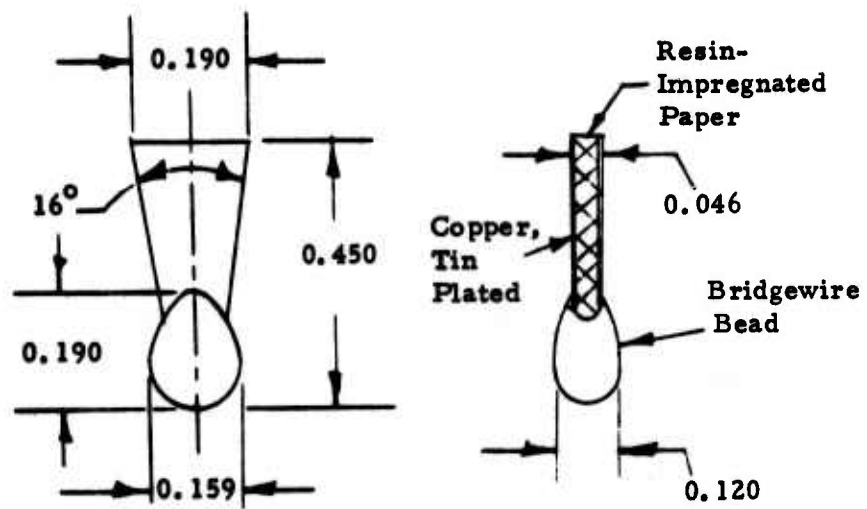


Figure VIII-4. Atlas M-100 Electric Match

TABLE VIII-10

ELECTRIC MATCH COMPOSITION<sup>(a)</sup>

First Coat

76.5% Lead Mononitroresorcinate  
8.5% Potassium Chlorate ( $\text{KClO}_3$ )  
15.0% 1/2 Sec. Nitrocotton, in Iso-Amyl Acetate

Second Coat

76.5% Lead Mononitroresorcinate  
8.5% Potassium Chlorate ( $\text{KClO}_3$ )  
15.0% 1/2 Sec. Nitrocotton, in Iso-Amyl Acetate

Third Coat

9.8% Charcoal  
88.0% Potassium Chlorate ( $\text{KClO}_3$ )  
2.2% 240 Sec. Nitrocotton, in Iso-Amyl Acetate

Fourth Coat - Lacquer

6 oz. 376 Sec. Nitrocotton  
1 gal. Ethyl Ether (2 parts by volume)  
Ethyl Alcohol (1 part by volume)

Fifth Coat - Lacquer

6 oz. 276 Sec. Nitrocotton  
1 gal. Ethyl Ether (2 parts by volume)  
Ethyl Alcohol (1 part by volume)

---

a. Atlas Aerospace Division, ICI United States, Inc., Valley Forge, Pennsylvania, Data Sheet #420, May 1970.

TABLE VIII-11

CHARACTERISTICS OF M-100 ELECTRIC MATCH<sup>(a)</sup>

Bridge Material	80-20 Nichrome .0012 - .0014-inch Dia.
Bridge Resistance, ohms	1.1 - 1.4
All Fire Current, amperes	0.50 for 50 msec
No Fire Current, amperes	0.25 for 5 sec
Test Current, Milliamperes	50
Leakage Resistance, Megohms (measured at 250 VDC)	50 min.
Temperature Storage Limit, min.	24 hours @ 200°F
Testing:	100% for resistance AQL of 0.10%, amb °F for ignition

Electrostatic; no fire when subjected to pin-to-pin discharge from 500 pf cap charged to 25 KV, < 1 msec pulse, 5000  $\Omega$  series resistance.

Static Sensitivity <sup>(b)</sup>	
Max. Energy 0% Firing, Millijoules	Min. Energy 100% Firing, Millijoules
18.0	22.5

Energy (millijoules) =  $CV^2 \times 10^{-3}$ , where c = micro farads and V = volts.

- a. Atlas Aerospace Division, ICI United States Inc., Valley Forge, Pennsylvania, Data Sheet #420, June, 1974.
- b. Redstone Arsenal Laboratories, "Component Studies", Report No. 3M7N23, October 1, 1957, pg. 24.



TABLE VIII-12

ELECTRICAL CHARACTERISTICS: M-100 SERIES ELECTRIC MATCHES

	<u>M-100</u>	<u>M-102</u>	<u>M-103</u>	<u>M-104</u>	<u>M-105</u>
Bridge Resistance, ohms	1.1 - 1.4	4.0 - 5.0	1.1 - 1.4	4.0 - 5.0	0.1 - 0.4
Test Current, milliamps	50	25	50	25	50
All-Fire	0.50a for 50ms	0.58a for 2ms	0.50a for 50ms	0.58a for 2ms	4.5a for 20ms
No-Fire	0.25a for 5 sec.	0.10a for 2 min.	0.25a for 5 sec.	0.10a for 2 min.	1.0a for 15 sec.
	Standard Match	Low Firing Energy	More Flame, Less Gas	Low Firing Energy, "Gasless"	High Firing Energy

Testing by Thiokol/Huntsville  
24 VDC, Ambient Temperature  
Photocell Sensing

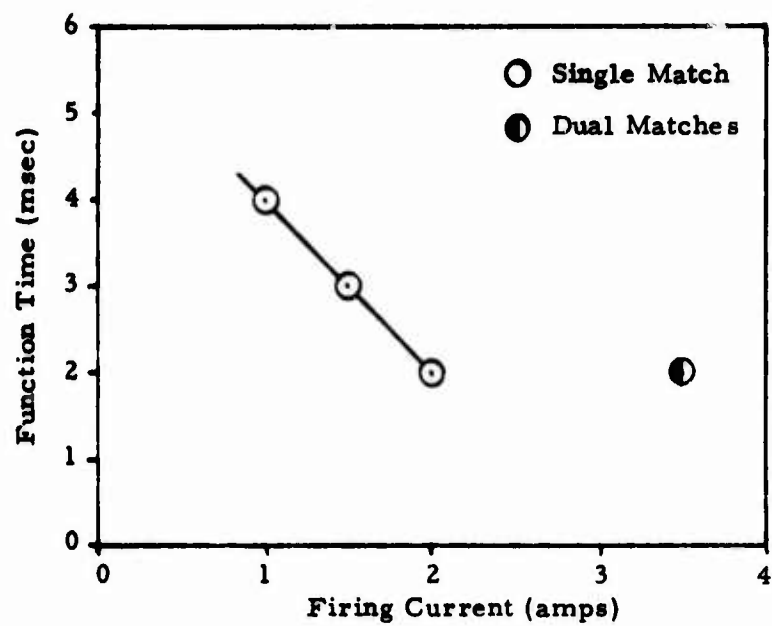


Figure VIII -5. Function Time versus Current for M-100 Electric Match

From a safety standpoint, the problem of protection against static electricity is far and away the most critical in the field of electro explosive devices. Table VIII-13 compares the Atlas match with an M3 type squib, which is commonly used in systems such as LAW and the M-58 Falcon rocket motor. As shown in this brief listing, the Atlas match is less susceptible to static discharge than the M3 squib. This is due to, in part, the absence of a metal case surrounding the Match bridgewire and pyrotechnic which, in the M3 provides a short discharge path between bridgewire and case. The susceptibility of the Match is therefore dependent more on its proximity to metal objects and if 'buried deep' in a high resistance mix or charge, is rather insensitive.

Table VIII-14 compares all-fire, no-fire current and no-fire power characteristics of several squibs and the Match, along with relative cost. The S-102 squib shown is produced by Du Pont and is used in the Air Force Maverick Missile system. The 706 (Celesco) squib was qualified for use in Project Mercury and also used in Tiros satellite systems. The Networks NEI-11 squib is used extensively in thermal batteries.

The no-fire current of the M-105 Match (1.0 amp for 15 seconds) delivers some degree of safety above that of the standard Match. The power dissipation of 6 watt-seconds is sufficient enough to suggest that further development could yield a higher-rated device.

The no-fire power rating might be increased by increasing heat dissipation through the inert metal components (electrode body), the bridge wire (through contact with inert parts, etc.), and through the bead mix itself.

With respect to electrostatic sensitivity, the Match is equivalent to other squibs available. As mentioned earlier, the absence of any metal case in the direct vicinity of the bridgewire prevents any lead-to-case arc.

In comparing other concepts studied, specifically the Pyrofuze<sup>®</sup> initiator, with the 1-amp, 1-watt requirement, one must consider the power output of the fuze and the available 'all-fire' current. A four inch length of .004 inch diameter Pyrofuze<sup>®</sup> will meet the 1-amp, 1-watt requirement (based on calculations only, not tested) for initiation of the wire. However, since the Pyrofuze<sup>®</sup> initiation temperature of 1200°F must be reached before Pyrofuze<sup>®</sup> function, the igniter pyrotechnic charge could easily be ignited by the 'hot' wire even though it fails to function normally. The all-fire current requirement for the four inch wire, for a function time of 0.010 or less, is  $\approx 8.5$  amps at 24 VDC. This is based on an assumption of 1.287 ohms bridge wire resistance and does not include any circuit resistance. Output from the four inch wire (.004 dia) is only 1.93 calories (compared to 22.6 for an M-100 Match).

In summary, the M-105 Match compares favorably with the 1-amp,

TABLE VIII-13

STATIC SENSITIVITY OF INITIATORS<sup>(a)</sup>

Initiator	Average Resistance, (ohms)	Bridgewire		Static Sensitivity (b)		
		Alloy	Average Length (inches)	Average Diameter (inches)	Max. Energy 0% Firing, Millijoules	Min. Energy 100% Firing Millijoules
M3	1.16	Pt	0.07	0.0010	7.5	14.0
Atlas Match	1.53	Ni-Cr	0.08	0.0017	18.0	22.5

223

M102 Atlas Match, No fires when subjected to < 1 msec pin-to-pin discharge pulse from a 500 pf capacitor charged to 25 KV through 5000Ω series resistance<sup>c</sup>.

a. Redstone Arsenal Laboratories, "Component Studies", 3M7N23, October 1, 1957, pg. 24.

b. Energy (millijoules) =  $CV^2 \times 10^{-3}$ , where C = micro farads and V = volts.

c. Atlas Aerospace Division, ICI United States, Inc., Mr. James McCann telecon October 27, 1975 to J. W. McCain, Thiokol/Huntsville.

BEST AVAILABLE COPY

TABLE VIII-14  
INITIATOR COMPARISON

Type Mfg.	Resistance (ohms)	No-Fire (amps)	All-Fire (amps)	No-Fire Power (watts)	Electrostatic Discharge (KV)	Relative Cost (Dollars)	Comments
Pyrofuse Wire (.004)	0.26	≈ 1.0	9.0	0.26	Not susceptible in use configura- tion	2.00 - 5.00 Estimated	Used in Nebworth Motor, high currents (10-20 amps) required.
Nichrome Wire (.005)	3.89	≈ 0.40 (300 sec)	4.0	≈ 0.40	Not susceptible in use configura- tion	2.00 - 5.00 Estimated	Used in 'hot wire' test igniters, etc. Hand labor.
M-100 Match, Atlas	1.40	0.25 (5sec)	0.50 (.05sec)	0.09	25	0.25	Used extensively in Thermal batteries, test motors, etc. Fully automated production.
M-105 Match, Atlas	0.40	1.00 (15sec)	4.50 (.02sec)	0.40	25	0.35	
M3, Callesco	1.16	0.45	0.80	0.23	10	6.95	Used in Falcons, LAW. Some hand labor required.
706, Callesco	≈ 1.00	0.27	0.55	0.07	3	5.40	Used in Tires satellite, more automated.
S102, DuPont	0.70	1.0 (300sec)	4.50	1.00	25	7.66	Used in Maverick
NEI-11, Networks	1.00	1.0 (300 sec)	3.50	1.00	25	5.75	Used in Thermal Battery.

1-watt no-fire squibs. Although it is not a 1-watt no-fire device, the cost differential is overwhelming. The potential cost-savings warrant further investigation into the use of the Match, even though further development would be required to yield a 1-watt no-fire device. The Matches are used extensively "as-is" in thermal batteries for ordnance and space applications (i.e., Eagle Pitcher) and by propulsion companies, including Thiokol/Huntsville for initiators in test motors, batch-check motors, etc.

#### Electric Match and Welding

Weld bonding was one of the techniques evaluated during the program for joining the forward closure or the nozzle to the case. If this technique were selected for low cost application, then it would be possible to have an igniter initiator inside the case during the welding operation. A test was conducted to determine if there might be an incompatibility.

Initiator sensitivity tests were conducted at CDC Industries to determine if significant currents are induced into the squib circuit wiring during the head end closure welding procedure (for weld bonding joining). Two series of tests were conducted, both employing the Atlas M-100 Electric Match. One series employed a shielded leadwire cable and the other used unshielded leadwire.

The test set-up and test circuit schematic are shown in Figure VIII-6. A Tektronix Type 555 dual beam oscilloscope was used to measure current flow through the test circuit. Data was recorded on a Polaroid scope camera. A measure of 1 volt across points A and B signifies a current flow of 0.002 amps ( $E = I \times R$ ;  $1.0 \text{ v} = 500 \Omega \times 0.002 \text{ A}$ ) through the test circuit.

Data from the tests are shown in Table VIII-15. No current flow was measured during the tests. Likewise, neither of the M-100 matches were initiated during repeated welding.

There was some uncertainty as to the exact synchronization of welder discharge and scope triggering during these tests; however no means was readily available at the test site to verify proper synchronization.

In summary, neither of the two Atlas M-100 matches was initiated by the welding operation. No current was measured in the test circuit. However, it is recommended that a similar test be repeated to verify these results before final conclusions as to the safety of the procedure is made.

#### CONCEPT SELECTION

As a result of the laboratory testing and engineering evaluation of those data and other information, two basic approaches were formulated for further evaluation in full-scale heavy-weight motors (TX-631).

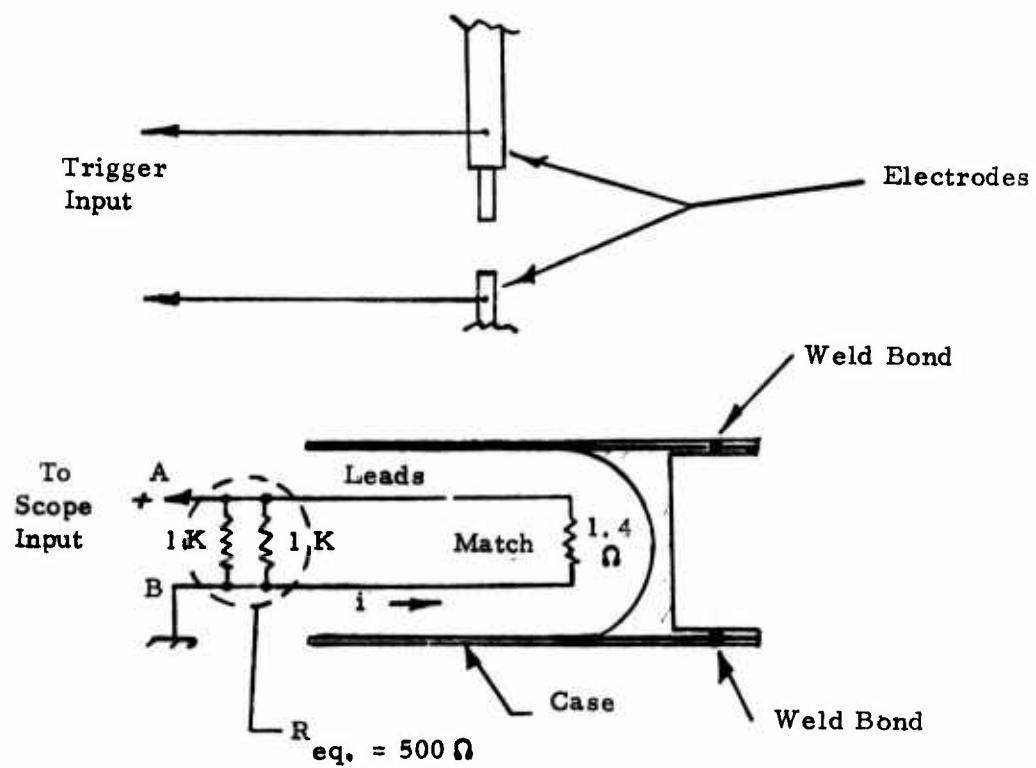


Figure VIII-6. Weld-Bond Initiator Sensitivity Test Set-Up



**TABLE VIII-15**  
**WELD-BOND INITIATOR SENSITIVITY TESTS**

<u>Test No.</u>	<u>Series No.</u>	<u>A &amp; B Resistance</u>	<u>Initiator</u>	<u>Current<sup>(a)</sup> (milliamps)</u>
1	1 (unshielded)	1.396Ω	M100	0
2	1	1.396Ω	M100	0
3	2 (shielded)	1.396Ω	M100	0
4	2	1.396Ω	M100	0
5	2	1.396Ω	M100	0

a. None measured.

Concept A, shown in Figure VIII-7, utilizes the initiator and pyrotechnic which received the highest ratings in previous studies: the Atlas M-100 electric match and magnesium/Teflon. The design incorporates dual matches for increased output and reliability. The matches and pyrotechnic are housed in a thin wall, plastic tube which seals these active components from moisture. This tube is contained within a premolded cavity in the foam mandrel (head end of the motor). Ignition wires are also molded into the mandrel, surrounded by plastic spaghetti tubing.

Concept B, shown in Figure VIII-8, utilizes a molded or roll-up propellant grain charge in place of the Mg/TFE pyrotechnic. Atlas matches serve as initiators. This concept requires no special moisture-sealing techniques since the propellant (i.e., TP-H8047) is not as susceptible as Mg/TFE. This concept might have been used if the previously described design had proven unsatisfactory. Laboratory tests were conducted with TP-H8047 propellant with acceptable delay times. However, if motor tests had indicated the need to use the TP-H8047 booster charge, additional laboratory tests would have been conducted.

#### FULL-SCALE MOTOR TESTS

Eight full-scale heavy weight motors (TX-631) were tested with consumable mandrels having integral igniters. Details of the mandrel are contained in Section VII. The subsequent discussions describe the ignition phase and igniter/mandrel interactions. Some pertinent information is listed in Table VIII-16.

#### First Test Group

The first TX-631 motor test (Mix T-634, Charge 1) with a leave-in-place consumable foam mandrel was singularly successful. Mandrel S/N 22, with an average density of 12 lb/cu ft, was inserted into the propellant cavity after the grain had been cut back. No rework of the foam was required to obtain a good fit of the mandrel in the cavity. The igniter was pre-assembled into the mandrel. After the mandrel was inserted, the head end closure and the nozzle assembly were installed on the case.

The igniter (Figure VIII-9) consisted of 20 grams of Size 3A Mg/TFE pellets initiated by dual (parallel) M-100 Electric Matches and was contained in a premolded cavity in the head-end portion of the foam mandrel. The motor was preconditioned to 70°F prior to the test.

Maximum pressure was less (3950 psia compared with 4270 psia) than had been experienced with Charge 2 of Mix T-622 without a consumable mandrel. Erosion appeared to be more uniform around the nozzle periphery, which is attributed to the slower filling of the chamber and thus less distortion of the flow field at ignition.

The igniter/mandrel appeared to function satisfactorily, igniting the

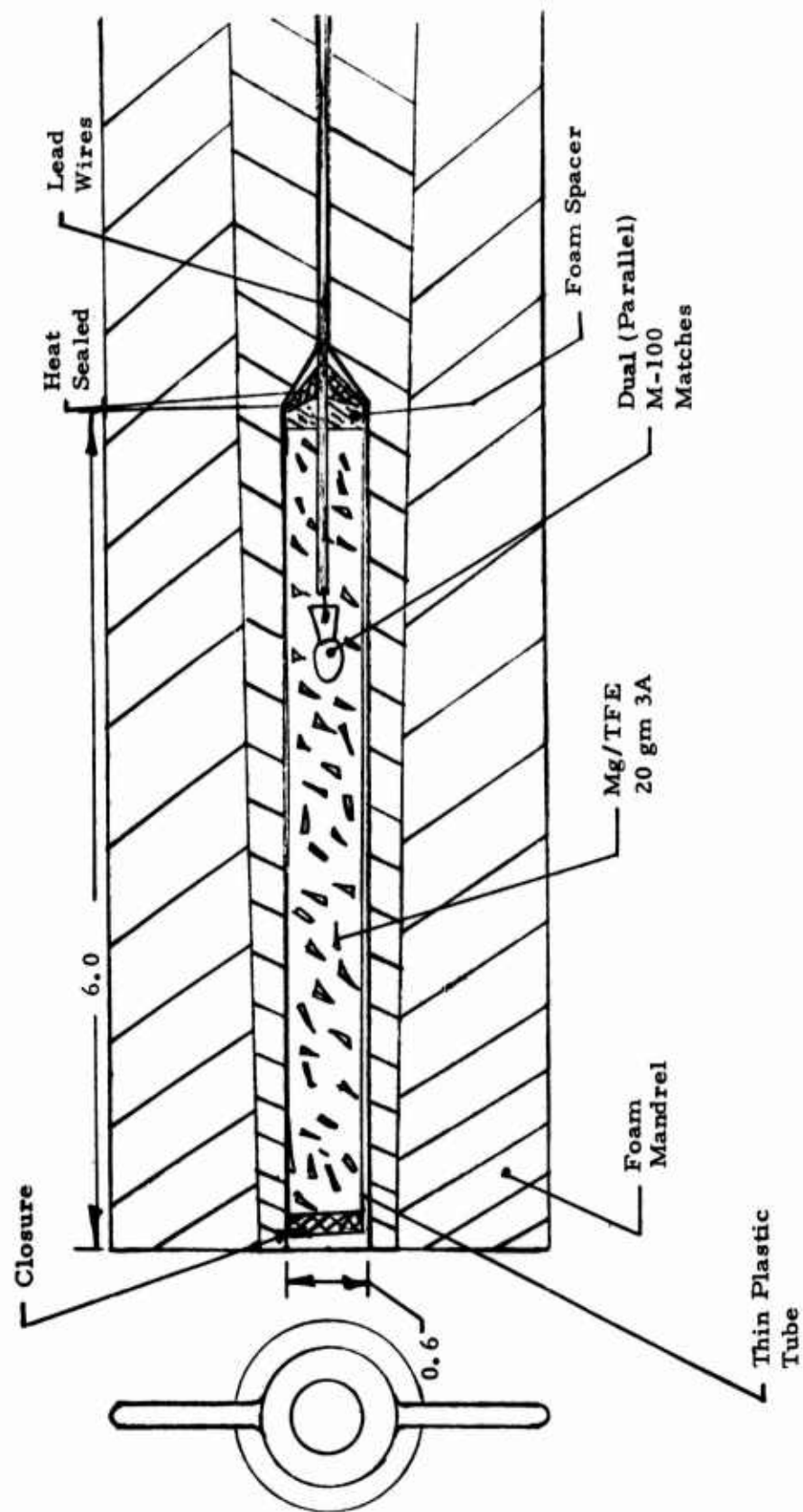


Figure VIII-7. Concept A, Leave-In-Place Igniter/Mandrel for TX-631 Motor

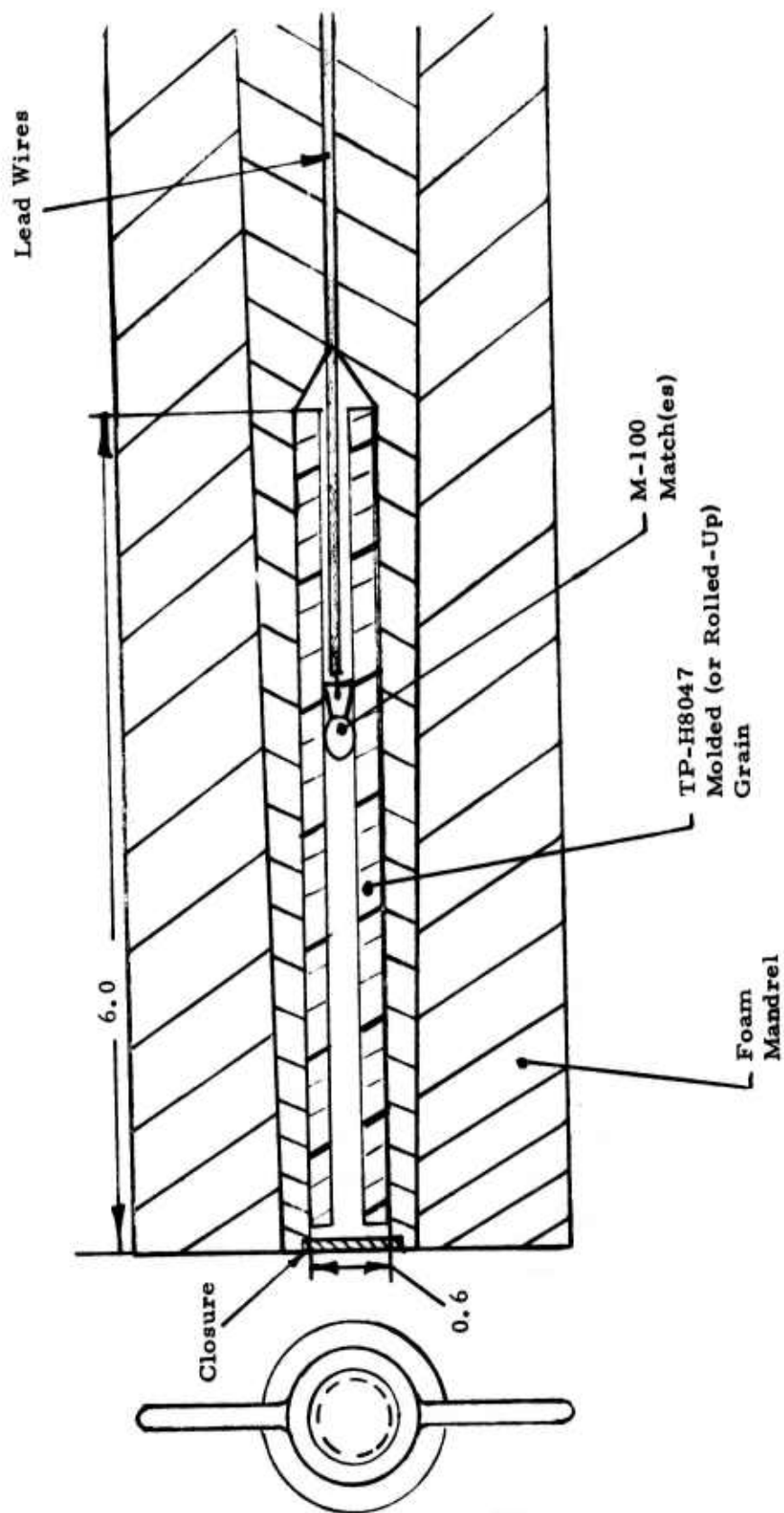


Figure VIII-8. Concept B, Leave-In-Place Igniter/Mandrel for TX-631 Motor

TABLE VIII-16

## IGNITER/CONSUMABLE MANDREL TESTS

TX-631 Designation (Mix-Charge No.)	Mandrel Average Density (lb/cu ft)	How Mandrel Used	Test Temp. (°F)	Igniter Charge (gms) <sup>(a)</sup>		Results
				Pellets	Powder	
T634-1	12.5	(b)	70	20	--	Satisfactory operation
T640-1	11.9	(b)	70	10	10	Satisfactory operation
T640-2	17.5	(b)	70	10	10	Satisfactory operation
T643-1	12.1	(b)	-65	10	10	Satisfactory operation
T643-2	11.9	(b)	165	10	10	2.675 sec hangfire
T634-2	11.7	(b)	165	20	20	0.339 sec hangfire (increased igniter charge from T634-2)
T684-1	14.3	(c)	70	10(d)	10(d)	0.155 sec hangfire
T684-2	11.9	(c)	70	10	10	Over-pressurization not associated with igniter/mandrel; 2.620 sec hangfire

a. Initiator was Atlas M100 Electric Match. Pyrotechnic was magnesium-tesflon.

b. Consumable mandrel inserted into grain cavity during final motor assembly.

c. Consumable mandrel used to form grain.

d. Mandrel cut back to propellant surface in cylindrical bore for distance of 1.5 inches from headend.

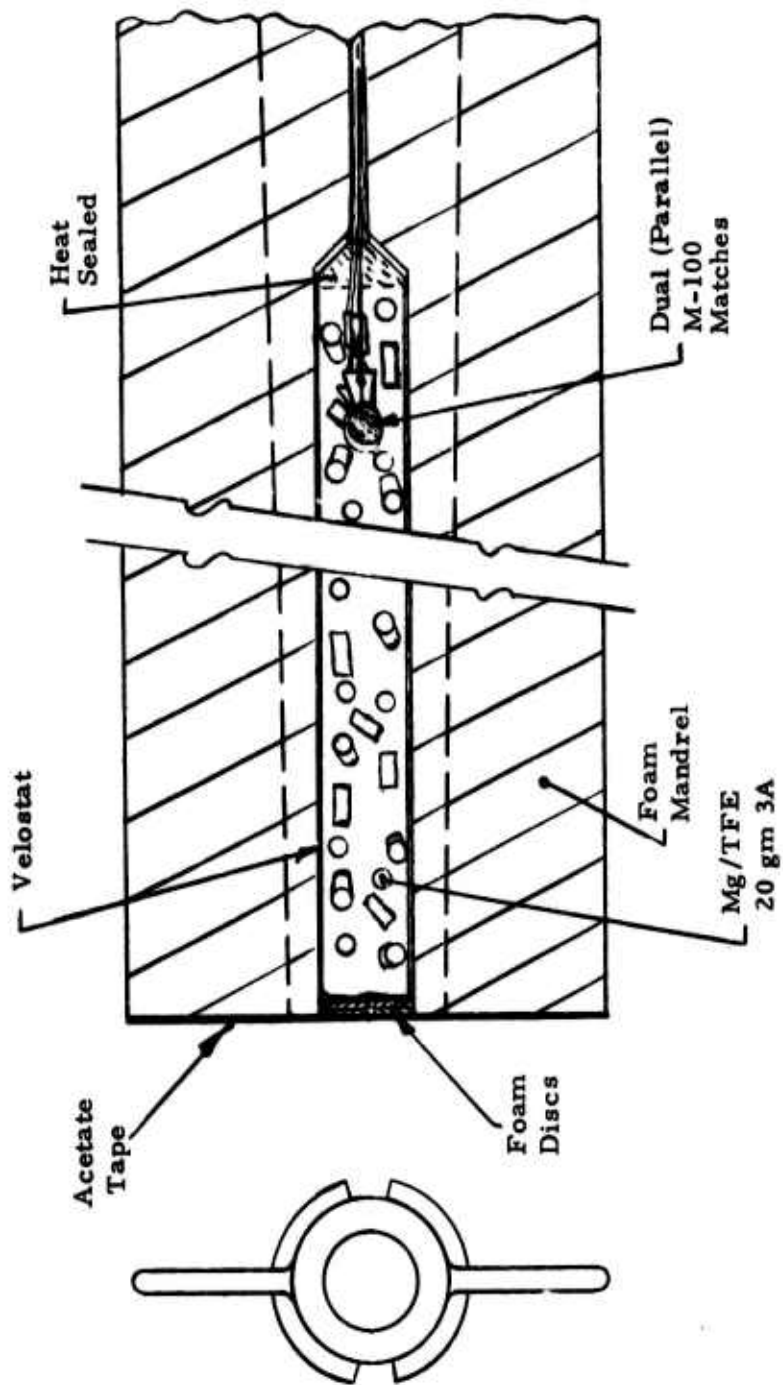


Figure VIII -9. Leave-In-Place Igniter/Mandrel for TX-631 Motor, Mix T-634, Charge 1

motor in less than 150 msec (switch closure to 50%  $P_{\max}$ ). Table VIII-17 compares the operation of the igniter/mandrel with the previously used head-end mounted igniter in Charges 1 and 2 of Mix T-622. These data show that the igniter/mandrel was somewhat slower in igniting the motor than the head-end mounted igniter and that the average transient  $dp/dt$  was lower.

Figure VIII-10 shows the ignition transient (pressure versus time) for these motors. The flame spread rate and subsequent pressure rise was very fast for the first two motors (high  $dp/dt$ ). However, for the motor with the integral igniter/mandrel, the pressure rise was not as sharp (lower  $dp/dt$ ). Possible explanations for this phenomenon include heat absorption and/or motor grain inhibition by the foam material which adds to delay time. An absence of any pronounced crack burning effects between the mandrel/motor grain was evident. The mandrel taper was such that only slight movement aft served to diminish these effects.

The ignition delay time and motor rise time would most likely be improved by slightly increasing the igniter charge weight or by substituting a quantity of Mg/TFE powder to decrease initiation-to-charge delay. Apparently much ignition energy is absorbed in the process of thermal and mechanical decomposition and ejection of the foam mandrel.

The low gas/solids ratio of the Mg/TFE ( $\approx 1:99$ ) pyrotechnic conceivably results in a much lower addition to motor  $dp/dt$  and  $P_{\max}$  by the igniter, which is certainly a desirable feature for the igniter/mandrel concept.

Evaluation of the high-speed movie coverage of the test-firing indicated no visible debris other than smoke being ejected from the motor and suggests that the mandrel was entirely consumed as the motor ignited.

In summary, the initial test of the leave-in-place igniter/mandrel was considered completely successful with no failure occurring and acceptable ignition delay being exhibited.

#### Second Test Group

The second test set evaluated a change in igniter charge from all pellets to a pellet/powder combination in conjunction with mandrels of two different densities (nominally 12 and 17 lb/cu ft), both with motors at 70°F.

TX-631 motors, Charges 1 and 2 of Mix T-640, were both successfully tested with leave-in-place mandrels. The igniters (Figure VIII-11) consisted of 20 grams Mg/TFE pyrotechnic (10 grams size 3A pellets and 10 grams 20/80 powder). The charge was initiated by dual (parallel) M-100 Atlas Matches. The charge was contained in a premolded cavity in the headend portion of the BX-289 foam mandrel.



TABLE VIII-17

TX-631 BALLISTIC DATA

IGNITION PHASE

First Test Group and Reference Firings

Motor	TSPR <sup>(a)</sup> (sec)	TD20 <sup>(b)</sup> (sec)	TD50 <sup>(c)</sup> (sec)	TPMAX <sup>(d)</sup> (sec)	PMAX <sup>(e)</sup> (psia)	dp/dt <sup>(f)</sup> (KPSI/sec)
T622-1	0.0135	0.0295	0.0331	0.0651	3853	321
T622-2	0.0125	0.0312	0.0349	0.0535	4268	346
T634-1	0.0875	0.1200	0.1325	0.2075	3951	95

a. TSPR	-	Time interval from application of firing voltage (TSW) to the first sustained pressure rise (seconds).
b. TD20	-	Time interval from TSW to where pressure equals 20% PMAX on the first sustained pressure rise (seconds).
c. TD50	-	Time interval from TSW to where pressure equals 50% PMAX on the first sustained pressure rise (seconds).
d. TPMAX	-	Time interval from TSW to the time of PMAX (seconds).
e. PMAX	-	Maximum pressure (psia).

f.  $\frac{dp}{dt} = \frac{P50 - P20}{TD50 - TD20}$

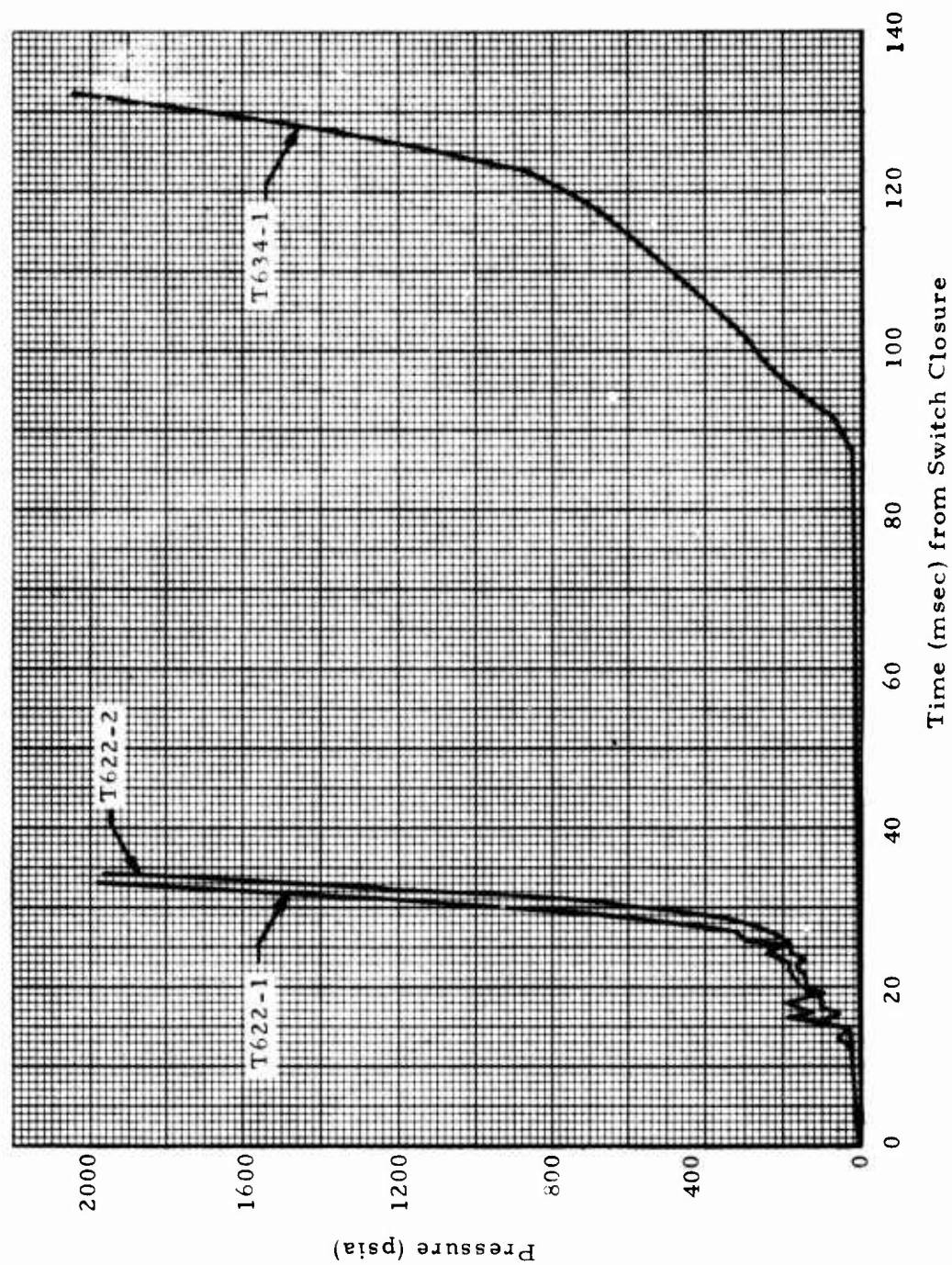


Figure VIII-10. TX-631 Motor Ignition Transients, First Test Group and References

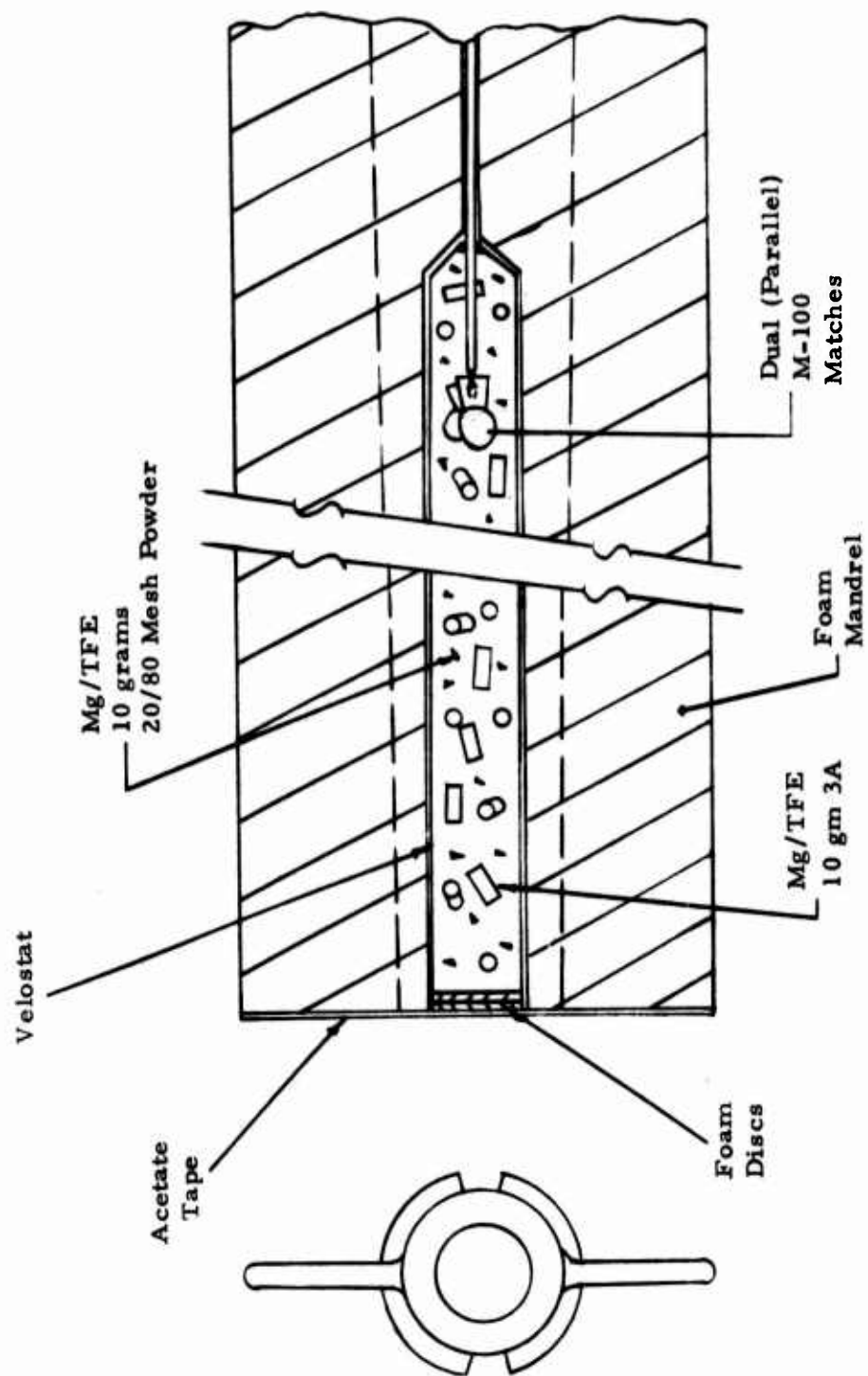


Figure VIII-11. Igniter/Mandrel for TX-631 Motors, Mix T-640, Charges 1 and 2

Motor T-640-1 employed a 12 lb/cu ft foam mandrel (S/N 24) and Motor T-640-2 employed a 17.5 lb/cu ft mandrel (S/N 28).

The change in igniter charge makeup from all size 3A pellets to 10 gm pellets plus 10 gm 20/80 powder resulted in a marked reduction in ignition delay (TSPR) from 87.5 msec for the previous motor (all pellets) to  $\leq 31$  msec for the latter motors. This reduction in ignition delay may be attributed to improved match-to-charge ignition and faster flame spread within the charge itself due to the presence of the 20/80 mesh powder.

As noted in Table VIII-18, TD50 for both motors was significantly improved from 133 msec (T-634-1) to  $\leq 46$  msec. This delay time is acceptable being well below the  $\leq 100$  msec goal.

The high-speed movie coverage of both tests were evaluated with no visible debris being ejected from either motor. The first visible sign of ignition was a small fireball followed by dark, heavy smoke. The next event was the ejection of a large, bright, magnesium-type fireball. A normal motor plume followed this event. All indications are that the mandrel was consumed entirely within the motor with no debris being ejected.

Figure VIII-12 depicts the ignition transient for these motors along with T-634-1, the first igniter/mandrel test, and T-622-2, a motor which used the standard head-end mounted igniter. As shown on the figure and by data in Table VIII-18, dp/dt for these motors was slightly higher than for the first mandrel test. The pressurization rate from TSPR to TD20 was also markedly higher. P<sub>MAX</sub> for T-640-2 with the 17.5 lb/cu ft mandrel was greater (higher spike of 4963 psia versus 3750 psia) than for T-640-1 which employed the 12 lb/cu ft mandrel.

To summarize, both igniters functioned satisfactory in terms of ignition delay time. The 17.5 lb/cu ft mandrel test showed an undesirably high ignition peak. The igniter charge weight and composition tested showed much improvement over the previously tested all-pellet charge and no changes were indicated at this time.

#### Third Test Group

Two TX-631 motors, Charges 1 and 2 of Mix T-643, were selected to evaluate the 12 lb/cu ft igniter/mandrel at low ( $-65^{\circ}\text{F}$ ) and high ( $165^{\circ}\text{F}$ ) test temperatures, respectively. Since favorable results in terms of ignition delay were obtained with the last two motors (T-640-1 and T-640-2) using the 20-gram charge (10 gm 3A pellets, 10 gm 20/80 mesh powder), temperature extremes were the next logical step in testing the concept.

The behavior of the foam mandrel/igniter at temperature extremes is perturbed by several factors including: (1) the foam material becomes stiffer and shrinks somewhat at low temperature, and becomes less stiff

**TABLE VIII-18**  
**TX-631 MOTOR BALLISTIC DATA: FIRST AND SECOND TEST GROUPS**  
**AND REFERENCE FIRING**

Motor	Igniter	TSPR <sup>(a)</sup> (sec)	TD20 <sup>(b)</sup> (sec)	TD50 <sup>(c)</sup> (sec)	TPMAX <sup>(d)</sup> (sec)	PMAX <sup>(e)</sup> (psia)	dp/dt <sup>(f)</sup> (KPSI/sec)
T622-2	Head End 10 gm charge	0.0125	0.0312	0.0349	0.0535	4268	346
T634-1	Mandrel, 12 lb/ft <sup>3</sup> foam 20 gm 3A pellets	0.0875	0.1200	0.1325	0.2075	3951	95
T640-1	Mandrel 20 gm (10 gm 3A pellets (10 gm 20/80 pellets) 12 lb/ft <sup>3</sup> foam	0.0270	0.0343	0.0463	0.085	3750	105
T640-2	Mandrel 20 gm (10 gm 3A pellets) (10 gm 20/80 pellets) 17.5 lb/ft <sup>3</sup> foam	0.0308	0.0350	0.0456	0.0777	4962	142

- a. TSPR - Time interval from application of firing voltage (TSW) to the first sustained pressure rise (seconds).
- b. TD20 - Time interval from TSW to where pressure equals 20% PMAX on the first sustained pressure rise (seconds).
- c. TD50 - Time interval from TSW to where pressure equals 50% PMAX on the first sustained pressure rise (seconds).
- d. TPMAX - Time interval from TSW to the time of PMAX (seconds).
- e. PMAX - Maximum pressure (psia).
- f. dp/dt - P50 - P20  
TD50 - TD20



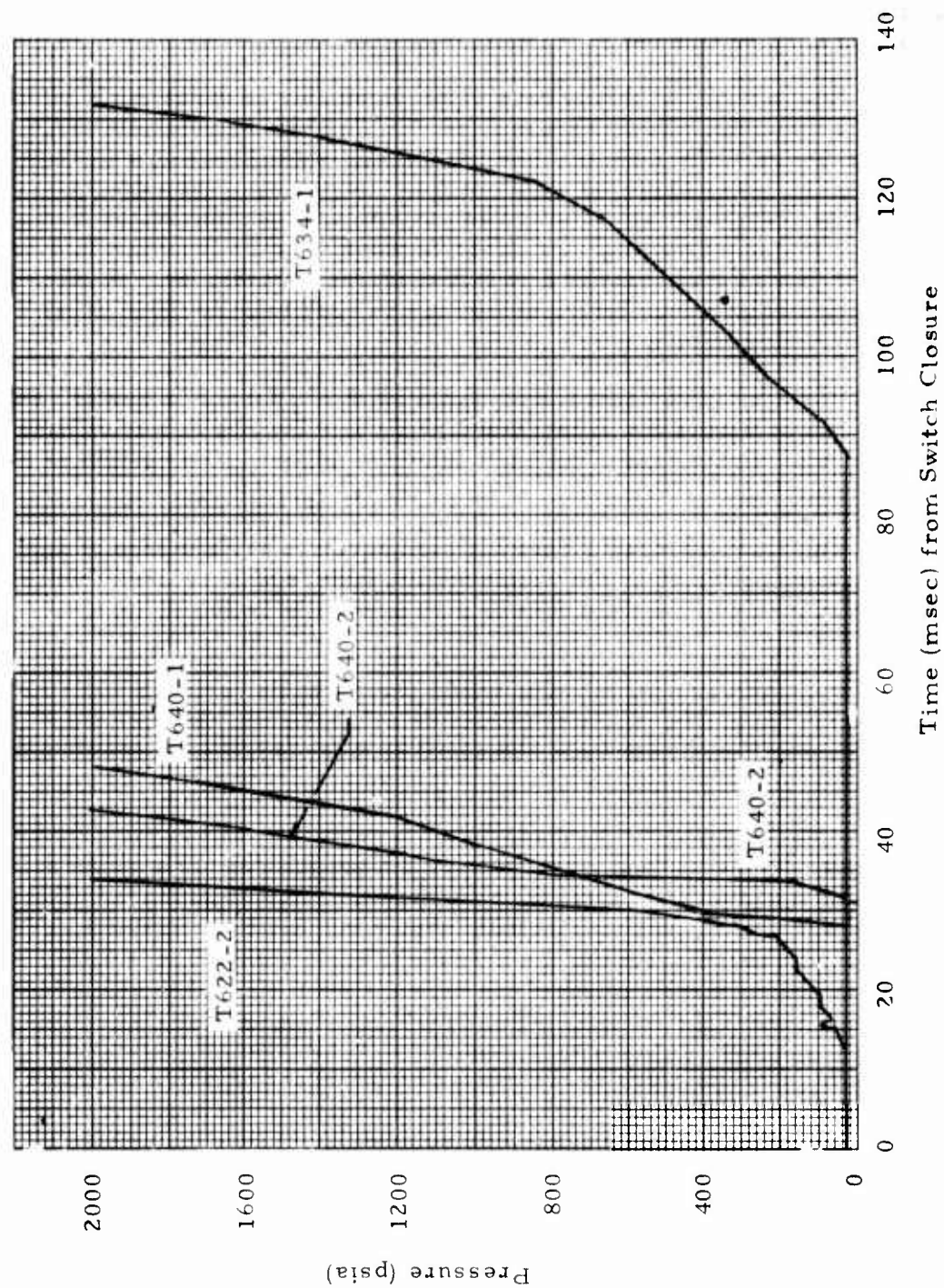


Figure VIII-12. TX-631 Motor Ignition Transients, First and Second Test Groups

and expands at high temperature and (2) the motor propellant flame spread rate and burning rate varies directly with temperature.

The factors in (1) may have either desirable or undesirable effects on igniter function. The increase in modulus at low temperature could foreseeably result in a longer time being required to break up and consume the mandrel material and/or expel it from the motor. The expected result (from this phenomena alone) would be an increase in initial motor  $P_{max}$ . The increase in delay time might be offset, however, by the increase in burning rate and flame spread rate as a result of increased pressure. In other words, the ignition delay at low temperature may be very near the 70°F delay due to these offsetting effects.

'Normal' motor characteristics dictate a reduction in ignition delay at high temperatures due to increased propellant burning rate and flame spread rate. In the case of pyrogen igniters, higher igniter output is also significant.

The foam mandrel/igniter high temperature performance is again somewhat complicated by the counteracting factors of 1) reduced foam modulus and 2) expansion of the foam core to give greater adhesion to the motor propellant.

The reduced core modulus would permit easier breakup and consumption and/or expulsion (tends to reduce delay); however, this results in a lower pressure which may contribute somewhat to delay (again counteracting factors).

The expansion of the mandrel material would tend to promote greater adhesion between the mandrel itself and the propellant. This effect could result in an increase in pressure and delay time due to increased difficulty in mandrel breakup and consumption/expulsion. Also, the reduced modulus and the greater adherence to the propellant could result in less distinctive breakup and/or more melting of the core material while it is still adhered to propellant. This 'coating' effect could result in some degree of inhibition of the propellant surface until such time as the propellant surface reaches autoignition temperature or the molten material is burned or swept away.

Table VIII-19 is an attempt to summarize various temperature 'effects' and relate their effect on mandrel/igniter, and subsequently motor, operation.

Test data for the third test group are summarized in Table VIII-20.

Motor T643-1 was successfully tested at -65°F. Ignition TSPR (0.029 sec) was somewhat shorter than a similar motor (T640-1) at 70°F.  $P_{max}$  was also slightly lower, 3705 psi versus 3750 psi for T640-1. No abnormalities whatsoever were noted. The high speed movie coverage was reviewed and appeared similar to other tests with no debris noted. Pressure versus time



**TABLE VIII-19**  
**IGNITER/CONSUMABLE MANDREL TEMPERATURE EFFECTS**

Characteristic	Result	Effect	Delay Time
<b>LOW TEMP</b>			
<u>Mandrel</u>			
1. Increased Foam Modulus	Stiffer Mandrel	More difficult to consume May increase P <sub>max</sub>	Increases Decreases
2. Shrinkage of Mandrel	Less bond to propellant	Less difficult to consume May lower P <sub>max</sub>	Decreases Increases
<u>Motor</u>			
1. -A Lower Burning Rate	Lower dp/dt		Increases
2. -A Slower Flame Spread	Decreased Burning Area Rate		Increases
<b>HIGH TEMP</b>			
<u>Mandrel</u>			
3. Reduced Foam Modulus	Softer Mandrel	Less difficult to consume Lower pressure	Decreases Increases
4. Expansion of Mandrel	Greater bond to propellant	More difficult to consume Higher pressure More melting at surface of propellant (inhibiting)	Increases Decreases Increases
<u>Motor</u>			
3. -B Higher Burning Rate	Higher dp/dt		Decreases
4. -B Faster Flame Spread	Increased Burning Area Rate		Decreases

BEST AVAILABLE COPY

TABLE VIII-20  
TX-631 MOTOR BALLISTIC DATA - THIRD, FOURTH, AND FIFTH TEST GROUPS

Motor	Igniter	TSPR(a) (sec)	TD20(b) (sec)	TD50(c) (sec)	TPMAX(d) (sec)	PMAX(e) (psia)	dp/dt(f) (kpsi/sec)	Temp.(°F)	Comments
T643-1	20 gm 10 gm-3A 12 pcf Mandrel	0.0292	0.0425	0.0545	0.0975	3705	87	-65.0	First temperature test of Mandrel/ Igniter
T643-2	30 gm 10 gm-3A 12 pcf Mandrel	2.675	2.720	2.7703	3.0900	2231.3	13	+165.0	High temperature test; Hangfire resulting.
T634-2	40 gm 20 gm-3A 12 pcf Mandrel	0.339	0.358	0.4025	0.5588	2648.8	18	+165.0	Second High temperature test. Igniter charge doubled. Hangfire resulted, but shorter (2.675) than before.
T684-1	20 gm 10 gm-3A 17 pcf Mandrel	0.155	0.3950	0.440	0.6350	2758.0	19	+70.0	First cast-in-place Mandrel/Igniter test. Standard charge. Hangfire resulted. (Ambient cure propellant)
T684-2	20 gm 10 gm-3A 12 pcf Mandrel	2.620	2.670	2.680	2.680	13,600	408	+70.0	Second cast-in-place Mandrel/Igniter test. Standard charge, but cut back 1.5 inches of inner core (headend) after cure to directly expose propellant surface to igniter charge. Motor failed after hang- fire, (similar to T643-2) into normal pressure rise.

- a. TSPR - Time interval from application of firing voltage (TSW) to the first sustained pressure rise, seconds.  
b. TD20 - Time interval from TSW to where pressure equals 20% P<sub>max</sub> on the first sustained pressure rise, seconds.  
c. TD50 - Time interval from TSW to where pressure equals 50% P<sub>max</sub> on the first sustained pressure rise, seconds.  
d. T<sub>PMAX</sub> - Time interval from TSW to the time of P<sub>MAX</sub>, seconds.  
e. P<sub>MAX</sub> - Maximum Pressure, psia.  
f. dp/dt - P<sub>50</sub> - P<sub>20</sub>  
TD50 - TD20

for this test is shown in Figure VIII-13. The standard 20-gram igniter was employed (see Figure VIII-11).

Motor T643-2 was tested at +165°F with a 2.675 second hang-fire resulting. Igniter operation appeared normal (700 psi  $P_{max}$ ) and as viewed from movie coverage was similar to all others with the exception that after the initial fire ball was ejected, normal motor operation failed to follow. What did follow was several seconds of extremely low pressure ( $\approx 18$  psia) operation, resulting in ejection of much dark smoke and an occasional small flame. After  $\approx 2.67$  seconds from switch closure, a pronounced increase in burning was noted followed immediately by 'normal' motor operation. An expanded igniter pressure versus time plot is shown in Figure VIII-14. Motor pressure versus time is shown in Figure VIII-15.

After carefully studying the data and movie coverage footage, a hypothesis was formulated as to the cause for the hangfire. As mentioned earlier, increased temperature results in expansion of the mandrel and greater adhesion to the propellant (ignition flame would not easily propagate between the mandrel and propellant). Also the reduced modulus would allow the burning charge to be ejected sooner with subsequent loss of heat effect to the propellant surface. This factor along with the possibility that a layer of molten mandrel material might still be adhered to the propellant surface was the basis for deciding to increase the charge weight from 20 to 40 grams for another high temperature test. The increased charge should contribute a significantly greater amount of heat toward the propellant surface and reduce or eliminate the hangfire condition.

It was recognized that for the mandrel to be inserted into the pre-formed propellant cavity, there must exist a gap of some finite dimension between the mandrel and propellant surface. As a result of the test of Motor T643-2, it was further recognized that lack of a gap could contribute to the hang-fire if the igniter combustion products were not sufficient to burn away the foam. A test was devised to determine if differential thermal expansion between the mandrel and propellant at 165°F did seal off whatever small gap might exist at 70°F.

The TX-631 case has identical attachment threads at both ends. Motor T643-2 was allocated to test effects of increased igniter charge, so a foam mandrel was installed as had been done on previous motors. Head-end caps were assembled on both ends of the case. Identical pressure transducers were installed on both ends with equal length air-filled, 1/4-inch diameter tubing. Transducer output was recorded on the digital data acquisition system and was played back on to a high-speed oscillograph. A nitrogen tank was attached to the forward closure (with respect to the grain configuration) through 1/4-inch tubing, a pressure regulator and a hand-operated valve. It was not intended to simulate ignition pressure transient, but merely to introduce a source of pressure at the forward end of the grain and measure the time interval between first pressure rise at the forward end and at the aft end.

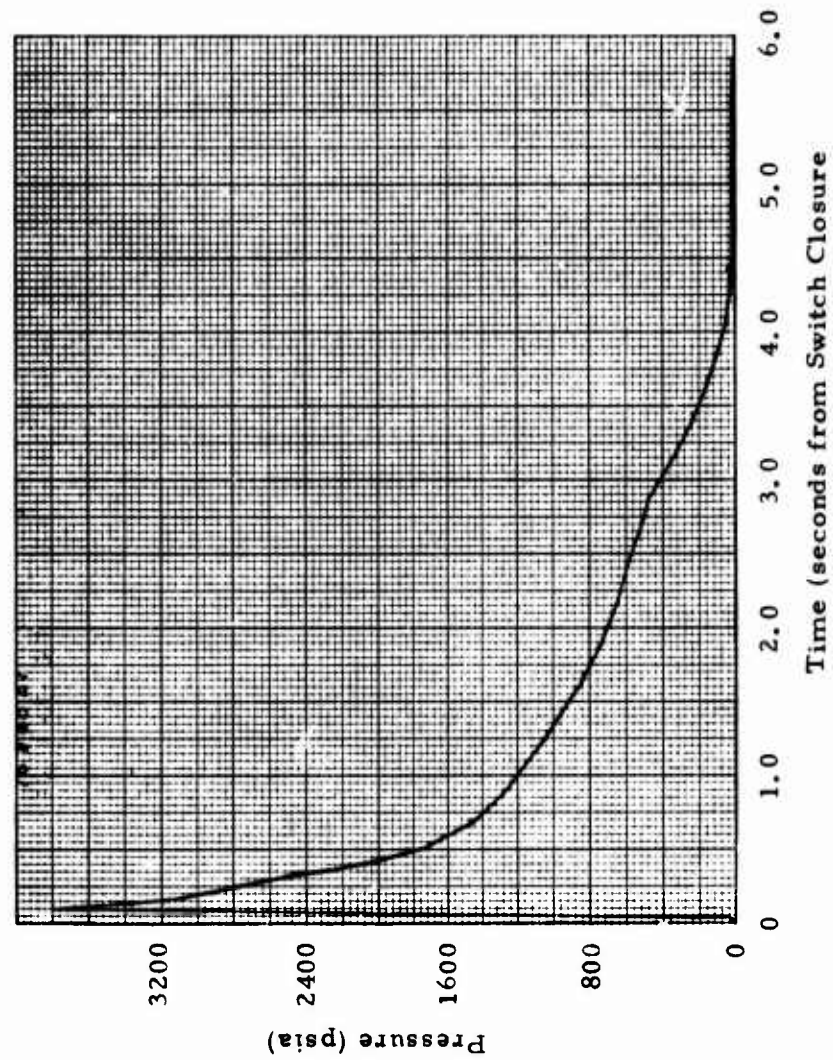


Figure VIII-13. Ballistic History, TX-631 Motor, Mix T-643, Charge 1, Fired at -65°F

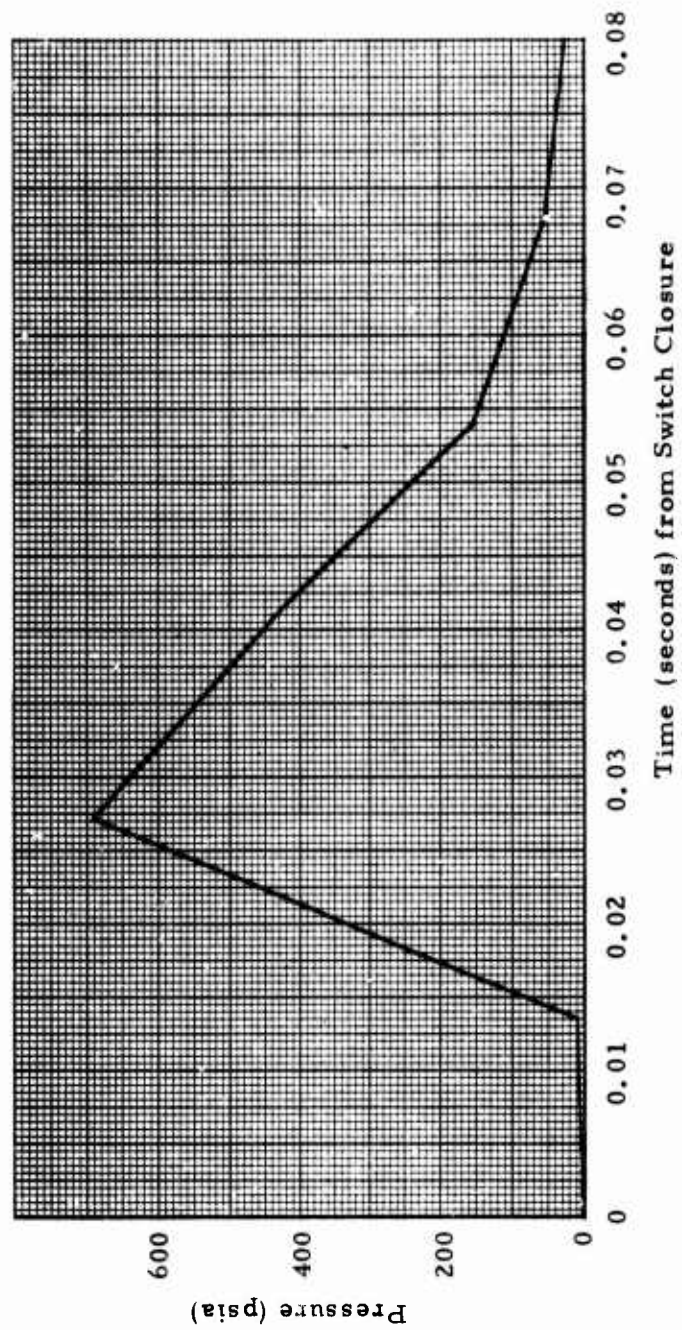


Figure VIII-14. Igniter Operation, TX-631 Motor, Mix T-643, Charge 2, Fired at 165°F

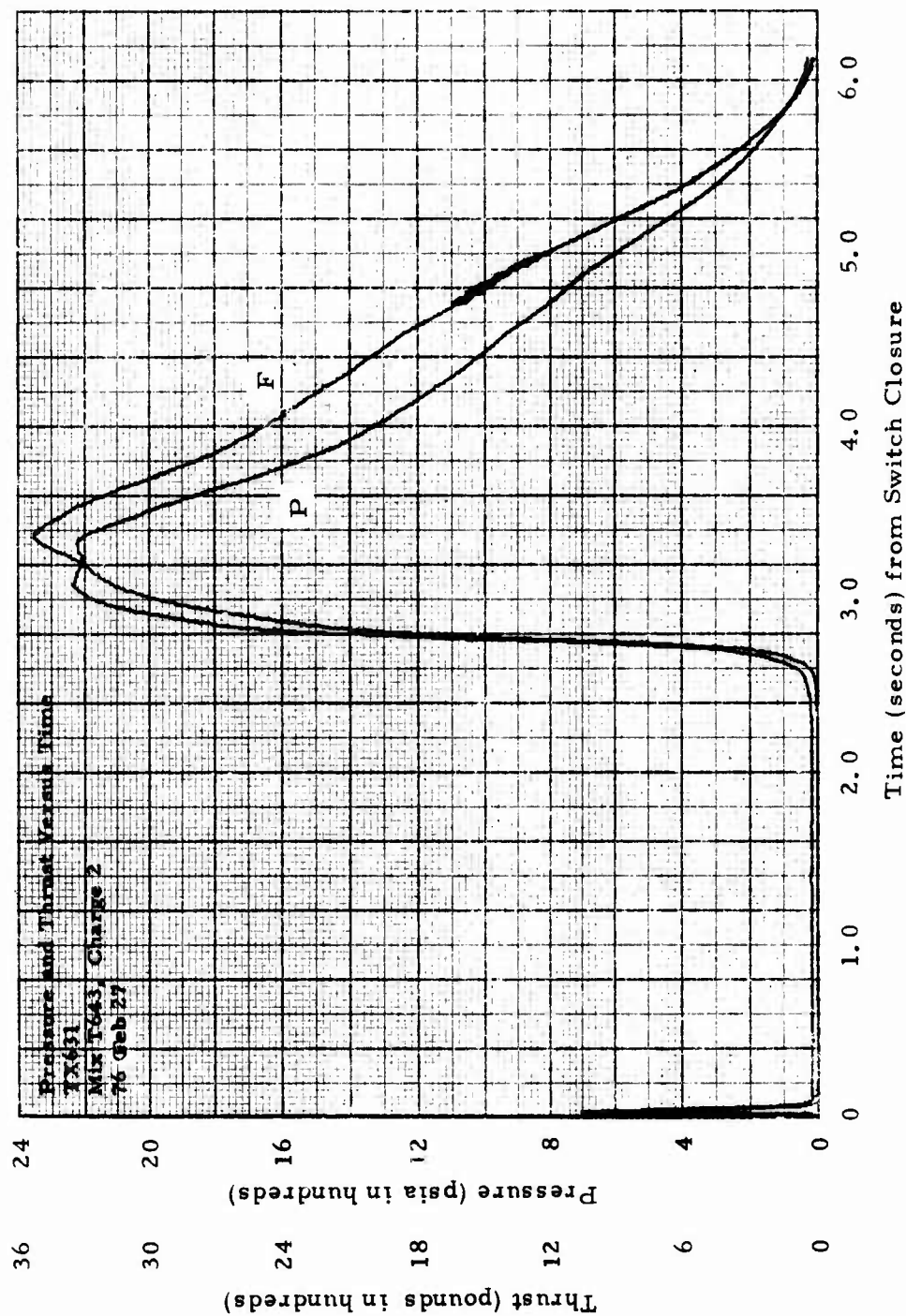


Figure VIII-15. Ballistic History, TX-631 Motor, Mix T-643, Charge 2, Fired at 165°F



After the test arrangement was assembled, it was conditioned to 70°F, installed in the test bay and attached to the nitrogen source. When the valve was opened, pressure at the two ends behaved as shown on Figure VIII-16. The high-speed playback revealed the aft end transducer responded 0.016 second after the forward end pressure started to rise.

The motor was then disconnected from the nitrogen and instrumentation (no other changes) and stored overnight in a 165°F conditioning oven. When it was brought back to the test bay, it was set-up and tested within ten minutes after removal from conditioning. Contrary to the insignificant delay observed at 70°F, the aft end pressure did not start to rise until 1.329 seconds after the forward end pressure first increased (Figure VIII-17). Note that any axial motion of the mandrel during the 70°F test would tend to open the gap between mandrel and propellant because of the taper of the propellant cavity. It was concluded that the differential thermal growth of mandrel and propellant did cause the gaps to close off.

Other hypotheses considered for the ignition delays in the 165°F tests of motors with mandrels were lack of exposed propellant, degradation of mandrel material and/or mold release coating, and degradation of the propellant surface at the mandrel interface. A simple test was made to determine the validity of these hypotheses. A slab of TP-H8208 propellant was clamped against the surface of an MR-22 coated foam mandrel. The assembly was placed overnight in a 170°F oven. When the sample was removed from the oven, the following observations were made:

1. Neither the TP-H8208 propellant, mandrel, foam, nor MR-22 coating were degraded by the 170°F exposure.
2. When first removed from the oven, the MR-22 coating was slightly tacky, but upon cooling the coating regained a normal hard surface.
3. The slab of TP-H8208 propellant "stuck" to MR-22 mold release on the mandrel surface, but could be peeled easily from the surface. The low grade bond at the mandrel/propellant interface appeared to fail cohesively in the MR-22 coating as there was evidence of the coating on both surfaces — mandrel and propellant.

This test showed that the MR-22 coated mandrel and TP-H8208 propellant would, under pressure at 170°F, create a low grade bond.

#### Fourth Test Group

Motor T634-2 was identical to T643-2 in mandrel density (12 lb/cu ft) and temperature (+165°F), but employed a 40 gram [20 gm 3-A pellets (Mg/TFE), 20 gms 20/80 powder (Mg/TFE)] charge. A hang-fire of much shorter duration than previously noted occurred (0.339 second vs 2.675 second). The motor exhibited a slightly higher  $P_{max}$  of 2649 psi and a higher  $dp/dt$  during ignition transient than the previous motor (Table VIII-20). The igniter  $P_{max}$



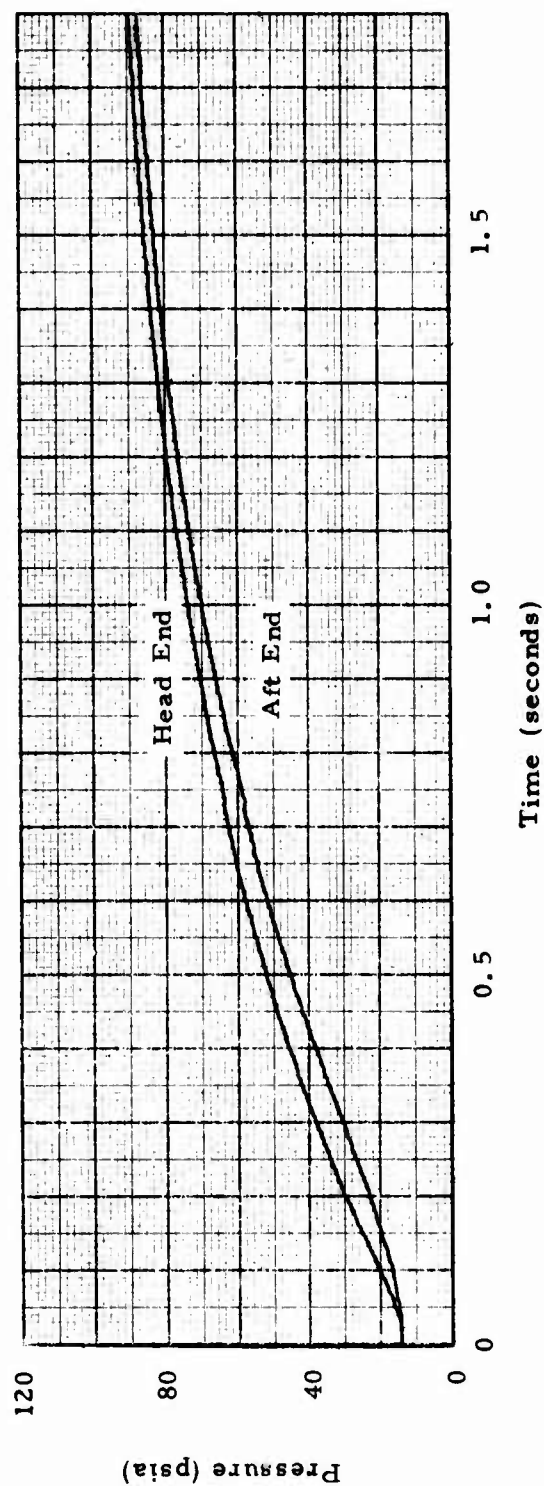


Figure VIII-16. Pressurization Test at 70°F on TX-631 Motor, Mix T-634, Charge 2

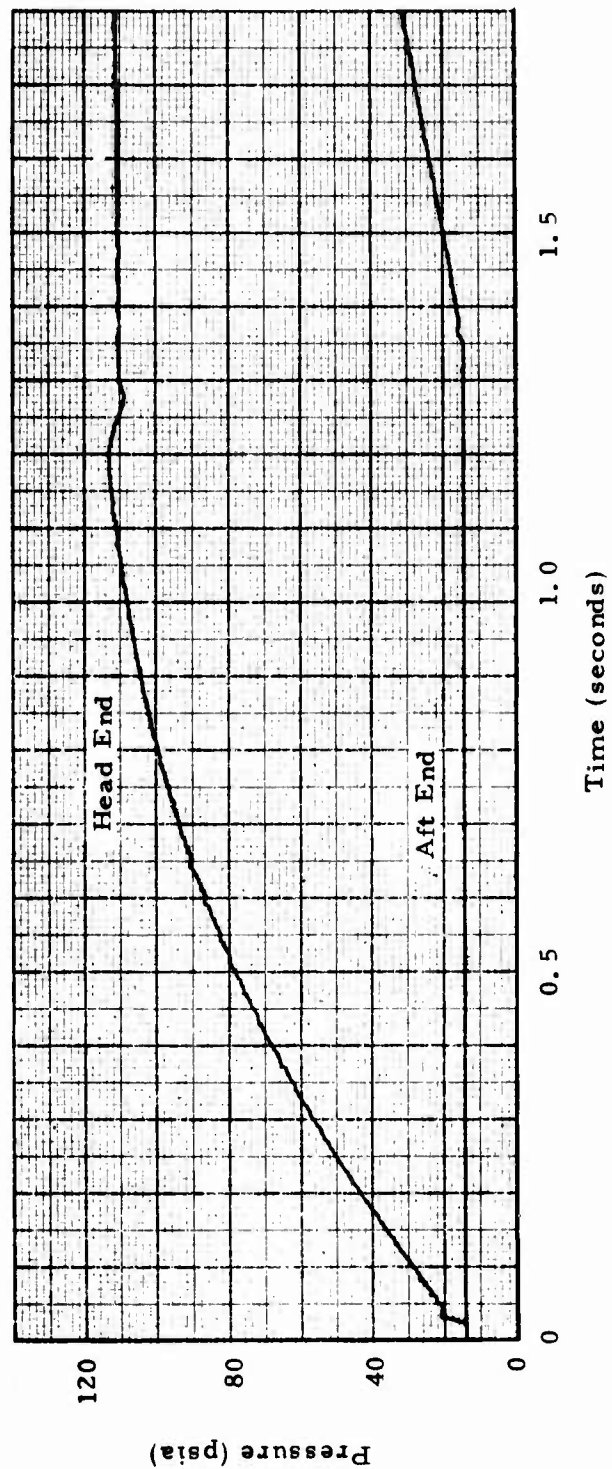


Figure VIII-17. Pressurization Test at 165°F on TX-631 Motor, Mix T-634, Charge 2

was higher as expected. An expanded pressure versus time plot is shown in Figure VIII-18; Figure VIII-19 shows the entire test. The delay of 0.339 second was still unacceptable.

Review of the movie coverage showed a larger fireball ejected at ignition, as expected. But the period of low pressure "smoldering", although greatly reduced, was still present. It was hypothesized that the ignition combustion products, being low in gas content (gas/solids ratio = 1/99), were still failing to 'sweep' the propellant surface clear of molten mandrel material which might be acting as an inhibitor.

Two alternative approaches to solution of the delay problem were addressed, namely: (1) adding an amount of 'gas producing' pyrotechnic ( $B/KNO_3$ ) to the igniter charge, or (2) providing a means to directly ignite a predetermined portion of motor propellant surface area. Both alternatives would attempt to use gaseous combustion products to "sweep" the propellant surface clean of foam material (molten foam or foam particles simply adhered to the surface). This should remove the inhibiting properties and allow rapid ignition of the propellant.

#### Fifth Test Group

The next two motors tested employed ambient temperature-cured propellant with cast-in-place foam mandrels. Previously, the mandrel and igniter were installed after normal casting and cure.

Due to an increase in the number of test variables, it was decided to:

1. Revert to the 20-gram igniter charge for the motors.
2. Cut back a portion of the center core of T684-2 at the headend to directly expose approximately 1.2 in<sup>2</sup> of propellant surface to the igniter charge (rather than change the charge composition), see Figure VIII-20.
3. Test both motors at 70°F.

Motor T-684-1 was cast with a 14 lb/cu ft mandrel and T-684-2 with a 12 lb/cu ft mandrel. For both motors, the igniter charge was identical (20 grams of Mg/TFE). Dual M-100 matches were used for initiation. The igniters were installed after propellant cure and prior to installation of the head-end cap.

T684-1 was successfully tested, but exhibited a longer than acceptable delay (TSPR = 0.155 second). The expanded pressure versus time plot indicates that a 100 psi pressure level was maintained for 0.200 second after the ignition peak before normal motor operation began.  $P_{max}$  for the motor was 2758 psi.  $Dp/dt$  during pressure rise was 19 KPSI/sec, indicating a rather slow transition (See Figures VIII-21 and VIII-22 and Table VIII-20).

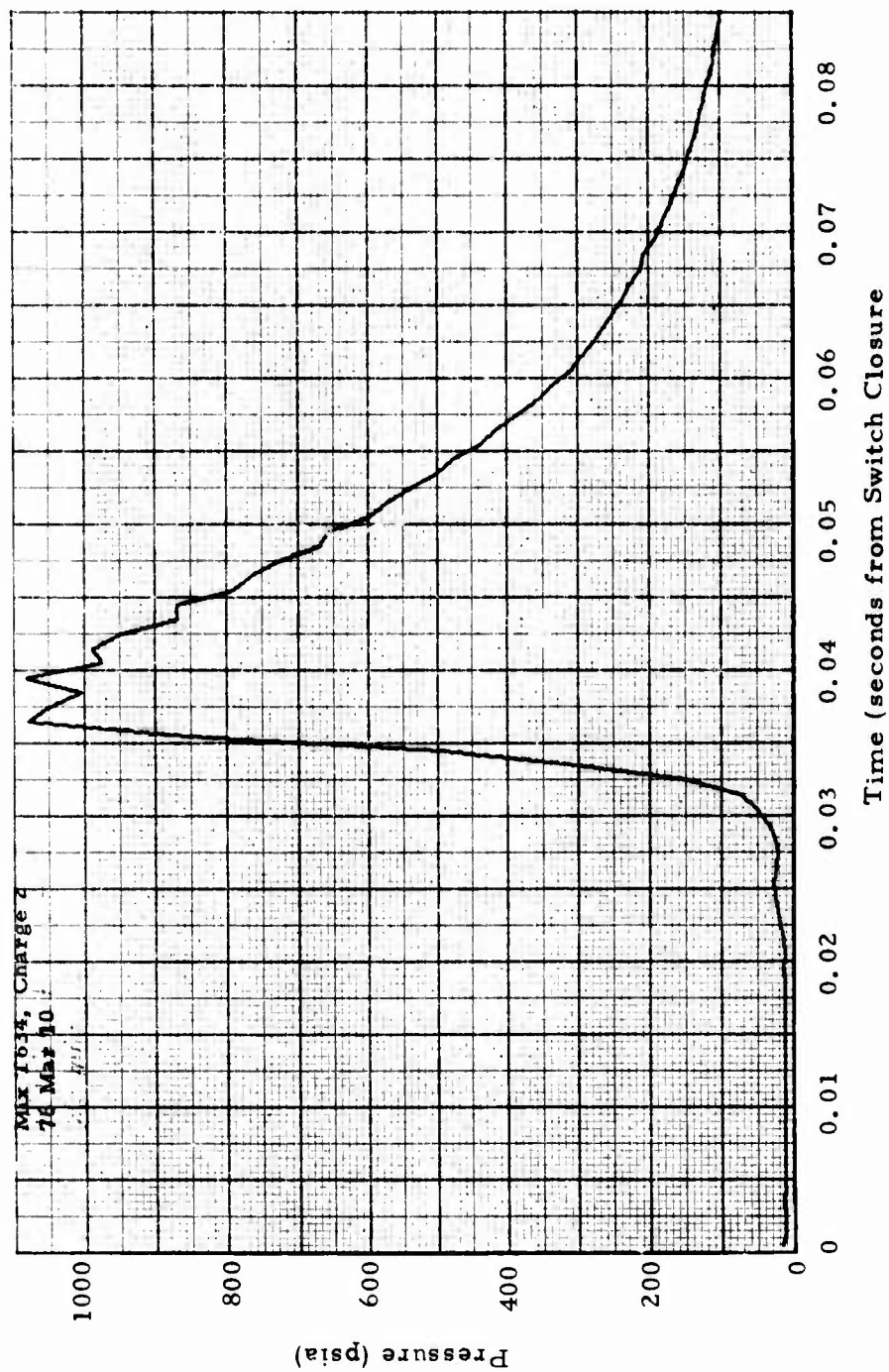


Figure VIII-18. Ignition Phase, TX-631 Motor, Mix T-634, Charge 2, Fired at 165°F

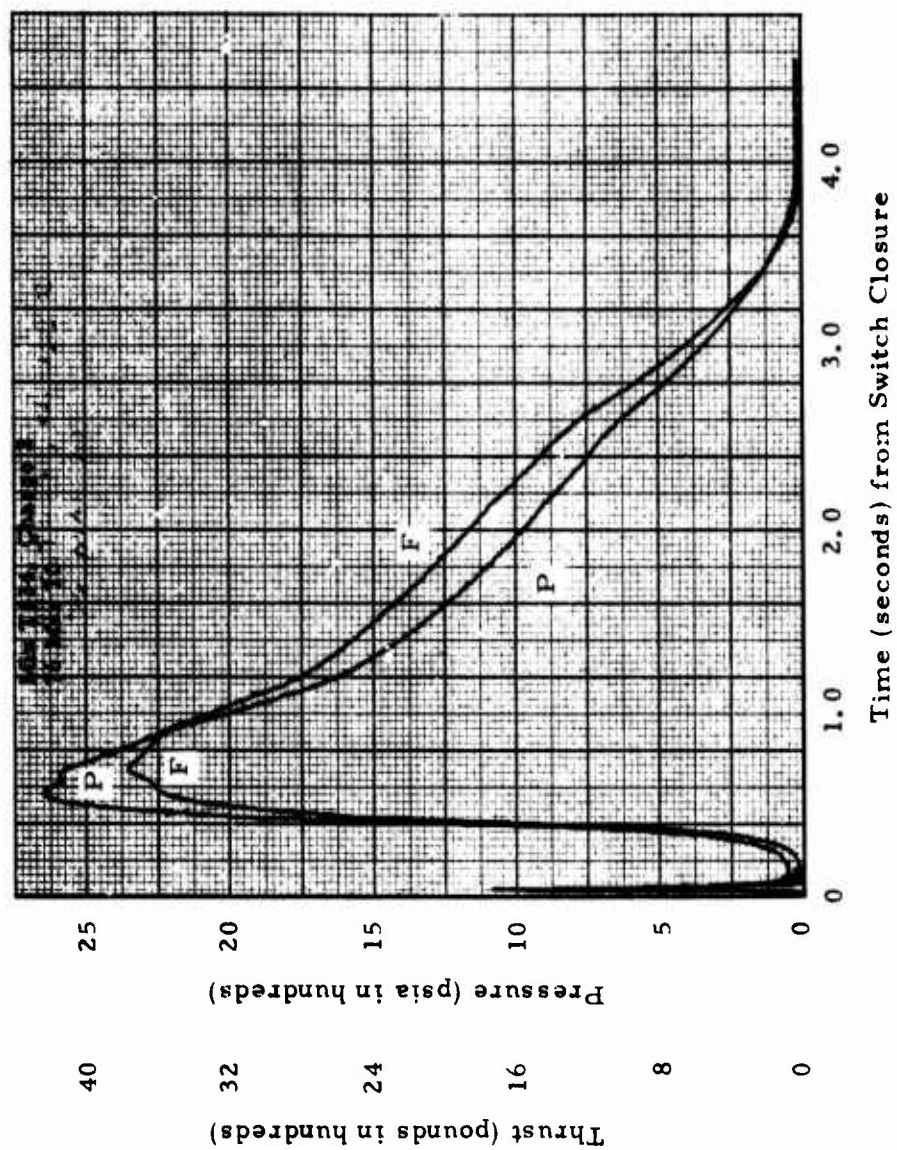


Figure VIII-19. Ballistic History, TX-631 Motor, Mix T-634, Charge 2, Fired at 165°F

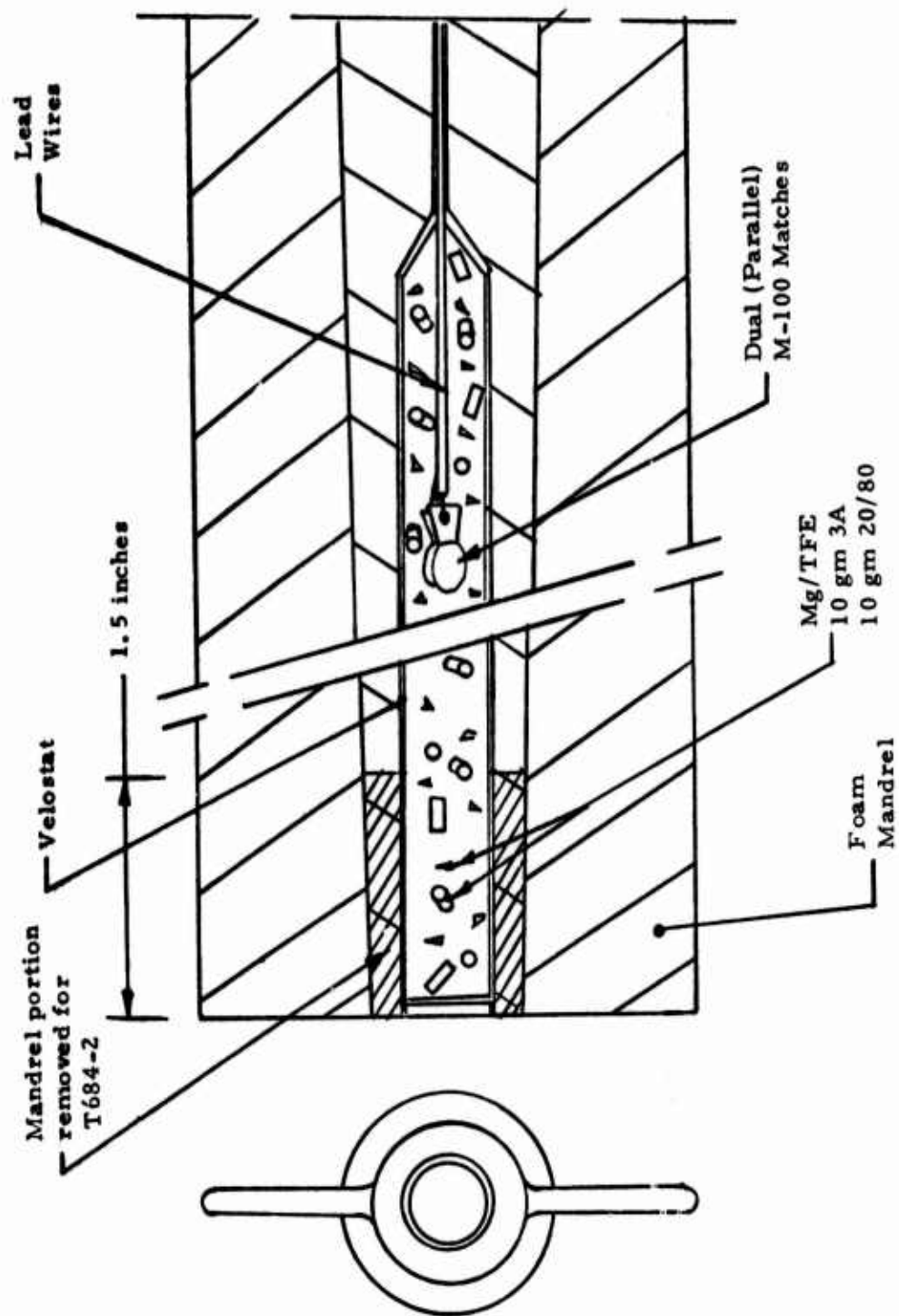


Figure VIII-20. Igniter/Mandrel for TX-631 Motors, Mix T-684, Charges 1 and 2



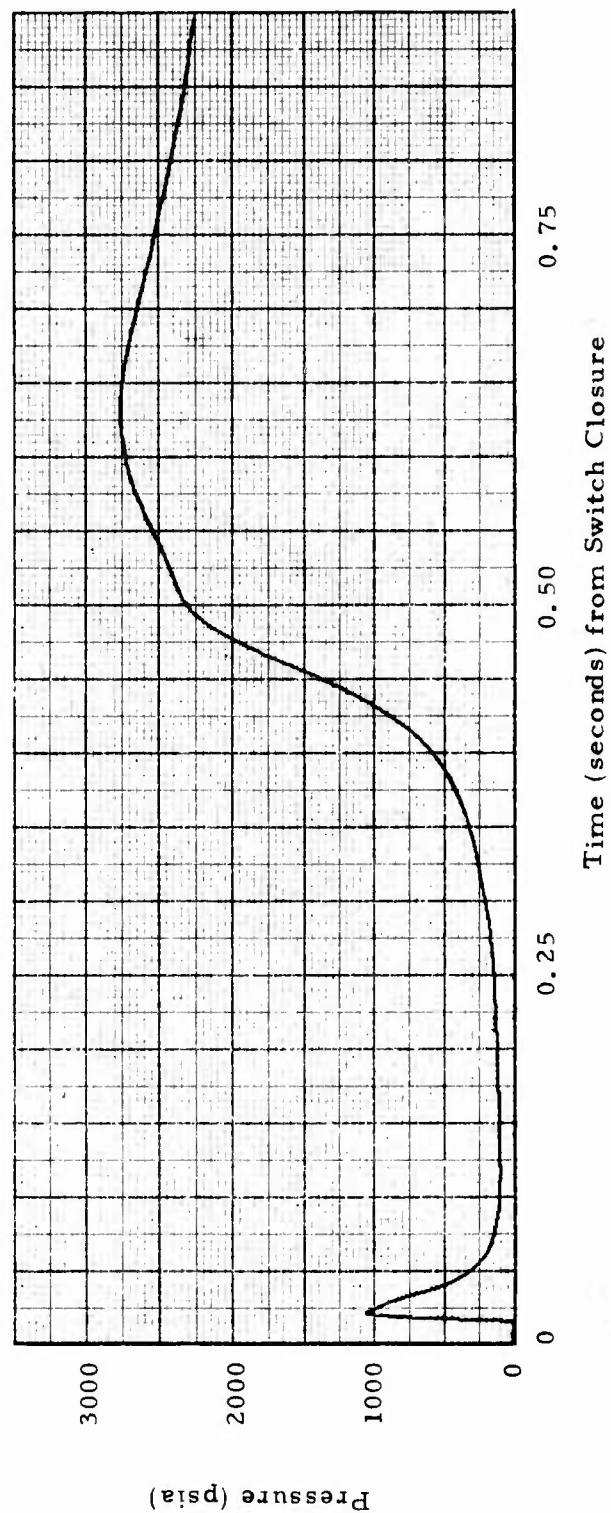


Figure VIII-21. Ignition Phase, TX-631 Motor, Mix T-684, Charge 1, Fired at 70°F



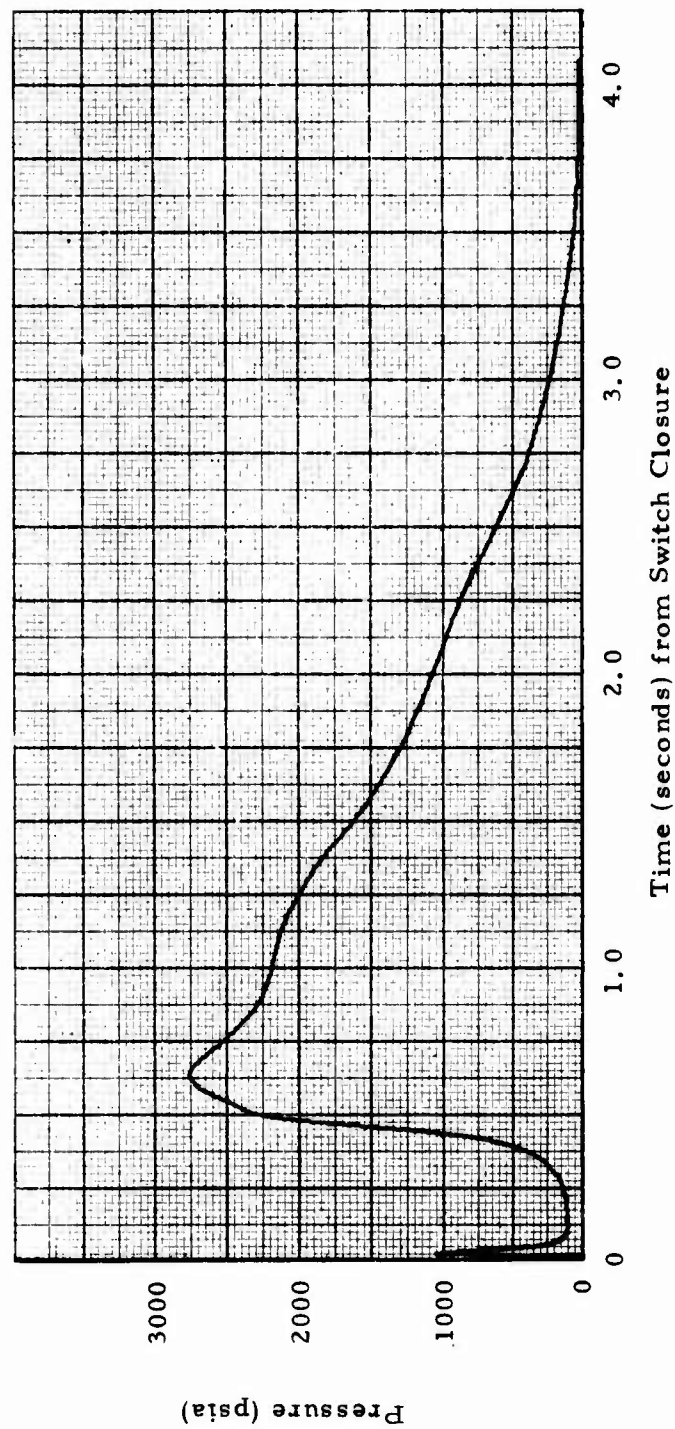


Figure VIII-22. Ballistic History, TX-631 Motor, Mix T-684, Charge 1, Fired at 70°F

Motor T684-2 exhibited a hangfire almost identical (2.620 seconds) to that of a previously tested motor (T643-2). Igniter  $P_{max}$  occurred at  $\approx 0.022$  second as was common to other motors. Pressure then decayed to well below 50 psia for  $\approx 2.6$  seconds, during which movie footage indicated little or no active burning, excepting continuous expulsion of dark, heavy smoke and an occasional small, low-pressure flame. At approximately 2.65 seconds after switch closure, a marked increase in burning was apparent followed by a brief period of what appeared as normal operation. Combustion in the plume appeared to stop momentarily, followed by a very bright and expanding plume (indicating high pressure), followed by the failure of the headend closure.

It is not readily apparent that exposing the  $\approx 1.2 \text{ in}^2$  of motor propellant in the headend was sufficient in reducing the delay time. The motor appeared to 'smolder' for  $> 2.0$  seconds as did T643-2. Apparently insufficient propellant surface area was ignited (or did ignite and was quenched) to successfully 'sweep' clean the propellant surface. A section of unburned propellant was recovered to which was still attached some charred mandrel material.

Pressure versus time plots are shown in Figure VIII-23.

There is no indication that the motor failure was associated directly with the igniter function. A detailed failure analysis is reported in Section VI.

#### CONCLUSIONS

Motor ignition delays at  $70^\circ\text{F}$  and  $-65^\circ\text{F}$  were acceptable ( $TD_{50} \leq 0.055$  second) for motors employing 20 gm Mg/TFE pellets/powder and M-100 Atlas Electric Match initiators when the consumable foam mandrels were inserted in the cavity after propellant cure was completed with conventional metal casting tooling. Ignition delays at  $165^\circ\text{F}$  were unacceptable with inserted mandrels and at  $70^\circ\text{F}$  with motors whose propellant was formed by consumable mandrels which were left in the propellant cavity.

Doubling the igniter charge to 40 gm significantly reduced the delay (from  $TD_{50} = 2.770$  second to 0.403 second), indicating that more energy release in the motor cavity during ignition phase would be a fruitful area of investigation. A first attempt to "sweep" clean the propellant surface by directly igniting a small portion of the motor headend propellant was not successful.

Much has been accomplished in ignition of motors using low cost, mandrel/igniter systems. Obviously, however, there remain several unanswered questions.

Based on the work accomplished to date, the following conclusions are in order:

1. Ignition of precured motors at ambient and low temperatures with acceptable delay times ( $< 100$  msec) is possible at this time,

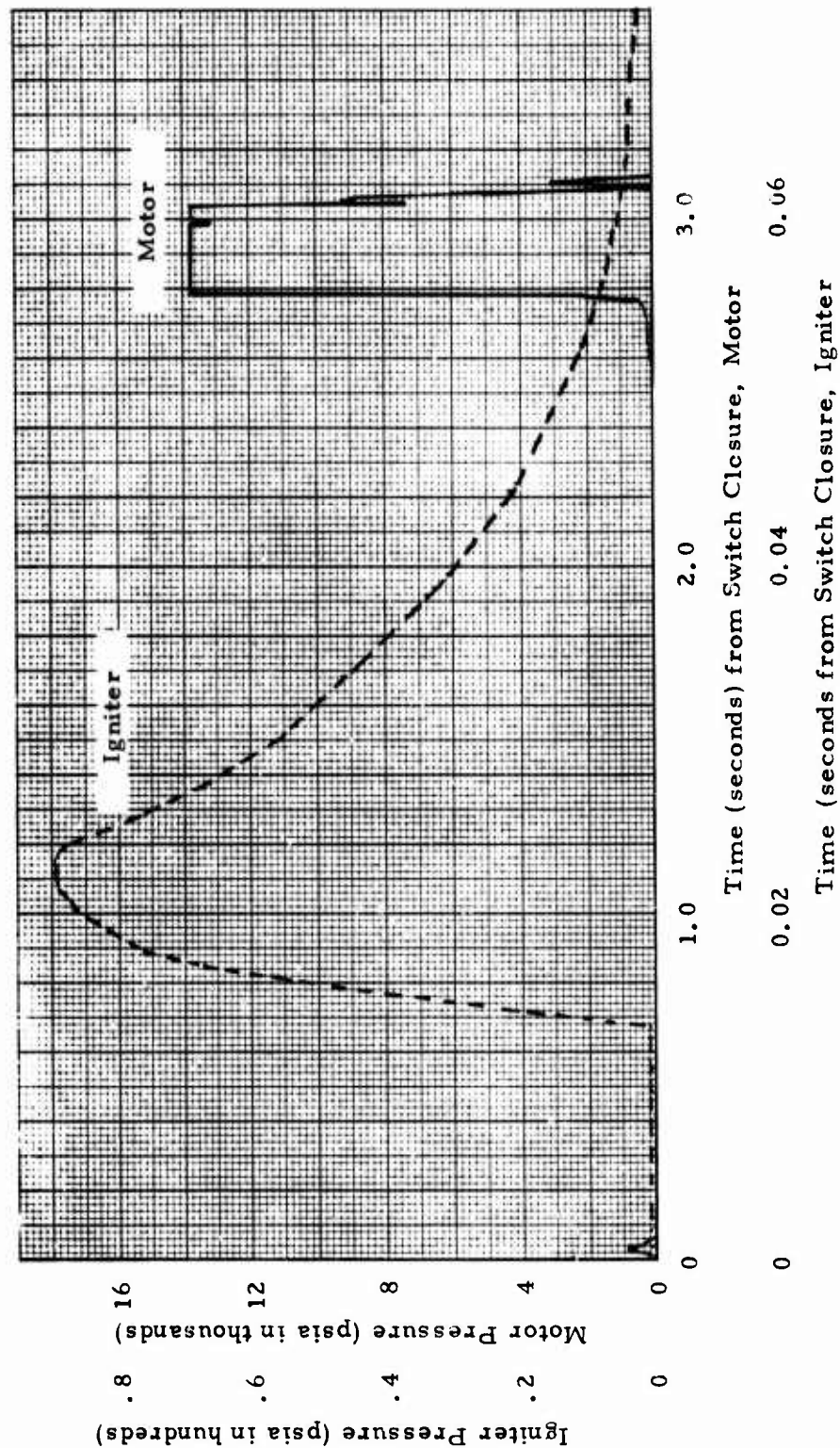


Figure VIII-23. Ballistic History, Igniter and TX-631 Motor, Mix T684, Charge 2, Fired at 70°F

- using low cost foam mandrels, pyrotechnics and initiators.
2. Use of the low gas-to-solids producing pyrotechnic Mg/TFE resulted in acceptable motor  $P_{\max}$  values.
  3. Low cost, M-100 series electric matches can be used to reliably initiate the igniter while maintaining a good degree of safety (the M-105 is a 1-amp no-fire match).
  4. Ignition of motors using cast-in-place mandrel/igniters is possible (T684-1); however, more work is required to develop an igniter/mandrel combination to meet ignition delay time goals.

#### REFERENCES

1. "Improved Low Cost Rocket Motor Processing and Component Development Study", Report No. AFRPL-TR-75-34, Booz, Allen Applied Research, Bethesda, Maryland, July 1975.
2. Department of the Army, "Compilation of Data on Army, Navy, and Commercial Standard Electric Squibs", Report No. 3J14N1, Redstone Arsenal, Alabama, January, 1956.

SECTION IX  
NOZZLE STUDY

## SECTION IX

### NOZZLE STUDY

Because of the severity of their environment, rocket motor nozzles have been costly to build and difficult to design. The purpose of these studies was to identify design approaches and materials amenable to low cost nozzles. Cost effectiveness, ease of fabrication and minimization of manufacturing steps were more significant than nozzle erosion effects and were considered ahead of performance degradation during material selection.

It was decided from the beginning that the material would be a compound suitable for transfer molding directly into a structural support shell (if it were found necessary to have such a shell). The as-molded part would have final dimensions everywhere except for the throat flashing, which would be removed as part of final processing.

### APPROACH

In order to satisfy the objective, it was necessary to consider much more than the cost of the nozzle itself since nozzle performance interacts with every other component of the rocket motor. The criteria for the nozzle design were established as:

- (1) Structural integrity,
- (2) Future availability,
- (3) Minimum unit-cost in production,
- (4) Performance and weight compatible with satisfying missile requirements at a minimum total motor cost, and
- (5) Tolerable risk that development or reliability problems would not prevent utilization of this design within reasonable development funding.

Each of these criteria were examined in the process of selecting the most attractive designs.

Structural integrity of various designs was assessed by use of finite-element type stress analyses. Rigorous analysis of every conceivable design would be prohibitive; thus, six basic design configurations were examined in a parametric manner to provide insight into the behavior of a large number of



specific designs. The six basic designs included three different internal profiles, each designed both with a metal supporting shell and as a free-standing all-plastic component. Each of these six basic designs was analyzed with three different levels of modulus assumed for the insulation material. A plot of tensile stress versus modulus was then generated and used in order to determine the stress induced in nozzles molded from a variety of materials. Thus, a margin of safety was computed for several dozen discrete designs. Additional design variations were evaluated by determining the effect of shell stiffness upon insulation stress.

Risk was assessed on the basis of calculated structural margin, complexity of the design, the novelty of the design or the material application, and anticipated problems of raw-material procurement. High structural and ablative margins of safety obviously provide a cushion for unanticipated problems in material strength, variations in manufacture, variation of loads, etc. The number of components fitting together and the complexity of joints between them generally increase the likelihood of having problems. Obviously, designs closely resembling proven components represent less risk than those unlike any previously tested.

Future availability of candidate materials was assessed by consideration of the raw materials required, the processing equipment required, the number of sources for the material type, and other applications for the material. Although firm quantitative data cannot be generated, recent experience provides some basis for projecting into the future. Candidate materials requiring fillers of asbestos or rayon fibers were downgraded because of supply problems. Asbestos production has been threatened because of restricted handling associated with its carcinogenic nature. Rayon of the type used in carbon-fibers has been dropped by several suppliers because of a diminishing demand for it as a tire cord. Likewise, proprietary products and those with limited sources are down-graded because production could be halted by either marketing decision or limited natural disaster.

The characteristic of nozzle design having the greatest effect upon overall motor performance is throat erosion. Throat erosion for several low-cost materials of interest could be determined only through motor firings since they had not previously been used for this application and since theoretical prediction techniques are tedious, expensive, and generally unreliable until "calibrated" for each material using motor-firing results. Thus, initial screening tests were conducted using TX3 ballistic-test motors (containing 3.1 pounds of propellant). Further evaluation of the better materials was performed using full-scale (TX631) motors containing 25.3 pounds of propellant. It was assumed that throat erosion rate had a linear effect on missile trajectory performance and thus could be ranked as a simple ratio to the baseline material characteristics.



All of the aforementioned factors

Structural margin-of-safety  
Relative throat erosion rate  
Relative risk  
Future availability

were combined into an "Index of Technical Merit", which consists of the algebraic product of several individual indices based upon criteria discussed previously. These indices are formed such that the maximum rating is unity and the minimum rating is zero. With this scheme, a design inadequacy from any one standpoint will cause a design to be eliminated without regard to an "overkill" capability evident from some other standpoint. Included in the overall index are a structural performance index (the hyperbolic tangent of twice the margin of safety), an ablative performance index (the hyperbolic tangent of the ratio of a reference throat erosion to the candidate's throat erosion), and an availability index (probability of continued economical production of component for next ten years).

Overall comparison of the various materials and design approaches were based on establishing a relationship between "Unit Nozzle Cost" and "Index of Technical Merit".

#### MATERIAL SELECTION

A list of candidate materials for use as the throat insert and/or as the complete ablative portion of the nozzle are tabulated in Table IX-1. Selections of the candidate materials were primarily based on the material costs. The selected materials can be divided into two areas: (1) materials which have been used previously in rocket motors and (2) materials which are low-cost commercial grades of plastics which might be usable. Contacts were made with fabricators (HITCO, C&D Plastics, Thermec, Haveg, Edler Industries and Wyatt Industries) to solicit information about materials which might be applicable for this design. Also, selection was made based on tensile strength, tensile modulus, specific gravity and impact strength as well as cost.

Physical property data were accumulated for the candidate materials and also are shown in Table IX-1. These properties are based upon information distributed by the respective suppliers. Caution should be exercised in using these properties, especially, tensile strength. Past experience has shown component tensile strengths to be considerably less than the "book values." In obtaining the "book value", the material is molded such that optimum tensile strengths are obtained since the measurements are obtained by using thin molded tensile coupons. In actuality, this optimum orientation is seldom, if ever, obtained in molded components. For example, the average

**TABLE IX-1**  
**LOW COST MOTOR - NOZZLE CANDIDATE MATERIALS (a)**

Material	Material Designation	Supplier	Tensile Modulus (psi x 10 <sup>6</sup> )	Tensile Strength (b) (lbs)	Fabrication Method	Erosion Resistance (c) TX-3/TX-631 %	Material Cost (\$/lb)	Unit Cost (\$/Unit)	Specific Gravity (g/cc)	Isod Impact (ft-lb/in)
Glass Phenolic Fabric (1/2" chopped roving)	FM16771	Fiberite	3.1	5000	Compression	100/104	1.44	13.06	1.85	9.0
Mineral-filled Phenolic	D23639	Durez	2.3	6000	Transfer	71/---	0.74	9.51	1.76	1.4
Mineral-filled Phenolic	D16090	Durez	1.7	6500	Transfer	87/---	0.43		1.67	0.45
Polyphenylene Sulfide (40% Glass Filled)	Ryton 4	Phillips 66	2.1	19500	Injection		3.10		1.60	1.4
Phenylene Oxide Fiber (20-30% Glass Filled)	Noryl	General Electric	1.2	14500	Injection		1.23		1.30	2.3
Asbestos Phenolic	153T	Raybestos/Manhattan	2.4	10200	Transfer		0.93		1.85	
Asbestos Phenolic	153C	Raybestos/Manhattan	2.9	11730	Compression	88/95	0.75	11.47	1.88	
Elastomerized Glass Phenolic	4E0253	HEXCEL	0.4	5200	Compression		5.00		1.79	
Glass-filled Phenolic	D23570	Durez	1.9	9500	Transfer	106/136	1.08	10.86	1.76	0.55
Glass-filled Diallyl phthalate	D22008	Durez	1.4	10000	Transfer		1.35		1.73	0.55
Glass-filled Alkyd	D24060	Durez	2.8	9500	Transfer		0.60		2.13	0.55
Wood-flour-filled Phenolic	D791B	Durez	1.2	6000	Transfer	86/---	0.40	7.25	1.38	0.29
Asbestos Phenolic	110R PD	Raybestos/Manhattan	3.0	7300	Compression	84/94	0.66	10.69		
Cellulose-filled Phenolic	D22532	Durez	1.3	7000	Transfer	101/130	0.48		1.37	0.37
Cellulose-filled Phenolic	FM3510	Fiberite	1.0	7000	Transfer	63/---	0.79	8.56	1.37	2.4
Cellulose-filled Phenolic	R25406	Reichhold	1.3	7100	Compression	98/---	0.53	7.62	1.37	0.50
Glass Phenolic (Fabric)	FM5042	U. S. Polymeric	2.25	7700	Compression		4.50		1.87	14
Glass Phenolic (Fiber)	FM5821	U. S. Polymeric	2.25	6860	Compression		3.50			
Glass Phenolic (Fabric)	FM5736	U. S. Polymeric	3.00	12009	Compression		3.50		1.9	15
Polyaryl ether	Arylon T	Uniroyal Chemical	0.32	7500	Injection		---		1.14	8.0

a. Updated August 1976.

b. Catalog values

c. Compared to baseline material, FM16771.

tensile strength of the baseline material, FM16771, based on four tests conducted by Haveg in January 1975 was approximately 3200 psi while the "book value" for the material tensile strength is listed as 5000 psi. Therefore, although Table IX-1 lists "book value", later calculations of structural margin of safety used tensile strengths discounted to 64% of "book value". This degradation factor was derived from tests of molded nozzle parts subjected to load tests.

## STRUCTURAL ANALYSIS

Nozzle designs which utilize low cost materials and processing for large production quantities have encountered significant problems in nozzle structural integrity and reproducible component performance. This section dealt with the design and structural analysis of the nozzle assembly. It is important to note that the driving force in this program was the design of a low-cost motor assembly (Figure IX-1). Therefore, the nozzle design with the greatest margin of safety was not necessarily the selected design. This selection was made based primarily upon an interrelation of material cost, production cost, margin of safety, erosion resistance and component reproducibility. This particular analysis was conducted to determine the margin of safety in the baseline design and the alternate configurations with the various nozzle candidate materials.

### Nozzle Geometries

The six nozzle geometries (Figures IX-2 through IX-7) examined in these analyses represent three internal profiles, each with and without a supporting 0.10 inch thick metal shell. The baseline represents a convergent-divergent nozzle profile of the simplest configuration. The two alternates offer lower exit-cone half angles, somewhat lower weight, and potentially lower material and mold-time costs. For each basic profile, the supporting shell reduced structural demands made on the throat material but added its own weight and cost to the system. Features of the designs are summarized below.

<u>Design No.</u>	<u>Structural Support</u>	<u>Exit Section</u>	<u>Subsonic Blast Tube</u>	<u>Figure No.</u>
Baseline	No	Conical	No	IX-2
1	No	Contoured	No	IX-3
2	No	Contoured	Yes	IX-4
3	Alum	Conical	No	IX-5
3s	Steel	Conical	No	IX-5
4	Alum	Contoured	No	IX-6
4s	Steel	Contoured	No	IX-6
5	Alum	Contoured	Yes	IX-7
5s	Steel	Contoured	Yes	IX-7

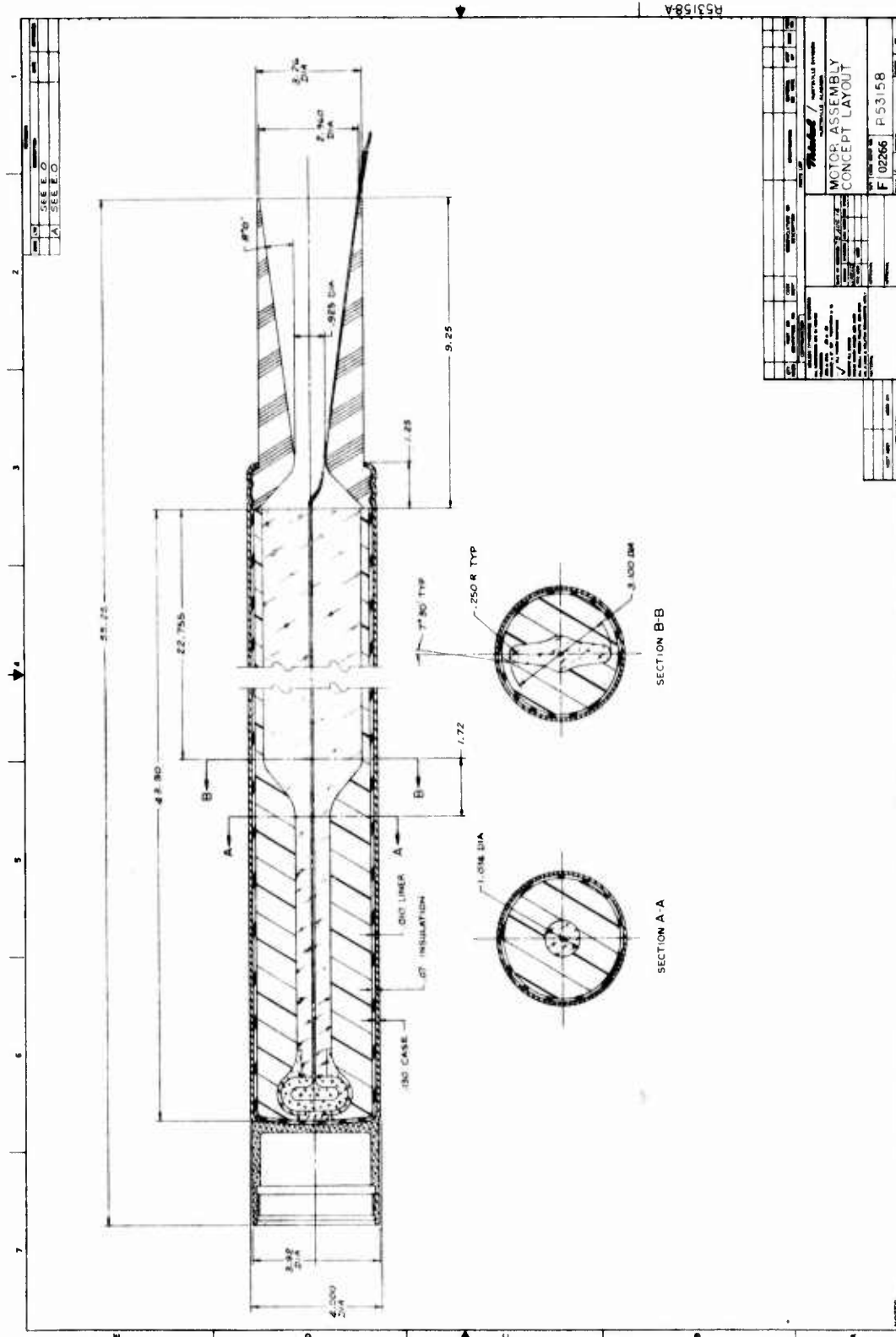
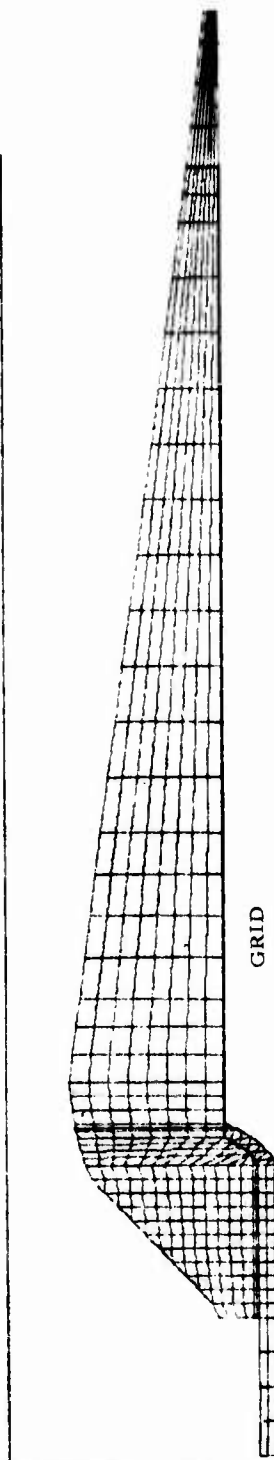


Figure IX-1. Baseline Design

$R = 0.000$   
 $Z = 0.000$

E2386 LOW COST NOZZLE DESIGN 1110-AAA0-

9.



$R = 0.000$   
 $Z = 0.000$

E2386 LOW COST NOZZLE DESIGN 1110-AAA0-

9.

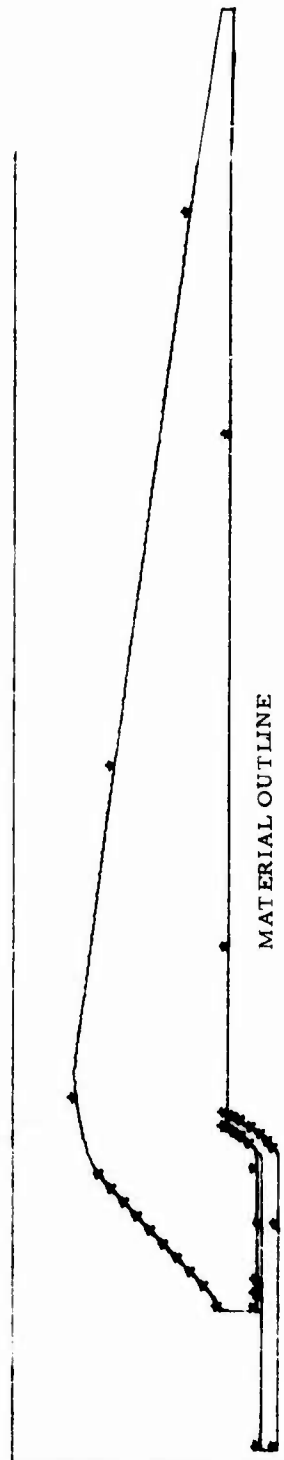


Figure IX-2. Nozzle Baseline Design (Grid and Material Outline)

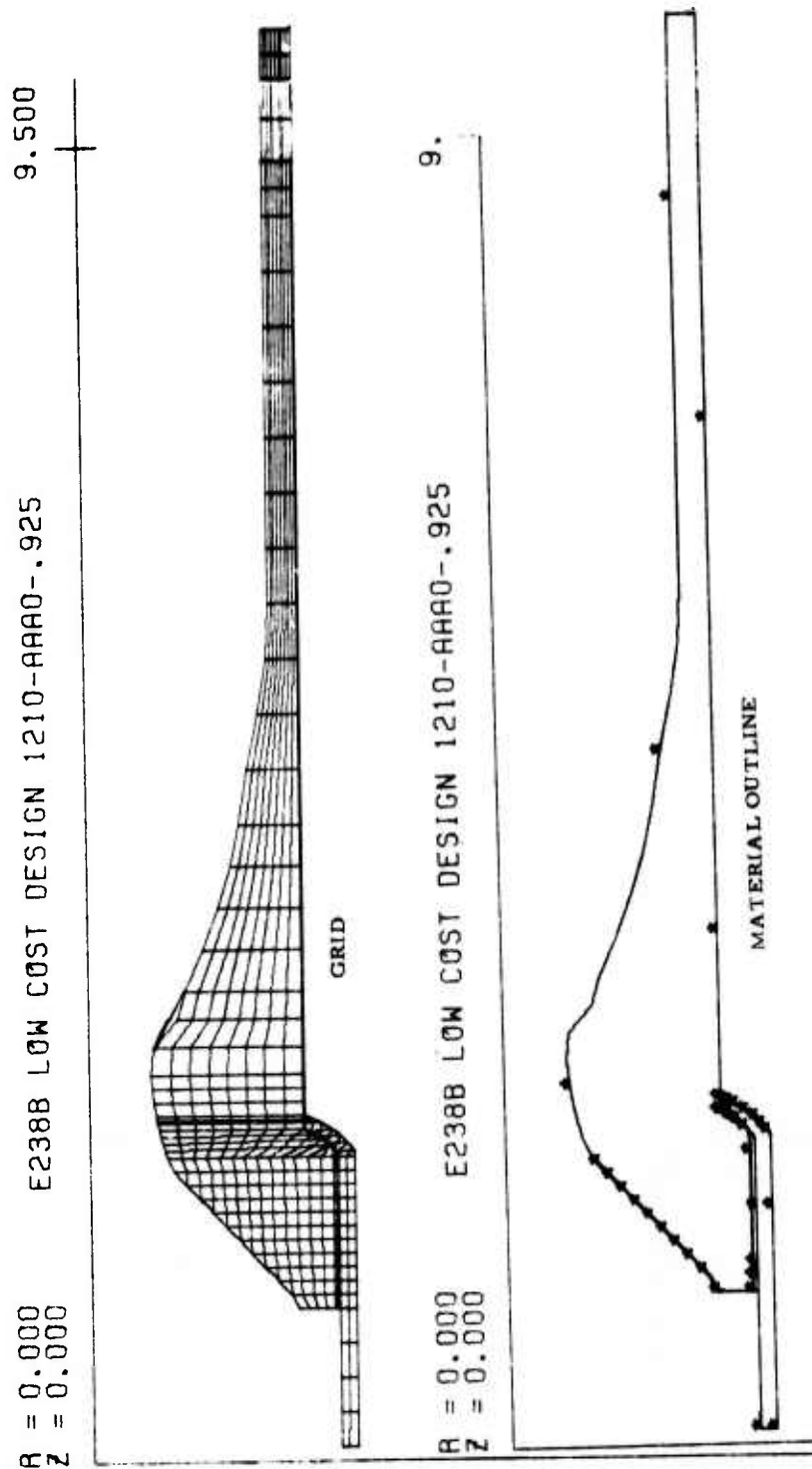


Figure IX-3. Design 1 (Grid and Material Outline)

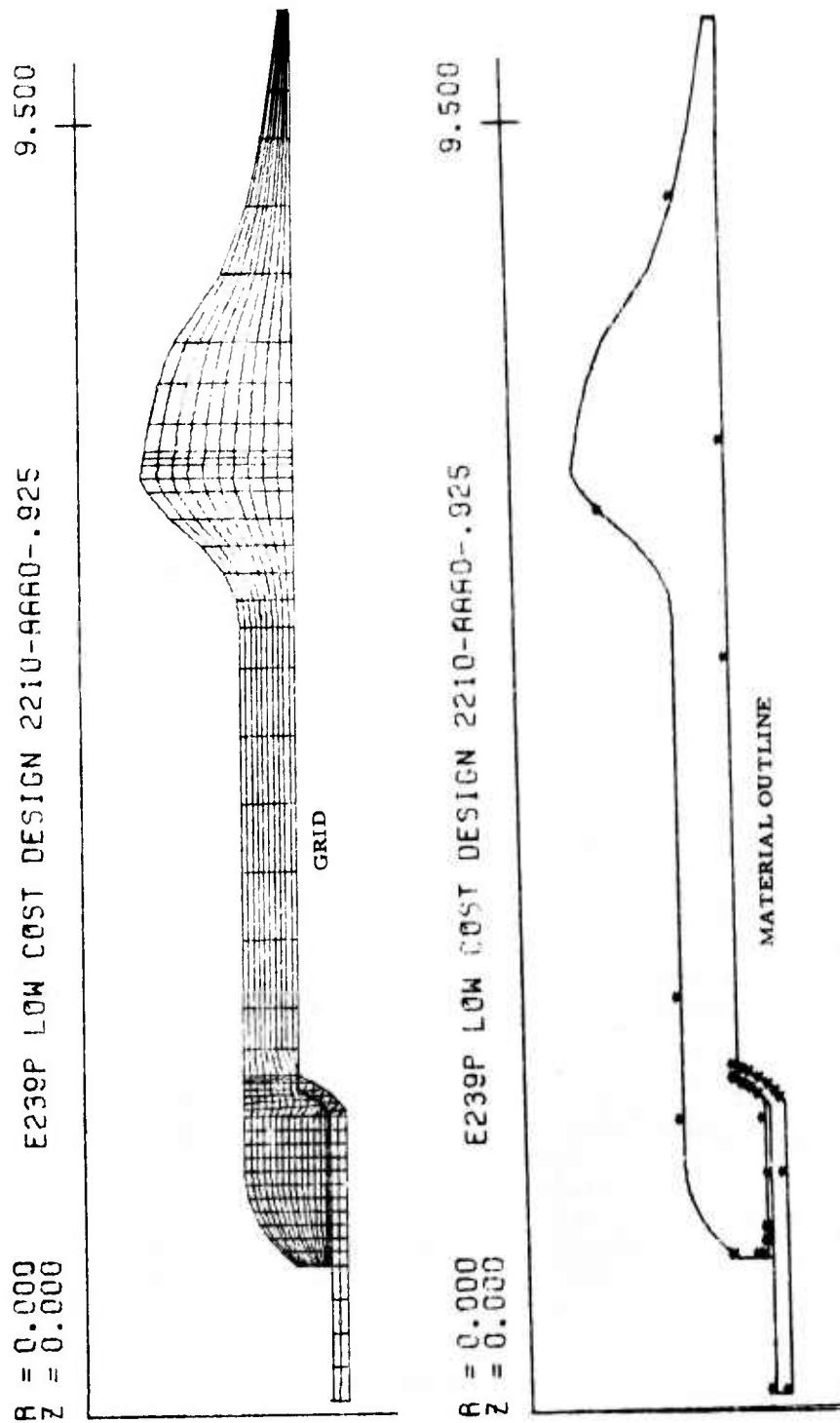


Figure IX-4. Design 2 (Grid and Material Outline)



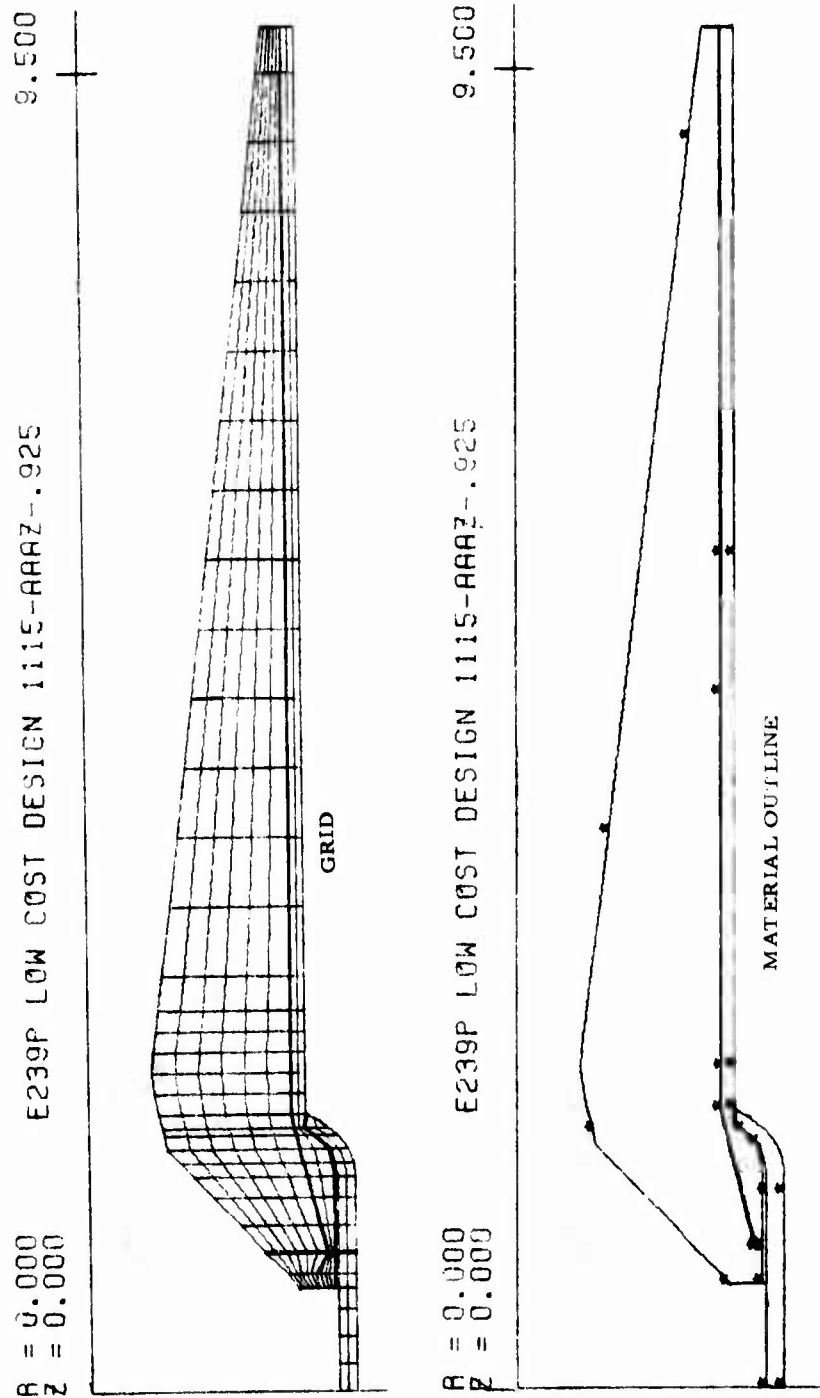


Figure IX-5. Design 3 (Grid and Material Outline)

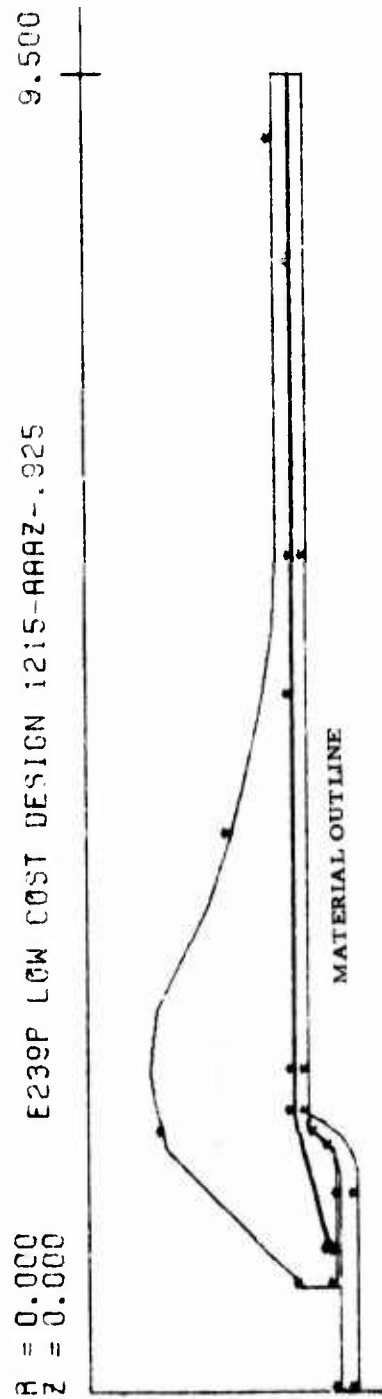
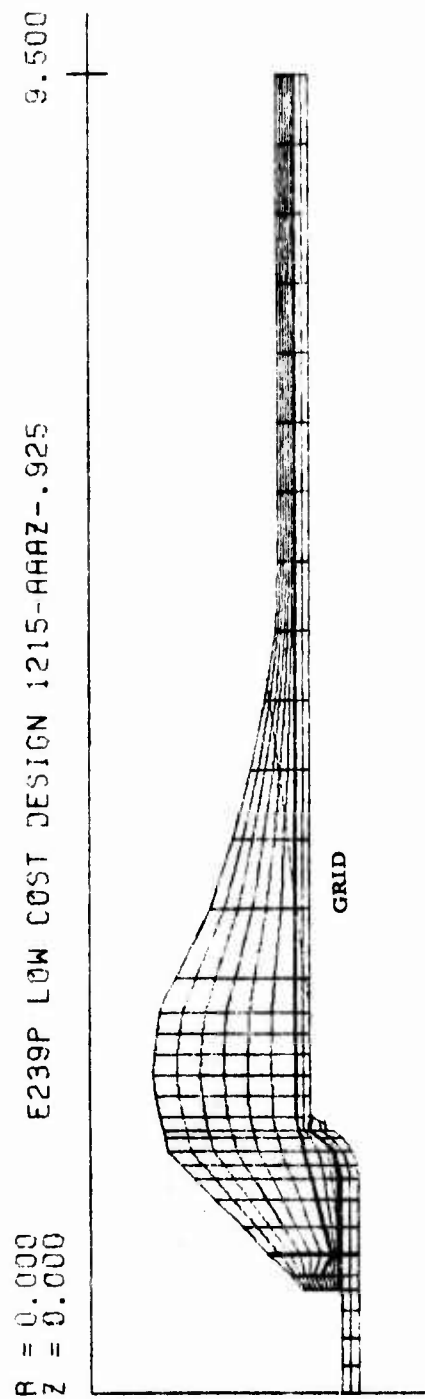


Figure IX-6. Design 4 (Grid and Material Outline)

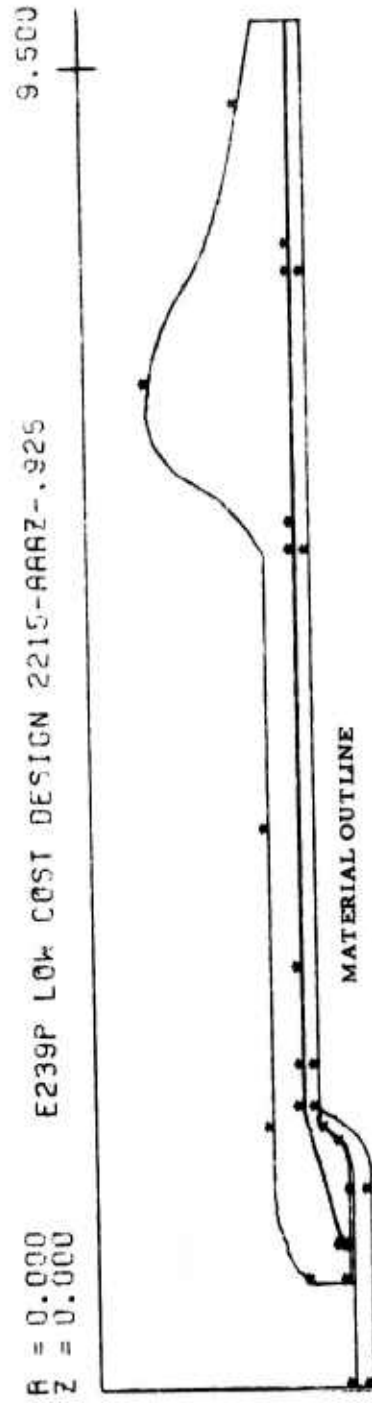
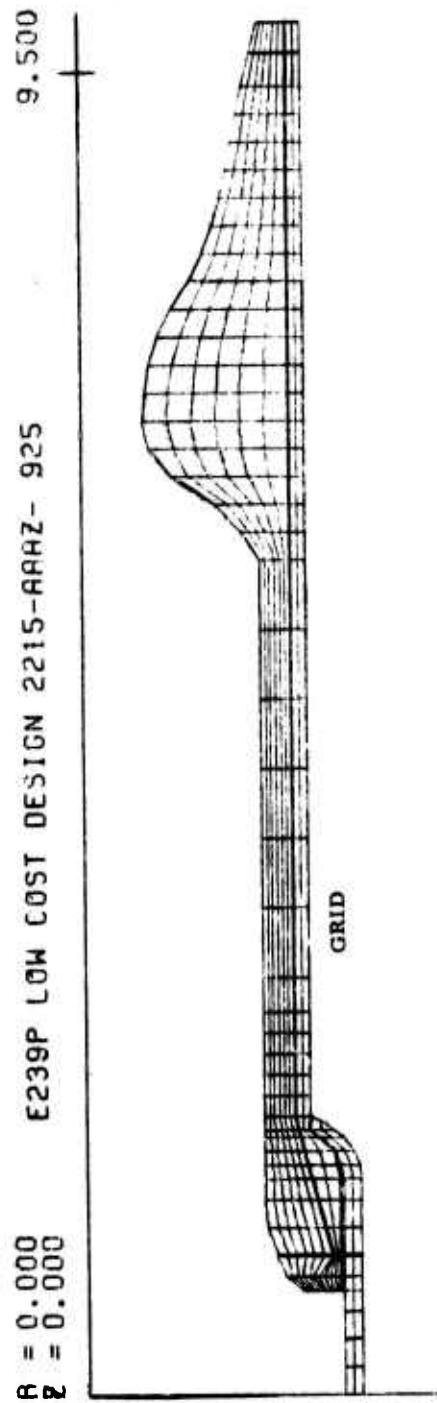


Figure IX-7. Design (Grid and Material Outline)

### Method of Analysis

An axisymmetric finite element stress analysis was conducted on each design. The computer code selected for this effort was the "Finite Element Nozzle Stress Analysis Program" developed as program "AMG054" and subsequently modified by Thiokol for more efficient utilization. The code used for this effort is identified as program E238B.

The pressure loads were applied along all appropriate surfaces of the blast tube and the nozzle inner surface. A reference pressure of 3640 psia was used in the analysis. The pressure distribution along the nozzle surface was computed on the basis of area ratio and thermodynamic principles, using 1.16 for the ratio of specific heats. With this pressure distribution applied to the appropriate surfaces of the nozzle, consideration of thrust as a load would be redundant.

The only displacement boundary condition imposed on the model was a zero longitudinal displacement prescribed for the model at the forwardmost row of nodal points contained in the aluminum shell. Thus, the case is fixed in one direction at a point sufficiently distant from the area of interest such that the results will be unaffected by any discontinuity arising at the point of fixed displacement.

Four distinct materials were modeled for each analysis, each with properties appropriate to the particular design configuration

Case	Aluminum
Structural Support Shell	Aluminum
	Steel
Bondline	TL-L700
Ablative	Various moduli

Table IX-2 lists typical values for one calculation. In order to encompass the wide range of modulus of elasticity of the candidate materials, each of the six major designs (both with and without aluminum structural support) were analyzed using modulus values of one, two and three million.

### Results

Figures IX-8 through IX-13 show effects of modulus on maximum hoop stress for the configurations that have no structural support and aluminum support shells. These relationships were used, along with the material modulus of elasticity, to calculate maximum induced hoop stress and concomitant margin of safety, which are displayed in Table IX-3.

TABLE IX-2

MATERIAL PROPERTY TABLE

	CONTINUUM			MATERIAL	PROPERTIES
Aluminum					
MAT. NO. = 1	E1= 1.0000D 07	NU21= 2.9000D-01		ALPHA1= 6.0000D-06	G13= 1.6700D 07
	E2= 1.0000D 07	NU31= 2.9000D-01		ALPHA2= 6.0000D-06	BFR= 0.0
	E3= 1.0000D 07	NU32= 2.9000D-01		ALPHA3= 6.0000D-06	BFZ= 0.0
Bondline					
MAT. NO. = 2	E1= 1.0000D 03	NU21= 4.9990D-01		ALPHA1= 6.0000D-06	G13= 3.3300D 02
	E2= 1.0000D 03	NU31= 4.9990D-01		ALPHA2= 6.0000D-06	BFR= 0.0
	E3= 1.0000D 03	NU32= 4.9990D-01		ALPHA3= 6.0000D-06	BFZ= 0.0
Glass Phenolic					
MAT. NO. = 3	E1= 3.0000D 06	NU21= 2.9000D-01		ALPHA1= 6.0000D-06	G13= 1.0000D 06
	E2= 3.0000D 06	NU31= 2.9000D-01		ALPHA2= 6.0000D-06	BFR= 0.0
	E3= 3.0000D 06	NU32= 2.9000D-01		ALPHA3= 6.0000D-06	BFZ= 0.0

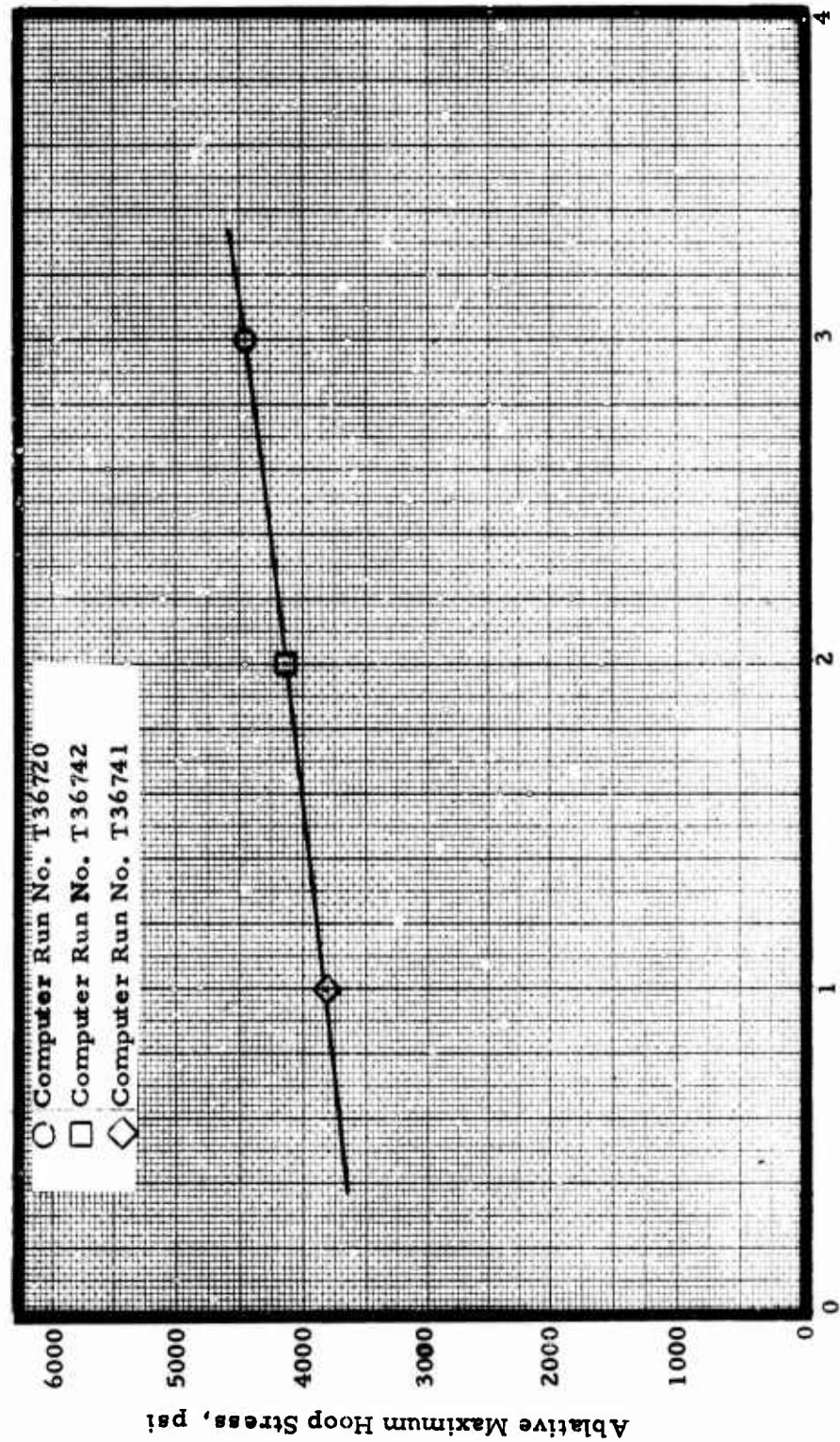


Figure IX-8. Effect of Varying Modulus on the Maximum Hoop Stress in Baseline Design



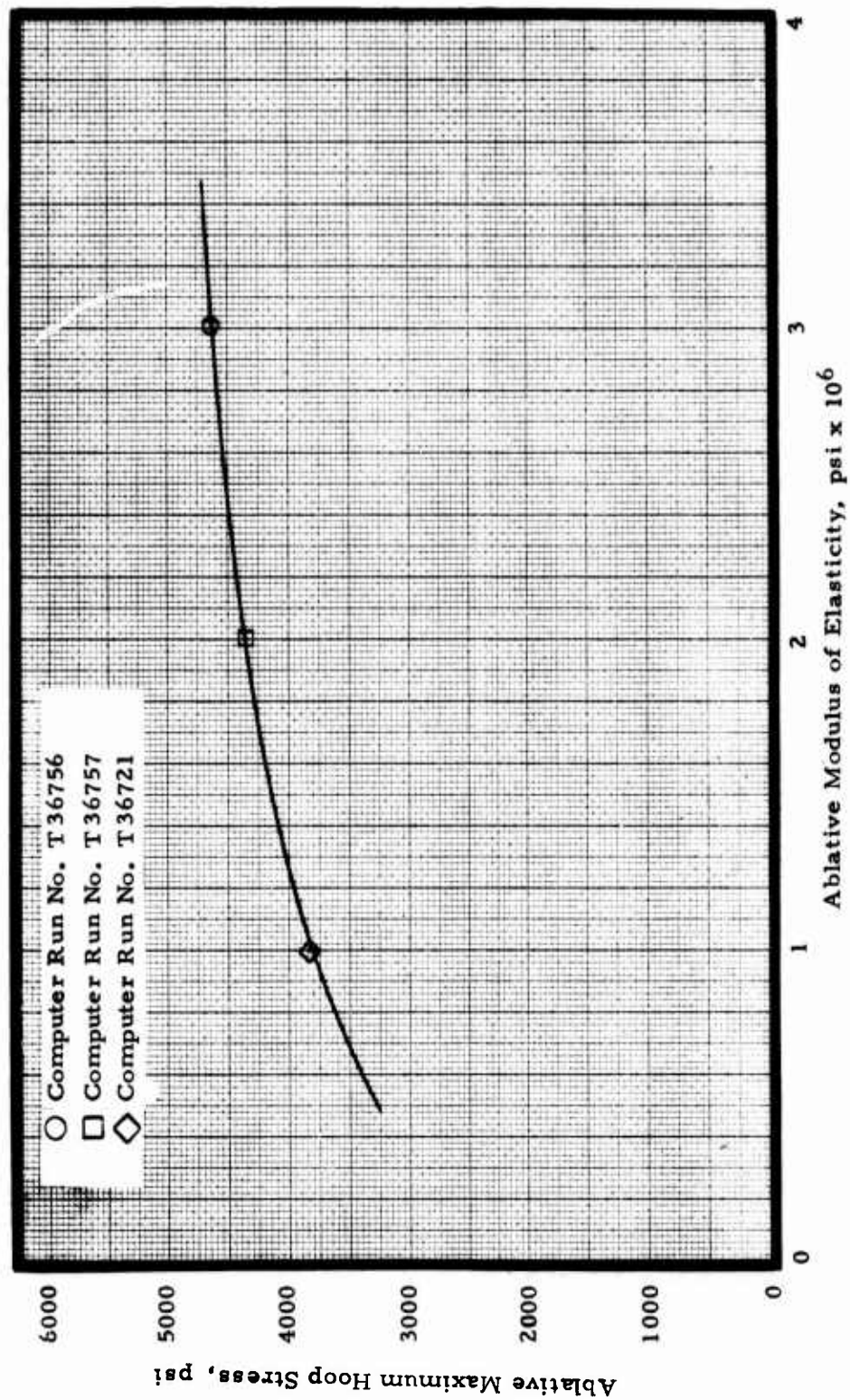


Figure IX-9. Effect of Varying Modulus on Maximum Hoop Stress in Design 1



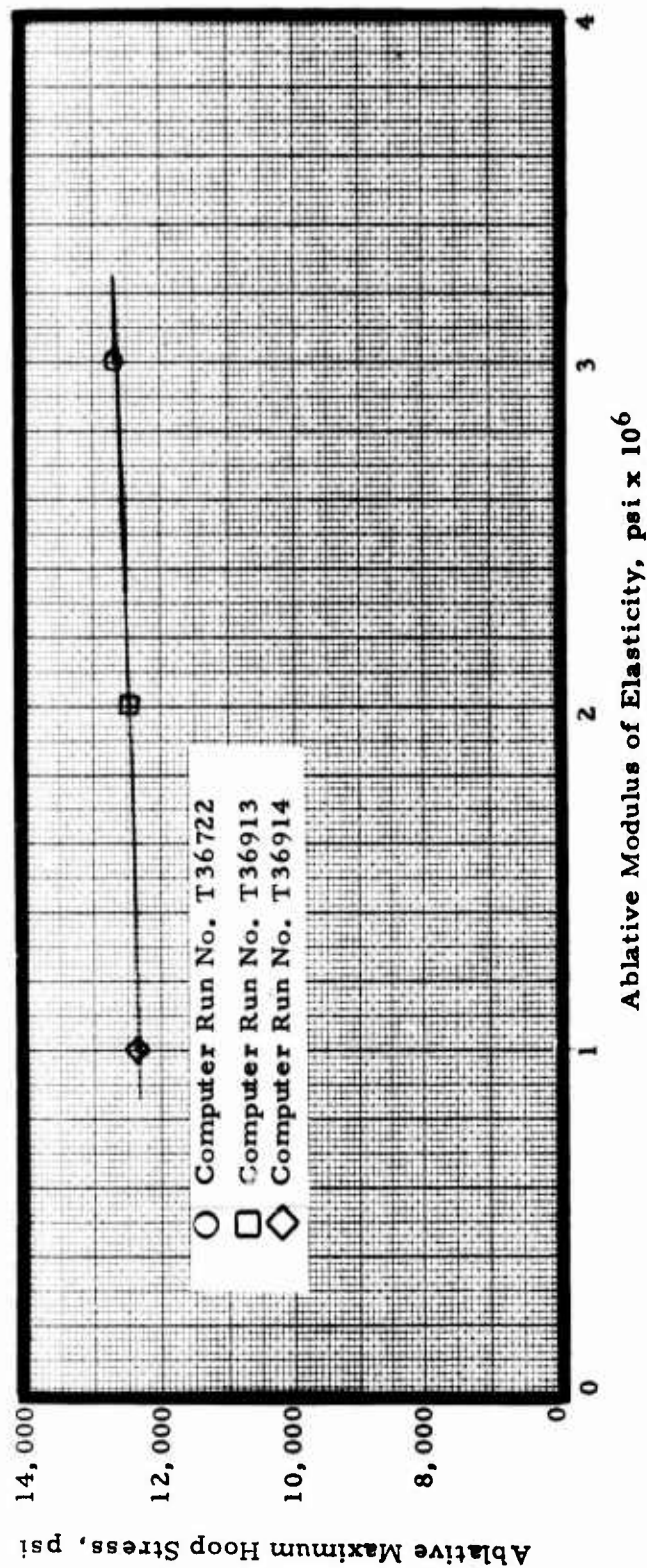


Figure IX-10. Effect of Varying Modulus on the Maximum Hoop Stress in Design 2

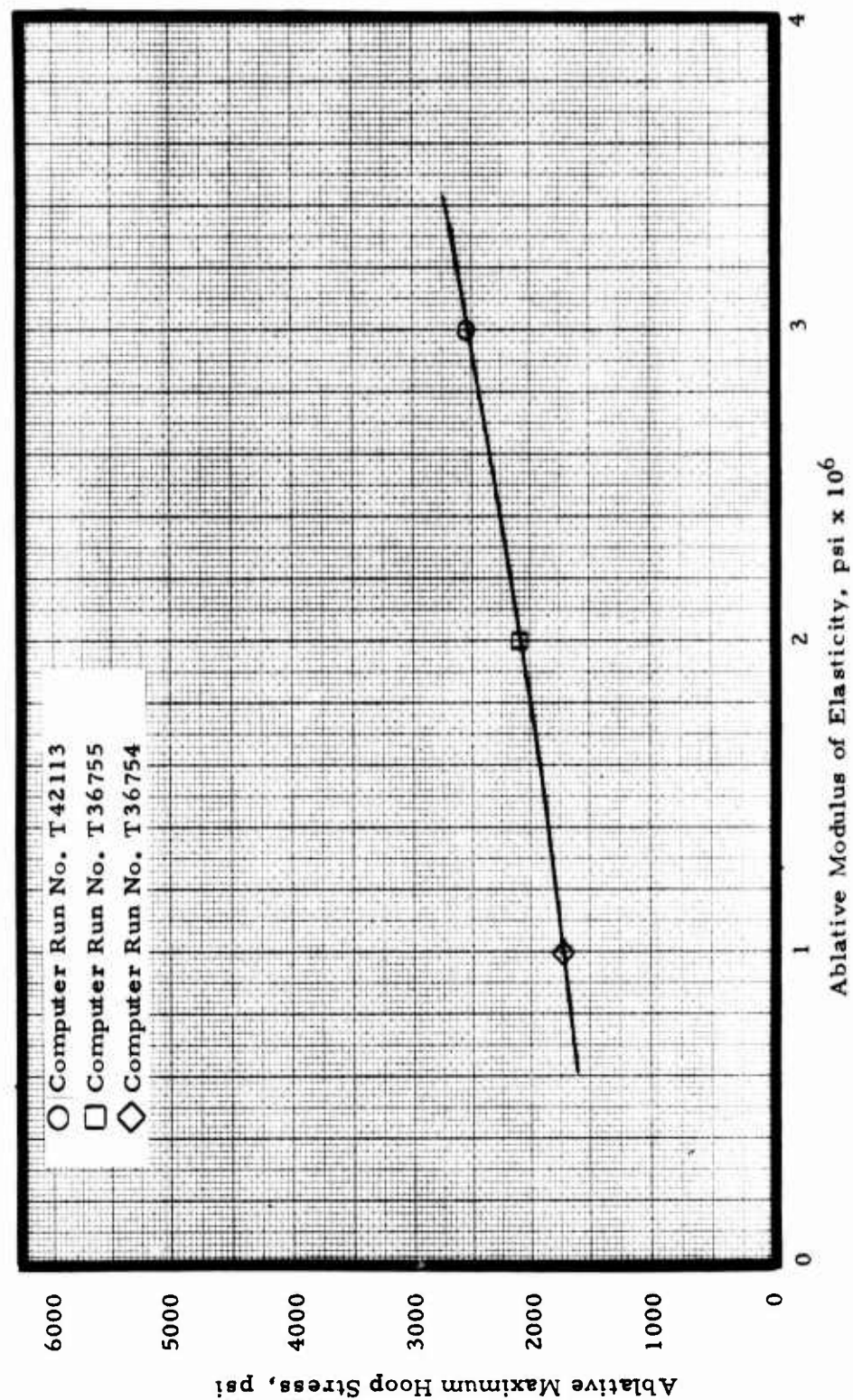


Figure IX-11. Effect of Varying Modulus on the Maximum Hoop Stress in Design 3

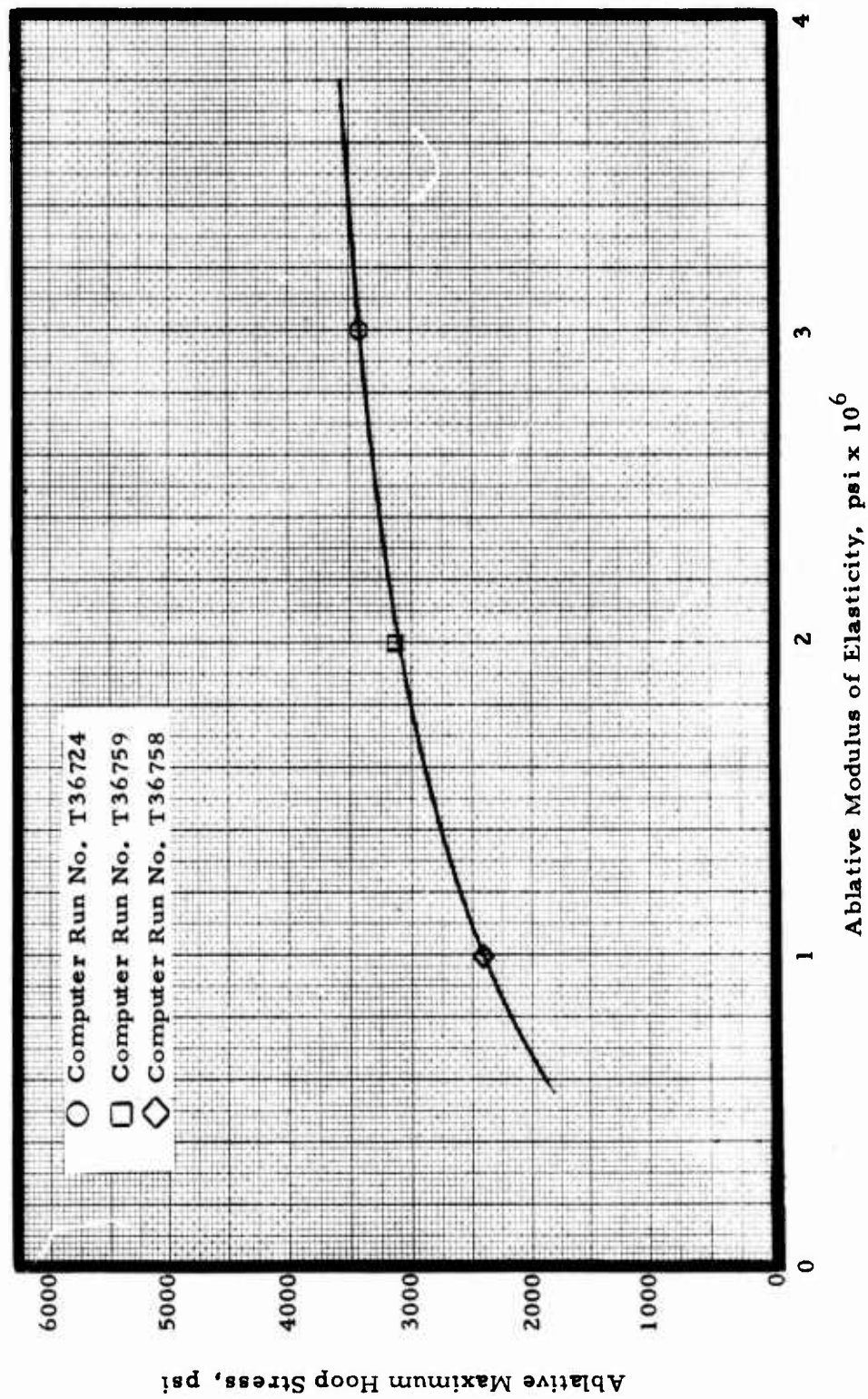


Figure IX-12. Effect of Varying Modulus on the Maximum Hoop Stress in Design 4

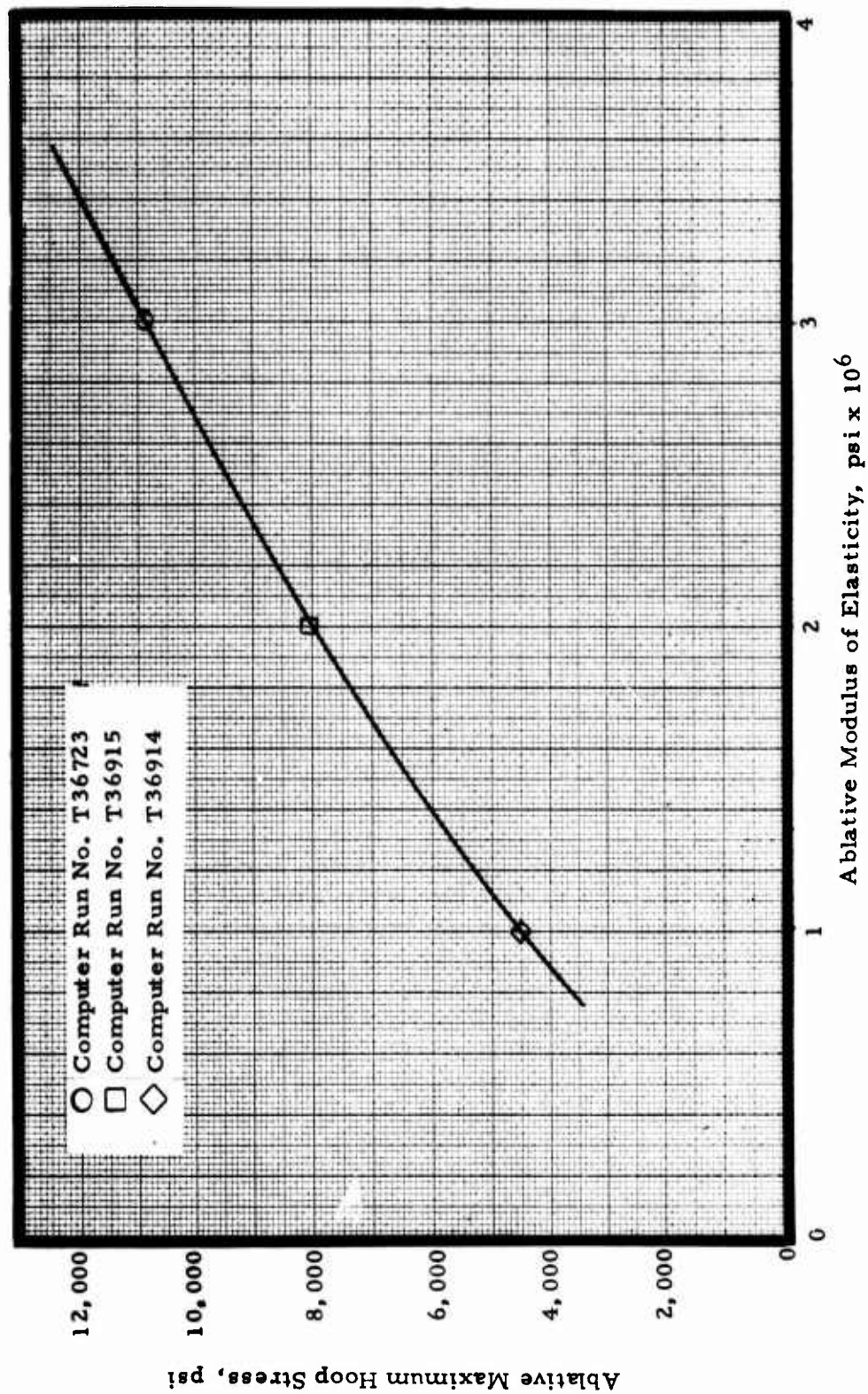


Figure IX-13. Effect of Varying Modulus on the Maximum Hoop Stress in Design 5



**TABLE IX-3**  
**INDUCED STRESSES AND MARGINS OF SAFETY FOR DESIGNS BASELINE THROUGH FIVE**

Material	Tensile Modulus (psi x 10 <sup>6</sup> )	Mat'l. Strength (psi)	Maximum Stress (psi)					Margin of Safety (c)									
			Design Baseline	Design 1	Design 2	Design 3	Design 4	Design 5	Design Baseline	Design 1	Design 2	Design 3	Design 4	Design 5			
Glass Filled Phenolic																	
FM16771	3.1	3200 (b)	4495	4650	12670	2625	3440	11150	-0.29	-0.31	-0.75	0.22	-0.07	-0.71			
FM5042	2.25	4928 (b)	4190	4450	12500	2180	3200	8720	0.18	0.11	-0.61	1.26	0.54	-0.43			
FM5821	2.25	4390 (b)	4190	4450	12500	2180	3200	8720	0.05	-0.01	-0.65	1.01	0.37	-0.50			
FM5736	3.0	7680 (b)	4450	4625	12640	2540	3420	10880	0.73	0.66	-0.39	2.02	1.25	-0.29			
4E0253	0.4	3328 (b)	3650	3120	12250	1555	1500	1500	-0.09	0.07	-0.73	1.14	1.22	1.22			
D23570	1.9	6080 (b)	4083	4320	12450	2050	3050	7700	0.49	0.40	-0.51	1.97	0.99	-0.21			
Glass Filled Dialyl Phthalate																	
D232008	1.4	6400	3935	4090	12390	1880	2760	6020	0.63	0.56	-0.48	2.40	1.32	0.06			
Glass Filled Alkyd																	
D24060	2.8	6080	4375	4580	12600	2425	3370	10300	0.39	0.33	-0.52	1.51	0.80	-0.41			
Mineral Filled Phenolic																	
D23639	2.3	3840	4207	4460	12530	2200	3220	8880	-0.09	-0.14	-0.69	0.75	0.19	-0.57			
D16090	1.7	4160	4020	4240	12420	1980	2950	7050	0.03	-0.02	-0.67	1.10	0.41	-0.41			
Asbestos Phenolic																	
153-RPD-T	2.4	6528	4240	4490	12530	2240	3258	9190	0.54	0.45	-0.48	1.91	1.01	-0.29			
153-RPD-C	2.9	7507	4415	4600	12620	2485	3400	10600	0.70	0.63	-0.41	2.02	1.21	-0.29			
110-RPD	3.0	4672	4450	4625	12640	2540	3420	10880	0.05	0.01	-0.63	0.84	0.37	-0.57			
Cellulose Filled Phenolic																	
D22512	1.3	4480	3905	4025	12380	1845	2680	5700	0.15	0.11	-0.64	1.43	0.67	-0.21			
R25406	1.2	4544	3875	3960	12350	1810	2608	5300	0.17	0.15	-0.63	1.51	0.75	-0.14			
FM3510	1.0	4480	3820	3810	12320	1740	2410	4560	0.17	0.18	-0.64	1.57	0.86	-0.01			
Wood Flour Filled Phenolic																	
D-791B	1.2	3840	3875	3960	12350	1810	2600	5300	-0.01	-0.03	-0.69	1.12	0.48	-0.28			
Thermoplastic																	
Ryton 4	2.1	12480	4145	4400	12490	2120	3150	8300	2.01	1.84	-0.00	4.89	2.96	0.50			
Noryl	1.2	9280	3875	3960	12350	1810	2600	5300	1.39	1.34	-0.25	4.13	2.57	0.75			
Arylon T	0.32	4800	3625	2975	12220	1530	1350	1000	0.32	0.61	-0.61	2.14	2.56	3.80			

a. Material strength is 64% of book value tensile strength based on previous tests on molded samples.

b. Results of tests with molded components

c.  $M.S. = f_u / \sigma - 1$

Supplementary analyses were performed to determine the effect of shell stiffness upon insulation stress. For this purpose, steel was substituted for aluminum as the back-up structure for each of the three basic supported configurations (Figures IX-5 through IX-7). Some results are summarized in Table IX-4 and are illustrated in Figure IX-14. The effect of this change upon the margin of safety of the various designs is shown in Table IX-5.

#### THROAT EROSION

Throat erosion for several materials was assessed in TX3 (3 lb) and full-scale TX631 (25 lb) motors. Engineering judgement was used to select the 10 materials (plus FM16771 baseline) evaluated in the TX3 motors. Bases for the selections were cost, availability and anticipated throat erosion characteristics. Results are listed in Table IX-6. Post-test examination showed uniform erosion except for Charge No. 8 and 9 (Figures IX-15 through IX-24).

Costs for the baseline nozzle design was used in conjunction with TX3 erosion to chose those materials for testing in the full-scale motor (Figure IX-25). The baseline material, FM16771, was tested in two motors to assure a good reference erosion value. A material suitable for injection molding, Ryton R4, was selected for that characteristic. The others were selected on the basis of erosion rate equal to that of FM16771 at significantly lower cost and on intermediate erosion resistance at somewhat lower cost. The wood-flour filled material (D791) had the same intermediate erosion resistance but at significantly lower costs; looking back, that material somehow should have been incorporated into the TX631 test program.

Results of the TX631 tests are listed in Table IX-7. Post-test condition of the nozzles are shown in Figures IX-26 through IX-32. There was gouging in all but two of the ablative nozzles.

<u>Amount of Gouging</u>	<u>Motor</u>	<u>Material</u>
Little or none	T643-2	153R PD
	T684-1	23570
Some	T634-1	16771
	T643-1	110R PD
Quite a bit	T622-1	16771
	T634-2	22532
Severe	T622-2	Ryton R4

A major reason for the gouging was the gas flow field at the aft end of the grain. Based on other motor programs, this type of environment can be improved through proper shaping of the grain aft surface and compatibility of entrance and throat materials. The circumferential grooves at the "X" position are obvious effects from circulation patterns of the combustion gases

TABLE IX-4  
RESULTS OF ANALYSIS OF SHELL

<u>Type Shell</u>	<u>Shell Maximum Stress, psi</u>		
	<u>Designs Baseline/3</u>	<u>Designs 1/4</u>	<u>Designs 2/5</u>
No Shell	4666	4637	12667
Aluminum Shell <sup>(a)</sup>	2638	3414	10446
Steel Shell <sup>(a)</sup>	2507	2599	4521

a. Shell thickness = 0.1 inch



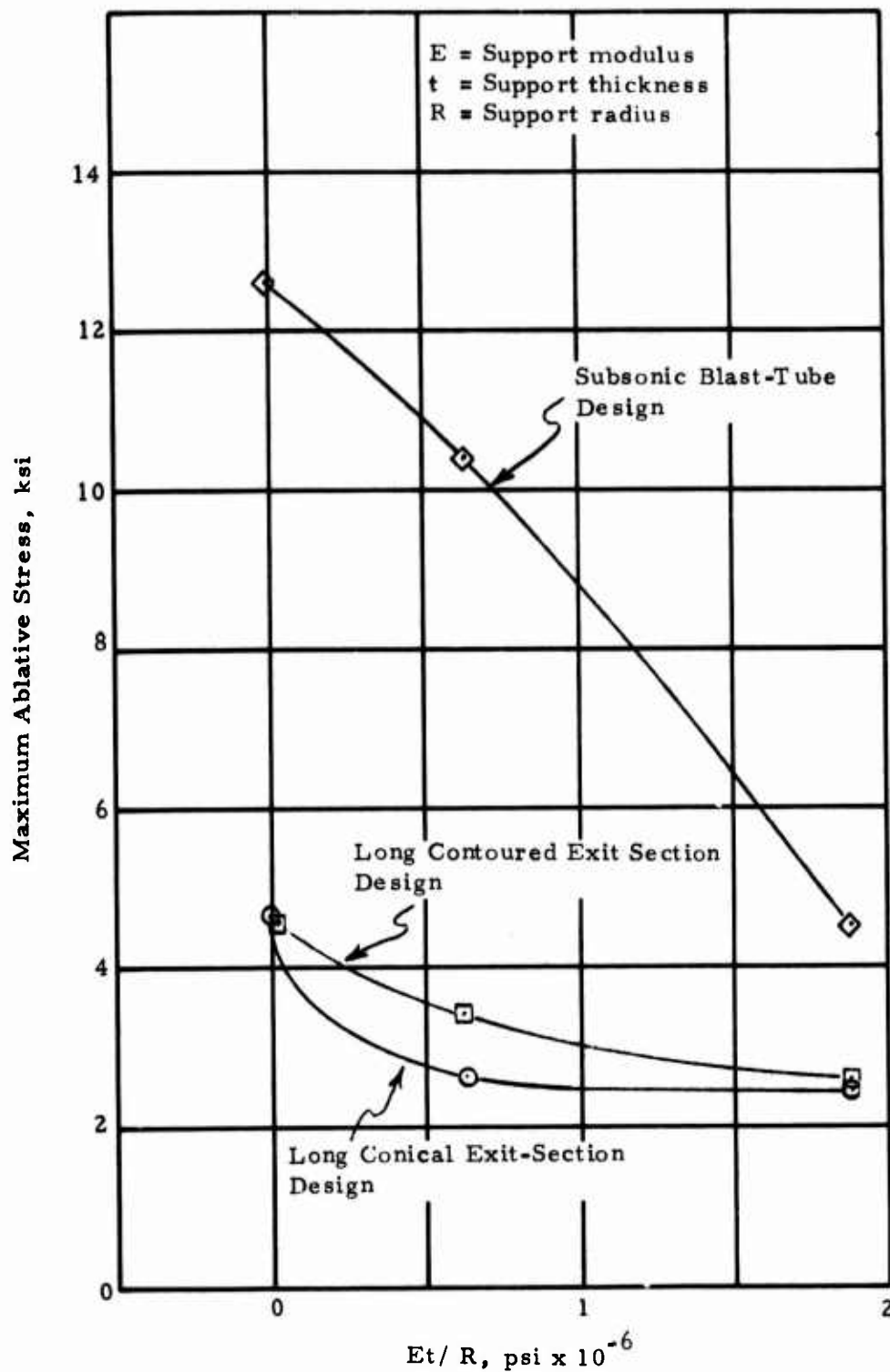


Figure IX-14. Effect of Structural Support Stiffness on Stress

TABLE IX-5

MAXIMUM STRESS AND MARGIN OF SAFETY  
FOR NOZZLES WITH STEEL SUPPORT SHELL

Material	Tensile Modulus (psi x 10 <sup>-6</sup> )	Mat'l. Streng. <sup>(a)</sup> (psi)	Maximum Stress (psi)			Margin of Safety <sup>(c)</sup>		
			Design 3s(b)	Design 4s(b)	Design 5s(b)	Design 3s(b)	Design 4s(b)	Design 5s(b)
<u>Glass Filled Phenolic</u>								
FM16771	3.1	3200	2495	2619	4826	0.28	0.22	-0.34
FM5042	2.25	4928	2072	2436	3774	1.38	1.02	0.31
FM5821	2.25	4390	2072	2436	3774	1.12	0.80	0.16
FM5736	3.0	7680	2414	2604	4709	2.18	1.95	0.63
4E0253	0.4	3328	1478	1142	650	1.25	1.91	4.12
D23570	1.9	6080	1948	2322	3333	2.12	1.62	0.82
<u>Glass Filled Diallyl Phthalate</u>								
D22008	1.4	6400	1787	2101	2605	2.58	2.05	1.46
<u>Glass Filled Alkyd</u>								
D24060	2.8	6080	2305	2566	4458	1.64	1.37	0.36
<u>Mineral Filled Phenolic</u>								
D23639	2.3	3840	2091	2451	3843	0.84	0.57	-0.00
D16090	1.7	4160	1882	2246	3051	1.21	0.85	0.36
<u>Asbestos Phenolic</u>								
153-RPD-T	2.4	6528	2129	2474	3977	2.07	1.64	0.64
153-RPD-C	2.9	7507	2362	2588	4588	2.18	1.90	0.64
110-RPD	3.0	4672	2414	2603	4709	0.94	0.79	-0.08
<u>Cellulose Filled Phenolic</u>								
D22532	1.3	4480	1753	2040	2467	1.56	1.20	0.82
R25406	1.2	4544	1720	1979	2294	1.64	1.30	0.98
FM3510	1.0	4480	1654	1835	1948	1.71	1.44	1.30
<u>Wood Flour Filled Phenolic</u>								
D-791B	1.2	3840	1720	1979	2294	1.23	0.94	0.67
<u>Thermoplastic</u>								
Ryton 4	2.1	12480	2014	2398	3592	5.20	4.20	2.47
Noryl	1.2	9280	1720	1979	2294	4.40	3.69	3.05
Arylon T	0.32	4800	1454	1028	433	2.30	3.67	10.09

a. Material strength is 64% of book value based on previous tests on molded nozzles.

b. 3s indicates steel was used in place of aluminum in Design 3, etc.

c. M.S. =  $f_{tu}/\sigma - 1$

TABLE IX-6  
NOZZLE MATERIAL EROSION TESTS

Chg. No.	Material	DTI	DTF	TX-3 Test Motor Parameters <sup>a</sup>					EREF/E
				E	WTPB	TWEB	PAVG		
1	FM16771	0.465	0.654	0.189	3.149	1.2362	1481.8	1.000	
3	110 RPD	0.466	0.690	0.224	3.130	1.1372	1409.9	0.844	
4	153 RPD	0.464	0.680	0.216	3.140	1.1668	1430.2	0.875	
5	D16090	0.465	0.682	0.217	3.138	1.1897	1409.2	0.871	
6	D22532	0.467	0.654	0.187	3.149	1.3906	1381.0	1.011	
7	D791	0.466	0.687	0.221	3.122	1.3101	1279.4	0.855	
8 <sup>b</sup>	FM3510	0.465	0.767	0.302	3.135	1.1557	895.6	0.626	
9 <sup>b</sup>	D23639	0.465	0.730	0.265	3.133	0.9356	1419.7	0.713	
10	R25406	0.465	0.658	0.193	3.133	1.3687	1340.6	0.979	
11	D23570	0.463	0.642	0.179	3.130	1.2734	1488.8	1.056	

a. All motors fired at 70°F.

DTI = Initial throat diameter, inches

DTF = Final throat diameter, inches

E = Total erosion (DTF - DTI), inches

WTPB = Weight of propellant burned, pounds

TWEB = Web time, seconds

PAVG = Average chamber pressure, psi

EREF/E = Erosion of FM16771/Erosion of candidate material

b. Gouged throat.

TABLE IX-7  
NOZZLE MATERIAL EROSION TESTS  
(EX-631)<sup>a</sup>

Mix and Charge No.	Material	DTI (inch)	DTF (inch)	E (inch)	WTPB (lb)	TWEB (sec)	PAVG (psi)	Temp. (°F)	EREF/E <sup>(c)</sup>
T622-1	FM-16771	1.047	1.327	0.280	25.33	2.3919	1438.7	70	0.963
T622-1 (b)	Ryton R4	1.507	1.925	0.868	25.27	3.2401	658.0	70	0.310
T634-1	FM-16771	1.049	1.308	0.259	25.20	2.280	1525.4	70	1.041
T643-1	110 RPD	1.048	1.336	0.288	25.20	2.7965	1168.4	-65	0.936
T643-2	153 RPD	1.048	1.332	0.284	25.20	1.1922	1916.6	165	0.949
T634-2	D22532	1.049	1.256	0.207	25.20	2.2975	1444.2	165	1.300
T684-1	D23570	1.050	1.248	0.198	25.20	1.8350	1765.6	70	1.360
T684-2	R25406	1.048	Motor dome blew off at $\approx$ 13600 psi during ignition						

a. All motors fired at 70°F.

b. Gouged severely.

c. EREF = average of both FM-16771 firings = 0.2695 inch.

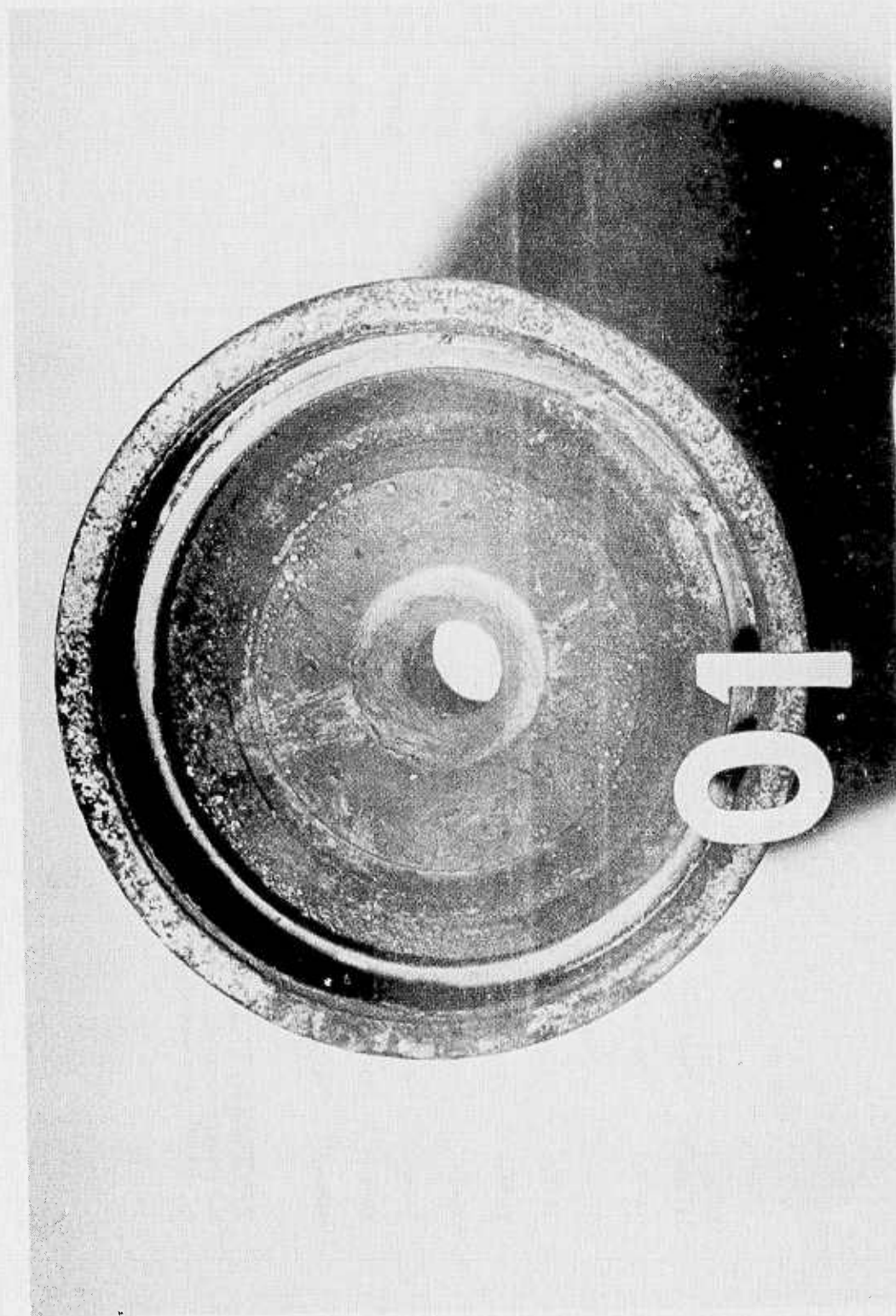


Figure IX-15. Post Test Condition of FM16771 in TX-3 Motor, Charge 1



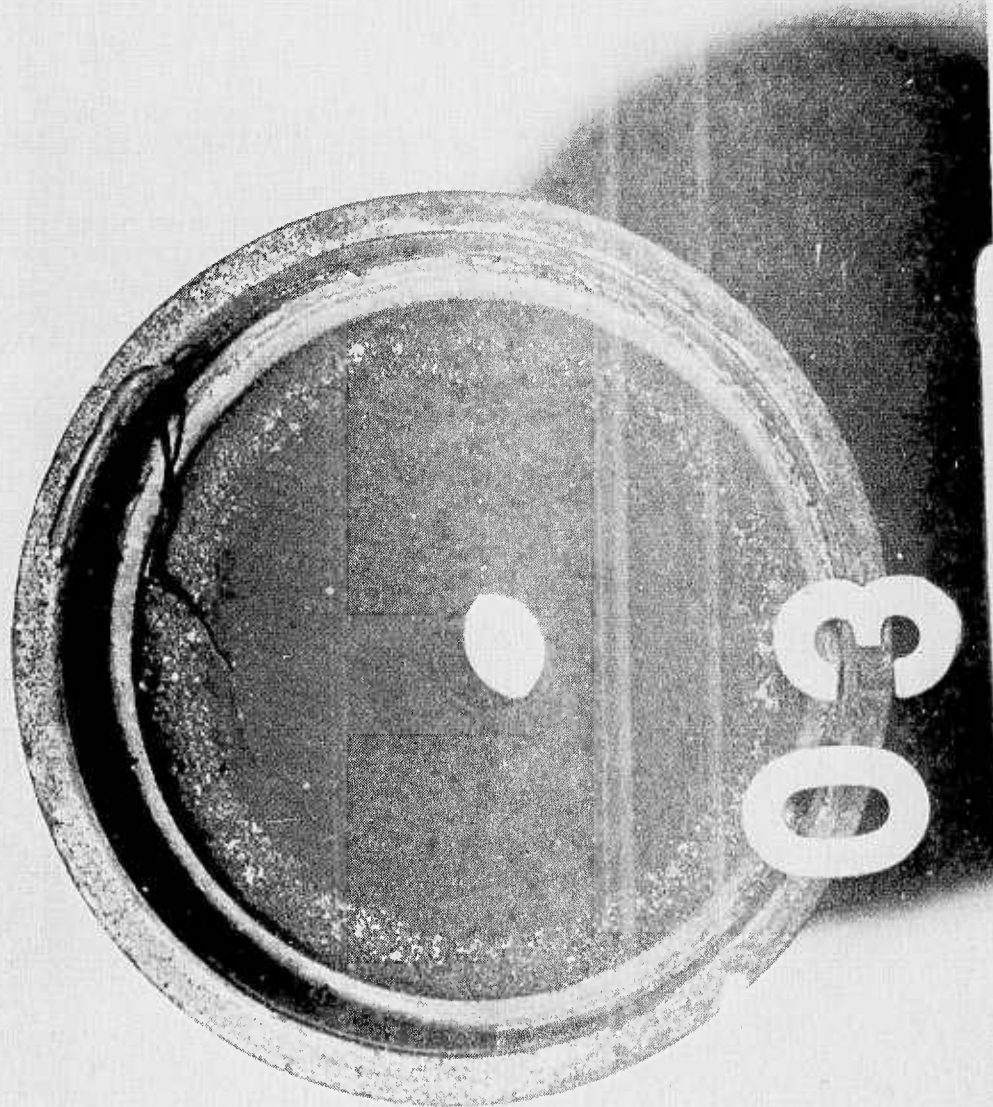


Figure XI-16. Post Test Condition of 110 RPD in TX-3 Motor, Charge 3

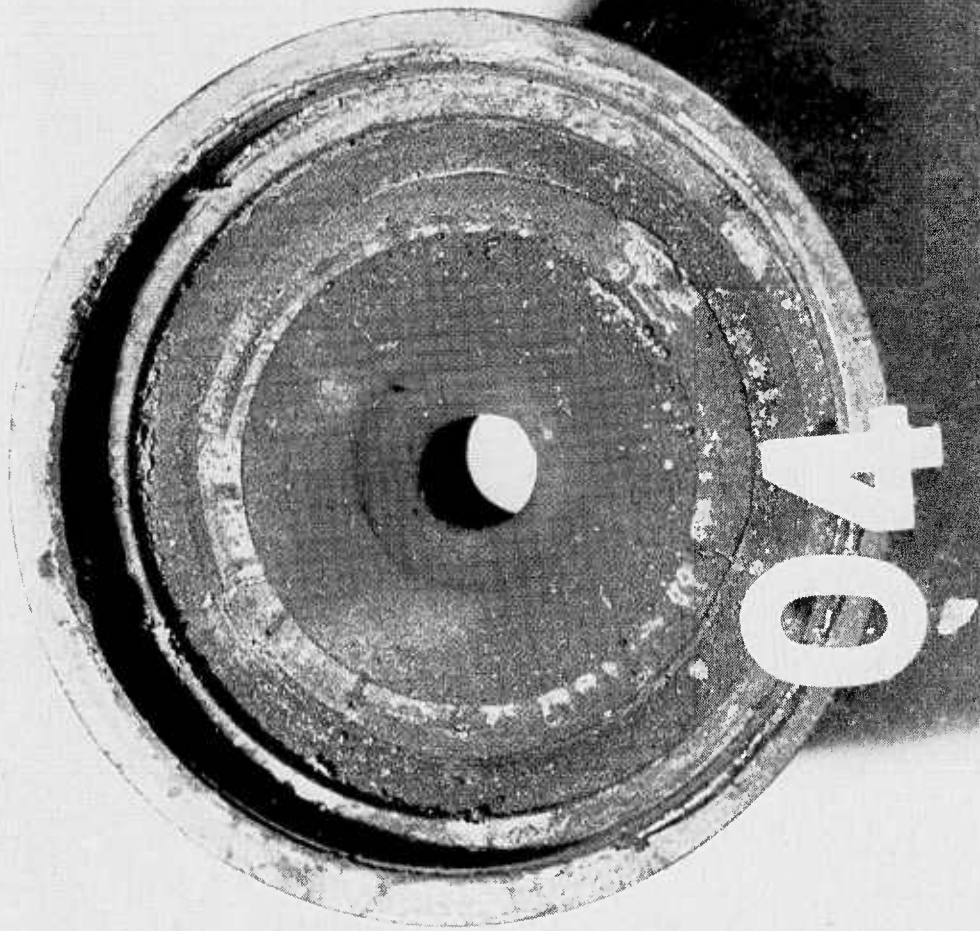


Figure IX-17. Post Test Condition of 153 RPD in TX-3 Motor, Charge 4



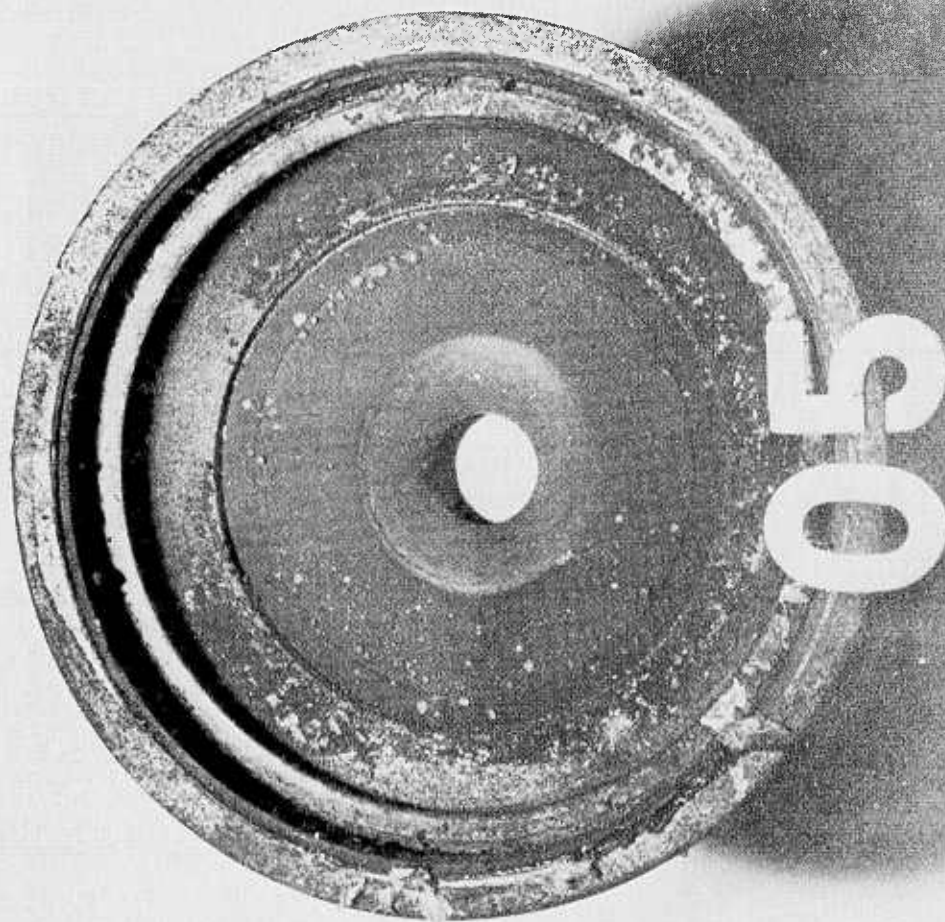


Figure IX-18. Post Test Condition of D16090 in TX-3 Motor, Charge 5

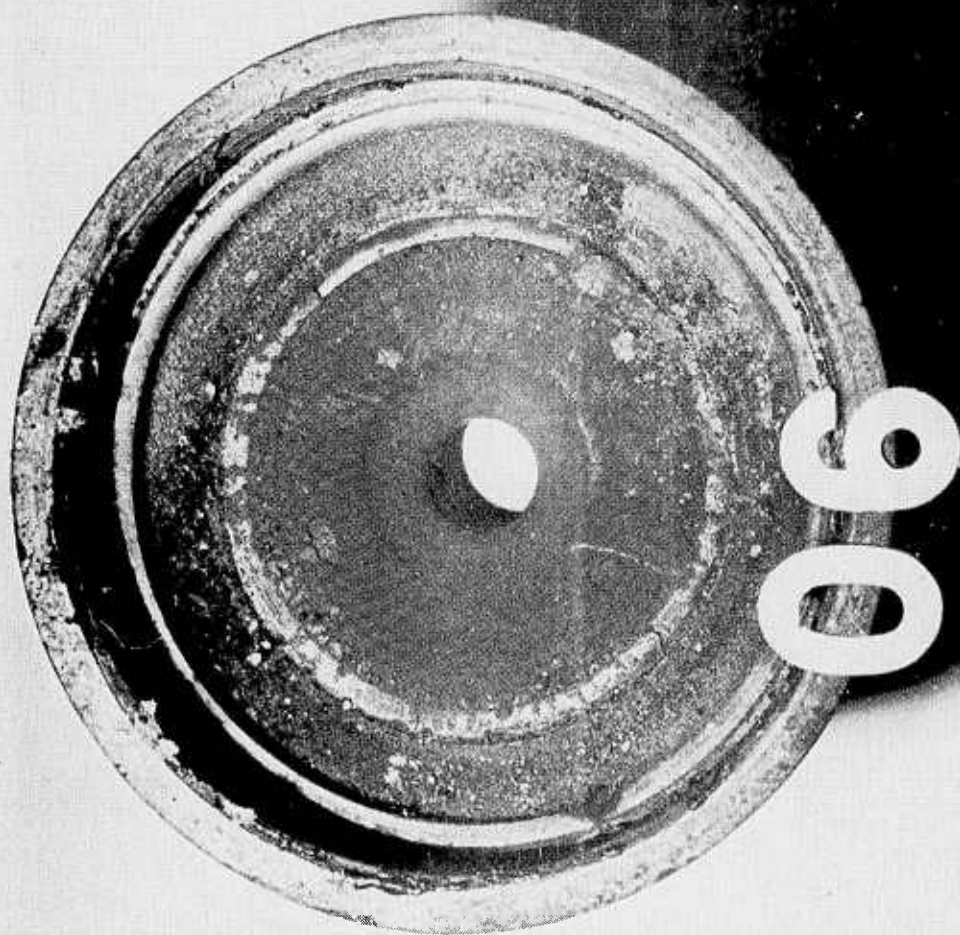


Figure IX-19. Post Test Condition of D22532 in TX-3 Motor, Charge 6

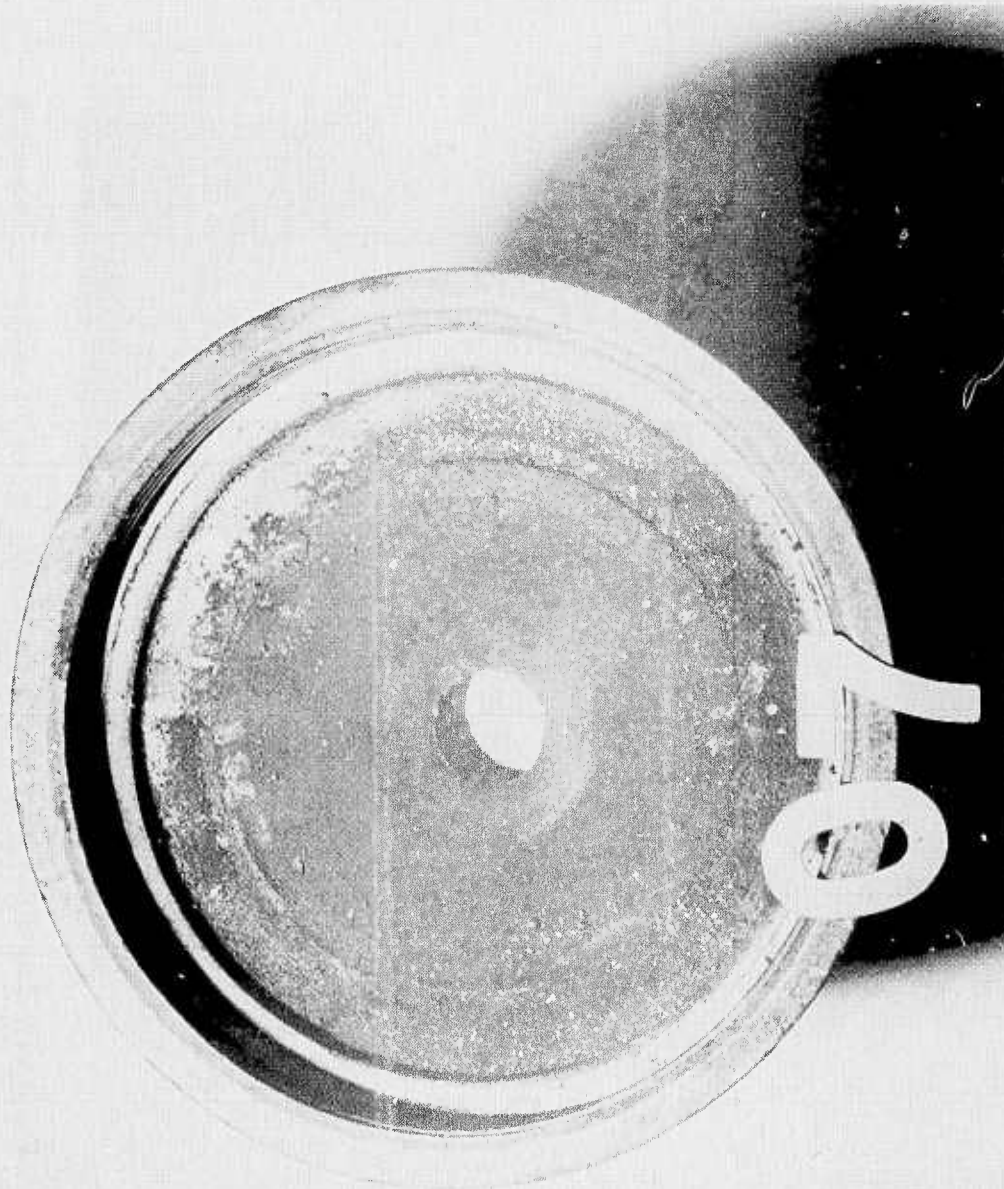


Figure IX-20. Post Test Condition of D791 in TX-3 Motor, Charge 7



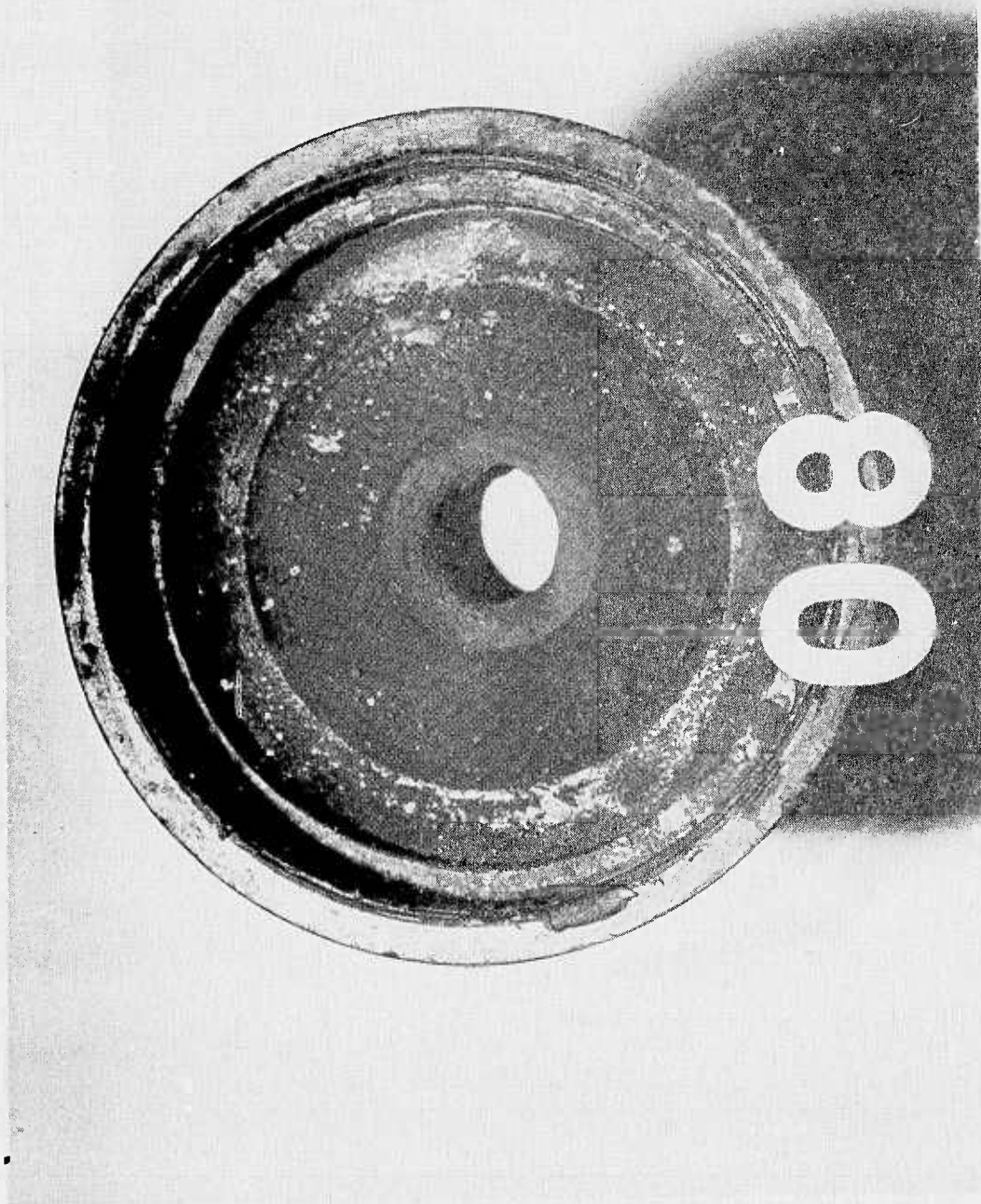


Figure IX-21. Post Test Condition of FM3510 in TX-3 Motor, Charge 8

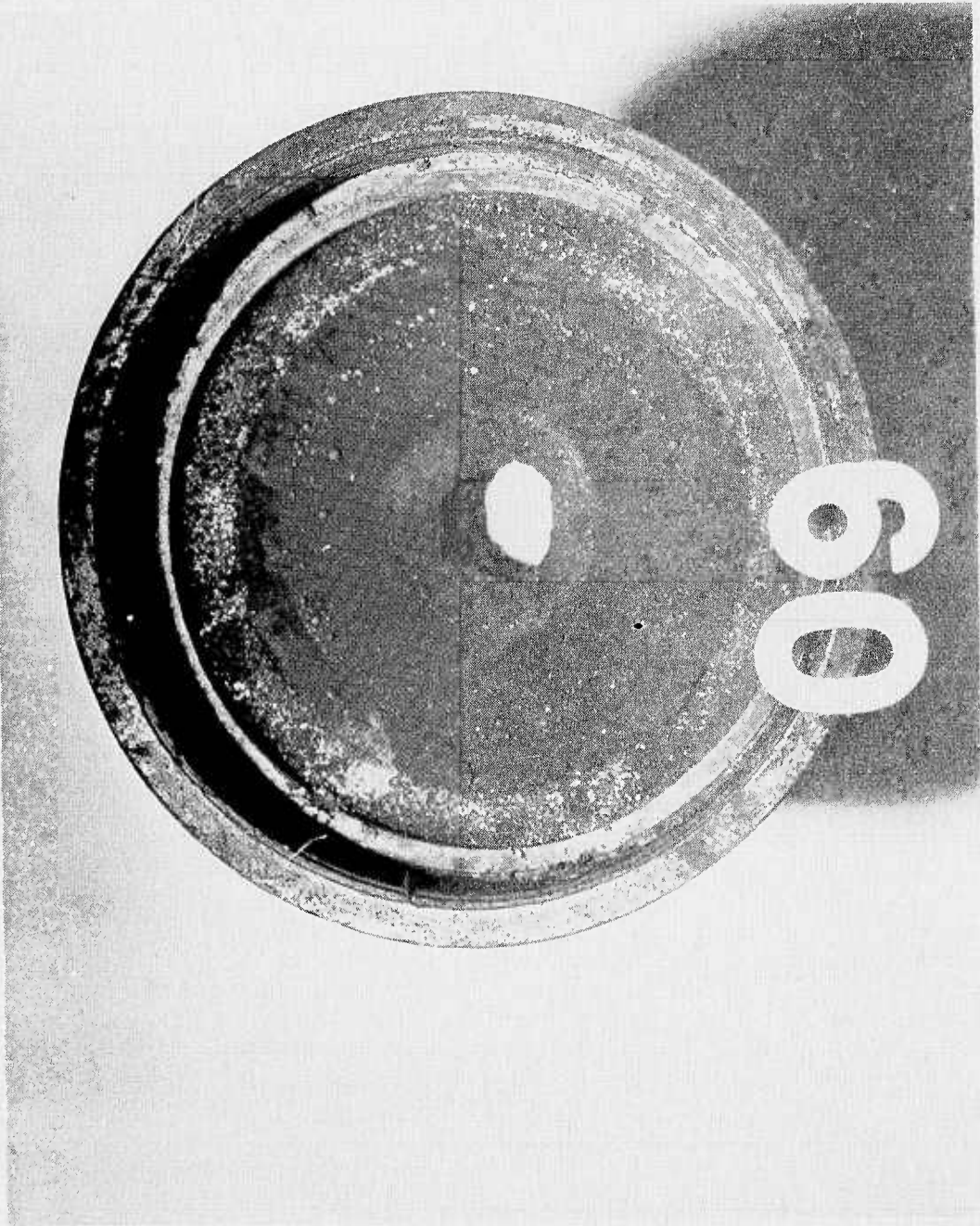


Figure IX-22. Post Test Condition of D23639 in TX-3 Motor, Charge 9



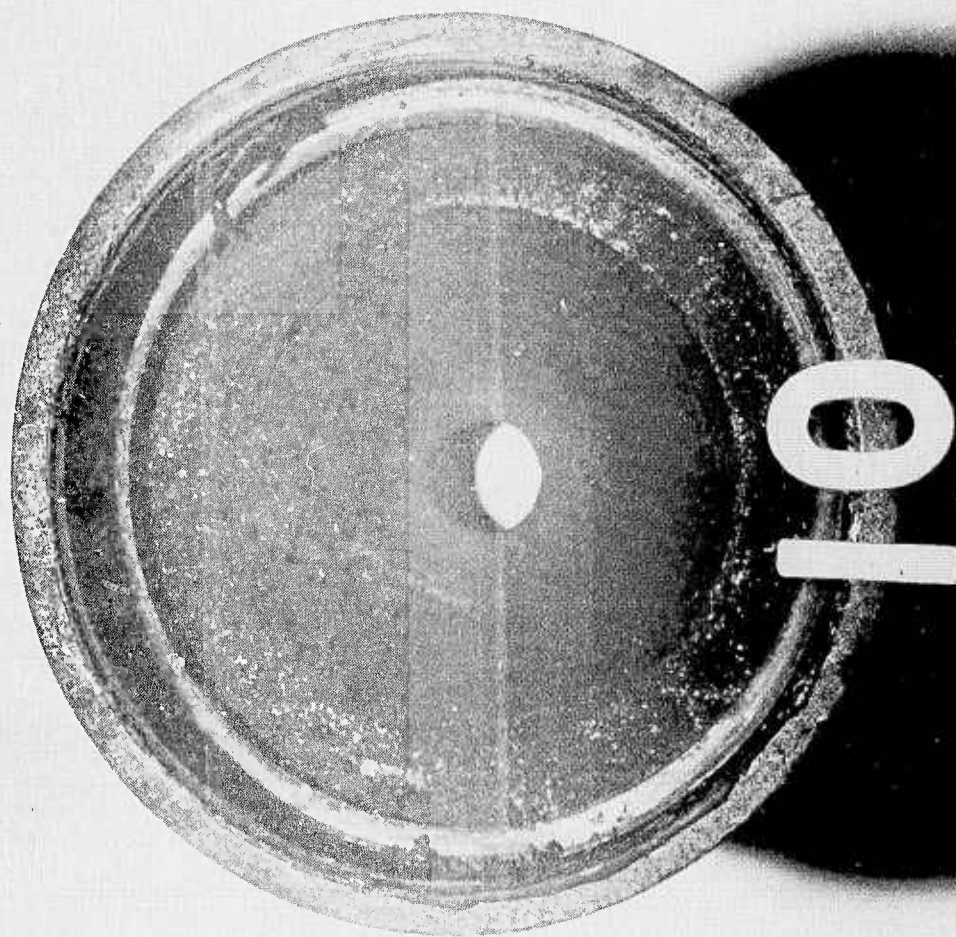


Figure IX-23. Post Test Condition of R25406 in TX-3 Motor, Charge 10

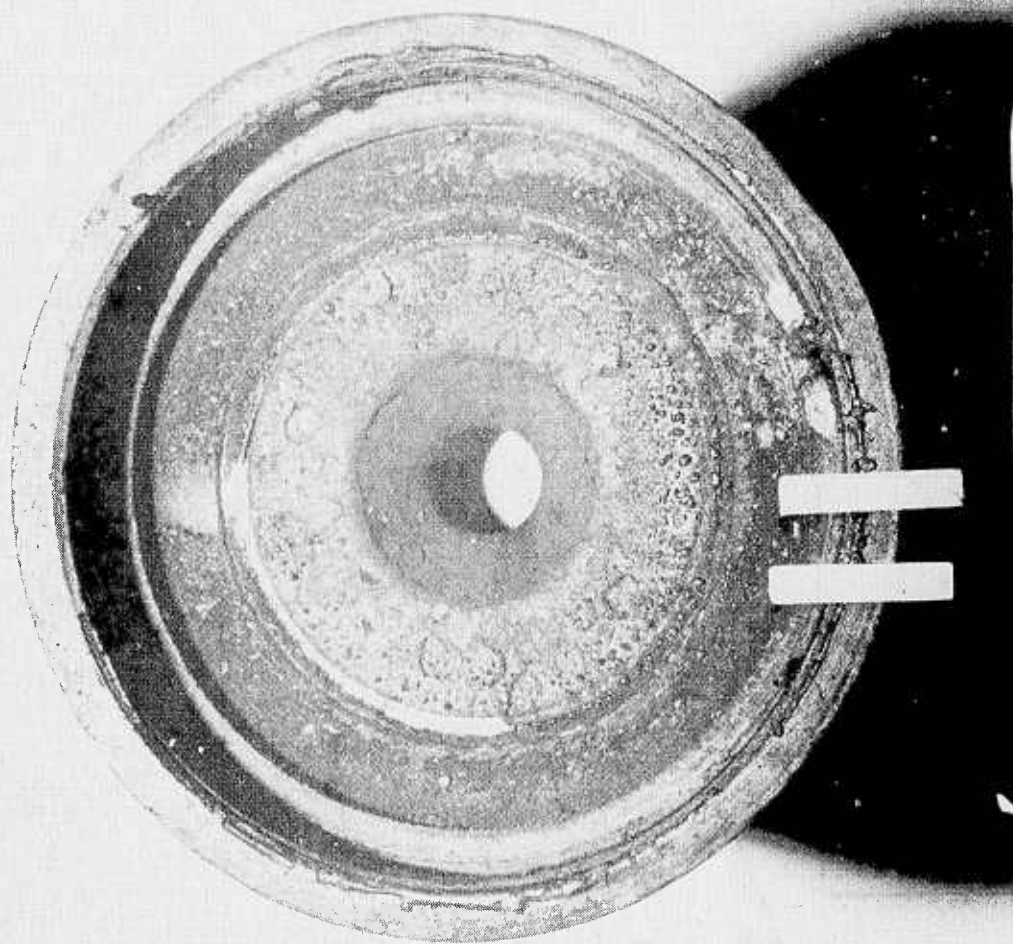


Figure IX-24. Post Test Condition of D23570 in TX-3 Motor, Charge 11



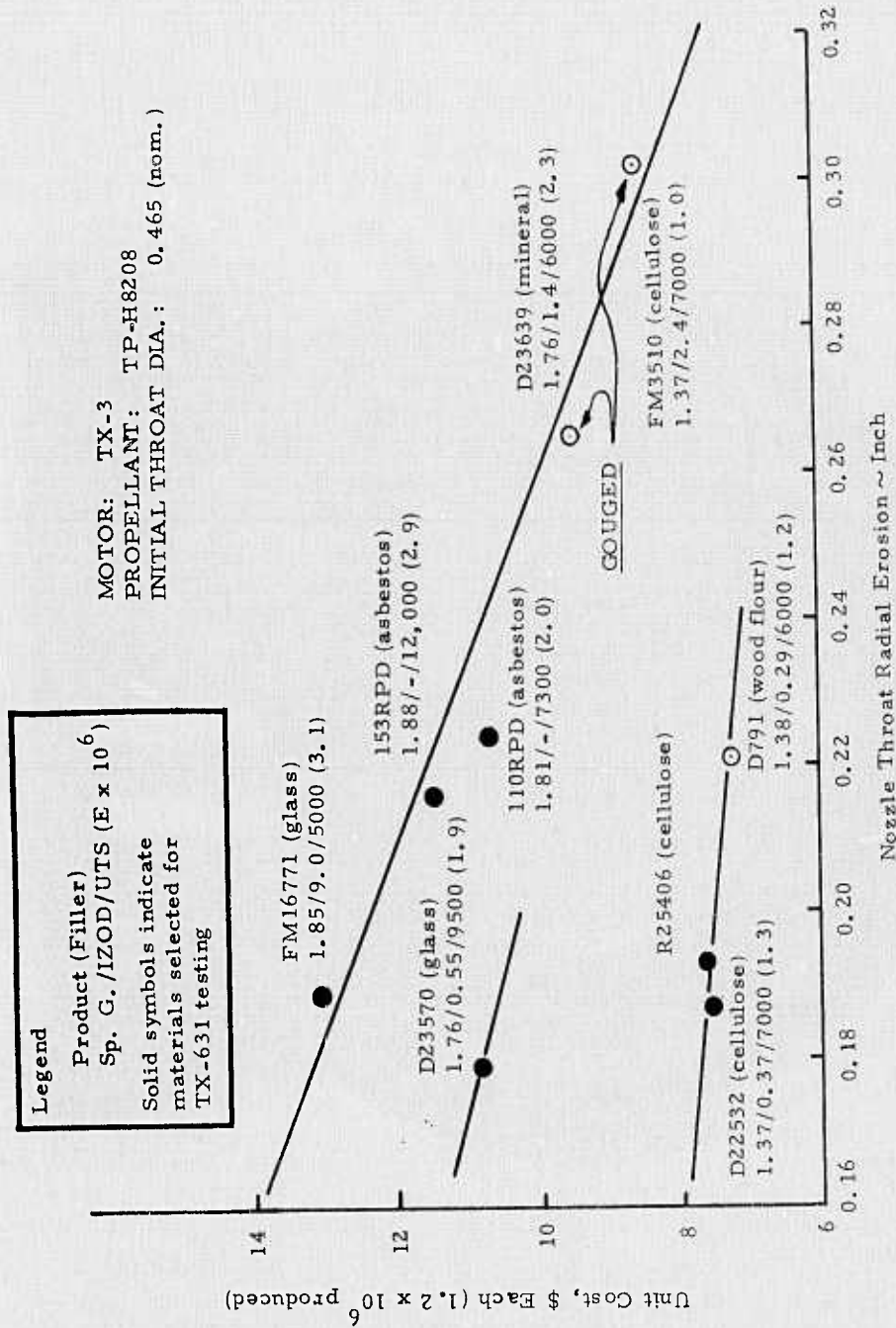


Figure IX-25. Unit Cost Versus TX-3 Throat Erosion

0° "Y"  
Propellant Valley

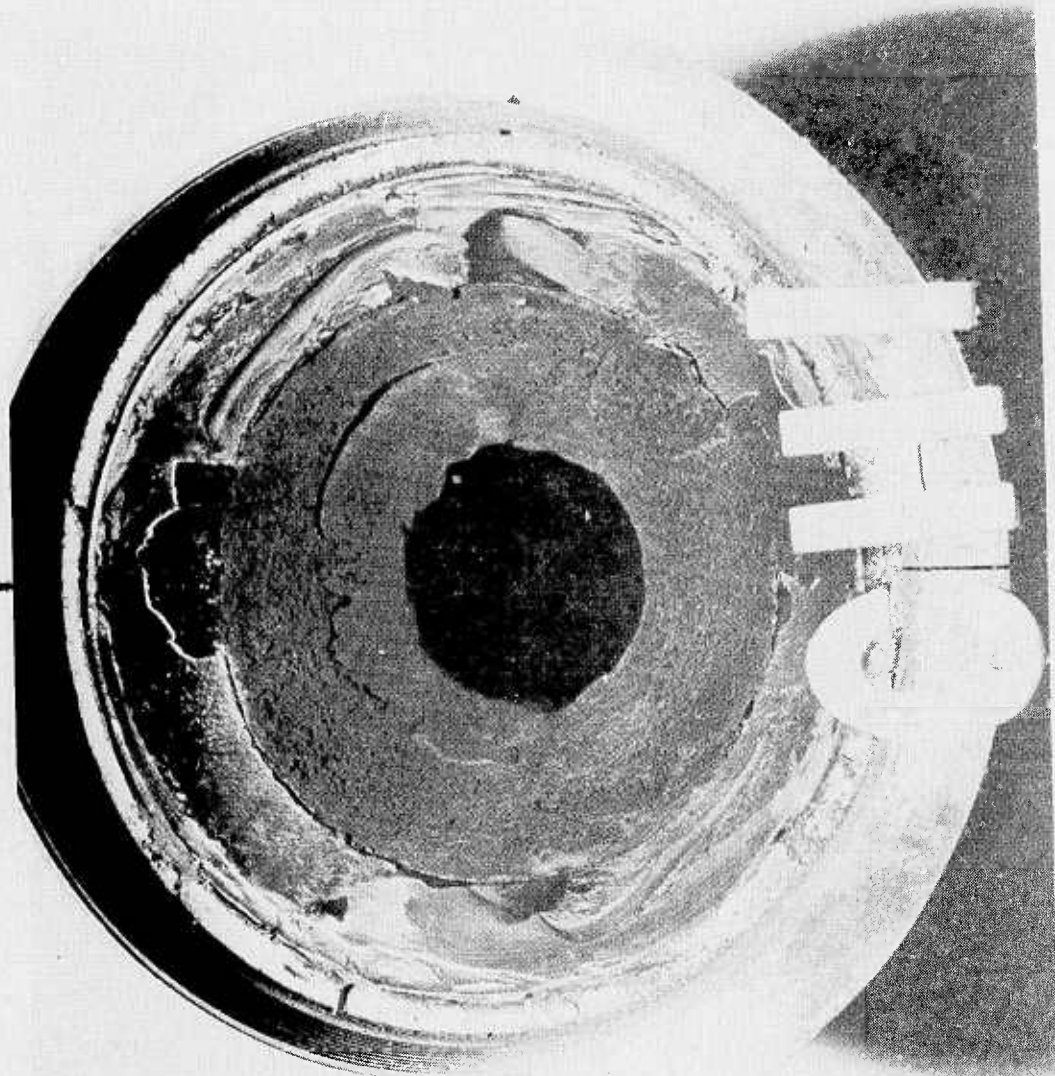


Figure IX-26. Post Test Condition of FM16771 in TX-631 Motor, Mix T-622, Charge 1

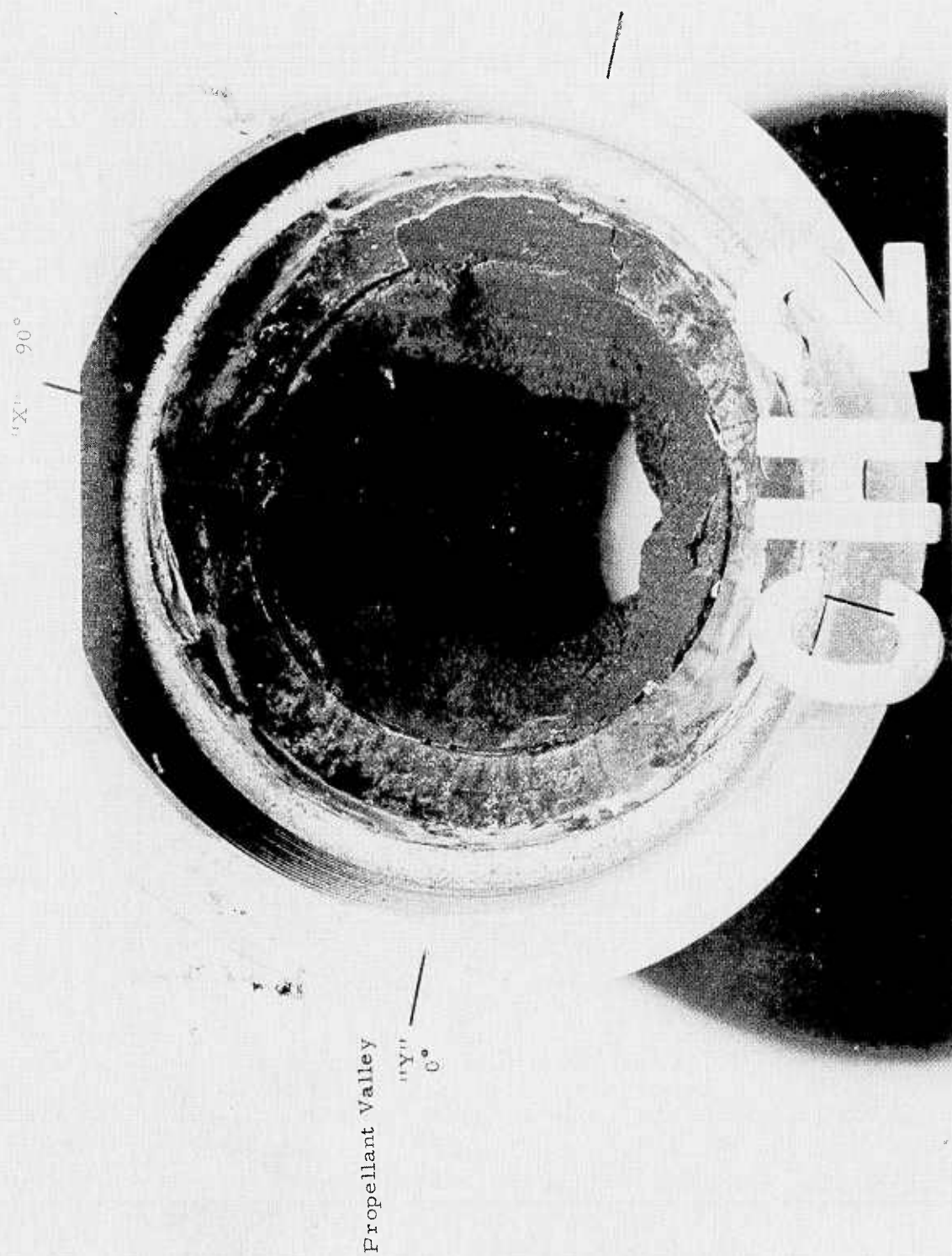


Figure IX-27. Post Test Condition of RYTON R4 in TX-631 Motor, Mix T-622, Charge 2



TX631  
MIX T634-1

Propellant Valley

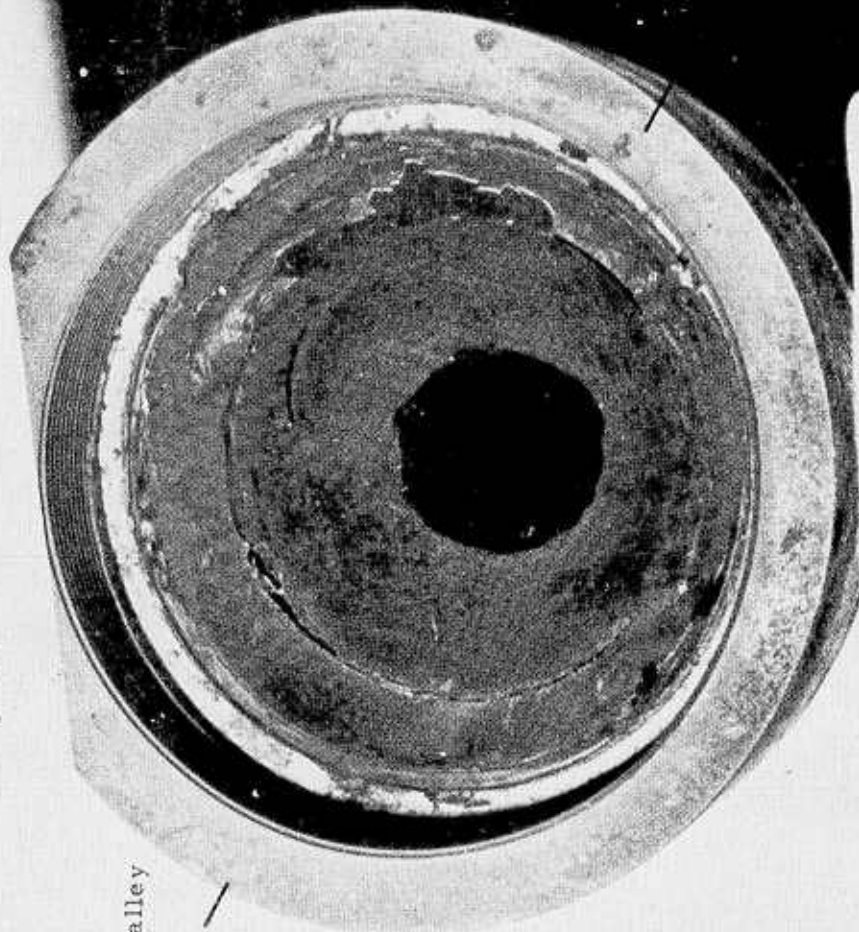


Figure IX-28. Post Test Condition of FM16771 in TX-631 Motor, Mix T-634, Charge 1

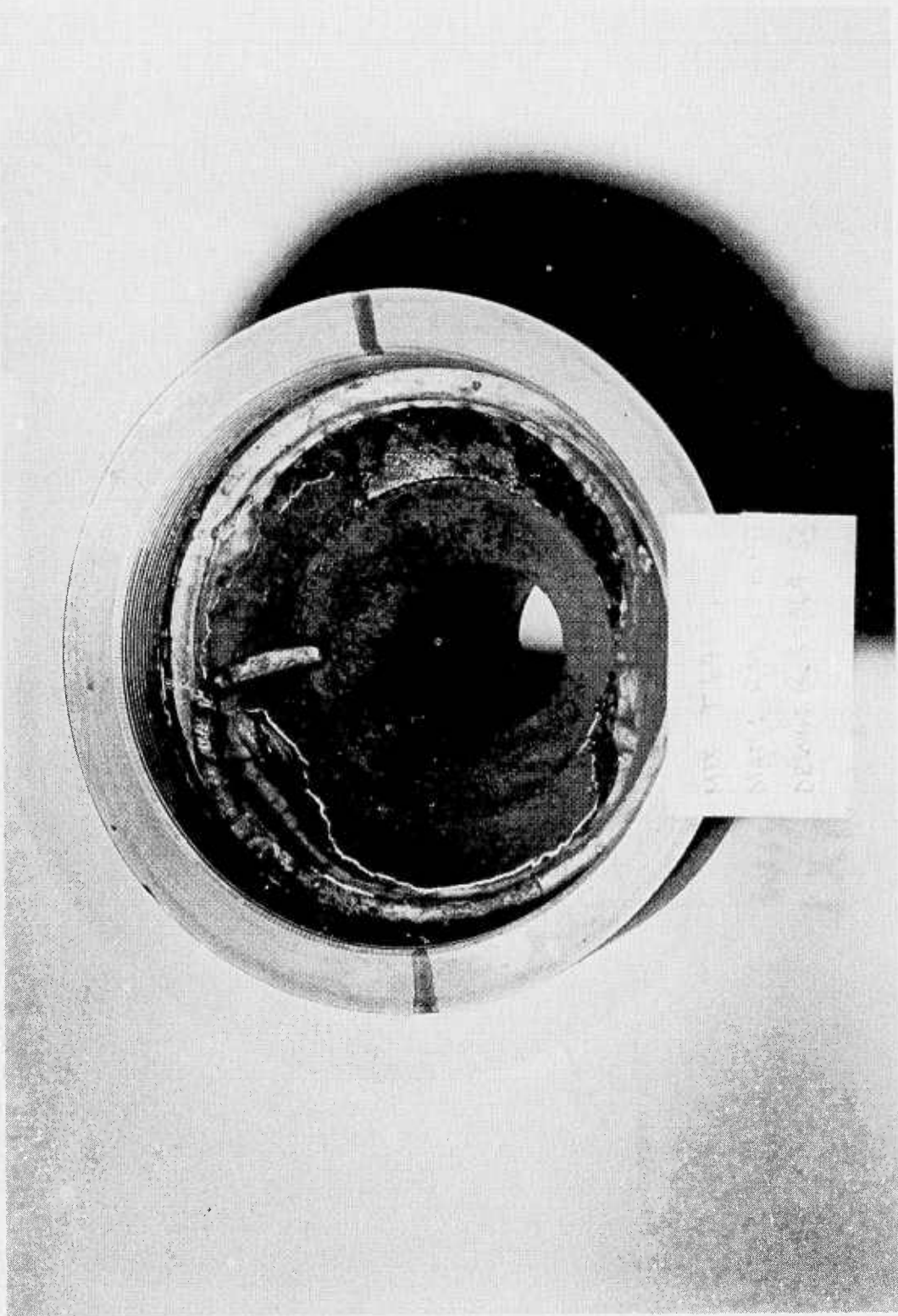


Figure IX-29. Post Test Condition of 100RPD in TX-631 Motor, Mix T-643, Charge 1

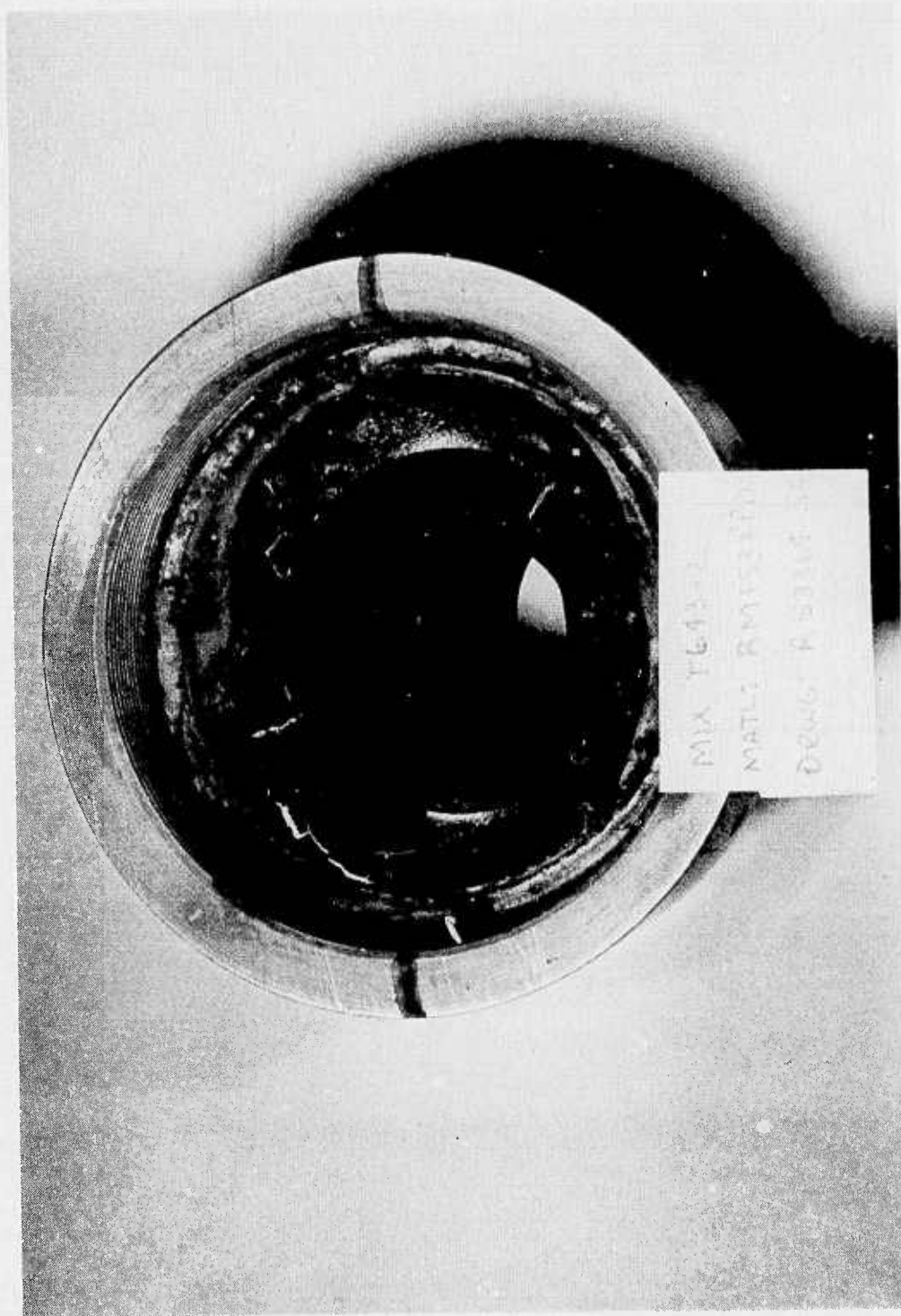


Figure IX-30. Post Test Condition of 153RPD in TX-631 Motor, Mix T-643, Charge 2



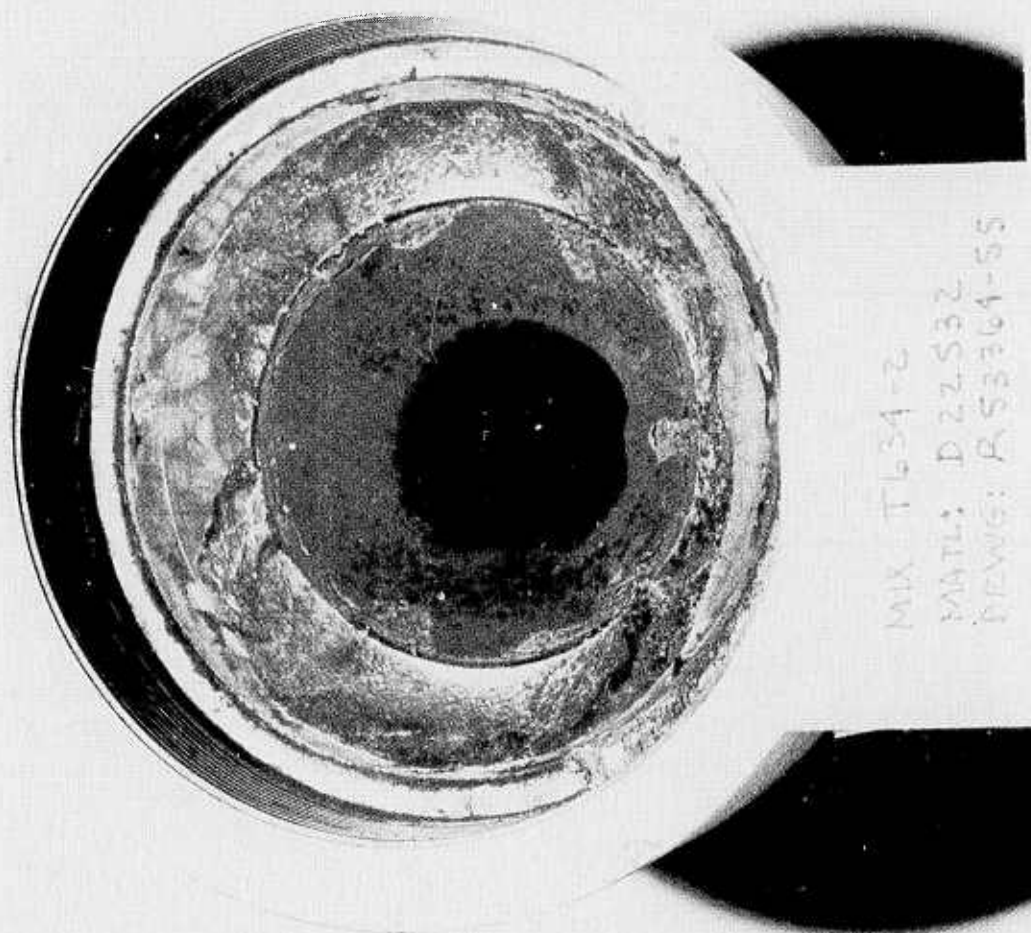


Figure IX-31. Post Test Condition of D22532 in TX-631 Motor, Mix T-634, Charge 2

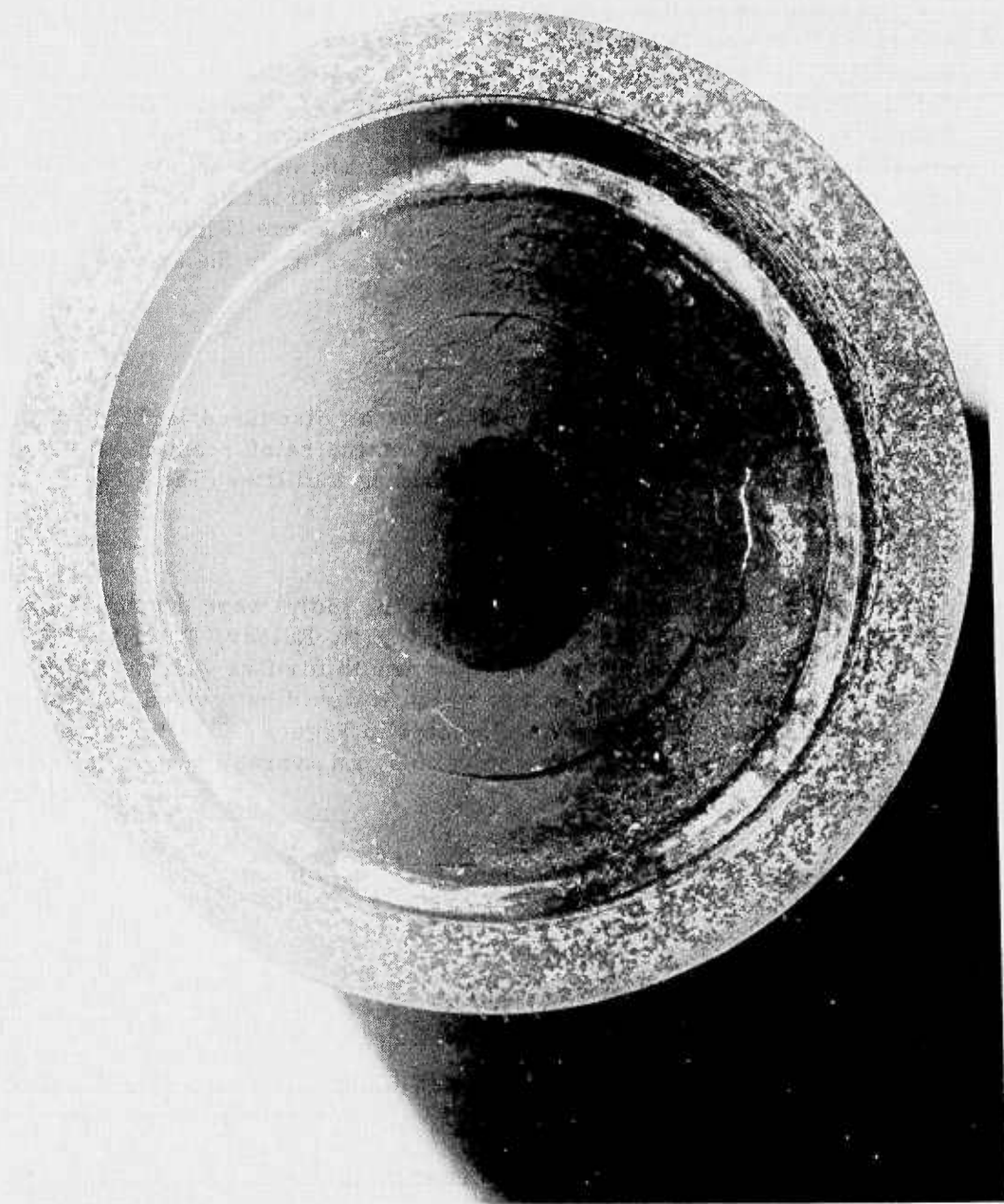


Figure IX-32. Post Test Condition of D23570 in TX-631 Motor, Mix T-684, Charge 1

behind the star points. A flight design would have these effects minimized or eliminated through a variety of techniques. The propellant can be extended into the nozzle entrance section which will greatly reduce the free volume in which circulation patterns can be established. The number of longitudinal slots can be increased (with complementary reduction in slot length) which will reduce the unfilled base area of the propellant grain.

Erosion measurements from TX3 and TX631 motors are compared in Figure IX-33 and Table IX-8. Total throat erosion in the TX631 motor (Table IX-7) is used as a basis for evaluation of the erosion resistance, with the erosion of FM16771 used as a baseline since a significant quantity of throat-erosion data has been accumulated for this reasonably economical material. Those materials tested in the TX3 and not selected for TX631 motor firings are evaluated on the basis of TX3 throat erosion, adjusted to TX631 motor conditions by use of a correlation curve (Figure IX-33) developed from data for materials fired in both motors. Finally the erosion index of merit was calculated and listed in Table IX-8.

#### AVAILABILITY

The availability index was calculated as discussed earlier. It is a composite of the estimated availability of resin, reinforcement, material compounding facilities and component molding facilities (Table IX-9).

#### COSTS

Four nozzle configurations for costing (only) were documented and sent out for quotations (Haveg, HITCO, Wyatt, Kaiser, Edler, and C&D Plastics) for molding 20,000 nozzles per month for five years. Each nozzle had twelve different materials out of which it would be molded. These four nozzles and their material list are depicted in Figure IX-34 through IX-38. From the quotations of the above companies, an average costing equation was derived.

$$C_u = C_p + V \rho_m (C_H + C_s C_m)$$

where

- $C_u$  = total unit price (\$/unit)
- $C_p$  = processing cost per molding (\$/unit)
- $V$  = volume of material in net molding ( $\text{in}^3$ )
- $\rho_m$  = material density ( $\text{lb}/\text{in}^3$ )
- $C_H$  = material preparation cost (\$/lb)
- $C_s$  = scrap and overhead rate (\$/\$)
- $C_m$  = unit cost of material (\$/lb)

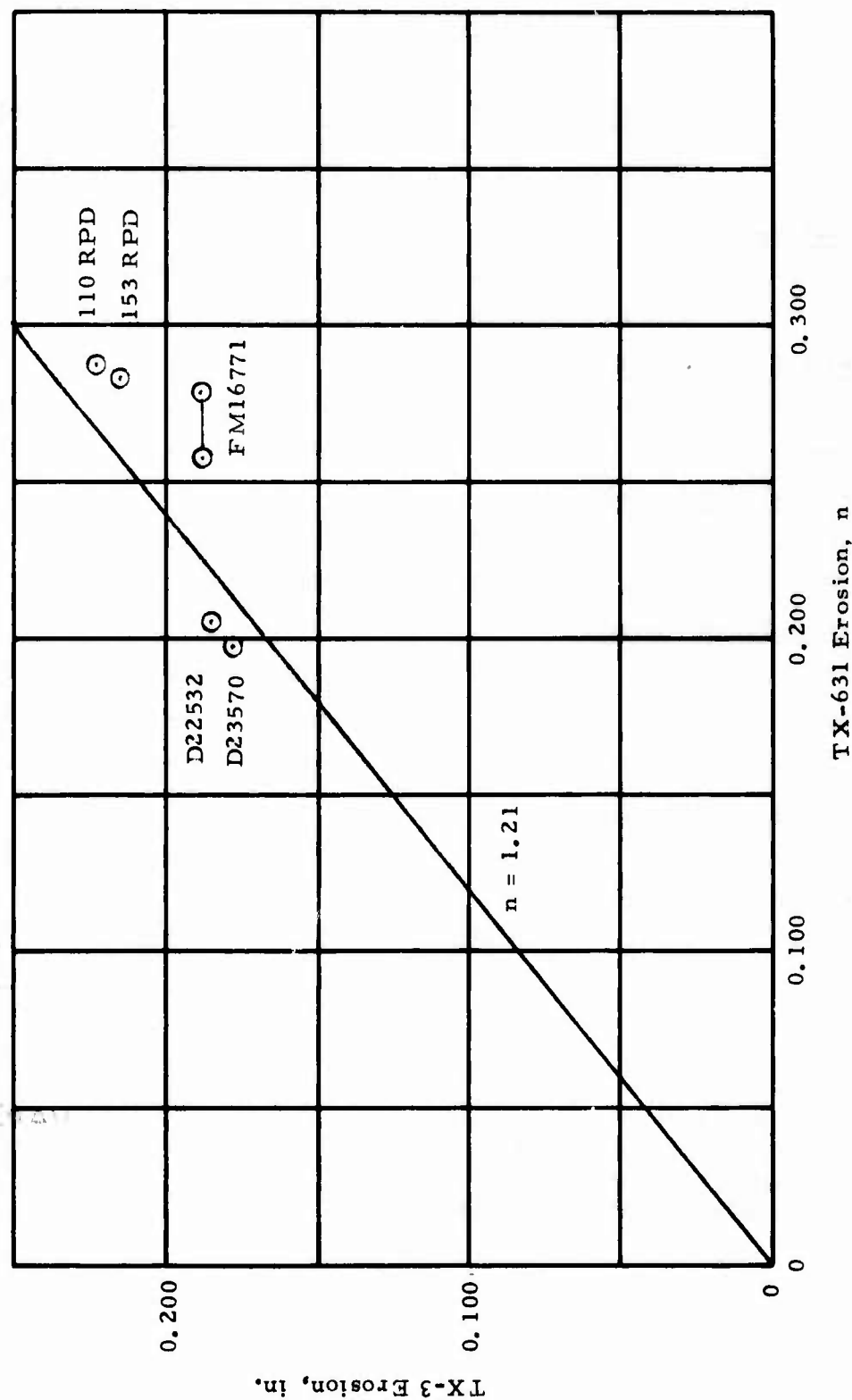


Figure IX-33. Correlation of Erosion In TX-3 and TX-631 Motors

**TABLE IX-8**  
**SUMMARY OF EROSION DATA**

<u>Throat Erosion (ΔD), in</u>		<u>(ΔD of 16771)/ΔD</u>		<u>Ablative Index of Merit<sup>a</sup></u>	
<u>TX-3</u>	<u>TX-631</u>	<u>in</u>	<u>in</u>		
<u>Tests</u>	<u>Tests</u>	<u>TX-3</u>	<u>TX-631</u>		
<u>Glass-Filled Phenolic</u>					
FM16771	0.189	0.2695 <sup>(b)</sup>	1.00	1.00	0.76
D23570	0.179	0.198	1.056	1.360	0.88
<u>Mineral-Filled Phenolic</u>					
D23639	0.265	-----	0.713	-----	0.61
D16090	0.217	-----	0.871	-----	0.70
<u>Asbestos-Filled Phenolic</u>					
153RPD	0.216	0.284	0.875	0.949	0.74
110RPD	0.224	0.288	0.844	0.936	0.73
<u>Cellulose-Filled Phenolic</u>					
D22532	0.187	0.207	1.011	1.300	0.86
R25406	0.193	(c)	0.979	-----	0.82
FM3510	0.302	-----	0.625	-----	0.55
<u>Wood Flour-Filled Phenolic</u>					
D791B	0.221	-----	0.855	-----	0.69
<u>Glass-Filled Thermoplastic</u>					
Ryton R4	-----	0.868	-----	0.310	0.30
Noryl	-----	-----	-----	-----	-----

- a. Unity is highest possible, calculated as  $\tanh [(\Delta D \text{ of FM16771})/\Delta D]$  from TX631 (if available) or TX3.  
b. Average of two tests.  
c. Motor failure unrelated to nozzle.

TABLE IX-9  
ESTIMATED PROBABILITY OF TEN-YEAR CONTINUED ECONOMICAL AVAILABILITY

	Resin Availability (a)	Reinforcement Availability	Compounding	Fabrication	Total Availability
Glass-Filled Phenolic					
FM16771	0.99	0.99	0.99	0.99	0.96
FM5042	0.99	0.98	0.98	0.99	0.94
FM5821	0.90	0.99	0.90	0.99	0.79
FM5736	0.90	0.98	0.98	0.99	0.86
4E0253	0.90	0.98	0.95 (f)	0.99	0.83
D23570	0.99	0.95	0.90 (f)	0.99	0.84
Mineral Filled Phenolic					
D23639	0.99	(c) 0.90 (c)	0.90 (f)	0.99	0.79
D16090	0.99	0.90 (c)	0.90 (f)	0.99	0.79
Asbestos Phenolic					
153RPD	0.98	(d) 0.80 (d)	0.95	0.99	0.74
110RPD	0.98	0.80 (d)	0.95	0.99	0.74
Cellulose Filled Phenolic					
D22532	0.98	(e) 0.90 (e)	0.90 (f)	0.99	0.79
R25406	0.98	0.90 (e)	0.95	0.99	0.83
FM3510	0.98	0.90 (e)	0.95	0.99	0.83
Wood-Flour Filled Phenolic					
D791B	0.98	0.99	0.99	0.99	0.95
Glass-Filled Thermoplastic					
Ryton R4	0.90 (b)	0.99	0.90 (f)	0.95	0.76
Noryl	0.95	0.99	0.95	0.99	0.88

a. Standard resins assumed to be replaceable by others.

b. Limited source and application.

c. Filler source not identified; could contain asbestos.

d. Asbestos in jeopardy because of EPA and OSHA attention to carcinogenic substance.

e. Filler source not identified; could require rayon.

f. Anticipated realignment of product line.



BEST AVAILABLE COPY

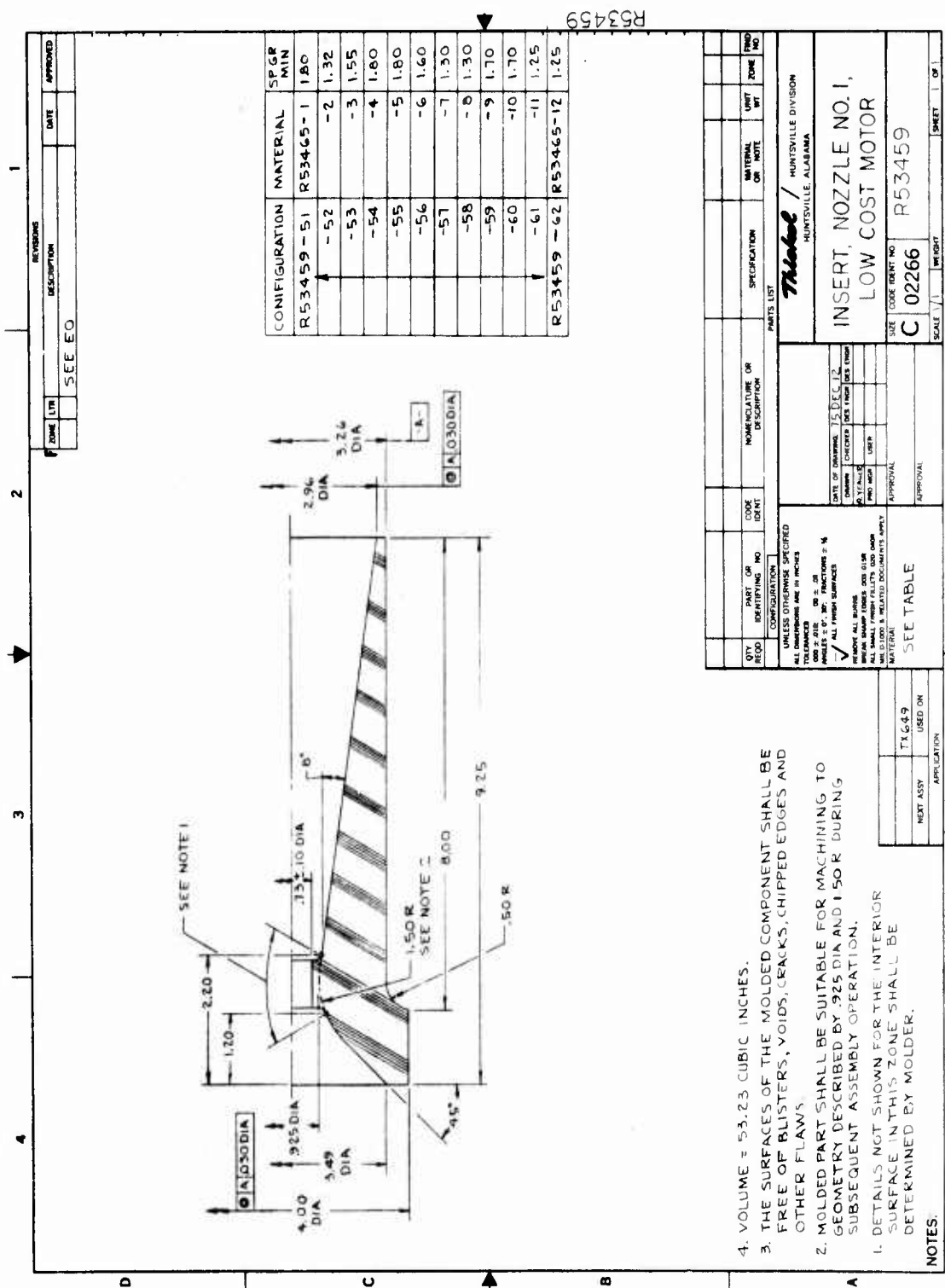


Figure IX-34. Costing Design I

BEST AVAILABLE COPY

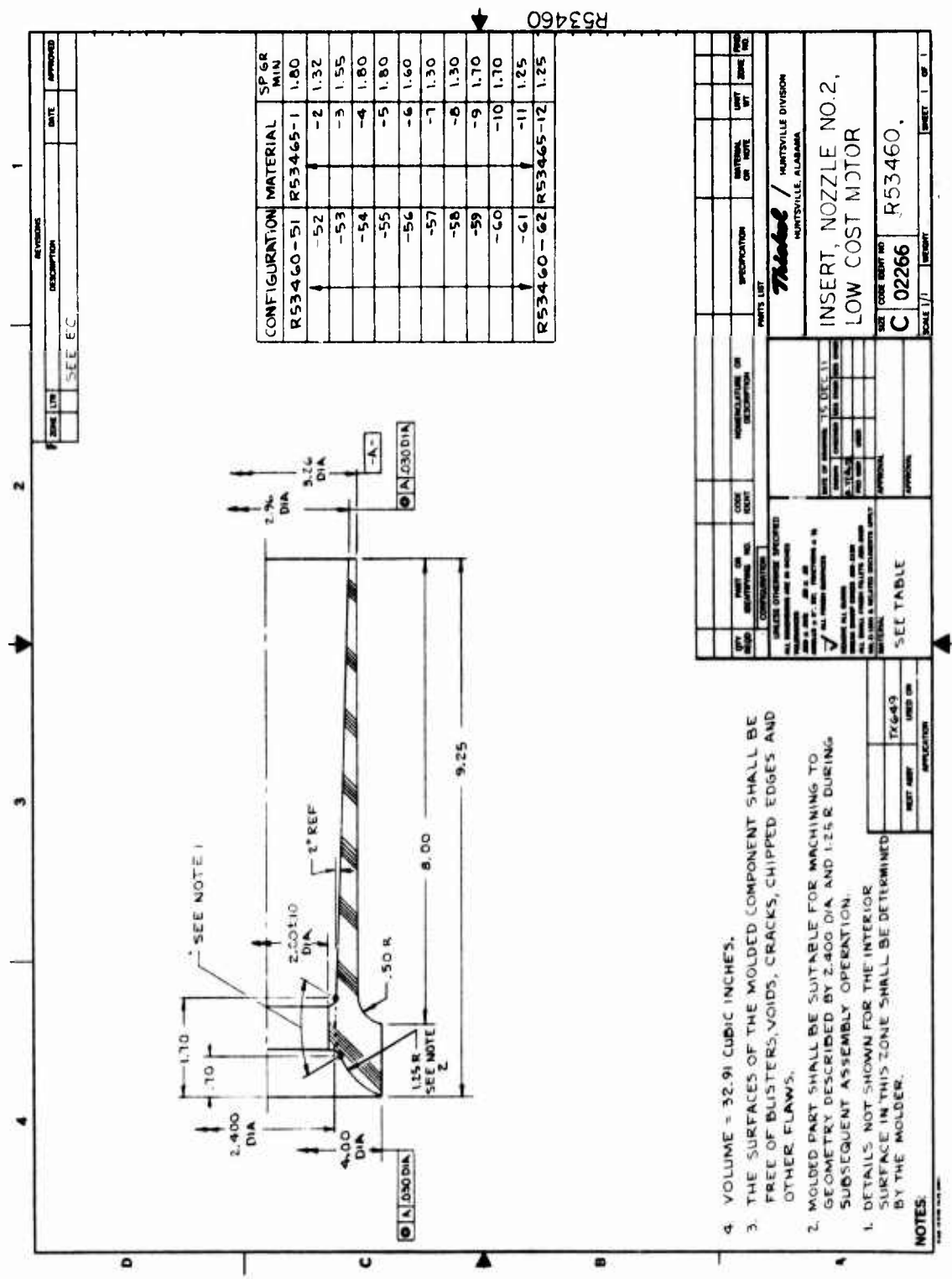


Figure IX-35. Costing Design 2

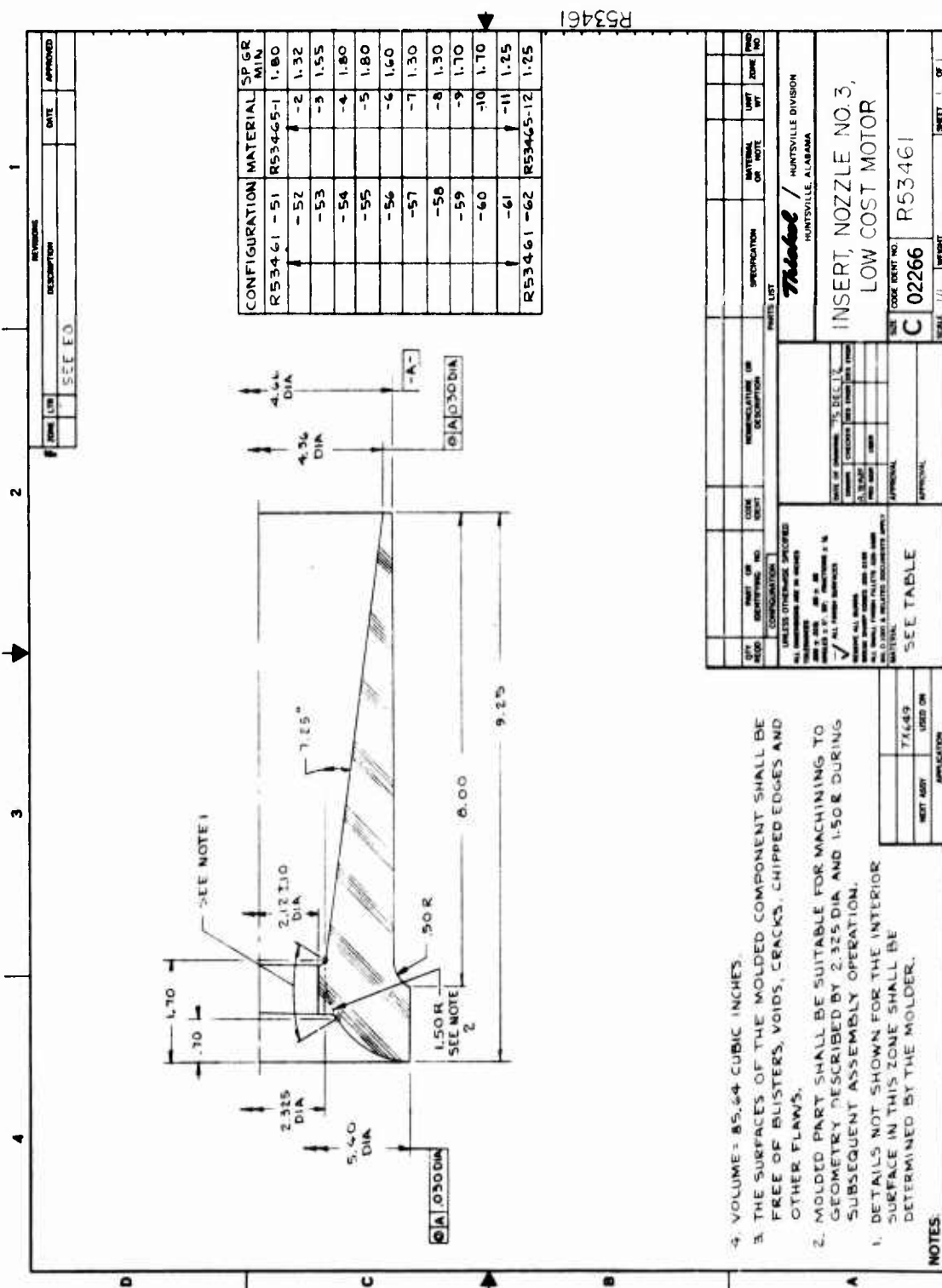


Figure IX-36. Costing Design 3

R53462



**Figure IX-37. Costing Design 4**



and where the collected data suggests the following:

$$\begin{aligned} C_p &= \begin{array}{l} 5.00 \text{ for fiber-reinforced thermosets} \\ 4.50 \text{ for filled thermosets} \\ 1.60 \text{ for injection moldable thermoplastics} \end{array} \\ C_H &= \begin{array}{l} 0.07 \text{ for thermosets} \\ 1.19 \text{ for thermoplastics} \end{array} \\ C_s &= \begin{array}{l} 1.465 \text{ for thermosets} \\ 0.527 \text{ for thermoplastics} \end{array} \end{aligned}$$

These factors are used in estimating costs of designs not specifically quoted.

Table IX-10 presents the overall cost of each nozzle configuration (9 in all) with twelve candidate materials. The cost of the compression molded plastic nozzle was based on the average of the three lowest costs from quotes or by using the cost equation if quoted information was not available. The cost of a back-up support is included where applicable.

#### SUMMARY AND CONCLUSIONS

The overall "Index of Technical Merit" for each design/material combination was calculated as the algebraic product of each of the individual indices. These are listed in Table IX-11.

The estimated costs of the various designs are plotted as a function of "Index of Technical Merit" in Figure IX-39. The characteristics of the plot reveal the typical zones of diminishing return, where increasing costs at one end reach a point where little benefit is gained, and at the other end where sacrifices in technical merit yield no significant reduction in cost. The recommended designs lie in the zone where the greatest curvature in the boundary is evident. Along this portion of the boundary, rational trade-offs exist and the final selection must be made on the basis of other factors. Design points that lie a significant distance from the boundary are generally poorer choices since each design represented by interior point is more costly than a design of comparable value and/or has less merit than one of comparable cost.

From the knee of the curve in Figure IX-39, the seven best nozzle candidates were picked, shown inside the dotted line. These are listed in order of increasing cost and merit index in Table IX-12. Four of the nozzles have a contoured exit cone which decreases cost due to less material usage, and also increases performance due to lower weight. All nozzles have an aluminum backup shell since that increased the merit index substantially.

Since this study was completed, it was learned that Durez was discontinuing their D22532 cellulose phenolic, and replacing it with a newer



**TABLE IX-10**  
**NOZZLE TOTAL COSTS(a)**

Design Code	Cost of Metal (\$)	Vol. of Insul (in <sup>3</sup> )	Overall Cost Evaluation						
			Long Straight Exit Cone	Long "Contoured" Exit Cone	Subsonic Blast Tube				
			Basic(b) 3(c)	3a(d)	1(b)	4(c)	4a(d)	2(b)	5a(d)
0	\$2.34			\$6.34	0	\$2.34	\$6.34	0	\$2.34
49.8	42.3	42.3			36.5	27.0	27.0	41.1	30.0
<b>Insulation Material</b>									
<b>Unit Costs (e)</b>									
<b>Glass-Filled Phenolic</b>									
FM-16771	12.72	13.89	17.89	10.62	11.44	15.44	11.35	11.94	15.94
D23570	12.27	13.48	17.48	10.18	11.34	15.34	10.95	11.51	15.51
FM5042	22.37	22.08	26.08	17.71	16.71	20.71	19.32	17.76	21.76
<b>Mineral-Filled Phenolic</b>									
D23639	9.80	11.42	15.42	8.47	9.86	13.86	8.95	10.19	14.19
D16090	8.83	10.49	14.49	7.57	9.06	13.06	8.03	9.31	13.31
<b>Asbestos-Filled Phenolic</b>									
153RPD	11.30	12.74	16.74	9.67	10.79	14.79	10.28	11.12	15.12
110RPD	10.53	12.01	16.01	9.02	10.27	14.27	9.57	11.62	15.62
<b>Cellulose-Filled Phenolic</b>									
D22532	8.52	10.21	14.21	7.32	8.82	12.82	7.77	9.09	13.09
R25406	8.62	10.31	14.31	7.42	8.89	12.89	7.85	9.17	13.17
FM3510	8.50	10.29	14.29	7.52	9.11	13.11	7.85	9.34	13.34
<b>Wood-Flour Filled Phenolic</b>									
D791B	7.03	8.96	12.96	6.30	8.09	12.09	6.55	8.26	12.26
<b>Glass-Filled Thermoplastic</b>									
Ryton R4	9.75	10.94	14.94	7.60	8.34	12.34	8.40	8.89	12.89

- a. Production Rate 20,000 per month for 5 years.  
b. Designs B, 1, and 2 are self-supporting.  
c. Designs 3, 4, and 5 use 0.1 inch thick aluminum back-up shells  
d. Designs 3s, 4s, and 5s use 0.1 inch thick steel back-up shells.  
e. Cost to Propulsion Contractor.

**TABLE IX-11**  
**INDEX OF TECHNICAL MERIT MATRIX**

Material	Mat'l Indices		Overall "Index of Technical Merit" (a)											
	Abl	Avail.	Long Straight Exit Cone			Long "Contour" Exit Cone				Subsonic Blast Tube				
			Basic (b)	3 (c)	3s (d)	1 (b)	4 (c)	4s (d)	2 (b)	5 (c)	5s (d)			
Glass-Filled Phenolic														
FM16771	0.76	0.96	(e)	0.30	0.37	(e)	(e)	0.30	(e)	(e)	(e)	(e)	0.69	0.40
D23570	0.88	0.84	0.56	0.74	0.74	0.49	0.71	0.74	(e)	(e)	(e)	(e)	0.69	0.40
FM5042	0.76	0.95	0.25	0.71	0.72	0.16	0.57	0.70	(e)	(e)	(e)	(e)	0.69	0.40
Mineral-Filled Phenolic														
D23639	0.61	0.79	(e)	0.44	0.45	(e)	0.17	0.39	(e)	(e)	(e)	(e)	0.69	0.40
D16090	0.70	0.79	0.03	0.54	0.54	(e)	0.37	0.52	(e)	(e)	(e)	(e)	0.69	0.40
Asbestos-Filled Phenolic														
153RPD	0.74	0.74	0.48	0.55	0.55	0.55	0.54	0.55	(e)	(e)	(e)	(e)	0.69	0.40
110RPD	0.73	0.74	0.05	0.50	0.52	0.01	0.34	0.50	(e)	(e)	(e)	(e)	0.69	0.40
Cellulose-Filled Phenolic														
D22532	0.86	0.79	0.20	0.67	0.68	0.15	0.59	0.67	(e)	(e)	(e)	(e)	0.69	0.40
R25406	0.82	0.83	0.22	0.68	0.68	0.20	0.62	0.67	(e)	(e)	(e)	(e)	0.69	0.40
FM3510	0.55	0.83	0.13	0.45	0.46	0.10	0.38	0.45	(e)	(e)	(e)	(e)	0.69	0.40
Wood-Flour Filled Phenolic														
D791B	0.69	0.95	(e)	0.64	0.65	(e)	0.49	0.63	(e)	(e)	(e)	(e)	0.69	0.40
Glass-Filled Thermoplastic														
Ryton R4	0.30	0.76	0.23	0.23	0.23	0.23	0.23	0.23	0.00	0.17	0.23	0.23	0.69	0.40
Noryl	----	0.88	----	----	----	----	----	----	(e)	----	----	----	0.69	0.40

- a. Calculated as product of (Index of Ablation) x (Index of Availability) x tanh 2 x M.S.), using structural M.S.  
b. Designs B, 1, and 2 are self supporting.  
c. Designs 3, 4, and 5 use 0.1 inch thick aluminum back-up shells.  
d. Designs 3s, 4s, and 5s use 0.1 inch thick steel back-up shells.  
e. Negative value indicates inadequacy, generally indicating need for thicker back-up tube or stronger insulation material (e.g., paper phenolic).

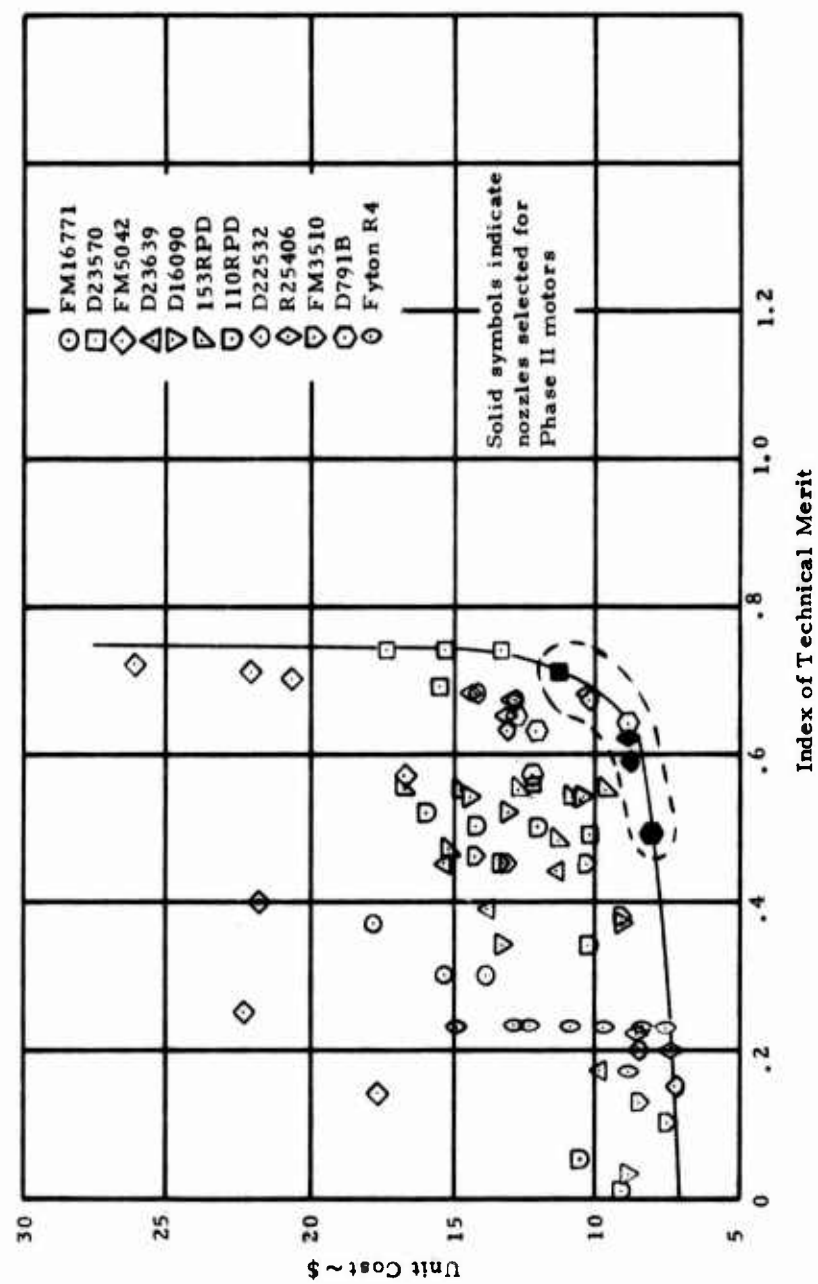


Figure IX-39. Cost Versus Index of Merit

TABLE IX-12

## RANKING OF BEST CANDIDATES

Material	Cost <sup>(a)</sup> (\$)	Merit Index	Design Number	Description of Nozzle
D791B	8.09	0.49	4	Long "Contour" Exit Cone with Aluminum Backup Shell
D22532 <sup>(b)</sup>	8.82	0.59	4	Long "Contour" Exit Cone with Aluminum Backup Shell
R25406	8.89	0.62	4	Long "Contour" Exit Cone with Aluminum Backup Shell
D791B	8.96	0.64	3	Long Straight Exit Cone with Aluminum Backup Shell
D22532 <sup>(b)</sup>	10.21	0.67	3	Long Straight Exit Cone with Aluminum Backup Shell
R25406	10.31	0.68	3	Long Straight Exit Cone with Aluminum Backup Shell
D23570	11.34	0.71	4	Long "Contour" Exit Cone with Aluminum Backup Shell

a. Cost to Propulsion Contractor; per unit; 1,200,000 units total production.

b. Delete due to discontinuation later this year.

compound called D123. Since this newer material had not been static fired, and the R25406 was very close in cost with a slightly better merit index, the D22532 was dropped from consideration and R25406 substituted.

The three materials selected for evaluation in Phase II motors were:

D791	Wood flour phenolic
D22532	Cellulose phenolic
D23570	Glass phenolic

#### VENDORS

The following vendors were contacted for technical consultation and/or budgetary price quotations during the course of the nozzle study:

C&D Plastics  
Gardena, Calif.

HITCO, Inc.  
Gardena, Calif.

Edler Industries  
Newport Beach, Calif.

Thermech Engineering  
Anaheim, Calif.

Haveg Industries  
Reinhold Aerospace Division  
Santa Fe Springs, Calif.

Wyatt Industries  
Houston, Texas

Kaiser Aerospace and Electronics  
San Leandro, Calif.

SECTION X

CASE STUDIES



## SECTION X

### CASE STUDIES

Traditionally case fabrication techniques used in rocket motor production are expensive and burdened with extensive quality control requirements. One objective of the current program is to explore alternate case fabrication techniques in an attempt to lower cost while maintaining reliability and safety. Four techniques were considered: (1) stock (i.e., mill run) tubing; (2) impact extruded; (3) wound metal laminate; (4) plastic laminate.

Results of these studies are summarized in subsequent paragraphs. Details of the work are contained in referenced appendices.

#### STOCK TUBING STUDY

##### Initial Investigation

This study was performed to investigate the feasibility of using stock tubing (steel or aluminum) for use as a case for the Low Cost motor. Results are summarized in the paragraphs below. Details of the study are in Appendix B.

Some 15 vendors (manufacturers and warehousemen) were contacted relative to tubing availability, size, type of material and costs. As a basis for cost, base price was requested and steel tubing was specified to either ASTM A513 (welded) or A519 (seamless) so that commonality existed.

Insofar as steel tubing was concerned, piping was considered but rejected due to limited size availability and relatively thick walls. A fuel transmission pipe per an American Petroleum Institute Standard was considered as promising by a Battelle study for the Missile Command. It is likely, however, that heat treating would prove a problem in conjunction with the wide composition range permitted by the API Specification. Thus, it was eliminated. Seamless tubing was also eliminated on the basis of a greater dimensional tolerance spread and since price was greater for thin walls. In addition it had somewhat lesser strength guarantees.

Consideration was given to the various types of welded tubing and subsequently drawn-over-mandrel. Type 1035 low carbon and 4130 low alloy tubings evolved as the most promising: the 1035 material based on cost, with a weight penalty, and the 4130 material on the basis of greater strength

1. Reference B-6 in Appendix B.

in a normalized condition plus the possibility of greater strengths in a heat treated condition. (1035 material cannot be heat treated to uniform strengths throughout in thick sections, only case hardened). Subsequently, a ROM cost on heat treatment of the 4130 tubing indicated it would likely be less cost competitive than the normalized tubing.

Of the various aluminum tubings screened, only the heat-treated alloys appeared usable based on required level of strength. For the thin wall material, drawn tubing, (or extruded and drawn) is required. On this basis and considering availability, alloys 2014 T6, 2024 T6 or T8, and 7075 T6 were the most feasible.

Mechanical and processing properties for the various types of steel and aluminum tubing were compared. These included corrosion and stress corrosion characteristics, tensile properties, temperature effects, fracture toughness, weldability, machinability, formability and heat treating properties. Cost and impulse performance effects were also considered.

The 1035 material stood out on the basis of cost, but it is questionable whether the weight (about 17 lbs) can be accommodated. 4130 steel tubing has greater costs associated with it but weighs less. Also, a minimum quantity of 1000 to 2000 ft would have to be ordered, limiting prototype availability to a high cost. The 2014 T6 and 2024 T8 aluminums are closely competitive, with stress corrosion considerations of importance associated with the former and weldability considerations associated with the latter. Heating may or may not be necessary for adequate forming for all of these materials.

The relatively high cost associated with heat treatment of the 4130 and the limited gain in performance appear to make its use for this particular application non-competitive. Likewise, since there was available only a .156 minimum wall thickness for the 7075 T6 tubing, its greater strength level would be non-competitive unless motor pressure is increased. That possible trade off has not been evaluated at this point. Thus both heat treated 4130 and 7075 T6 material are considered as not being cost competitive at this point in the study. This leaves 1035 and 4130 DOM tubing and 2014 T6 and 2024 T8 (or possibly T6) tubing as being the most practical ones to consider for ballistic performance effects.

#### Expanded Investigation

The initial study was based on having a material/case wall thickness combination capable of withstanding a nominal maximum operating pressure of about 3000 psia. This pressure level represented the best estimate of motor operating conditions at the time the tubing study was initiated. Subsequent performance studies indicated that motor pressure can be reduced significantly below 3000 psia. If a particular class of tubing has a minimum available wall thickness associated with it, then there is no advantage to

reducing the operating pressure below the level corresponding to the minimum available wall thickness. Therefore the data base for the stock tubing study was expanded so that the trade off between cost and pressure level could be made. The basic findings of the initial study are still valid and the expanded effort was limited to the six materials carried into final considerations (steel 1025, 1035 and 4130; aluminums 2014, 2024, and 7075) and two others.

As ballistic performance calculations do not result in a single "final design", no really definite conclusion can be reached in this supplemental study insofar as a firm recommendation is concerned. However, the expanded study does indicate that if ballistic calculations indicate low pressure or performance values such that a heavier wall case is acceptable, then 6061 T6 aluminum could prove an attractive tubing material for case use. It has excellent corrosion resistance, weldability and formability and acceptable fracture toughness although its machinability is less than ideal. In addition, it is cheaper than alternative aluminum alloys. Its use should be seriously considered for  $P_{\max}$  at 70°F values of up to about 2450 psi.

Another possible alternative material, 5052 H36 aluminum, was briefly considered--mainly to include a non-heat treatable alloy in the study. Prior efforts had not considered it because of the strength limitations. Although its tensile properties were equal to 6061 T6 aluminum, pricing considerations prevented its subsequent consideration when they were compared with 6061 T6.

#### Summary of Tubing Characteristics

Characteristics and properties discussed in detail in Appendix B are presented here for a direct comparison of the different steel and aluminum alloys.

Tensile properties for steel tubing are in Table X-1. Those for aluminum tubing are contained in Table X-2 and compared with properties of the selected steel tubing.

Tolerances of the various steel tubings are listed in Table X-3 and Table X-4 has tolerances for drawn aluminum tubing.

Advantages and disadvantages of the selected tubings are given in Table X-5

#### IMPACT EXTRUDED CASE STUDY

Properties of several aluminum alloys were reviewed to determine which would be most suitable for use in impact extrusions. Five were selected for further consideration (Table X-6 ). The tensile values are the minimum property limits for the alloys in the indicated temper per MIL

TABLE X-1  
TENSILE PROPERTIES FOR STEEL TUBING

I. SEAMLESS MECHANICAL TUBING<sup>(a)</sup>

<u>Material</u>	<u>Ult. Tens. Str. (psi)</u>	<u>Strength (psi)</u>	<u>Elongation in 2 in. (%)</u>
Hot Rolled			
1025	55,000	35,000	25
1035	65,000	40,000	20
Cold Worked			
1025	75,000	65,000	5
1035	85,000	75,000	5

II. ELECTRIC RESISTANCE WELDED  
CARBON AND ALLOY STEEL  
MECHANICAL TUBING<sup>(b)</sup>

As Welded			
1025	56,000	40,000	12
1030	62,000	45,000	10
1035	66,000	50,000	10
Welded and Mandrel Drawn (DOM)			
1025	75,000	65,000	5
1025(c)	85,000	78,000	8
1030	85,000	75,000	5
1035	90,000	80,000	5
4130N	105,000	85,000	10

a. Per ASTM A519-71 - values given as "typical."

b. Per ASTM A513-70 - values specified as minimum (except for 1026 as noted).

c. Values "Typical Minimum" per Ohio Steel Tube Co., Shelby, Ohio.

TABLE X-2  
TENSILE PROPERTIES  
(Room Temperature)

<u>Material</u>	<u>Ultimate Tensile Strength (psi)</u>	<u>Tensile Yield Strength (psi)</u>	<u>Hardness R<sub>b</sub> Minimum</u>	<u>Elongation % in 2 in.</u>
<b>Steel Tubing (Mandrel Drawn)</b>				
AISI 1025 <sup>(a)</sup>	75,000 (70,000) <sup>(f)</sup>	65,000 (60,000)	82 (77)	5 (10)
AISI 1035 <sup>(a)</sup>	90,000 (85,000)	80,000 (75,000)	90 (85)	5 (10)
AISI 4130 <sup>(b)</sup> (N)	103,000	93,000		
(H. T.)	150,000	132,000		
<b>Aluminum Tubing (Drawn Tube)</b>				
2014 T6 <sup>(c)</sup>	65,000	55,000		7
2024 T8 <sup>(d)</sup>	66,000	58,000		5
7075 T6 <sup>(c)</sup>	77,000	66,000		7
T73 <sup>(e)</sup>	66,000	56,000		

a. Minimum values per ASTM A513-70.

b. Cyro - Tec, Inc., Huntsville, Alabama.

c. Minimum values per "Aluminum Standards & Data" - The Aluminum Association.

d. Minimum values per "Alcoa Aluminum Tubular Products" Section AE2A-1.

e. Minimum values per WW-T-700/7A.

f. Values in Parentheses for stress relieved tubing.

TABLE X-3  
TOLERANCE COMPARISON FOR 4-INCH OUTSIDE  
DIAMETER TUBING (a), (b)

A. SEAMLESS MECHANICAL TUBING

Hot Finished

<u>Outside Diameter</u>	<u>Wall Thicknesses</u>
$\pm .031$	$\pm 14$ to $15\%$ depending on thickness or $\pm .018$ to $\pm .025$ (over applicable range thicknesses)

Cold Worked (Unannealed or finish annealed)

<u>Outside Diameter</u>	<u>Inside Diameter</u>	<u>Wall Thickness</u>
$+ .015$	$+ .005$	$\pm 10\%$ or $\pm .012$ to
$- .000$	$- .015$	$\pm .018$ over applicable range of thicknesses

B. ELECTRIC-RESISTANCE-WELDED CARBON AND ALLOY  
STEEL MECHANICAL TUBING (c)

As Welded from Hot Rolled Steel  
(Flash Controlled to .010" max.) (d)

<u>Outside Diameter</u>	<u>Wall Thickness</u>
$\pm .190$	$+ .005$ $+ .010$ to $- .012$ $- .020$

As Welded from Cold Rolled Steel  
(Flash Controlled to .010" max.) (d)

<u>Outside Diameter</u>	<u>Wall Thickness</u>
$\pm .010$	$+ .003$ $- .007$

Mandrel Drawn (or Drawn over mandrel-DOM) (b)

<u>Outside Diameter</u>	<u>Inside Diameter</u>	<u>Wall Thickness</u>
$\pm .006$	$\pm .006$	$\pm .005$ over applicable range of thicknesses

- 
- a. Per ASTM A-519-71.
  - b. Where all three dimensional tolerances are given, only two of the dimensions can be specified for ordering purposes.
  - c. Per ASTM A513-70.
  - d. Flash controlled to 0.010 in. max. normally produced to outside diameter and wall thickness tolerances.



TABLE X-4

TOLERANCES FOR DRAWN

ALUMINUM TUBING (a), (b), (c)

DIAMETER (INSIDE OR OUTSIDE)

<u>Definition</u>	<u>Interpretation</u>	<u>Value (inch)</u>
Allowable deviation between mean and specified diameter	Average diameter	$\pm 0.008$
Allowable deviation of diameter at any point from specified diameter	Ovalness	$\pm 0.016$

WALL THICKNESS

Allowable deviation between mean and specified wall thickness	Average thickness	$\pm 0.006$
Allowable deviation of wall thickness at any point from specified wall thickness	Eccentricity	$\pm 10\%$ of specified thickness

BOW 0.010 per ft

- 
- a. Aluminum Standards and Data, The Aluminum Association, 420 Lexington Ave., NYC, 1969.
  - b. Outside diameter of 4 inches; wall thickness of 0.121 to 0.203 inch.
  - c. Can specify only two of the three (ID, OD, wall).

TABLE X-5

SUMMARY OF ADVANTAGES  
AND DISADVANTAGES  
SELECTED STOCK TUBINGS

<u>Material</u>	<u>Advantages</u>	<u>Disadvantages</u>
1035	<ol style="list-style-type: none"> <li>1. Inexpensive</li> <li>2. Readily available</li> <li>3. Weldable</li> <li>4. Machinability good</li> <li>5. Reasonable formable depending on degree and process</li> </ol>	<ol style="list-style-type: none"> <li>1. Heavier wall required</li> <li>2. Nil ductility. Transition temperature may be limiting factor.</li> <li>3. More susceptible to general corrosion (requires good corrosion protection)</li> </ol>
4130	<ol style="list-style-type: none"> <li>1. Highest strength (thin wall)</li> <li>2. Fairly good corrosion resistance when protected by coating</li> <li>3. Weldability and machinability should be good</li> <li>4. Fracture toughness high</li> <li>5. Could be heat treated if necessary</li> </ol>	<ol style="list-style-type: none"> <li>1. Higher cost than 1035</li> <li>2. limited availability--(minimum order 4000 to 8000 lb range or 1000 to 2000 ft)</li> <li>3. Better low temperature properties than 1035</li> <li>4. Forming may be a problem</li> </ol>
2024	<ol style="list-style-type: none"> <li>1. Lightest weight</li> <li>2. Good general corrosion resistance and stress corrosion resistance in T6 or T8 tempers</li> <li>3. Low temperature capabilities good</li> <li>4. Fracture-toughness poorer than steel, but probably adequate</li> </ol>	<ol style="list-style-type: none"> <li>1. High cost</li> <li>2. May be difficult to form--requiring heating and time limits to achieve</li> <li>3. Resistance weldable only is practical</li> <li>4. High temperature capabilities limited</li> <li>5. Allowable tolerances of standard tubing are greater than those of DOM Steel Tubing</li> </ol>
2014	<ol style="list-style-type: none"> <li>1. Light Weight</li> <li>2. Good general corrosion resistance</li> <li>3. May be fusion welded (as compared to 2024)</li> </ol>	<ol style="list-style-type: none"> <li>1. High cost (lower than 2024)</li> <li>2. May be difficult to form--requiring heating and time limits to achieve</li> <li>3. Susceptible to stress corrosion cracking in T3, T4, T6 conditions</li> </ol>

(Continued on next page)

TABLE X-5. (Continued).

<u>Material</u>	<u>Advantages</u>	<u>Disadvantages</u>
2014 (contd.)	4. Low temperature capabilities good 5. Fracture toughness poorer than steel but probably adequate	4. High temperature capabilities limited 5. Allowable tolerances of standard tubing are greater than those of DOM Steel Tubing

TABLE X-6

## ALLOYS FOR IMPACT EXTRUDED CASES

Alloy	F <sub>tu</sub> <sup>(a)</sup> (ksi)		F <sub>ty</sub> <sup>(a)</sup> (ksi)		Elong. <sup>(a)</sup> (%)		Wall Thick. <sup>(b)</sup> (in.)		Case Length <sup>(c)</sup> (in.)		Case Wt. <sup>(d)</sup> (lb.)		Wt. Increase <sup>(e)</sup> (%)	
	L	LT	L	LT	L	LT	L	LT	L	LT	L	LT	L	LT
7075-T6	78	76	70	66	7	5	.115		44.75		6.16		---	
7075-T73	68	65	58	55	7	--	.134		45.66		7.28		18.3	
2024-T81	64	64	56	55	4	--	.136		45.76		7.56		22.7	
2014-T6	60	60	53	49	7	5	.145		46.21		8.20		33.2	
2024-T4	57	54	42	37	12	--	.162		47.07		9.19		49.4	

a. MIL - Handbook - 5B.

b. Minimum wall thickness based on burst pressure of 4375 psi and F<sub>tu</sub> in LT direction.

c. Case length to yield constant volume in case (500 cu. in.).

d. Weight of case exclusive of end closure and forward skirt.

e. Weight increase over 7075 - T6 case.

Handbook 5B. The wall thicknesses required to meet a minimum burst pressure of 4375 psi were calculated using the ultimate tensile strength in the LT or hoop direction. The case length and case weight were determined to give a constant volume of 500 in<sup>3</sup> in the case. However, the weight of the end closure and forward skirt were neglected since this will be essentially constant for each alloy. The percent weight increase was determined over the 7075-T6 baseline case.

Some factors considered in selection of the alloys and tempers for the impacted extruded case are as follows:

(a) Alloy 7075 in the T6 temper will yield the lowest weight case but is the most difficult to extrude and will have the poorest tolerances and surface finish in the as-extruded condition. Relative extrusion pressure is 2.3 for 7075 compared to 1.8 for 2XXX series alloys (Alloy 1100 = 1.0).

Wall thickness tolerances obtainable are approximately  $\pm .010$  to  $\pm .015$  in. as-extruded. The cost of an impact extruded case will probably be 1.5 to 1.7 times the cost of 2014 or 2024 cases, respectively, based on relative costs of extruded tubing. Alloy 7075 has relatively poor stress corrosion in the T6 temper but it can be improved by heat treating to the T73 temper. This will result in an 18% weight increase and about 10% cost increase. The properties of 7075 cannot be improved by cold working after extrusion and any sizing to improve tolerances would have to be performed in the annealed temper (O) or the solution heat treated temper (W).

(b) Alloy 2024 is typically specified in extrusions in the T4 and T81 tempers, among others. The T4 temper results from natural aging after solution heat treating. Temper T81 is produced by cold working after the solution heat treat and then artificial aging, resulting in both improved strength and resistance to stress corrosion. The cold working can be done in conjunction with any sizing operation to improve the tolerance of the case. However, because of the rapid natural aging of 2024, cold working has to be done within about two hours of solution heat treating or else the extrusion must be refrigerated. Wall thickness tolerances of about  $\pm .005$  to  $\pm .010$  can be obtained in the as-extruded condition. The cost differential between the T4 and T81 tempers will probably be 15 to 20% because of the additional working and heat treatment involved for T81.

(c) Alloy 2014-T6, produced by solution heat treating and artificial aging the extrusion, will probably result in the lowest overall cost for the impact extruded case, based on costs obtained for extruded tube and fabrication experience of the 2.75" rocket. However, the case weight will be approximately 33% greater than a case of 7075-T6. Extrusion characteristics and tolerances that can be obtained are comparable to those of 2024.

Two cases were then designed with 7075-T6 as impact extrusions. One (Thiokol drawing R53148) features an integral forward closure and forward skirt (Figure X-1 ). Propellant would be loaded into this case from the aft end; then a separate nozzle would be attached to the case with the selected joining technique. The second case (Thiokol drawing R53152) has an integral nozzle support shell (Figure X-2 ). Propellant would be loaded into this case from the forward end after first installing the nozzle ablative liner. Then a forward closure would be joined to the case.

A sub-contract was given to Norris Industries, Vernon Special Military Products Division, Los Angeles, California to perform an engineering analysis to determine the lowest cost method to impact extrude case described on the aforementioned drawings. These drawings were also to be evaluated to identify means of reducing the final cost. Materials to be considered were those listed in Table X-1 . However, Norris Industries chose not to include the two 2024 alloys for the following reasons.

- (1) Alloy 2024-T81 was considered a special condition for plate materials which develops properties which probably are not uniformly achievable in an extruded rocket motor case.
- (2) Alloy 2024 is not as readily worked as Alloy 2014, is more expensive than 2014, and has lower mechanical properties than 2014. Thus it offers no advantages which justified further consideration.

Details of the Norris Industries study are continued in the following paragraphs.

#### Summary and Conclusions

The original Scope of Work was divided into eight tasks.

1. Review original drawings.
2. Select general methods of manufacture for each individual part.
3. Perform detailed analysis of the production feasibility of each part through every phase of the operational sequences.
4. Establish inspection procedures and requirements necessary to insure final part acceptance.
5. Outline required part modifications or final product specifications.
6. Finalize operational sequences.
7. Provide modified final product drawings.
8. Produce a final report.

Each motor case, with its three alternate materials or material conditions, was subjected to the above procedure. Upon completion of this analysis, the following conclusion was reached.



BEST AVAILABLE COPY

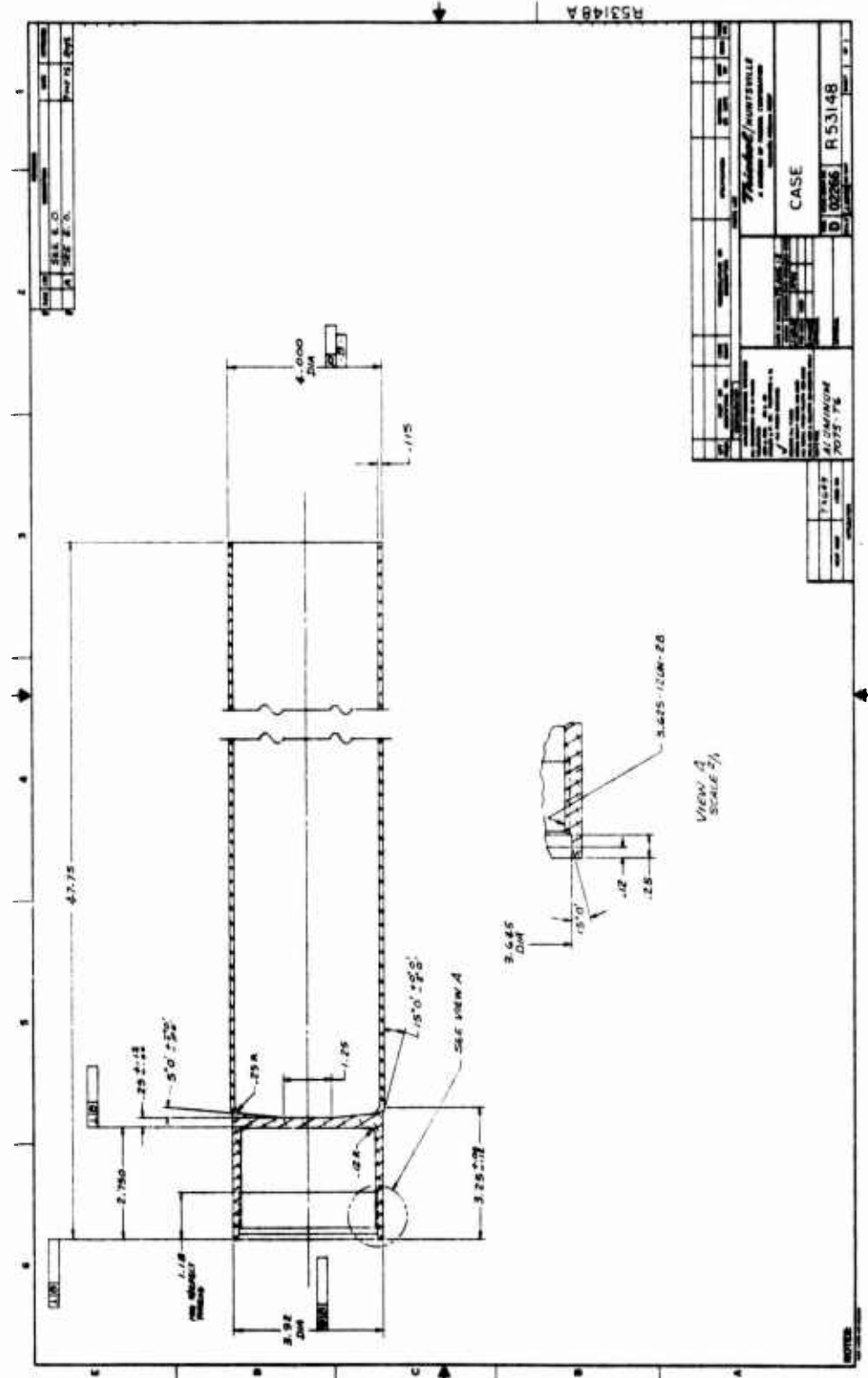


Figure X-1. Integral Forward Closure Impact Extruded Case

BEST AVAILABLE COPY

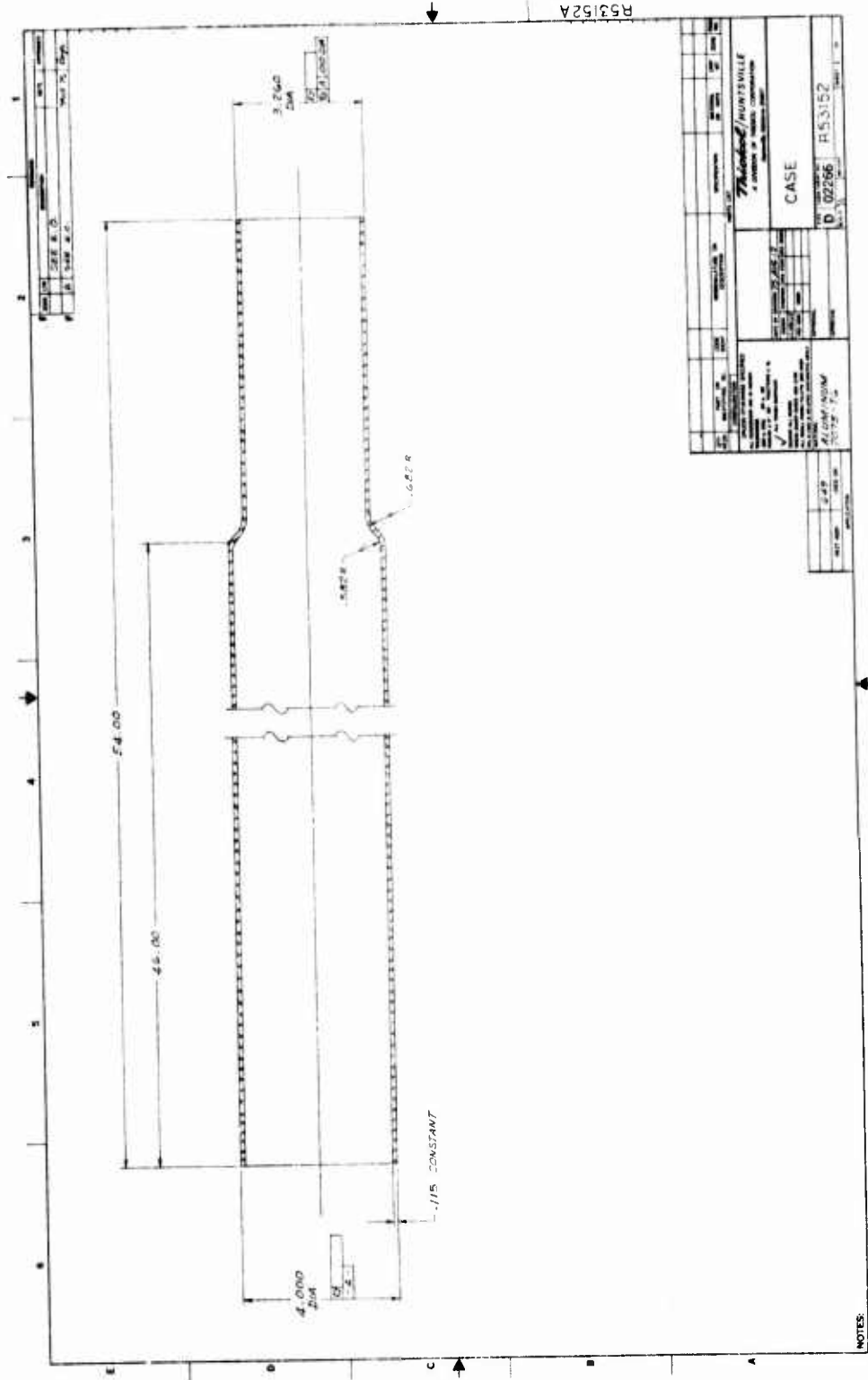


Figure X-2. Integral Nozzle Support For Impact Extruded Case

The most economical method of manufacturing an impact extruded aluminum rocket motor case similar to Thiokol Part Number R53148 or R53152 would be to produce the cases from 2014 aluminum alloy, process the parts through the operational sequence outlined, solution heat treat and age to the T-6 condition.

#### Integral Forward Closure (R53148)

The following steps will be required to manufacture the case with integral forward closure:

1. Purchase Material and Inspect
2. Oil and Upset
3. Anneal
4. Apply Solid Film Lubricant
5. Extrude
6. Pre-Iron
7. Machine Forward Section and Timing Shoulder
8. Anneal
9. Apply Lubricant
10. 1st Iron
11. Anneal
12. Apply Lubricant
13. 2nd Iron
14. Clean
15. Solution Heat Treat and Quench
16. Apply Lubricant
17. Final Iron
18. Salvage Straighten if Necessary
19. Age
20. Bore, Face Bulkhead, Counterbore and Thread
21. Trim Overall Length
22. Final Inspect
23. Surface Preparation
24. Pack and Ship

Norris drawing P703 (Figure X-3 ) was prepared to show changes recommended to improve producibility, to reduce costs and to show attainable tolerances. A summary of the recommendations for R53148 are as follows:

1. The internal and external surface finishes should be 125 RMS maximum, except as noted on Norris Drawing P-703 (Figure X-3 ).
2. The sidewall thickness in the 4.000 inch diameter area on the rocket motor case made of 2014 material could be reduced approximately 10%. This reduction of wall thickness can be obtained by advantage of the 2014 material response characteristic to cold working in the solution heat treated condition. By adding cold work

BEST AVAILABLE COPY

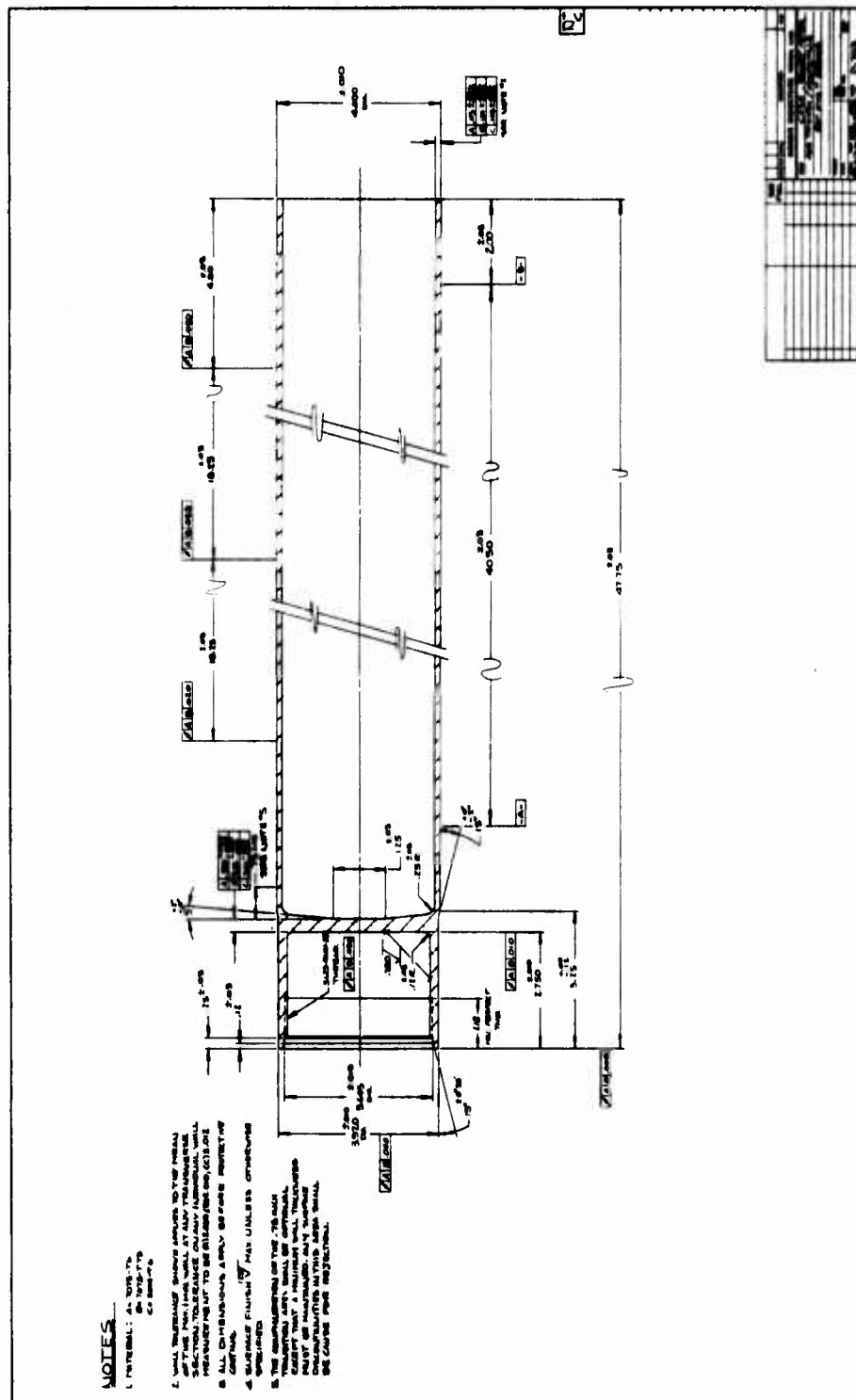


**Figure X-3. Modified Design of Integral Forward Closure**

into the part at this point, an increase of wall strength amounting to at least 10% is realized. This increase can be converted into a reduction of wall thickness and overall product material content.

3. The integral bulkhead thickness should be increased from 17% to 26% (depending on the material and heat treat level selected). Calculations performed during the evaluation show that if the present bulkhead thickness is maintained, possible deflection or failure could occur. An increase in bulkhead thickness would insure product integrity under hydrotest and firing pressures.<sup>1</sup>
4. The bulkhead thickness tolerance could be reduced from the present  $\pm .120 / - .000$  to  $\pm .050 / - .000$  without affecting the product cost or producibility.
5. All runout, bow and perpendicularity requirements should be measured in relationship to the external 4.000 inch body diameter. The means to establish this relationship would be to locate the rocket motor case horizontally on rollers spaced approximately 40.50 inches apart on the 4.000 inch body diameter. Then all dimensions would be checked relative to this longitudinal axis.
6. The internal 3.625-12 UN-2B thread should have a runout requirement measured in relationship to the external 4.00 inch body diameter. If inspected in this manner, the means of attaching mating parts will be checked and insure final assembly with less total product runout.

Raw material requirements are

7075 T6	8.8 lbs.
7075 T73	9.8 lbs.
2014 T6	10.5 lbs.

#### Integral Nozzle Shell (R53152)

The following steps will be required to manufacture the case with integral nozzle shell.

1. Purchase Material and Inspect
2. Oil and Upset
3. Anneal
4. Apply Solid Film Lubricant
5. Backward Extrude
6. Anneal
7. Machine Bulkhead, Timing Shoulder and Trim Overall Length

---

1. Design ultimate pressure = 4500 psi

8. Apply Lubricant
9. Forward Extrude
10. Trim Open End
11. Anneal
12. Apply Lubricant
13. Reduce Bulkhead End
14. Clean
15. Solution Heat Treat and Quench
16. Apply Lubricant
17. Final Body and Expand Bulkhead End
18. Salvage Straighten if Necessary
19. Age
20. Remove Bulkhead
21. Trim to Final Length
22. Final Inspect
23. Surface Preparation
24. Pack and Ship

Norris drawing P704 (Figure X-4 ) was prepared to show changes recommended to improve producibility, to reduce costs and to show attainable tolerances. A summary of the recommendations for R53152 are as follows:

1. The internal and external surface finishes should be 125 RMS maximum.
2. The sidewall thickness in the 3,260 diameter area should be allowed to be 15-20% thicker than the sidewall thickness in the 4,000 diameter area. This would eliminate one operation (thining the wall to the size now required). This recommendation is not on the Norris Drawing or included in the estimates.
3. The sidewall transition area between the 4,000 inch diameter and the 3,260 inch diameter must be 15-20% thicker than the 4,000 inch diameter final wall thickness as there is no practical method of maintaining a constant thin wall uniformly in this area.
4. The sidewall thickness in the 4,000 inch diameter area on the rocket motor case made of 2014 material could be reduced approximately 10%. This reduction of wall thickness can be obtained by taking advantage of the 2014 material response characteristic to cold working in the solution heat treated condition. By adding cold work into the part at this point, an increase of wall strength amounting to at least 10% is realized. This increase can be converted into a reduction of wall thickness and overall product material content.
5. All runout, bow and perpendicularity requirements should be



BEST AVAILABLE COPY

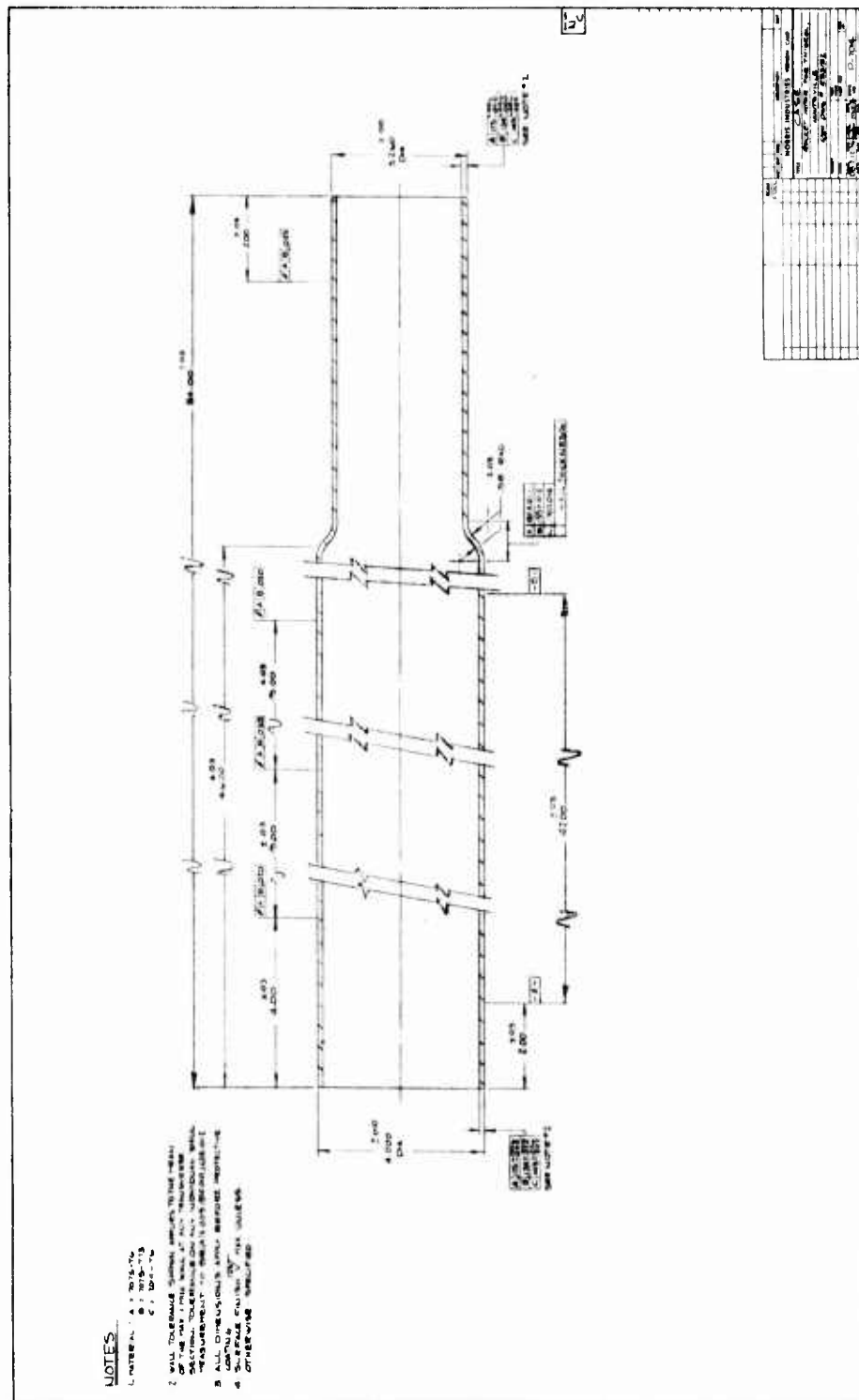


Figure X-4. Modified Design of Integral Nozzle Shell Case

measured in relationship to the external 4.000 inch body diameter. The means to establish this relationship would be to locate the rocket motor case horizontally on rollers spaced approximately 42.00 inches apart on the 4.000 inch body diameter. Then all dimensions would be checked relative to this longitudinal axis.

Raw material requirements are:

7075 T6	10.0 lb.
7075 T73	11.1 lb.
2014 T6	11.7 lb.

#### WOUND METAL/PLASTIC LAMINATE CASE

New and significant improvements in strength-to-weight ratios have been achieved by the use of fiber and metal laminates to fabricate pressure vessels. Cost and technical information were examined so these approaches could be included in the final cost/performance comparison. It was determined that the cost of a limited number of units prohibited experimental evaluation in this current program, so, with AFRPL approval, it was decided to include them only in the analytical evaluation. Both plastic fiber and metal laminate cases have been extensively manufactured for pressures similar to those expected for the subject four-inch motors. Attachment of end closures were adaptable to the approaches being examined herein. Thus it is reasonable to consider the basic case fabrication techniques to be state-of-the-art.

#### Wound Metal Cases

Work has been conducted on wound metal cases (also known as "strip laminate" cases) since the mid-1950s at Thiokol/Huntsville, Aerojet and Hercules (ABL). The latter effort resulted in operational capability to fabricate cases of ultra-high strength maraging steel strips, as a licensee of Imperial Metals Industries, England, who originally developed the process. Cost and technical information was requested from both ABL and Imperial Metals.

Close tolerances can be held without increase in costs because of automated construction and use of high-accuracy tooling. On 49 samples of a 23.6 inch diameter case the maximum out-of-squareness for the case end was 0.014 inch while the mean value was about 0.006 inch (Reference III-1). On a sample of 45 cases of 5.2 inches diameter, the combined bow and ovality was rarely over 0.01% of the length (which was 44.3 inches). No data was available on inside diameter tolerance. However, it was assumed to be relatively small and suitable for bonding end closures or nozzles directly into the wound tube since this is the basic fabrication technique itself for the IMI/Hercules process.

Behavior of the laminate under cyclic pressure load is satisfactory (Reference X - 1), although this characteristic is not too critical to a one-time-use rocket motor. The case resin can withstand cyclic environmental conditions of temperature (58°F to 166°F) and relative humidity (60 to 90%). High temperature resins are available for applications where aerodynamic heating may be a factor.

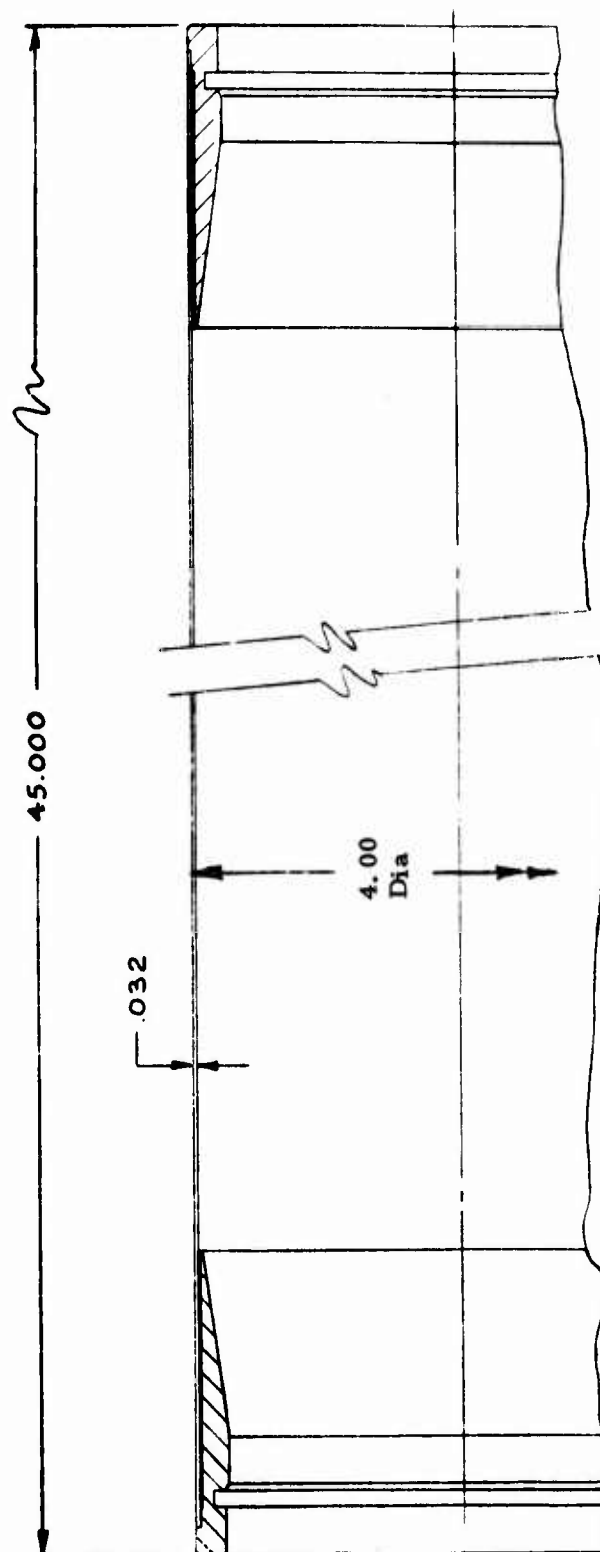
A sketch of a 4-inch diameter, 45-inch long case was supplied by Hercules, along with weight and ROM cost data (Figure X - 5). The costs included the bonded end rings as shown.

#### Plastic Laminate Case

Filament wound cases have been used for several years because of attractive physical properties (Table X- 7 ). Absolute ultimate strength of E-glass in epoxy resin is better than the best of the aluminum materials (7075-T6) and the non-heat treatable steels (AISI 1035). In terms of strength-to-density ratio the filament case surpasses even the heat treated 413X series of steel. Until recently filament wound cases have been so expensive to manufacture that this use was reserved for ultra high performance systems. However, it is now possible to obtain small pressure vessels with integrally wrapped forward closures or nozzles that are very cost competitive with more traditional case fabrication techniques.

The nature of the technical risks associated with FWC must be scrutinized against a detail system specification. Because of the following technical concerns, the FWC were examined as a separate class:

1. Assurance of an acceptable factor of safety and known reliability for safe life design of a man rated, mission critical, or equipment-cost-critical system depends on
  - a. NDI (non-destructive inspection) methods which cannot quantitatively assess initial and cumulative flaw damage.
  - b. A proof test factor selection which is limited since case integrity is degraded an unknown amount under proof loading, and since yield and ultimate of FWC nearly coincide.
  - c. Environmental effects of moisture, heat, UV radiation and fungus which must be avoided by protecting the round with a container or environmental controls.



Design Data	
Part	Weight
Steel Tube	5.0 lb
Steel End Rings	1.5 lb
Total	6.5 lb
Burst Pressure	
4500 psi	

Unit Cost \$27  
20,000 per month  
for 5 years

Figure X-5. Strip Laminate Case Assembly

TABLE X-7

## DESIGN MECHANICAL PROPERTIES OF SEVERAL CASE MATERIALS

Material	Method of Fabrication	F <sub>tu</sub> (ksi)	F <sub>ty</sub> (ksi)	E (psi x 10 <sup>6</sup> )	Specific Strength (in x 10 <sup>3</sup> )	Specific Stiffness (in x 10 <sup>6</sup> )	ρ (lb/in <sup>3</sup> )
4132 Steel	Forge, draw, spin, upset	180	163	29.0	576	102	0.283
7075-T6 Alum.	Impact extrude, upset	78	68	10.4	673	103	0.101
2014-T6 Alum.	Impact extrude, upset	62	53	10.8	541	110	0.098
6XXX-T6 Alum.	Impact extrude, weld	41	35	11.0	357	112	0.098
E-Glass/Epoxy	Filament wound	109	---	4.8 - 5.4	1 380	~ 65	0.079
1035 Steel	DOM tubing	90	80	29	318	102	0.283

2. Bending and torsion loads can induce undesirable propellant strains because the modulus of an E-glass-epoxide is 1/6 that of steel and 1/2 that of aluminum.
3. Since case wall thickness is higher than some steels, FWC may not be suitable for a volume limited design.

Several materials and manufacturing methods were examined (Figure X- 6). The filamentary materials included S-glass, E-glass, both aerospace and commercial grades of the polyaramids ("KEVLAR 49 and 29") and miscellaneous hybrids of these and boron and graphite. The matrix material were largely epoxides since polyimides and polyphenylquinoxylene are still too costly and difficult to process. The fabrication techniques screened were filament winding with and without layup of broad goods, and braiding. K-glass, a commercial form of E-glass, in an epoxide anhydride matrix built up by filament winding showed the best cost advantage and lowest development risk. Progress of the newer braided composite technology bears engineering surveillance for future applications.

The basis of engineering cost estimates was an early 1976 design and cost quote on a similar system. All data were scaled from the quoted lot size (160, 000 units) and case dimensions (8" diameter, 70" length, 0.133" thickness) from one reputable case fabricator.

In order to capitalize on the capability features of filament winding two designs are proposed for the subject application (Figure X- 7 ). Both incorporate a pinned closure joint (for either the forward closure or the nozzle). The case holes are wound around mandrel pins with continuous filaments for optimum strength and longitudinal integrity. Both include a skirt stub for payload attachment. Data for the integrally wound headend style (Figure X- 7 ) do not include nozzle, pins, or assembly costs (which should be about the same for any case). The predicted unit cost in lots > 160,000 units would range from 55% to 70% of the cost of an integral head impact extruded aluminum case.

The integrally wound case cylinder-nozzle style (Figure X- 7 ) was costed with an aluminum forward closure designed for strain compatibility with the FWC cylinder wall. The predicted unit costs in lots > 160,000 units range from 80% to 120% of the cost of the integral head impact extruded aluminum case alone (without nozzle). Thus it is apparent that filament wound composite cases are very competitive in costs and on physical properties (except for stiffness). There are certain reservations about its use in a severe field environments and on the matters mentioned above. The filament wound composite case:

- o Requires system technical risk assessment
- o Exhibits obvious cost effectivity



Unidirectional Composite Tensile Stress/Strain Curves

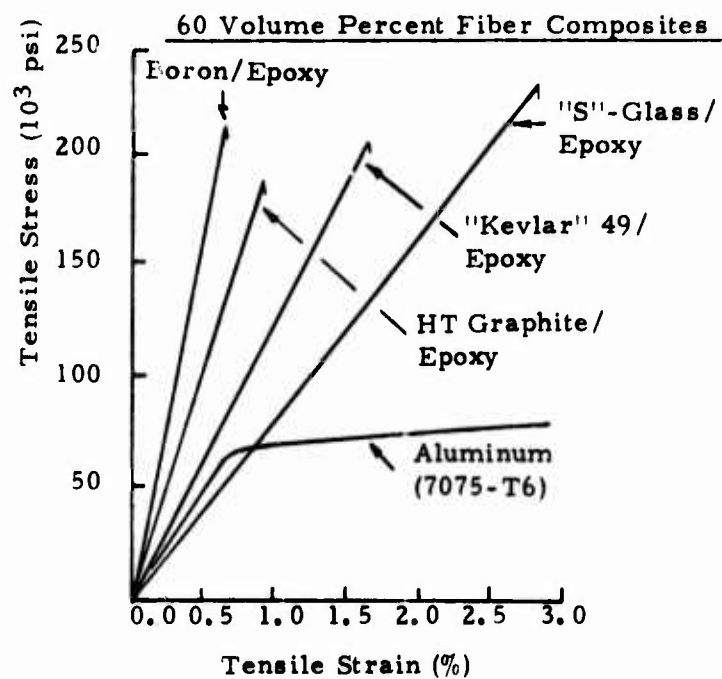
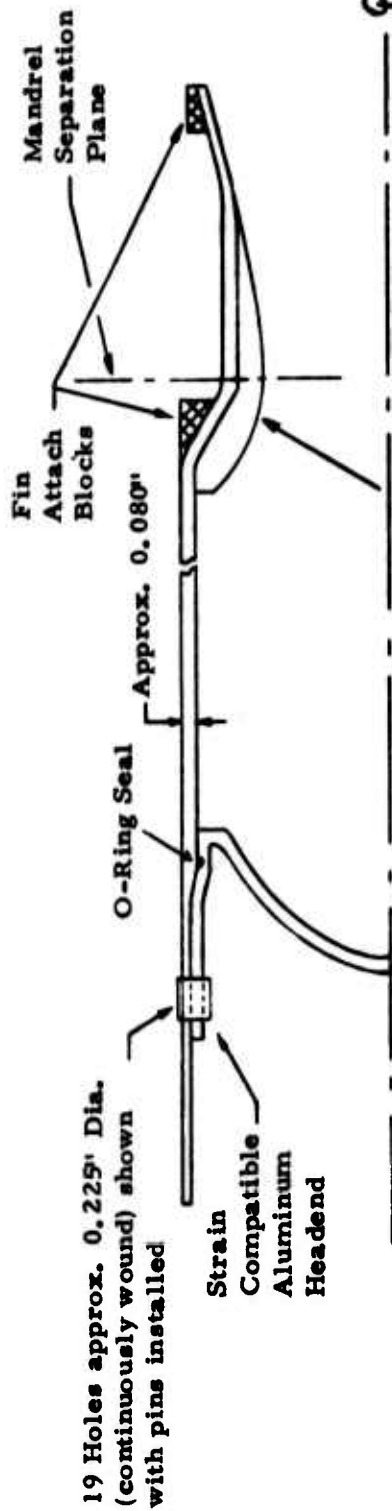
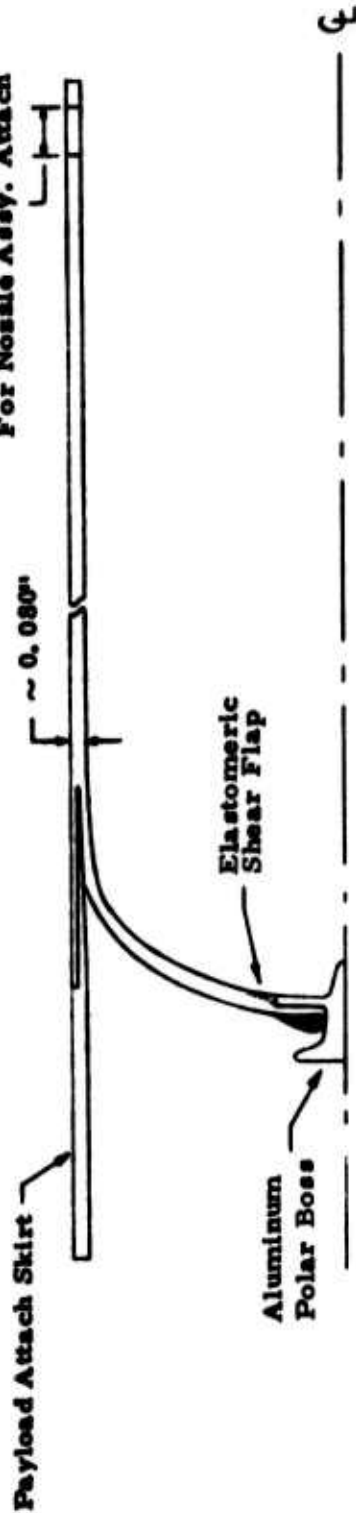


Figure X- 6. Comparison of Filament Wound Case Materials

(Continuous Filament Wound)  
19 Holes approx. 0.225" Dia.  
For Nose Assembly. Attach



Integrally wound  
throat insulation  
silica-phenolic (typical)

Figure X-7. Filament Wound Composite Cases

- o Shows a motor performance increase if high specific strength (2:1 over 7075-T6 aluminum) can be utilized without a penalty for specific stiffness (1:1.6 below 7075-T6 aluminum), or if motor design is not volume critical.

Additional test evaluations and system compatibility studies are recommended.

#### VENDOR CONTACTS

##### Stock Tubing

See Appendix B

##### Case Impact Extrusions

Martin Marietta Aluminum  
Torrance, Calif.

Norris Industries  
Los Angeles, Calif.

Lite-A-Loy Corp.  
Spartanburg, S. Carolina

##### Strip Laminate Case

Imperial Metal Industries  
Kidderminster  
Worcestershire, England

Hercules, Inc.  
Alleghany Ballistics Lab  
Cumberland, Maryland

#### REFERENCE

1. "The Application of the IMI Strip-Laminate Process to the Manufacture of Rocket Motor Bodies", by G. C. J. Haefeli, Imperial Metals Industries Limited, Summerfield Research Station; Kidderminster, Worcestershire, England, Oct 1968.

SECTION XI  
CLOSURE/JOINING STUDY

## SECTION XI

### CLOSURE/JOINING STUDY

There are an extremely large number of closure configurations and methods of joining them to cases of various types. Since some joining techniques are not feasible with certain case/closure combinations, the matrix of possibilities is not symmetrical. By the same token, even though a particular combination of case/closure/joining technique is technically feasible, the prime requisite of "low cost" will further reduce the number of arrangements that might be considered. Table XI-1 lists the possible arrangements of the cases considered in this program, three general types of closures and several methods of joining the two parts together, keeping in mind that some of these arrangements are more attractive than others. More details about the joining techniques are given in Table XI-2.

All types of welding operations with a metal strip laminate case raises the question of what effect there might be on the adhesive used to bond the laminates together; therefore these are less attractive than bonding closures in place. In addition the bonding technology for the metal strip laminate case has been developed. Although shear pins, either with O-ring or adhesive sealant, can be used with a variety of cases, the equipment and additional operations needed do not seem practical for cases where other joining techniques can be employed. On the other hand, plastic laminate cases have a scarcity of joining techniques; shear pin holes can be formed as the case is wrapped and thus this technique is viable for this type of case. The same reasoning applies to the rivet bonding, where number of assembly operations, number of components and protrusion of rivets out of the missile envelope make other joining techniques more attractive.

With these and other considerations, an investigation of manageable scope was undertaken.

- a. Laboratory tests were performed to evaluate some joining techniques

- Friction welding
  - Weld bonding
  - Rivet bonding
  - Tapered bondline<sup>1</sup>
  - Electromagnetic forming

- b. Other joining techniques could be evaluated only through analysis because equipment and set-up costs were prohibitive

---

1. Performed as part of company-sponsored research and reported here for completeness.

BEST AVAILABLE COPY

TABLE XI-1  
POTENTIAL ARRANGEMENTS

Case Type	Form of Closure	Adhesive			Welding			Electron Beam			Mechanical		
		Straight Bondline	Tapered Bondline	Weld Bond	Laser	Friction		ESSJ	Rivet Bond	Crimp Bond	Retainer	Shear Pin	
Impact Extruded (Aluminum)	Molded Plastic	X							X		X	X	
	Plastic with Metal Shell (a) Formed Metal (b)	X		X	X	X	X	X	X	X	X	X	
Stock Tubing (b)	Molded Plastic	X	X						X	X	X	X	
	Plastic with Metal Shell (a)	X	X	X	X	X	X	X	X	X	X	X	
	Formed Metal (b)	X	X	X	X	X	X	X	X	X	X	X	
Laminate Metal (Steel)	Molded Plastic	X							X			X	
	Plastic with Metal Shell (a) Formed Metal (b)	X		X	X	X	X	X	X	X	X	X	
Laminate Plastic	Molded Plastic	X										X	
	Plastic with Metal Shell (a) Formed Metal (b)	X		X	X	X	X	X	X	X	X	X	

a. A typical example is nozzle ablative material in metal structural support shell.  
b. Either aluminum or steel.



TABLE XI-2

JOINING METHOD SUMMARY

Method	Description of Method	Advantages	Disadvantages	Scalability (size)	Discussion of Methods for Evaluation
Adhesive Bonding	Adhesive is applied to surface to be joined and is allowed to cure.	<ul style="list-style-type: none"> <li>No high temperatures</li> <li>No large capital equipment costs</li> <li>Can be used on loaded motor</li> <li>Disimilar materials can be joined</li> </ul>	<ul style="list-style-type: none"> <li>Requires controlled fit-up (except on tapered seat)</li> <li>Adhesives can be "messy"</li> <li>Probably not applicable to large motors</li> <li>Surface preparation critical for good bond</li> <li>Temperature limited by adhesive</li> <li>Aging unknown</li> <li>Cannot be disassembled</li> </ul>	Potential limited by diameter considerations. Feasible up thru 15-in size at moderate chamber pressures.	Experimental effort in progress for bonding plastic closures to tapered aluminum tubing. Has potential for lightweight, low cost joining method.
Electromagnetic Solid State Joining (ESSJ)	Workpiece is placed in single turn induction coil. Coil is driven by 3-10 KHz AC to heat material to "stick" temperature. AC then removed and 1-6 KJ capacitor bank is dumped into coil. Eddy currents in workpieces cause metals to diffuse into one another. Currents in coil run 50-80 K amps. EM pressures to 50,000 psi.	<ul style="list-style-type: none"> <li>No filler material</li> <li>Applicable to larger motors--up to 12-15" D</li> <li>Highly repeatable quality "weld"</li> <li>Disimilar metals can be joined</li> <li>Can be used on loaded motors (maybe)</li> </ul>	<ul style="list-style-type: none"> <li>High capital equipment cost</li> <li>Method is considered in process development stage by Thermtool, Inc.</li> <li>May require preheating of materials for high speed operations and therefore difficult to use on loaded motor.</li> <li>Cannot be disassembled</li> </ul>	Should be feasible at 15-in size. Capacitor bank size is critical from investment standpoint.	ESSJ vendor will not perform evaluation in the near future.
Inertia/Friction Welding	One of two concentric pieces is turned at high speed while other is held stationary. The two are then pressed together and frictional heat causes the parts to weld.	<ul style="list-style-type: none"> <li>No filler material</li> <li>Disimilar metals can be joined</li> <li>Applicable to larger motors--up to 30" D.</li> <li>High production rates</li> <li>Automated operation</li> </ul>	<ul style="list-style-type: none"> <li>Cannot be used on loaded motor easily</li> <li>Substantial equipment costs</li> <li>Thin wall tube must be supported to prevent collapse</li> <li>Contact surfaces must be cleaned (aluminum)</li> <li>Cannot be disassembled</li> <li>Must provide for flashing</li> </ul>	Demonstrated up to 30-in diameter	Good potential for low cost, high production rate. Evaluation needed for application to thin wall tubing.
Electron Beam (EB) Welding (in-or out-of-Vacuum Chamber)	High power electron beam is directed at weld zone. Kinetic energy of electrons transferred to workpiece, causing local vaporization and melting, producing the weld.	<ul style="list-style-type: none"> <li>No filler material</li> <li>Might be usable on loaded motor</li> <li>Minimum energy input to workpiece--highest known energy concentration <math>10^6</math> watts/cm<sup>2</sup></li> <li>Highly repeatable quality weld</li> <li>Weld speed to <math>\approx 300</math>"/sec</li> </ul>	<ul style="list-style-type: none"> <li>High capital equipment cost</li> <li>Shielded facility required for out-of-chamber EB welding</li> <li>Pumpdown of EB welding chamber slow &amp; limits rate</li> <li>Requires close fit-up tolerances</li> </ul>	No limit if "tension" weld used. Shear welds will require consideration of bending loads which might cause excessive "peel stresses"	Cost and feasibility studies will be made. No major problems in application foreseen.

TABLE XI-2 (Continued)

Method	Description of Method	Advantages	Disadvantages	Scalability (size)	Discussion of Methods for Evaluation
Weldbonding	Combination of adhesive bond and spotwelding. Takes advantage of best features of both.	<ul style="list-style-type: none"> <li>Adhesive forms seal and provides shear strength and spot weld provides peel strength</li> <li>Fit-up less critical than spot weld</li> <li>Adhesive can be cured before or after welding</li> </ul>	<ul style="list-style-type: none"> <li>Surface preparation critical for good bond</li> <li>Adhesive aging is unknown factor</li> <li>Cannot be disassembled</li> <li>Temperature limited by adhesive</li> </ul>	Potential greater than straight adhesive joint. Will satisfy 15 inch requirements	Experimental evaluation needed because of possible problems associated with tolerances and alignment. Potential for application to loaded motors.
(a) Snap Ring, (b) Ortmann Shear Key, (c) Threaded Retainer Ring or Threaded Closure	(a) Spring steel snap ring holds closure in place (b) threaded wire used; (c) ring screwed onto case or closure screwed onto case	<ul style="list-style-type: none"> <li>Can be disassembled with proper design</li> <li>Can be used on loaded motor</li> <li>State-of-art approach</li> </ul>	<ul style="list-style-type: none"> <li>Snap ring groove or thread machining required</li> <li>O-ring seal required</li> </ul>	Diameter limited. Weight excessive at 15 inch diameter.	To be used for baseline design. Costs can be obtained from previous experience.
Mechanical Crimped or Rubber Pad Formed or Swaged	Case is mechanically or electromagnetically crimped into closure shear grooves or other suitable interface.	<ul style="list-style-type: none"> <li>No filler material</li> <li>Automated assembly-high production rates</li> <li>Can be used on loaded motor</li> <li>Tolerance stack-up is not critical</li> <li>Can be used with adhesive bonding</li> </ul>	<ul style="list-style-type: none"> <li>Cannot be disassembled</li> <li>O-ring seal may be required if adhesive not used</li> <li>Provisions must be made to support ablatives where applicable</li> </ul>	Potential limited by diameter considerations because of "stiffness" needed to make joint. Can be done at larger diameters if joint can be backed up during forming.	One method, tapering of tube by spinning, being evaluated in combination with adhesive bonding. Other methods will be evaluated for feasibility and costs
Thermal Shrink Fit	Inner piece is cooled and/or outer piece is warmed. Resultant thermal expansion/contraction allows assembly of pieces which have an interference when at the same temperature	<ul style="list-style-type: none"> <li>No filler material</li> <li>Simple assembly</li> <li>Might be usable on loaded motor with tight tolerances on case I. D. and closure O. D.</li> </ul>	<ul style="list-style-type: none"> <li>High temperature differences required for stackup of loose manufacturing tolerances--may reduce strength of case</li> <li>Case thickness to withstand stresses from fit and produce gas seal is excessive if no O-ring is used.</li> <li>Stress corrosion cracking potential</li> </ul>	Definitely diameter limited	Does not appear feasible because of high temperature, close tolerance requirements.
Laser Welding	High power laser beam is focused on workpiece, resultant heat produces weld.	<ul style="list-style-type: none"> <li>No filler material required</li> <li>Is usable on loaded motor</li> <li>Applicable to larger motors with high enough laser power</li> <li>Multiple work stations from one work station by time sharing or split beam</li> </ul>	<ul style="list-style-type: none"> <li>Weld thickness limited by available laser power</li> <li>Requires close fit-up tolerances</li> </ul>	No limit at reasonable material thicknesses using "tension" weld	Has potential for high production rate but equipment costs are high. Will be evaluated for costs

Laser welding  
Electron beam welding  
Electromagnetic forming

c. Stress analyses were performed on

Weld bonding  
Friction welding

Electromagnetic solid state joining (ESSJ) was eliminated from consideration at the start because the patent-holding vendor considered the process not yet ready for development or exploratory investigations.

### STRESS ANALYSIS

Stress analyses using the "Finite Element Nozzle Stress Analysis Program E-238B" were conducted on the weldbonded head end closure and the friction welded head end closure. These two different concepts are shown, respectively, in Figure XI-1 and XI-2 which presents their stress analysis grid as well as material divisions.

Each model was restricted in the axial direction at elements 16,22 to 20,22 or 15,33 to 19,33, as the case may be, to simulate attachment to the pressure test equipment cap. Also, each model was restrained at element 1,1 to 1,5 or 1,11 in the radial direction to enable it to simulate its attachment to its mirror image. The pressure loads on either model was 5000 psia which was distributed over all interior surfaces of the closure, adhesive joint, and case, depending on the configuration. The materials and their properties used in the analysis are shown in Tables XI-3, XI-4, and XI-5.

Table XI-3 presents the results of the weldbonded head end closure showing that the maximum stress (hoop) of 61405 psi is in the case and allows a slight margin of safety at 5000 psi. The first part to fail should be the case at approximately 5200 psi since it has the least margin of safety.

Table XI-4 shows the stress analysis of the friction welded head end closure. As can be seen, the stresses in both the closure and weld are substantially higher than the material strength. (The properties of the weld were assumed the same as those of the weaker steel.) These high stresses are due to two reasons: (1) the geometry of the joint and (2) the inability of the model using E-238 to cope with the actual situation.

### LABORATORY TESTS

#### Friction Welding

The friction welded test closure is shown in Figure XI-3. A "flash trap" is incorporated in the end closure to eliminate the necessity of machining the weld flash from the I.D. for cost savings in production. The thickness of the closure can be reduced for weight savings in a flight version but

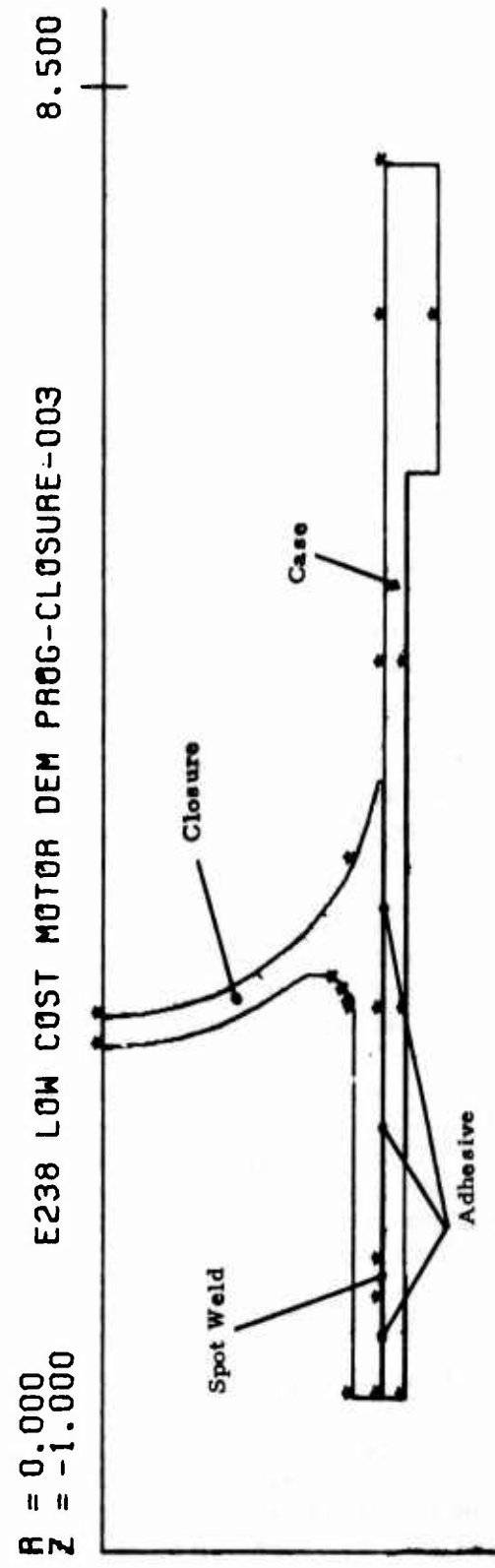
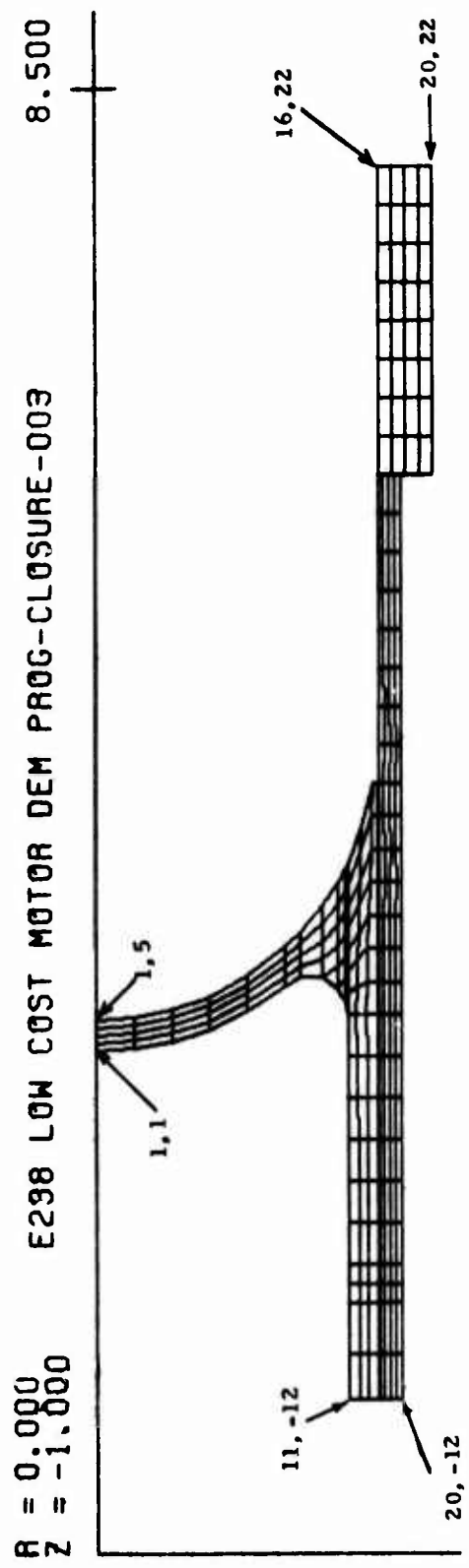


Figure XI-1. Weld Bonded Head End Closure

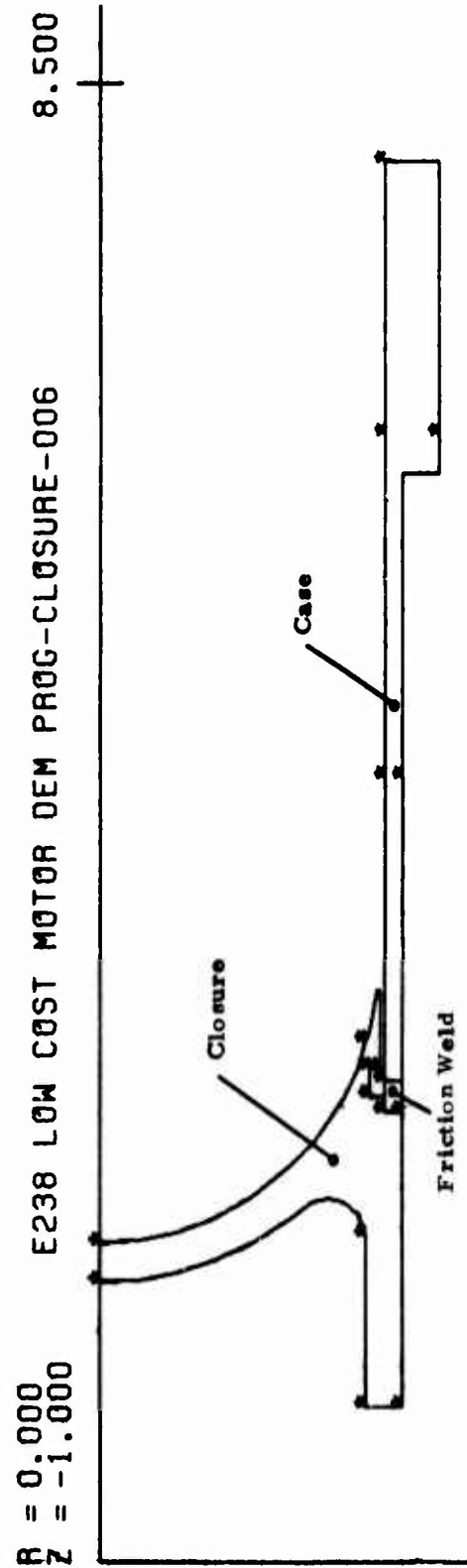
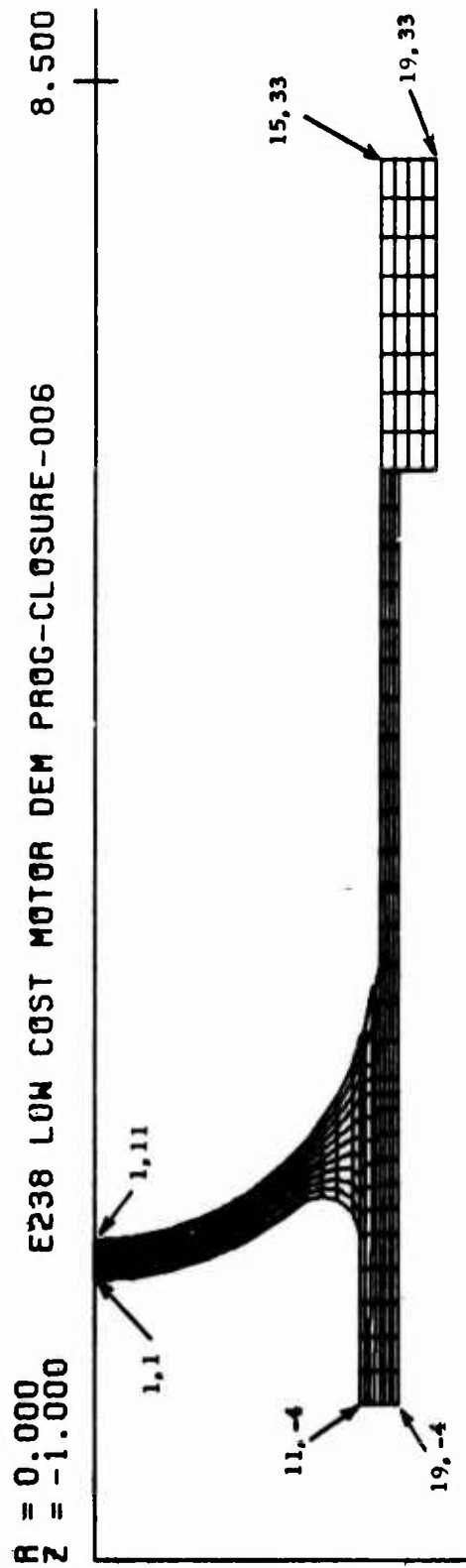


Figure XI-2. Friction Welded Head End Closure

TABLE XI-3  
RESULTS OF STRESS ANALYSIS OF  
WELD BONDED HEAD END CLOSURE

Part	Material	Maximum Stress, $\sigma$ (psi) and (Element Location)	Material Strength, $F_{tu}$ (psi)	Margin of Safety (a), (b)
Closure	Aluminum 6061-T6	36,311 (1,1)	42,000	0.16
Adhesive	EA9309	830 <sup>(c)</sup> (15,4)	2,140	1.58
Spot Weld	---	20,220 (15,-9)	42,000	1.08
Case	Aluminum 2024-T8511	61,405 <sup>(d)</sup> (16,9)	64,000	0.04

---

a.  $M.S. = \frac{F_{tu} - 1}{\sigma}$

b. Stress analysis pressure = 5000 psia.

c. Tensile shear.

d. Hoop stress was highest for this part.



TABLE XI-4

RESULTS OF STRESS ANALYSIS OF  
FRICTION WELDED HEAD END CLOSURE

<u>Part</u>	<u>Material</u>	<u>Maximum Stress, <math>\sigma</math> (psi)</u> <u>and (Element Location)</u>	<u>Material</u> <u>Strength, <math>F_{tu}</math></u> <u>(psi)</u>	<u>Margin of</u> <u>Safety</u> <u>(a), (b)</u>
Closure	1025 Steel	68,211 (14, 6)	55,000	-0.19
Weld	----	101,457 (15, 7)	55,000	-0.46
Case	1026 Steel	82,949(c) (15, 14)	85,000	0.02

a. Hoop stress was highest for this part.

b.  $M.S. = \frac{F_{tu} - 1}{\sigma}$

c. Stress analysis pressure = 5000 psia.

TABLE XI-5  
MATERIAL PROPERTY TABLE

C O N T I N U U M				M A T E R I A L			P R O P E R T I E S		
<u>Aluminum 6061-T6</u>									
Mat. No.= 1	E1=	1.0000D	07	NU21=	3.3000D-01	ALPHA1= 0.0	G13= 3.7594D	06	PHI= 0.0
	E2=	1.0000D	07	NU31=	3.3000D-01	ALPHA2= 0.0	BFR=0.0		
	E3=	1.0000D	07	NU32=	3.3000D-01	ALPHA3= 0.0	BFZ=0.0		
<u>EA9309</u>									
Mat. No.= 2	E1=	1.0000D	03	NU21=	4.9900D-01	ALPHA1= 0.0	G13= 3.3600D	02	PHI= 0.0
	E2=	1.0000D	03	NU31=	4.9900D-01	ALPHA2= 0.0	BFR=0.0		
	E3=	1.0000D	03	NU32=	4.9900D-01	ALPHA3= 0.0	BFZ=0.0		
<u>Spot Weld</u>									
Mat. No.= 3	E1=	1.0000D	07	NU21=	3.3000D-01	ALPHA1= 0.0	G13= 3.7594D	06	PHI= 0.0
	E2=	1.0000D	07	NU31=	3.3000D-01	ALPHA2= 0.0	BFR=0.0		
	E3=	1.0000D	07	NU32=	3.3000D-01	ALPHA3= 0.0	BFZ=0.0		
<u>Aluminum 2024-T8511</u>									
Mat. No.= 4	E1=	1.0000D	07	NU21=	3.3000D-01	ALPHA1= 0.0	G13= 3.7594D	06	PHI= 0.0
	E2=	1.0000D	07	NU31=	3.3000D-01	ALPHA2= 0.0	BFR=0.0		
	E3=	1.0000D	07	NU32=	3.3000D-01	ALPHA3= 0.0	BFZ=0.0		
<u>1025 Steel</u>									
Mat. No.= 1	E1=	2.9000D	07	NU21=	2.9000D-01	ALPHA1= 0.0	G13= 1.1240D	07	PHI= 0.0
	E2=	2.9000D	07	NU31=	2.9000D-01	ALPHA2= 0.0	BFR=0.0		
	E3=	2.9000D	07	NU32=	2.9000D-01	ALPHA3= 0.0	BFZ=0.0		
<u>Friction Weld</u>									
Mat. No.= 2	E1=	2.9000D	07	NU21=	2.9000D-01	ALPHA1= 0.0	G13= 1.1240D	07	PHI= 0.0
	E2=	2.9000D	07	NU31=	2.9000D-01	ALPHA2= 0.0	BFR=0.0		
	E3=	2.9000D	07	NU32=	2.9000D-01	ALPHA3= 0.0	BFZ=0.0		
<u>1026 Steel</u>									
Mat. No.= 3	E1=	2.9000D	07	NU21=	2.9000D-01	ALPHA1= 0.0	G13= 1.1240D	07	PHI= 0.0
	E2=	2.9000D	07	NU31=	2.9000D-01	ALPHA2= 0.0	BFR=0.0		
	E3=	2.9000D	07	NU32=	2.9000D-01	ALPHA3= 0.0	BFZ=0.0		

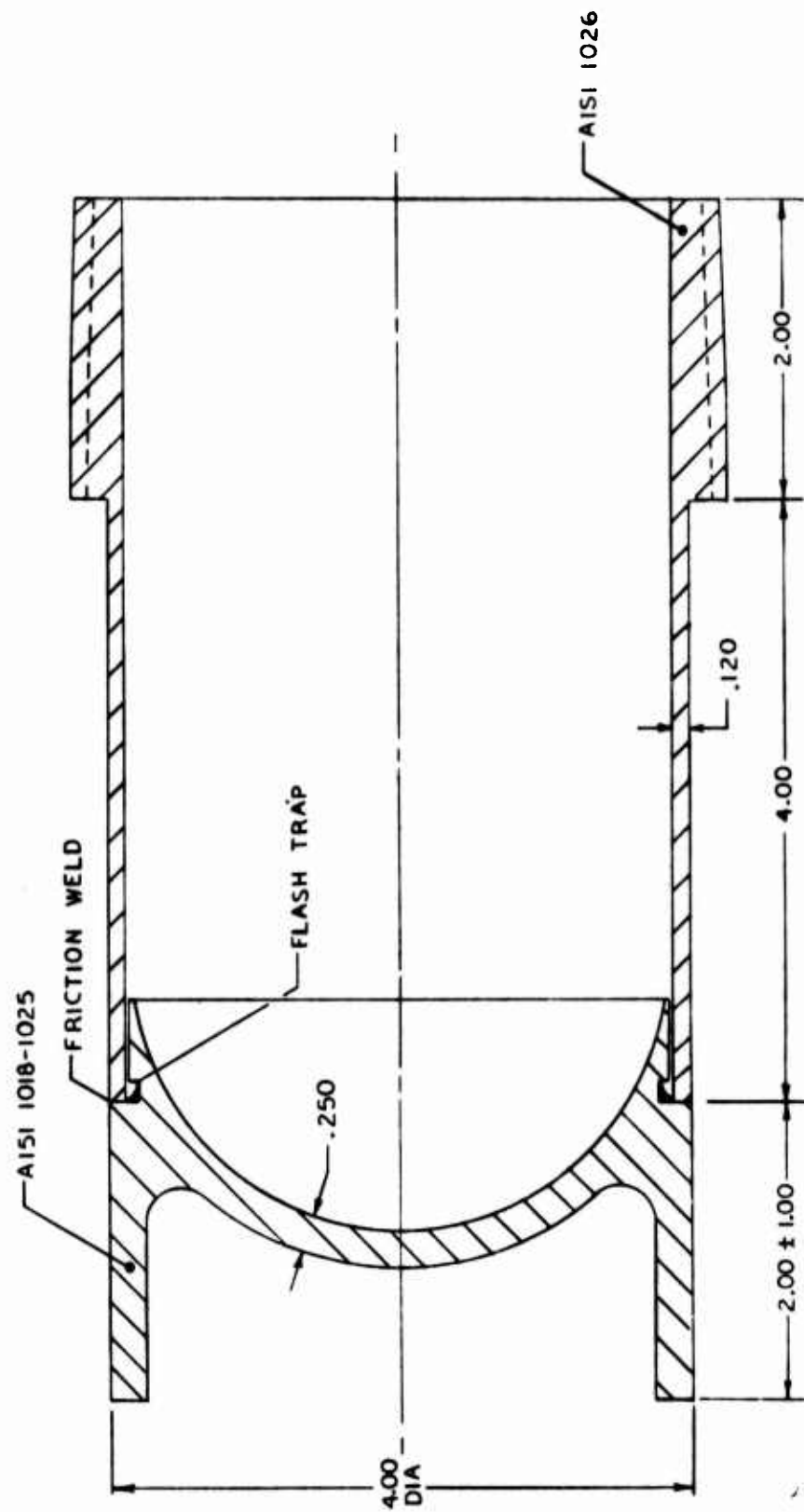


Figure XI-3. Friction Weld Test Chamber

was purposely designed heavy for adequate support of the holding device required for welding. For production, backup tooling can be used for support of thinner closures if necessary. The case was machined from AISI 1026 seamless tubing 4.5" O.D. x 0.375" wall. Prior to welding the wall thickness was machined to final size only over a length of approximately 1" to allow the thicker tube section to support the gripping force. Then the case was machined to final dimensions after welding.

The eight friction welded test chambers were completed at Interface Welding and received at Thiokol. Examination of the chambers indicated all had acceptable external weld flashing; however, one had slight extension of the flash from the "flash trap" into the chamber interior. The temperature attained on the closure interior during welding was monitored with a "Tempilabel" (a label with temperature-sensitive spots which change color over a range of temperatures) and determined to be between 350°F to 400°F on the surface. A room temperature hydrotest of 5000 psi with no failure or evidence of yielding was completed on one test chamber.

A pressurization test at -65°F was successfully performed to the design pressure of 5000 psi on a friction welded test chamber. This test was performed at -65°F because of the fact that many steels undergo embrittlement at low temperatures (below the nil-ductility transition temperature-NDTT). No testing was done at the upper temperature requirement of +160°F because of the negligible strength degradation of steels at this temperature. Tensile tests were performed on specimens cut from a welded chamber to determine weld strength. The average ultimate strength of four tests was 109,700 psi with all fractures in the 1026 tube rather than at the weld interface. The minimum longitudinal tensile strength of this tube material is 85,000 psi. Based on stress analysis the burst pressure of the friction welded should be approximately 6250 psi, assuming the hoop stress is the same as the longitudinal strength of the tube determined by the tensile tests. The friction welded interface was examined by metallography and found to have narrow heat affected zones of approximately .03" in the closure and .02" in the tube with recrystallized microstructures. The original interface between the two parts could not be distinguished because of the forging during upset. The forged region has the characteristics of a tempered martensite microstructure and is approximately .025 wide.

#### Weldbonding

The effects of bondline clearances on concentricity between the case and closure, as well as variation of weldbond strength around the circumference was established on test specimens shown in Figure XI-4. Results from these tests were expected to permit determination of tube and closure tolerances that will be required to produce reliable weldbonded closures. Three sets of test specimens with clearances of .005", .010" and .015" on the radius were weldbonded, with eight spot welds equally spaced around the circumference. A room temperature curing adhesive was applied before welding. Total-indicator-readout measurements were used to determine

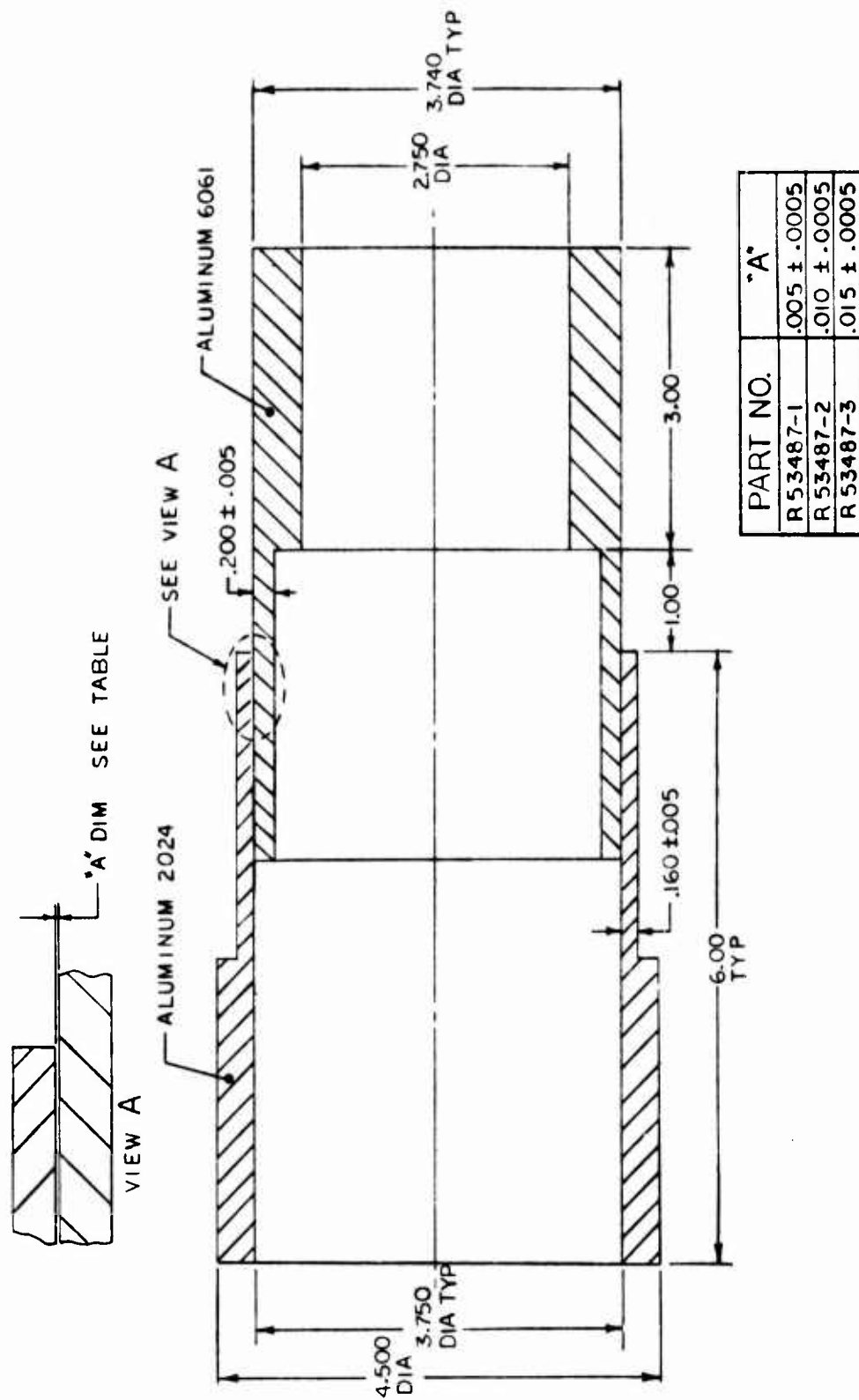


Figure XI-4. Weldbond Test Specimens

concentricity between tubes; the lap shear tensile specimens were cut, each to include a weld, and pull tested. Quality of adhesion and spot welds was evaluated by the lap shear tests and any necessary changes then made in welding or adhesive parameters before weldbonding the test chambers.

The test chamber design to be utilized for performing burst tests is shown in Figure XI-5. The case is machined from 2024-T 3511 tubing 4.5" O.D. x .375" wall thickness to permit use of a threaded pipe cap for pressurization. The end closure material is 6061-T6 bar stock with a bond clearance of .005" between it and the case.

Weld bond evaluation was conducted utilizing aluminum tube and closures and based on a General Electric Co. study (Reference XI-5) for the Army Missile Command to greatly reduce the experimental effort required. This project evaluated the weldbonding and postweld sealing of 7075-T6 aluminum alloy with six adhesives and three primers/couplers under the following test conditions:

- a. Standard weldbond joint assembly
- b. Varying cross section of the weldbond area
- c. Standard atmospheric exposure prior to assembly and welding
- d. Thirty day high humidity and salt fog exposure
- e. Ninety day high humidity and salt fog exposure
- f. Twelve month high humidity and salt fog exposure

Three thicknesses of the aluminum sheet and three surface preparation methods were included in the G.E. test program. The major differences that needed to be considered for closure applications were: A different alloy and thicker material was used and cylindrical rather than flat parts were joined. Because of these differences the test program required a preliminary investigation of surface preparation methods for the aluminum alloy to be used, weld schedule establishment and tolerance requirements for the tube I. D. and closure O. D.

Weldbond fabrication of test specimens and chambers was initiated with preliminary tests to establish bonding and welding parameters. A set of cylindrical test specimens with nominal bond-line clearances of 0.005, 0.010 and 0.015 inch were weldbonded and T.I.R. measurements obtained to determine eccentricity were 0.007, 0.023 and 0.35 inch, respectively. Tensile tests were made on eight specimens cut from the weldbonded cylinders each containing a weld, with the following results:

Test Specimen No.	Bond Gap, (in.)	Avg. Lap Shear (psi)	Remarks
R53487-1	0.005	2175	Only 2 of 8 welds formed nuggets, poor adhesive bonding.
R53487-2	0.010	1630	
R53487-3	0.015	1833	



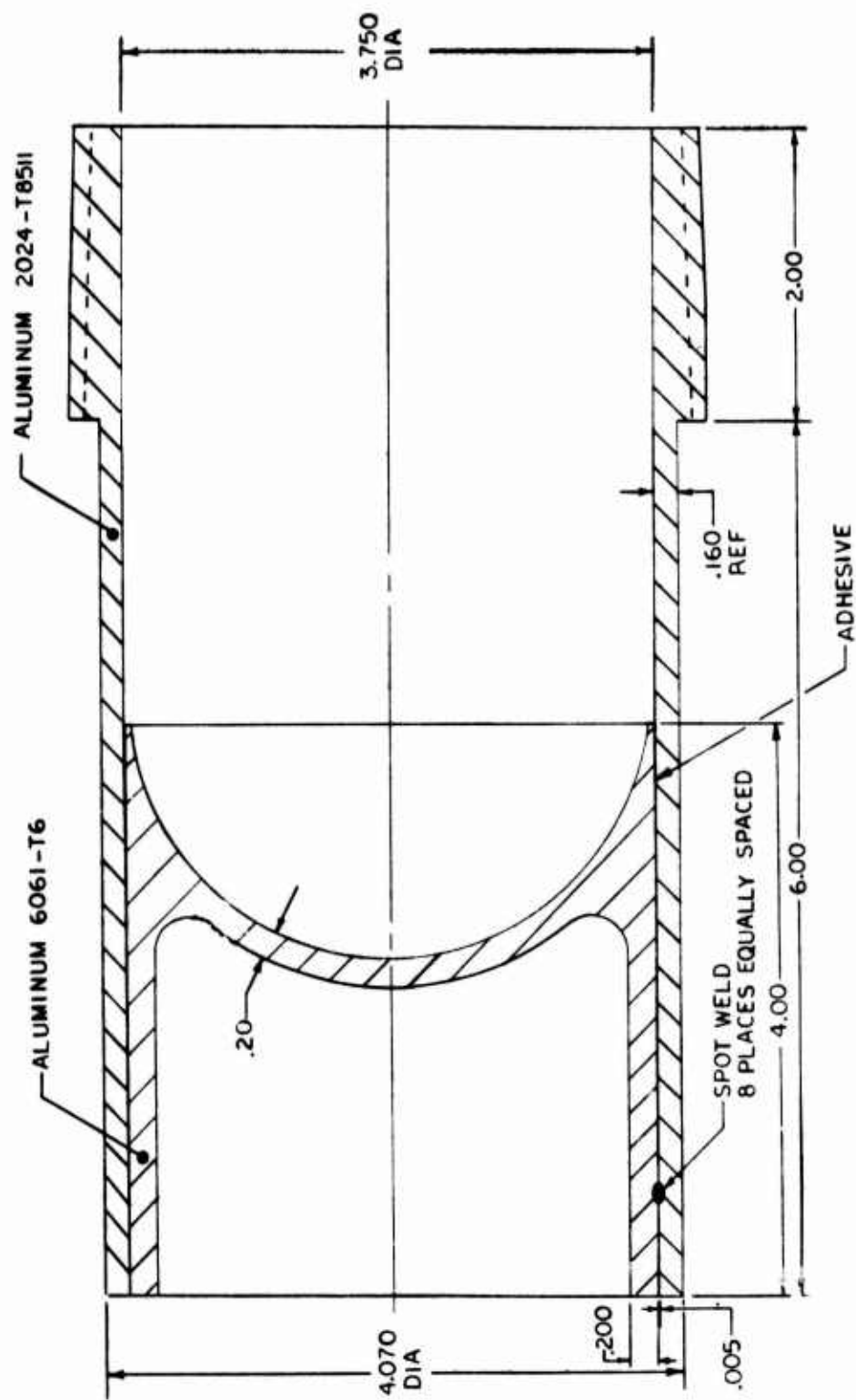


Figure XI-5. Weldbond Test Chamber

The cleaning procedure and welding parameters were revised and one test specimen weldbonded with a bond gap of 0.005 inch. The average lap shear strength was 2940 psi, all eight welds exhibited nuggets and adhesive bond characteristics were improved.

A test chamber was weldbonded using the same parameters and pressurized to 5000 psi with no failure at room temperature. The chamber was then heated to 165°F and pressurized to 2300 psi before failure in the shear mode. Stress analysis of the bond area indicated a minimum of 830 psi lap shear strength is required for a pressure of 5000 psi. Results from the pull tests shown above indicate the room temperature lap shear strength obtained by weldbonding is greater than that required by a factor of 2 to 3.5. However, the lap shear strength obtained at 165°F, based on a ratio  $2300 \div 5000 \times 830$ , was only 380 psi.

The manufacturer's data for the adhesive, Hysol EA 9309, indicates a lap shear strength of 750 psi at 180°F, whereas recent tests at Thiokol on another program yielded a strength of only 200 psi at 170°F for the same adhesive. Thus for the weldbond process to successfully withstand 5000 psi at 165°F, other adhesives must be tested to establish their strength at this temperature. The welds, although not as temperature sensitive as the adhesive, are not capable of withstanding the pressure bonds when unsupported by an adhesive.

Another cylindrical test specimen (R53487-1-3) with 0.005" bond clearance was weldbonded with the weld schedule modified for the last four spot welds by increasing the weld energy from 90% to 95%. This was done to overcome the current shunting effect of the previous welds which reduces the size of the weld nugget and, correspondingly its strength. The same cleaning procedure was used as previously (caustic etch with nitric acid desmut); however, a cloth was used to dry the parts after the final rinse rather than air drying. After weldbonding, tensile tests made on coupons cut from the specimen showed an average lap shear strength of 1293 psi. The weld nuggets were more uniform in size than the previous test but the adhesion bond to the aluminum surface was poor, probably because of contamination of the surfaces by the cloth. For comparison a previous test specimen, with an average lap shear strength of 2940 psi, showed good adhesive characteristics. These results exemplify the necessity for maintaining clean bond surfaces and that the weldbond strength is more dependent on the adhesive rather than weld strength. A test chamber (R53491-2) weldbonded with the same weld schedule and cleaning procedure as test specimen R53487-1-3 was, however, successfully pressurized to 5000 psi at room temperature, although it did fail by leaking at 1200-1500 psi on repressurization. There was no movement of the closure with respect to the case, as in a previous test indicating failure occurred by peeling because of the poor adhesive bond rather than shear of the adhesive and welds.

The experimental evaluation of weldbonding conducted thus far indicates that it is a feasible method of joining motor case assemblies; however, more effort is needed than time permitted to evaluate other adhesives and weld schedules to improve the weldbond strength, particularly at elevated temperatures. Also, a welder with a higher KVA rating (400 KVA) than the one available (200 KVA) would give improved strength for the metal thickness involved as was recommended by the welder manufacturer, Vendor B.<sup>1</sup>

#### Rivetbonding

Rivetbonding of closures, as an alternate joining method, used test chambers fabricated for weldbonding. This method involves drilling matching holes in the case and closures, applying an adhesive and installing blind fasteners. This operation can be fully automated. Rivetbonding offers an advantage over weldbonding in that no case-to-closure contact is required as in welding, allowing a more uniform bondline and concentricity. A major disadvantage is cost of drilling hole and fasteners. Preliminary hydrostatic testing has been conducted on two test chambers; however, the established goal of 5000 psi was not attained at room temperature. Failure occurred in the form of leakage.

#### Tapered Bondline

A separate project<sup>2</sup> investigated the feasibility of an adhesive bonded plastic closure in a swaged (tapered) aluminum case. Two aluminum case materials and four plastic closure materials bonded with several adhesives were assessed. Twelve test cases were fabricated and hydrostatically tested at room temperature with five meeting or exceeding the design limit pressure of 4500 psi. The successful configuration was a 6061-T6 machined case, a 40% glass-filled, injection molded polycarbonate closure and a Hysol EA 9309 modified epoxy adhesive. Again, problems with adhesive strength were encountered at high temperature.

#### Electromagnetic Forming (EMF)

A design concept for joining a closure to tubing was provided by Maxwell Laboratories using electromagnetic forming in combination with an adhesive (Figure XI-6). They furnished test data on a similar design utilizing a 4" O.D. x .188" wall 2024-T3 aluminum tubing and O-ring seal which failed at 7000 psi. The design requires machining of the tube I.D. which could be accomplished for a forward closure during machining of warhead threads with little or no additional cost. A machining vendor stated that the tube ends would be faced off as a turning operation to provide the proper length; the facing tube used for the aft end can be shaped to cut the internal configuration shown at the upper left of Figure XI-6. Since the set-up for turning will already be made, providing the EMF seat will not entail additional costs.

1. Vendors identified by code letters to protect price quotations.
2. Company sponsored research reported here for completeness.



## COMPARISON OF JOINING METHODS

The joining methods were evaluated qualitatively according to the factors listed in Table XI-6 and rated from one through five with the higher rating the best. A discussion of each method is given in the following paragraphs. Cost estimates obtained for each method are given in Table XI-7. Effort was directed toward joining methods that would be applicable to the metal stock tubing types determined to be promising candidates in the "Stock Tubing Study" as well as plastic and strip laminate tubes and impact extruded cases.

### Welding Methods

#### o Laser Welding

Laser welding utilizes a high energy laser beam to form a weld which has very narrow fusion and heat affected zones similar to electron beam welding. Its major advantages are that it requires no vacuum or X-ray shielding and can utilize a split beam for making two welds simultaneously or time sharing. A major disadvantage is the high initial cost of the equipment and limited availability. For high production welding of closures to tubing, fixtures for aligning and rotating the assemblies under the beam would be required and costs for this were included in the equipment estimate. Set-up and alignment of the butting surfaces is critical, similar to EB welding and a shielding gas is necessary, particularly for aluminum alloys. Operating costs were assumed to be comparable to EB welding, for which data are available. Laser welding could be used on a loaded motor provided the weld joint is greater than about 1/4" from the propellant.

#### o Electron Beam Welding

Electron beam welding can be performed in three different modes: in-vacuum, partial vacuum, or out-of-vacuum. For in-vacuum welding the entire assembly is placed in the vacuum chamber or seals provided such that only the area to be welded is in the vacuum. Production rates for in-vacuum welding are low because of pump time. A dual chamber system can increase production rates by pumping in one chamber while welding in the other but equipment costs are higher than for out-of-vacuum and would barely maintain production of 20,000 per month with no allowance for downtime (Reference XI-1).<sup>1</sup> Out-of-vacuum welding can be conducted at higher production rates, has lower equipment cost and can be used on loaded motors provided the weld is sufficiently removed from the propellant as with laser welding. For protection of the weld and greater penetration, helium effluent is used when welding aluminum and this cost, including operating and maintenance expenses, were estimated for both aluminum and steel (Reference XI-2).

---

1. References are given at the end of this section.

TABLE XI-6  
COMPARISON OF JOINING METHODS

	Application to				8" and 15" Motors	Can Be Disassembled	Surface Preparation	Storage Temperature Capability	Use With Loaded Motors	Use With Installed Igniter	Tooling Costs	Assembly Costs	No. of Assembly Operations	O-Ring Required	Tolerances Required	No. of Components	Automated Assembly	Ease of Assembly	Inspection of Assembly
	Aluminum Cases	Steel Cases	Plastic Strip Laminate Cases	Metal Strip Laminate Cases															
Laser Welding	3	5	1	1	5	1	3	5	4	4	1	3	4	5	3	5	4	3	3
Electron Beam Welding	3	5	1	1	5	1	3	5	4	4	4	4	4	5	3	5	4	3	3
Friction Welding	4	5	1	1	3	1	5	5	1	1	5	4	5	5	5	5	5	5	5
Weldbonding	3	4	1	2	3	1	1	2	5	5	3	3	2	5	2	3	3	2	1
Rivethbonding	5	5	5	3	4	3	1	2	5	5	4	3	1	5	3	1	4	2	4
Electromagnetic Forming	5	4	1	1	2	1	1	2	5	5	5	5	4	5	5	3	4	3	4
Taper Bonding	5	3	5	2	3	1	1	2	1	1	4	3	4	5	3	3	4	5	4
Threaded Retainer	5	5	3	2	4	5	5	5	5	5	4	2	4	1	2	2	3	4	5
Snap Ring Retainer	3	3	3	2	2	5	5	5	5	5	4	1	4	1	1	2	2	4	5
Straight Bonding	5	5	5	5	3	1	1	2	5	5	4	4	4	5	1	3	4	4	4
RATING: 5 - Excellent 4 - Good 3 - Fair 2 - Poor 1 - Worst or Impractical																			



BEST AVAILABLE COPY

TABLE XI-7  
JOINING COSTS EVALUATION<sup>(a)</sup>

Joining Method	Vendor <sup>(b)</sup>	Work Performed by Propulsion Contractor	Equipment, Development or Tooling Costs		Operating and Maintenance Cost	Labor Cost <sup>(d)</sup>		Services and/or Parts Costs	Total Cost
			Total	Each <sup>(c)</sup>		Time (min)	Cost (\$)		
Laser Welding	B	Yes	800,000	0.67	0.07 <sup>(e)</sup> 0.05 <sup>(e)</sup>	1	0.37		(Al) 1.11 (Stl) 1.09
Electron beam Welding In Vacuum	B	Yes	550,000	0.46	0.05	3	1.11		1.62
	C	No						1.25 to 1.65	1.25 to 1.65
Electron Beam Welding Out of Vacuum	D	Yes	300,000	0.25	0.07 <sup>(f)</sup> 0.05 <sup>(g)</sup>	1	0.37		(Al) 0.69 (Stl) 0.67
Friction Welding	A	No	12,000	0.01				(Al) 1.55 (Stl) 1.20	(Al) 1.56 (Stl) 1.21
	E	Yes	94,000	0.08	0.02	1	0.37		0.47
Weld Bonding	B	Yes	100,000 <sup>(h)</sup>	0.08	0.04	2	0.74	(Adhesive) 0.20	1.04
Electromagnetic Formed Bond	J	Yes	50,000	0.04	0.02	1	0.37	(Adhesive) 0.20	0.63
Tapered Bond	G	Yes	54,000	0.04	0.05	1 1/2	0.58	(Adhesive) 0.20	0.87
	H	No <sup>(i)</sup>	120,000	0.10		1/2	0.18 <sup>(j)</sup>	(Adhesive) 0.20 (Forming) 2.00 to 3.00	2.28 to 3.38
Straight Bond	---	Yes	10,000	0.01		1/2	0.18	(Adhesive) 0.20	0.39
Thread	I	No <sup>(j)</sup>	20,000	0.02		1/2	0.18 <sup>(j)</sup>	(Al case) 1.65 (Al Closure) 0.90 (O-ring) 0.13	(Al) 2.88
				0.02		1/2	0.18	(Stl case) 1.33 (Al Closure) 0.90 (O-ring) 0.13	(Stl) 2.56
	J	No <sup>(j)</sup>	20,000	0.02		1/2	0.18 <sup>(j)</sup>	(Al case) 1.98 (Al Closure) 0.90 (O-ring) 0.13	(Al) 3.21
				0.2		1/2	0.18	(Stl case) 2.67 (Al Closure) 0.90 (O-ring) 0.13	(Stl) 3.90
Snap Ring Retainer	J	No <sup>(j)</sup>	14,500	0.01		1/2	0.18	(Al case) 1.73 (Snap Ring) 0.60 (O-ring) 0.13	(Al) 2.65

- a. Costs (in dollars) to Propulsion Contractor, per operation and/or part, except where indicated.  
b. Vendors identified by code letters to protect cost quotations.  
c. Total production of 1,200,000 motors at rate of 20,000 per month.  
d. Labor costs at \$23.00 per hour, which includes factor for "non-touch" support labor.  
e. Assumed same as out-of-vacuum EB welding.  
f. Helium effluent recovered.  
g. Air effluent.  
h. Includes \$10,000 for equipment to automatic mix, meter, and apply adhesive.  
i. A vendor will form the tapered seal on the case and the propulsion contractor will bond in the closure.  
j. Vendor will machine the components and the propulsion contractor will assemble.

#### o Friction Welding

This process involves rotating one part with an attached flywheel and holding the other stationary. Then the two parts are forced together. Heat generated from the friction is sufficient to soften but not melt the faces of the parts. Just before rotation ceases the parts bond and the remaining flywheel energy hot works the metal interface, expelling impurities and voids and refining the grain structure. Friction welding is adaptable to welding aluminum and steel alloys to themselves or to dissimilar metals.

The friction welding process offers the advantages of high production rates, minimum tolerance and joint preparation requirements and a means of automatically determining weld quality by measurement of the weld upset. Disadvantages are that it cannot be readily accomplished on a loaded motor without special design provisions and the weld flash must be removed on the O. D. and I. D. unless a flash trap is provided in the joint design for the latter. Both steel and aluminum alloys are weldable; however, aluminum requires more careful joint preparation and this is reflected in the higher cost for aluminum welds, as quoted by Vendor A.<sup>1</sup> Inspection of weld quality is by visual examination of the weld flash and measurement of the total length change of the assembly, which can be maintained within  $\pm 5\%$  of the nominal upset determined during establishment of the weld schedule.

The large difference in friction welding costs for the two examples on Table XI-7 reflect the difference in welding equipment. Vendor A must stop the entire rotating components while the welder bought from Vendor E has a clutch so that only the chuck must be stopped. Similar equipment used by McDonnell-Douglas in Tulsa, Okla. makes three friction welds on 3-inch diameter heat pipes in 45 seconds (Reference XI-3). Friction welding for the heat pipe fabrication was selected because of its "high speed, low cost, unskilled operator requirement, high reliability and reproducibility and the very low criticality of joint preparation and tolerances" (Reference XI-3 and XI-4).

#### Adhesive Bonding

The methods considered for adhesive bonding (straight and tapered bondline), weldbonding, rivetbonding, and electromagnetic forming, (EMF/Bond), utilize a room temperature curing adhesive as sealant in combination with mechanical support. Cost estimates for these processes include equipment costs (\$10,000) for automatic mixing, metering and applying the adhesive to the bond surfaces. Surface preparation costs were not included because it is assumed that surface preparation would be performed beforehand for liner application, painting, etc., and need not be repeated for the adhesive bonding. Adhesive material costs were obtained from Vendor Q who provided an estimate of the quantity required per square foot (.10 lb) and the same area was assumed for each type of joint (48 in<sup>2</sup>). Cost of a typical adhesive is \$.05/lb when procured in 5 gallon units (45 lbs/unit) at the rate of 16 units per month or \$.85/lb in 100 unit quantities, yielding a cost per joint of approximately \$.20.

1. Vendors are identified by code letters when costs are attributed by source.

On the basis of the results of this program, in-house literature surveys, and cognizance of adhesive developments, it is recognized that an adhesive with room-temperature cure characteristics has not been identified for bonding plastic to metal, particularly for use at elevated temperatures (i.e., 170°F). Numerous adhesives are available to bond metal to metal for use at such temperatures (those meeting MMM-A-132), but there is not a similar selection for plastic-to-metal bonding.

o Weldbonding

Weldbonding is a relatively new process of joining metal parts and utilizes a combination of resistance welding (commonly spot welding) and adhesive bonding to form a pressure tight joint with higher properties than can be produced by either method. The process has been used on aluminum alloys but probably could also be adapted to steel materials. Cleaning of the mating parts is critical to the process; however, weldability of the metal must be considered as the prime requirement. The high strength aluminum alloys, 2014, 2024 and 7075 considered for the case material, have an "ease of welding" factor of B - "Makes good welds but special practices are required; can be welded only over a narrow range of machine settings". Advantages of weldbond over adhesive bonding for joining closures are:

1. Greater strengths can be achieved in both peel and shear directions and at higher temperatures.
2. The case does not have to be crimped or tapered to provide a mechanical reinforcement to the joint.
3. Weld bond joints resist aging effects better than adhesive joints.
4. Weld bond has potential for application to loaded motors.

Disadvantages are:

1. Greater capital investment is required for the welding machine
2. Tolerances of mating parts may be more critical to maintain concentricity and axial alignment of case and closure.

Based on the experimental evaluation, weldbonding would be feasible for joining but at relatively high risk. Both aluminum and steel tubing can be joined but steel offers an advantage over aluminum because of closer tolerances of the drawn tubing, better adhesion characteristics and lower weld energy requirements during spot welding. The welder recommended by Vendor B

for aluminum (400 Kva) would give a production rate of about 60 joints per hour so cost estimates were based on two shifts per day to yield a production rate of 20,000 per month. Major operating and maintenance costs are electricity, cooling water and dressing and/or replacement of electrodes and is estimated at \$0.04 per joint. The equipment includes a device which would automatically position and index the assembly between the electrodes for each weld at an estimated cost of \$15,000. Inspection of the weldbonded joint would be difficult by nondestructive methods so quality control would have to be done on a destructive sampling basis, as is normally done in spotwelding.

o Electromagnetic Forming

This process, involving the use of a high energy magnetic field to form metal, is capable of high production rates (up to 1000 operations per minute) with relatively low equipment costs. Its use in combination with adhesive is considered here, although an O-ring could also be used. The process is more applicable to high electrically conductive metals such as aluminum but has been applied to steels. The design and equipment costs for forming a joint to a closure established by Maxwell Laboratory involves machining of the tube I. D. If this machining is done at the same time as threading of the tube for a warhead, then little or no cost need to be added for the extra operation. For joining the nozzle to the aft end, this machining cost would have to be done when the tube is cut to length. Operating costs were based on estimates for typical EMF operations provided in the Metals Handbook (Reference XI-6). Inspection of the final assembly can be performed by visual inspection of the formed crimp and by destructive test sampling of the adhesive bond. Tolerance requirements of the tube and closure can be relatively loose (within aluminum tube ovality tolerances).

o Taper Bondline

The tapered bondline process evaluated involves tapering a tube by swaging or other forming technique and bonding in a matching closure with an adhesive. Cost estimates for swaging were provided by Vendor H using the method of "straight-line" swaging. This consists of forcing the tube into a tapered die and then forcing a punch into the tube to expand the reduced end to the required angle on the I. D.; therefore swaging cannot be done on a loaded motor. Steel or aluminum tubing can be swaged although the harder aluminum alloys (7000 series) and steel would have to be in the annealed condition. The aluminum alloy 2024-T3 was successfully swaged by this process. Assembly of the joint would be easy and merely involves application of adhesive, dropping a closure into the case and allowing the adhesive to cure.

The tapered seat can also be "shrink formed", as illustrated at the top of the next page.



This process can be used on the final closure of a loaded motor, as well as to form a tapered seat for the first closure to be installed. The serious questions which must be answered through an experimental investigation are: (a) What is degree of "spring back" when the tube is formed onto a semi-rigid plastic or metal nozzle or closure, rather than on to a rigid tooling mandrel? ; (b) Can the mating parts be held in alignment?

#### o Straight Bondline

Bonded closures which have a constant diameter bondline are characterized by strain-complatable closures and cases at the interior interface. Close dimensional control is required because bondline thickness is a critical parameter.

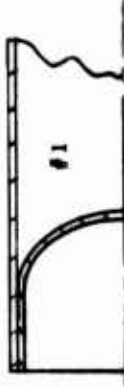



#### Mechanical Retainers

Mechanical retainers represent joining techniques that are state-of-the-art, having been used on nozzles of small rocket motors and on igniters of larger motors. They were included in this study to determine the cost advantage of the more unusual joining techniques. Cost estimates were obtained for machining threads on steel and aluminum cases and a snap ring groove on aluminum cases. It was estimated that threads and O-ring grooves could be machined on the mating part (closure or nozzle) for half the cost of the case threading cost. It was assumed that there would be no additional costs for machining just an O-ring groove on the mating parts for a snap ring retainer.

#### Closure Cost Studies

The closure types evaluated for costs were of four basic configurations, as shown on Table XI-8, using three representative materials---aluminum, 6061-T6; steel 1018-1025; and plastic, glass reinforced polycarbonate. Fabrication methods considered were impact extrusion, forging or extrusion and injection molding for the three materials, respectively. Cost estimates were obtained from vendors using closure designs and materials evaluated for friction welding, weldbonding and taper bonding and are shown in Table XI-8. For other configurations and materials, estimates were based on calculated weights times cost per pound determined from the quotes, with machining costs estimated where not available.

TABLE XI-8  
CLOSURE COST EVALUATION<sup>(a)</sup>

	Material	Aluminum 6061-T6	Steel 1018/1025	Plastic Glass Filled Polycarbonate
 #1		2.62	4.64	3.10
 #2		2.64	---	1.70 <sup>(e)</sup>
 #3		3.40 <sup>(b)</sup>	6.15 <sup>(b)</sup>	---
 #4		3.00 <sup>(c)</sup>	5.42 <sup>(d)</sup>	1.89

- a. Costs to Propulsion Contractor.  
b. Vendor K, including threads (or warhead attachment).  
c. Vendor L.  
d. Vendor M.  
e. Vendor N.



Costs for impact extruded preforms of aluminum 6061-T6 were obtained from Vendor L and Vendor P and ranged from \$2.75 to \$2.91 for Configuration 4 at weight 1.1 lbs. Prices for hot extruded steel closures similar to configuration 3 but with a hemispherical dome ranged from \$.8075/lb for 1018 steel to \$.8200/lb for 1025 steel. Weight of this closure is 3.0 lbs for a total cost of \$2.56 of the preform. Costs for finish machined parts including threads for a warhead were provided by Vendor K and were \$3.40 for aluminum and \$6.15 for steel plus \$110,000 tooling and equipment costs. Injection molded plastic closure cost obtained from Vendor N was \$1.70 for Configuration 2 with a weight of 0.55 lbs and was used to estimate prices of the other plastic closures.

### SUMMARY

The closure configurations were selected to provide a variety of possible combinations of closures and joining techniques. These combinations are listed on Table XI-9, where closure, joining, and warhead threading costs have been combined. Inspection of Table XI-9 reveals the following hierarchy:

<u>Closure</u>		<u>Joining</u>		<u>Can be Used On</u>
<u>Configuration</u>	<u>Material</u>	<u>Technique</u>	<u>Cost (\$)</u>	<u>Loaded Motor</u>
Flat Plate	Aluminum	Friction Weld	3.87	No
Conventional	Plastic	Straight Bond-		
		line	3.94	Yes
Flat Plate	Aluminum	Electron Beam		
		(OV)	4.09	Yes
Taper	Plastic	Taper Bondline	4.22	No
Reverse Dome	Aluminum	Straight Bond-		
		line	4.66	Yes
Reverse Dome	Aluminum	EMF Bond	4.90	Yes
Reverse Dome	Aluminum	Electron Beam		
		(OV)	4.96	Yes

Taken by themselves, the most attractive joining techniques are listed below and are compared with the more conventional methods.

	<u>Costs (\$)</u>	<u>Can be Used on</u>
		<u>Loaded Motor</u>
Straight Bondline	0.39	Yes
Friction Weld	0.47	No
EMF-Bond	0.63	Yes
Electron Beam Weld (OV)	0.69	Yes
Taper Bondline	0.87	No
Snap Ring (Alum)	2.65	Yes
Threaded (Alum)	3.21	Yes

TABLE XI-9  
TOTAL COSTS FOR COMBINATIONS OF CLOSURES AND JOINING TECHNIQUES (a), (b), (c)

Config. No.	Configuration	Closures		Joining Technique						
		Material	Cost (\$)	Weight (lb)	Friction Weld	EMF Bond	Electron Beam(OV)	Taper Bond	Straight Bond	Snap Ring
1	Reverse Dome	Alum	2.62	1.0	---	4.90	4.96	---	4.66	6.92
		Steel	4.64	1.9	---	6.92	6.98	---	6.68	8.94
		Plastic	3.10	1.0	---	---	---	---	5.14	7.40
2	Taper	Alum	2.64	1.0	---	---	---	5.16(e)	---	---
		Steel	---	---	---	---	---	---	---	---
		Plastic	1.70	0.6	---	---	---	4.22(e)	---	---
3	Flat Plate	Alum	3.40(d)	1.1	3.87(e)	---	4.09	---	---	---
		Steel	6.15(d)	3.0	6.62(e)	---	6.84	---	---	---
		Plastic	---	---	---	---	---	---	---	---
4	Conventional	Alum	3.00	1.1	---	5.28	5.34	---	5.04	7.30
		Steel	5.42	3.1	---	7.70	7.76	---	7.46	9.72
		Plastic	1.89	0.6	---	---	---	---	3.93	6.19
Joining Costs		---	---	0.47	0.63	0.69	0.87	0.39	2.65	

a. All with aluminum case.

b. All include costs (\$1.65) for warhead attachment threads, where cost was not included in original component estimate.

c. Costs to Propulsion Contractor.

d. Includes warhead attachment threading cost as part of basic closure cost.

e. Cannot be used on loaded motors.

There are five joining techniques that are not too different in cost (compared with the entire motor) which offer the motor designer considerable flexibility. Two techniques employ adhesive only (albeit one with special case forming). Friction welding, even though it cannot be used on loaded motors, provides a means of joining dissimilar metals and complex parts which may be more difficult with extrusions or machining. Electron beam offers the same advantage as friction welding and can be used on loaded motors. Electro-magnetic forming in combination with adhesives is one of the more attractive means of closing a loaded motor.

Additional investigations are warranted in the following areas:

- (1) Identify an adhesive with room-temperature cure for bonding plastics to metals for use at elevated temperatures (i.e., 170°F).
- (2) Conduct an experimental program and perform coast analysis of the rivet-bonding joining technique to define the potential more fully.
- (3) Conduct an experimental program on the shrink-forming technique to answer questions about "spring-back" when incorporating a plastic interior part and alignment between mating parts.

#### REFERENCES

- (1) Personal communication with Sciaky Brothers, Inc.
- (2) Westinghouse ENGINEER, October 1974.
- (3) "Friction-Welded Heat Pipes Stabilize Arctic Soil", Metals Progress, February 1976.
- (4) Personal communications with McDonnell-Douglas/Tulsa personnel.
- (5) Final Report - Contract DAAH01-72- -0027, "Missile Hardware Fabrication Weldbond/Sealant Technology (December 1973 - October 1974), " Ray Cole; General Electric Co., Huntsville, Alabama.
- (6) Metals Handbook, Vol. 4 - "Forming".

#### VENDOR CONTACTS

##### Closure Manufacture

Cliff Manufacturing Co.  
33800 Lakeland Boulevard  
Eastlake, Ohio 44094

##### Type

Al Impact Extrusion

VENDOR CONTACTS (Continued)

Closure Manufacture (continued)

Type

Martin Marietta Aluminum  
19200 S. Western Ave.  
Torrance, California 90509

Al Impact Extrusion

Bram Metallurgical-Chemical Co.  
245 W. Cheltenham Ave.  
Philadelphia, Pennsylvania 19144

Al Impact Extrusion  
Steel Cold Extrusion

Metal Impact Corp.  
10450 W. Lunt Ave.  
Rosemont, Illinois 60018

Al Impact Extrusion  
Steel Extrusion

Lovell Extrusion Co.  
690 W. Maple Road  
Troy, Michigan 48064

Steel Extrusion

Babcock and Wilcock  
P. O. Box 401  
Beaver Falls, Pennsylvania 15010

Steel Forging

Welding Equipment and Services

Type

Sciaky Bros., Inc.  
4915 West 67th Street  
Chicago, Illinois 60638

Electron Beam and  
Resistance Welding Equip.

Fusion Labs Division  
EBTEC Corporation  
120 Shoemaker Lane  
Agawam, Massachusetts 01001

Electron Beam Welding  
Equipment and Services

Interface Welding  
Carson, Calif.

Welding Services

General Electric Co.  
Huntsville, Ala.

Welding Service, Weldbond  
Development

VENDOR CONTACTS (Continued)

Machining and Welding Vendors

Type

OMNECO  
13561 Desmond St.  
Tacoima, Calif. 91331

Case manufacturing and  
machining

Weber Machine Inc.  
901 W. 12th St.  
Long Beach, Calif. 90813

Case manufacturing and  
machining

Norris Industries  
Military Products Division  
Vernon, Calif.

Case manufacturing and  
machining

Adhesives

Type

Hysol Division  
The Dexter Corp.  
Richardson Central Bldg. C-5  
725 S. Central Expressway  
Richardson, Texas 75080

Aerospace Adhesives

Hardman Incorporated  
Belleville, New Jersey 07109

Adhesives  
Mixing and Metering  
Equipment

Electromagnetic Forming

Type

Maxwell Laboratories, Inc.  
9244 Balboa Ave.  
San Diego, California 92123

Electromagnetic Forming  
Equipment and Services

Advanced Kinetics, Inc.  
1231 Victoria Street  
Costa Mesa, California 92627

Electromagnetic Forming  
Equipment and Services

Herf Industries  
452 Hoffman Road  
Little Rock, Arkansas 72209

Electromagnetic Forming  
Equipment and Services

VENDOR CONTACTS (Continued)

Tube Forming

Type

Diversico Industries, Inc.  
3609 48th Ave. No  
Minneapolis, Minnesota 55429

Swaging and others

Coast Metal Craft  
18518 Suzanna Road  
Compton, California 90221

Spinning

Fenn Mfg. Co.  
Newington, Conn.

Swaging

Grotnes Machine Works Co.  
Chicago, Ill.

Forming Equipment

Flagpoles, Inc.  
E. Setauket, N. Y.

Spinning & swaging

Plastic Closures

Type

C&D Plastics, Inc.  
Gardena, Calif.

Plastics molding

Value Engineered Components  
P. O. 523  
Old Cullman Rd.  
Arab, Ala. 35016

Plastics molding



SECTION XII

INSULATION/LINER STUDY

## SECTION XII

### INSULATION/LINER STUDY

While materials for insulation used in tactical rocket motors are not excessively expensive, the total cost for installation, cure, and quality control makes this component's cost of real significance to the total rocket motor cost. Therefore, the thrust of this study was to identify and evaluate one or more materials with adequate thermal protection properties which could be adapted to high speed application in automated production schemes.

The insulation system is dictated in large part by the grain design selected for a motor. Section XIII contains a detailed discussion of the different concepts. "Cartridge-loaded" grains use a relatively rigid sleeve in which propellant is cast and cured before being inserted into the case, either with or without an adhesive to bond the cartridge to the case. This same insulation sleeve can be installed in the case (again either with or without adhesive) and then the propellant cast and cured. The latter approach produces the common "case bonded" grain if the insulation sleeve is bonded to the case or if sleeve is rigid when compared to the relatively flexible propellant.

It can be seen that both the case-bonded and cartridge-loaded grains require (or may require, depending on the final design arrangement):

- a. Adhesive to bond the insulation sleeve to the case
- b. Insulation sleeve to contain propellant and/or to provide thermal protection to the case
- c. Bond promoter to enhance the bond between insulation sleeve and propellant.

Therefore, one area of the Insulation/Liner Study was concerned with identifying and evaluating in laboratory tests materials suitable for the three functions listed above.

Another method of insulating the case is to use a "mastic" insulation, a polymer filled with a material to enhance its erosion resistance. This material must be "swept", sprayed, or otherwise distributed along the case in a suitable pattern, after which the propellant is cast and cured, resulting in a case-bonded grain. Therefore, a second area of investigation was the formulation and initial characterization of a mastic insulation.

The traditional technique of assuring a good bond between propellant and various substrates (e.g., case or insulation) is to interpose a "liner" that consists of the same polymer as used in the propellant and various additives for bonding enhancement. It was difficult to break with tradition; so as a backup to the exploratory investigations into "low cost" techniques, a conventional liner was formulated for this application and carried through initial evaluation. It was recognized that the use of liner would incur significant cost penalties because of the added costs that go with a multi-constituent material.

All three areas of investigation had imposed one inviolable ground rule: all cure had to take place at "ambient" temperature so as to be compatible with the ambient-temperature cure propellant and its manufacturing philosophy of "no high temperature cure ovens".

#### INITIAL SCREENING

There were many materials from which to choose several to subject to laboratory evaluation. Initial screening was necessary to pare those available to a manageable number. Past experience, technical judgement, cost, availability, and environmental considerations were used.

##### Liner

An ambient temperature cure liner (designated TA-H731A) was already formulated for earlier applications and thus became the starting point (Table XII-1). Other work with similar systems showed that a bond promoter incorporated in a liner greatly improved its bond characteristics. Because of the need to restrict the total scope of work, an immediate decision was made to modify TA-H731A to the same sort of formulation, even though there was a three-fold increase in cost. The new material was designated TA-H732A.

##### Mastic Insulation

Basic work was necessary to formulate an ambient-temperature cure insulation filled with a material to increase erosion resistance. There was no direct experience from which to start. The initial screening involved selection of the filler material:

Carbon black	because of	Low cost
Milled glass	because of	Most experience
Ground silica	because of	Erosion resistance

All three have been used in other insulations with various polymers, so processing experience was considerable. Polyisoprene (TI-R300) was listed as a back-up choice.

TABLE XII-1  
RATIONALE FOR MATERIAL SELECTION  
LINER AND MASTIC INSULATION

<u>Material</u>	<u>Cost (\$/lb)</u>	<u>Experience</u>	<u>Processing (ability)</u>	<u>Remarks</u>
<u>Liner:</u>				
TA-H731A	1.25	Extensive	Good	Ambient cure
TA-H732A	4.56	Little	Good	Ambient cure
TL-H755A	4.31	Extensive	Excellent	145°F cure
-----				
TL-H754A	1.45	Moderate	Excellent	145°F cure
<u>Mastic Insulation:</u>				
TI-H706A (a)	0.90	This study	Good	Ambient cure
TI-H707A (b)	1.30	This study	Good	Ambient cure
TI-H708A (c)	1.44	This study	Good	Ambient cure
TI-R300	3.75	Extensive	Good	Cost more to install.
-----				
TI-O700A	1.56	Extensive	Poor	Contains a toxic ingredient.
V-44	6.50	Moderate	Fair	High pres. and temp.
41RPD	3.02	Extensive	Poor	

- a. Carbon filler.  
b. Glass filler.  
c. Silica filler.

### Insulation Sleeve

Thermoplastic materials were selected for the insulation sleeve because of their potential for low-cost high-volume manufacture (Table XII-2). Polystyrene, styrene-acrylonitrile, and polyethylene/polypropylene were eliminated because their low deflection temperature was used as a measure of inability to withstand the rocket motor environment. Polyurethane (a thermoset material), polysulfone, and polyphenylene sulfide were eliminated because of their high cost. The remaining three are glass-filled nylon, ABS and polycarbonate, which have high deflection temperature, low-to-moderate cost and high tensile strength. Numerous vendors are available for injection molding the final part.

### Adhesives

ECCO-BOND 45 and APCO 1252 were the commercial products selected for bonding the insulation sleeve to the case (Table XII-3). Their cost, compared to other products, is low; both are ambient temperature cure and have acceptable processing characteristics. The two liners, TA-H731A and TA-H732A, were also taken into laboratory evaluation because of low raw material cost and because there might be a need for an elastomeric adhesive. The other materials listed in Table XII-3 were attractive because of considerable experience in their use, but they were too costly or had processing/curing compromises which were unacceptable.

Bonding propellant to thermoplastic with just a primer or bond promoter was the preferred approach to reduce manufacturing costs. Because of the uniqueness of the application, it was decided to evaluate a relatively large number of materials. They are the eleven shown above the line in Table XII-4. The last three (Z-6040, A-187, and A-1893) were chosen because they were very effective in earlier investigations where cost was not so important; they were considered as "fall-back" candidates. Those shown below the line in Table XII-4 were eliminated because of high processing costs, no experience, no source or similarity to other selected products. Those at the top of the list have final costs of the same order as the raw material costs of liner compounds.

### Summary

Table XII-5 summarizes all the materials selected for laboratory evaluation. A similar listing is given in Table XII-6 but which includes trade names, class of material and a more detailed description of their function. Included in Table XII-6 are some materials used in the mastic insulation compounds. Costs and sources of the selected materials are shown in Table XII-7.

### LINER

Starting with the basic formulation of TA-H731A (Table XII-8), a new compound, TA-H732A, was prepared by adding a bond promoter, HX-868.

TABLE XII-2  
RATIONALE FOR MATERIAL SELECTION  
INSULATION SLEEVE MATERIAL

<u>Material</u>	<u>Deflection Temp. (°F)</u>	<u>Cost (\$/lb)</u>	<u>Processing Temp. (°F)</u>	<u>Specific Gravity</u>	<u>Tensile Strength (1000 psi)</u>
Nylon <sup>(a)</sup> J-10/10 <sup>(b)</sup>	475-490	1.10	520-650	1.34-1.38	19-28
ABS <sup>(a)</sup> G-1200/20 <sup>(b)</sup>	310-330	0.90	500-550	1.20-1.36	8-19
Polycarbonate <sup>(a)</sup> G-50/20 <sup>(b)</sup>	290-305	1.50	520-650	1.25	12-21
<hr/>					
Polystyrene	195-220	0.80	450-625	1.20-1.28	9-15
Styrene- Acrylonitrile	195-230	0.70	450-575	1.20-1.46	9-15
Polyethylene - Polypropylene	235-280	0.68	450-550	1.04-1.28	9-15
Polyurethane	200-225	2.50	350-450	1.33-1.55	5-10
Polysulfone	340-365	3.90	700-750	1.38-1.55	15-20
Polyphenylene Sulfide	280-315	3.85	600-700	1.65	21

a. Glass filled.

b. Fiberfil Division, Dart Industries.



TABLE XII-3  
RATIONALE FOR MATERIAL SELECTION  
INSULATION SLEEVE/CASE ADHESIVE

<u>Material</u>	<u>Cost (\$/lb)</u>	<u>Experience</u>	<u>Processing (ability)</u>	<u>Remarks</u>
ECCO-BOND 45	7.20	Considerable	Excellent	Ambient cure - excellent bond
APCO 1252	7.39	Moderate	Good	Ambient cure - excellent bond
TA-H731A	1.25	Considerable	Fair	Elastomeric
TA-H732A	4.56	Limited	Excellent	Elastomeric
EA-901	11.35	None	Good	Slow curing
EA-919	8.75	Considerable	Poor	Too low viscosity
EA-946	11.00	Considerable	Good	Slow curing
Eastman 910	88.00	Considerable	Poor	Too brittle
EA-934	9.15	Considerable	Good	Slow curing
EA-9309	8.95	Considerable	Good	Slow curing

TABLE XII-4

## RATIONALE FOR MATERIAL SELECTION

## PRIMERS AND BOND PROMOTERS (PROPELLANT/INSULATION SLEEVE)

<u>Material</u>	<u>Cost (\$/lb)</u>	<u>Experience</u>	<u>Processing Cost</u>	<u>Remarks</u>
Chemlok 205/234	0.87/1.51	Extensive	Low	
Chemlok 217	1.05	Slight	Low	
Chemlok 218	1.10	Slight	Low	
Chemlok 233	1.53	Slight	Low	
Chemlok 205	0.87	Extensive	Low	
Chemglaze 9924	1.01	None	Moderate	
Z-6077	6.30	None	Moderate	
XZ-8-0903	7.50	None	Moderate	
Z-6040	28.85	Moderate	Moderate	Very effective in past tests
A-187	10.00	Moderate	Moderate	Very effective in past tests
A-1893	8.75	Little	Moderate	
-----				
Chemlok 220	1.43	Little	Low	Very similar to 205
Chemlok 234	1.51		Low	Can not use directly to case
Chemlok 207	2.34	Very little	Low	Similar to 205
Chemlok 207/234	2.34/1.51	None/much	Low	Very similar to 205/234
Thixon AB894	2.40	Considerable	High	
Thixon D16282	3.00	None	High	
Chemglaze 9924	1.53	None	High	
Triisostearic	----	None	High	No source identified
isopropyl titanate				
N, 4-dinitroso-	----	None	High	No source identified
N-methylaniline				
p-nitroso-phenol	75.60	None	High	
p-nitroso-diphenyl-	----	None	High	No source identified
amine				

TABLE XII-5

MATERIALS SELECTED FOR EVALUATION

<u>Insulation Sleeve</u>	<u>Insulation Sleeve Adhesive</u>
Nylon <sup>(a)</sup> (J-10/10)	ECCO-BOND 45
ABS <sup>(a)</sup> (G-1200/20)	APCO 1252
Polycarbonate <sup>(a)</sup> (G-50/20)	TA-H731A & TA-H732A
<u>Primers and Bond Promoters</u>	<u>Liner</u>
<u>Propellant/Insulation Sleeve</u>	
Chemlok 205/234	TA-H731A
Chemlok 217	TA-H732A
Chemlok 218	TA-H755A
Chemlok 233	
Chemlok 205	
Chemglaze 9924	
Z-6077	<u>Mastic Insulation</u>
XZ-8-0903	TI-H706A
Z-6040	TI-H707A
Z-187	TI-H708A
Z-1893	TI-R300

a. Glass filled.

TABLE XII-6

MATERIALS FOR LINER AND INSULATION STUDIES

<u>Class</u>	<u>Material</u>	<u>Description</u>
Catalyst	DBTDA	Dibutyltin diacetate
Catalyst	DBTDL	Dibutyltin dilaurate
Catalyst	ZnO	Zinc oxide
Catalyst	Et <sub>3</sub> N	Triethyl amine
Filler	CAB-O-SIL	Ground silica filler
Filler	Carbon	Carbon black filler
Filler	Glass	Milled glass filler
Adhesive	APCO 1252	Epoxy Adhesive
Adhesive	ECCO-BOND 45	Epoxy Adhesive
Adhesive	EA-946	Epoxy Adhesive
Sleeve Material	POLYCABOFIL	Glass filled polycarbonate
Sleeve Material	ABSAFIL	Glass filled acrylonitrile-butadiene-styrene co-polymer
Sleeve Material	NYLAFIL	Glass filled nylon
Primer	Chemlok 205	Metal to rubber primer (adhesive)
Primer	Chemlok 234	Rubber to rubber primer (adhesive)
Primer	Chemlok 217	Metal to rubber primer (adhesive)
Primer	Chemlok 218	Metal to rubber primer (adhesive)
Primer	Chemlok 233	Metal to rubber primer (adhesive)
Primer	Chemglaze 9924	Metal to rubber primer (adhesive)
Bond Promoter	Z-6077	Organosilane bond promoter
Bond Promoter	XZ-8-0903	Organosilane bond promoter
Bond Promoter	Z-6040	Organosilane bond promoter
Bond Promoter	A-187	Organosilane bond promoter
Bond Promoter	A-1893	Organosilane bond promoter

TABLE XII-7  
COST OF MATERIALS

<u>Materials</u>	<u>Source</u>	<u>Cost</u>
<u>Primers</u>		
Chemlok 205	Hughson Chem	6.95/gal
234	"	12.05/gal
217	"	8.35/gal
218	"	9.95/gal
233	"	12.30/gal
Chemglaze 9924	Hughson Chem.	7.95/gal
<u>Bond Promoters</u>		
Z-6077	Dow Corning	50.00/gal
XZ-8-0903	"	60.00/gal
Z-6040	"	28.85/lb
A-187	Union Carbide	10.00/lb
A-1893	"	8.75/lb
<u>Adhesives</u>		
APCO #1252	Applied Plastics, Inc.	14.78/qt
ECCO-BOND-45	Emmerson & Cuming, Inc.	14.40/qt
<u>Insulation Sleeve</u>		
ABS (J-10/10)	Fiberfil Division	0.90/lb
	DART Industries	
Nylon (G-1200/20)	"	1.10/lb
Polycarbonate (G-50/20)	"	1.50/lb
<u>Liner &amp; Insulation</u>		
TI-H706A	Thiokol Corporation	0.90/lb
TI-H707A	"	1.30/lb
TI-H708A	"	1.44/lb
TA-H731A	"	1.25/lb
TA-H732A	"	4.56/lb

TABLE XII-8

LINER FORMULATION

<u>Material</u>	<u>TA-H731A</u>		<u>TA-H732A</u>	
Filler	Carbon	3.00% <sup>(a)</sup>	Carbon	20.00%
Polymer	R45M	75.74%	R45M	60.02%
Cure Agent	DDI	21.16%	DDI	13.97%
Cure Catalyst	DBTDL	0.10%	DBTDL	0.01%
Bond Promoter			HX-868	6.00%

a. Carbon content may vary from 3 to 40%, depending on application.



Investigations during the SAM-D development program showed the large improvement resulting from this approach. It was those data that caused an immediate modification to TA-H731A. As will be shown later, there are good indications that the bond promoter is not needed for the ambient-temperature cure application.

Tests were conducted to determine the effect of cure catalyst concentration on cure time of the TA-H731A compound (Figure XII-1). The data show that the onset of cure can be adjusted over a fairly broad range without measurably affecting the final cure time.

Peel and adhesion data were obtained for two mixes of ambient cured propellant bonded to TA-H732A. Good bond was obtained from both mixes (Table XII-9).

#### MASTIC INSULATION

Essentially new formulations were devised for the mastic insulations, even though again TA-H731A served as the starting point. Because the mastic insulation was one of the prime candidate thermal protection systems, it was desired to reduce the cost as much as possible. Polymer and fillers did not offer any leeway, so cure agents and cure catalysts were investigated.

Several binder mixes were made to evaluate various curing agents and cure catalysts (Table XII-10). Processing data such as potlife, cure time, viscosity and physical properties were obtained from each mix. Potlife is a qualitative measure of how long the material could be processed. Cure time is the elapsed time after cure agent addition at which a penetrometer reading of 10 is observed (Figure XII-2).

The criteria used for selecting a formulation (in addition to cost) was potlife (working time) and a cure time compatible with the expected propellant cure conditions. It appears that about two hours would be a reasonable working time for using a large insulation mix by spray, sling or sweep application to a large number of motors in a production run. Propellant could be cast in the motors after approximately 8 - 10 hours of liner precure at ambient temperature. The best estimate is that 8 days will be required for the propellant to cure at ambient temperature. By selecting a liner cure time of  $\approx 100$  hours, there will be sufficient time for chemical reaction to take place between the liner and propellant and still be assured that the liner will be fully cured before the propellant. This cure condition should result in the best bond of liner to propellant.

From the data on Table XII-10 an insulation formulation was selected that provided the best all around characteristics. This is the formulation using TDI curing agent and 0.1%  $\text{Et}_3\text{N}$  cure catalyst with R45M

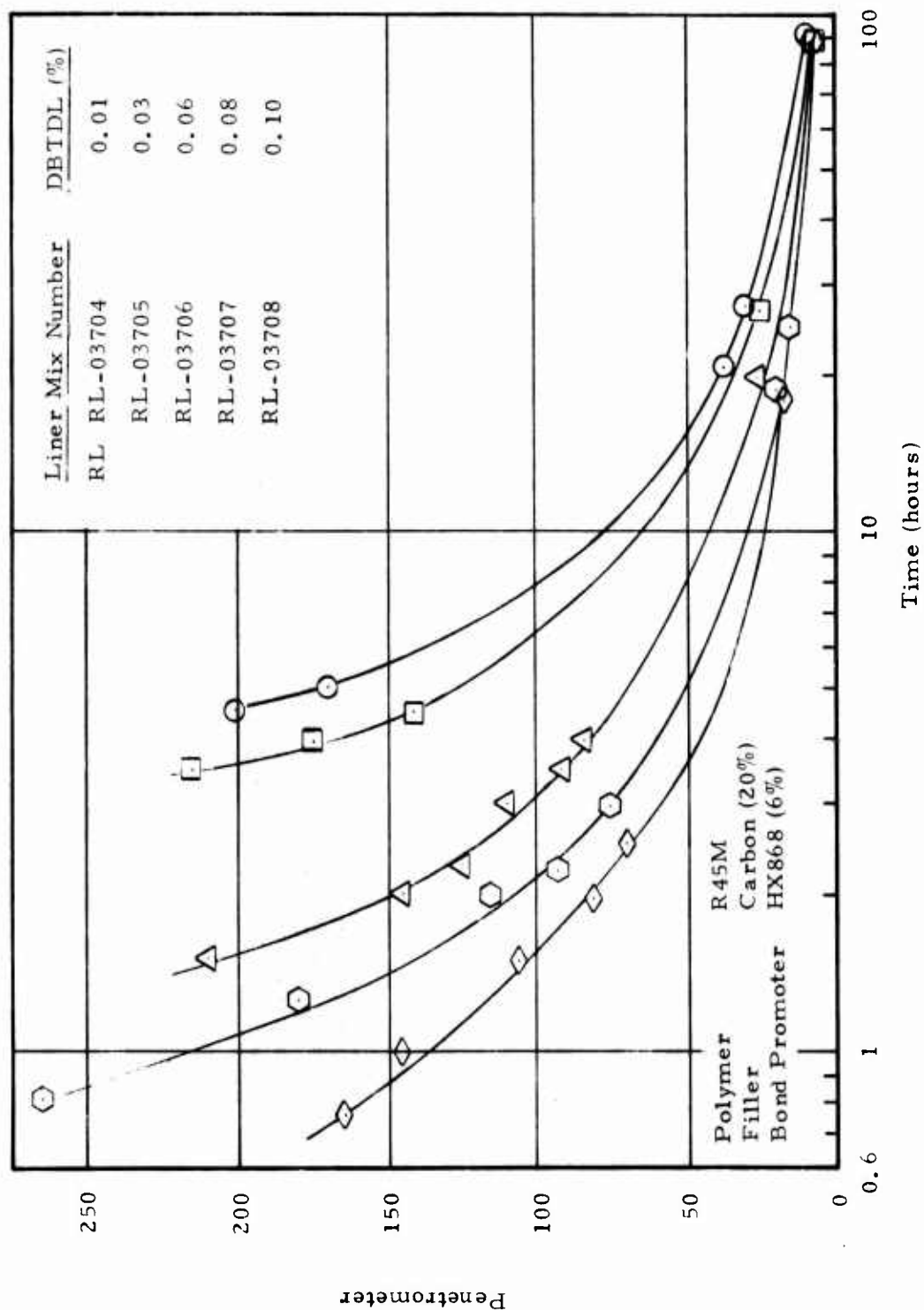


Figure XII-1. Effect of DBTL Concentration on Cure Rate of Liner

TABLE XII-9

PROPELLANT BOND TO TA-H732A LINER<sup>(a)</sup>

		Peel <sup>(b)</sup> (pli)		Adhesion <sup>(b)</sup>	
<u>T-630/RL-03715:</u>					
Test Temp., °F	-65	+77	+170	-65	+77 +170
Bond Values	52 (3B)	8.9 (3B)	2.5 (3B)	524 (3B)	141 (3P&B) 93 (3P&B)
<u>T-656/RL-03777:</u>					
Test Temp., °F	--	--	--	-65	+77 +170
Bond Values	--	--	--	787 (3TCP)	141 (3TCP) 76 (3TCP)

a. Ambient temperature cured propellant (DTS-7984). TA-H732A cured 48 hours at 77°F prior to propellant casting.

b. Number and letter in parenthesis indicates number of tests and mode of failure: B = Bond, P = Propellant, TCP = Thin Coat Propellant.

TABLE XII-10

## MASTIC INSULATION CURING AGENT AND CATALYST STUDY

Polymer: R45M  
 Filler: Carbon  
 P/CA: 1/1.0

Curing Agents	Cure Catalyst		Tests					RL No.
	Type	%	Carbon	Gassing	Potlife	Cure Time	Viscosity	Stress/Strain psi/in per in
DDI	Dibutyltin dilaurate	0.1	40%	None	10 min	24 hrs	0.84	299 526 03695
TDI	Dibutyltin dilaurate	0.1	40%	None	10 min	50 hrs	0.48	336 286 03694
DDI	DBTDA	0.1	40%	None	3 min	4 hrs	(a)	(a) (a) 03696
TDI	DBTDA	0.1	40%	None	3 min	20 hrs	1.21	(a) (a) 03700
DDI	ZnO	0.1	40%	None	2 hrs	300 hrs	0.20	225 785 03697
TDI	ZnO	0.1	40%	None	2 hrs	100 hrs	0.22	285 540 03701
DDI	Et <sub>3</sub> N	0.1	40%	None	3 hrs	370 hrs	0.20	187 812 03698
TDI <sup>(b)</sup>	Et <sub>3</sub> N	0.1	40%	None	1.5 hrs	100 hrs	0.21	354 546 03702

a. Cured in mixing bowl.

b. Lowest cost of those in test series.

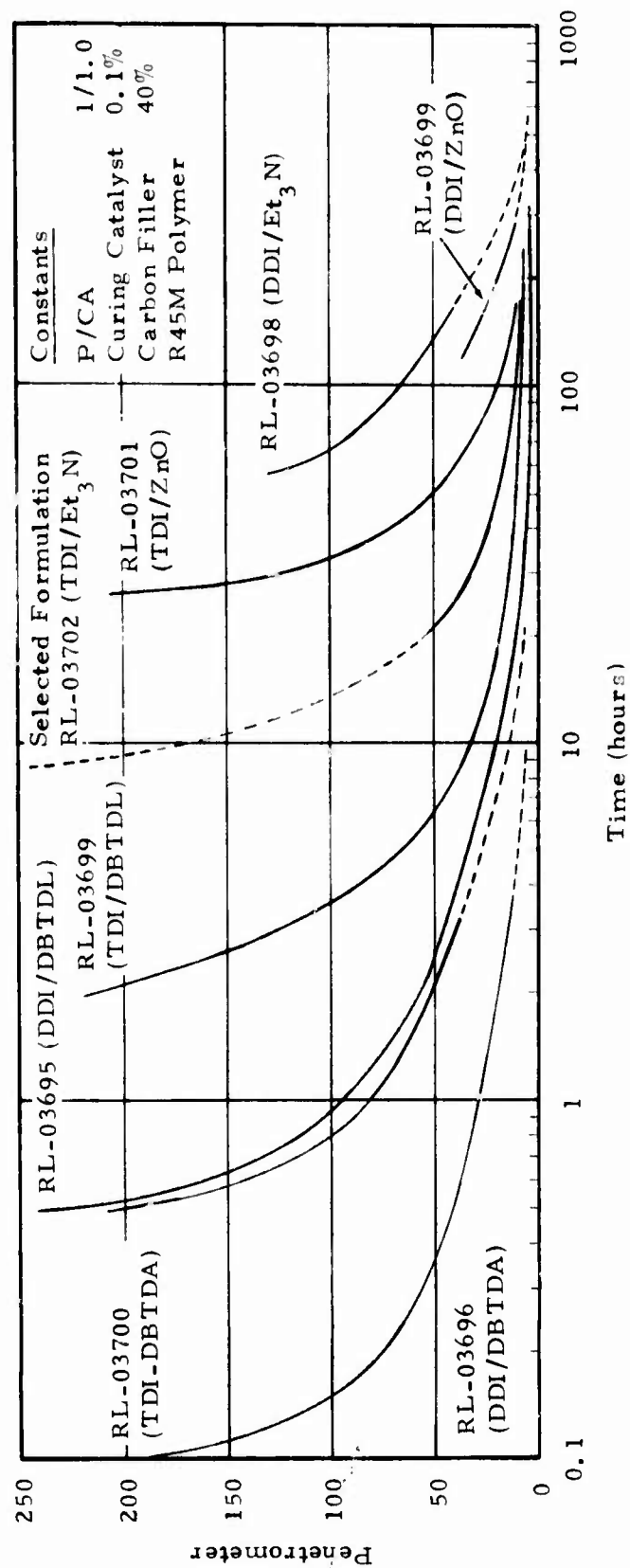


Figure XII-2. Mastic Insulation Cure Time with Various Curing Agents and Catalysts

polymer (RL03702). A potlife of 1.5 to 2 hours and a cure time of 100 hours is compatible with the expected manufacturing techniques. Viscosity of 0.2 Kp allows the material to be "sling lined" in several layers or to be centrifugal cast. Stress and strain are both high. The combination of Et<sub>3</sub>N/TDI has the lowest cost of any other catalyst/cure agent considered. The formulation containing zinc oxide (RL03701) is an acceptable backup to the selected formulation.

Next, additional mixes were made where the filler content was increased to the maximum reasonable level and still have a workable material. The goal was to achieve 40% (by weight) filler, but it was found that concentrations this high resulted in unacceptable processing characteristics. The fillers and filler levels finally selected were carbon (40%), milled glass (30%), and silica (10%). Complete formulations are given in Table XII-11 and other data for the individual compounds are listed in Tables XII-12, XII-13, and XII-14. Cure rate information is shown on Figure XII-3.

The processing data and physical properties are shown in Tables XII-15 and XII-16. Stress and strain are still generally acceptable, although the strain for the glass-filled material is some what low. The addition of glass and silica reduced potlife and increased EOM viscosity from that observed with carbon filler. However all three materials are still viable candidates as long as the selected manufacturing technique is compatible with material characteristics. The shorter potlife is of no consequence where continuous mixing and application is employed. Higher viscosity is a positive attribute when the material is to be troweled, swept or extruded directly into the case. In addition the proportion of cure agent can be reduced which will increase potlife with little effect on cure time.

Adhesion bond data were obtained for the bond of propellant to TI-H706A, TI-H707A and TI-H708A insulations (Table XII-16). It appears that the insulation with milled glass (TI-H707A) or with carbon (TI-H706A) bonds better to aluminum and propellant than the insulation with silica (TI-H708A). The physical properties of all materials are acceptable at all temperatures except for the TI-H708A at 165°F.

As indicated in Table XII-11 the insulation formulations TI-H706A, TI-H707A and TI-H708A do not contain the bond promoter HX-868. Several insulations mixes were made in which HX-868 was added because previous experiences indicated significant improvements might be realized. Mixes made with and without HX-868 were tested at -65, 77 and 170°F to evaluate the bond to ambient cured propellant (Table XII-17). There is not a significant



TABLE XII-11  
FORMULATION FOR MASTIC INSULATIONS

<u>Material</u>	<u>TI-H706A</u>		<u>TI-H707A</u>		<u>TI-H708A</u>	
Filler	Carbon	40.00%	Milled Glass	30.00%	Silica	10.00%
Polymer	R45M	55.96%	R45M	65.29%	R45M	84.00%
Cure Agent	TDI	3.94%	TDI	4.61%	TDI	5.90%
Cure Catalyst	Et <sub>3</sub> N	0.10%	Et <sub>3</sub> N	0.10%	Et <sub>3</sub> N	0.10%

TABLE XII-12  
PROPERTIES OF TI-H706A INSULATION  
(40% Carbon)

Bulk Modulus, psi	200,000
Hydrostatic Compressibility, % @ 2000 psi	0.998
Specific Heat, cal/gm°C	$3.47 \times 10^{-1}$
Thermal Conductivity, cal/cm-sec°C	$5.084 \times 10^{-4}$
Bond to DTS-7984 propellant, (a) adhesion, psi at 77°F	106
Pot Life, hrs.	1.5
Cure Time, hrs. at 77°F	100
EOM Viscosity, Kp	0.21
Stress, psi at 77°F	395
Strain, % at 77°F	469

a. Propellant cured at ambient for 8 days.

TABLE XII-13  
PROPERTIES OF TI-H707A INSULATION  
(30% Milled Glass)

Bulk Modulus, psi	118,000
Hydrostatic Compressibility, % @ 2000 psi	1.70%
Specific Heat, cal/gm°C	$3.685 \times 10^{-1}$
Thermal Conductivity, cal/cm-sec°C	$3.375 \times 10^{-4}$
Bond to DTS-7984 propellant, <sup>(a)</sup> adhesion, psi at 77°F	151
Pot Life, hrs.	0.5
Cure Time, hrs. at 77°F	144
EOM Viscosity, Kp	0.7
Stress, psi at 77°F	466
Strain, % at 77°F	100

a. Propellant cured at ambient for 8 days.

TABLE XII-14

PROPERTIES OF TI-H708A INSULATION  
(10% Silica)

Bulk Modulus, psi	
Hysrostatic Compressibility, %	
Specific Heat, cal/gm°C	
Thermal Conductivity, cal/cm-sec°C	
Bond to DTS-7984 propellant, (a) adhesion, psi at 77°F	44
Pot Life, hrs. at 77°F	0.5
Cure Time, hrs. at 77°F	138
EOM Viscosity, Kp	1.4
Stress, psi at 77°F	337
Strain, % at 77°F	586

a. Propellant cured at ambient for 8 days.

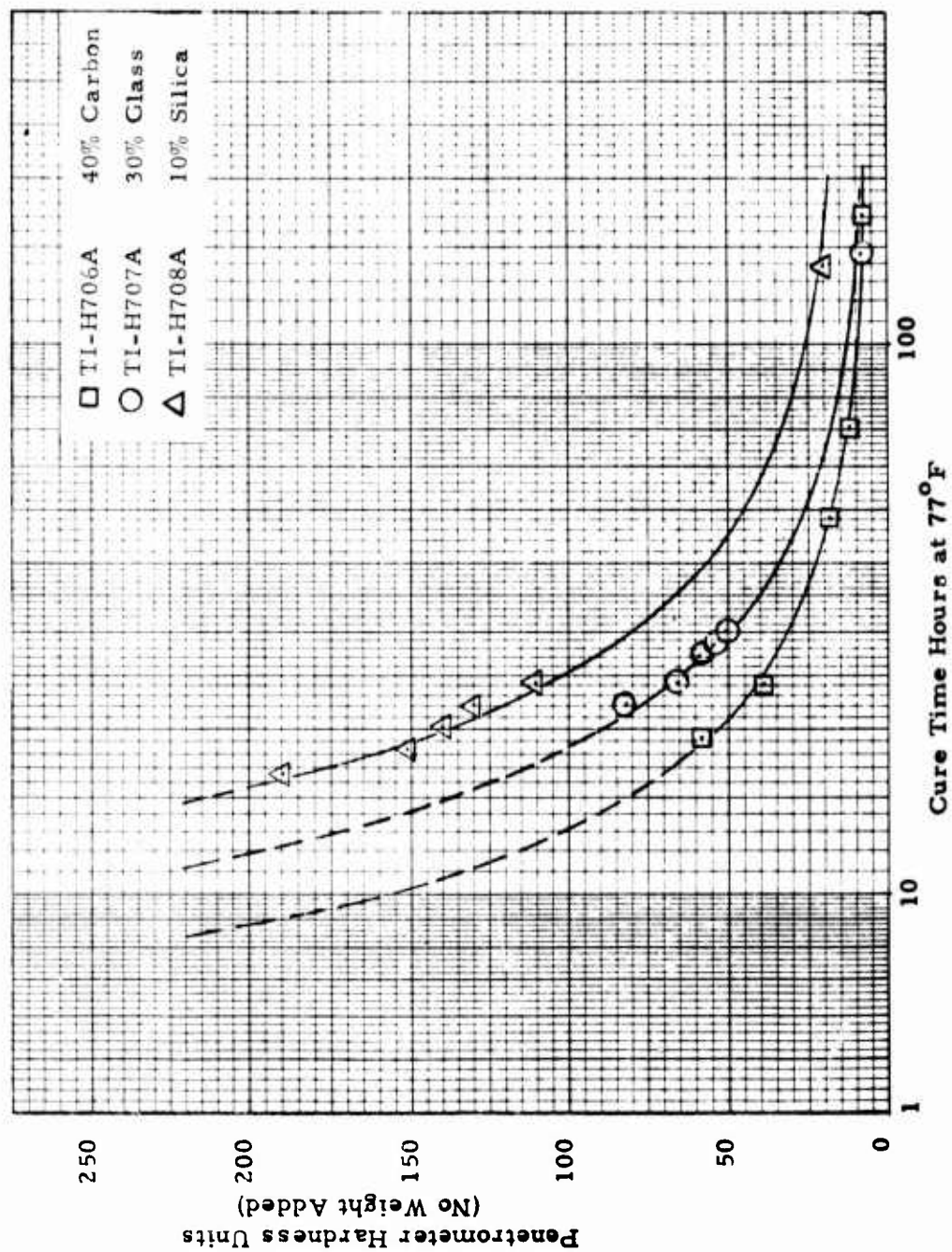


Figure XII-3. Cure Rate of Mastic Insulation

TABLE XII-15

## MASTIC INSULATION - PROCESSING CHARACTERISTICS

Filler	Formulation	Potlife (hrs.)	Cure Time (hrs.)	Viscosity (kp)	Test Temperature				
					Polymer	Cure Agent	Cure Catalyst	P/CA	
40% Carbon	TI-H706A	1.5	100	0.21	77°F	R45M	TDI	Et <sub>3</sub> N (0.1%)	1.0/1
10% Silica	TI-H708A	0.5	138	1.40					
30% Milled Glass	TI-H707A	0.5	144	0.70					

TABLE XII-16  
MASTIC INSULATION BOND, PHYSICAL, AND EROSION PROPERTIES

Material Designation	Filler		Bond to Aluminum Case		Prop. (a) to Insulation		Insulation Properties			Torch Erosion Test		
	%	Type	(psi) at		(psi) at		Stress (psi)	Strain (%)	at			
			-65°F	77°F	-65°F	165°F					-65°F	77°F
TI-H706A	40	Carbon	927	225	129	852	106	32	1589/469	395/469	221/256	Good
TI-H707A	30	Milled Glass	342	130	68	759	151	55	2163/29	466/105	241/41	Poor
TI-H708A	10	Silica	600	64	33	634	44	16	1861/570	337/586	69/282	Excellent

a. Mix T-656.



TABLE XII-17  
EFFECT OF BOND PROMOTER HX-868 ON MASTIC INSULATION BOND TO PROPELLANT (a)

Mix No. (RL-)	Material	Partial Comp.	(b) Tensile Adhesion (psi) at		
			-65°F	77°F	170°F
03777	TA-H732A	DDI/HX-868 DBTDL 206	787	(3TCP, liner pulled loose from plate)	141 (3TCP) 76 (1 P 1 50% P 50% B-L-steel, 1 B-L-steel)
03778	TI-H706A	TDI/Et <sub>3</sub> N 40% Carbon	852	(3TCP)	106 (3TCP) 32 (3P)
03779	TI-H706A (modified)	Same as 03778 + 6% HX-868	837	(2TCP:1 70% TCP, 30% P)	109 (3TCP) 65 (3 P)
03780	TI-H707A	TDI/Et <sub>3</sub> N, 30% Glass	759	(3TCP)	151 (3P) 55 (3P)
03781	TI-H707A (modified)	Same as 03780 + 6% HX-868	831	(3P)	135 (3P) 90 (3P)
03782	TI-H708A	TDI/Et <sub>3</sub> N 10% Silica	634	(3 B-P-mat.)	44 (3TCP) 16 (3TCP)
03783	TI-H708A (modified)	Same as 03782 + 6% HX-868	334	(3 B-P-mat.)	42 (3TCP) 24 (3TCP)

a. Insulation cured 48 hours at 77°F prior to propellant (Mix T-656) application.

b. The number in parenthesis indicates the number of replicates tested and the letters indicate the mode of failure, TCP = thin coat of propellant, P = propellant, I = insulation, B-P-mat. = bond between propellant and material, B-L-steel = bond between liner and steel, B. T. = broken tab.

difference in the bond of the propellant to the insulation with or without the HX-868. TA-H732A is shown on the same table as a baseline or target for the bond of propellant to the insulation. It appears that TI-H707A is comparable to the bond of TA-H732A to propellant. TI-H706A has acceptable bond characteristics. It was during this series of tests that it was realized that liner TA-H731A may be just as good as the TA-H732A (with bond promoter). Additional investigations are warranted if the need for a liner should arise.

A series of acetylene/oxygen torch erosion tests were conducted with the three insulation sleeve materials and the three mastic insulations (Table XII-18). A sample of TI-R300 insulation was used as a control for these tests. Each sample was approximately 0.10-inch thick. A torch was held about three inches from the surface until a hole was burned through the sample. The time required for burning through was measured from the time the torch was applied until the sample burned through. The TI-H708A was the best of the insulation materials. After 12 seconds exposure of the TI-H708A material to the torch, the torch was inadvertently removed from the sample before it burned through. None of the materials were quite as good as the TI-R300 insulation used as the control.

Mastic insulations were compared as shown below. TI-H706A (carbon filled) was selected for evaluation in a TX-631 motor. It showed good bond and has the lowest cost. Erosion resistance in a motor environment was to be determined by the TX-631 tests.

	Relative Ranking (1 = Best)		
	TI-H706A (Carbon)	TI-H707A (Glass)	TI-H708A (Silica)
Cost	1	2	3
Erosion Resistance	2	3	1
Bond to Aluminum			
-65°F	1	3	2
+77°F	1	2	3*
+165°F	1	2	3
Bond to Propellant			
-65°F	1	2	3
+77°F	2	1	3*
+165°F	2	1	3

\*Considered unacceptable

TABLE XII-18  
OXYGEN/ACETYLENE TORCH EROSION TEST

<u>Materials</u>	<u>Time (seconds) to Burn Through 0.10 inch Thickness</u>
<u>Reference Material:</u>	
TI-R300 (Polyisoprene)	25
<u>Mastic Insulation:</u>	
TI-H706A, 40% Carbon	10
TI-H707A, 30% Milled Glass	3
TI-H708A, 10% Silica	No burn through after 12 seconds <sup>(a)</sup>
<u>Insulation Sleeve:</u>	
J-10/40, Nylon	12
G-1200/20, ABS	12
G-50/20, Polycarbonate	17

a. Torch inadvertently removed before burn-through.

## INSULATION SLEEVE

Four adhesive materials were evaluated for bonding the sleeve materials to the aluminum case. Adhesion bond samples were made using the candidate materials, an adhesive and an aluminum plate. In the case of evaluating bond to aluminum, two aluminum plates were used (see Figure XII-4). The data shown on Table XII-19 shows ECCO-BOND-45 to be superior to APCO 1252. TA-H732A is slightly superior to TA-H31A when bonding to aluminum, polycarbonate, ABS and nylon.

Other bond data were obtained for TA-H732A and ECCO-BOND-45 adhesives to the three sleeve materials (Table XII-20). Excellent bond was obtained with the ECCO-BOND-45 to the polycarbonate, ABS, and nylon materials at -65, 77 and 165°F. The bond of the TA-H732A was somewhat less than for the ECCO-BOND-45, but still in an acceptable range for a high elongation type material.

Propellant adhesion samples were made to the three sleeve materials using various primer and bond promoters between the sleeve and the propellant (Table XII-21). The best primer for bonding ambient cured propellant to the cartridge materials was Chemlok 233. The best bond promoter was A-187.

Table XII-22 contains stress and strain values for the cartridge materials at various temperatures.

Cartridge sleeve materials were compared as shown below. Complete tubes could not be obtained because of costs and schedule considerations, so erosion test specimens were made from samples on hand for bond testing. These specimens were installed in the aft end of a TX631 motor to obtain preliminary erosion information. Two materials could be accommodated in the two-slotted motor. Only the polycarbonate and ABS could be heated and formed to match the case interior surface. From these data it should be possible to evaluate erosion resistance of all three.

	Relative Ranking (1 = Best)		
	Polycarbonate	ABS	Nylon
Cost	3	1	2
Erosion Resistance	1	2	2
Bond to Aluminum (all temp.)	OK	OK	OK
Bond to Propellant	OK	OK	OK
Strain Capability			
-65°F	1	3	2
+77°F	1	2	1
+165°F	2	3	1

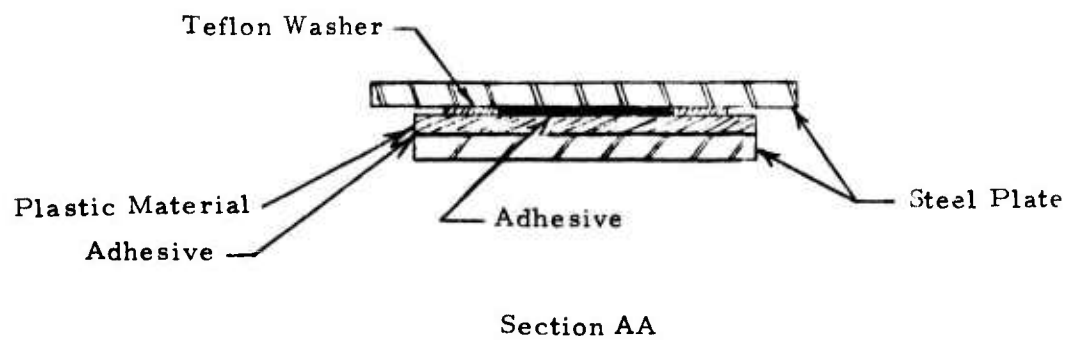
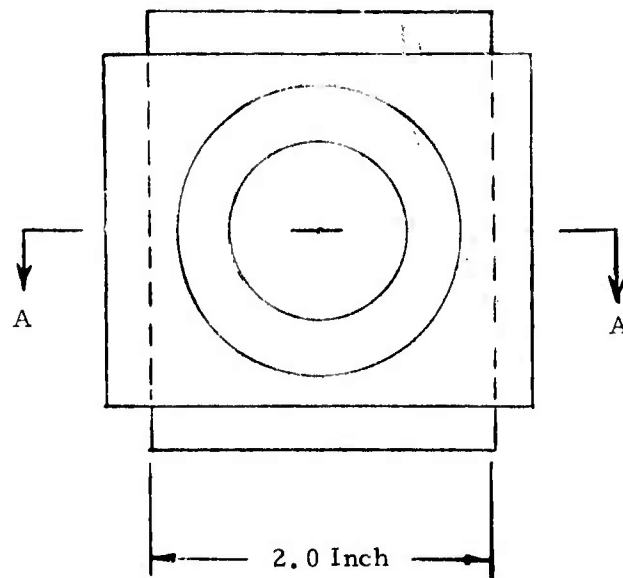


Figure XII-4. Double Plate Test Device for Insulation Sleeve Materials.

TABLE XII-19

ADHESIVES FOR INSULATION SLEEVES  
(Bonding Sleeve to Case)

Candidate Adhesives	Tensile Adhesion (psi)						
	Steel (G.B.) <sup>(a)</sup>	Alum. (G.B.) <sup>(a)</sup>	Polycarbonate		ABS		Nylon J-10/40
			Plain	G.B. <sup>(a)</sup>	Plain	G.B. <sup>(a)</sup>	
APCO #1252	----	53.6	76.6	---	69.6	---	43.6 ---
ECCO-BOND-45	1500	850	631	876	408	247	261 576
Liner TA-H731A	----	105	128	---	93.3	---	107.6 ---
Liner TA-H732A	----	121	119	---	106	---	108 ---

a. G.B. = grit blasted.

**TABLE XII-20**  
**BOND OF SELECTED SLEEVE SYSTEMS**

<u>Selected System</u>	<u>Tensile Adhesion<sup>(a)</sup>(psi) at</u>		
	<u>-65°F</u>	<u>77°F</u>	<u>165°F</u>
Polycarbonate/ECCO-45	840 (3B)	1846 (3B)	197 (3B)
ABS/ECCO-45	1102 (3B)	1049 (3B)	201 (3B)
Nylon/ECCO-45	52 (2B)	1814 (3B)	175 (3B)
Polycarbonate/TA-H732A	987 (3B)	177 (3B)	52 (3B)
ABS/TA-H732A	944 (3B)	229 (3B)	65 (3B)
Nylon/TA-H32A	399 (3B)	246 (3B)	76 (3B)

a. The number in parenthesis indicates the number of replicates tested and letter indicates the mode of Failure: B = Bond. Test sample per Figure XII-4.



TABLE XII-21

## PROPELLANT BOND TO INSULATION SLEEVE

Primers:	Tensile Adhesion <sup>(a)</sup> (psi) at 77°F		
	Polycarbonate	ABS	Nylon
Chemlok 205/234	87 (3 TCP)	65 (3 P)	123 (3 P)
Chemlok 217	110 (3 TCP)	119 (3 P)	125 (3 P)
Chemlok 218	42 (1-50% B-P-mat. and 50% TCP; 1-TCP, 1-B-P-mat.)	19 (3 B-P-mat.)	45 (3 B-P-mat.)
Chemlok 233	146 (3 TCP)	143 (3 P)	173 (3 P)
Chemlok 205	111 (3 TCP)	81 (3 TCP)	109 (3 TCP)
Chemglaze 9924	18 (3 B-P-mat.)	38 (3 TCP)	86 (3 TCP)
<b>Bond Promoters:</b>			
Z-6077	55 (3 TCP)	24 (2 B-P-mat.; B.T.)	46 (2 B-P-mat.; B.T.)
XZ-8-0903	42 (3 B-P-mat.)	52 (3 B-P-mat.)	33 (3 B-P-mat.)
Z-6040	108 (3 P)	32 (3 B-P-mat.)	78 (3 B-P-mat.)
A-187	123 (3 P)	28 (3 B-P-mat.)	72 (3 B-P-mat.)
A-1893	20 (2 TCP; B.T.)	45 (3 TCP)	38 (3 TCP)

a. The number in parenthesis indicates the number of replicates tested and the letters indicate the mode of failure, TCP = thin coat of propellant, P = propellant, I = insulation, B-P-mat. = bond between propellant and material, B.T. = broken tab.

TABLE XII-22  
PHYSICAL PROPERTIES FOR INSULATION  
SLEEVE MATERIALS

	Tensile Ultimate Stress (psi)/ Ultimate Strain (%) <sup>(a)</sup> at		
	<u>-65°F</u>	<u>77°F</u>	<u>165°F</u>
<u>Adhesives:</u>			
APCO #1252	(b)	(b)	(b)
ECCO-BOND-45	(b)	(b)	(b)
EA-946	(b)	2530/103	(b)
TA-H731A	625/642	119/737	102/318
<u>Sleeve Materials:</u>			
Polycarbonate (G 50/20)	14439/7.5	10647/6.8	9537/6.4
ABS (G 1200/20)	7487/2.6	6255/3.9	5147/3.8
Nylon (J 10/40)	14938/5.0	14342/7.0	11634/14.6

- a. Values shown are results of one test series at Thiokol.  
b. Not available from vendors.

### Cartridge Sleeve Fabrication

The feasibility of producing cartridge sleeves from the three baseline materials (three types of glass filled thermoplastics) by injection molding was investigated. The basic materials and dimensional envelope were defined and discussed with the engineering and management staff of a thermoplastic parts vendor. By dividing the tapered cylindrical section (Figure XII-5) into four jointed 11-inch long segments, and then joining to a forward closure, five pieces can be individually injection molded. Joining is by solvent weld for polycarbonate. Tolerances would be on the order of  $\pm 0.006$  to  $0.008$  inch on the 4-inch diameter, with mold and material parameter characterization being required. Another method of fabrication was discussed and found feasible, but probably 20 to 50% more expensive. The technique is that of extruding a single, straight walled cylinder (Figure XII-6), possible grinding to the taper, and joining to a closure (Figure XII-7).

Other discussions with a second vendor elicited their interest in the feasibility of injection molding the complete part, or extruding a large quantity of glass filled thermoplastic tube. Both appear feasible methods. Tolerances on the diameter for the molded part would be approximately  $0.015$  inch. The most significant problem with a "monolithic" molding results from warpage (ovality). This deviation is expected to run  $\pm 1/16$  inch on the diameter. Differences in glass distribution and orientation at various locations within the part will cause localized residual stresses and subsequent deflection (warpage) when the part is removed from the dies.

These two vendors and three others provided budgetary cost quotations for the analyses reported in Section XIII.

### FULL-SCALE MOTOR TESTS

Erosion resistance can be evaluated only qualitatively in the laboratory. Two tests with TX-631 motors were arranged to obtain erosion data on three candidate materials.

The compound TI-H706A (carbon filled) was selected as the mastic insulation because it was the lowest cost of the three; all other properties and characteristics were acceptable. The mastic insulation was used to insulate the entire motor case to find how well it could be applied. The mastic was poured into the motor case and roughly "swept" to the desired .150-inch thickness. The case was then placed on a set of rollers and rotated at approximately 100 rpm for 3 hours. A second coat was applied in a like manner to bring total thickness to 0.250 inch and rotated for 16 hours (over night) at room temperature. The insulation surface appeared very smooth and uniform. No additional preparation was made to the surface prior to casting with propellant.

Polycarbonate and ABS thermoplastics were chosen for the second motor test. Polycarbonate showed the best erosion resistance in laboratory tests, but it has the highest cost. ABS had the worst erosion resistance but the lowest cost. Both had acceptable bond characteristics and physical properties. Since sleeves could not be obtained, material specimens on hand for

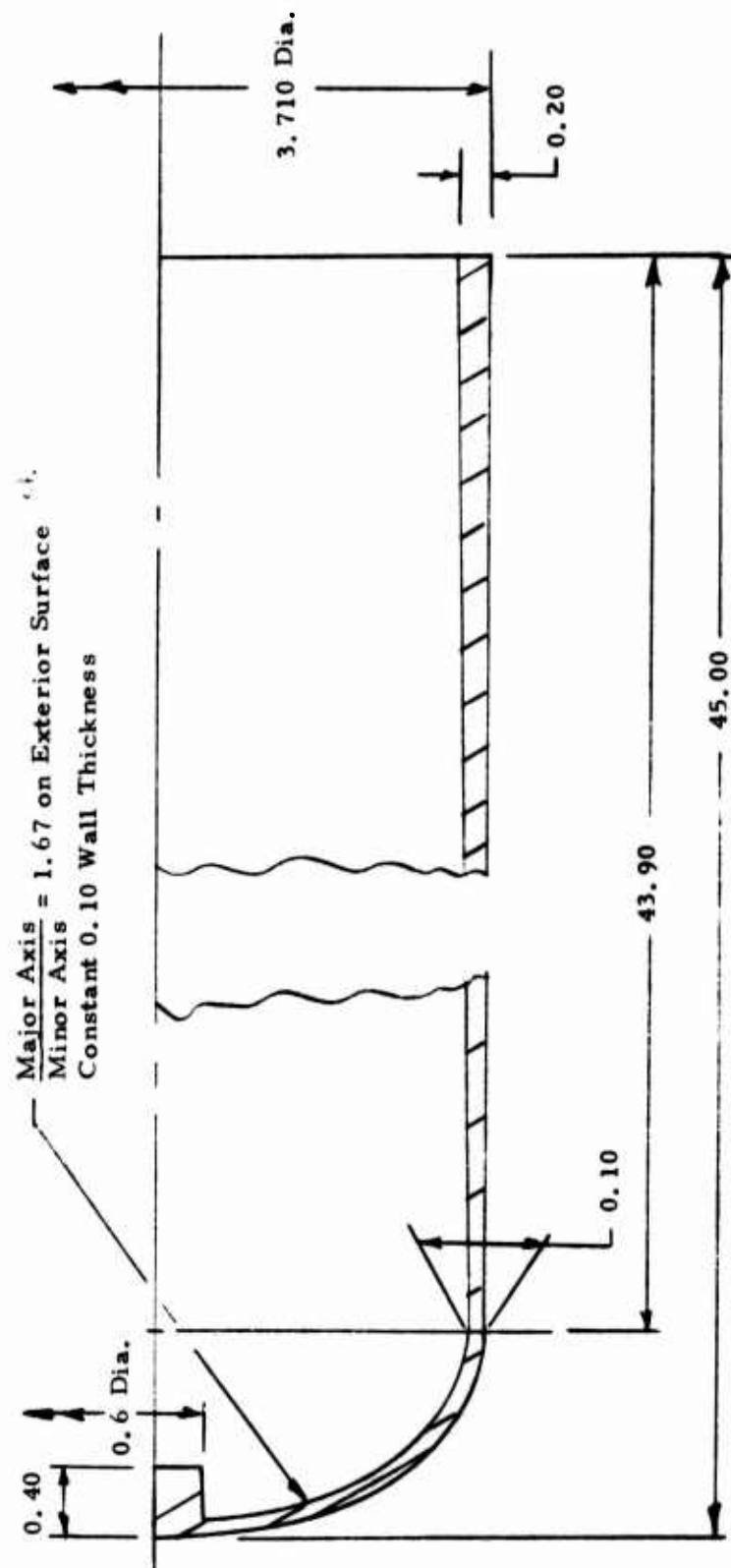


Figure XII-5. Molded Integral Case Insulation Concept.

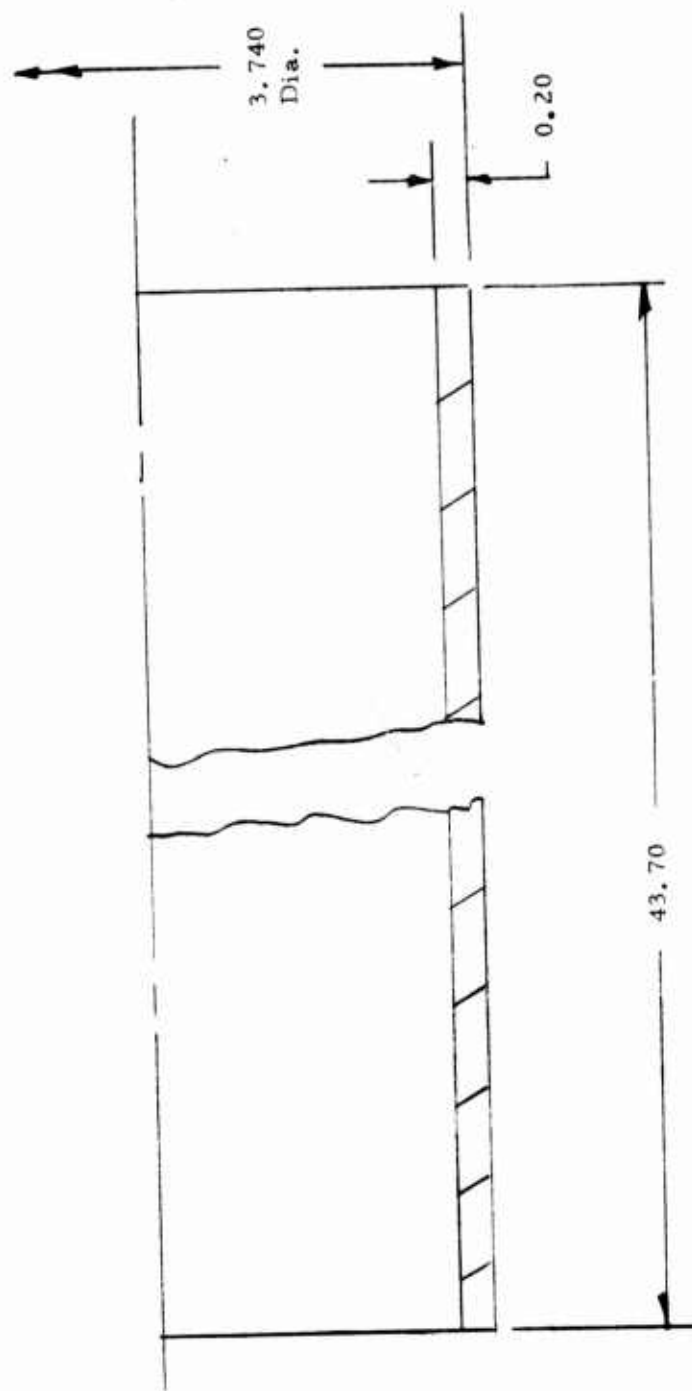


Figure XII-6 Extruded Insulation Sleeve Concept.

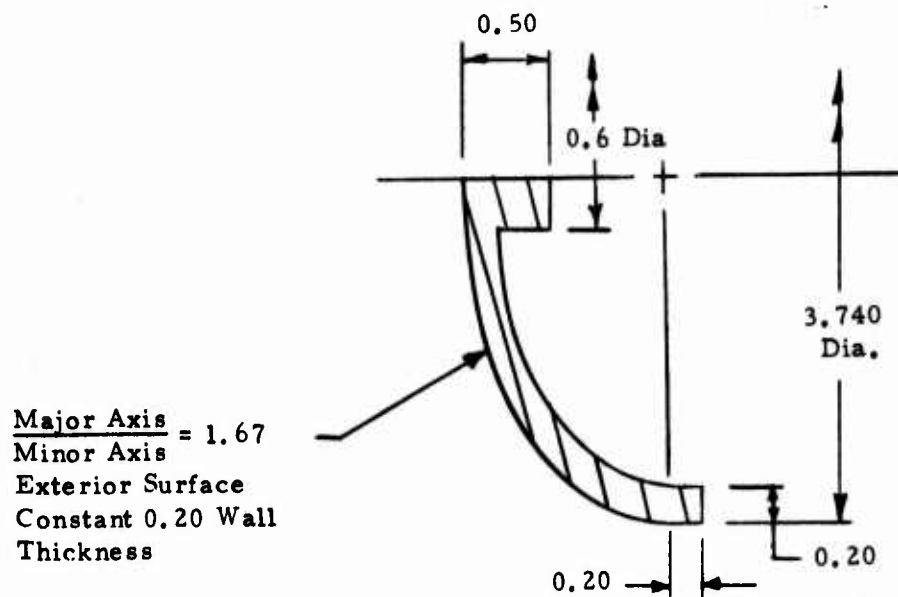


Figure XII-7. Molded Forward Closure Insulation Concept.

bond tests were cut into narrow strips and installed in line with propellant valleys at the aft end of the grain (one sample in each valley).

Two slots were cut out of the TI-R300 polyisoprene<sup>1</sup> insulation in the aft end of the motor. These slots were 180° apart. In one slot a 5-inch long piece of the ABS sleeve material was bonded and the other slot received the polycarbonate material, both bonded with ECCO-BOND-45 adhesive. All surfaces (TI-R300 and sleeve materials) were then primed with Chemlok 234 (the usual primer for TI-R300), which was cured for 4 hours at 170°F. A coat of TA-H732A liner was slush coated on the entire internal surface and cured for 48 hours at 77°F. The motor was then cast with propellant.

Details of the static tests are contained in Section VI. The motor containing the mastic insulation (T684-2) failed at ignition due to over-pressurization. No erosion data were obtained. Post-test investigations determined the failure was due to exposure of a large extra burning surface, but the origin of the surface could not be determined.

The motor with the thermoplastic samples (T684-1) experienced a 0.15 second hang-fire, but a good erosion comparison could be made. The erosion pattern is illustrated in Figure XII-8. Polycarbonate was relatively unscathed while 0.150 inch was ablated from the aft end of the ABS sample. Almost all the ABS was ablated at the forward end of the sample because of flow separation at the junction of the ABS and polyisoprene.

The test of T684-1 motor gave an initial indication of erosion resistance of ABS and polycarbonate thermoplastics in a rocket motor, but additional tests are required for an exact evaluation. If the relative ranking of the two materials is assumed correct, polycarbonate is the more attractive insulator. On an equal cost basis<sup>2</sup>, the polycarbonate can be 60% (see Table XII-7) as thick as the ABS.

Required thickness of ABS = 0.150 inch ablated, plus  
0.050 inch safety factor  
= 0.200 inch  
Thickness of polycarbonate = 0.120 inch for equal cost

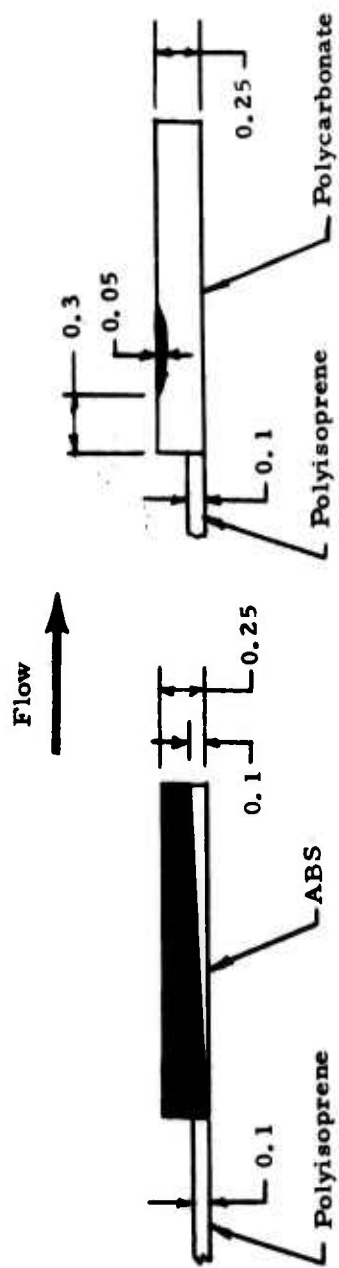
This is a reasonable thickness, but there is no way to be sure it is an adequate thickness until more motor test data are obtained.

#### MATERIAL SELECTION

A single material was selected for each of the various insulation/liner functions, using bond characteristics and cost as primary criteria. The selected materials are shown in Table XII-23, along with various other factors

1. Usual way of insulating the TX-631 motor.
2. Cost per pound of raw material, assuming fabrication costs are identical.





NOTES: (1) Shaded region shows material removed during motor operation

(2) Both samples coated with Chemlok 234 (0.002 in) and liner TA-H732A (0.010 in) prior to propellant loading

Figure XII-8. Erosion Patterns on ABS and Polycarbonate Insulation Samples in TX-631, Mix T684-1

**TABLE XII-23**  
**SUMMARY OF LINER/INSULATION MATERIALS SELECTED FOR**  
**PHASE II EVALUATION**

Selected Material	Use	Source	Availability	Cost (\$/lb.)	EPA Restrict.	Cure Temp.	Erosion (mil./sec.)	Physical Properties at 77°F			Versatility	Remarks
								Ultimate Stress (psi)	Ultimate Strain (%)	Bond		
TA-H732A (a)	Linear	Thiokol Corp.	Excellent	4.56	None	Ambient	N.A.	207	252	Excellent	Excellent	Best bond to prop.
TI-H706A	Insulation	Thiokol Corp.	Excellent	0.90	None	Ambient	10	395	469	Excellent	Excellent	Lowest cost
Chemlok 233	Bond Primer (b)	Hughson Chem.	Excellent	1.53	None	Ambient	N.A.	N.A.	N.A.	Excellent	Excellent	Best of all mat. tested
TA-H731A	Adhesive (c)	Thiokol Corp.	Excellent	1.25	None	Ambient	N.A.	119	737	Excellent	Excellent	Lowest cost
Polycarbongde	Insulation Sleeve	Dart Industries	Excellent	1.50	None	N.A.	6	10,647	5.8	Excellent	Good	Good erosion resistance

a. TA-H731A is potential alternate, at \$1.25/lb., pending additional experimental evaluation.  
b. Propellant-to-insulation sleeve.  
c. Case-to-insulation sleeve.  
d. Laboratory comparison.

which were considered. Figure XII-9 also illustrates the insulation systems. It was further decided that the selected mastic insulation (TI-H706A) and two thermoplastic insulation sleeves (polycarbonate for high erosion resistance and ABS for low cost) should be evaluated further in Phase II full scale motors.

TA-H731A liner was selected to bond the insulation sleeve to the case. Its bond characteristics are satisfactory, as are those of the other three materials (Table XII-19), besides which the subject interface does not have critical structural strength requirements. As developed in Section XIII, an adhesive is used between the sleeve and case to support the grain during motor pressurization. Cost of the TA-H731A raw materials is the lowest of those evaluated.

TA-H731A	\$1.25 per lb.
TA-H732A	4.56
ECCO-BOND-45	7.20
APCO-1252	7.39

However, mixing costs must be included in the total cost associated with using a compounded material. Details are contained in Table XII-24 and summarized below:

	<u>Cost Per Motor to Propulsion Contractor</u>	
	<u>TA-H731A</u>	<u>ECCO-BOND-45</u>
Raw Material	\$0.30	\$1.67
Mixing (Labor and Equipment)	0.16	---
Application (Labor & Equipment)	<u>0.38</u>	<u>0.38</u>
Total	\$0.84	\$2.05

Thus, even with mixing costs included, TA-H731A liner is lower cost.

Chemlok 233 was selected for bonding the propellant to the insulation sleeve. Its bond characteristics were significantly higher for all three thermoplastics than those of the other materials considered (Table XII-21). The two next best materials were Chemlok 217 and Chemlok 205, while A-187 was satisfactory for polycarbonate. Chemlok 205/234 combination was acceptable for nylon sleeves, but has a significant cost penalty because of its two-component approach. Of the acceptable adhesives, Chemlok 233 is the highest cost per pound but such a small amount is used (estimated 0.002 inch thick) that the cost per motor is only about \$0.065. Use of Chemlok 217 would drop the material cost to \$0.044 and application costs would be the same. This small cost difference is insignificant and so the material giving the best

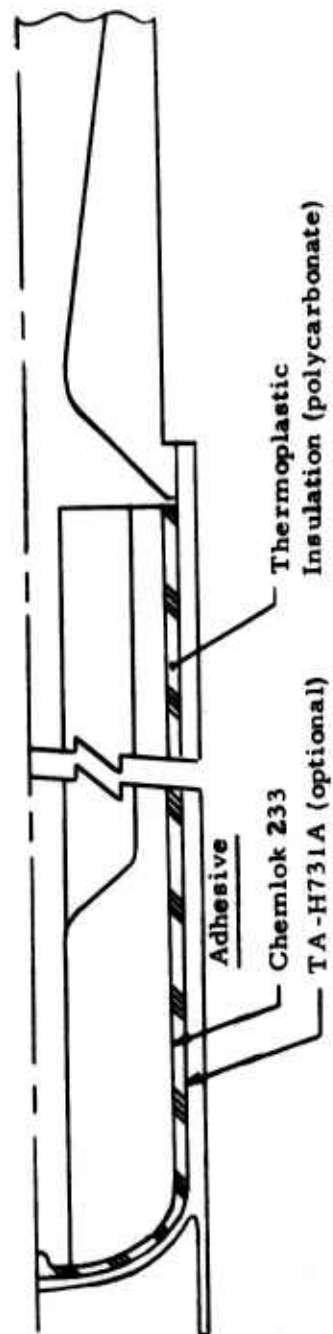
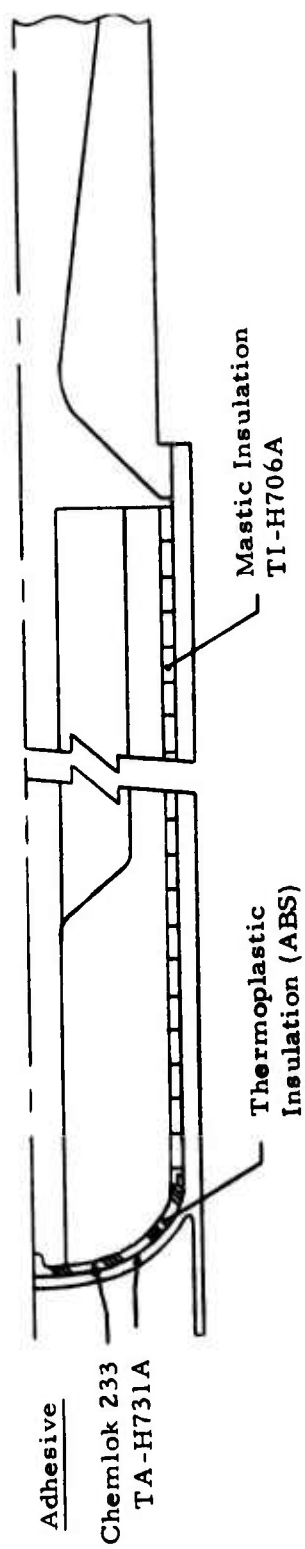


Figure XII-9. Selected Insulation Systems.

TABLE XII-24  
COSTS FOR  
CASE-TO-INSULATION SLEEVE  
BOND SYSTEM<sup>(a)</sup>

ADHESIVE MATERIAL

Assume nominal clearance between case and sleeve = 0.010 in.  
Density = 0.04 lb/cu in  
Weight = 0.21 lb per motor  
Assume 10% excess material applied  
Cost for TA-H731A at \$1.25/lb = \$0.30 per motor  
ECCO-BOND-45 at \$7.20/lb = \$1.67 per motor

APPLICATION

Labor

Assume both materials can be sprayed equally well  
1 minute per sleeve (including transfer) = 60 sleeves per hour  
40 motors per hour required for design production rate  
Thus need 1 station  
Using 2/3 man per station = 0.016 mh/sleeve  
At \$23.00 per mh  
Labor<sup>(2)</sup> = \$0.38 per motor

Equipment

Sprayer only, assume insignificant cost

MIXING

Labor

1 mixer needed  
1/3 man per mixer = 0.008 mh/sleeve  
At \$23.00 per mh<sup>(b)</sup>  
Labor = \$0.13 per motor

Equipment

1 mixer at \$30,000  
Amortized over 1,200,000 motors  
Equipment = \$.030 per motor

TOTAL PER MOTOR	TA-H731A	\$0.84
	ECCO-BOND-45	\$2.05

- 
- a. Cost to Propulsion Contractor  
b. Labor rate includes factor for "non-touch" support labor

bond characteristics should be used. For completeness, an estimate was made of the total cost for the propellant-to-insulation sleeve bond system (see Table XII-25 for details).

	Cost to Propulsion Contractor (per motor)
Adhesive (Chemlok 233)	\$0.065
Application Labor	0.383
Equipment	<u>0.016</u>
TOTAL	\$0.464

TI-H706A was selected as the mastic insulation. It is the lowest cost mastic (Table XII-7), ranked second in erosion resistance (Table XII-18), and ranked either first or second in bond characteristics (Table XII-16), all of which were satisfactory.

TA-H732A was selected as the liner, should a need arise for its use. It showed acceptable bond to propellant (Table XI-9). A cost savings can be realized by using the TA-H731A version which does not contain HX868 bond promoter, a very expensive ingredient. Tests with and without HX868 in the mastic insulations showed little difference in the bond characteristics. Additional tests are warranted for the liner.

Glass-filled polycarbonate was selected as the insulation sleeve. Although it is the most expensive (per pound) of the three thermoplastics considered, its better resistance to erosion may allow a thinner part to such an extent that cost per sleeve could be the same for polycarbonate and ABS (which is 60% the cost of polycarbonate).

#### SUMMARY AND RECOMMENDATIONS

The following materials were selected for Phase II evaluation:

- a. TA-H731A to bond insulation sleeve to case
- b. Polycarbonate as primary insulation sleeve
- c. ABS as secondary insulation sleeve
- d. TI-H706A as mastic insulation
- e. Chemlok 233 to bond insulation sleeve to propellant

Other findings from this investigation were:

- a. TA-H732A is a suitable liner for bond to propellant.

TABLE XII-25  
COSTS FOR  
PROPELLANT-TO-INSULATION SLEEVE  
BOND SYSTEM<sup>a</sup>

ADHESIVE MATERIAL

Assume thickness = 0.002 inch  
Density = 0.04 lb/cu in  
Weight = 0.042 lb per motor  
For Chemlok 233 at \$1.53/lb  
Material cost = \$0.065 per motor.

APPLICATION

1 minute per sleeve (including transfer) =  
60 sleeves per hour  
40 motors per hour required for design production rate  
Thus need 1 station  
Using 2/3 man per station = 0.016 mh/sleeve  
At \$23.00 per mh<sup>b</sup>,  
Labor = \$0.383 per motor

EQUIPMENT

Applicator (1 at \$20,000)  
Amortized over 1,200,000 motors  
Equipment = \$0.016 per motor

TOTAL PER MOTOR	\$0.464
-----------------	---------

- a. Cost to Propulsion Contractor.  
b. Labor rate = \$23.00 per hour and includes factor for "non-touch" support labor.



- b. There does not appear to be any improvement in the bond of TA-H732A, TI-H706A, TI-H707A, or TI-H708A to the insulation sleeve by incorporating HX868 bond promoter in the compounds.
- c. Erosion resistance of mastic insulation in laboratory tests ranked: 1st: TI-H708A (with silica); 2nd: TI-H706A (with carbon); 3rd: TI-H707A (with glass)
- d. Erosion resistance of thermoplastic insulation sleeves ranked: 1st: polycarbonate; 2nd: ABS and nylon

The following investigations are recommended:

- a. Evaluate TA-H731A as liner to validate that HX868 is not needed.
- b. Tailor TA-H731A and adapt equipment for spray application.
- c. Conduct additional laboratory evaluation of all selected bond systems at temperature extremes and after service-life aging.
- d. Characterize thermoplastic materials, viz, glass-filled polycarbonate and ABS for thermal properties to facilitate insulation analyses.

Note that insulation on the forward dome, as illustrated in Figures XII-7 and XII-9, may not be needed if the forward closure for the pressure vessel is made of a heat, resistant plastic (e.g., glass-filled polycarbonate) and if the design provides for some degradation of pressure capability where the inner surface is ablated. The heating environment at the forward closure is less severe, relatively, than elsewhere in the motor; it will be fairly straightforward to combine the pressure vessel and insulation functions in a single component.

SECTION XIII

GRAIN DESIGN AND PERFORMANCE STUDY

## SECTION XIII

GRAIN DESIGN AND PERFORMANCE STUDY

Ballistic and trajectory analyses were performed to evaluate the effects of nozzle throat erosion rate, case strength level, propellant performance characteristics, thrust profile and insulation thickness on missile performance. Additional studies determined cost and performance differences between case bonded and cartridge loaded grains and between molded thermoplastic and mastic insulations. These studies started, in effect, with preparation of a baseline motor preliminary design, which is described in Section III.

Since the baseline motor was designed, an additional performance requirement was imposed---velocity out of an 8.4 ft.<sup>1</sup> launch tube of 200 ft/sec. All other original requirements (Section III) were maintained, with the reduced diameter at the aft end being 3.29 inches (providing a nozzle exit diameter of 2.96 inches). Design pressure factors were as in Section III. Drag coefficient is detailed in Appendix C. Baseline nozzle throat erosion rate (Section III) was used as the baseline rate in this study. Increases in erosion rate were incorporated into the calculations as multipliers on the rate, while keeping the same pressure exponent of 0.824. Nozzle exit divergence half angle was 8 degrees for the baseline motor calculations, but in the subject study when initial throat diameter was varied from 0.925 inch, the exit angle was changed to maintain the original nozzle length. Case wall thickness and concomitant case weight was adjusted to be compatible with the maximum pressure calculated for any given design perturbation. The baseline propellant for this study (and the Section III design) contains 88% total solids made up of 12% aluminum and 76% AP; other propellants considered are described in Table XIII-1. Propellant burn rate was held constant for portions of the study and varied for others, as discussed in the following text.

GENERALIZED PERFORMANCE STUDY

The propellant grain has a cylindrical-perforation in the forward portion and two longitudinal slots in the aft portion. The number of slots can be changed to three or more (up to a limit imposed by cross-sectional dimensions) without affecting the general findings of the subject study.

First phase of the subject study varied the length of the longitudinal slots to determine the effect on internal ballistic behavior and concomitant trajectory characteristics. Calculations were made with the following sets.

## Propellant Formulations

Total Solids (%)	88	86	86
Aluminum (%)	12	12	15

1. The length of the launch tube was estimated by the investigator from information available about the probable length of the warhead and the known motor length.

TABLE XIII-1

PROPELLANT CHARACTERISTICS

Formulation (TS/AL)	88/12	86/12	86/15
Characteristic Velocity, $C^*$ (ft/sec)	5215	5195	5220
Density, Cured, $\delta_f$ (lb/cu in)	0.0630	0.0617	0.0621
Burn Rate at 1000 psia, $r_b$ (in/sec)	0.42	0.42	0.42
Pressure Exponent, $n$	0.5	0.5	0.5
Temperature Coefficient of Pressure, $\pi_k$ (per °F)	0.001	0.001	0.001

Case Ultimate Strength (psi)	78,000
	60,000
	42,000
Throat Erosion Rate (% of baseline rate)	100
	150
	200
	250

Typical results are illustrated in Figures XIII-1, XIII-2 and XIII-3. Maximum pressure (Figure XIII-1) is dependant on grain configuration and throat erosion rate for a given initial throat diameter<sup>1</sup> and propellant formulation. For the short slots the grain configuration is highly progressive but high throat erosion rates cause maximum pressure to be lower. Burnout velocity increases with decreasing slot length (Figure XIII-2) which reflects the influence of higher propellant weight with the shorter slots. Thrust history is regressive with the longer slots and progressive with the shorter slots (Figure XIII-3). A typical thrust and pressure history is shown in Figure XIII-4. One of the more interesting findings comes from Figure XIII-2, which shows that burnout velocity is little affected by throat erosion rate at the smaller slot lengths. This would indicate that non-reproducibility of throat erosion rate at these conditions would have smaller influence on missile performance than at the longer slots.

It was known from the baseline motor design (Section III) that a launch angle of -30 degrees was physically incompatible with a launch altitude of 6000 feet and a slant range of 12,000 feet. Preliminary calculations showed a -28 degree launch angle would be appropriate. The subject study further considered launch angle with the results shown in Figure XIII-5. For two widely different set of conditions, launch angle was varied to determine its effect on slant range. It was found that a change of one degree in launch angle caused a 340 feet change in slant range. Thus it is argued that since the original -28 degree angle was more-or-less arbitrarily selected, it is acceptable to assume that launch angle can be a unique value for each design point. Furthermore the slant range calculated for all sets was close to 12,000 feet so that it can be stated the slant range requirement is met at all design points.

Another generalized result of the subject study is shown in Figure XIII-6. Anytime the burnout velocity requirement was met (ratio greater than 1.0), the impact velocity for that design point was also greater than the required value. The points shown on Figure XIII-6 are performance levels from a large number of design sets (throat erosion rate and slot length) for the two basic conditions shown on the figure, which represent the highest and the lowest performance systems considered in the study. From this it is concluded that meeting the burnout velocity requirement begets meeting

1. An initial throat diameter of 0.925 inch, determined in the baseline motor design (Section III), was used throughout this study (until as noted). Subsequent discussions will show the effect of varying initial throat diameter.

88% Total Solids  
 12% Aluminum  
 Initial Throat Diameter, DTI = 0.925  
 Baseline RE = 0.033 in/sec at 1000 psia

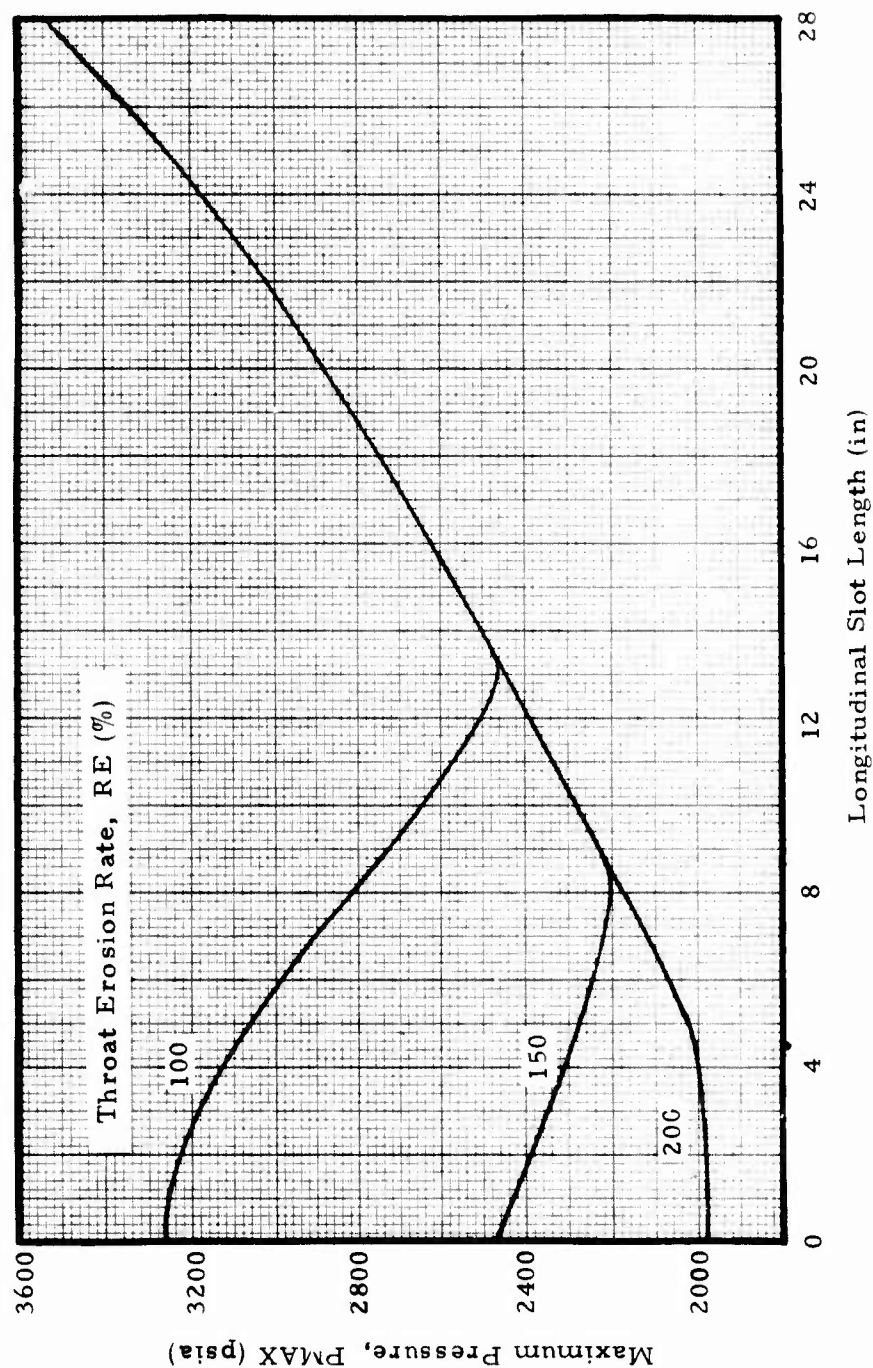


Figure XIII-1. Variation of Maximum Pressure With Slot Length

88% Total Solids  
 12% Aluminum  
 Baseline RE = 0.033 in/sec at 1000 psia  
 Case Ultimate Strength = 78,000 psi

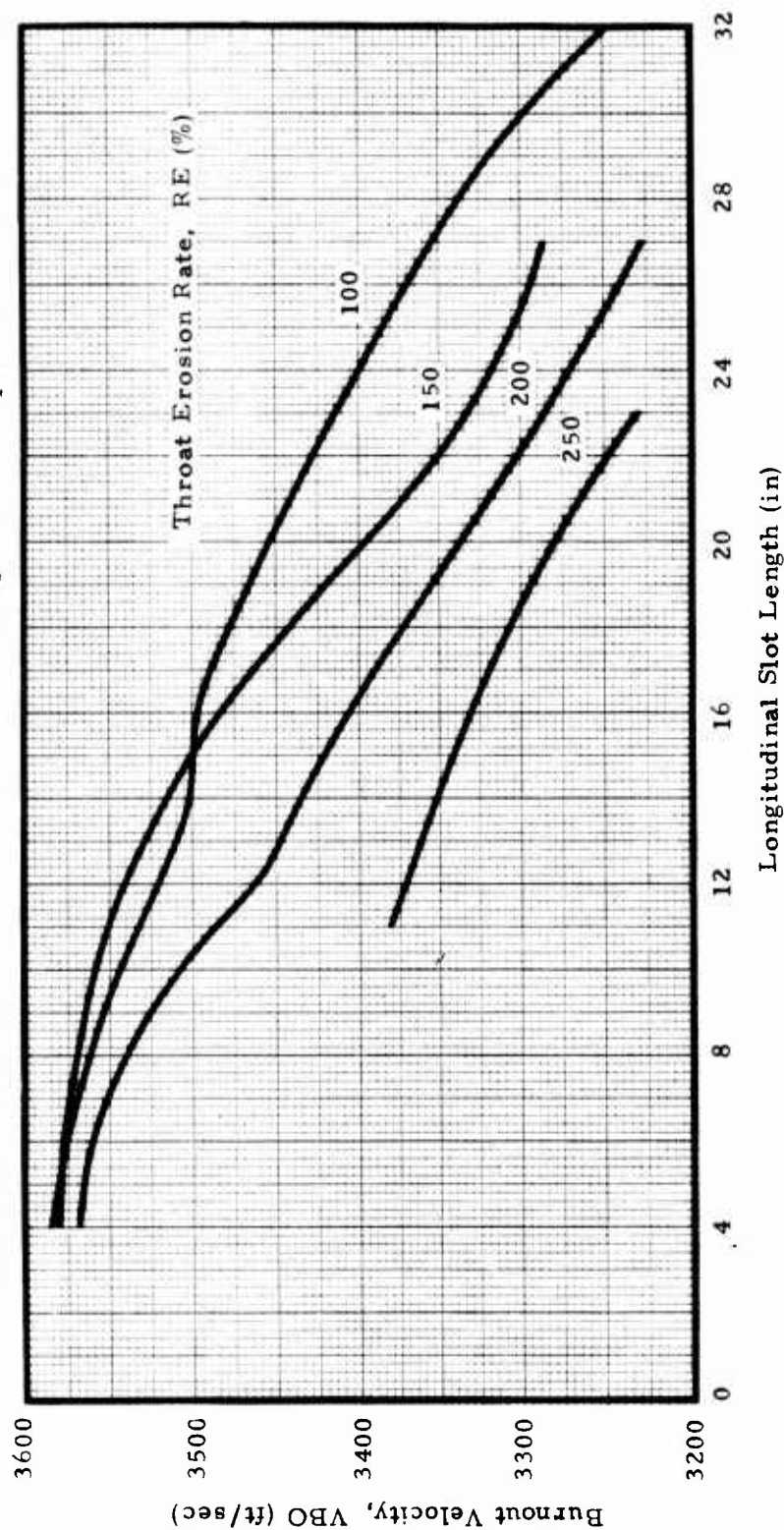


Figure XIII-2. Variation of Burnout Velocity with Slot Length



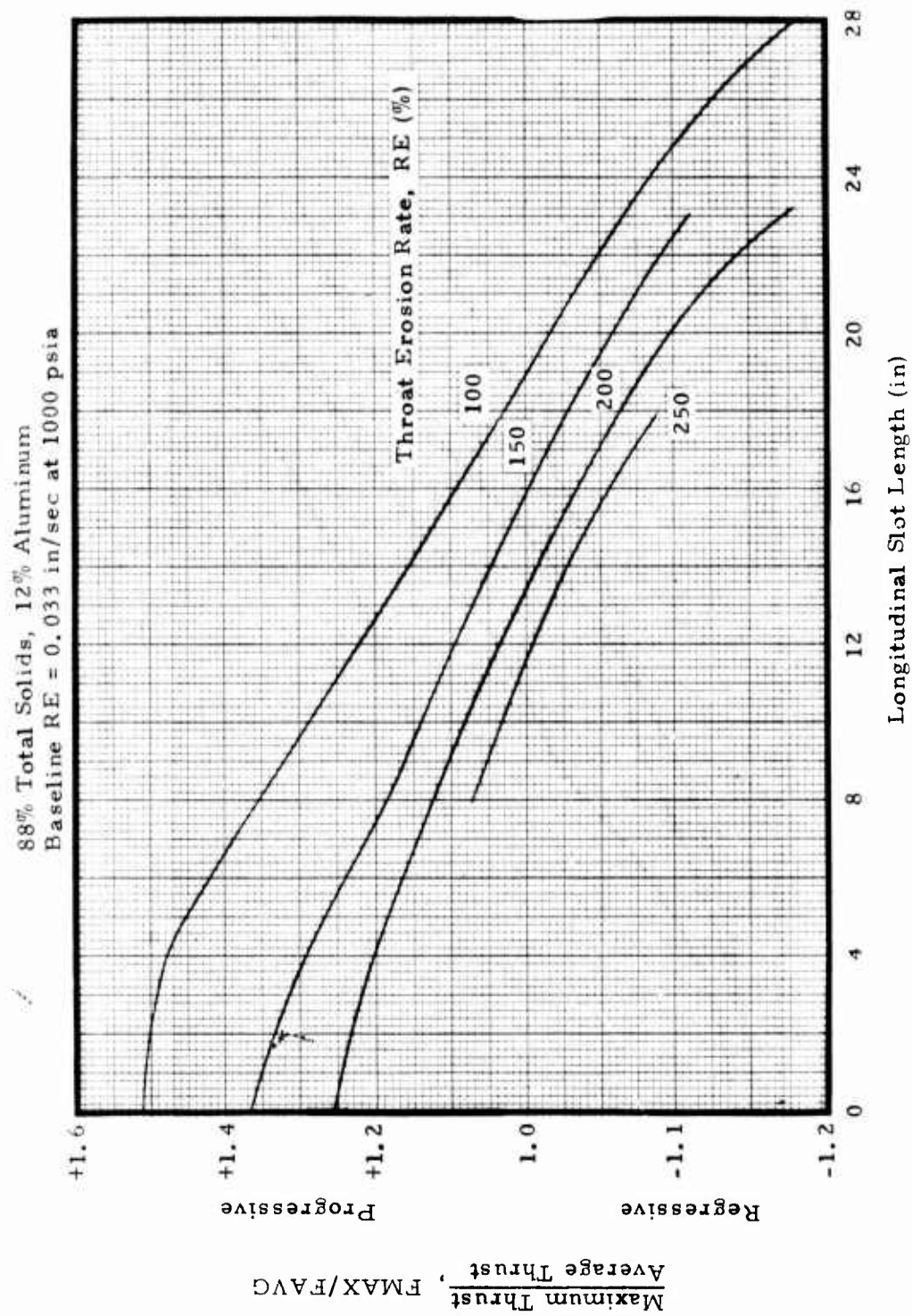


Figure XIII-3. Variation of Thrust Profile with Slot Length

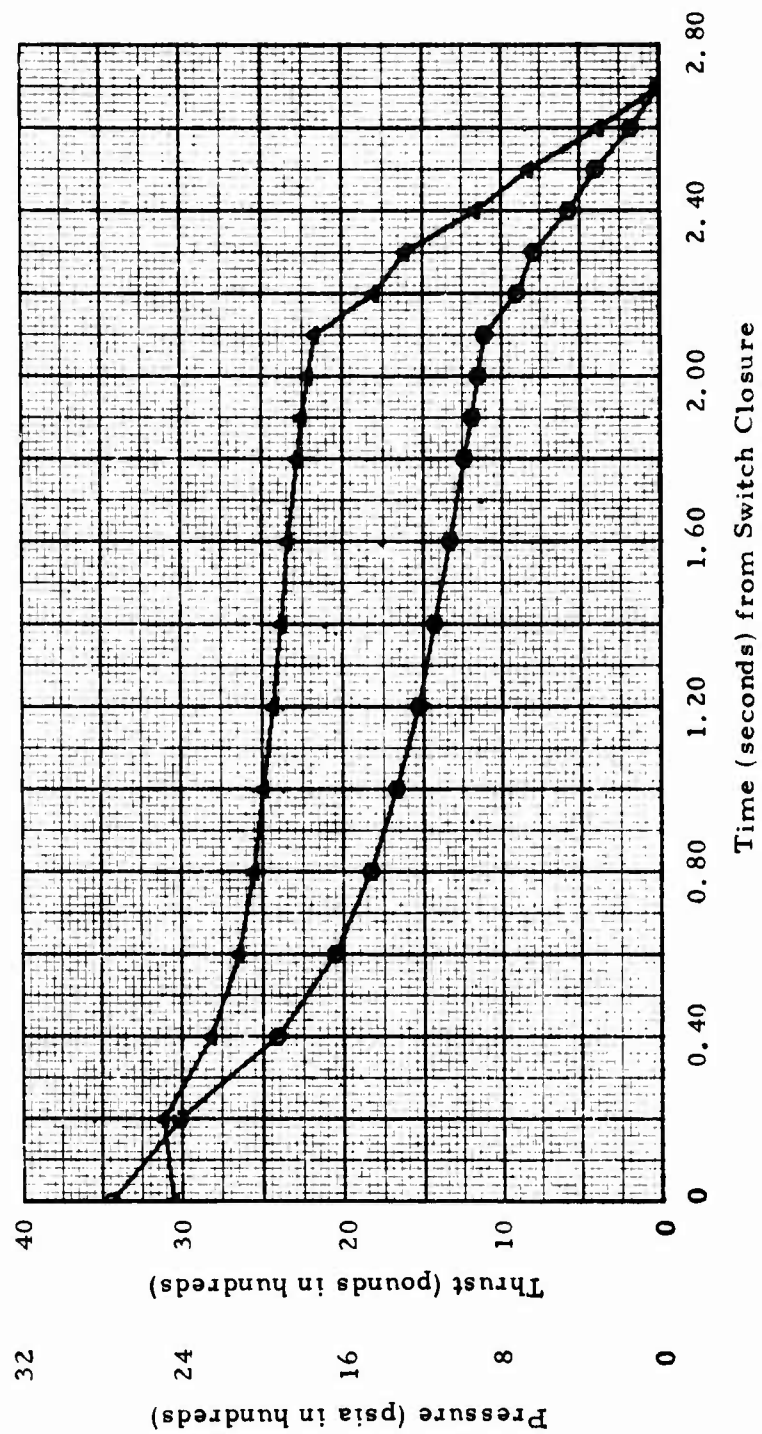


Figure XIII-4. Typical Pressure and Thrust Histories

	<u>I</u>	<u>II</u>
Total Solids (%)	88	86
Aluminum (5)	12	15
Rate at 1000 psia	.42	.32
Case Strength (ksi)	78	42
Nozzle Erosion Rate (% of Baseline)	200	200
Burn Out Velocity (ft/sec)	3520	3250
Maximum Pressure (psia)	2180	2380
Slot Length (in)	8	10
Thrust Trace Shape	Prog.	Level
FMAX/FAVG	1.12	1.0

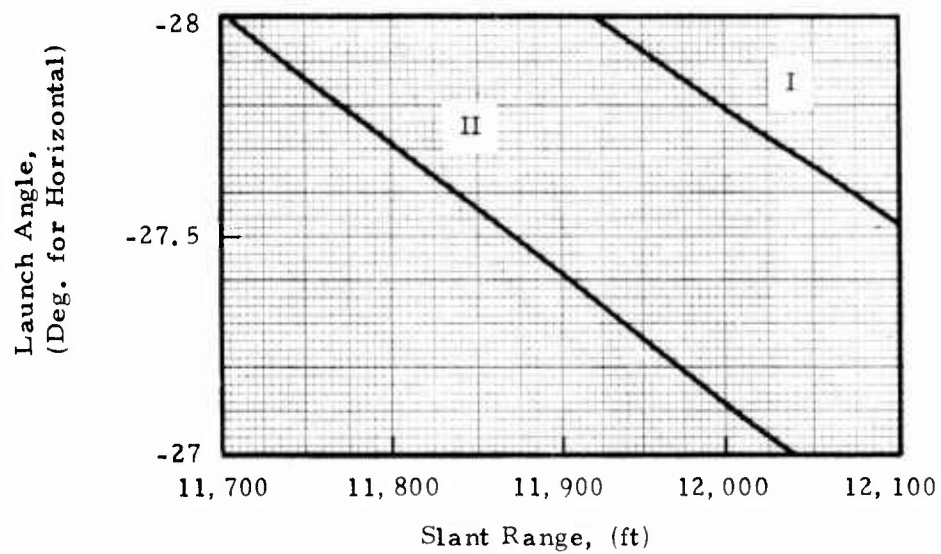


Figure XIII-5. Effect of Initial Launch Angle on Slant Range

Points shown represent performance delivered by following combinations:

<u>Total Solids</u>	<u>Alum.</u>	<u>Cas: Stg.</u>
88%	12%	78,000 psi
86%	12%	42,000 psi

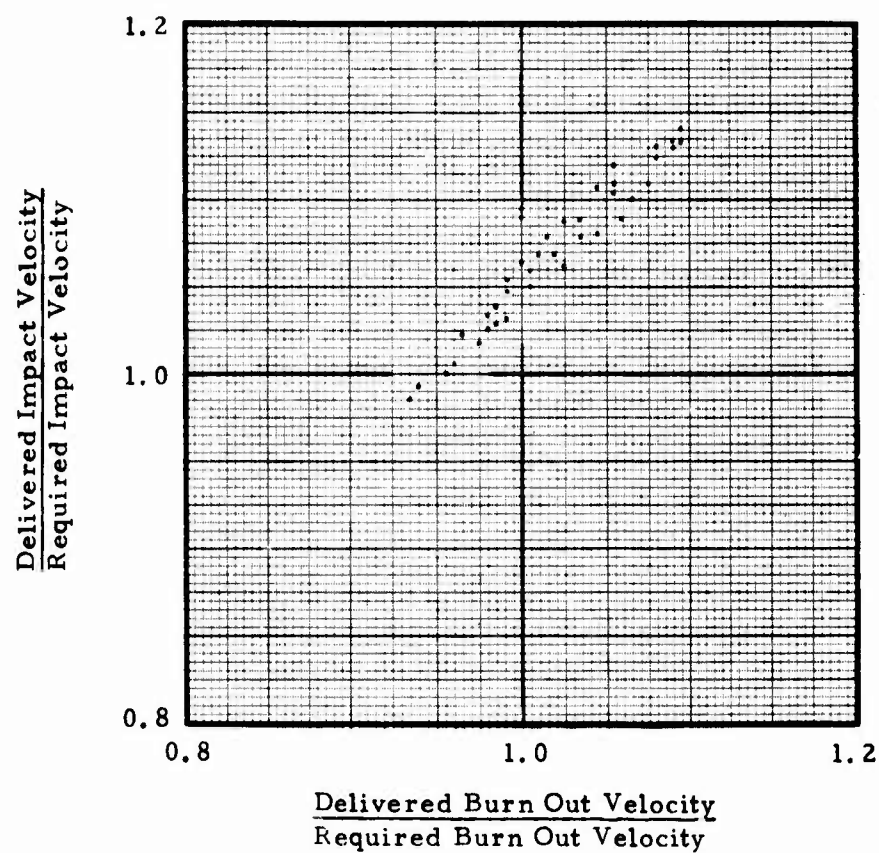


Figure XIII-6. Relationship Between Burnout Velocity and Impact Velocity for Selected Conditions

the impact velocity requirement for the entire spectrum of design points considered in the subject study.

One last generalized finding is that thrust history alone does not greatly affect the missile performance (Table XIII-2). Three idealized thrust histories, all producing 5000 lb-sec total impulse, produced essentially identical performance results. Thus the effect of thrust history (as described by the ratio of maximum thrust to average thrust) shown on subsequent figures is caused mostly by the change in total impulse resulting from changing longitudinal slot length with the accompanying change in propellant weight.

Plots of thrust ratio ( $F_{MAX}/F_{AVG}$ ) versus slot length (e.g., Figure XIII-3) were used to determine the slot length at which  $F_{MAX}/F_{AVG}$  was equal to 1.0, 1.1, and 1.2. At these same slot lengths, the concomitant burnout velocity was found from plots such as Figure XIII-2. These values were used to create a series of illustrations to show the influence of thrust history ( $F_{MAX}/F_{AVG}$ ), case ultimate strength ( $\sigma_u$ ) and throat erosion rate (RE) on burnout velocity (VBO).

All of the combinations above a burnout velocity of 3290 ft/sec represent design points that satisfy all performance requirements. With a case ultimate strength of 78,000 psi, there are many possibilities (Figure XIII-7). For example, even when total solids are reduced to 86%, throat erosion rates of 200% (of baseline) can be used and still meet requirements (with a level thrust history). Conversely, a thrust history that is 20% regressive can be provided with the same propellant at RE = 100% in a motor that meets the VBO requirement.

On the other hand, when  $\sigma_u = 60,000$  psi is incorporated, the region above VBO = 3290 ft/sec is greatly reduced in area (Figure XIII-8). None of the design points with 86% total solids, 12% aluminum propellant exceeds required VBO. Thrust histories must be neutral or only slightly regressive.

The same information in a different form is shown in Figures XIII-9, XIII-10, and XIII-11 for the three propellant formulations. Again the region above VBO = 3290 ft/sec encompasses those design points that meet requirements.

These calculations reveal the need to use a propellant having high energy content and density in order to provide the most flexibility to the design process. With a propellant of 88% total solids, 12% aluminum (or even greater aluminum content), the final design can consider incorporation of nozzles with high throat erosion rate and cases with low strength levels, both of which will lead (hopefully) to lower costs.

TABLE XIII-2

EFFECTS OF THRUST HISTORY

Total Impulse (lb/sec)	5000
Burn Time (sec)	2
Total Missile Weight (lb)	87.57
Propellant Weight (lb)	25.16

	<u>20% Progressive</u>	<u>Level</u>	<u>20% Regressive</u>
VBO (ft/sec)	2808	2801	2794
VIMP (ft/sec)	2469	2466	2463
SR (ft)	11,768	11,805	11,842



Case Ultimate Strength,  $\sigma_u = 78,000$  psi  
 Baseline RE = 0.033 in/sec at 1000 psia

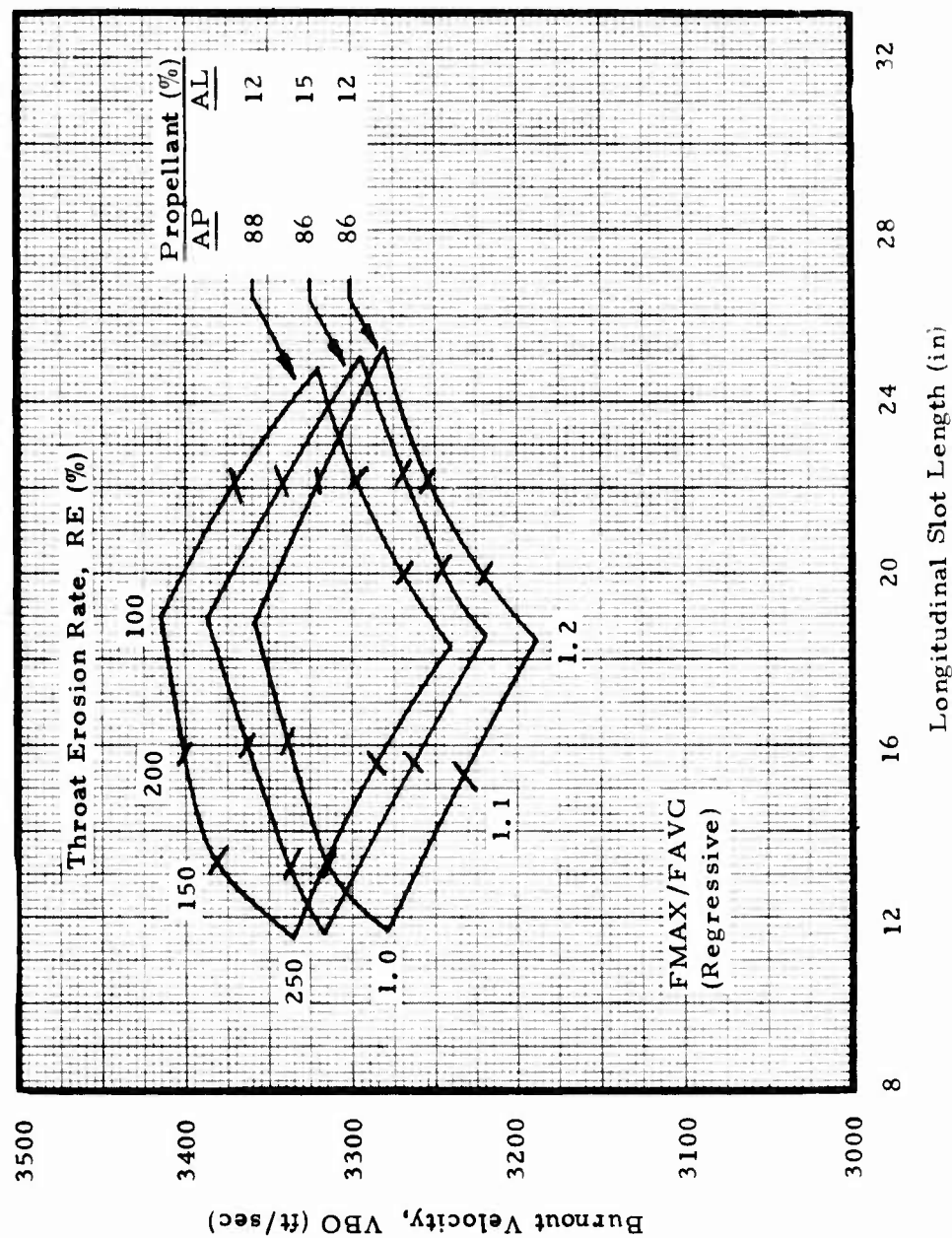


Figure XIII-7. Performance Map of Possible Motor Designs,  $\sigma_u = 78,000$  psi



Case Ultimate Strength,  $\sigma_u = 60,000$  psi  
 Baseline RE = 0.033 in/sec at 1000 psia

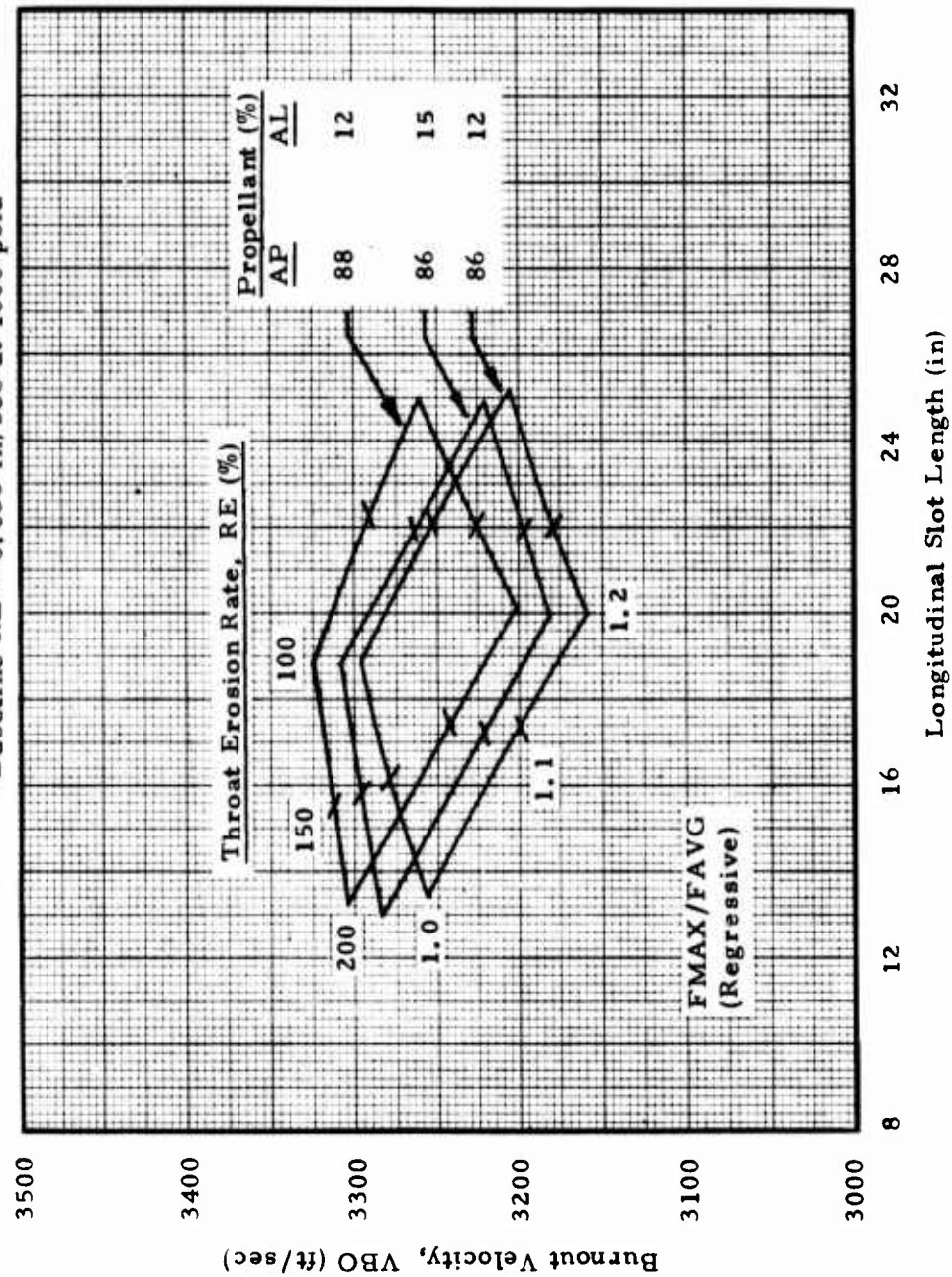


Figure XIII-8. Performance Map of Possible Motor Designs,  $\sigma_u = 60,000$  psi

88% Total Solids  
12% Aluminum

Baseline RE = 0.033 in/sec at 1000 psia

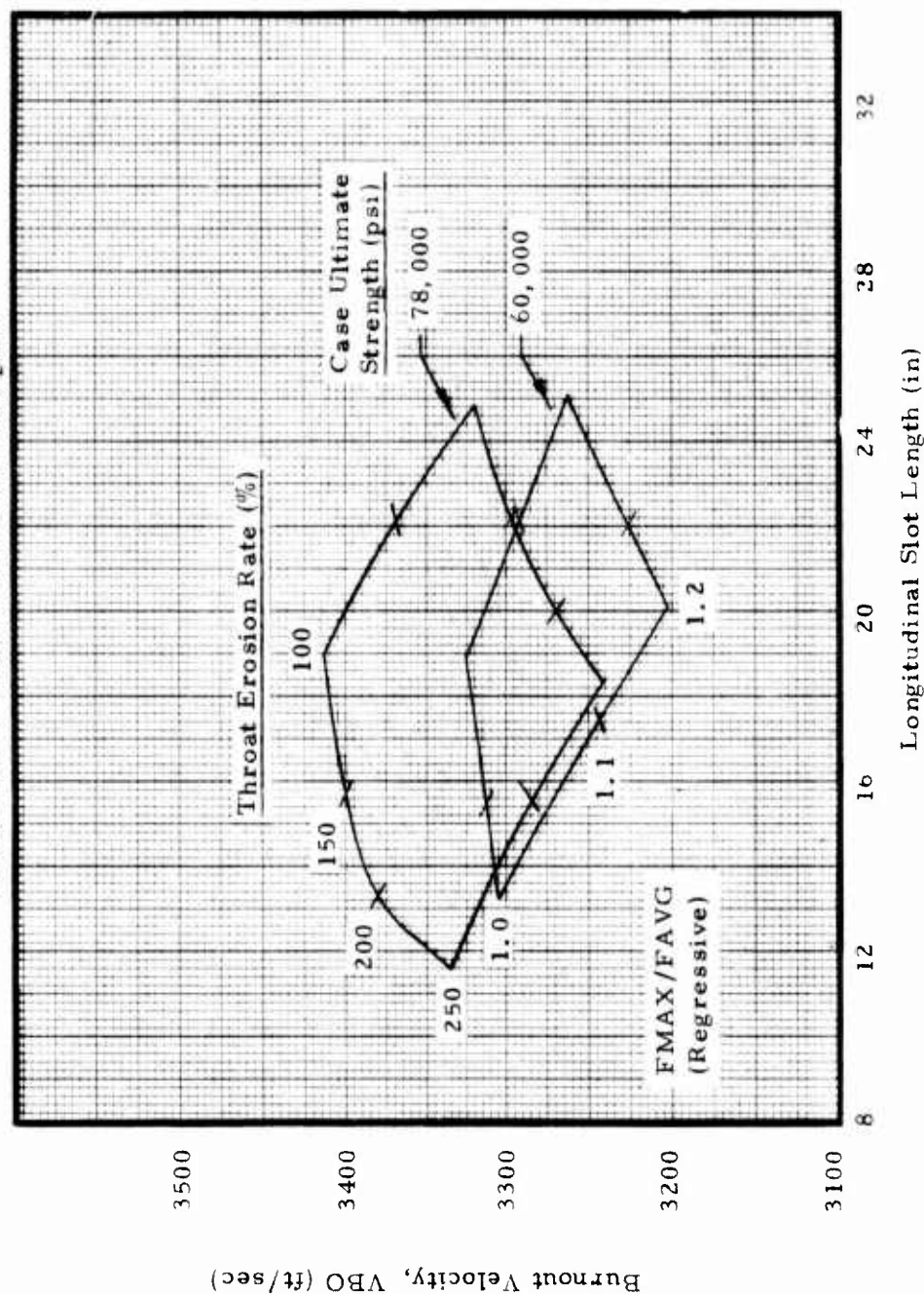


Figure XIII-9. Performance Map of Possible Motor Designs, 88% Total Solids

86% Total Solids  
 12% Aluminum  
 Baseline RE = 0.033 in/sec at 1000 psia

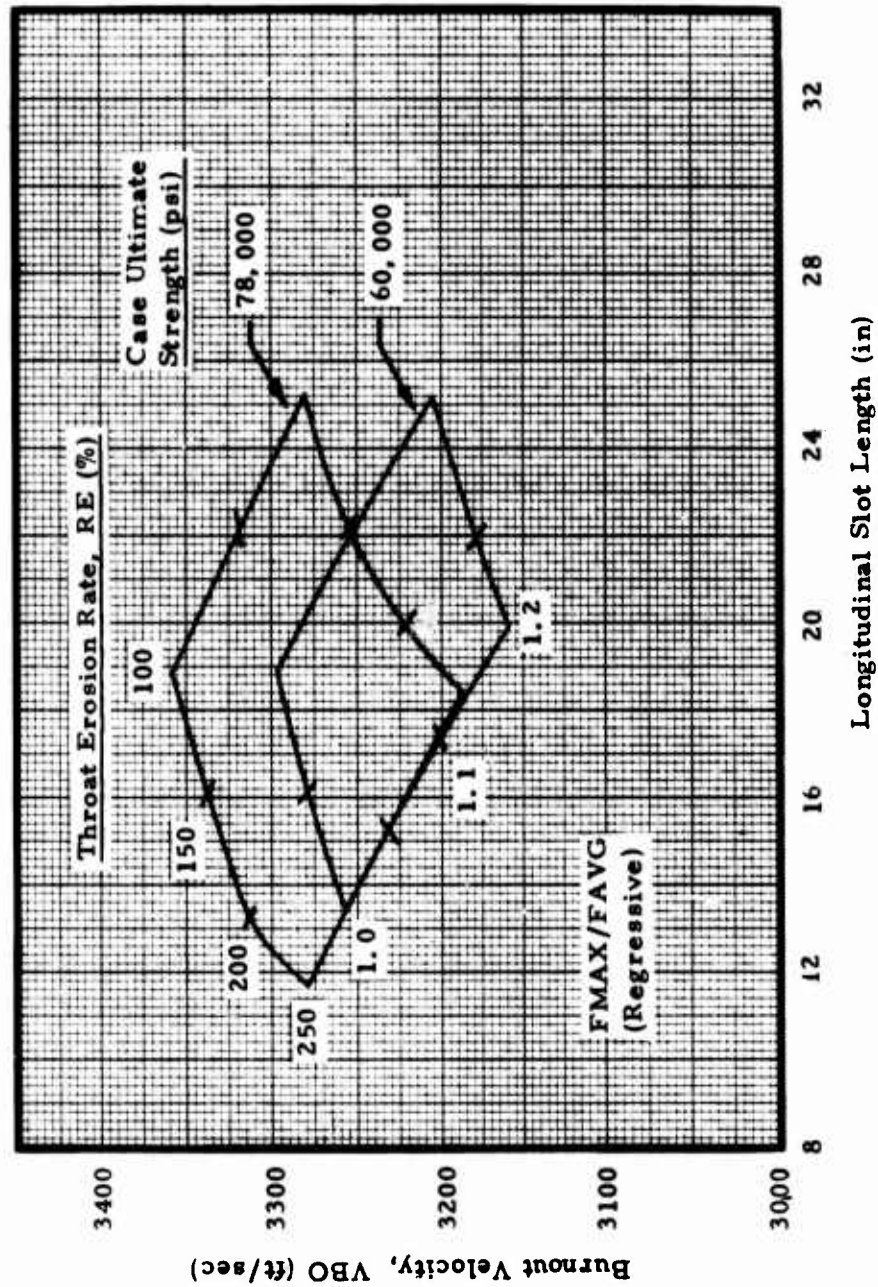


Figure XIII-10. Performance Map of Possible Motor Designs, 86% Total Solids

86% Total Solids  
 15% Aluminum  
 Baseline RE = 0.033 in/sec at 1000 psia

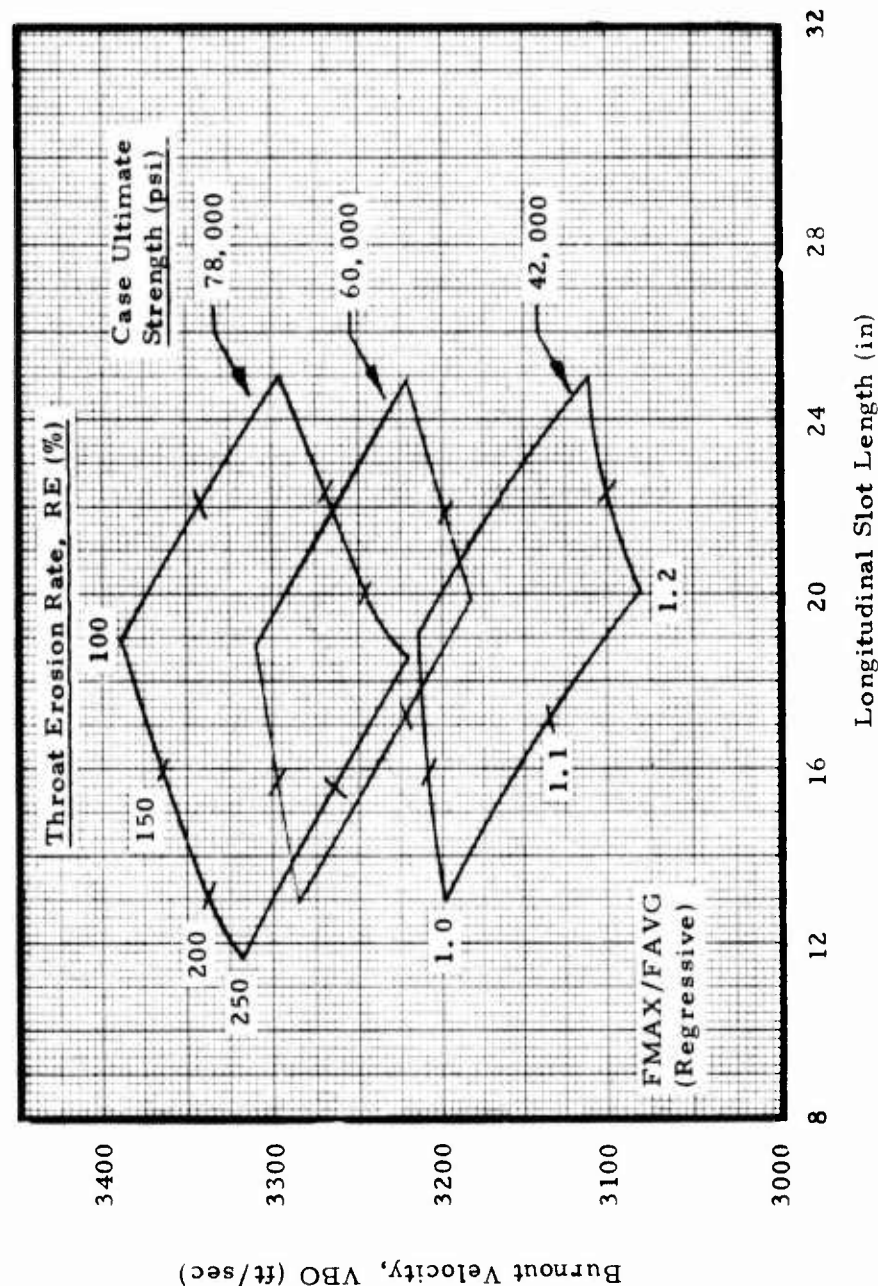


Figure XIII-11. Performance Map of Possible Motor Designs, 86% Total Solids



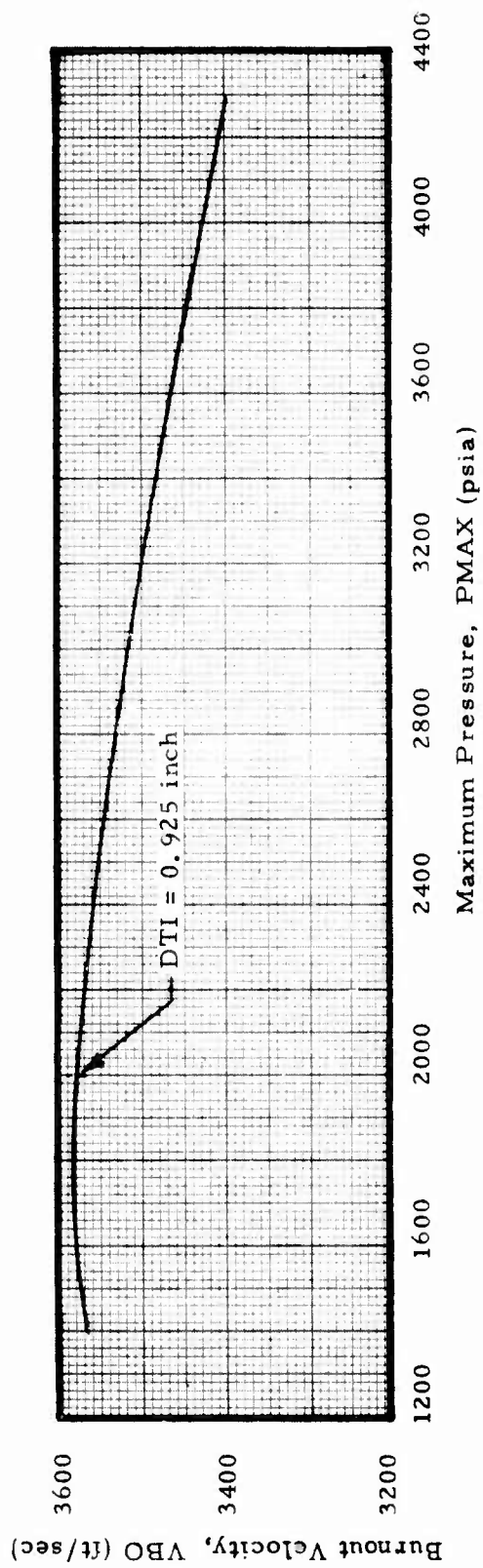
Since all preceeding calculations were made with an initial throat diameter (DTI) of 0.925 inch (from the Section III baseline motor design), a check was made to see if performance could be improved by changing the DTI. For a given grain geometry (slot length), changes in DTI produce corresponding changes in maximum pressure. At the conditions shown on the figure, DTI was varied to give a range of P<sub>MAX</sub>, from 1400 psia to 4300 psia (Figure XIII-12). The maximum VBO occurred at a pressure of 2000 psia, which indicated that the use of DTI = 0.925 inch was producing design points not too far from optimum.

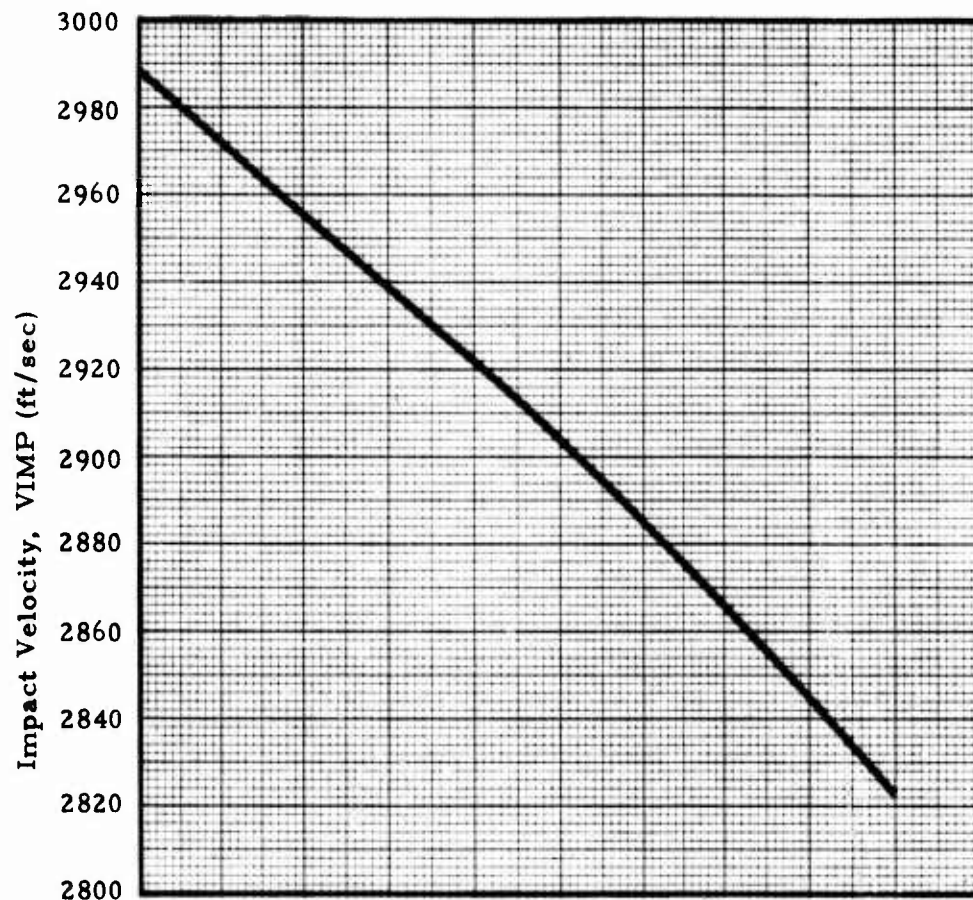
Next was a determination of the effect of burn rate on missile performance (Figure XIII-13). The burn rate used throughout the subject study (0.42 in/sec at 1000 psia) is in the range of ambient-temperature cure propellants available at Thiokol and other contractors (Reference XIII-1).<sup>1</sup> In these calculations longitudinal slot length was adjusted so that P<sub>MAX</sub> = 2380 psia and F<sub>MAX</sub>/F<sub>AVG</sub> = 1.0 at RB = 0.32, 0.42 and 0.50 in/sec at 1000 psia. It was found that a rate of 0.42 in/sec produced the highest VBO (albeit there was little difference). Slant range increased with increased burn rate, while impact velocity decreased. The conclusion is that propellant burn rate RB = 0.42 in/sec at 1000 psia is satisfactory for use in this study and that the study results are valid for a range of burn rates, with a level thrust history.

A new performance requirement was that missile velocity out of the launch tube (VTUBE) be at least 200 ft/sec. This requirement throws a whole new complexion on the characteristics of the final motor. High VBO dictates high total impulse, which calls for high propellant loading density (for a given propellant formulation), which in turn indicates relatively low initial burning surface when the grain configuration is designed to experience relatively sharp thrust tail-off. The latter is desirable because propellant burned at thrust less than vehicle drag does not increase VBO. Furthermore burning cannot continue to impact because of terminal guidance considerations. This entire situation leads to a conflict: a design which causes VTUBE to increase experiences a decrease in VBO. This point is illustrated in Figure XIII-14. For the conditions shown on the figure, slot length and DTI were varied. The points on Figure XIII-14 having the same symbol represent identical grain geometry with different DTI. VTUBE of 200 ft/sec was never achieved. At VBO = 3290 ft/sec (the missile performance requirement) VTUBE of about 155 ft/sec is the best that can be expected.

Note that Figure XIII-14 propellant, case ultimate strength, and throat erosion rate are the best that were explored in this study. Higher performance propellant will improve the situation. Even then it may be necessary to forego some low cost features, such as low strength cases and high erosion rate nozzles, so as to obtain the desired performance goals. As it usually happens, the missile/motor performance requirements will dictate a certain base level for motor characteristics. Low cost features which can provide those characteristics will be used; those that cannot, will not be used.

1. References are given at the end of this Section.





88% Total Solids, 12% Aluminum  
 Throat Erosion Rate, RE = 200% of Baseline  
 Case Ultimate Strength,  $\sigma_u = 42,000$  psi

PMAX = 2380 psia  
 FMAX/FAVG = 1.0  
 Pressure Exponent,  $n = 0.5$

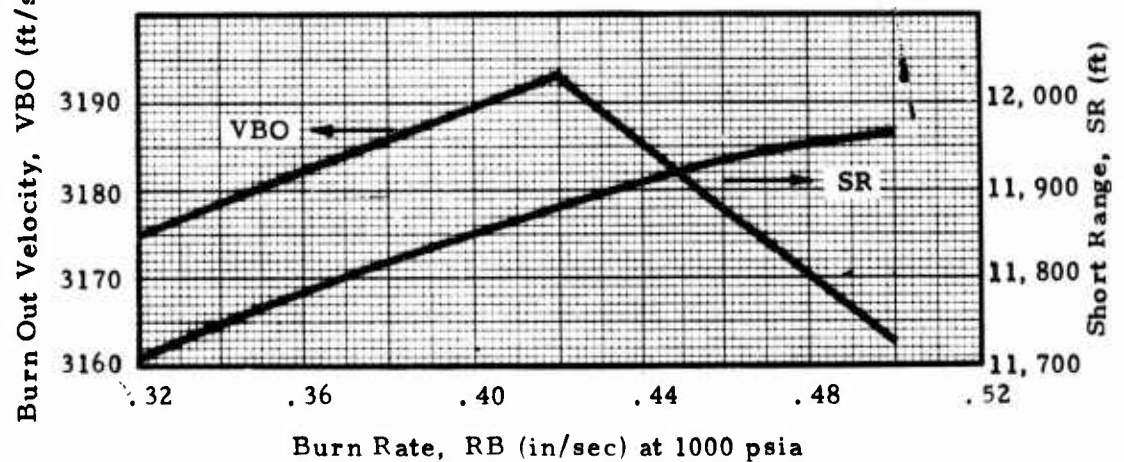
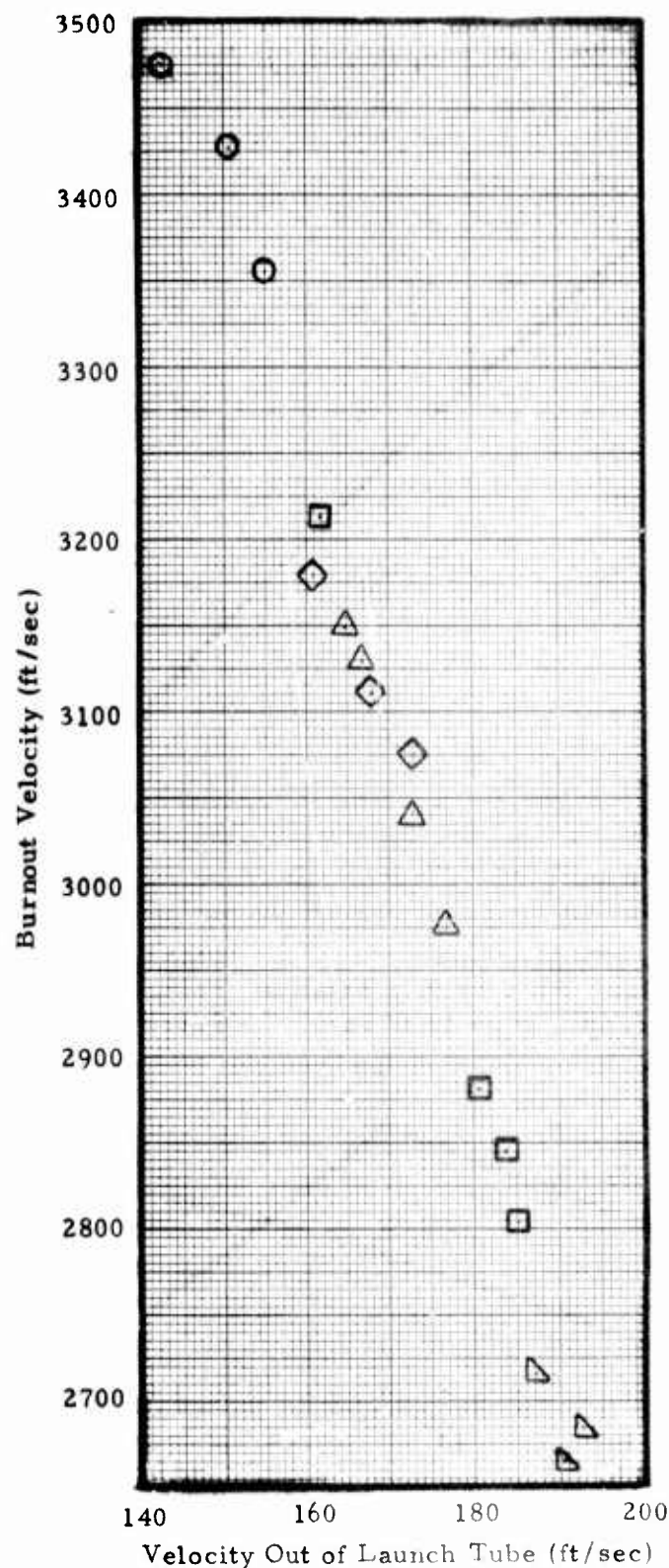


Figure XIII-13. Effect of Burn Rate on Missile Performance





88% Total Solids  
 12% Aluminum  
 Case Ult. Stg. =  
 78,000 psi  
 Throat RE = 100%  
 Burn Rate, RB =  
 0.42 in/sec at  
 1000 psia  
 Launch Tube Length  
 8.4 ft

Figure XIII-14. Relationship Between Burnout Velocity and Velocity Out of Launch Tube at Constant Burn Rate

To summarize the findings of this portion of the performance study:

1. Required missile performance can be furnished with
  - o Nozzle throat erosion rate up to 250% of baseline
  - o Case ultimate strength level as low as 60,000 psi
  - o Level to 20% regressive thrust history

The exact limits depend on propellant formulation.

2. Maximum flexibility in selecting motor component design and materials can be achieved with propellant having 88% total solids and 12% aluminum (within the bounds of this study. Propellant with higher specific impulse and density would provide even greater flexibility).
3. Velocity out of the launch tube and burnout velocity are incompatible requirements, within the limits of this portion of the study.

#### RELATIONSHIP BETWEEN COST AND PERFORMANCE

The following study was done to show how missile performance levels might affect the case cost if stock tubing of 2024-T81 aluminum were used. Figure X-35 shows how case cost<sup>1</sup> varies with allowable PMAX; Figure XIII-1 shows the variation of imposed PMAX with longitudinal slot length. Information on these two plots are combined in Figure XIII-15 to illustrate how slot length will cause changes in case tubing cost. Costs are the same for RE = 150% and 200% below slot length of 14 inches because the imposed pressures below this slot length (Figure XIII-1) are less than the pressure capability of the thinnest wall tubing available (Figure X-33).

Burnout velocity was shown as a function of slot length in Figure XIII-2. When these values are combined with Figure XIII-15, the effect of VBO on case costs can be observed (Figure XIII-16). An interesting result is that a VBO of about 3460 ft/sec can be provided at a case cost of about \$5.65 per ft. when using a nozzle having RE = 150% or 200% of baseline rate, whereas the use of material having RE = 100% would dictate case cost from \$6.65 to \$7.25 per foot. Low throat erosion combined with the short slots results in higher PMAX than the high RE, but VBO is about the same for all RE at the short slot length; thus tubing with thinner walls can be used with the higher RE at short slot length than can be used with lower RE; thinner walls result in lower cost. Note that thrust profile is not considered in this discussion.

---

1. Base price of material. Does not include cutting or finishing costs.

88% Total Solids  
 12% Aluminum  
 Baseline RE = 0.033 in/sec at 1000 psia  
 Tubing - 2024 T81 Aluminum

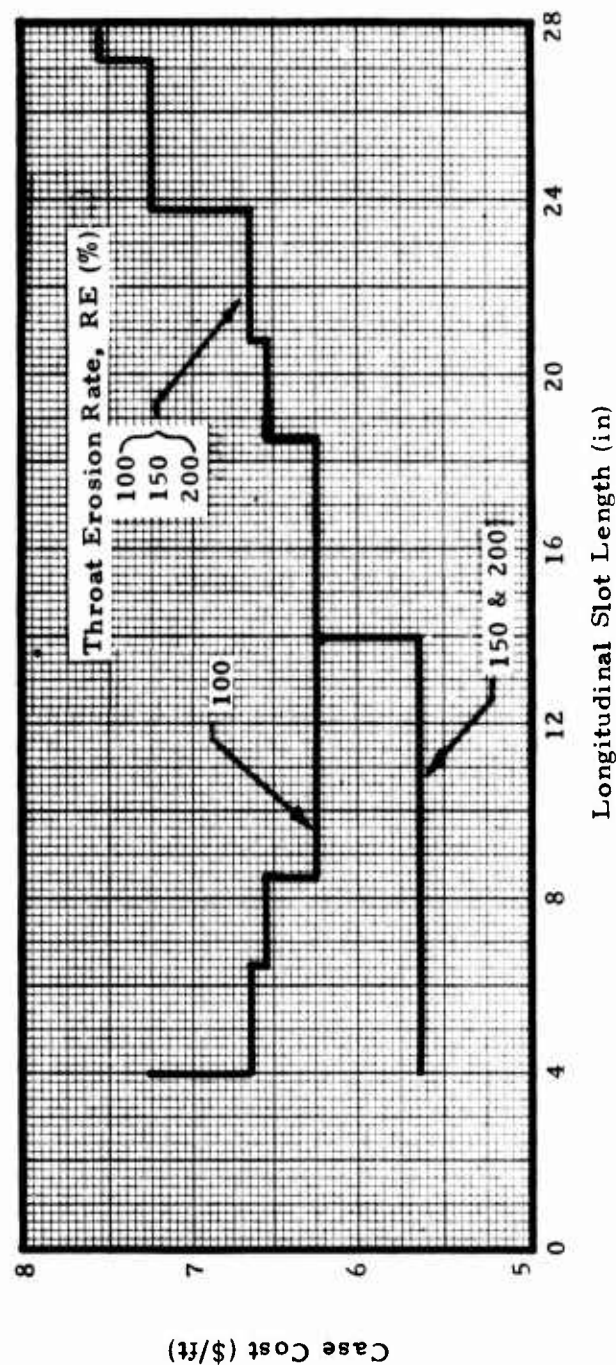


Figure XIII-15. Cost of Stock Tubing Cases

88% Total Solids  
 12% Aluminum  
 Case Ultimate Strength = 60,000 psi  
 Baseline RE = 0.033 in/sec at 1000 psia  
 Tubing - 2024 T81 Aluminum

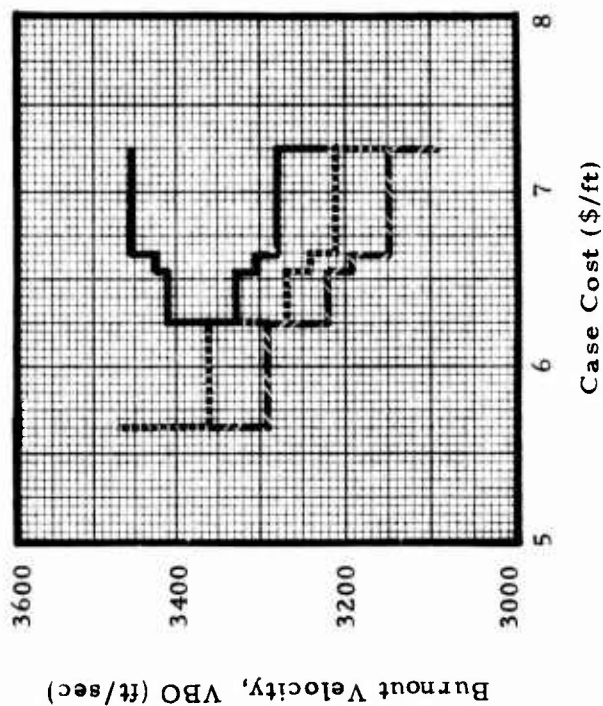
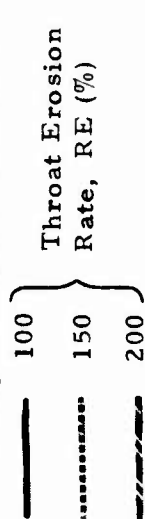


Figure XIII-16. Cost to Obtain Specified Burnout Velocity

Thrust profile varies with longitudinal slot length as shown in Figure XIII-3. When this relation is combined with the case costs of Figure XIII-15 the effect of FMAX/FAVG on case costs can be examined (Figure XIII-17). For any given thrust profile, the higher RE allows the use of lower cost cases than does the lower RE. For example, at FMAX/FAVG = 1.1 (regressive), the case would cost

\$6.25 per foot for RE = 200%  
\$6.55 per foot for RE = 150%  
\$6.65 per foot for RE = 100%

For a given RE a specified FMAX/FAVG occurs at a shorter slot than for a lower RE. The same logic as used in the preceding paragraph produces the effect seen in Figure XIII-17.

In summary, this portion of the grain design study, when combined with results from the stock tubing study, has shown that

- (1) For a given burnout velocity or thrust profile, the use of high throat erosion rate nozzles will allow the use of lower cost case tubing.
- (2) There are subtle interrelations that must be considered when "minimizing" motor costs.

#### BURN RATE STUDY

Performance studies just described were performed with a propellant burn rate of 0.42 in/sec at 1000 psia, whose pressure exponent,  $n$  (in the relationship  $RB = a P^n$ ) was 0.5. A burn rate study centered on level thrust profile<sup>1</sup> showed burn rate to be a weak influence on burnout velocity. It was also found that velocity out of the launch tube, VTUBE, and burnout velocity, VBO, were incompatible requirements at a particular burn rate (Figure XIII-14). The subject study is a preliminary investigation to determine if a higher propellant burn rate would result in higher initial thrust (i.e. higher VTUBE) while not causing too much degradation of delivered total impulse (i.e., reduced VBO).

Certain design features were held constant:

- a. Propellant contained 88% total solids, of which 12% was aluminum, which had the highest energy content of any formulation considered in the study.
- b. Throat erosion rate was 0.033 in/sec at 1000 psia, which was the Baseline rate, and the lowest of any considered.

---

1. FMAX/FAVG = 1.0 (Figure XIII-13).

88% Total Solids  
 12% Aluminum  
 Baseline RE = 0.033 in/sec at 1000 psia  
 Tubing - 2024 T81 Aluminum

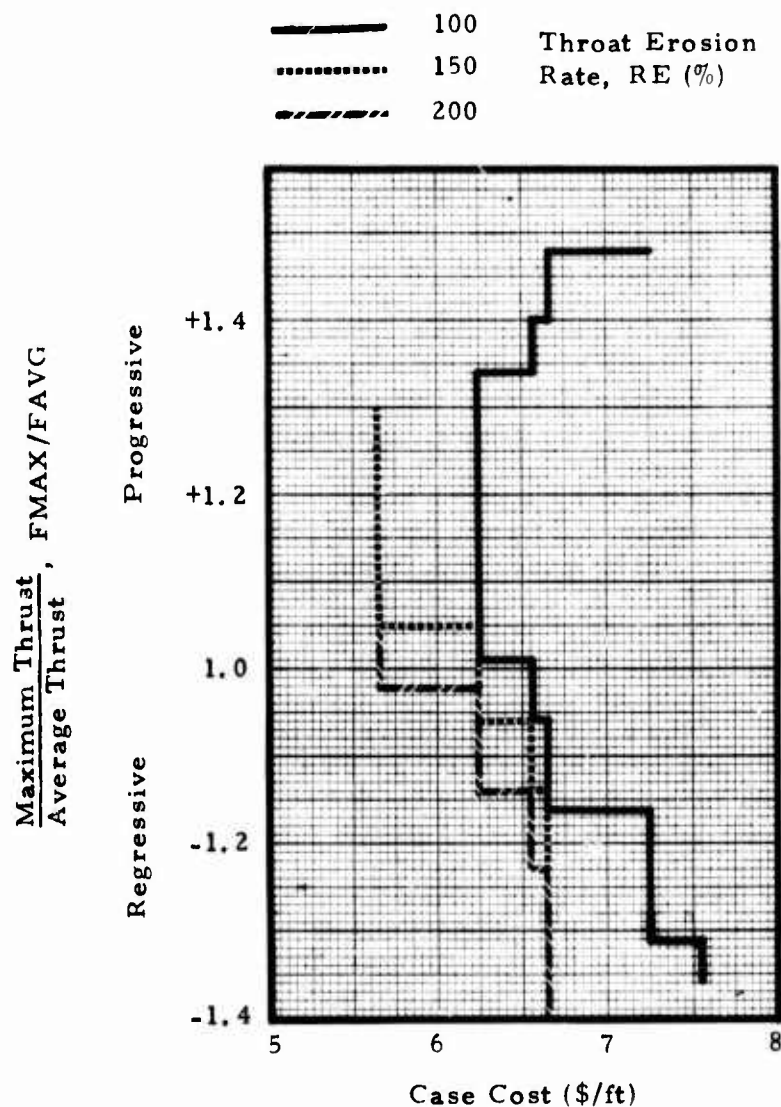


Figure XIII-17. Effect of Thrust History on Stock Tubing Case Costs



- c. Case ultimate strength was 78,000 psi, equivalent to 7075-T6 aluminum, which was the highest strength considered in the study.
- d. The grain had two longitudinal slots, 28 inches long, and a cylindrically perforated port in the remaining length with a 70% web fraction.

Case ultimate strength, propellant formulation and throat erosion rate were chosen to provide the highest possible performance. Slot length was selected on the basis of preliminary calculations which showed slots longer than 28 inches caused drastic decrease in VBO without significant improvement in VTUBE.

Internal ballistic and trajectory calculations were made with a series of propellant burn rates. At each burn rate, initial throat diameter was varied to produce a range of maximum pressure. From this the appropriate missile performance was obtained at a maximum pressure (at 70°F) of 3500 psia. Typical thrust and pressure histories are shown in Figure XIII-18.

Results of these computations (Figure XIII-19) show that VTUBE can be increased by incorporating a propellant with higher burn rate. Whereas VTUBE was about 160 fps at the base burn rate of 0.42 in/sec, it can be increased to 200 fps with a burn rate of about 0.82 in/sec (at 1000 psia). Concurrently, VBO stays about 3300 fps. Impact velocity, VIMP, shows a continuous decrease with increasing burn rate, going from almost 3000 fps at RB = 0.42 in/sec to about 2850 fps at RB = 0.82 in/sec. On the other hand, VBO experienced an increase (to 3350 fps) at RB = 0.65 in/sec, followed by a decrease at higher burn rates.

The subject calculations represent only an initial examination of the burn rate effects on VBO, VTUBE and VIMP. Much more extensive studies must be performed before the desired propellant burn rate can be established finally. The matrix must include systematic variations in longitudinal slot length and maximum pressure. The calculations described previously showed that VBO is decreased (from that of the Baseline motor) by higher throat erosion rate, lower proportions of total solids and/or aluminum in the propellant, and lower case ultimate strength. Thus there is the possibility that there is a "best" burn rate for each combination of these features.

#### GRAIN DESIGN STUDY

Propellant can be loaded into motors in one of two ways: (1) "Case bonded" propellant grains result when insulation and liner are applied to the case interior surfaces in such a manner that the materials are bonded to the case and then the propellant is cast into the prepared case. Upon completion of cure, the propellant is bonded to the case through liner/insulation system;



Propellant: 88% Total Solids  
 12% Aluminum  
 Throat Erosion: 100% of Baseline  
 Baseline Throat Erosion: 0.033 in/sec at 1000 psia  
 Maximum Chamber Pressure at 70°F: 3516 psia  
 Case Ultimate Strength: 78,000 psia  
 Two Longitudinal Slots: 28" long  
 Propellant Burn Rate: 0.84 in/sec at 1000 psia  
 Pressure Exponent,  $n = 0.5$   
 Initial Throat Diameter: 1.335 inches

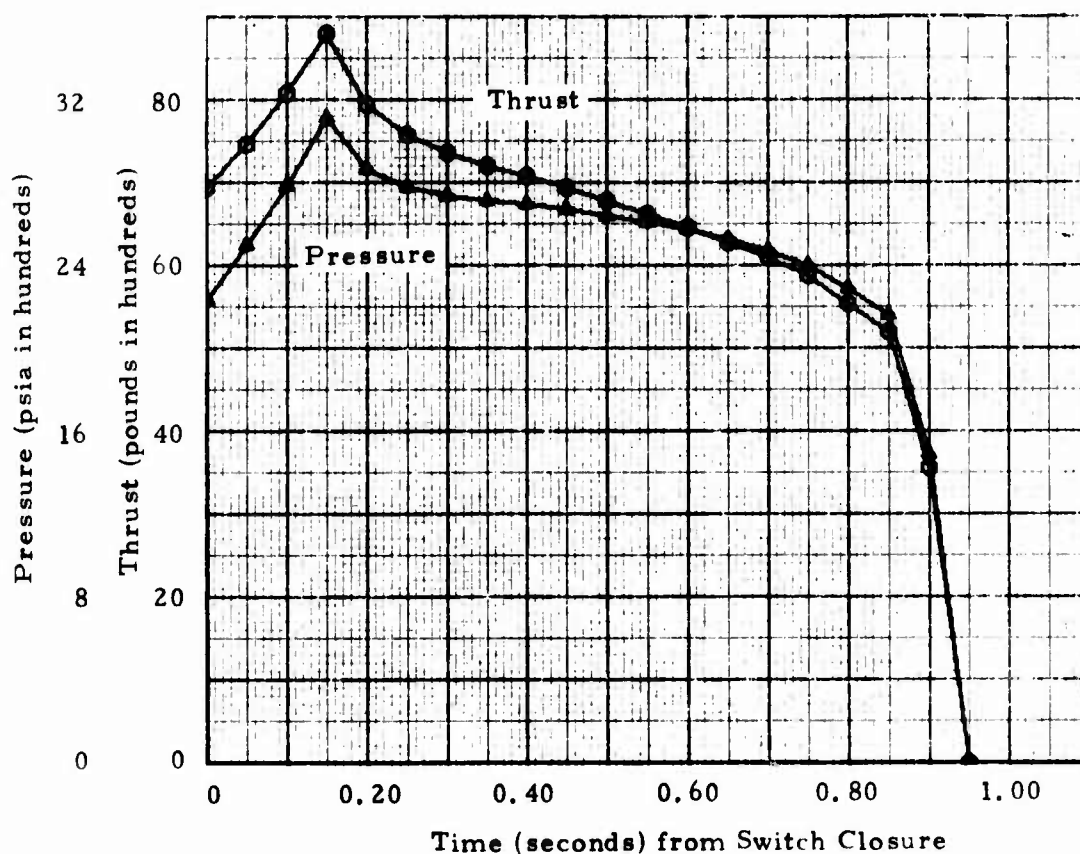


Figure XIII-18. Typical Pressure and Thrust Histories of Flight Motor, Fired at 70°F

Propellant: 88% Total Solids  
12% Aluminum

Throat Erosion: 100% of Baseline  
Baseline Throat Erosion: 0.033 in/sec at 1000 psia  
Maximum Chamber Pressure at 70°F: 3500 psia  
Case Ultimate Strength: 78,000 psia  
Two Longitudinal Slots, 28 inches long  
Pressure Exponent,  $n = 0.5$

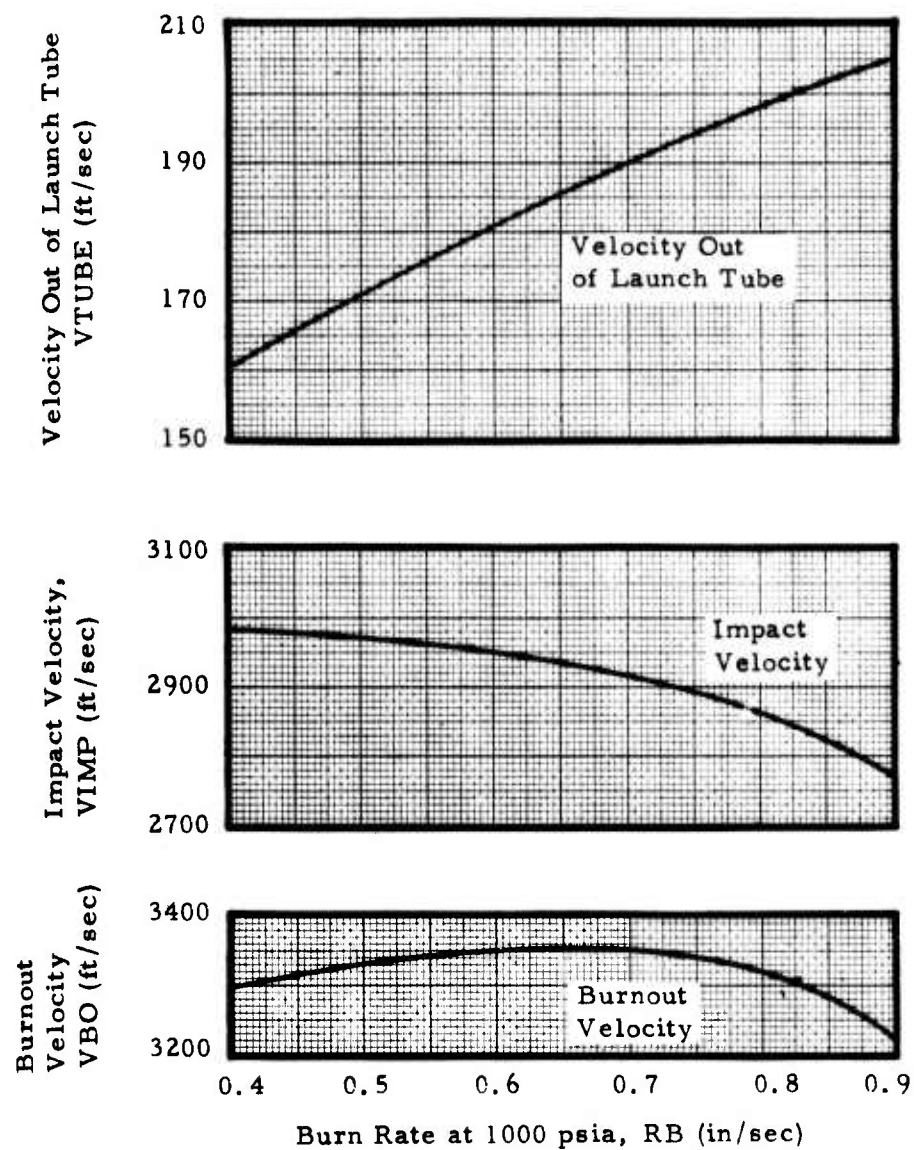


Figure XIII-19. Variation of Missile Performance With Propellant Burn Rate

(2) "Cartridge loaded" propellant grains result when the insulation covers the entirety of the case interior and is so rigid (or is so supported) that propellant can be cast into it without use of the case. Upon completion of cure, the propellant is already bonded to the insulation and then the complete "cartridge" is installed in the case, either with or without adhesive to bond the unit to the case.

There are several technical comparisons made in selecting one approach over the other, not the least of which is the experience background of a particular propulsion contractor. If the insulation for the cartridge grain is flexible, then the propellant can shrink inward during cure and bore strains are greatly reduced. Another way to achieve the same results is to apply the insulation after the propellant is cured, where the propellant was cast and cured in special tooling. On the other hand, if the insulation for the cartridge grain is rigid, there will be no differences in cure-induced bore strains between the case-bonded and cartridge grains since either case or insulation will prevent inward shrinkage. There must be some finite gap between the cartridge and case for installation and this gap represents volume no longer available for propellant. If this gap is not filled with an adhesive during installation, the grain must have some retention device to hold it in place during handling and at initial pressurization. Absence of the gap-filling adhesive may result in a large pressure differential across the cartridge sleeve which could result in structural failure of the sleeve or cartridge. The gap is larger at low storage temperature, but this is a result of one of the advantages of the cartridge grain, viz, the bore strains at low temperature are reduced because the grain can contract without being constrained by the case (provided the insulation sleeve has the same coefficient of thermal contraction as does the propellant). The cartridge-loaded grain will be over-insulated if the particular propellant configuration does not dictate insulation on all the case because of the need to provide a "container" for the propellant. There is some practical size limit for cartridge grains because of handling considerations rather than for insulating requirements. The opening in the case through which the cartridge is inserted must be as large as the case ID. The cartridge grain offers significant improvements in design flexibility. It is simple to incorporate propellants with two different burn rates by installing separate cartridges. Complex grain geometries can be formed with multiple segments. By making it easy to not bond the forward end of the grain to the forward case closure, the cartridge grains eliminate the need for split flaps. Reject grains, or mixes, result in cases being thrown away (or reclaimed) for case-bonded grains, whereas only the insulation sleeve is lost in the cartridge-loaded approach.

However, it was not an objective of this study to make a completely technical evaluation of case-bonded versus cartridge grains, since so much of the technical choice depends on the particular application. Rather, wherever possible, the technical merits were judged equal for the two approaches. The main thrust of the subject study was a cost comparison of cartridge grains

and case-bonded grains. At the same time a comparison was made with a mastic insulation which included both cost and performance considerations. A part of the latter investigation determined the influence of case strength and density.

#### Assumptions for Cost Comparisons

The following assumptions were formulated for these cost comparisons:

- a. Both the loaded propellant cartridge and the empty insulation sleeve will be bonded into the case.
- b. Nozzle attachment technique is identical for all three types, and it includes an adhesive.
- c. Casting tooling and equipment are identical for all three types.
- d. Dimensions and tolerances are the same for the insulation sleeve that serves as the container in the cartridge-loaded technique or that is bonded directly into the case for the case-bonded technique; thus the sleeve costs are identical for the two items.
- e. A composite labor cost of \$23.00 per hour of "touch" labor was used as the labor cost to the propulsion contractor. As such it includes all overhead burdens, but no fee. In addition to the labor costs actually required to accomplish a given task, it includes a factor that accounts (on an average basis) for the "non-touch" labor such as inspectors, foremen, and clerks that support the production worker.
- f. Costs of facilities, equipment and vendor-supplied motor components are given as cost to propulsion contractor.

#### Comparison of Cartridge and Case-Bonded Grains

Because of the emphasis put on high-speed, automated production of insulation components, the sleeve materials used in this study were filled thermoplastics; another insulation considered was a filled mastic which could be swept or spun into the case. Details about the materials and their characteristics are in Section XII.

The possible combinations of case, insulation and grain manufacturing techniques are illustrated in Figure XIII-20. The two major categories are the two grain manufacturing techniques: case-bonded and cartridge-loaded. Cartridge grains can use only a sleeve insulation, designated Type I. Case-bonded grains can use either sleeve or mastic insulation, designated Type II and III, respectively. Two types of case are shown on Figure XIII-20 stock tubing and impact extruded, but others (such as metal strip laminate

or plastic laminate) could be added to the matrix without changing the basic approach. Regardless of the case type, sleeve insulation can be bonded, or not bonded, to the case, whether the propellant is case-bonded or cartridge-loaded. Thus, as far as cost comparisons are concerned, there are only three basic grain/insulation systems. Major processing steps for each of the three types are outlined below:

#### Type I

- Cast propellant into insulation sleeve
- Cure propellant
- Install in case (either bonded to case, or not)
- Cure adhesives

#### Type II

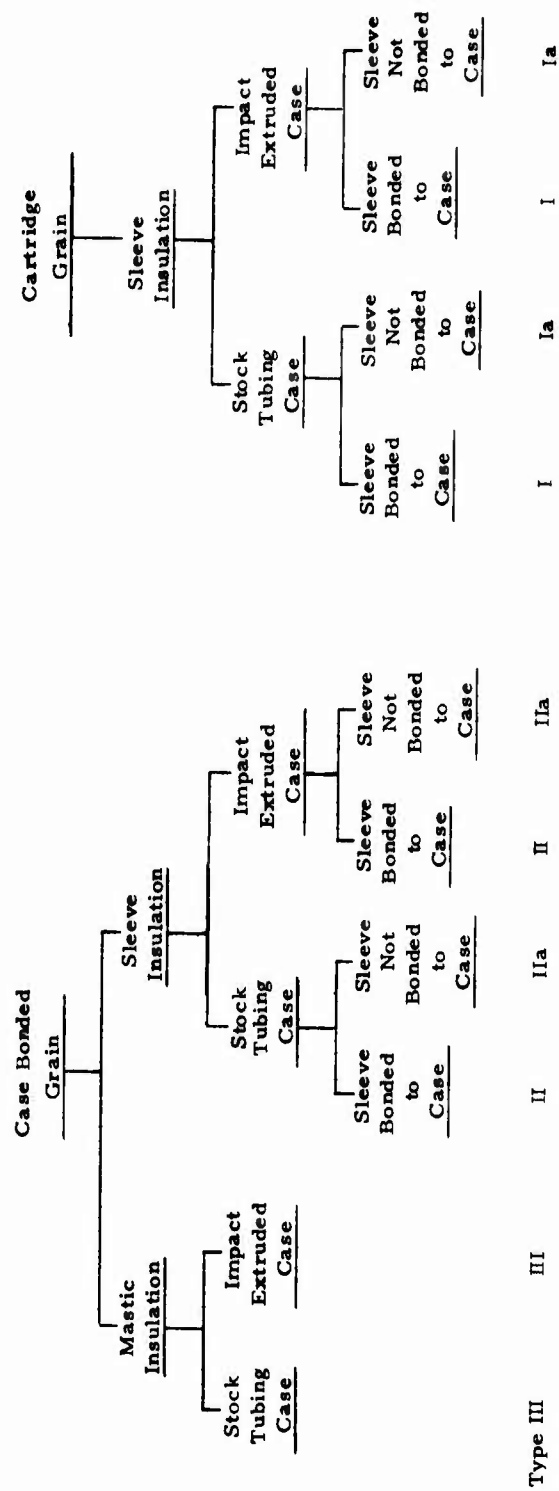
- Install insulation sleeve in case (either bonded to case, or not)
- Cast propellant
- Cure propellant and adhesives

#### Type III

- Apply mastic insulation to case
- Cast propellant
- Cure propellant, insulation and adhesives

Detail processing steps were formulated for each type. Care was exercised that trivial steps were not included in the manufacturing sequence such that one type system appeared to be more complex and costly than the others. These sequences are shown in Tables XIII-3, XIII-4, and XIII-5.

Processing steps for the three insulation/grain types are compared in Table XIII-6. It was assumed that a given step costs the same for all three types. Further, if a particular type required a certain processing step that the other did not, then that step represented a cost differential between the types. For example, even the mastic insulation (Type III) requires receipt and acceptance inspection of a molded forward closure insulation and the associated costs should be the same as for the Type I and II insulation sleeves, even though the latter are larger items. But in addition to the molded insulation, Type III requires receipt and acceptance inspection of the mastic insulation raw materials, and thus this processing step represents a cost differential between Type III and the other two. Another example where costs were assumed equal for the three types is illustrated by the step listed as "Install molded insulation (grain) in case" in Table XIII-6. Each of the three has some item installed in the case: Type I a loaded propellant cartridge, Type II an empty insulation sleeve, and Type III a forward dome insulation. Although there will be detail differences in the automated equipment to accomplish the three different operations, it is not unreasonable to assume that the equip-



Strip laminate cases can be included in such a matrix with the same insulation possibilities as shown herein

Figure XIII-20. Insulation/Grain Systems to be Studied



ment and labor costs will not be significantly different. Thus for this step there is no cost differential between the three types. Similar logic was followed throughout the preparation of Table XIII-6.

#### Comparison of Type I and Type II Grains

Type I system was compared to Type II and then Type II was compared to Type III to obtain cost differentials between the three types of grain/insulation systems.

Type I has the following cost penalties:

- a. An extra degreasing operation (Step 11) is required before bonding the loaded grain into the case.
- b. An extra cure cycle is needed for bonding the propellant cartridge into the case and the nozzle into the case.
- c. Consultation with thermoplastic vendors determined the as-received insulation sleeve will not be round (with respect to the case). Unless special rounding tooling is provided, a larger gap must be provided between cartridge and case for assembly, since the cured grain cannot be deformed. This larger gap translates into a performance penalty for Type I. In keeping with the basic philosophy of providing equal performance for all systems, there will be rounding fixtures as part of the casting stand for Type I grains. Each set of rounding fixtures must stay with the grain until cure is complete. The case serves as the rounding device in Type II.

Type II has only one cost penalty. Individual propellant grains rejected because of grain integrity defects or entire mixes rejected because of physical properites or ballistics being out of tolerance result in entire motors being unacceptable for delivery. Obviously the insulation sleeve and case are associated with reject propellant in the case-bonded technique; additionally, there are a nozzle and the costs of attaching it to the case which must be part of the cost penalty because of the selected overall manufacturing technique.<sup>1</sup> Since many of the low-cost nozzle joining techniques do not provide for later dis-assembly, once the motor is put together, the nozzle would be destroyed during any reclamation attempt. Furthermore the insulation sleeve would be rendered unusable. Therefore it was assumed that reject motors with Type II grains would be discarded with no attempt to reclaim any components. Note that the insulation sleeve and propellant casting and curing activities are costs that cannot be recovered with either Type I or Type II grains and thus do not

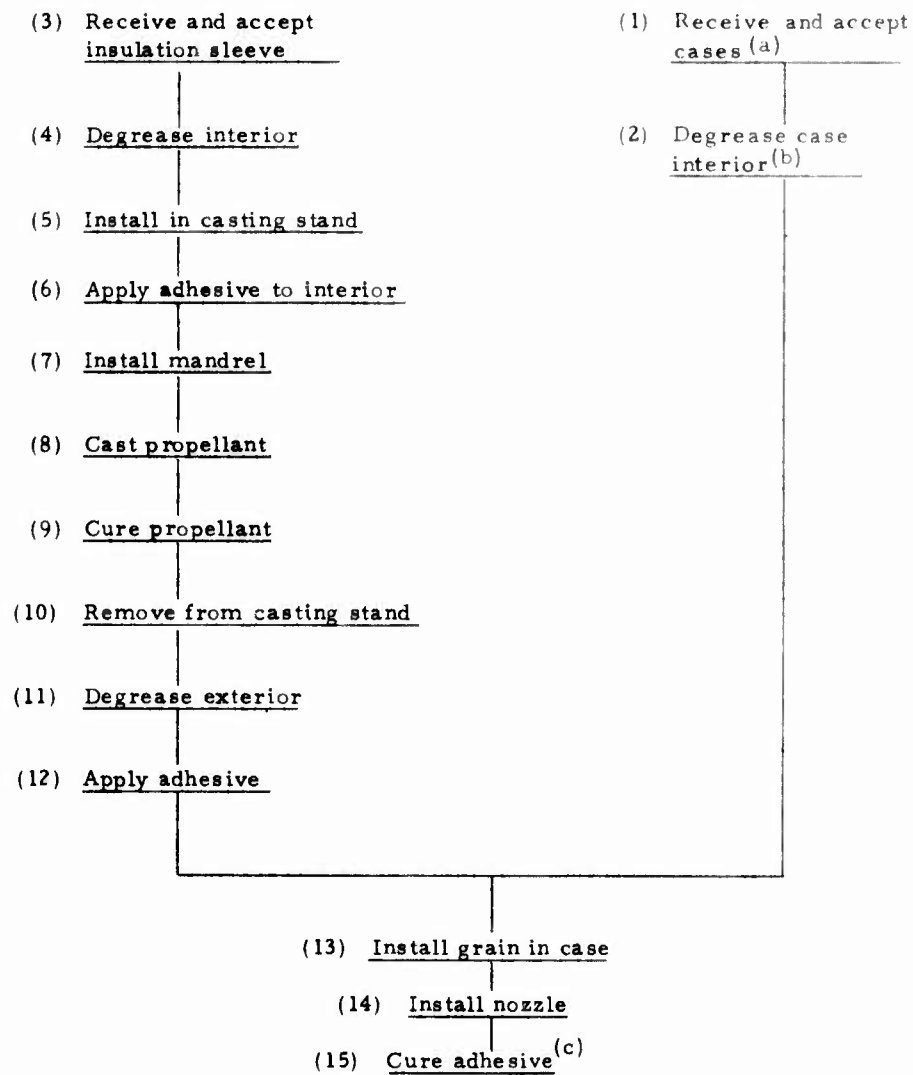
---

1. Immediately after propellant casting is complete, the nozzle will be installed and all cure will be accomplished simultaneously.



TABLE XIII-3  
PROCESSING STEPS FOR TYPE I INSULATION SYSTEM

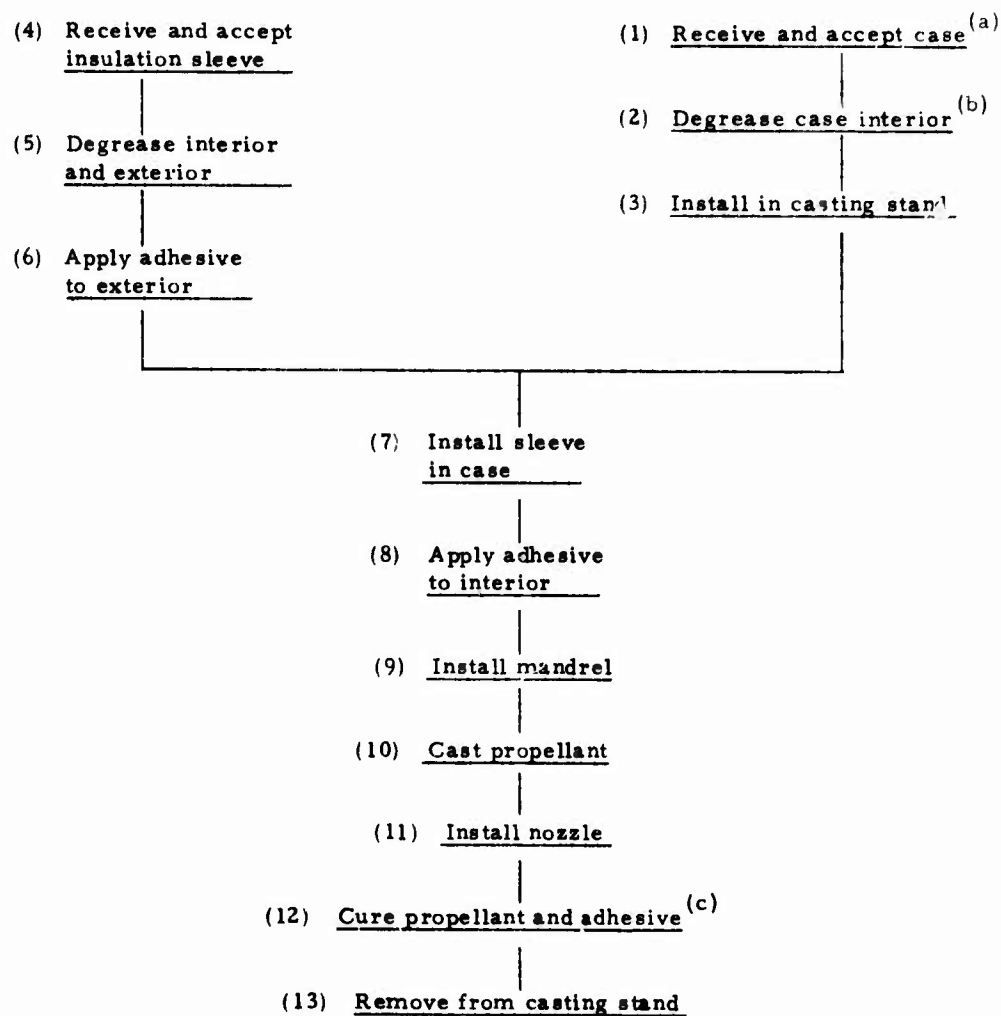
Cast Propellant Into Insulation Sleeve  
Cure Propellant  
Install in Case  
Cure Adhesives



- a. Assume forward closure already present.  
 b. Needed only if design calls for bonding grain in case (Type I). Also not needed if cases degreased by vendor.  
 c. Not needed if nozzle attachment does not require adhesive and if grain not bonded to case (Type Ia).

TABLE XIII-4  
PROCESSING STEPS FOR TYPE II INSULATION SYSTEM

Install Insulation Sleeve in Case  
Cast Propellant  
Cure Propellant and Adhesives



a. Assume forward closure already present.

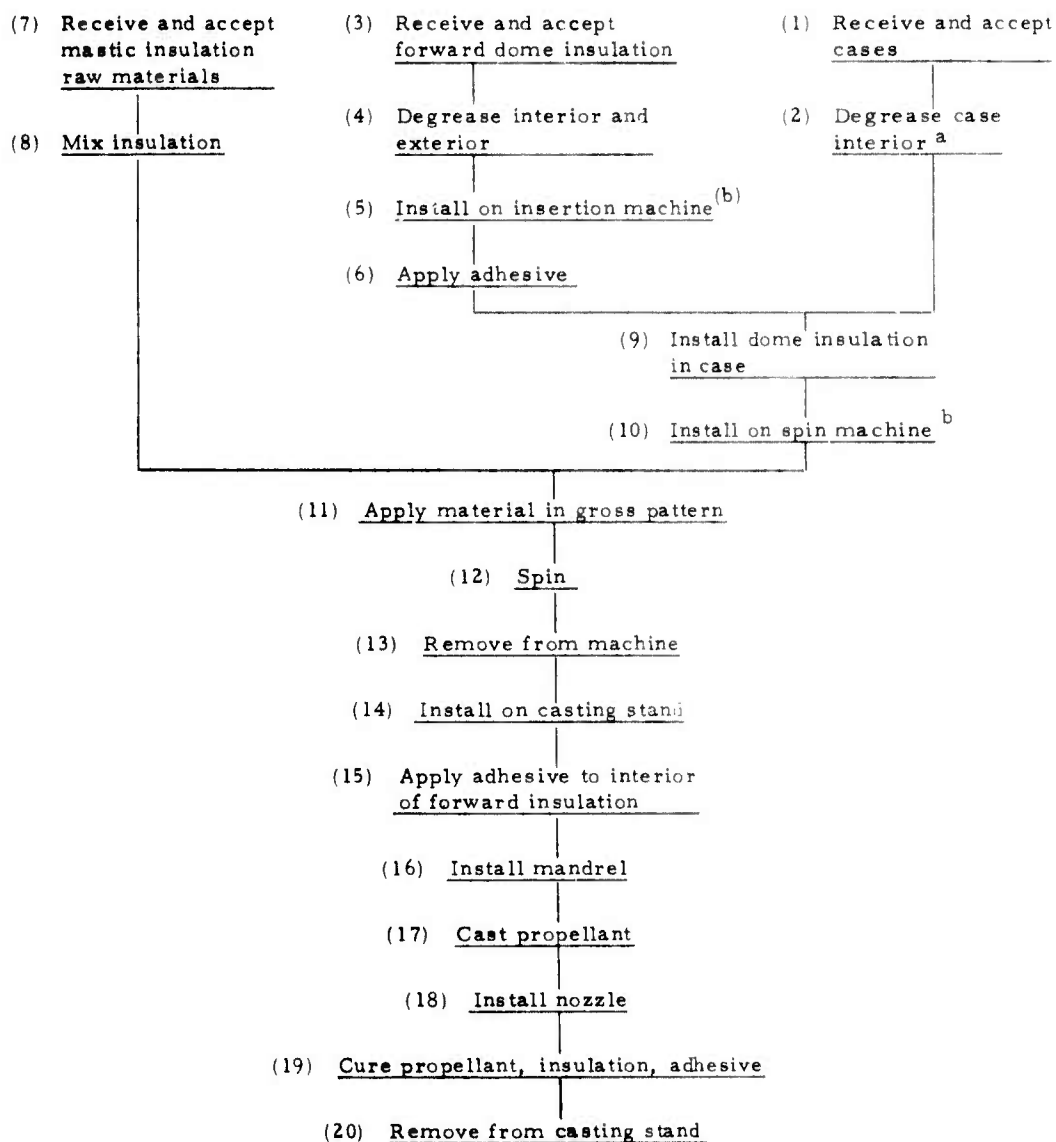
b. Needed only if design calls for bonding grain in case (Type II). Also not needed if cases degreased by vendor.

c. Not needed if nozzle attachment does not use adhesive and if grain not bonded to case (Type IIa).

TABLE XIII-5

PROCESSING STEPS FOR TYPE III INSULATION SYSTEM

Apply Mastic Insulation to Case  
Cast Propellant  
Cure Propellant, Insulation and Adhesives



a. Not needed if cases degreased by vendor.

b. May be same machine. This step considered "trivia?" and not counted against Type III costs.

TABLE XIII-6  
COMPARISON OF PROCESSING STEPS

Step Description	Step Number		
	Insulation Type		
	I	II	III
Receive and accept case	1	1	1
Degrease case interior	2	2	2
Receive and accept molded insulation	3	4	3
Degrease interior and exterior of molded insulation	4	5	4
Degrease exterior of molded insulation (sleeve)	11	---	---
Apply adhesive to exterior of molded insulation	12	6	5/6
Receive and accept mastic insulation raw material	---	---	7
Mix mastic insulation	---	---	8
Install molded insulation (grain) in case	13	7	9
Install on spin machine	---	---	10
Apply insulation in gross pattern	---	---	11
Spin	---	---	12
Remove case from spin machine	---	---	13
Install on casting stand	5	3	14
Apply adhesive to interior of molded insulation	6	8	15
Install mandrel	7	9	16
Cast propellant	8	10	17
Install nozzle	14	11	18
Cure propellant, insulation, adhesive	9	12	19
Remove from casting stand	10	13	20
Cure nozzle and case/grain adhesive	15	---	---

represent a cost differential between the two systems. It was assumed the proportion of reject grains would be the same for Type I and Type II since nothing in either grain manufacturing technique would inherently result in more or fewer rejects.

Detailed calculations of the cost penalties are given in Tables XIII-7 and XIII-8, for Type I and Type II grains, respectively.

Type I grains have the following cost penalties with respect to Type II grains:

Extra degrease step	\$1.15
Extra cure cycle	1.19
Rounding operation	<u>1.39</u>
	\$3.73 per motor

Type II grains have the following cost penalties with respect to Type I grains:

Reject mix (or grain) results in discarding case, nozzle, and labor/equipment to install the nozzle. Expected reject rate of 1% is that portion of "throw-away" costs that must be carried by each delivered motor.

Case	\$26.58
Nozzle	8.09
Attachment	<u>0.63</u>
	\$35.30
	0.35 per delivered motor

From these calculations, the Type I grain costs  $\$3.73 - 0.35 = \$3.38$  more than Type II grains. Further calculations were made to verify this conclusion.

- a. Type I penalty was decreased to \$1.10 by eliminating the rounding step (\$1.39), halving the labor costing of the extra degrease step (\$0.575) and halving the labor cost of the extra cure cycle (\$0.575)
- b. Type II penalty was increased to \$0.36 by tripling the labor required to attach the nozzle from one minute to three minutes

Case	26.58
Nozzle	8.09
Attachment	
Equipment (same as before)	0.23
Labor (\$0.37 before)	<u>1.15</u>
Per reject motor	\$36.05
Per delivered motor	0.36

TABLE XIII-7

TYPE I GRAIN COST PENALTIES<sup>(a)</sup>

Extra degrease operation <sup>(b)</sup> (1/20 mh)	\$1.15
Extra cure cycle	
Transfer units to oven (1/20 mh)	\$1.15
Additional cure facilities	\$0.04
<p>Production rate of 20,000 motors per month          Adds 667 motors per day to cure facilities          At estimated 1/3 sq ft per motor          Requires about 220 sq ft of oven per day of cure time          At about \$25 per sq ft construction cost          Each day of cure requires about \$5000 of facility          For 9 days cure time, total facility = \$45,000          Amortized over          Total production run of 1,200,000 motors</p>	
Rounding Operation	
Labor (1/40 mh to install, 1/40 mh to remove) <sup>(c)</sup>	\$1.15
Tooling	\$0.21
10,000 sets at \$25 each	
Amortized over 1,200,000 motors	
Equipment for installing and removing tooling	\$0.03
Machine to install \$20,000	
Machine to remove \$20,000	
Amortized over 1,200,000 motors	

- a. Cost to Propulsion Contractor, per motor.  
 b. Assume that no additional facilities are required.  
 c. Labor rate of \$23.00 per hour cost to propulsion contractor includes factor for "non-touch" support labor.

TABLE XIII-8

TYPE II GRAIN COST PENALTIES<sup>(a)</sup>

For each reject motor, the following cost factors<sup>(b)</sup> represent penalties

Case	\$26.58
Integral forward closure, impact extruded, 2014-T6 aluminum	
Nozzle	8.09
D791 wood flour phenolic with aluminum structural support shell	
Nozzle attachment to case	0.63
Electromagnetic pulse forming with adhesive bonding; includes facilities, equipment, maintenance, adhesive, and labor <sup>(c)</sup>	
<hr/>	
TOTAL	\$35.30

Assume 1% reject rate

Cost of each delivered motor must be increased by 1% of the cost of the non-recoverable costs associated with reject motors for those costs unique to Type II grains.

Cost penalty per delivered motor \$ 0.35

- a. Cost to Propulsion Contractor, per motor.
- b. It is recognized additional costs are "lost" with a reject motor, e.g., insulation sleeve and propellant casting; these costs are unique to Type II grains.
- c. See Section XI for details.



This comparison again shows that Type I grains cost  $\$1.19 - 0.36 = \$0.83$  more than Type II grains.

It is concluded the lowest cost grain design is obtained by installing an insulation sleeve in the case, casting propellant, installing the nozzle and then concurrently curing all adhesives and propellant (i.e., the case-bonded grain), when compared with a cartridge-loaded grain.

#### Comparison of Type II and Type III Grains

Type II grains have just one cost penalty associated with it, when compared to Type III. A large, and thus more expensive, molded insulation is needed for Type II, where the molded insulation sleeve extends the full length of the case. Type III grains have a molded forward closure insulation which can be made of glass-filled ABS (the least expensive thermoplastic considered). Thus the cost penalty incurred by using Type II grains is the difference in costs of the two different molded insulation components.

Type III grains have the following cost penalties:

- a. Raw materials (polymer, filler, cure agent, etc) must be purchased, received and accepted for use in the mastic insulation.
- b. The mastic insulation must be mixed, either as a batch or in a continuous mixer.
- c. The insulation must be applied to the case interior. Several conventional application techniques are suitable. "Sweeping" uses a long blade oriented lengthwise through the motor and separated from the case interior surface by a distance which is a function of the desired insulation thickness. After the mastic is more or less uniformly spread on the wall, the case is rotated with the blade held stationary. The insulation is thus "swept" to the final configuration. Another "sweep" is a disk that is withdrawn from the case after the insulation is applied as before. The latter technique involves less complicated equipment but insulation thickness cannot be varied along the length of the motor. The former technique can use a blade shaped to vary the mastic thickness. Experience with both techniques has shown that total insulation thickness must be increased significantly above the amount required for thermal protection to account for the numerous defects which are inherent in the technique (even when using vacuum deaerated material).

Another application technique is "spinning", or "centrifugal casting". Again the material is applied to the case more-or-less uniformly, but the final shaping is accomplished by spinning the case about its longitudinal axis at a relatively high rate. The centrifugal force causes most of the entrapped air bubbles to move to the interior surface or to be flattened. The quality of the final insulation is much better than with sweeping and only a 10% allowance for defects is needed. One drawback is that only a constant insulation thickness can be provided readily. The centrifugal casting technique was selected

for the subject cost study and later performance analyses. The extra steps associated with this technique are (a) install case on spin machine; (b) apply insulation to case in gross pattern; (c) spin; (d) remove from spin machine. Sweeping the mastic insulation would require almost identical steps and thus the costs would not be too much different.

The extra costs incurred for Type III grains are detailed in Table XIII-9, and summarized below:

	<u>Cost to Propulsion Contractor (\$ per Motor)</u>
Raw Material	\$3.60
Labor	4.03
Equipment	0.10
Tooling	0.15
	<u>\$7.88</u>

Based on quotes on similar parts and materials, cost of the forward closure insulation was estimated to be \$1.25 each, made from glass filled ABS thermoplastic. This part represents an additional cost attributed to the Type III grain. The cost penalty associated with Type II grains is the cost of the insulation sleeve. Combining these effects,

$$\left[ \begin{array}{l} \text{Net Cost of Using} \\ \text{Type III Grains} \end{array} \right] = \left[ \begin{array}{l} \text{Cost of Type II} \\ \text{Insulation Sleeve} \end{array} \right] - \$1.25 - \$7.88$$

Thus, if the Type II insulation sleeve costs less than \$9.13, Type III grains will be more expensive to produce.

Several vendors were contacted for budgetary estimates of 1,200,000 insulation sleeves (at the rate of 20,000 per month) made from different thermoplastic materials. A wide range of costs resulted for the configurations described in Section XII, Insulation/Liner Study.

<u>Material</u>		<u>Sleeve Wall Configuration</u>	<u>Costs to Propulsion Contractor<sup>1</sup></u>
<u>Resin</u>	<u>Filler</u>		
ABS	30% glass	Constant	\$9.78
ABS	30% glass	Tapered	4.02
Polycarbonate	20% glass	Tapered	15.08
Polycarbonate	20% glass	Tapered	8.52
Nylon	43% glass	Tapered	7.02

1. \$ per unit, including tooling amortized over 1,200,000 motors.

TABLE XIII-9  
TYPE III GRAIN COST PENALTIES<sup>(a)</sup>

Raw Material Costs

4 lb per motor \$0.90 per lb. \$3.60

Raw Material Receiving and Acceptance

52 manhour per month = 0.0026 mh/motor N/A

Labor

Mixing - 1 mixer per application station = 2 mixers  
1 man per mixer = 2 men

Application - 3 minutes per case =  
20 cases per station per hour =  
2 stations required<sup>(b)</sup>  
1 man per station = 2 men

Spin 6 minutes per case (including transfer) =  
10 cases per station per hour = 4 stations  
2 stations per man = 2 men

Rework 1 man for all stations

Total labor = 7 men for 40 cases per hour  
= 0.175 manhour per case<sup>(c)</sup> \$4.03

Equipment

0.10

Mixer (2 each at \$30,000)  
Applicator (2 each at \$20,000)  
Spin machine (4 each at \$5000)  
Total = \$120,000 amortized over 1,200,000 motors

Tooling

Aft end dam (one per motor, throw-away) 0.15  
\$7.88

- a. Costs per motor to Propulsion Contractor.  
b. 20,000 motors/month = 240,000 motor/year.  
2000 clock hours/year/shift for 3 shifts = 6000 clock hours/year.  
240,000/6000 = 40 motors/clock hour required production rate.  
c. Labor rate of \$23.00 per hour cost to Propulsion Contractor, includes factor for "non-touch" support labor.

These are shown in Figure XIII-21, along with a line that shows how the cost of the thermoplastic insulation determines whether the mastic insulation will result in savings or extra costs. Since there were several budgetary cost estimates below the break-even point of \$9.13, it appears reasonable to conclude that Type II grains (case-bonded with thermoplastic insulation) are lower cost than Type III grains (case-bonded with mastic insulation). Therefore, within the confines of this study, Type II grains are lower cost than the other two approaches.

#### GAP BETWEEN INSULATION SLEEVE AND CASE

Once it was determined that case-bonded grains with thermoplastic insulation sleeves resulted in the lowest cost system, the question of whether or not to use adhesive between the sleeve and case was addressed. Elimination of the adhesive (except only at the forward closure to restrain the grain) would probably result in lower cost (a little). One of two events can occur during initial motor pressurization if the gap is unfilled. If the insulation/case interface is properly designed the gap can pressurize at almost the same rate as the chamber, which results in almost no differential pressure across the insulation sleeve and grain. Flow passages must be provided for this approach to function properly and the passage between chamber and gap must be carefully controlled. The second possibility consists of the gap lagging far behind the chamber pressurization which causes full motor pressure to act across the insulation sleeve and grain.

The subject calculations determined if the insulation sleeve (acting as though the propellant grain was not present) could expand across an unfilled gap without exceeding the strain or tensile strength capabilities of a particular material. If the gap eventually is pressurized to essentially chamber conditions, then the neglect of the load carrying capabilities of the grain (particularly during rapid load application) causes these calculations to give pessimistic results. However, if the gap is never pressurized to chamber conditions, then at some point during motor operation it is possible to have full pressure differential acting across the insulation sleeve.

Some additional considerations were:

a. The design gap between insulation, sleeve and case does not have to be different for the unbonded approach as opposed to the bonded approach.

b. Since the main purpose of the adhesive would be to support the grain against pressurization deformation, there does not have to be complete coverage. A relatively inexpensive technique then would be to spray a thin coat of adhesive on the exterior of the sleeve just before it is inserted into the case. The case would wipe off any excess (which could be caught on a simple throw-away paper collar) as the sleeve is inserted.

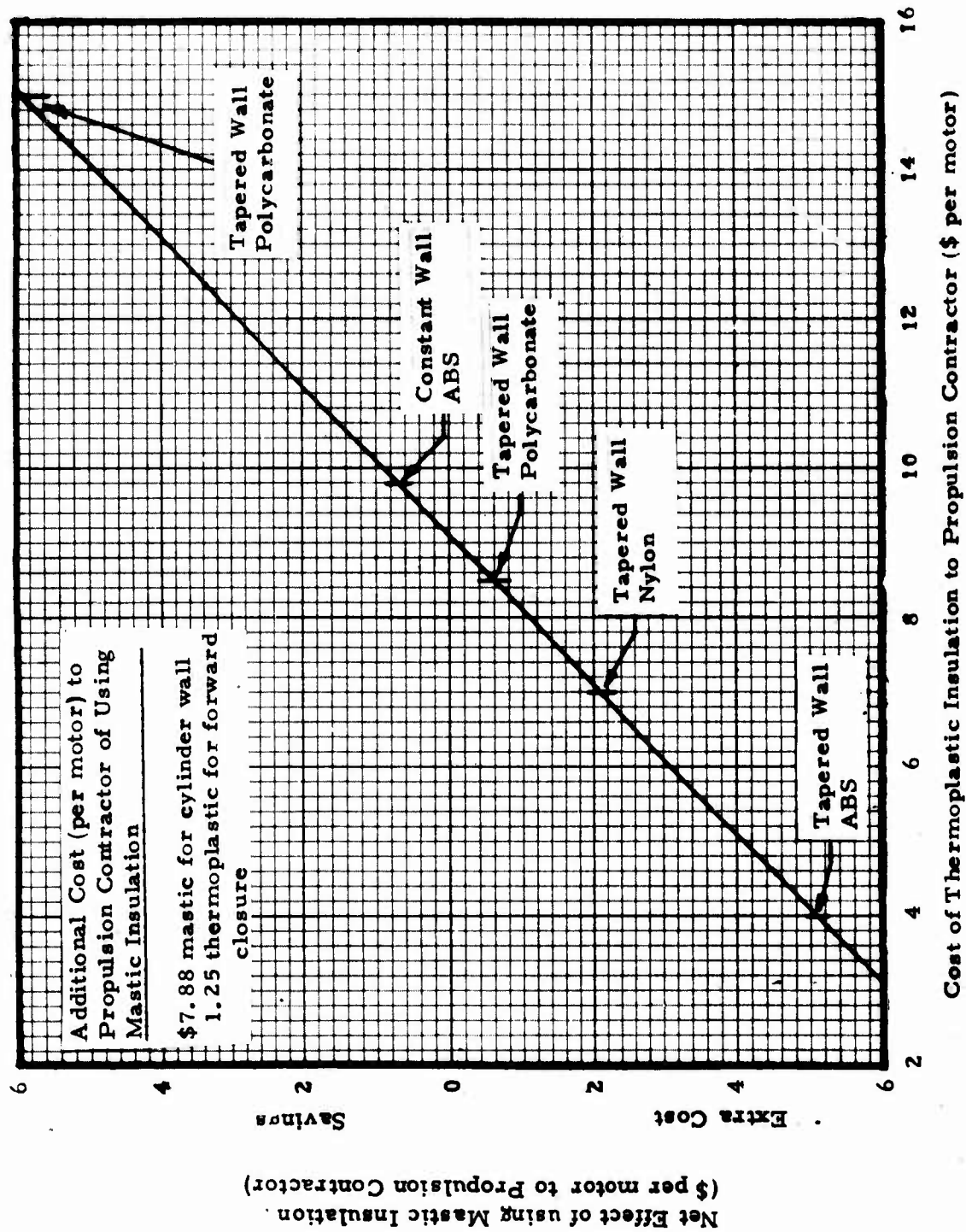


Figure XIII-21. Cost Effects of Mastic Insulation Compared to Case Bonded Thermoplastic Insulation

c. Effects of ovality and bow of the case and insulation sleeve were neglected for this study because the empty sleeve can be deformed as it is inserted into the case.

The relationships between gap and induced stress and strain in the insulation sleeve are:

$$\epsilon_i = \frac{\Delta R}{R}$$

$$\sigma_i = \frac{(\Delta R)(E)}{R}$$

where  $\epsilon_i$  = induced strain in sleeve (in/in)  
 $\sigma_i$  = induced stress in sleeve (psi)  
 $\Delta R$  = gap between sleeve and case (in)  
 $R$  = inside radius of case (in)  
 $E$  = modulus of sleeve material (psi)

These equations are plotted in Figure XIII-22, the latter for values of modulus that are found for several filled thermoplastics.

Resin	Material <sup>1</sup>		Ultimate Properties @ 70°F		
	% Glass	Designation	Tensile Strength (10 <sup>3</sup> psi)	Elongation (in/in)	Modulus (10 <sup>6</sup> psi)
ABS	20	J-1200/20	12	0.015	0.90
Polycarb	40	J-50/40	20	0.014	1.70
Polycarb	20	J-50/20	15	0.020	0.90
Nylon	40	J-10/40	29	0.027	1.45

Ultimate mechanical properties of the four materials also are shown on Figure XIII-22, which indicates the maximum unpressurized gaps which can be tolerated.

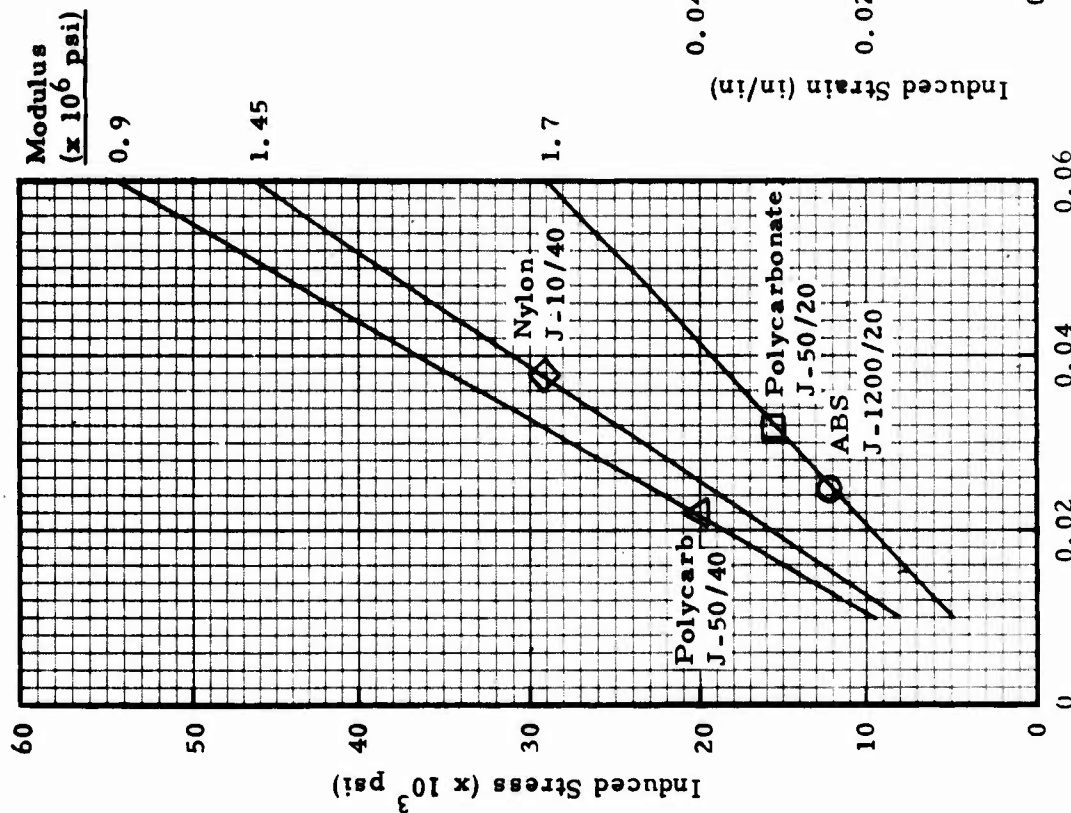
The gap between sleeve and case which might be expected depends on tolerances of the two parts and design minimum gap. Maximum gap occurs when case inside diameter is at maximum tolerance and sleeve outside diameter is at minimum tolerance.

#### Impact extruded aluminum case (See Section X)

Outside diameter = 4.00 ± 0.01 inch  
 Thickness = 0.134 + 0.006/-0.000 inch  
 ∴ Maximum ID = 3.742 inches  
 Minimum ID = 3.710 inches  
 So that total spread = 0.032 inch

1. Fiberfil Division, Dart Industries, Inc.

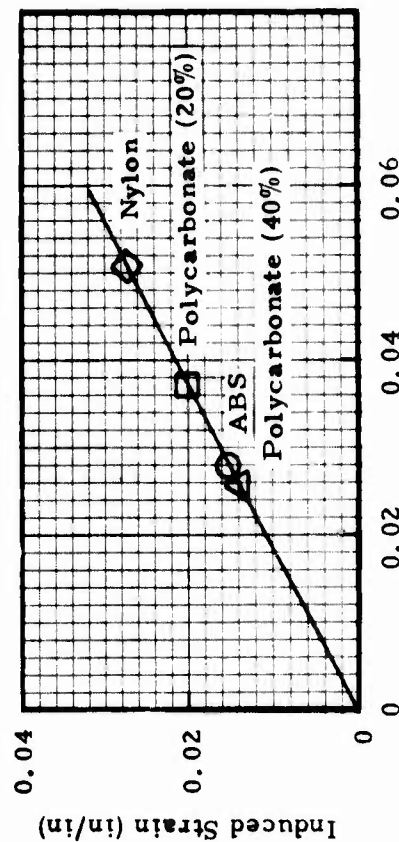




Symbols indicate ultimate properties of materials.

Assumptions:

- (1) Propellant does not take any pressure load.
- (2) Gap is pressurized at rate much slower than chamber so that full chamber pressure is across sleeve.



Unpressurized Gap Between Case and Insulation Sleeve (in)

Figure XIII-22. Capabilities of Insulation Sleeve Materials



Aluminum stock tubing (See Appendix B)

Assume ID and thickness specified for drawn tubing  
Inside diameter = nominal  $\pm 0.016$   
Thickness = 10% of nominal  
Using OD = 4 inches and thickness = 0.165 inch  
 $\therefore$  Maximum ID = 3.686 inches  
Minimum ID = 3.654 inches  
So that total spread = 0.032 inch

Steel stock tubing (See Appendix B)

Assume inside diameter is specified for DOM<sup>1</sup> tubing  
Inside diameter = nominal  $\pm 0.006$  inch  
So that total spread = 0.012 inch

Insulation Sleeve<sup>2</sup>

Outside diameter = Nominal  $\pm 0.003$  to  $0.005$  inch

The maximum gap which might be expected (under extreme conditions) is

maximum gap = Total spread in case ID, plus  
Design minimum gap, plus  
Total spread in sleeve OD

Assuming a design minimum gap of 0.010 inch,

<u>Case</u>	<u>Maximum Gap (in)</u>
Impact extruded aluminum	0.047
Aluminum stock tubing (drawn)	0.047
Steel stock tubing (DOM)	0.027

Referring to Figure XIII-22, a gap of 0.047 inch will induce strain of 0.025 in/in in the sleeve. Neither the two polycarbonates nor the ABS materials have sufficient strain capability to withstand this deflection. The nylon sleeve could provide that level of strain. The gap of 0.047 inch induces stresses of

~ 23,000 psi in the ABS and 20% filled polycarbonate  
~ 36,000 psi in the nylon  
~ 43,000 psi in the 40% filled polycarbonate

all of which exceed the materials capabilities.

1. Consultation with thermoplastic parts vendor
2. Drawn over mandrel

The closer tolerance to which steel DOM tubing can be manufactured shows a large influence on available insulation sleeve materials. The maximum gap of 0.022 inch induces strain of 0.012 in/in which can be provided by all sleeve materials (albeit a small margin of safety for the 40% filled polycarbonate). The induced stress can be withstood by all materials except the 40% filled polycarbonate.

It is concluded that an adhesive should be used between the sleeve and case to restrict grain movement where the cases are aluminum impact extruded or stock tubing. It is not necessary to include an adhesive when using DOM steel tubing. Additional analyses and investigations should be performed prior to a final design. Hoop tensile tests of various filled thermoplastic materials from several vendors will give a more accurate representation of material capabilities. Viscoelastic analyses of the propellant/insulation sleeve/case system will provide a more accurate estimate of induced loads, taking into account the load carrying capabilities of the propellant grain.

#### EFFECT OF INSULATION THICKNESS ON PERFORMANCE

As discussed previously, centrifugal casting is the preferred technique for applying mastic insulation because it results in fewer voids. Motor firing results reported in Reference XIII-2 were used to estimate thickness required for the mastic insulation. One motor with mastic insulation<sup>1</sup> experienced 1.78 times the erosion as an identical motor with polyisoprene insulation. The propellant composition was similar to that anticipated for the current application (88% total solids, 12% aluminum), and the average pressure level was similar. The mastic insulation in the Reference XIII-2 motor was centrifugal cast. Based on the TX631 tests of the current investigation (See Section XII, Insulation/Liner Study), 0.10 inch of polyisoprene would be required for this application. Thus the thickness needed for the mastic insulation is  $(1.78)(0.10) = 0.178$  inch, as a minimum. Examination of the insulation samples from the Reference XIII-2 motor showed there could be voids that were 10% of the thickness. Since the initial application of the mastic in the case and subsequent spinning will not produce exactly the same thickness throughout the case, an additional 10% allowance was included. Thus the nominal thickness of the mastic insulation is  $(1.1)(1.1)(0.178) = 0.215$  inch at the aft end of the grain.

As yet, there is no direct comparison between erosion resistance of thermoplastic and mastic insulations. For the time being it is necessary to assume that minimum thickness requirement is the same for the two classes of material (0.178 inch). Based on consultation with several thermoplastic part vendors, the wall thickness tolerance of  $\pm 0.001$  inch can be expected, which means the thermoplastic insulation sleeve would have a nominal thickness of 0.179 inch. As before, a minimum design clearance of 0.010 inch between case and sleeve was allowed for assembly, and so the effective thickness of the sleeve (for performance calculations) is 0.189 inch. For

---

1. HTPB polymer filled with 40% carbon.

some now obscure reason, the performance analyses described in subsequent paragraphs incorporated a sleeve thickness of 0.200 inch, which unduly penalizes the thermoplastic sleeve approach.

Additional considerations for the performance calculations were:

- a. Both sleeves and mastic insulation have constant thickness around the periphery at a given longitudinal location. The thermoplastic sleeve is penalized in performance by imposing this condition because the molding die can easily provide varying thickness.
- b. Mastic insulation was held constant over its entire length, but thermoplastic sleeves were allowed to vary, in thickness, stepwise or continuously.

Trajectory simulations were made with various insulation configurations. Results are presented in Figure XIII-23, along with the conditions for the calculations. There is a large penalty associated with having insulation of constant thickness over the entire length, where the thickness is established by the most severe conditions at the grain aft end. An approach to improve performance is to provide the maximum thickness just in the area of the longitudinal slots and some lesser thickness over the rest of the case (center perforate section). Another method would be to have a continuous taper over the full length.

<u>Insulation Thickness (in)</u>	<u>Burnout Velocity (ft/sec)</u>
Constant 0.20	3050
Slots 0.20 CP 0.10	3150
Slots 0.20 CP 0	3280
Taper 0.2 (aft) to 0.05 (fwd)	3350

Table XIII-10 shows a comparison of both performance and costs (from Figure XIII-21, Tables XIII-7 and XIII-8) of several insulation systems. Thermoplastic used as either a cartridge sleeve or as an insulation has 40 ft/sec additional burnout velocity because of its smaller nominal thickness. A tapered thermoplastic insulation (either in a single step or continuously) allows from 90 to 300 ft/sec more burnout velocity to be realized over even the thermoplastic constant wall thickness insulation. Motors with mastic insulation cost \$0.60 each more than do those with thermoplastic insulation and case bonded grains, which are also \$3.38 less expensive than motors with cartridge-loaded grains.

Propellant: 88% total solids, 12% aluminum  
 Two slots, 23 inches long; grain web fraction: 0.70  
 Propellant burn rate: 0.42 in/sec @ 1000 psia  
 Initial throat diameter: 0.925 in; exit diameter: 2.96 inches  
 Nozzle throat erosion rate: Baseline, 0.033 in/sec @ 1000 psia  
 Case ultimate strength: 78,000 psi  
 Motor length: 53 inches; diameter 4 inches

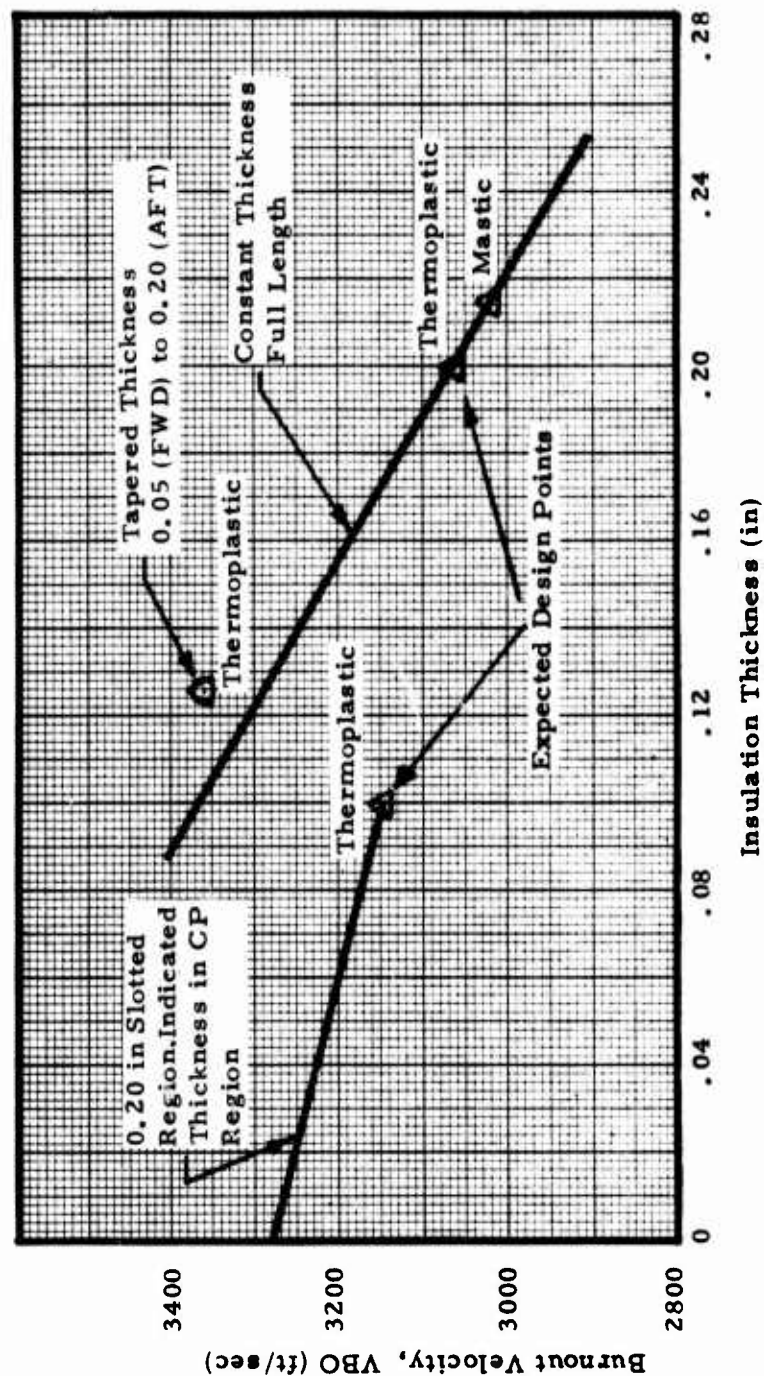


Figure XIII-23. Effect of Insulation Thickness on Missile Velocity

TABLE XIII-10

COMPARISON OF COST AND PERFORMANCE  
CASE INSULATION

<u>Insulation</u>	<u>How Used</u>	<u>Cost Relative to Case Bonded Grain (a)</u>	<u>Burnout Velocity (ft/sec)</u>	<u>Insulation Wall Thickness Configuration</u>
Thermoplastic	Cartridge Sleeve	+\$3.38 +\$3.38	3060 3150 to 3350	Constant Tapered
Thermoplastic	Case insulation <sup>(b)</sup> (Case bonded grain)	0 0	3060 3150 to 3360	Constant Tapered
Mastic	Case insulation	+\$0.60	3020	Constant

- a. Cost to Propulsion Contractor.  
b. Tapered wall polycarbonate.

This study shows lowest cost and highest performance with case bonded grains with molded thermoplastic insulation sleeves having wall thickness that varies over the length of the motor.

#### EFFECT OF CASE STRENGTH ON PERFORMANCE

Additional trajectory analyses determined the joint effect of case material and insulation thickness (Figure XIII-24). The most attractive steel stock tubing, AISI 1026 (See Appendix B), incurs a severe performance penalty in spite of its high ultimate strength. Even though a steel case can tolerate more temperature rise during motor operation than can an aluminum case (thus required insulation thickness is less) the difference is not enough to compensate for the lower strength-to-density ratio of the steel.

#### VENDOR CONTACTS

The following vendors were contacted for technical consultation and/or budgetary cost estimates:

AMOCO  
St. Paul, Minn.

Meridian Plastics  
Shelby, N. C.

Millington Plastics  
Upper Sandusky, Ohio

Modern Plastics  
Benton Harbor, Mich.

Plexco  
Knoxville, Tenn.

Value Engineered Components  
Arab, Ala.

#### REFERENCES

1. AFRPL-TR-73-68, "Demonstration of Ambient Temperature Cure Propellant", Aerojet Solid Propulsion Co., August 1973.
2. C-74-1023, "Static Test Report TX-646-2, Motor D1", Thiokol/Huntsville.



Constant Insulation Thickness

Propellant: 88% total solids, 12% aluminum

Two Slots, 23 inches long

Grain Web Fraction: 0.7

Propellant Burn Rate: 0.42 in/sec @ 1000 psia

Initial Throat Diameter: 0.925 inch

Nozzle Throat Erosion Rate: Baseline, 0.033 in/sec at 1000 psia

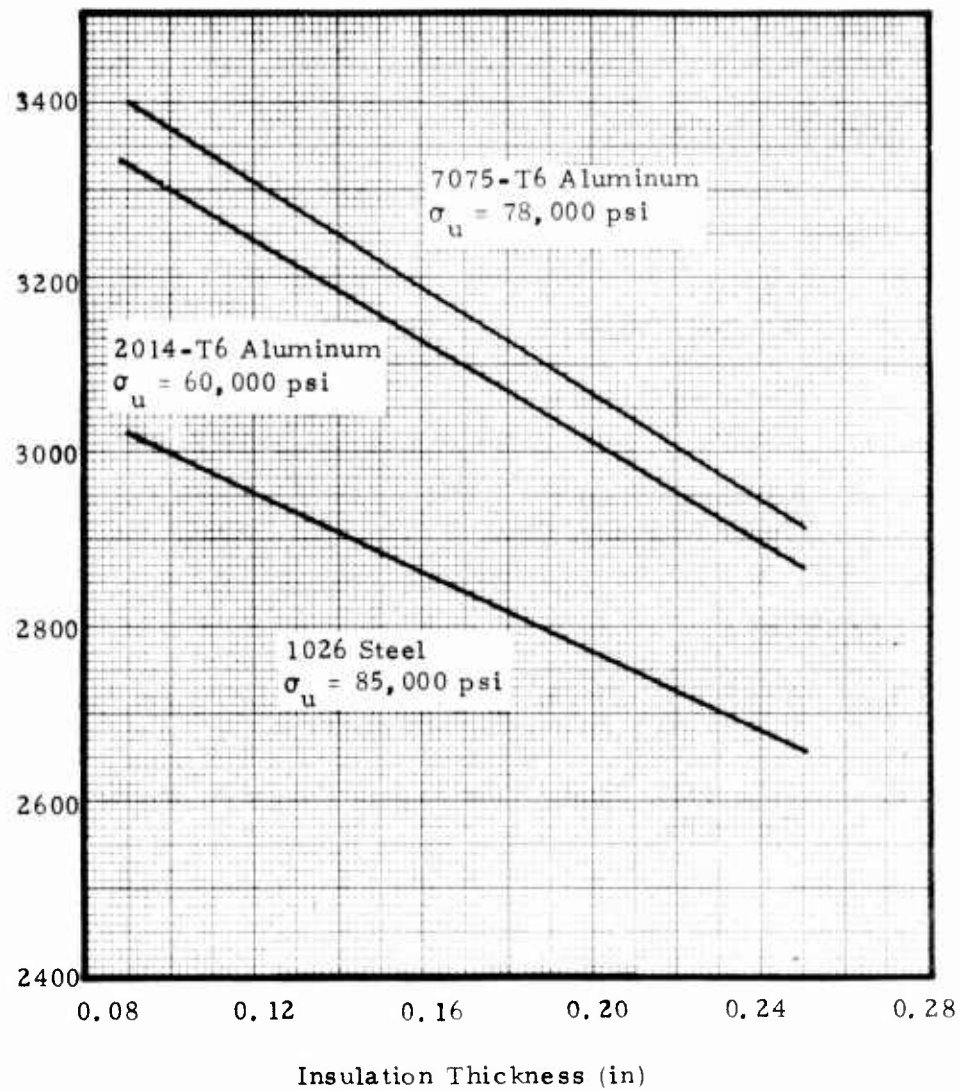


Figure XIII-24. Effect of Case Material and Insulation Thickness on Burnout Velocity



SECTION XIV

COST COMPARISONS

## SECTION XIV

### COST COMPARISONS

Each rocket motor component can be chosen individually on the basis of lowest cost, acceptable performance, technical feasibility, etc. Where a large number of candidates were reviewed for each component, it was necessary to examine the combinations, rather than the individuals, to determine which might be "best". As would be expected, the comparisons showed there was no "best" arrangement, but instead, a spectrum from which to choose.

The usual tradeoff is cost versus performance and those were the variables selected for this study. "Cost" was cost to propulsion contractor to buy and assemble forward closure, case, and nozzle; "performance" was the weight of those components. It was assumed that costs to insulate the cases and load propellant were identical for all combinations. For the purposes of this study it was not necessary to include those costs.

Table XIV-1 summarizes the costs and weights used in the combinations. The plastic laminate case (filament wound composite) was not included because of some technical misgivings, even though it will be one of the more attractive case because of both weight and cost. For any case made from tubing, it doesn't matter whether the forward closure or the nozzle is attached first. Whatever joining technique is used on the first-made joint is acceptable whether the joint is at the forward closure or the nozzle. Therefore, for simplicity in this study, it was assumed the forward closure is attached first, then the propellant loaded, and finally, the nozzle attached. Obviously, for the impact extruded cases with integral forward closure or integral nozzle support, the case configuration dictates the last-made joint.

Case weights and costs were taken from available information and where possible the pressure capabilities were made consistent (Table XIV-2). Adhesive costs were added to the combinations with the case having integral nozzle support because the nozzle ablative would be procured without a shell and must be bonded into the case; in all other joining techniques using adhesive, that cost is included in the basic cost. Costs for providing warhead attachment threads and mating surface preparation are included. Shipping charges are not included.

All nozzles have contoured exit cones and aluminum support shells (except as discussed above). Cost of providing a snap ring for steel cases was assumed to be the same as for aluminum cases. Joining with straight bondline (i.e., constant diameter) was combined only with the strip laminate case because the close tolerances needed for that technique are inherently provided in the strip laminate case, whereas more expensive joint preparation would be needed for tubing or extruded cases.

Some components listed on Table XIV-1 were not included in the final

TABLE XIV-1

COMPONENT WEIGHTS AND COSTS

<u>Component or Operation</u>	<u>Configuration</u>	<u>Material</u>	<u>Cost<sup>(a)</sup> (\$)</u>	<u>Weight (lb)</u>
Case	Integral HE (Impact extruded)	2014-T 6	26.58	10.5
		7075-T 6	28.12	8.8
		7075-T 73	29.19	9.8
	Integral NE (Impact extruded)	2014-T 6	26.78	9.6
		7075-T 6	28.44	7.6
		7075-T 13	29.56	8.8
	Steel Tubing	1026	7.41	21.5
		1035	7.59	19.0
		4130N	14.78	16.1
	Alum Tubing	2014	23.02	9.2
		2024	24.95	9.2
		7075-T 6	28.84	7.5
	Strip Laminate	Steel	27.00	6.5
Nozzle	Alum Shell	D791	8.09	3.0
	Steel Shell	D791	12.09	5.0
	W/O Shell	D791	6.30	1.8
	Alum Shell	D22532	8.82	3.0
	W/O Shell	D22532	7.32	1.8
	Alum Shell	D23570	11.34	3.5
	Steel Shell	D23570	15.34	5.5
	W/O Shell	D23570	10.18	2.3
Closure	Reverse Dome	Alum	2.62	1.0
		Steel	4.64	1.9
		Plastic	3.10	1.0
	Taper	Alum	2.64	1.0
		Plastic	1.70	0.6
	Flat Plate	Alum	3.40	1.1
		Steel	6.15	3.0
	Conventional	Alum	3.00	1.1
		Steel	5.42	3.1
		Plastic	1.89	0.6

(Continued on next page)

TABLE XIV-1 (continued)

Component or Operation	Configuration	Material	Cost <sup>(a)</sup> (\$)	Weight (lb)
Joining (Empty cases)	Straight Bondline	---	0.39	---
	Friction Weld	---	0.47	---
	EMF-Bond	---	0.63	---
	Electron Beam (OV)	---	0.69	---
	Taper Bondline	---	0.87	---
	Snap Ring (alum)	---	2.65	---
	Snap Ring (steel)	---	2.65	---
Joining (Loaded Cases)	Straight Bondline	---	0.39	---
	EMF-Bond	---	0.63	---
	Electron Beam (OV)	---	0.69	---
	Snap Ring (alum)	---	2.65	---
	Snap Ring (steel)	---	2.65	---
Threading	---	Alum	1.65	---
		Steel	1.33	---
Adhesive	---	---	0.20	---

a. Cost to Propulsion Contractor.

TABLE XIV-2

CASE COMPARISONS

<u>Type</u>	<u>Material</u>	<u>Wall Thickness (in)</u>	<u>PMAX @70°F (psia)</u>	<u>Length (in)</u>	<u>Weight (lb)</u>	<u>Cost<sup>(a)</sup> (\$)</u>
Strlp Laminate Tubing	Steel	0.032	2620	45	6.5	27.00
	Steel-1026	0.134	3295	45	21.5	7.41
	-1035	0.120	3100	45	19.0	7.59
	-4130N	0.100 <sup>(b)</sup>	2970	45	16.1	14.78
	Alum-2014-T6	0.165	3080	45	9.2	23.02
	-2024-T81	0.165	3130	45	9.2	24.95
	-7075-T6	0.156 <sup>(b)</sup>	3430	45	7.5	28.84
Impact Extruded (Integral HE)	Alum-2014-T6	0.145	2620	45	10.5	26.58
	-7075-T6	0.115	2620	45	8.8	28.12
	-7075-T73	0.134	2620	45	9.8	29.19
Impact Extruded (Integral NE)	Alum-2014-T6	0.145	2620	45	9.6	26.78
	-7075-T6	0.115	2620	45	7.6	28.44
	-7075-T73	0.134	2620	45	8.8	29.56

a. Cost to Propulsion Contractor.

b. Only quote, only thickness found.

calculation because inspection revealed that they gave lower performance for higher costs (e. g., 7075-T73 impacted extruded cases cost more and weigh more than 7075-T6 cases). In other instances, certain components were not carried into final calculations because they represented intermediate costs or performance and the interest was in the best and the more conservative ( e. g., D22532 nozzle ablative was intermediate cost, had intermediate weight, and showed intermediate technical index of merit).

Results of the calculations are given in Figure XIV-1. The lower line forms the boundary of the entire group and represents the lowest weight/lowest cost combinations. As discussed earlier, there was no "best" combination. The points making up the lower boundary are listed in Table XIV-3.

The middle line on Figure XIV-1 delineates typical motors that used the same advanced joining techniques and closures of those motors on the lower boundary, but they incorporate a more conservative nozzle ablative material (glass phenolic instead of wood flour phenolic). The upper line in Figure XIV-1 shows the typical more conventional arrangements; those with the conservative nozzle ablative and a snap ring retention.

Forward Closure & Joining  
Case  
Nozzle & Joining

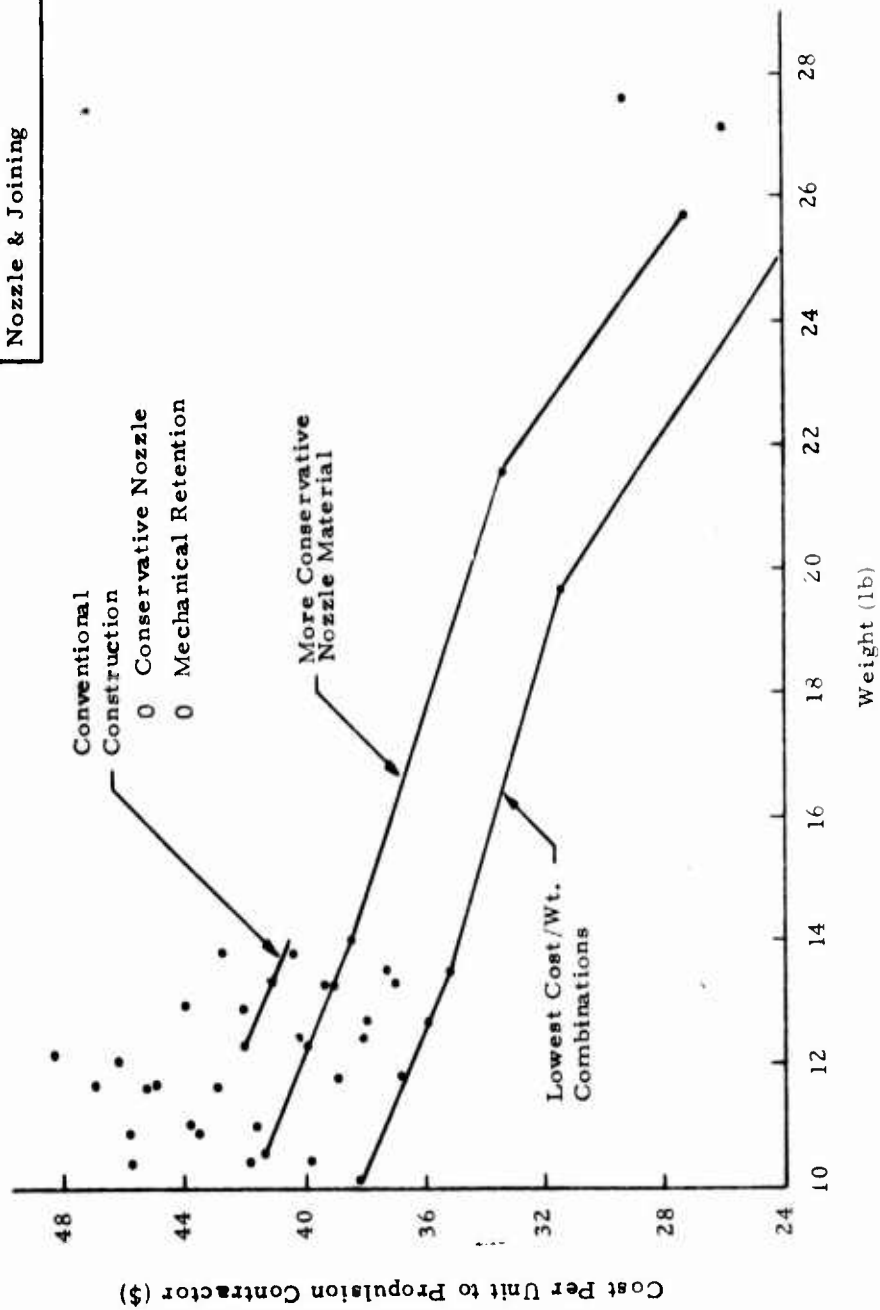


Figure XIV-1. Cost Comparisons



TABLE XIV-3

LOWEST COST / LOWEST WEIGHT COMBINATIONS

Forward Closure	Forward Joining	Case	Aft Joining	Nozzle (a)	Weight (lb)	Cost (b) (\$)
Plastic Dome (c)	Straight Bondline	Steel Strip Laminate	Adhesive	D791 <sup>d</sup>	10.1	38.15
N/A	N/A	Integral HE (7075-T6 Alum)	EMF-Bond	D791	11.8	36.76
Taper-Plastic	Taper Bond	Alum Tubing 2014-T6	EMF-Bond	D791	12.7	35.88
Aluminum Flat Plate	Friction Weld	Alum Tubing 2014-T6	EMF-Bond	D791	13.3	35.47
N/A	N/A	Integral HE (2014-T6 Alum)	EMF-Bond	D791	13.5	35.22
Plastic Dome (c)	Snap Ring	Steel Tubing (4130N)	Snap Ring	D791	19.7	31.39
Plastic Dome (c)	Snap Ring	Steel Tubing (1026)	Snap Ring	D791	25.1	24.02

- a. All with contoured exit section and aluminum shell.  
 b. Cost to Propulsion Contractor  
 c. Conventional configuration.  
 d. Wood-flour phenolic molding.

SECTION XV

PHASE II MOTOR CONFIGURATIONS

## SECTION XV

### PHASE II MOTOR CONFIGURATIONS

The second phase of the subject contract will involve the testing of selected components in full-scale (4-inch diameter) motors. Component and manufacturing techniques found to be promising in cost reduction potential will be evaluated under conditions of temperature extremes and vibration. They will also be compared on the basis of absolute cost per unit and the ability to meet missile performance requirements.

The final task in Phase I was to select the components and motor configurations to be evaluated in Phase II. The starting point for such a selection was the lowest cost/lowest weight combinations identified in Section XIV, where the final results are presented in Table XIV-3.

Table XV-1 lists the configurations selected for Phase II which are also illustrated in Figure XV-1. The lowest weight combination on Table XIV-3 cannot be evaluated in the current program because of the high cost for a small number of steel strip laminate cases. The impact extruded cases with integral forward closure is considered a state-of-the-art fabrication technique and, thus, need not be evaluated or simulated as part of Phase II. The nozzle joining technique proposed for use with the impact extruded case---electromagnetic forming with bonding (EMF-Bond) will be incorporated on other Phase II motors. Steel tubing, while offering extremely low cost, suffers extreme performance penalties because of its low strength-to-weight ratio (Section XIII); therefore steel tubing was not included in Phase II testing.

Thus the features which should be evaluated in full-scale motor tests are (concentrating on the "lowest weight" combinations listed in Table XV-1):

- o Aluminum tubing as case material
- o Plastic tapered closure, with associated swaging of the case tubing
- o Friction welded closure
- o EMF-Bond joining
- o Wood flour phenolic nozzle ablative

Other investigations during Phase II result in these further details of Phase II motors:

- o Glass-filled polycarbonate case insulation
- o Glass-filled ABS case insulation
- o Carbon-filled mastic insulation

- o Cellulose-phenolic nozzle ablative
- o Glass-phenolic nozzle ablative

Polycarbonate insulation has the potential for best erosion resistance at cost equal to or less than ABS or mastic insulations (Section XII). However, ABS has lower cost per unit thickness and cost of mastic insulation relative to the thermoplastics depends to a great extent on the cost of the latter. In addition there needs to be additional motor evaluation of relative erosion resistance of the three materials. Thus it was decided to incorporate all three---polycarbonate, ABS, and mastic---in Phase II motors. The thermoplastics will be bonded to the case with TA-H731A liner and to the propellant with Chemlok 233.

Nozzles with lowest absolute cost will use D791 wood flour phenolic ablative material, which had the lowest Technical Index of Merit of those finally selected for additional evaluation (Section IX). Cellulose-phenolic had excellent erosion resistance at only slightly higher cost and was also selected for Phase II tests. The most conservative nozzle material is glass-phenolic and is included in Phase II as a back-up to the other more experimental materials. The Phase II testing will provide a direct comparison of erosion resistance of the three materials. All three materials will be installed in an aluminum structural support shell.

Three of the more attractive low cost joining techniques---friction welding, EMF-Bonding, and taper-bonding---are included in Phase II motors because they are compatible with aluminum stock tubing. Straight bondline joining is most suitable for strip laminate cases, which are not included in Phase II. Electron beam welding cannot be considered because of the high initial investment. It was decided to include a mechanical retention system---a snap ring---as a back-up to the EMF-Bond for the last-made joint.

EMF-Bonding on a loaded motor will be simulated even though the technique is suitable for use on a loaded motor. There is not a facility with EMF equipment that can process explosive-carrying hardware. An adapter that mates with threads on the case tubing (Figure XV-1) will have dimensions duplicating the tube/nozzle interface. The adapter and nozzle will be sent to the EMF vendor, assembled and then returned to Thiokol for attachment on the loaded motor.

Another concession to high tooling cost involves the thermoplastic case insulation. Full-length moldings will be prohibitively priced because of tooling and process development costs. Instead the insulation sleeve will be assembled from short length (about four inches) segments made in a "sample" cavity.

Ambient-temperature cured propellant (DTS-7984) will be cast in a case-bonded configuration using a foamed polyurethane mandrel which will remain in the motor. The propellant will be "pour-cast" and the casting assembly will be vibrated during the operation to alleviate void formation. Igniter pyrotechnic charge will be magnesium-teflon pellets initiated with an Atlas Match.

In summary (referring to Table XV-1), Phase II motors will have the following salient features and test objectives.

Low Cost Design No. 1

- o Third lowest weight pressure vessel, which has the third highest cost
- o Most likely case insulation
- o Lowest cost nozzle ablative
- o Determine nozzle thrust alignment with EMF joining

Low Cost Design No. 2

- o Fourth lowest weight pressure vessel, which has the fourth lowest cost
- o Best nozzle ablative on cost/performance basis
- o Potentially lowest cost case insulation

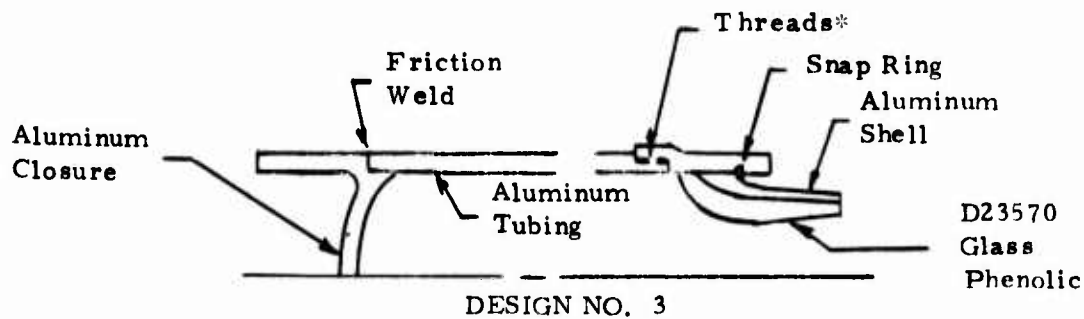
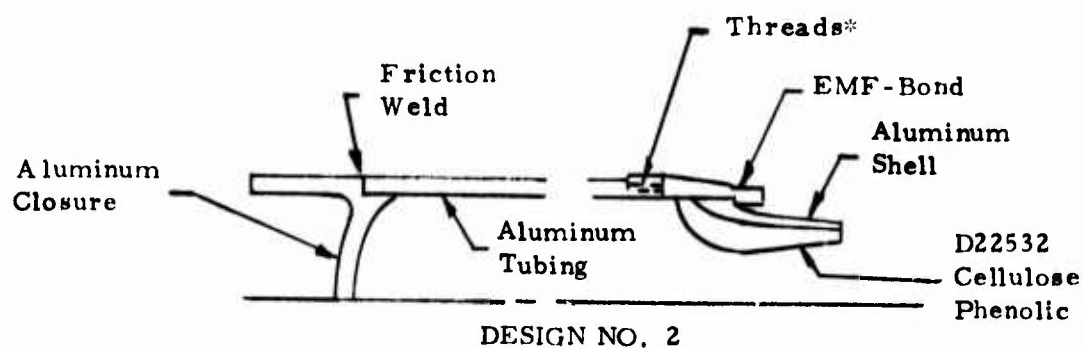
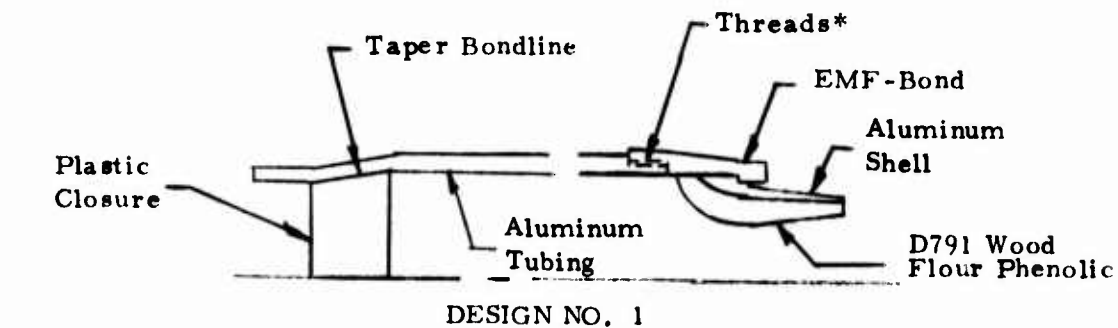
Low Cost Design No. 3

- o Back-up aft joining technique
- o Most conservative nozzle ablative
- o Back-up case insulation

TABLE XV-1

PHASE II MOTOR CONFIGURATIONS

Feature	Configuration		
	No. 1	No. 2	No. 3
Propellant	Ambient-Temp. cured	Ambient-Temp. cured	Ambient - Temp. cured
Grain Configuration	Case Bonded	Case Bonded	Case Bonded
Grain Manufacturing	Pour casting with vibration	Pour casting with vibration	Pour casting with vibration
Mandrel	Foam, leave-in-place	Foam, leave-in-place	Foam, leave-in-place
Igniter Pyrotechnics	Magnesium-teflon pellets	Magnesium-teflon pellets	Magnesium-teflon pellets
Forward Closure	Plastic/taper	Alum (FW)	Alum (FW)
Forward Joining Technique	Taper-bond	Friction Weld	Friction Weld
Case	Aluminum stock tubing	Aluminum stock tubing	Aluminum stock tubing
Aft Joining Technique	EMF-Bond	EMF-Bond	Snap Ring
Nozzle Ablative	Wood-flour	Cellulose	Glass
Nozzle Support Shell	Aluminum	Aluminum	Aluminum
Case Insulation	Polycarbonate	ABS	Carbon Mastic



\*Feature included to facilitate demonstration testing within reasonable program expenditure

Figure XV-1. Motor Configuration Selected For Phase II Evaluation



APPENDIX A  
BALLISTIC ANALYSIS OF TP-H8245  
PROPELLANT (MIX T-600)

APPENDIX A  
BALLISTIC ANALYSIS OF TP-H8245 PROPELLANT  
(MIX T-600)

BURNING RATE

TX-395 Motors

Charges 1 through 12 of Mix T-600 of TP-H8245 propellant were loaded as TX-395 motors and these motors were static tested at -65, 70, and 160°F. The test results are summarized in Table A-1, and pressure versus time traces for the motors are given on Figures A-1 through A-6. A summary plot of burning rate versus pressure is shown on Figure A-7.

A multiple linear regression program (VR 7036) for the Monroe 1880 calculator was used to determine the coefficients of the burn rate equation:

$$\ln r = b_0 + b_1 (\ln P) + b_2 (T) + b_3 (T) (\ln P) \quad (1)$$

Resulting coefficients were:

$$\begin{aligned} b_0 &= -4.0547 \\ b_1 &= 0.44707 \\ b_2 &= -0.0022002 \\ b_3 &= 0.00039805 \end{aligned}$$

This is the correlation shown with the data on Figure A-7. Equation (1) explained 99.76% of the variation in  $\ln r$ , and both the regression and the individual coefficients are significant at a probability level greater than 99%. The residual error was 0.0117 (corresponding to a coefficient of variation of approximately 1.2%). Equation (1) expresses burn rate at all temperatures and Equation (2) shows that exponent is a function of temperature and independent of pressure.

$$n = \frac{\partial \ln r}{\partial \ln P} = b_1 + b_3 T \quad (2)$$

Figure A-8 is a plot of the burn rate exponent,  $n$ , versus temperature.

### Cured Strands

Eleven cured strands, each 2 inches long, were tested in a pure nitrogen atmosphere at 70°F. The data are summarized in Table A-2. A least squares linear regression program was used on the Monroe 1880 to calculate burn rate as a function of pressure:

$$\ln r = b_0 + b_1 \ln P \quad (3)$$

The resulting coefficients were:

$$\begin{aligned} b_0 &= -4.08696 \\ b_1 &= 0.45840 \end{aligned}$$

Equation (3) had a standard deviation of  $\ln$  rate at a given value of  $\ln$  pressure ( $S_{y, x}$ ) equal to 1.49% and a standard deviation of slope ( $S_{b_1}$ ) equal to 0.0063. This correlation is plotted with the strand test data and the TX-395 data on Figure A-7. The TX-395 and strand burn rates at 70°F agreed reasonably well.

### TEMPERATURE EFFECTS

The direct use of Equation (1) eliminates the need for  $\pi_k$  and  $\sigma_k$  values in ballistic calculations. For discussion purposes,  $\pi_k$  and  $\sigma_k$  calculations are presented below.

$$\pi_k$$

Figure A-9 is a plot of motor pressure versus temperature on different  $K_N$  lines. Equation (4):

$$\ln P = b_0 + b_1 \ln K_N + b_2 T + b_3 T \ln K_N \quad (4)$$

was the model for the multiple linear regression program to determine  $\ln$  pressure as a function of temperature and  $\ln$  area ratio ( $K_N$ ). The resulting coefficients were

$$\begin{aligned} b_0 &= -2.66009 \\ b_1 &= 1.72693 \\ b_2 &= -0.008539 \\ b_3 &= 0.0016903 \end{aligned}$$

This correlation explained 98.64% of the variation in  $\ln P$  with a standard error of 0.051. The overall relation was significant at a probability level greater than 99%. Coefficients  $b_0$ ,  $b_1$  and  $b_2$  were significant at a probability near 95%. The correlation using approximate values of  $K_N$  are presented with the data points on Figure A-9.

From Equation (5):

$$\pi_k = \frac{\partial \ln P}{\partial T} \bigg/_{K_N} = b_2 + b_3 \ln K_N \quad (5)$$

$\pi_k$  calculated for the approximate  $K_N$ 's used are seen below:

$K_N$	$\pi_k$
240	0.000653
290	0.000794
340	0.001102
400	0.001588

$\sigma_k$

The multiple linear regression program was used to determine  $\sigma_k$  in the same manner as  $\pi_k$  calculations. The model was:

$$\ln r = b_0 + b_1 \ln K_N + b_2 T + b_3 T \ln K_N \quad (6)$$

and the resulting coefficients were:

$$\begin{aligned} b_0 &= -5.25865 \\ b_1 &= 0.775164 \\ b_2 &= -0.00731863 \\ b_3 &= 0.00149192 \end{aligned}$$

This correlation explained 98.52% of the variation in  $\ln$  rate with a standard error of 0.029. The overall regression and the individual coefficients  $b_0$  and  $b_1$  were significant at a probability level greater than 99%. Coefficients  $b_2$  and  $b_3$  were significant at a probability level greater than 95%. The correlation is presented with the data on Figure A-10.

From Equation (7):

$$\sigma_k = \frac{\partial \ln r}{\partial T} \bigg/_{K_N} = b_2 + b_3 \ln K_N \quad (7)$$

Below are the values of  $\sigma_k$  for the approximate values of  $K_N$  shown on Figure A-10:

<u><math>K_N</math></u>	<u><math>\sigma_k</math></u>
240	0.00086
290	0.00114
340	0.00138
400	0.00162

TABLE A-1  
TX-395 MOTOR DATA FOR TP-H8245 PROPELLANT  
(Mix T-600)

<u>Charge</u>	<u>Temp. (°F)</u>	<u>K<sub>N</sub></u>	<u>P (psia)</u>	<u>r<sub>b</sub> (in/sec)</u>
1	-65	239.8	879	0.347
2	-65	296.6	1182	0.395
3	-65	355.8	1535	0.440
4	-65	412.7	2118	0.500
5	70	236.7	966	0.391
6	70	293.5	1298	0.447
7	70	329.1	1716	0.505
8	70	392.2	2583	0.631
9	160	242.9	1046	0.424
10	160	283.2	1384	0.486
11	160	324.0	1820	0.576
12	160	402.3	2759	0.688

TABLE A-2

CURED STRAND DATA FOR TP-H8245 PROPELLANT  
(Mix T-600)

(Tests on 2-inch long strands in nitrogen atmosphere,  
at 70°F)

<u>Pressure (psia)</u>	<u><math>r_b</math> (in/sec)</u>
200	0.190
400	0.268
600	0.314
800	0.354
1000	0.390
1200	0.428
1400	0.473
1600	0.494
1800	0.529
2000	0.544
2200	0.575



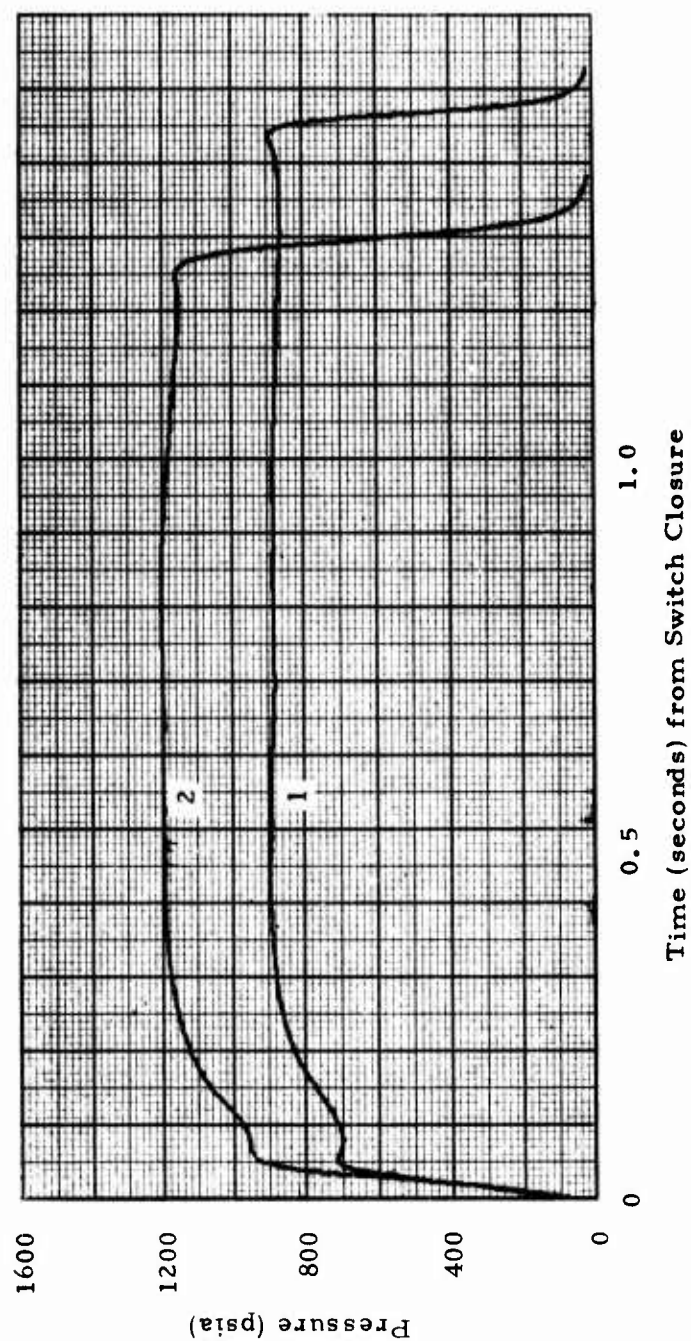


Figure A-1. Ballistic History, TX-395 Motors, Mix T-600, Charges 1 and 2,  
Fired at -65°F

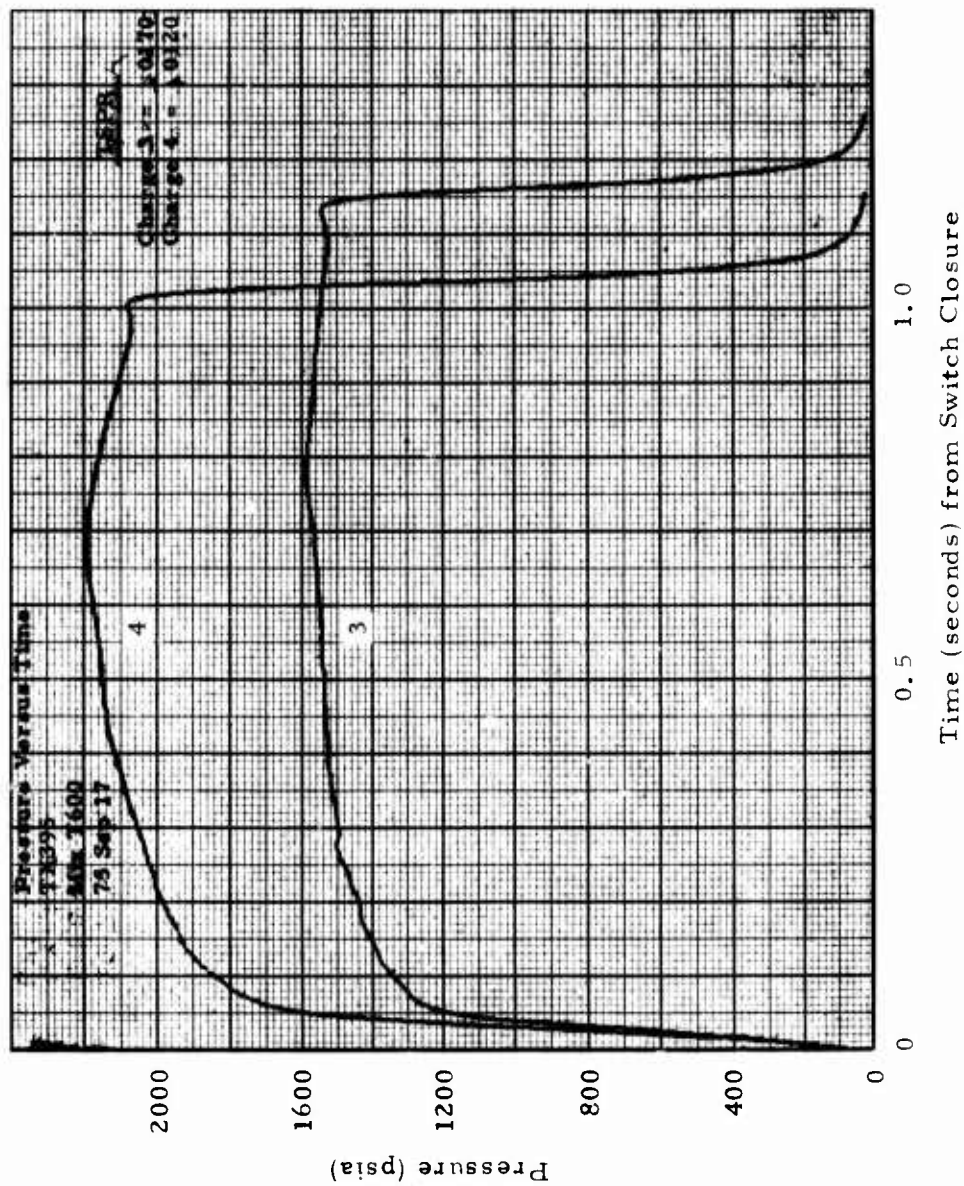


Figure A-2. Ballistic History, TX-395 Motors, Mix T-600, Charges 3 and 4, Fired at -65°F

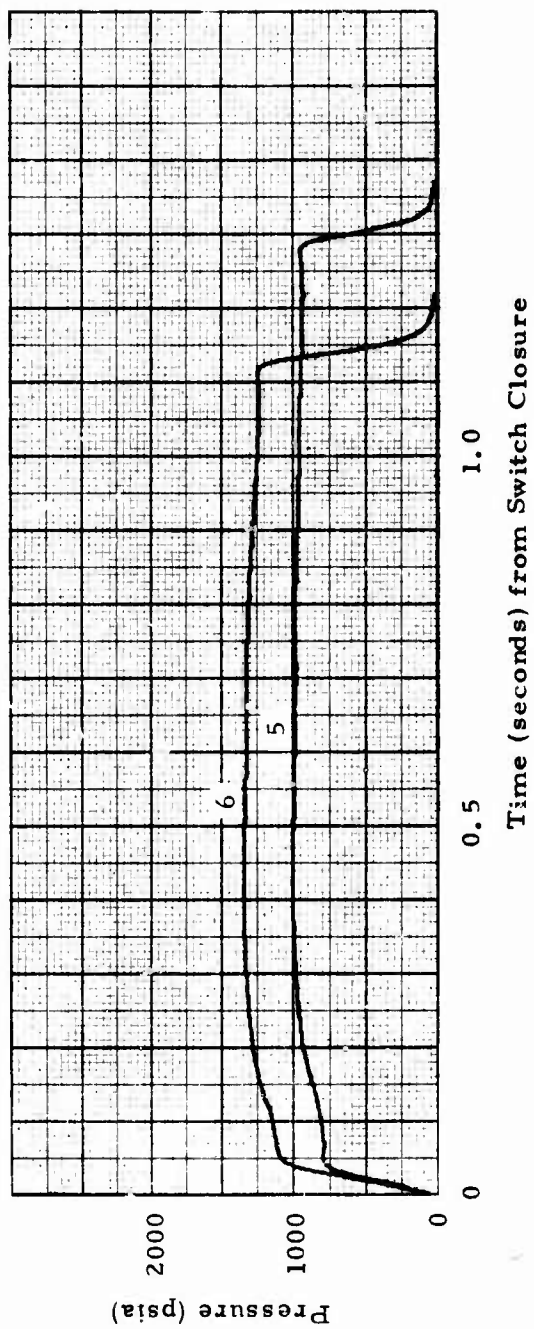


Figure A-3. Ballistic History, TX-395 Motors, Mix T-600, Charges 5 and 6, Fired at 70°F

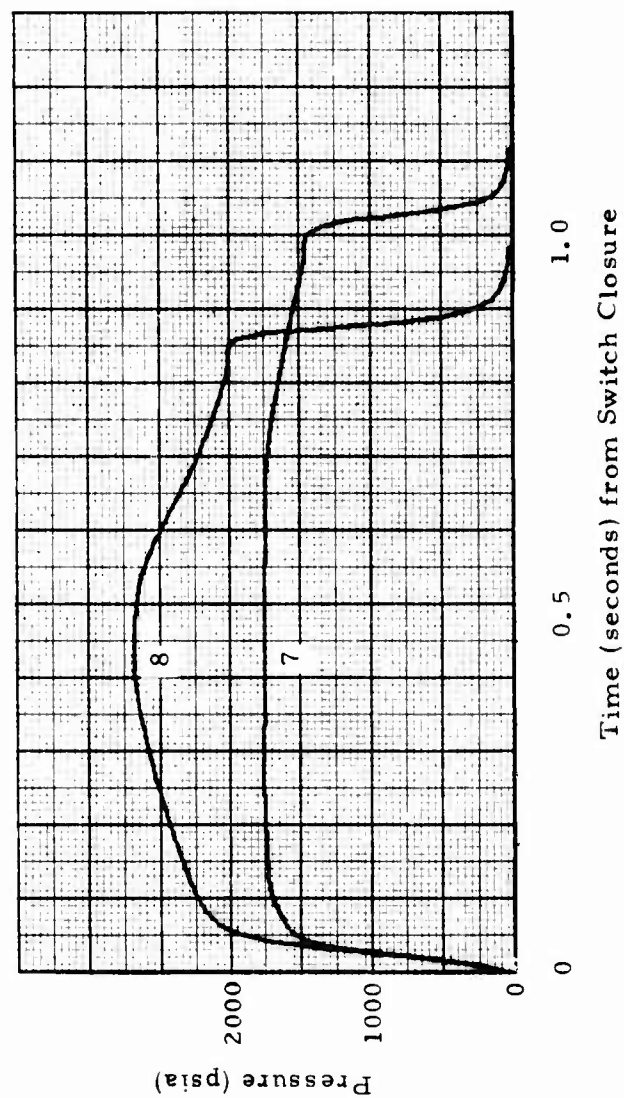


Figure A-4. Ballistic History, TX-395 Motors, Mix T-600, Charges 7 and 8, Fired at 70°F

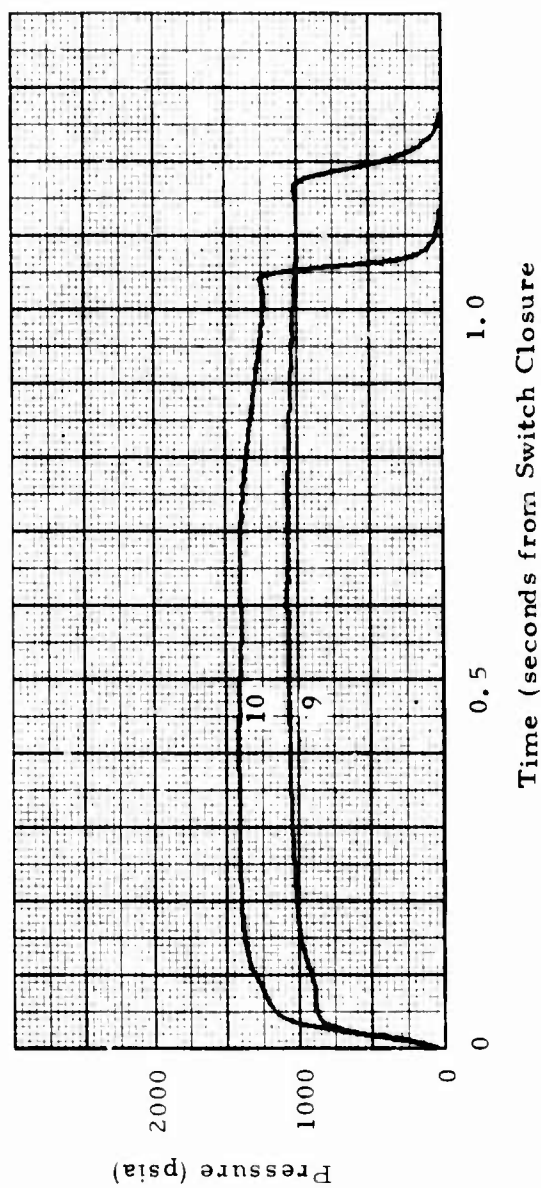


Figure A-5. Ballistic History, TX-395 Motors, Mix T-600, Charges 9 and 10,  
Fired at 160°F

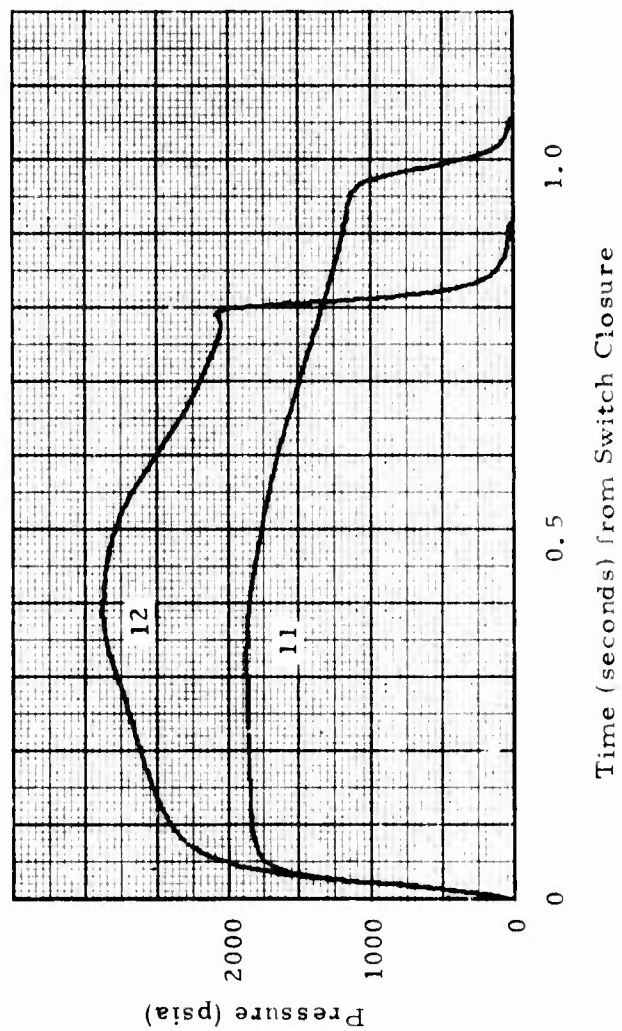


Figure A-6. Ballistic History, TX-395 Motors, Mix T-600, Charges 11 and 12, Fired at 160°F



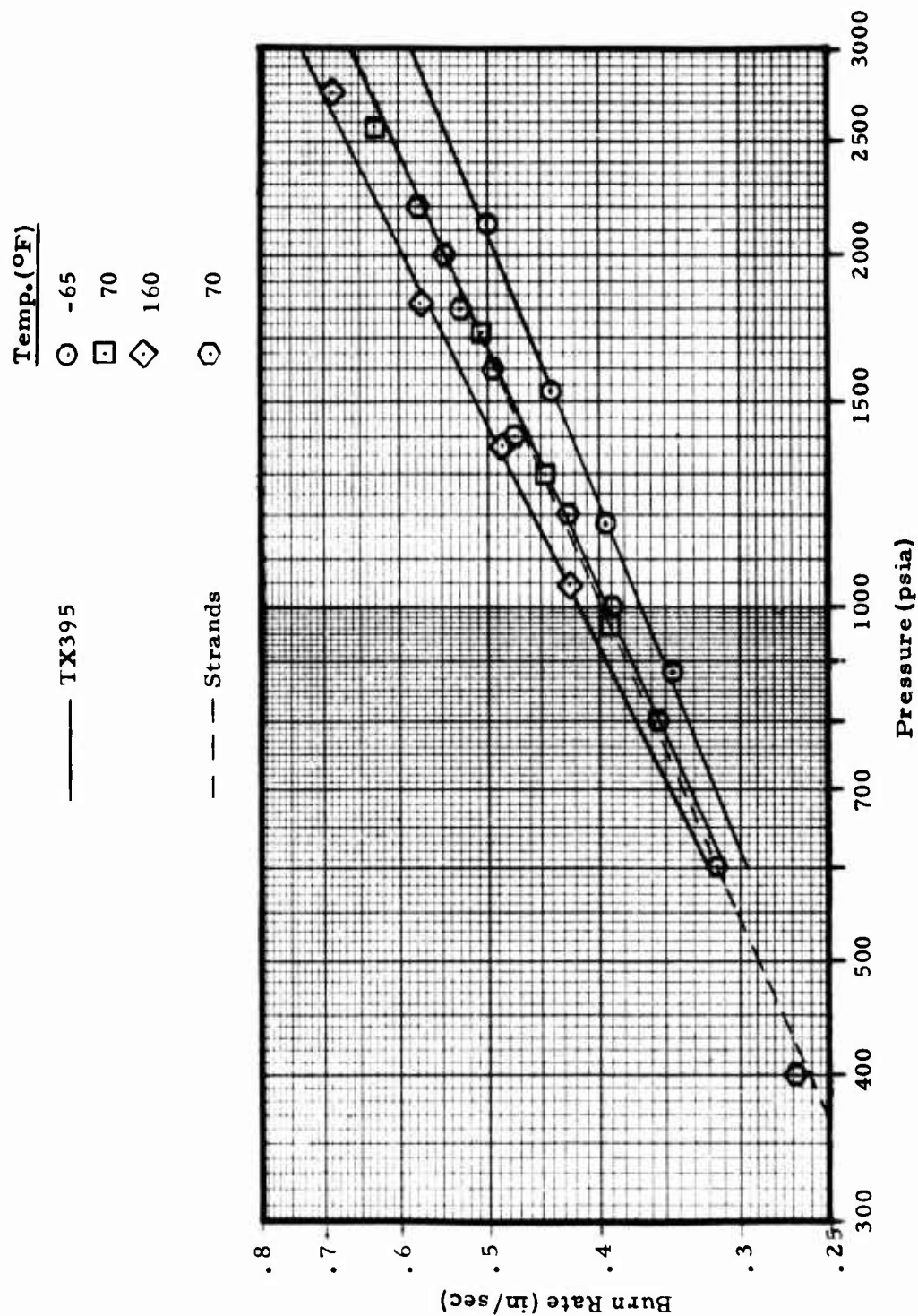


Figure A-7. Burning Rate versus Pressure for TP-H8245 Propellant (Mix T-600)



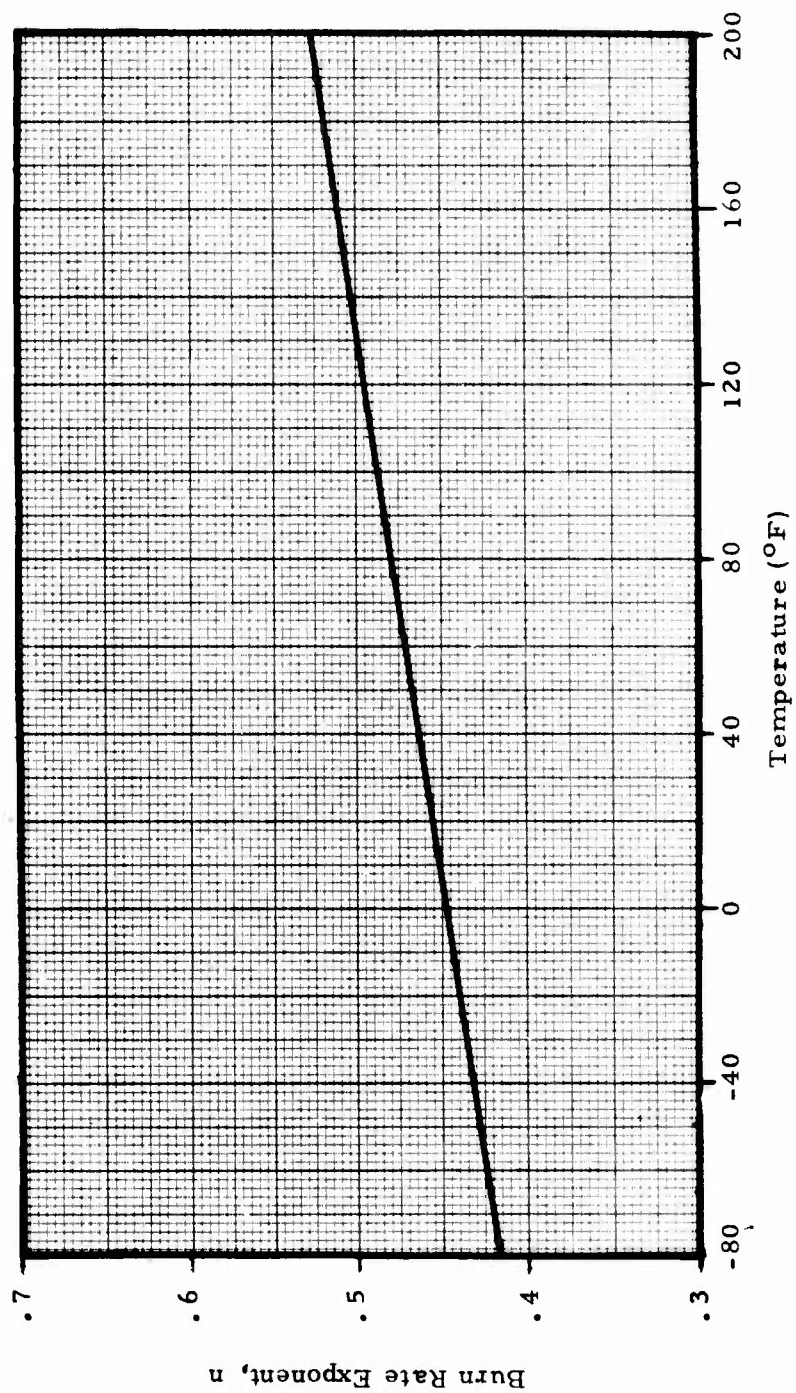


Figure A-8. Temperature Effect on Burning Rate Exponent, TP-H8245 Propellant (Mix T-600)

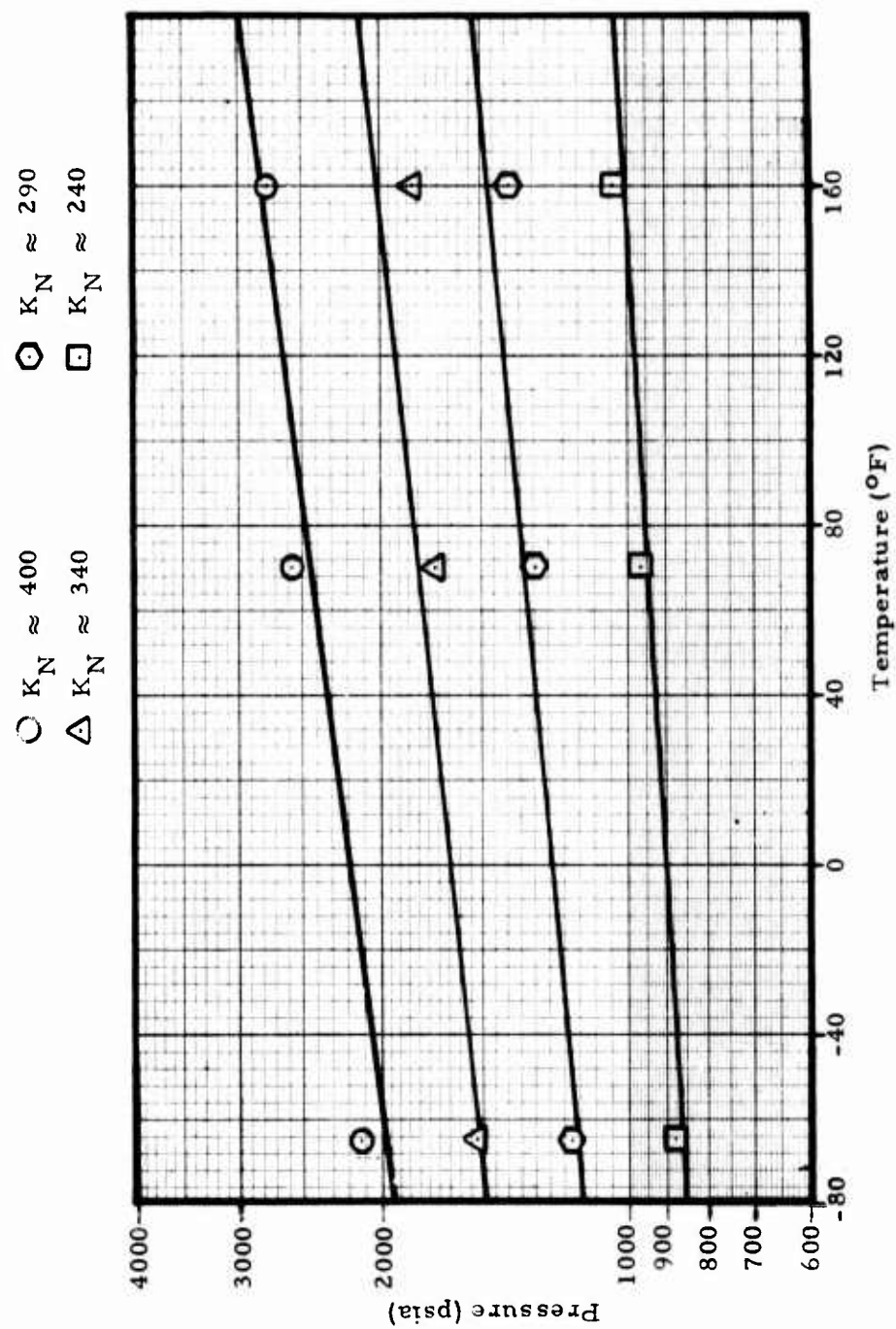


Figure A-9. Temperature Effect on Pressure, TP-H8245 Propellant (Mix T-600)

$\square$   $K_N \approx 240$   
 $\circ$   $K_N \approx 290$   
 $\triangle$   $K_N \approx 340$   
 $\odot$   $K_N \approx 400$

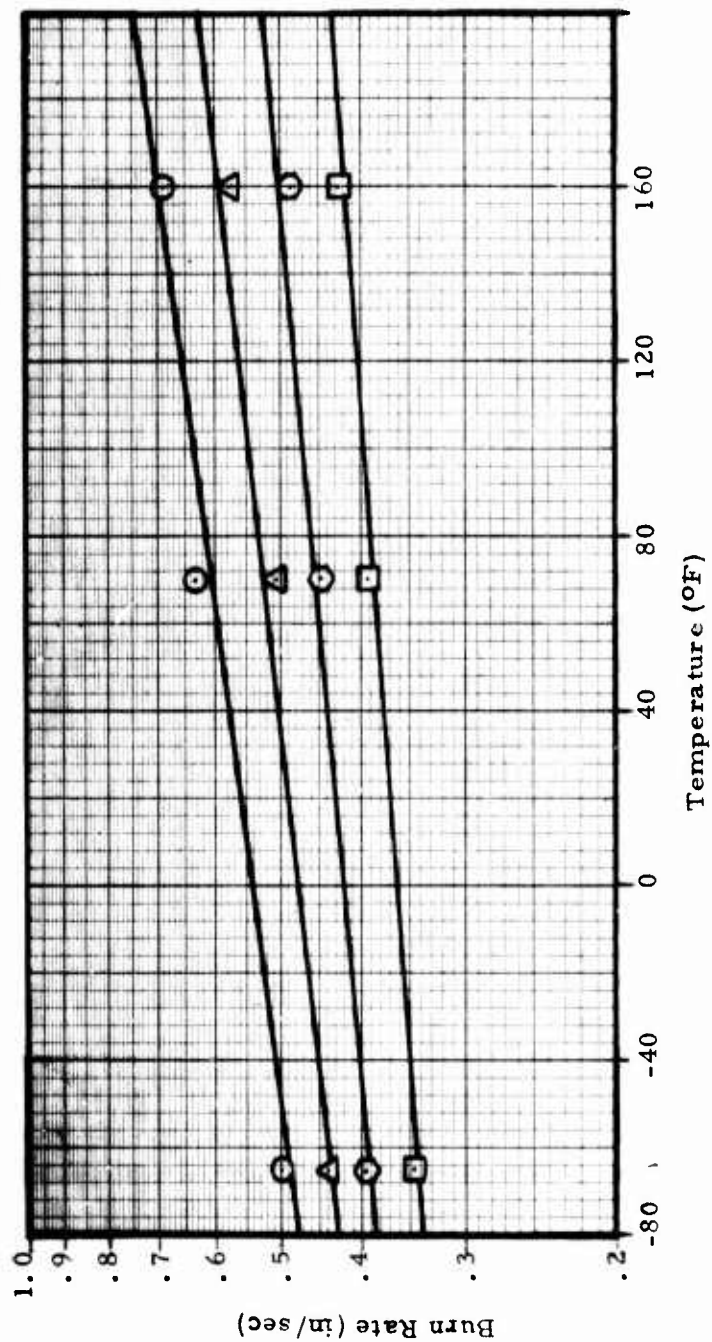


Figure A-10. Temperature Effect on Burning Rate, TP-H8245 Propellant (Mix T-600)

APPENDIX B  
STOCK TUBING STUDY

## APPENDIX B

### STOCK TUBING STUDY

#### STEEL TUBULAR PRODUCTS

##### Background

The general family of steel tubular products commonly available is broken down on Figure B-1. As may be seen, the general family can be divided into pipe, pressure tubing, and mechanical tubing. Clarification of certain general differences may be of initial interest. Pipe can be differentiated from tubing in both availability and generally used dimensional designations. Insofar as availability, pipe is limited to a relatively small number of sizes while tubing is available over a very broad range. As far as designation, piping (under 12 in. outside diameter) carries indicated sizes that roughly match the inside diameter of the pipe. For a given size pipe, the outside diameter is standard, leaving the inside diameter to fluctuate according to wall thickness (or schedule) with the schedule number increasing with wall thickness. The system evolved from the necessity of holding the outside diameter constant for coupling purposes. The standard method of designating tubing is by outside diameter. Thus, a 4 in. pipe (standard weight or schedule 40) has an outside diameter of 4.5 inches and a wall thickness of .237 inches while a 4 inch tube has an outside diameter of 4 inches and a wall thickness which is specified more properly in decimal form (as .238 inch), but often in the older manner of Birmingham Wire Gage (BWG) Number (.238 inch equals #4 BWG).

Another possibly confusing point is the difference between pressure pipe and pressure tubing. Generally speaking (besides these differences noted above) the difference is use, with pressure pipe being used for applications for which no heat is applied externally. By contrast, as indicated by Figure B-1, pressure tubing is used for boiler applications.

As indicated by Figure B-1, pipe and pressure tubing are classified according to intended use while mechanical tubing is classified according to the method used to manufacture it. Two broad tubing classes exist--seamless and welded. There are various types of processes used for making seamless tubes such as piercing and rolling, extruding, or cupping and drawing but such additional descriptive terms are not generally used in further classifying seamless tubing. Likewise, there are a large number of welding processes which can be utilized such as furnace welding (butt or lap, electrical resistance welding, fusion (gas or electric) welding, etc. Again, however, it is not

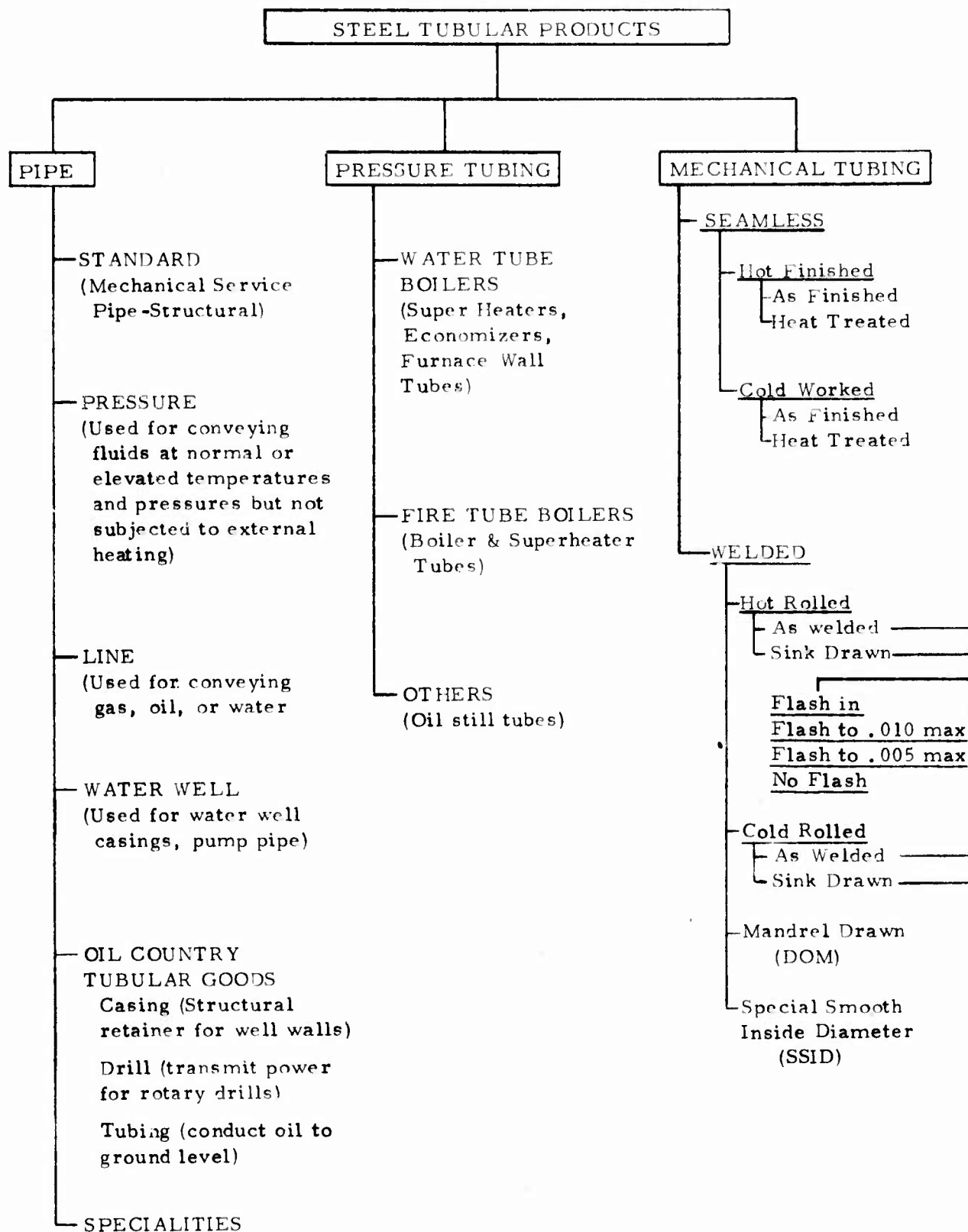


Figure B-1. Steel Tubular Products

general practice to break down the classification of welded tubing into sub-classes by types of welding.

Further sub-classifications of seamless tubing usually specify hot finish or cold worked. Hot rolled finishes include as-rolled or thermally treated (annealed, normalized, or quenched and tempered). Cold worked finishes include as-worked (cold worked), thermally treated (annealed, normalized, or quenched and tempered) with pickling as required, special smooth inside diameter (SSID), cylinder finish, and polished outside diameter (OD). Anneals are further classified as finish, stress relief, medium and soft in order of increasing ductility (and decreasing strength and machinability).

Welded tubing is classified further as made from hot-rolled or cold-rolled steel and being in one of the following six types and conditions (Ref. ASTM A513):

1. As-welded from hot rolled steel
2. As-welded from cold rolled steel
3. Sink-drawn from hot rolled steel
4. Sink-drawn from cold rolled steel
5. Mandrel-drawn (or drawn-over-mandrel, DOM)
6. Special smooth inside diameter (SSID)

Sink drawn tubing is a type (flash in, etc., --see below) which has been drawn through a die without a mandrel and thus cold finished only on the exterior surface. Mandrel Drawn Tubing is cold rolled material tubing with the interior flash removed (see below) and which has been drawn through a die and over a mandrel so that both wall surfaces are cold drawn.

As the welded tubing (originally sheet) is welded, a weld flash is formed along the joint. Normally this flash is removed from the outside diameter but the extent of flash removal from the inside diameter of Types 1 and 2 above, must be further specified if finishes other than "flash-in" are desired.

Flash-in tubing (to ASTM A513) may have welding flash on the inside diameter to the extent that it does not exceed either the wall thickness or 3/32" (.094"), whichever is less. At additional cost, the tubing can be furnished to either flash controlled to .010" max., flash controlled to .005" max., or no flash.

Additional finishing of the inside tube surface (over and above commercial grade which is standard) for more precise tolerances can be obtained.



If additional smoothness is required, such as for hydraulic or pneumatic cylinder applications, SSID or special honed tubing is obtainable.

### Preliminary Screening

The very great diversity of steel tubular products initially made the problem of selection appear a rather large one. Specifications such as ASTM A513 and A519 list a vast array of types and sizes. After initial contacts with quite a number of tubing manufacturers and some steel supply houses, however, it became clear that no such diversity of choice of steel tubing actually existed. Logically enough, the combinations of material, process, and economic limitations determine availability.

The basic criteria in considering stock tubing for use is one of economics. This in turn translates into ready availability and little or no additional machining; that is, the processing to produce the tubing initially and to then transform it into a rocket motor case should be as minimal as is feasible.

Insofar as availability, it became fairly clear after some initial screening, that the 4-inch outside diameter needed would exceed the capabilities of quite a number of tubing manufacturers. Initial contacts to vendors who advertised capability in tubing of the 4-inch size were made, as were a number of steel warehousing operations, in order to ascertain what could be expected in the way of availability in terms of size and type of steel.

Probably the most disconcerting fact that became apparent was while carbon steels in the lower carbon content range (that is, up to about .25%) were commonly available in the size and wall thickness range of interest, low alloy or alloy steel tubing could not be found. To clarify further this statement, the low alloy steel tubing was generally available in 4-inch outside diameter stock, but the wall thicknesses available were normally about two to two-and-a-half times what can be efficiently utilized for a 3000 psi pressure vessel. The high strength quality of these steels, which is the very thing that makes their use attractive for a motor case, also tends to limit their availability insofar as tubing manufacture is concerned. To utilize the thicknesses of the more readily available 4130 steel tubing with reasonable efficiency, it is expected that motor pressures in the vicinity of 6000 psi would be required--considerably above expectations for the Baseline motor of this study. A source for 4130 tubing was sought as other materials were being considered.

Technical Report RK-CR-75-28, "Development and Fabrication of Motor Cases Utilizing Tube Mill Products" by H. W. Mishler and D. G. Howden of the Battelle Columbus Laboratories (for the U. S. Army Missile Command, Redstone Arsenal, Alabama) and dated June, 1975, presented

an interesting possible material for use in rocket motor case fabrication. Use of electric-resistance-welded fuel transmission pipe per American Petroleum Institute (API) Standard 5LX was discussed. Basically, the material utilized for the pipe was a carbon manganese steel--0.30 max. Carbon, 1.35 max. Manganese, 0.04 max. Phosphorous, and 0.05 max. Sulfur. The composition is essentially that of low carbon steel of about AISI (American Iron and Steel Institute) 1027 composition. The report explored heat treatments of the 5LX material to yield strength levels of over 100 ksi and recommended further study of the material although conceding that the present API standard left composition limits too wide to enable consistent heat treatment except on an individual tube basis. It further concluded that the as-presently-manufactured quality of the 5LX pipe might well be suspect and that aspect also needed further exploration. In our opinion, serious questions are posed regarding heat treating distortion and cracking effects on the thin wall four foot long tube and the complications associated with heat treating steel of such wide composition limits. These concerns were serious enough in nature to eliminate consideration of the 5LX material from this study.

As a general category, piping appears to be of limited practical consideration due to a combination of limited size and materials availability. After screening the various commonly available pipes (via ASTM Specifications and suppliers' literature), it was concluded that piping offered no advantage over mechanical tubing. A number of applicable pressure tubing-type specifications were reviewed (ASTM 106, 200, 213, 268, 269, 271, 312, 335, 423, 450) to ascertain whether these types of products might be appropriate for use. Generally, it was found that specified minimum yield strengths were too low to be considered (on the order of 30 to 40,000 psi maximum). For the few instances of higher yield strengths, the 75,000 psi value given was merely about the equivalent of some of the cold worked carbon steel mechanical tubing and the alloys specified elements (as 8-9% nickel) which would add significantly to the cost of the material. Thus, primary attention for steel was focussed on the more readily available low and medium carbon steel mechanical tubing and on locating a source for the thin wall 4130 tubing.

Since the term "low carbon steel" covers a broad range of steels (containing up to .30 to .40% C for our purposes) it became necessary to screen the numerous types in some way to limit the possible choices. Low carbon steels are commonly available from AISI 1010 through AISI 1040, the 10XX series standing for nonsulfurized carbon steels, and the last two numbers indicating the carbon content. That is 1010 has a nominal carbon of 0.10% (commonly with a range of .08 - .13%), while 1040 has a nominal carbon content of 0.40% (range of 0.37 - 0.44%).

Several factors lead to rather quickly limiting the number of available low carbon steels which could include, at the extreme, 23 different grades between 1010 and 1040, inclusive (as listed in Vol. 1 of the Metals Handbook by the American Society for Metals - 8th Edition).

In the first place, the material strength increases with carbon content--thus, for a weight sensitive application (neglecting cost for a moment) one would instinctively rather use a steel with the highest carbon content (strength). For a given outside tubing diameter (i.e., 4 inches), the higher the available strength, the thinner the required wall thickness to accommodate a given pressure. The thinner the wall, of course, the lighter the weight of the tubing (motor case).

In considering cost of low carbon tubing, it was established in discussion with fabricators that the pricing structure of this tubing was such that carbon content did not affect price per se up to and including a level of AISI 1025. Between 1025 and 1026 there was a price structure change. This fact was then used for setting the lower limit for carbon content. In terms of cost per unit there is no advantage of using a steel less than 1025 since the tubes with lower carbon contents (with their concomitant lower strengths) would weigh more and thus cost more than tubes with the higher carbon contents.

The setting of an upper limit for type of low carbon steel to be considered was somewhat less exact. As stated previously, as carbon content goes up steel becomes progressively more difficult to both work and to weld. The number of tubing fabricators available varies inversely with the carbon content of the steel desired. Thus, while there is a large number of fabricators who will furnish tubing of 1010 or 1020 material, only a few will fabricate tubing over 1025 and only one fabricator was located who would go to 1040. There may be others, of course, since not all fabricators could be screened but their numbers would be quite small. Since it was desirable to achieve some basis of commonality in the comparison of steel tubing, the decision was made early in the study to achieve this commonality by utilizing American Society for Testing and Materials (ASTM) Specifications for quotation purposes. Thus, Specification A513 was utilized for Electric-Resistance-Welded Carbon and Alloy Steel Mechanical Tubing and Specification A519 was utilized for Seamless Carbon and Alloy Steel Mechanical Tubing. Since the former specification was limited to 1035 (maximum carbon) material, it was decided to set the upper carbon steel composition at 1035, despite the possibility of getting 1040 material from at least one fabricator. It should be pointed out that although the A519 specification is written to cover many alloy steels, it is most unrealistic to assume these are all readily available.

Thus, it was initially decided to limit the consideration of carbon steel tubing to AISI 1025, 1026, 1030 and 1035 and, as stated above, to any 4130 low alloy tubing if a suitable size could be located.

#### Seamless Versus Welded Steel Tubing

Seamless tubing is manufactured by simultaneously piercing the center of a round heated billet while rolls contacting the external billet surface squeeze the part and the billet is being rapidly rotated and drawn through the rolls and

over the piercing point. The pierced billet is subsequently subjected to further rolling over a mandrel (in one of several possible ways) to further reduce the outside diameter and wall thickness as a consequence. Additional rolling is performed for sizing as necessary. If greater dimensional accuracy, strength, smaller diameters or wall thicknesses are necessary than those produced by hot-rolling, there can be additional cold drawing through a die and over a mandrel. Prior to cold drawing, annealing is necessary to soften the material and promote easier cold working. Pickling is also necessary to remove the scale resultant from the hot rolling operations.

Welded tubing starts with flat rolled stock which is gradually roll-formed into a cylindrical cross section. The butt edges of the formed material are then fused together by electric resistance welding (arc may be used in some instances but not under ASTM A513). After welding, weld flash is removed, outside and inside to the degree desired. Due to the welding operation, mechanical properties are nonuniform in the tube. Thus, normalizing and cold drawing (over a mandrel) operations are performed to increase strength, and improve uniformity of properties, tolerances, surface finish, and machinability. As with seamless tubing the cold drawing operation reduces outside diameter and wall thickness.

The brief background on processing helps to explain some of the differences in allowable tolerances and certain inherent limitations for both seamless and welded tubing. For example, the hot-rolled type of seamless tubing, cannot be obtained in "thin" wall sizes. It would appear from data obtained that for a hot-rolled seamless 1025 material, a wall thickness of about .180 inch borders on the minimum for the 4-inch diameter. With cold drawing specified, quotes were obtained down to a .134 inch wall for the same material and down to .120 wall with an even harder (1035) material. Intuitively, if the differences in the processes involved are considered, it would seem that for thin-walled tubing, the welded type would hold the edge price-wise since there would likely to be closer control of the "raw stock" going into the process. The initial processing requires less cold working to achieve the final sizes when compared to seamless-hence lower cost for a given thickness. This supposition is reflected in the generally higher costs of the seamless tubing. (One would expect seamless tubing to gain the cost advantage at some point as required wall thickness increases since less cold working becomes involved and welding becomes more difficult).

Likewise, it might be expected that welded thin wall tubing could be held to tighter tolerances than seamless over most of the cross section (i.e., except for the weld area) since the "raw stock" input can be to tighter tolerances. This supposition also is reflected by permissible tolerance variations for both types as given by Table B-1.

The comparison of tensile properties for the two types of tubing indicates little difference in properties unless it is noted that ASTM 519 values are "typical"

**TABLE B-1**  
**TOLERANCE COMPARISON FOR 4-INCH OUTSIDE**  
**DIAMETER TUBING (a), (b)**

**A. SEAMLESS MECHANICAL TUBING**

**Hot finished**

<u>Outside Diameter</u>	<u>Wall Thicknesses</u>
$\pm .031$	$\pm 14$ to $15\%$ depending on thickness or $\pm .018$ to $\pm .025$ (over applic- able range thicknesses)

**Cold Worked (Unannealed or finish annealed)**

<u>Outside Diameter</u>	<u>Inside Diameter</u>	<u>Wall Thickness</u>
$+ .015$	$+ .005$	$\pm 10\%$ or $\pm .012$ to
$- .000$	$- .015$	$\pm .018$ over applicable range of thicknesses

**B. ELECTRIC-RESISTANCE-WELDED**  
**CARBON AND ALLOY STEEL**  
**MECHANICAL TUBING**

**As Welded From Hot Rolled Steel**  
 (Flash Controlled to  $.010''$  max.)<sup>(c)</sup>

<u>Outside Diameter</u>	<u>Wall Thickness</u>
$\pm .190$	$+ .005$ to $+ .010$ $- .012$ to $- .020$

**As Welded from Cold Rolled Steel**  
 (Flash Controlled to  $.010''$  max.)<sup>(c)</sup>

<u>Outside Diameter</u>	<u>Wall Thickness</u>
$\pm .010$	$+ .003$ $- .007$

**Mandrel Drawn (or Drawn over mandrel-DOM)**

<u>Outside Diameter</u>	<u>Inside Diameter</u>	<u>Wall Thickness</u>
$\pm .006$	$\pm .006$	$\pm .005$ over applic- able range of thick- nesses

(Continued on next page)

TABLE B-1. (Continued).

- 
- a. Per ASTM A-519-71.
  - b. Where all three dimensional tolerances are given, only two of the dimensions can be specified for ordering purposes.
  - c. Flash controlled to 0.010 in. max. normally produced to outside diameter and wall thickness tolerances.



while A513 values are specified as minimum. The difference could well reflect the somewhat poorer tolerance capabilities of the seamless tubing. A tensile property comparison is given by Table B-2.

Since tolerances are wider for seamless tubing than for welded tubing and strength levels are equal to or less than those of welded tubing, the only basis for picking seamless tubing over welded tubing would be cost. However, a comparison of the costs of the two types indicated that on an equivalent thickness basis the welded tubing was less expensive. Comparison of costs between these two types was made from data furnished by a single supplier so difference data is not masked by possible price differences between two suppliers. As examples of the cost differences between seamless and welded (DOM) tubing: - a 1035 material seamless tubing in a wall thickness of .120 inches was quoted (by Babcock and Wilcox) for a base price equivalent at \$2.26 per foot while a .125 inch thick DOM welded tubing of the same material was quoted at \$2.18 per foot. Likewise, a .125 inch wall in a 1030 seamless material was \$2.35 per foot while a .134 inch wall for DOM welded tubing of the same material was \$2.33 per foot.

Thus, for the application with which this report is concerned seamless tubing was eliminated from further consideration.

#### Welded Tubing Considerations

Initially, two types of welded tubing were compared - the as-welded (flash controlled to .010 inch max) hot-rolled material and the mandrel-drawn material. Flash controlled to .010 inch maximum was chosen since it was felt that the flash-in material permitted too much weld flash (.094 inch) for a rocket motor case. Likewise, it was believed a .010 inch maximum could be tolerated and that there was no need to pay extra to go to a .005 inch maximum flash or to a special smooth inside diameter.

Table B-1 indicates that although outside diameter tolerances are not too different between DOM and hot-rolled types, the wall thickness tolerances are best for the DOM tubing. Control over wall thickness is most important in considering motor pressure and the reliability associated with a particular pressure.

Minimum tensile properties between as-welded and DOM tubing (as listed by Table B-2) became the limiting factor in a decision as to the type of welded tubing to use. DOM tubing generally has minimum yield strengths which are about 60% greater than the as-welded tubing--a reflection of the added cold-work. Typically, ultimate strengths are generally about one-third greater for the DOM material. The difference in strength levels translates into an approximate 50% increase in weight required for the as-welded tubing versus the DOM tubing. By comparison, the cost savings would be approximately



**TABLE B-2**  
**TENSILE PROPERTIES FOR STEEL TUBING**

**I. SEAMLESS MECHANICAL TUBING<sup>(a)</sup>**

<u>Material</u>	<u>Ult. Tens. Str. (psi)</u>	<u>Yield Strength (psi)</u>	<u>Elongation in 2 in. (%)</u>
<b>Hot Rolled</b>			
1025	55,000	35,000	25
1035	65,000	40,000	20
<b>Cold Worked</b>			
1025	75,000	65,000	5
1035	85,000	75,000	5

**II. ELECTRIC RESISTANCE WELDED  
CARBON AND ALLOY STEEL  
MECHANICAL TUBING<sup>(b)</sup>**

**As Welded**

1025	56,000	40,000	12
1030	62,000	45,000	10
1035	66,000	50,000	10

**Welded and Mandrel Drawn (DOM)**

1025	75,000	65,000	5
1026 <sup>(c)</sup>	85,000	78,000	8
1030	85,000	75,000	5
1035	90,000	80,000	5
4130N	103,000	93,000	10

a. Per ASTM A519-71 - values given as "typical".

b. Per ASTM A513-70 - values specified as minimum (except for 1026 as noted).

c. Values "Typical Minimum" per Ohio Steel Tube Co., Shelby, Ohio.

12% for the as-welded tubing compared to the DOM material. It was felt the weight penalty was too much to pay for the cost savings in this instance, particularly since the DOM material offered the added advantages of closer tolerance control, no inside weld flash, and a more uniform structure with its associated greater reliability. Thus, the remainder of effort for steel tubing considered only the DOM type tubing.

It should be pointed out that for the welded tubing comparisons, costs for both types of welded tubing came from each of two suppliers with the cost differences being relatively the same for both.

#### Summary of Preliminary Screening of Steel Tubular Products

At this point in the study, the number of classes of steel tubular products had been narrowed through consideration of costs, tolerances and strength levels.

- a. Piping, as a general category, was eliminated from further consideration because it offered no advantages over mechanical tubing.
- b. API fuel transmission pipe was eliminated because of concern about heat treating distortion and the complications associated with heat treating material having a wide allowable composition range.
- c. Seamless mechanical tubing was eliminated because welded tubing has smaller allowable tolerances, equal or greater strength levels, and lower costs for equivalent thicknesses.
- d. As welded hot-rolled tubing was eliminated because drawn-over-mandrel (DOM) welded tubing has 60% higher strength levels with only a 12% higher costs, smaller allowable tolerances, no inside weld flash, and a more uniform structure.
- e. As-welded cold-rolled tubing was eliminated because the strength of the tubing, although from cold-rolled material, is still limited by the weld efficiency which has not yet benefited by the increased cold-working benefits of drawing the tube between a die and mandrel.
- f. Pressure piping was eliminated because specifications generally required yield strengths which were too low for a rocket motor case.
- g. Steels with composition less than 1025 were eliminated because there is no price advantage for steels with lower carbon contents (and concomitant lower strength levels).
- h. Steels with composition greater than 1035 were eliminated because only one supplier for higher carbon steels could be located, thus portending future availability problems.

- i. A search was instituted for a supplier of 4130 steel tubing having "thin" wall thickness.

## ALUMINUM TUBULAR PRODUCTS

### Background

There are three broad classes of aluminum tubular products-extruded, welded and drawn. Further breakdown can be made based generally on use. Figure B-2 gives some of the more commonly used items in each category, the names being descriptive of the process used to produce them. Extruded tube or pipe is formed by forcing (or extruding) a hot metal billet through a die; welded tube is produced by the forming and then seam-welding of sheet metal longitudinally into a tubular product; drawn tube is that which has been further formed to dimensions by cold drawing through a die and over a mandrel to provide cold-worked surfaces to tighter tolerances than extrusions provide and to further strengthen non-heat treatable types of aluminum.

### Materials

Basically there are two broad categories of aluminum available--heat treatable and non-heat treatable. The initial strength of the non-heat treatable alloys depends on hardening effects of the various alloying elements. Further strengthening of these alloys (generally the wrought 1000, 3000, or 5000 series) can be accomplished by varying degrees of cold working since they are work-hardenable. The degree of cold working is designated by an "H" suffix given to the alloy designation along with a number code to further specify degree of temper or cold work. Elevated temperature treatments can be given to these alloys in the work hardened condition to soften (anneal) or stabilize the hardening effects as desired.

The heat treatable wrought alloys (commonly the 2000, 6000 and 7000 series) can have enhanced strength by virtue of the addition of alloying elements such as copper, manganese, zinc, and silicone. These elements are increasingly soluble in aluminum as temperature increases thus providing the means for increasing strength of the aluminum by thermal treatment. Copper is the primary alloying ingredient of the 2000 series, silicone and manganese in the 6000 series, and zinc in the 7000 series. The suffix "T" is added to the thermally treated alloy to designate the type of thermal treatment to which the product is subjected and hence is an indication of strength level.

### Preliminary Screening

For the purposes of this tubing study, it was clear that, practically speaking, only those alloys could be considered that had high strength capabilities. A second consideration was, of course, that a given alloy be readily available in a tubular form of the 4-inch O.D. size of interest for the motor case. With these two points in mind, the choice of possible materials was rapidly narrowed from the number of alloys available.

# ALUMINUM TUBULAR PRODUCTS

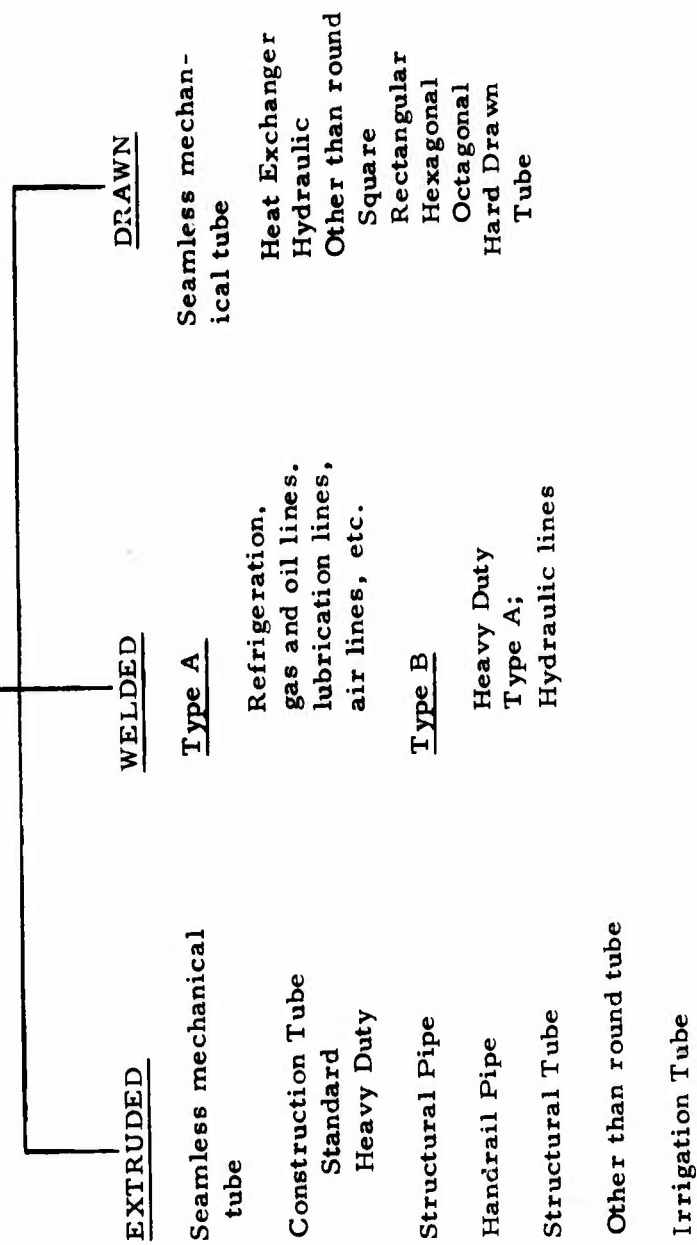


Figure B-2. Aluminum Tubular Products

Initially, the "Aluminum Standards and Data Book" of the Aluminum Association (Ref. 3) was consulted in order to "screen in" those available tubes having the most favorable mechanical property limits (tensile strength). From the initial screening, it appeared that the following alloys deserved further consideration:

<u>Alloy</u>	<u>Tensile Strength Range (ksi)</u>		<u>Elongation in 2 in. (%)</u>
	<u>Ultimate</u>	<u>Yield</u>	
2014	50-60	29-53	9-12
2024	57-66	38-56	4-12
2219	42-58	26-42	6-14
5456	41-42	19-26	12-14
6061	26-38	12-35	8-16
6066	40-50	24-45	8-14
6070	48	45	6
6262	38	35	10
7001	89	82	5
7075	66-78	58-70	7

At this point, to further converge on possible choices, required wall thicknesses for the various alloys listed were calculated on the basis of  $t = \frac{1.5 p r}{S}$ , with the 1.5 serving as an estimated safety factor multiplier,  $p = 3000$  psi, and  $r = 2$ . The value of  $S$  for this initial screening was the maximum tensile ultimate for each of the alloys listed. The results were as follows:

<u>Alloy</u>	<u>Preliminary Required Wall Thickness(in)</u>
2014	.150
2024	.136
2219	.155
5456	.214
6061	.237
6066	.180
6070	.188
6262	.237
7001	.101
7075	.115

On the basis of these calculations, any alloys requiring over 0.2" wall were arbitrarily rejected as not competitive. Thus 5456 (the only non-heat treatable one on the initial list), 6061, and 6262 were eliminated from further consideration, leaving 2014, 2024, 2219, 6066, 6070, 7001, and 7075 to be considered.

The availability of the seven remaining alloys for tubular products

(extrusions or drawn items) was screened using manufacturers literature and contacts and this resulted in further reducing the list of candidates by eliminating 2219, 6066, 6070, and 7001, leaving three materials as the most readily available alloys--2014, 2024 and 7075.

With the preliminary thickness and a number of possible alloys determined, a number of "standard" aluminum tubular products were screened to ascertain whether any might be suitable and possibly less expensive, with the results below.

Standard and Heavy-Duty Seamless Construction Tube: In the 4 in. OD size, the "standard" wall thickness is .050 inch and the "heavy duty" wall thickness is .072 inch. Both thicknesses were much too light for further consideration.

Handrail Pipe: Available diameters were too small.

Seamless Pipe: Available in .226 and .318 inch thicknesses only in 6061-T6, 6063-T6, and 3003-H 112 alloys. These do not appear competitive due to the very thick walls (Subsequently, a comparative price check was made and confirmed that economics did not justify their use).

Cylinder Tube: Alloy (6063)--too low in strength

Structural Pipe: Not available as standard item in required size or alloy.

Irrigation Tube: Wall thicknesses too thin.

Type II Hard Drawn Tube: Sizes too small.

Essentially, the screening eliminated all products except standard extruded or drawn tubing which are available in a wide variety of sizes and thicknesses. Further, the requirement for a thin wall tube dictated that it be extruded and drawn--that is, drawing would be the final type of tubing preparation process.

At this point, then, the aluminum tubing choice had narrowed down to drawn tubing of either the 2014, 2024, or 7075 types.

#### MATERIAL COMPARISONS

On the basis of preliminary considerations, the wide initial choice of materials and types of tubing was narrowed down to welded and drawn over mandrel tubing incorporating AISI 1025, 1035, and 4130 type steels and extruded and drawn tubing of 2014, 2024, and 7075 types of aluminum. With the narrowing of the number of materials to six, it became practical to consider a broad range of properties for the six. The following criteria were considered to

be sufficient to form a basis for further narrowing of the selection:

#### Mechanical Properties

- Corrosion resistance (general)
- Stress corrosion resistance
- Tensile properties (ultimate strength, yield strength, elongation)
- Temperature effects on mechanical properties
- Fracture toughness properties

#### Processing Properties

- Weldability
- Formability
- Machinability
- Heat treating characteristics

#### Physical Properties

- Weight (per foot)
- Standard tolerances (mill run)
- Size availability

#### Economic Properties

- Cost per foot (mill run)

The criteria as listed are covered in the succeeding paragraphs on a comparison basis between the various materials.

#### Corrosion Resistance (General)

Comparing the steel materials, the 1025 and the 1035 steels vary primarily in carbon content and slightly in manganese (with the 1035 being higher in both). It has been established (Ref. 9) that carbon as itself or as carbide has little effect on atmospheric corrosion or that in fresh water. Thus, there is equivalence between the 1025 and the 1035 materials. When the 4130 material is compared, however, it is superior from the corrosion aspect since it does contain .80 to 1.10% Chromium.

Generally speaking, the corrosion resistance of aluminum to environmental-type corrosion is much superior to steel. (It should be pointed out that in speaking of corrosion resistance herein, consideration was given only to the raw, unprotected material, i.e., not protected by plating, organic coatings,



etc., which would normally be used to provide such protection). The performance of aluminum is due, of course, to the oxide coating which develops naturally over the surface when in contact with air or other oxidizing agents. This film is normally stable in contact with solutions having a pH of about 4.5 to 8.5. Strong acids and alkalies do, however, destroy the protective film and can attack the base metal beneath.

Appropriate coatings are available for both steel and aluminum materials which would minimize concern with corrosion and it is assumed such would be used in any design. It is outside the scope of this report to consider differences in finishing costs, but it is expected to be about the same for all materials.

### Stress Corrosion

Static stress within a part can combine with specific environmental conditions to result in circumstances of failure at loads normally considered of little consequence. The resultant cracking under conditions of a corrosive environment is known as stress corrosion cracking and factors associated with the mechanism are stress (including possible residual or internal stresses), time, environment, and the structure of the alloy involved (pure metals appear to be immune from this type of failure). The stresses involved are tensile in nature and the time to failure is inversely proportional to the corrosiveness of the environment and the magnitude of the stress.

Generally speaking, of the metals under considerations, the steels are much less susceptible to stress corrosion cracking than the aluminums. With the steels (in contrast to the aluminums), the presence of a relatively low stress or a more dilute solution in combination with a relatively high stress condition is needed to cause stress corrosion cracking. Solutions which contain concentrations of chlorides or hydrogen sulfide seem particularly damaging.

While pure aluminum is resistant to stress corrosion cracking, some alloys have cracked in conditions caused only by exposure to atmosphere and tap water. There is little doubt that stress corrosion cracking is of generally more concern with the higher strength aluminum alloys than with steels. In these higher strength alloys, only small amounts of moisture are necessary to promote stress corrosion. Differences in alloy and temper result in differing susceptibilities to stress corrosion cracking. For instance, alloys 2014 and 7075 in the T6 condition and 2014, 2024 and 2219 in the T3 and T4 temper condition are susceptible to stress corrosion cracking. On the other hand, 2024 in the T6 or T8 temper and 7075 in the T73 condition are decidedly more resistant to that mode of failure. For 7075 alloy, however, the T73 condition (a proprietary process) is available only in sheet stock.

Technical personnel at Norris Industries stated that extruded 2.75-inch cases of 2014-T6 alloy had not experienced any problems with stress corrosion. Thus, it appears that, although laboratory tests rank stress corrosion resistance of 2024-T6 or T8 superior to 2014-T6, it does not present a significant factor for the subject application.

### Tensile Properties

Table B-3 gives a comparison of the tensile property data for candidate materials. It may be noted that, with the exception of 7075 T6, the values for the aluminum alloys are relatively similar. Without considering any other properties (i.e., weight, cost, etc.) steel tubing has the definite advantage, 7075 T6 aluminum would be the "best" of the aluminum and better than the 1025 steel tubing.

### Temperature Effects on Mechanical Properties

In the utilization of materials, consideration must be given to both low and high temperature effects on material properties. Lacking specific information on the high temperature limit which might be applicable, an arbitrary figure of +200°F was used to assess effects.

Although specific values are lacking insofar as low temperature toughness for all materials, some generalizations can be made for the various steel types based upon their composition. In carbon steels, notch toughness decreases with increased carbon content from .15 to .80%. That is, transition temperature is increased and energy absorption is decreased as measured by Charpy V notch testing. Manganese content of up to about 1.5% lowers the transition temperature. Sulfur up to about .040% seems to have no effect on low temperature properties or transition temperature while the phosphorus content appears to have a detrimental effect.

In comparing the two types of low carbon steel tubing (1025, 1035) from the aspect of low temperature service capability only, it seems clear that the carbon content is the overriding factor and that the higher carbon content of the 1035 would result in a decreased low temperature toughness capability despite the increase in manganese content. It should be emphasized that a quantitative value for either can not be quoted. Even if test data for impact energies or nil ductility temperatures were available, their applicability to a specific design would be quite questionable.

Heat treated low alloy steels (4130) are superior to carbon steels from the aspect of low temperature effects--again without quantifying data. Thus, when rating low temperature capabilities, 4130 is superior, 1025 is second best and 1035 is the least acceptable although there is no assurance they would not all be satisfactory. Only testing could answer that question.

Low temperature properties of aluminum show little basis for concern. Below zero degrees F, tensile strengths show slight improvement while elongation values may slightly decrease and impact properties remain about the same as room temperature values. Compared to steel--especially the 1025 and 1035 types, the aluminum alloys show advantages for low temperature service.

**TABLE B-3**  
**TENSILE PROPERTIES OF TUBING (AMBIENT TEMPERATURE)**

Material	Ultimate Tensile Strength (psi)	Tensile Yield Strength (psi)	Hardness R <sub>b</sub> Min.	Elongation in 2 in. (%)
<b>Steel Tubing (Mandrel Drawn)</b>				
AISI 1025 (a)	75,000 (70,000) <sup>(f)</sup>	65,000 (60,000)	82 (77)	5 (10)
AISI 1035 (a)	90,000 (85,000)	80,000 (75,000)	90 (85)	5 (10)
AISI 4130 <sup>(b)</sup> (N)	103,000	93,000		
(H, T.)	150,000	132,000		
<b>Aluminum Tubing (Drawn Tube)</b>				
2014 T6 <sup>(c)</sup>	65,000	55,000		7
2024 T8 <sup>(d)</sup>	66,000	58,000		5
7075 T6 <sup>(c)</sup>	77,000	66,000		7
T73 <sup>(e)</sup>	66,000	56,000		8

a. Minimum values per ASTM A513-70.

b. Cyrotec, Huntsville, Alabama.

c. Minimum values per "Aluminum Standards & Data" - The Aluminum Association.

d. Minimum values per "Alcoa Aluminum Tubular Products" Section AE2A-1.

e. Minimum values per WW-T-700/7A.

f. Values in parenthesis for stress relieved tubing.

For elevated temperature service considerations, the carbon steels can generally be expected to perform adequately to temperatures up to about 700°F. For alloy steels (i.e., 4130), a temperature of +200°F (see first paragraph, this section) would be expected to reduce the ultimate tensile strength to about 98.5% of the room temperature value and tensile yield strength about 94.5% of the room temperature value. These values are for exposure times up to 1/2 hour, hence are conservative.

Aluminum alloys however experience a decrease in tensile properties with increasing temperatures--the greatest effects being between about 212°F to 400°F. An increase in toughness accompanies the decrease in tensile properties. Practically speaking, exposure time to a high temperature of only 200°F for a time of only seconds may have no effect on tensile properties.

### Fracture Toughness Properties

Flaws may be present in a component as a result of its fabrication, environment or service. Such flaws could take the form of voids (as in castings), weld or base metal inclusions or cracks, or discontinuities as a result of design or fabrication. A sufficiently severe flaw can cause component failure under conditions (loads) which ordinarily do not result in failure.

The ability of a component (particularly one in a brittle material) to resist failure from a flaw depends upon the size of the flaw, the geometrical form of the component, and the fracture toughness of the material. The latter is a method of expressing the resistance of a material to fracture and of its tolerance (or lack of) to flaws.

If a particular flaw-containing material has very limited tendency towards plastic flow and for geometries inducing triaxial states of stress, an elastic type of failure is maintained until a failure stress is attained, after which a brittle type failure results from crack propagation from the flaw. Failure, being brittle in nature, happens very quickly.

There has evolved an analytical tool which includes the relationship between the size of the flaw, the geometry of the encompassing component, and the gross (non-magnified) stress in the material. The stress intensity factor derived from the theoretical relationship of the above factors is called the stress intensity factor and designated "K". For generalization purposes, for every material subject to brittle fracture, a lower limit or "critical" value of K exists and this value is designated as  $K_{Ic}$ --the critical plane-strain fracture toughness value.

Generally, data exist only for the higher strength alloys and for fairly thick sections (plates). To what extent these data can be extrapolated to specific component design and to drawn tubing in particular other than as a

general guideline is uncertain. However, such data as are presently available are given on Table B-4.

No data were available for the 1025 and 1035 steels as these are normally not particularly susceptible to this type failure and not amenable to testing due to high fracture toughness values.

Data for 4330 steel are given in lieu of 4130, but are expected to be relatively the same.

### Weldability

Considering the carbon steels first, weldability of those containing less than about .30% carbon is very good by all commercial methods. Thus, the 1025 material is considered to be superior to the other materials from this aspect. As carbon content increases (to that of the 1035 material), weldability decreases somewhat. It is not certain whether or not pre-heating and postheating would be necessary with the 1035 material, but satisfactory welds would be expected to be attained without a great deal of difficulty.

AISI 4130 is also readily weldable by most methods, particularly in the non-heat-treated condition. With more advanced techniques of welding such as electron beam, it is possible to weld the material in the high strength (quench and tempered) condition while minimizing the weld heat effects (heat affected zone).

Regarding the aluminum tubing, of the three types considered (2014, 2024 and 7075) welding is a much more difficult proposition than with the steels.

Fusion welding of 2014 is possible by either a tungsten inert gas or metal inert gas process. Usually the weld is about twice the thickness of the material it joins in recognition of its lesser load carrying capabilities and the part is used in the as-welded state. Successful resistance welds are possible by the use of special practices but brazing and soldering operations are not recommended.

The 2024 aluminum can be resistance welded in the heat treated condition by using special techniques. Welding in the annealed condition is not recommended.

The last of the three alloys (7075) is not normally fusion welded. Resistance welding is possible but is more difficult than with 2024 alloy.

Summing up weldability, the order of preference is 1025, 1035, 4130, 2014, 2024, and 7075.

TABLE B-4  
CRITICAL PLANE STRAIN FRACTURE TOUGHNESS <sup>(a)</sup>

<u>Material</u>	<u>Form</u>	<u>Yield Strength (ksi)</u>	<u>Avg. Fracture Toughness (ksi√in)</u>
<u>Steel:</u>			
4330	Forging	191 (ultimate)	96
<u>Aluminum:</u>			
2014 T6	Forging	63.8	28
2024 T851	Plate	59 - 66	24
7075 T6511	Extrusion	64 - 66	34

a. Section 9 of Reference B-14.

## Formability

The term formability is relative since these are various types. In general, assuming the same amount of cold work, the steel with the higher carbon content will be the least formable when considering the carbon grades. Considering the fact that the steel tubing under consideration has been cold worked already, it would be difficult to attempt to quote specific figures to indicate formability. As a broad measure however, the minimum percent elongation would be one indication. For both 1025 and 1035, this value is 5% (in 2 inches), indicating that further formability would likely be somewhat limited. Using elongation as the criteria, 4130 steel tubing would generally be comparable--having minimum elongation values of 5 to 7% depending upon tensile strength (heat treat condition). At a nearly equivalent strength level as 1025 and 1035 the 4130 steel would be expected to have somewhat greater (i.e., maximum) degree of formability.

The heat treated condition of the aluminum alloys with which we are concerned directly affects formability. A few general statements may aid in further understanding the formability problems. Refer to the next section for a more comprehensive discussion of heat treating of aluminum.

The annealed or "O" condition is the most easily formed. Next in ease of forming are alloys in the "W" condition--materials that have been freshly solution heat treated and quenched. After forming, these can be subsequently aged, either naturally or artificially to higher strength levels. Alloys can be stored in the "W" temper at low temperatures for some time to retard aging effects and keep formability at essentially this level.

If the material has been solution heat treated at the mill but not artificially aged (designated T3, T4, or W)--it may generally be subjected to minor bending, stretching or drawing. However, those items of material in the T6 condition (solution treated and artificially aged) are quite strong and have lost much ductility. As a consequence, even mild forming operations are apt to cause fracture. Comments on the forming of specific alloys of interest follow below.

Aluminum alloy 2014 has a range of formability capabilities which range from good in the "O" condition to limited in the T6 condition. Mild forming can be done in the T3 or T4 conditions but is susceptible to spring-back. In the T6 condition, 2014 is comparable to 7075 T6. It is possible to hot-form 2014 in the T6 condition at 350-700°F but maximum time-at-temperature requirements exist for this type of elevated conditioning and must be strictly followed. Hot forming can be done in the T4 condition but must be followed by aging to the T6 condition. It is generally more practical to hot-form the T6 condition.

The formability of 2024 aluminum alloy is generally similar to 2014 in



that while the "O" condition has rather good forming characteristics, the heat treated conditions possess limited properties. The T4 condition can be bent and stretched to some degree, but no shrinking can be performed. The T3 forming properties are somewhat inferior to the T4 condition. "As is" T6, T62, T81 and T86 conditions should be subjected only to dimpling. Formability improves a good bit with temperature increase. If the T3 or T4 conditions are hot-formed, their corrosion resistance is degraded. If subjected to hot-forming at elevated temperatures, the material in either of those conditions should subsequently be artificially aged to the T6, T81 or T86 conditions.

In the "O" condition, alloy 7075 is less formable than 2024-O, while in the W condition these properties are about the same as 2024 W. At room temperature, the formability of 7075 T6 is very limited but can be improved considerably by elevated temperatures of 300 to 425°F. At the elevated temperatures, time exposure should be strictly limited.

Insofar as a comparison of formability of the various materials is concerned, it appears obvious that none of the materials being considered can be considered clearly superior to the others if consideration is given to forming in the higher strength condition--that is, heat treated. The aluminums are complicated by the necessity to limit the time-temperature requirements to a combination which is compatible with the condition originally obtained from the mill (probably T6) and then the necessity for retreating to that condition after forming. Due to the relatively thin walls being considered, a system of satisfactory heating and cooling which minimizes the possibility of distortion will have to evolve. With respect to forming processes, thorough consideration of all aspects is needed before any final decision is reached on material.

#### Machinability

Commonly, the general term "machinability" refers to turning and machinability indices are usually based upon that quality of a material. The low grade carbon steels tend to be somewhat soft and gummy in an annealed condition but improve with cold work. The medium carbon steels get harder with carbon content (becoming more brittle) and machining is usually improved with annealing, particularly as the carbon content gets closer to .5%--the medium upper limit.

A brief comparison of recommended cutting speeds for 1025 versus 1035 material using high speed steel tools indicates that 1025 cold finished material of a Rockwell B hardness in the range of 82 can be machined (rough turning, finish turning, boring, drilling) at a speed of some 14 to 25% greater than the 1035 material of a Rockwell B hardness of around 90. Other things being equal, the 1025 material is superior. As carbon content and hardness increase over .35%, tool wear and production rate would get progressively worse.

For the 4130 low alloy type of steel, machining operations are best performed in the normalized and tempered or annealed conditions. Machining can be expected, in general, to be more difficult for alloy steels than for the low and medium carbon grades.

On a general comparison basis, for metals with similar mechanical properties, metal removal (by various machining processes) from aluminum requires less expenditure of power than metal removal from steel. Thus, aluminum is considered superior from that aspect.

Within the family of aluminums, most wrought alloys have excellent machinability. Heat treatable alloys (as 2014, 2024, and 7075) are better machined in the various heat treated conditions. Machinability ratings for the alloys under consideration are as follows:

2014 T6	B
2024 T8	B
7075 T6	B

with the B rating indicating "curled or easily broken chips and good to excellent finish. Thus, they can be considered as approximately equal in machinability and superior to the steels being considered from an energy expenditure view point. No difficulty would be expected in machining any of the materials considered.

#### Heat Treating Characteristics

Hardenability (or essentially the capacity to be transformed into martensite) is low for the low carbon steels. Although they are often case or skin hardened by a number of methods such as carburizing, they are ordinarily cold worked to provide uniform increases in strength throughout their cross sections. The 1025 and 1035 tubing material considered in this report has been cold drawn to achieve the strength levels indicated on Table III. For quenching and tempering purposes, the general lower carbon limit for consideration is that of AISI 1040 material. This does not mean that it would be impossible for, say, a 1035 material to be heat treated to a high strength level. However, in the tubing sizes being considered, a good bit of development effort would likely have to be performed to establish that such a process was feasible from the viewpoint of attaining uniform properties, with little distortion and no cracking. Such considerations seem to run somewhat contrary to the basic idea of "stock tubing" being utilized. Hence 1025 and 1035 tubing were considered only in the cold worked condition. Normalizing may be desirable from the aspect of improving toughness (hence low temperature properties) at some minor sacrifice of tensile properties.

One of the reasons (perhaps the basic one) for considering the use of

AISI 4130 material is its capability to be heat treated. Since its hardenability is rather low, only thinner sections can be considered for hardening. It is expected however that wall thicknesses of up to perhaps 0.125 inch could be heat treated to about the 160-180 ksi ultimate tensile strength level and with a minimum of distortion. For large numbers of parts it becomes more feasible since possible fixturing to minimize distortion could be amortized over the large numbers involved.

The availability of tubing in thin enough walls to enable it to be competitive with carbon steel tubing became a limitation for 4130.

All of the aluminum alloys being considered are heat treatable to various degrees. As pointed out in previous sections, heat treatment of these alloys is tied directly to concerns about stress corrosion capabilities and also to subsequent forming capabilities.

The most common heat treating tempers are T4 and T6. Along with T8, these are explained further below. The first step in heat treating aluminum alloys is called solution heat treatment and consists of an elevated temperature treatment required to put the soluble elements into solid solution. A rapid quench puts the alloy into a temporarily stable state in which the metal is quite workable (the "W" temper). The structure at room temperature (or above) begins an aging process during which precepitation of the constituents progresses from the saturated solution. This process is called aging or room temperature precipitation and results in a structure which is much stronger. Some alloys continue to age harden at room temperature for long periods of time. Heating for a controlled period of time at slightly elevated temperature can result in a still further increase in strength. This last process is called artificial aging or precipitation hardening.

A T3 temper condition denotes an item which has been solution treated, then cold worked to increase strength. The T4 condition refers to a product which has been solution treated and naturally aged to a substantially stable condition--no cold working (or at least no credit given for cold working enhancement effects). A T6 condition applies to a product which has been solution treated then artifically aged and has not been cold worked after solution heat treatment. The T8 condition refers to a product which has been solution treated, cold worked to improve strength, then artifically aged.

As indicated previously, 2014 in the T3, T4 and T6 conditions is particularly susceptible to stress corrosion cracking as is 7075 in the T6 condition and 2024 in the T3 and T4 conditions. On the other hand, 2024 in the T6 or T8 condition and 7075 in the T73 or T76 conditions are decidedly superior as far as stress corrosion cracking. Since the T73 and T76 conditions are available in sheet material only, no further mention will be made of them.

Minimum tensile properties attained for tubing at various required heat treat levels are shown in Table B-3.

#### Wall Thicknesses and Weights

As was indicated previously, preliminary wall thicknesses were based on:

$$t = \frac{1.5 p R}{S}$$

where:  $t$  = Required wall thickness (inches)  
 $p$  = An assumed pressure of 3000 psi  
 $R$  = Outside radius of tubing (2 inches)  
 $S$  = Ultimate tensile strength (minimum) of the material being considered  
and 1.5 was used as a factor of safety for pressure

A more refined calculation was used subsequently to provide a closer approximation of required wall thickness as follows:

1. Assumed maximum expected operating pressure (MEOP) of 1.10 ( $p$ ) or 1.10 (3000) = 3300 psi
2. A burst pressure/MEOP ratio of 1.25
3. A hydrotest pressure/MEOP ratio of 1.10
4. A minimum yield pressure/hydrotest pressure ratio of 1.10

This gave a burst pressure of 4125 psi,  
a hydrotest pressure of 3630 psi and,  
a minimum yield pressure of 4000 psi

From these values,  $t = \frac{p' R'}{S'}$  was evaluated

with:  $t$  = required wall thickness (in.)  
 $R'$  = the radius of the mean wall thickness (in.)  
 $S'$  = the minimum ultimate or minimum yield strength (psi)  
 $p'$  = burst pressure (psi)--used with matching value of  $S'$ .

Of necessity, these values will have to be further refined as ballistic performance iterations provide more information on motor performance.

Wall thickness requirements were then translated into nominal weights as follows:

$$W = C (D - t) t$$

where W is the weight per foot (lb/ft) of the tubing considered,  
D is the outside diameter (inches),  
t is the required thickness (inches),  
C is a constant, based on material density and is 10.68 for steel;  
3.8053 for 2014 and 7075 aluminum, and 3.7684 for 2024 aluminum.

The following values resulted:

<u>Material</u>	<u>Wall Thickness (in.)</u>	<u>Weight (lb/ft)</u>
1025 (DOM)	.134	5.173
1035 (DOM)	.109	5.916
4130 (normalized)	.087	4.973
4130 (heat treat to 150 ksi ult.)	.065	2.732
2014 T6	.140	2.056
2024 T8	.140	2.036
7075 T6	.156	2.282

#### Mill Tolerances

The following tolerances apply to the various DOM steel tubing and are per ASTM A513-70, Reference 4. (Only two of the three dimensions specified can be applicable to an order)

<u>Outside Dia. (in.)</u>	<u>Inside Dia., (in.)</u>	<u>Wall Thickness (in.)</u>
± .006	± .006	± .005

The standard (Aluminum Association) tolerances of aluminum tubing are called out somewhat differently as can be noted on Figure B-3. However, at any point, the worst condition can be

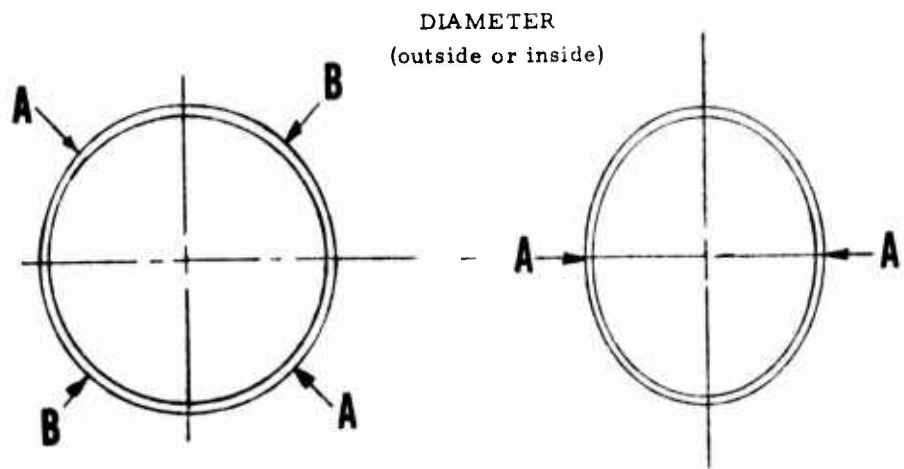
<u>Outside Diameter (in.)</u>	<u>Wall Thickness (in.)</u>
± .016	± .014 to ± .016

#### Cost

Table B-5 lists the cost per foot of the candidate materials.

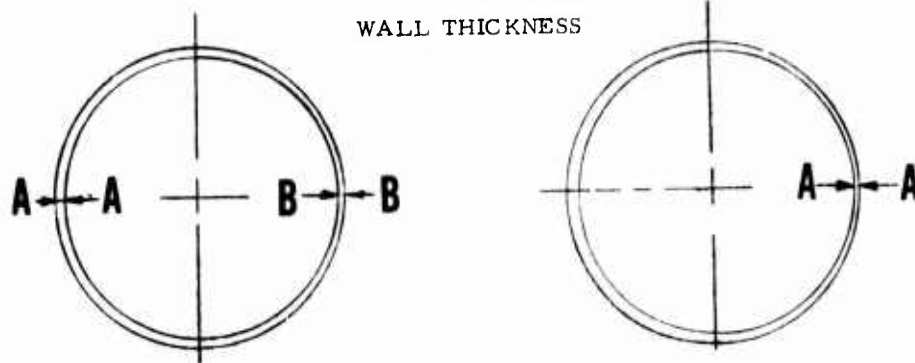
#### Summary of Material Considerations

Two factors of interest were noted when the six materials remaining for consideration were screened. For one thing, on comparing the 1025 steel material with the 1035, it is clear that the 1035 is much stronger. In addition, although there may be a adjustment in price between 1025 and 1035 materials, the increase in strength and accompanying decrease in required thickness appear from price quotes to more than make up for any material adjustment.



Allowable Deviation  
Between Mean Diameter,  
 $1/2 (AA + BB)$ , and Specified  
Diameter (O. D. of 4")  
 $= \pm .008''$

Allowable Deviation of  
Diameter at any Point (A-A)  
from Specified Diameter  
(Ovalness)  
 $\pm .016''$



Allowable Deviation Between  
Mean Wall Thickness,  $1/2 (AA + BB)$ ,  
from Specified Wall Thickness  
 $= \pm .006''$

Allowable Deviation of Wall  
Thickness at any Point (A-A) from  
Specified Wall Thickness (Eccentricity)  
 $\pm 10\%$  of Specified  
Wall Thickness  
(Min. of  $\pm .003''$ )  
 $\pm .014''$  and  $\pm .016''$

Figure B-3. Aluminum Tubular Products Applicable Standard Tolerances

The result is that the 1035 material is not only stronger, but cheaper as well. For this reason, no further consideration was given to using AISI 1025 steel.

Secondly, the minimum wall thickness for which a quotation for an 7075-T6 aluminum could be obtained was .156 inch. Thus, although the material is slightly higher in strength than either the 2014 T6 or the 2024 T8 aluminum, the additional strength could not be efficiently utilized and the price was also higher. For these reasons, the 7075 T6 material was effectively eliminated from consideration, particularly since it offered little in the way of advantage for forming, machining, or welding over the other two alloys.

Thus, there were four contending materials remaining for more thorough evaluation--AISI 1035 and 4130 steel and 2014 T6 and 2024 T8 aluminum.

Of these, the potential of 4130 will be discussed first. The only quote that was obtainable for this material was for normalized tubing (per ASTM 513)--DOM type with 103 ksi ultimate tensile strength and 93 ksi tensile yield strength. Such strengths would translate into a nominal wall thickness of about .087 inch.

The vendor who quoted felt, upon further inquiry, that it might be possible to fabricate a wall thickness of about .065" nominal but was unwilling to quote heat treatment because of distortion fears. (That thickness translated into a heat treatment level of about 150 ksi ultimate tensile strength.)

A specialty heat-treating company was contacted to ascertain the feasibility of heat-treating the 4130 material. After discussion, they felt it would be quite feasible to heat treat (martemper) without much distortion (perhaps requiring the use of fixtures). Their estimated price for heat treatment (on a 20,000 unit per month basis) was \$22.50 per unit. Not including the extra transportation costs involved, the heat treatment increased the case material cost by some 260% in comparison with the normalized DOM material. The net weight savings would be just over three pounds.

In considering the relative merits of the 2014 T6 and 2024 T8 aluminum alloys other than cost, two important factors seem to stand out. First, the 2024 T8 material cannot be readily fusion welded, although it can be resistance welded. Thus for any design contemplating the necessity of fusion weld, as an overriding factor, 2014 T6 should be considered.

More important is the susceptibility of 2014 T6 to stress corrosion as compared to this being of no concern if 2024 T8 is utilized. Other factors being equal, the 2024 T8 material should be considered as being a more reliable choice.



TABLE B-5

COST OF 4-INCH O.D. TUBING MATERIALS

	<u>Wall Thickness (Nom., in.)</u>	<u>Base Price (\$ per foot)</u>
<u>Steel:</u>		
AISI 1035 DOM (as drawn)	0.109	2,178
AISI 1035 DOM (stress relieve)	0.120	2,003
AISI 4130 DOM	0.100	3,940
<u>Aluminum (extruded and drawn):</u>		
2014 T6	0.140	5,497
2024 T81	0.140	5,773
7075 T6	0.156	7,689

### Cost Versus Performance

In order to more closely evaluate tubing costs, it is necessary to measure not only the direct cost of the various materials but to obtain some idea of their relative effect on motor performance. For instance, the use of thinner wall material not only results in a lighter case (on an equal density basis), but also enables the loading of a greater amount of propellant (which partially compensates for the added weight in the instance of a steel case).

To relate relative performance versus cost for the various tubings, certain performance values were assumed:

1. A propellant weight of 20 pounds
2. A propellant specific impulse of  $250 \frac{\text{lb sec}}{\text{lb}}$
3. A loaded tube length of 42 inches
4. A "base" tubing material of 2024 T8

The results are depicted on Figure B-4 and tabulated in Table B-6. As can be seen from the table, a total loaded tube weight was obtained which consisted of the weight of the tube plus 20 lbs. of propellant plus or minus the propellant differential weight resulting from varying case wall thickness as required for each material. The propellant differential and total weight was used to adjust total impulse. Subsequently a "Case Loaded Specific Impulse" was obtained by dividing the total impulse by the total weight. The base value (2024 case) was assigned a value of 100 and other materials ranked accordingly.

The tubing price obtained from quotes of material prices was normalized by assigning a value of 100 to 2024 also. The "case loaded specific" values were plotted against the relative prices and are given on Figure B-4. Observing the results clearly shows the inefficiency of using the 7075 T6 "thicker wall" material and the relatively high cost of heat treating each unit of 4130 steel. (Possibly this could be reduced by heating longer tubing sections, but the optimum length versus acceptable distortion would have to be developed).

It is also clear that only a minor difference exists between using 2014 T6 and 2024 T8, and that, relatively, both 4130 (DOM, normalized) and AISI 1035 (DOM) material decrease in cost at a greater rate than they affect performance. However, this approach says nothing about absolute performance--i.e., a lower limit which is higher than can be achieved by a particular material. Possible use of the 1035 material, in particular, must be modeled into a performance program before its use proves feasible.

As a summary, the advantages and disadvantages of 1035, 4130, and 2024 T8 are given in Table B-7. Some data are not available and would likely have to be obtained by testing for further proof of feasibility.

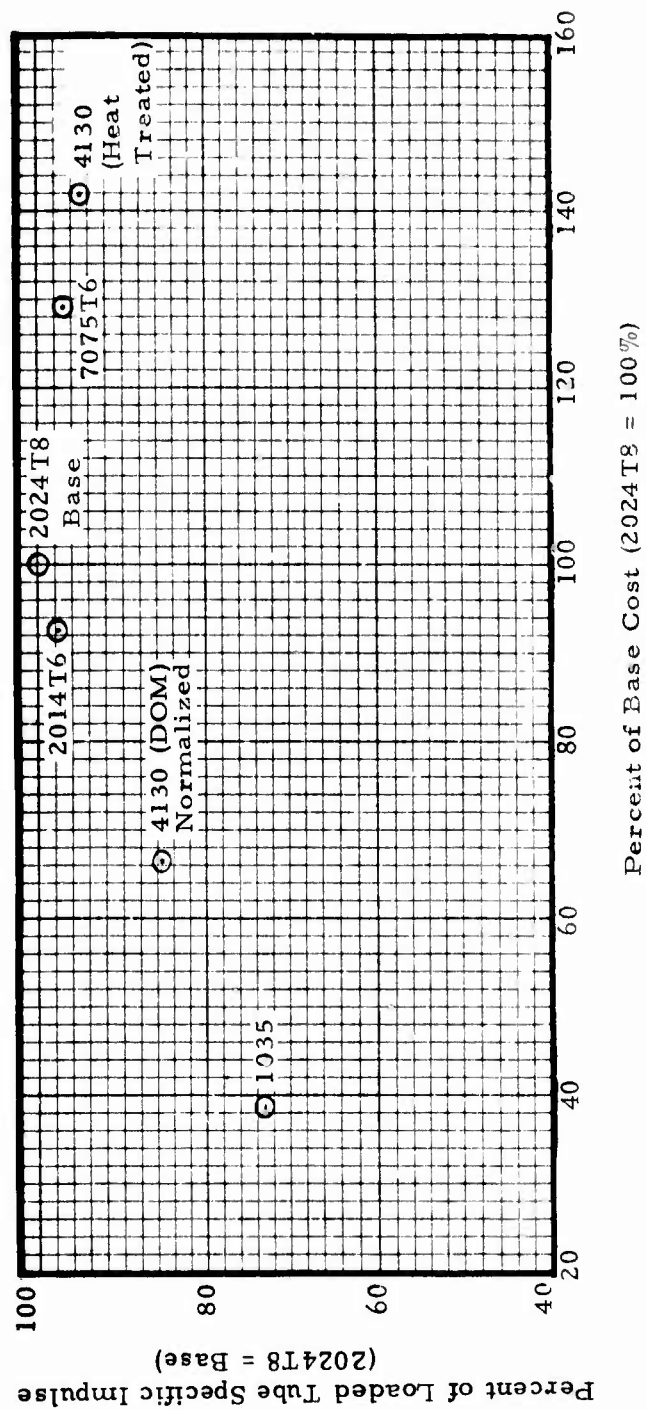


Figure B-4. Relative Performance Versus Cost of Selected Stock Tubing

**TABLE B-6**  
**FACTORS OF COMPARISON FOR SELECT TUBING (2024 T8=BASE)**

Material	Condition	Req'd Wall Thickness (in)	$\Delta$ Propellant Weight	$\Delta$ Propellant Impulse	Case Weight (lb)	Relative Case Wt. (%)
2024	T8	.140	0	0	7.13	100
2014	T6	.148	-0.25	-62.5	7.60	106.6
7075	T6	.156 (a)	-0.49	-122.5	7.99	112.1
4130	N.	.087	+1.67	+417.5	12.71	178.3
4130	HT 150K	.065	+2.37	+591.5	9.55	133.9
1035	C.W.	.120	+0.62	+155	17.45	244.7

Material	Total Weight (20 lb Prop. $\pm$ AP Case Wt)	Total Impulse	Case Loaded Specific = Total Impulse / Total Weight	Tube Price (42")
2024	27.13	5000	184.3	\$20.81
2014	27.35	4937.5	180.5	19.24
7075	27.5	4877.5	177.4	26.91
4130N	34.38	5417.5	157.6	13.79
4130NT	31.92	5591.5	175.2	36.29
1035	38.07	5155	135.4	8.00

a. Limited by processing.

TABLE B-7

## SUMMARY OF ADVANTAGES AND DISADVANTAGES OF SELECTED STOCK TUBING

Material	Advantages	Disadvantages
1035	<ol style="list-style-type: none"> <li>1. Inexpensive</li> <li>2. Readily available</li> <li>3. Weldable</li> <li>4. Machinability good</li> <li>5. Reasonably formable depending on degree and process</li> </ol>	<ol style="list-style-type: none"> <li>1. Heavier wall required</li> <li>2. Nil ductility. Transition temperature may be limiting factor.</li> <li>3. More susceptible to general corrosion (requires good corrosion protection)</li> </ol>
4130	<ol style="list-style-type: none"> <li>1. Highest strength (thin wall)</li> <li>2. Fairly good corrosion resistance when protected by coating</li> <li>3. Weldability and machinability should be good</li> <li>4. Fracture toughness high</li> <li>5. Could be heat treated if necessary</li> </ol>	<ol style="list-style-type: none"> <li>1. Higher cost than 1035</li> <li>2. Limited availability - (minimum order 4000 to 8000 lb range or 1000 to 2000 ft)</li> <li>3. Better low temperature properties than 1035</li> <li>4. Forming may be a problem</li> </ol>
2024	<ol style="list-style-type: none"> <li>1. Lightest weight</li> <li>2. Good general corrosion resistance and stress corrosion resistance in T6 or T8 tempers</li> <li>3. Low temperature capabilities good</li> <li>4. Fracture-toughness poorer than steel, but probably adequate</li> </ol>	<ol style="list-style-type: none"> <li>1. High cost</li> <li>2. May be difficult to form--requiring heating and time limits to achieve</li> <li>3. Resistance welding only is practical</li> <li>4. High temperature capabilities limited</li> <li>5. Allowable tolerances of standard tubing are greater than those of DOM steel tubing</li> </ol>

(Continued on next page)

TABLE B-7. (Continued)

<u>Material</u>	<u>Advantages</u>	<u>Disadvantages</u>
2014	<ol style="list-style-type: none"> <li>1. Light Weight</li> <li>2. Good general corrosion resistance</li> <li>3. May be fusion welded (as compared to 2024)</li> <li>4. Low temperature capabilities good</li> <li>5. Fracture toughness poorer than steel but probably adequate</li> </ol>	<ol style="list-style-type: none"> <li>1. High cost (lower than 2024)</li> <li>2. May be difficult to form--requiring heating and time limits to achieve</li> <li>3. Susceptable to stress corrosion cracking in T3, T4, T6 conditions</li> <li>4. High temperature capabilities are limited</li> <li>5. Allowable tolerances of standard tubing are greater than those of DOM steel tubing</li> </ol>

Table B-8 compares the tolerance range which can be expected from the mill products of these materials.

Table B-9 summarizes data regarding the present (October 1975) base prices (lowest prices without extras) for steel and aluminum tubings along with the minimum order required to obtain base prices and the present projected delivery.

### EXPANDED INVESTIGATIONS

The previous study of possible stock tubing usage resulted in a narrowing of candidate tubing materials to six types--1026, 1035 and 4130 steel tubing of the welded and drawn over mandrel type and 2014 T6, 2024 T8 and 7075 T6 aluminum of the drawn type. The previous study was intentionally limited to a maximum expected operating pressure (MEOP) of 3300 psi since it appeared the motor operating characteristics would be generally near that figure.

Subsequently, ballistic analyses indicated the possibility that much lower pressures might be feasible. Thus, the stock tubing effort was expanded to cover a range of pressures. The feasibility of lower pressures led to the investigation of two more types of materials--6061 T6 and 5052 H36 aluminum. The former was investigated as it is a widely used stock material and the latter to serve as a basis for comparison for non-heat treatable aluminum, being about the same strength level as 6061 T6. In addition, 6061 material can be obtained in a wide range of wall thicknesses.

### Tubing Wall Thicknesses

The initial approach for the extended portion of the study was to consider available wall thicknesses for stock tubing and to calculate a corresponding allowable burst pressure. The relationship between burst pressure, MEOP and maximum pressure at 70°F was established by utilizing appropriate estimates and margins of safety as follows:

Upper temperature limit	+ 160°F <sup>1</sup>
Estimate of $\pi_k$	0.10%/°F
Burst pressure/MEOP	1.4 <sup>2</sup>
Statistical coefficient of variation (±12% = 3 c v limits)	4% assumed

1. Program RFQ and MIL-R-25532.
2. MIL-R-25532, Paragraph 3.8.4.1.2.1.



TABLE B-8

TOLERANCE COMPARISON  
STEEL TUBING (DOM) VERSUS ALUMINUM TUBING

	<u>Steel (DOM)</u>	<u>Aluminum (Drawn)</u>
Diameter (Outside or Inside) (in.)	$\pm .006$	$\pm 0.008$
Wall Thickness (in.) (in range of interest)	$\pm .005$	$\pm 0.006$
Bow (in.)	.030 per 3 ft length plus .010" per each additional foot  (.040 max for a 42" cut length)	.010 per foot of length  (.040 max for a 42" cut length)
Ovalness (in.)	$\pm .006$	$\pm .016$

TABLE B-9

PRICE AND AVAILABILITIES  
OF "BASE" QUANTITIES  
(As of October 1975)

<u>Material</u>	<u>Base Price Per Foot</u>	<u>Minimum Order for Minimum (Base) Price</u>	<u>Projected Delivery</u>
1035 DOM (.120" wall)	\$2.18	75,000 lbs. (15,000 ft)	2 to 3 months
4130 DOM (.087" wall)	\$3.94	4000 to 8000 lbs. (1000 to 2000 ft)	8 to 9 weeks
2024 T8 (.140" wall)	\$5.77	5000 lbs. (2450 ft)	10 weeks
2014 T6 (.140" wall)	\$5.50	5000 lbs. (2430 ft)	10 weeks

then:

$$\frac{\text{MEOP at } 160^{\circ}\text{F}}{P_{\text{max at } 70^{\circ}\text{F}}} = [1.12] [e^{(0.001)(160^{\circ}\text{F} - 70^{\circ}\text{F})}] = 1.2255$$

and:

$$\frac{\text{Burst pressure at } 160^{\circ}\text{F}}{P_{\text{max at } 70^{\circ}\text{F}}} = 1.4 (1.2255) = 1.716$$

In addition to the 1.716 factor, allowable maximum tolerances were utilized to ascertain maximum diameters and minimum wall thicknesses in arriving at values of allowable  $P_{\text{maximum}}$  at  $70^{\circ}\text{F}$  which corresponded to standard tubing sizes.

Figure B-5 is a plot of  $P_{\text{maximum}}$  at  $70^{\circ}\text{F}$  versus tubing wall thickness for stock tubing of various materials. The "stair-step" effect results from the fact that any given thickness of tubing can only take up to one level of  $P_{\text{max}}$  at  $70^{\circ}\text{F}$  and this value of pressure cannot be exceeded until the next thickness of stock tubing is available for use. It is clear from the plot that the strength levels of 6061 T6 and 5052 H36 are the same and that 1035 and 2024 T81 tubing are somewhat stronger than 1026 and 2014 T6, respectively. Shown also on the plot are single points representing a single wall thickness for both normalized 4130 steel tubing and 7075 T6 tubing. Limited pricing information on these less-standard items coupled with their limited availability precluded more extensive consideration of them. As indicated, 1026 and 1035 steel tubing (in a 4-inch outside diameter) can be obtained in minimum thicknesses of 0.109 inches while 2024 T81 and 2014 T6 can be obtained in minimum thicknesses of 0.134 inches. The cut-off points for maximum wall thicknesses were somewhat arbitrary. However it should be pointed out that calculations for allowable pressures (or wall thicknesses) would decline in accuracy at around 0.2 inch wall thickness where thin-wall vessel equations (as used herein) would cease to become applicable and thick wall equations would be appropriate. The upper limit for the 1026 and 1035 materials was arbitrarily based on the fact that they will be weight-limited in the thicker walled sizes.

Figure B-6 gives a series of cost<sup>1</sup> versus wall thickness for the same materials as covered by Figure B-7. The "equal thickness" cost advantage of the low carbon steel tubing is demonstrated in this figure as is the cost advantage of 6061-T6 over the 5056-H36 material. With regards to the latter, it may be recalled from Figure B-5 that these aluminums have equal strength (pressure) capabilities so that the 6061-T6 material has (as will be seen later) a definite cost advantage. It may also be seen that the slight strength advantage of 2024-T8 over 2014-T6 is accompanied by a relatively greater

1. These costs utilized base prices (i.e., relatively large amounts) and do not include any amounts to cut the tube to desired lengths.

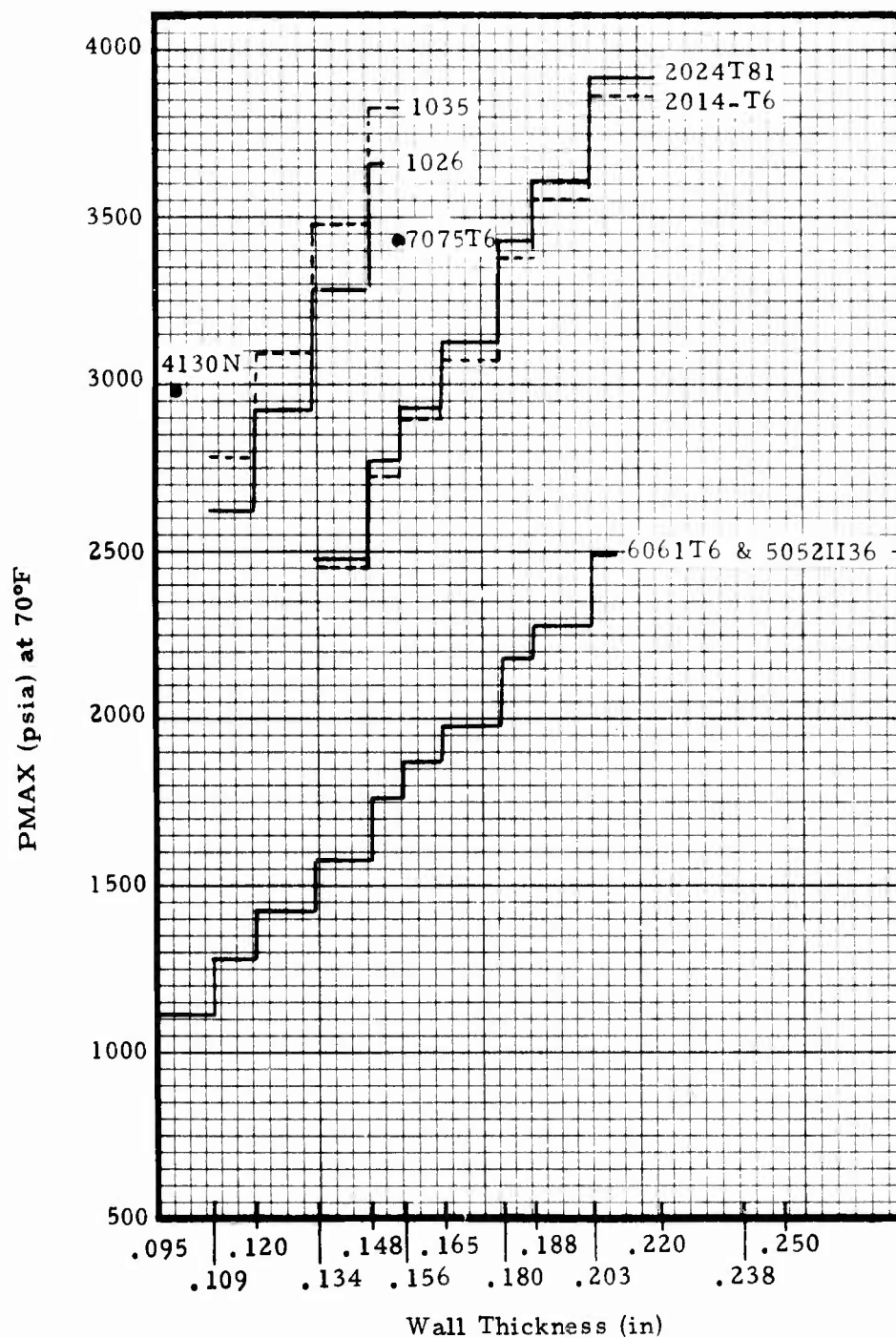


Figure B-5. Allowable Maximum Pressure at 70°F Versus Wall Thickness for Selected Stock Tubing

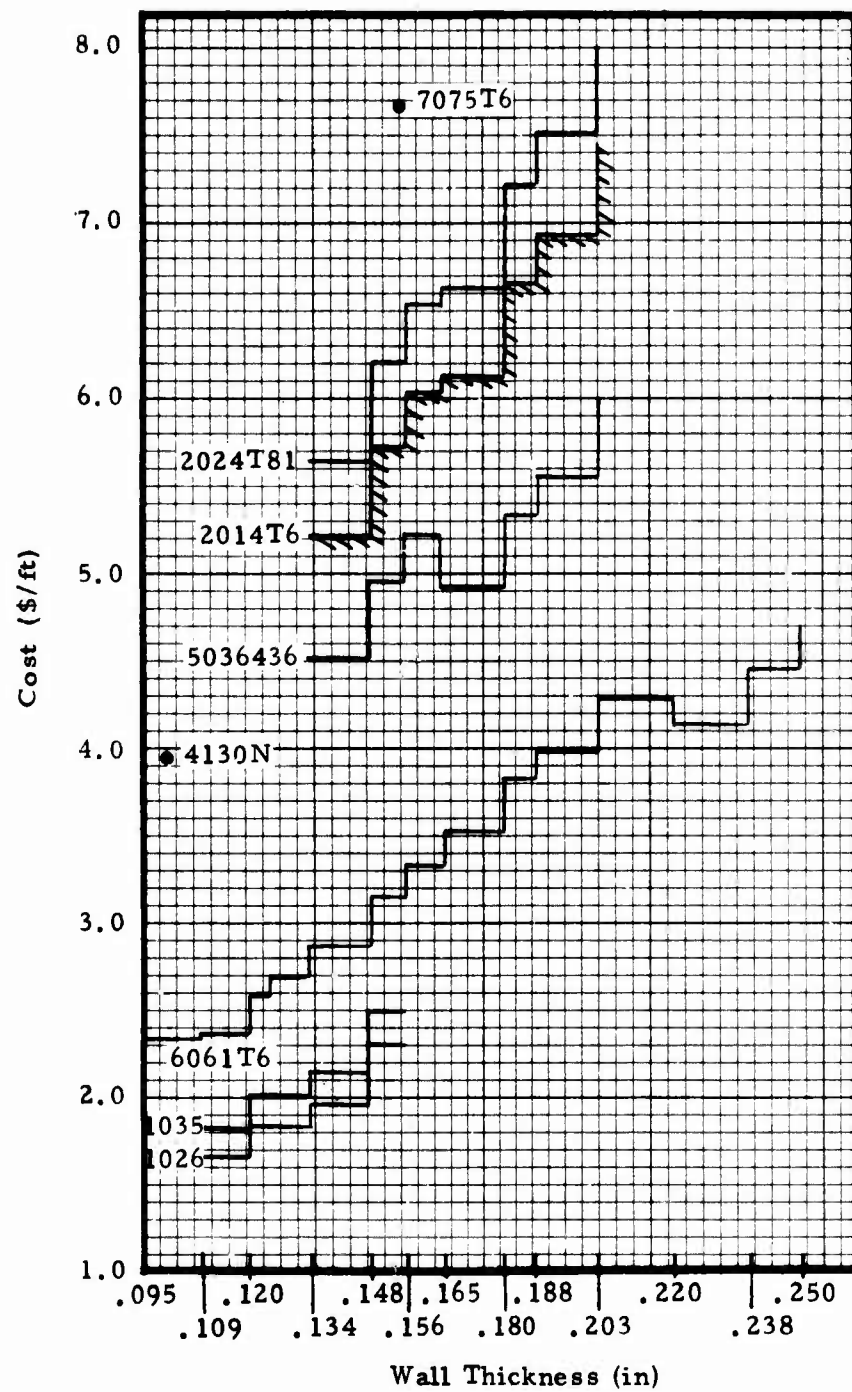


Figure B-6. Cost of Selected Stock Tubing Versus Wall Thickness

increase in cost per foot. A rather interesting aspect of pricing can be noted in the pricing structure of the 6061-T6 and 5056-H36 materials, whereby a thicker wall material may actually cost somewhat less. This may be noted at the 0.220 inch wall thickness level for 6061-T6 and the 0.165 inch wall thickness for 5056-H36 material.

Since cost vs. wall thickness (Figure B-6 and  $P_{\max}$  at 70°F vs. wall thickness (Figure B-5) are rather difficult to visualize relative to motor performance, Figure B-7 presents a comparison of  $P_{\max}$  at 70°F versus stock tubing cost (\$ per foot basis) for the same materials considered previously. As can be noted from Figure B-7, the cost of the carbon steel tubing is less than the other material on a pressure-equivalent basis. Likewise, the pressure capabilities increase at a faster rate relative to the costs in comparison with the aluminum alloys considered. Of the latter, 6061-T6 was the least expensive alloy while 5052-H36, despite having the same strength is priced higher. The 2014-T6 and 2024-T81 materials are relatively higher priced but have pressure capabilities about the same as the carbon steels.

#### Tubing Weights

The higher cost of the high strength aluminum alloys notwithstanding, these materials have the natural advantage of light weight over the steel tubing materials considered. An idea of the magnitude of the weight difference may be seen from Figure B-8 which is a plot of wall thickness versus weight (lb/foot) for the various tubing materials. Since the various steel tubings weigh the same for a given wall thickness, they can be represented by one line. On the other hand, the densities of the various aluminum alloys are somewhat different which results in the slight differences in weight noted on the figure.

A more meaningful comparison of the various materials insofar as weight can be seen on Figure B-9 which plots  $P_{\max}$  at 70°F versus tubing weight on a pound per foot basis. The depiction reflects the weight differences on an equivalent allowable pressure (i.e., strength) basis. The rather large difference in steel and aluminum tubings on this equivalent pressure basis can be clearly noted.

#### Loaded Tubing Mass Fraction

In a rocket motor case, the tubing wall thickness in addition to affecting the weight of the case (i.e., at a constant density of material) also affects the space available for loading of propellant within the case if a fixed outside diameter is assumed. That is, a relatively thinner wall not only permits the case to be lighter in weight but makes additional free space available for the loading of propellant. Thus, the weight concern of wall thickness are further magnified in their effects on performance. Figure B-10 indicates the extent to which wall thickness of tubing affects a parameter designated "Loaded Case Mass Fraction", which is merely the ratio of the pounds of propellant loaded



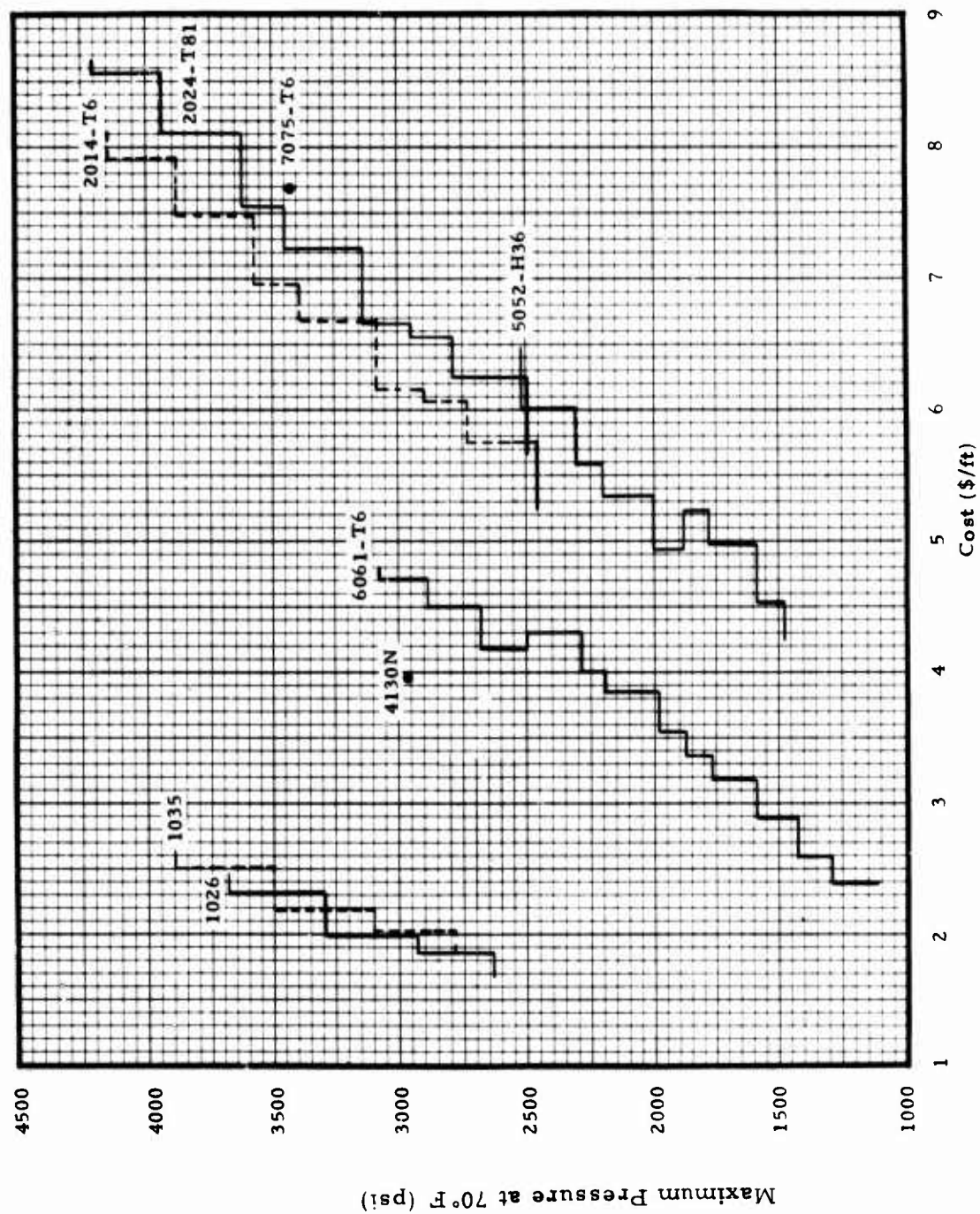


Figure B-7. Allowable Maximum Pressure at 70°F Versus Cost of Selected Stock Tubing



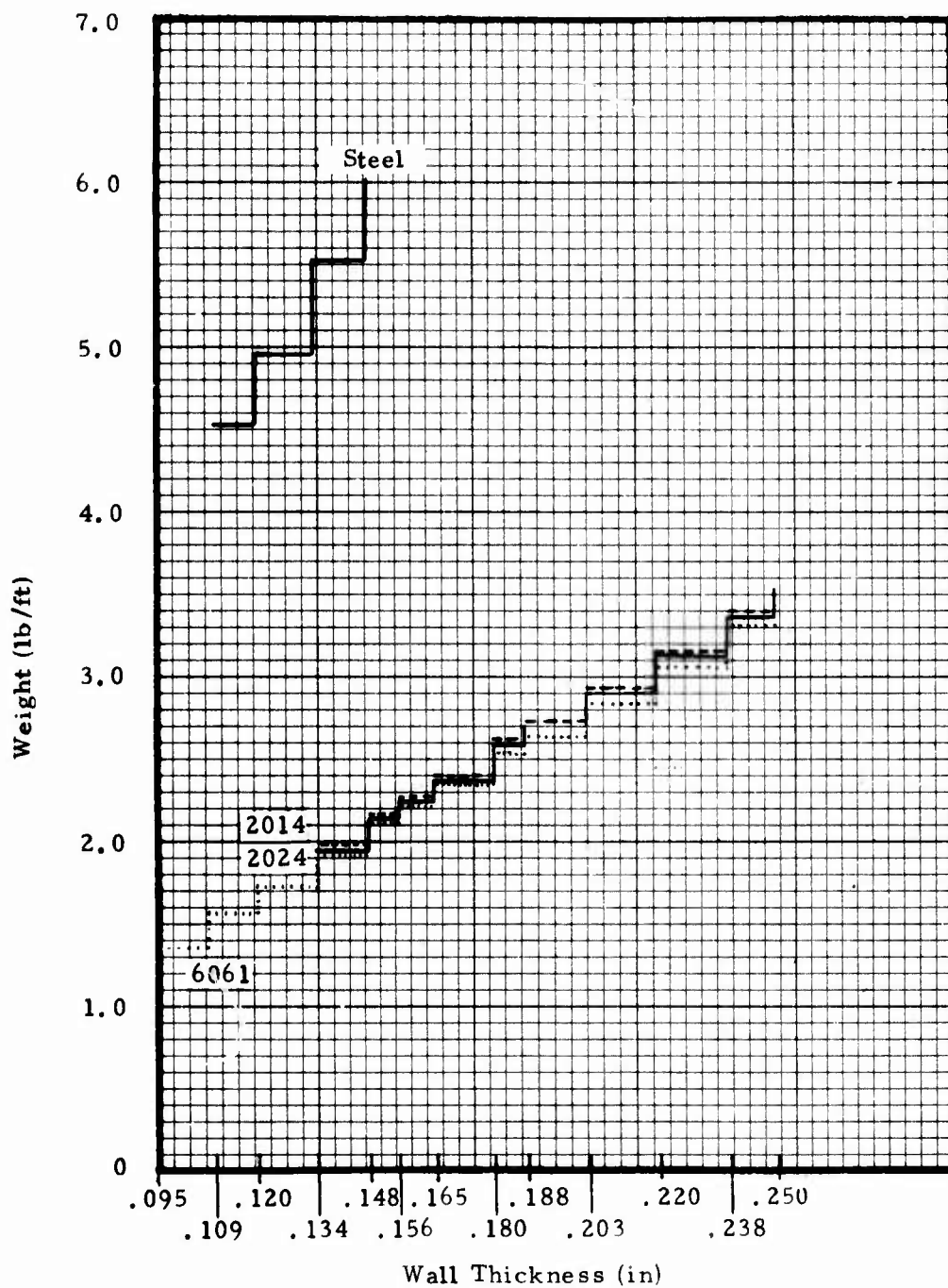


Figure B-8. Weight of Selected Stock Tubing Versus Wall Thickness.

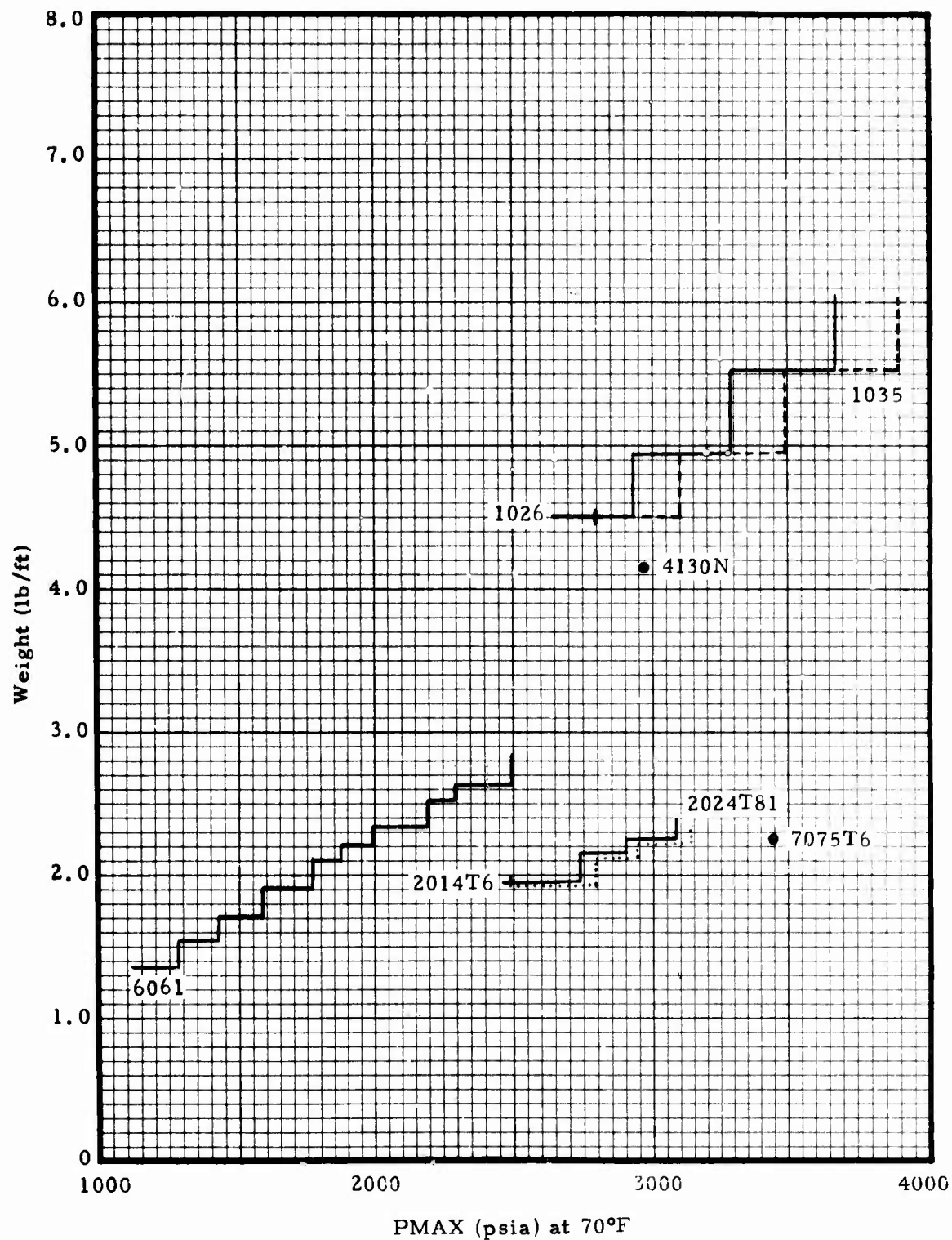


Figure B-9. Weight of Selected Stock Tubing Versus Allowable Maximum Pressure at 70°F

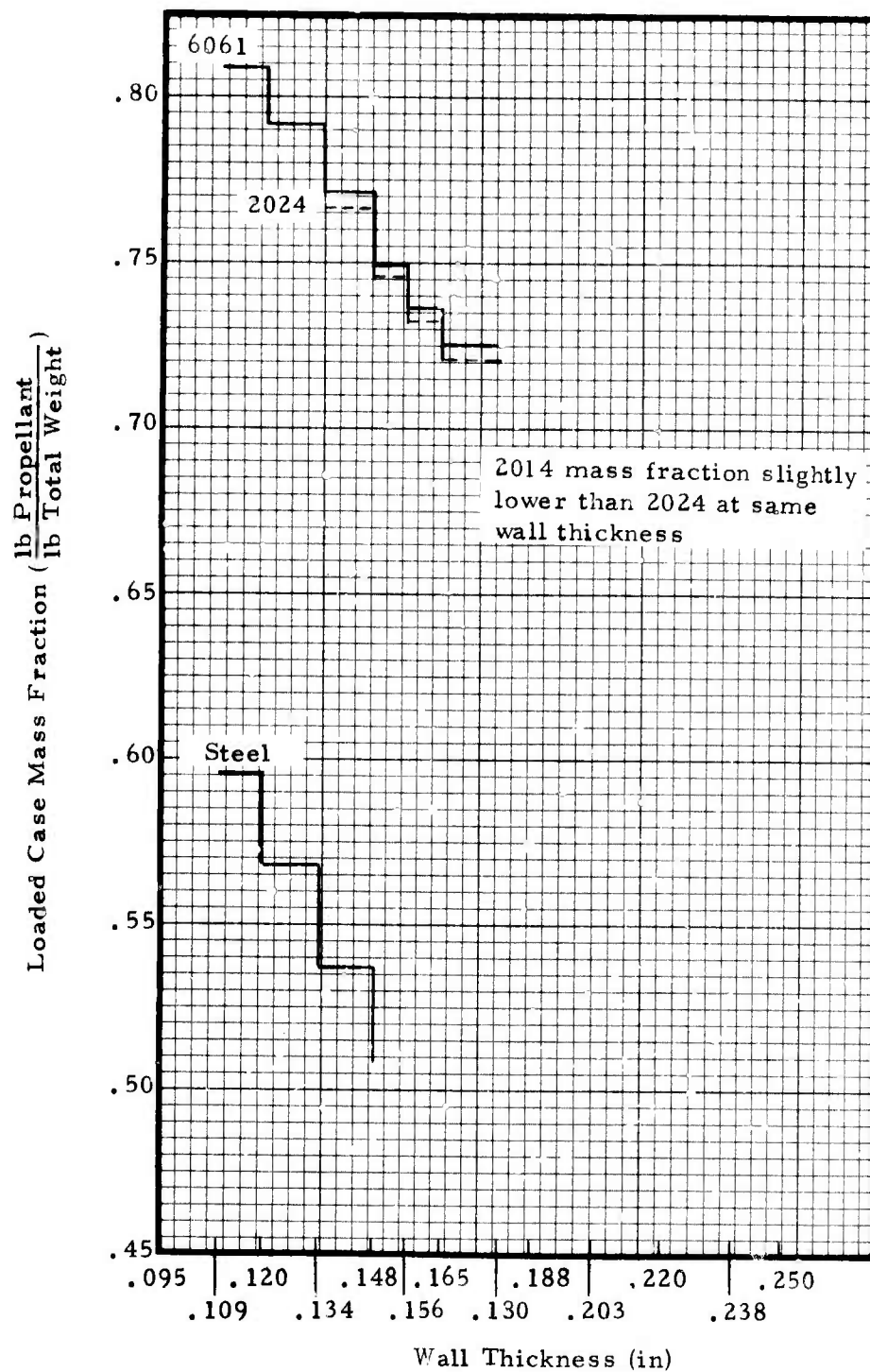


Figure B-10. Effects of Wall Thickness on Loaded Case Mass Fraction for Selected Stock Tubing

into a 42 inch long tube to the total weight (tube plus propellant) of the loaded tube. The propellant inner bore was held constant.

Again, however, values at equivalent pressures provide a more meaningful picture and these data are plotted on Figure B-11. The plots indicate a somewhat different picture. For example, the loaded case mass fraction of 6061-T6 is much closer to that of the carbon steel tubing material on an equivalent pressure basis than on the absolute weight basis as seen on Figure B-10. It further becomes clear that the highest loaded case mass fraction when carbon steel is used will be about 60%, while the use of 2014-T6 or 2024-T81 aluminum tubing will result in a mass fraction of about 75% at the same pressure capability.

The tradeoff of mass fraction versus tubing cost is depicted by Figure B-12 which shows the cost penalty paid for requiring the higher mass fractions. Figure B-11 indicates about a 20% increase in obtainable mass fraction is possible (at a  $P_{max}$  70°F of 2500 - 2600 psi) when using 2014 or 2024 aluminum instead of 1026 or 1035 steel (mass fractions of 0.75 and 0.60, respectively). Figure B-12 shows the 20% increase in mass fraction is achieved at an increase in cost of about 210% (from about \$1.70 per foot for the 1026 - 1035 steel to over \$5.20 per foot for the 2014 aluminum). Fabrication differences are ignored in these figures. Putting this on an absolute basis, the steel cases would weigh about 10 lbs. more and would load about 0.8 lbs. more propellant. The relative significance of tubing cost or mass fraction must be determined by the performance requirements specified for the motor.

#### Properties of 6061-T6 Aluminum

Since the prior study of material properties did not include 6061-T6 aluminum as a possible candidate, the properties will be covered in the following paragraphs.

General Corrosion Characteristics, i.e., those associated with general environmental usage, of 6061-T6 aluminum are much superior to those of either 2014-T6 or 2024-T81. The rating based on salt spray and immersion tests are "B" for 6061-T6 and "D" for the other two alloys on an A to E scale in decreasing order of merit.

In comparing stress corrosion characteristics of 6061-T6, it rates a value of "A" -- no known instance of failure in service or in laboratory tests. Thus from the aspect of corrosion resistance, 6061-T6 aluminum rates superior to other types of material considered.

The tensile properties of 6061-T6 drawn tubing, as indicated in the earlier report on stock tubing, is considerably less than either 2014-T6 or 2024-T81. The 6061-T6 ultimate tensile strength is a minimum of 42,000 psi (vs. 65,000 psi for 2014-T6 and 66,000 psi for 2024-T8). Ultimate yield strength for the 6061-T6 is 35,000 psi (vs. 55,000 and 58,000 psi, respectively

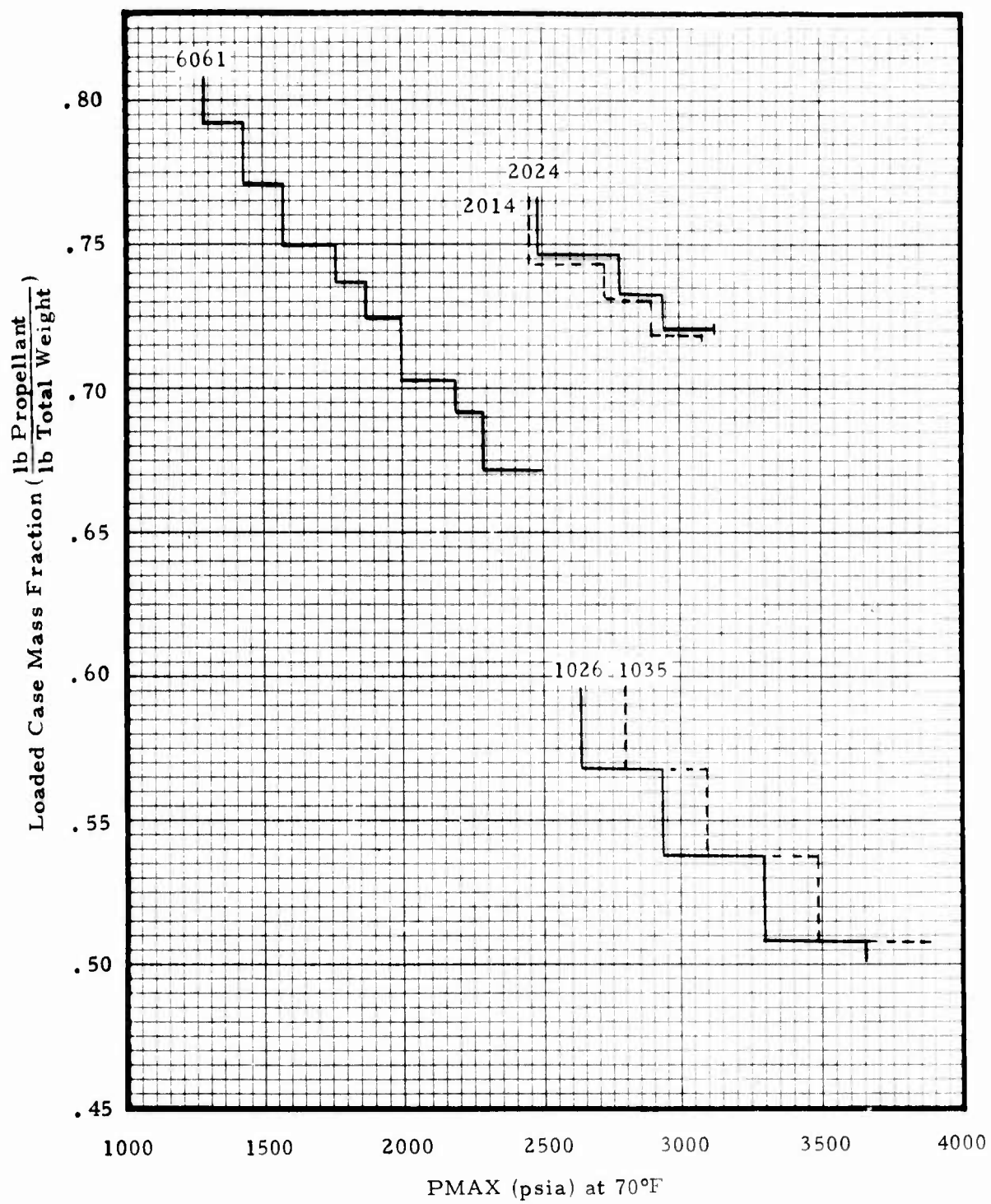


Figure B-11. Loaded Case Mass Fraction as Function of Allowable Maximum Pressure at 70°F



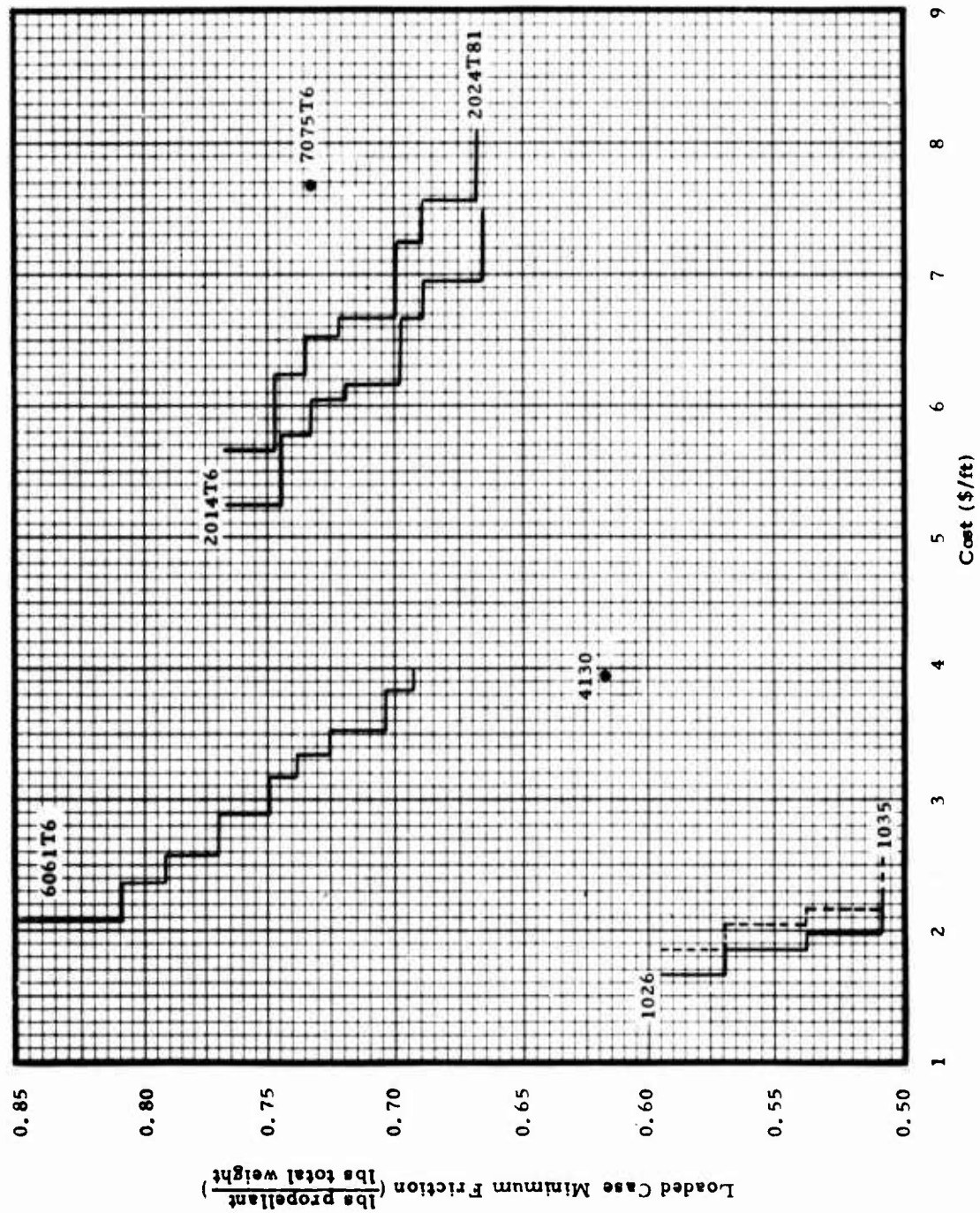


Figure B-12. Loaded Case Min. Friction Versus Cost of Selected Stock Tubing

for the other alloys). On the other hand the minimum percent elongation is greater, as would be expected, for the 6061-T6--being 10% minimum (vs. 7% and 5%).

The high temperature exposure effects on 6061-T6 are similar to those of the other aluminum alloys considered and, practically speaking, short term exposures (on the order of seconds) of elevated temperatures may have little effect on tensile properties, per se. Low temperature effects on tensile properties of 6061-T6 will also be similar to those of other aluminum alloys previously discussed, in that they will tend to increase tensile strength slightly.

Although the plane strain fracture toughness value for 6061-T6 material was not immediately available, a value for 6061 T651 should be applicable and this is a  $K_{IC}$  value of 27 ksi for 1 1/2" plate at room temperature. It is thus generally comparable to 2014-T6 alloy in fracture toughness.

The weldability of 6061-T6 is excellent by all commercial methods. Using 4043 filler rod, re-heat treated welds have about the same tensile strength as the parent alloy. Welding processes do not appear to affect the corrosion resistance of 6061-T6. Thus, this alloy ranks higher in weldability than all of the aluminum alloys previously considered.

Formability of 6061-T6 is slightly better than any of the other aluminum alloys considered. However, for even better forming properties, the alloy can be formed in a T4 condition and then artificially aged to the T6 condition.

In contrast to the superior welding and forming properties of 6061-T6, its machinability rating is somewhat inferior to the other aluminum alloys of comparison and it would rank last in this category, having a "C" rating.

Insofar as heat treating characteristics, as was indicated above, no effect on corrosion resistance by heat treatment is to be expected. The T6 condition as previously discussed for 2014 is indicative of an alloy which has been solution treated and then artificially aged with no subsequent cold work. Thus, the 6061-T6 would be heat treated in a similar manner to the 2014 and rank the same.

#### VENDOR CONTACTS

Aluminum Company of America	Carol Amberson Mr. Collins Kay Scott	Birmingham, Ala.
Babcock and Wilcox Co.	Mr. Gary Huey Mr. Lou Maleszewski	Atlanta, Ga.
Capital Pipe Co.	Mr. Wm. Riley	Atlanta, Ga.



Central Steel Tube	Mr. Jonn Maxheim	Clinton, Iowa.
Cryotec, Inc.	Mr. Ralph Mr. Wiseheart	Huntsville, Ala.
Murray, A.B, Co.	Mr. Philip Belejchak	McKeesport, Pa.
Ohio Steel Tube	Mr. Mahn	Shelby, Ohio
O'Neal Steel Co.	Mr. Gilmore	Birmingham, Ala.
Rex, J. W., Co.	Mr. Joe Wiser	Lansdale, Pa.
Reynolds Metals	Mr. Carl Jennings	Birmingham, Ala.
Ryerson, J. T. & Sons	Mary Lee	Chattanooga, Tn.
Specialty Pipe and Tube	Mr. Banfield	Warren, Ohio
Tull, J. M., Metals Co.	----	Atlanta, Ga.
U.S. Steel	Mr. Jack Horton	Birmingham, Ala.
Werner, R. D., Co.	Mr. R. Werner	Greenville, Pa.

#### REFERENCES

1. Aerospace Structural Metals Handbook, AFML-TR-68-115; Mechanical Properties Data Center, Belfour Stulen Inc., Traverse City, MI., 1975
2. Alcoa Product Data, Aluminum Tubular Products, Aluminum Company of America; Pittsburgh, Pa. 15219. The following sections:
 

AE2A	"Aluminum Tubular Products"	May 1, 1975
AE2A-1	"Drawn Tube"	June 20, 1967
AE2B	"Standard Items"	April 10, 1974
AE2C	"Tool and Pipe Available Without Charge"	Sept 29, 1967
AE2D	"Pipe and Construction Tube"	April 23, 1975
AE2E	"Dimensions and Weights"	June 1, 1973
3. Aluminum Standards and Data, The Aluminum Association; 420 Lexington Ave., NYC 10017; 1969
4. Annual Book of Standards, Part 1, American Society for Testing and Materials; Philadelphia, Pa., 19103; 1972

5. Custom Made Regal and Ohio DOM Tubing, Product Bulletin EW-2f; Ohio Steel Tubing Co., Shelby, Ohio, 44875, March, 1975
6. Development and Fabrication of Motor Cases, Utilizing Tube Mill Products, H. W. Mishler and D. G. Howden, Battelle Columbus Laboratories, Columbus, Ohio 43021, Technical Report RK-CR-75-28; US Army Missile Command, Redstone Arsenal, Alabama; June, 1975.
7. Materials Reference Issue - Vol. 47, No. 6; Machine Design, Penton Publishing Co.; Cleveland, Ohio; March, 1975
8. Materials Selector 76, Materials Engineering, Vol. 82, No. 4, Sept, 1975; Reinhold Publishing Co., Stamford, CN.
9. Metals Handbook, 8th Edition; American Society for Metals; Metals Park, Ohio. Individual Volumes as follows:  
 Volume 1 - "Properties and Selection of Metals"  
 Volume 2 - "Heat Treating, Cleaning, and Finishing"  
 Volume 3 - "Machining"  
 Volume 4 - "Forming"
10. Ryerson Products in Stock, Processing Services, Joseph T. Ryerson & Son Inc., 1972.
11. Seamless Mechanical Tubing, United States Steel, Pittsburgh, Pa., 15230; January, 1972.
12. Seamless Pressure Tubing, United States Steel, Pittsburgh, Pa., 15230; June, 1971.
13. Steel and Aluminum Data Book, Joseph T. Ryerson & Son Inc., 1975.
14. Damage Tolerant Design Handbook, Metals and Ceramics Information Center, Battelle Columbus Laboratories, Columbus, Ohio.

#### MILITARY HANDBOOKS

15. Metallic Materials and Elements for Aerospace Vehicle Structures; MIL-HDBK-5B, 1 Sept., 1971
16. Steel and Wrought Iron Products; MIL-HDBK-723A, 30 Nov., 1970.

#### FEDERAL SPECIFICATIONS

17. Aluminum Alloy, Bar, Rod, Shapes, Structural Shapes, Tube, and Wire, Extruded, General Specification for; Federal Specification QQ-A-200D, August 20, 1970.
18. Aluminum Alloy Bar, Rod, Wire, and Special Shapes; Rolled, Drawn, or Cold Finished, 7075; Federal Specification QQ-A-225/9D, August 24, 1971.
19. Tube, Aluminum and Aluminum Alloy, Drawn, Seamless, General Specification for; Federal Specification WW-T-700E/GEN, July 24, 1972.

#### MILITARY SPECIFICATIONS

20. Aluminum Alloy, Extruded Rod, Bar and Shapes, 7001; Military Specification MIL-A-52242A (MR); 15 August, 1969.
21. Tubing, Chrome-Molybdenum, 4130 Steel, Seamless and Welded, Aircraft Quality; Military Specification MIL-T-6736B; 3 May, 1965.
22. Tubing, Steel (Low Carbon), Mechanical Round; Military Specification MIL-T-3520B, 6 February, 1975.

APPENDIX C  
DRAG COEFFICIENT FOR 4-INCH DIAMETER  
LOW-COST MOTOR

APPENDIX CDRAG COEFFICIENT FOR 4-INCH DIAMETER  
LOW-COST MOTOR

Prior to formulating a baseline design and performing subsequent performance analyses, it was necessary to obtain an estimate of the drag coefficient for a typical 4-inch diameter air launched missile. At the suggestion of the AFRPL Project Officer, the drag information contained in Reference 1 was used in order to maintain continuity with previous trajectory analyses.

Drag of several missiles reported in Reference 1 were applicable. Unfortunately, only power-off drag was available for a 4-inch ATR missile. Preliminary calculations indicated the rocket motor would operate over a significant portion of the missile total flight time, so it would unrealistically penalize missile performance if a power-off drag coefficient was used for the entire flight. However, both power-on and power-off drag was listed for the Sparrow missile. A comparison of the ATR and Sparrow missiles was made:

	Throat Area (in <sup>2</sup> )	Nozzle Expansion Ratio	Missile Diameter (in)	Ratio of Nozzle Exit Area to Missile Frontal Area
ATR	1.178	4.54	4.0	0.334
Sparrow	4.230	5.00	8.0	0.330

Because the ratios of exit area to frontal area were almost the same, it was assumed that the ratio of power-on drag coefficient to power-off drag coefficient was about the same for the two missiles. Therefore

$$\left[ C_{D_{on}} \right]_{ATR} = \left[ C_{D_{off}} \right]_{ATR} \times \left[ \frac{C_{D_{on}}}{C_{D_{off}}} \right]_{Sparrow}$$

The ratio for Sparrow was calculated from listings in Reference 1 (Figure C-1). Then, calculations were made for the ATR (Figure C-2).

---

Reference 1. "Nozzleless Rocket Motor Application Study", AFRPL-TR-72-136, December 1972.

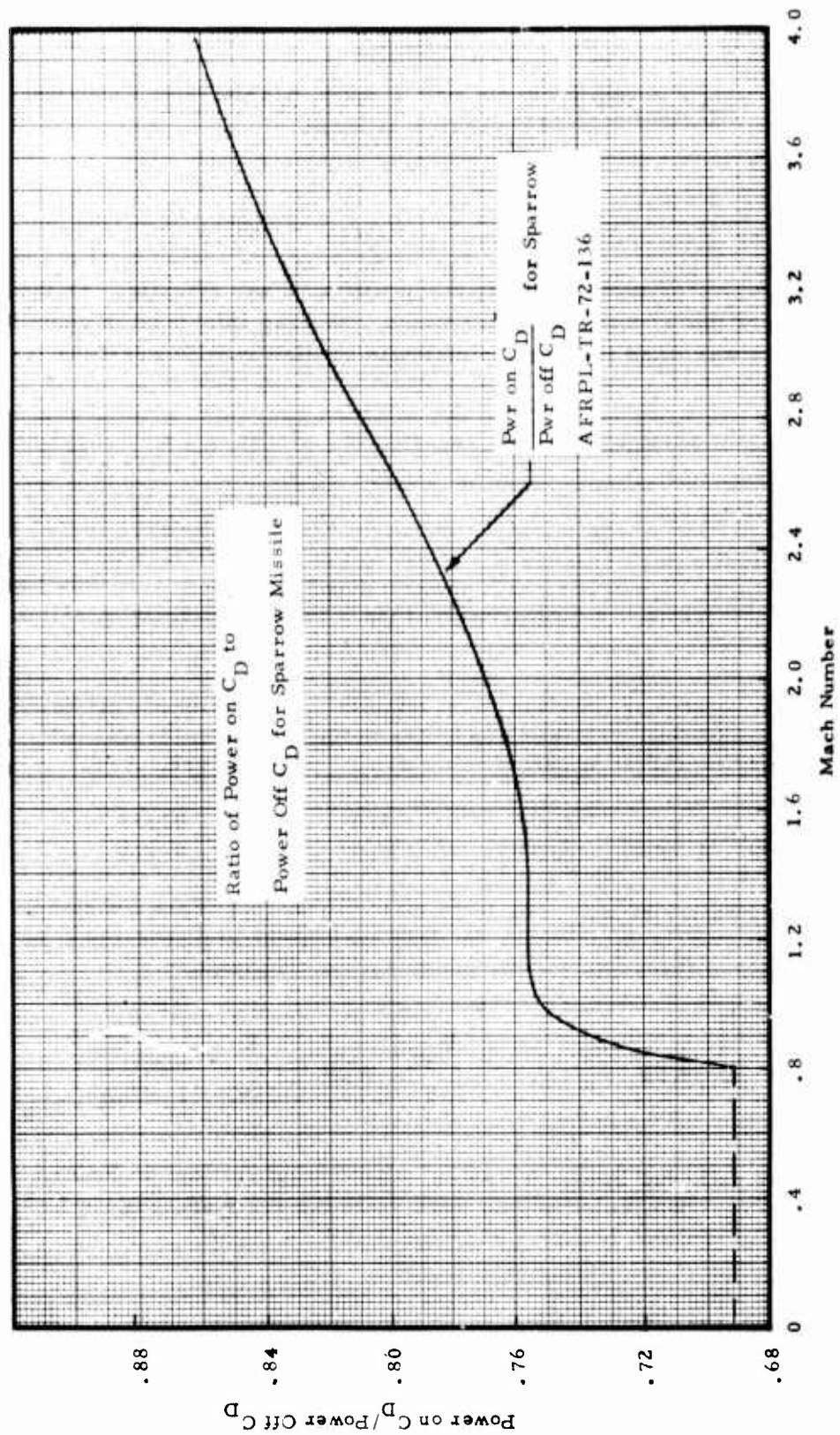


Figure C-1. Ratio of Power on  $C_D$  to Power Off  $C_D$  for Sparrow Missile



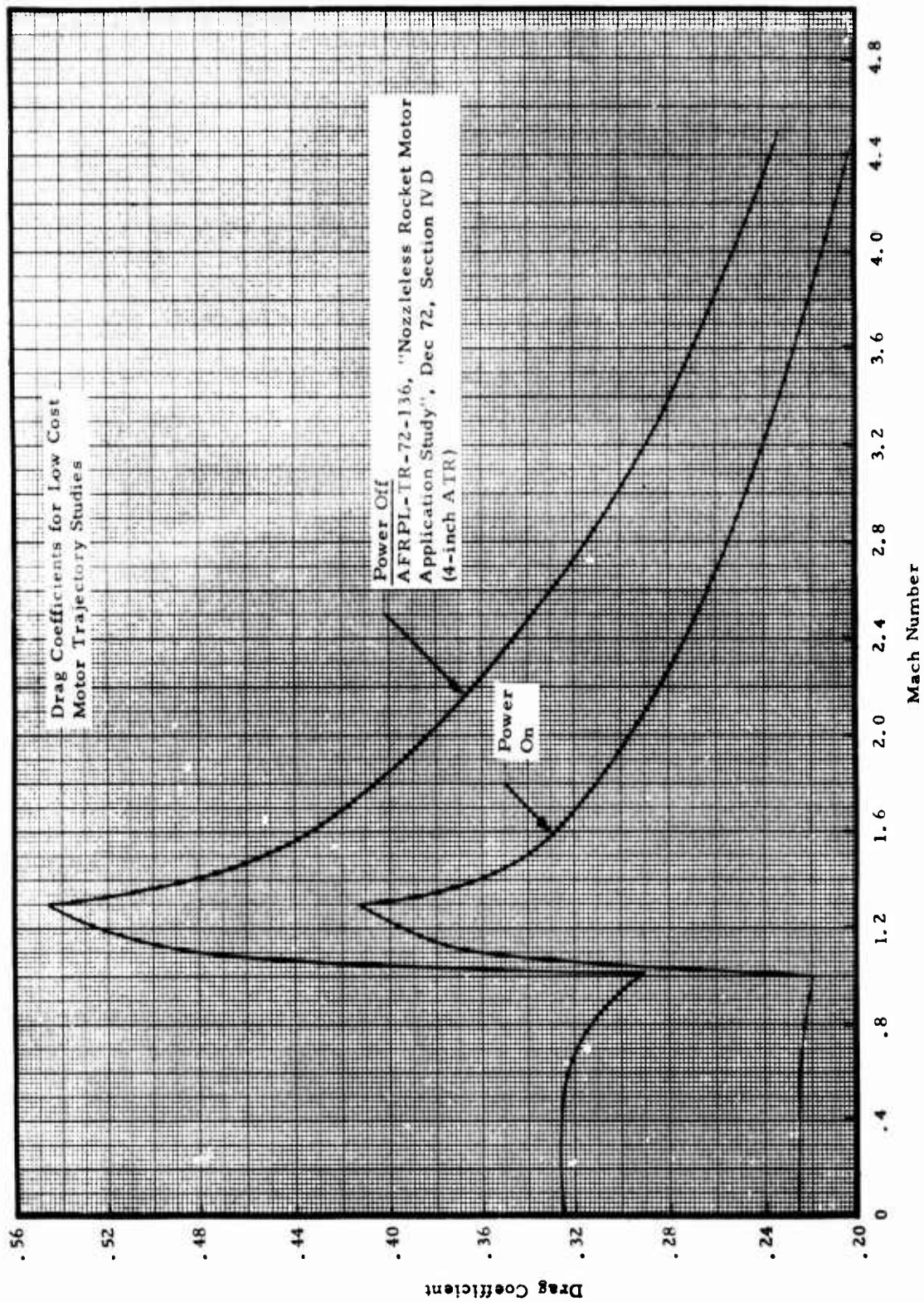


Figure C-2. Drag Coefficients for Low Cost Motor Trajectory Studies